

Some parts of this thesis may have been removed for copyright restrictions.

If you have discovered material in AURA which is unlawful e.g. breaches copyright, (either yours or that of a third party) or any other law, including but not limited to those relating to patent, trademark, confidentiality, data protection, obscenity, defamation, libel, then please read our [Takedown Policy](#) and [contact the service](#) immediately

SEDIMENTOLOGY, PALYNOLOGY
AND DIAGENESIS
OF THE NAMURIAN
IN NORTH WALES

BY
SIFATUL QUADER CHOWDHURY

THESIS SUBMITTED FOR THE DEGREE OF
DOCTOR OF PHILOSOPHY
AT THE
UNIVERSITY OF ASTON IN BIRMINGHAM

APRIL 1986

*To
my mother and father
who have always hoped
for the best*

ACKNOWLEDGEMENTS

Writing a thesis, at any level and of any size, is never a single-handed effort. Behind the backdrop lie invaluable contributions of a host of people and institutions who have directed their efforts - concrete and abstract - to the constant goal of this achievement.

It is a pleasure to record my gratitude to Dr. P. Turner whose valuable and relevant advice, enthusiastic supervision and unfailing encouragement have inspired me to do such a variety of works.

I am also greatly indebted to Dr. Mavis A. Butterworth for her help in palynological interpretations and for providing constant guidance and endless discussion.

I would like to extend my gratitude to Professor D.D. Hawkes, the head of the Geological Science Department, Aston University, for kindly providing the facilities and would like to thank Dr. D.J. Vaughan and all other academic staff of the Department of Geological Sciences, Aston University, for their intellectual contributions which served eventually as ingredients to my thesis. Special thanks are also due to Dr. Maureen Davis, Chemist, British Gas, for her direct help in vitrinite reflectance measurements and to Dr. M.A. Sweeney, Lecturer, Geology Department, University of Zambia, for his continuous help throughout this project. Acknowledgement is also made to the technical staff of the department headed by Mr. E. Hartland, to Mr R.J. Howell of the Department of Metallurgy for his technical assistance and to Mr Harvinder Singh Ubhi, Design Engineer, for his drafting works. I am also very grateful to Miss. Isobel Maciver and to Miss. Elaine Anderson, for their incredible cooperation particularly at the end of this work.

The wonderful service provided by the Aston University Interlibrary Loan System is gratefully acknowledged.

And last, but not least, my thanks are due to a very especial and kind lady, Mrs. Helen Higson, for her continuous moral support, able typing at such short notice and keeping her smiling face always at me.

This study was supported by grants from the Association of Commonwealth Universities, London, United Kingdom. This award is acknowledged with gratitude.

SUMMARY

This thesis presents a variety of geochemical, diagenetic and palynological studies of the Namurian of North Wales. Particular attention has been paid to the Gronant Chert and the Cefn-y-Fedw Sandstone Group.

Seven miospore assemblages have been recognised, which confirm that the study sequences range from the Viséan-Namurian Boundary to Namurian C in age (apart from two coal samples which are found to be Basal Westphalian A in age). Four new taxa from the Rhyd-y-Ceirw Coal Band are described.

On the basis of sedimentological investigation and palynofacies study six major deltaic subenvironments have been distinguished:

i) interdistributary bay shales/shallow marine sandstones; ii) distributary channel sandstones; iii) natural levee sandstones; iv) abandoned channel sandstones; v) swamp shales and vi) coal associations.

Selected major and trace element geochemistry of the Gronant Chert and the Llanarmon-yn-ial cherty flags reveal the origin, conditions of deposition, rate and mechanism of sedimentation and their diagenetic history. The major sources of diagenetic silica in the Gronant Chert are considered to be organic (sponge spicules + radiolarians). The proposed model for the Gronant chertification includes: host limestone >> dissolution and migration of opal-A >> precipitation of opal-CT + organic matter processes of methanogenesis + fermentation + sulfate reduction >> opal-CT to quartz inversion (mg^{2+} released and promoted dolomitization) >> inward diffusion of CaCO_3 >> increase of acidity (result: silica + marcasite and dissolution of carbonates) >> chert-carbonate reversals and multiple replacement reversals >> vadose diagenesis >> limonitization of pyrite.

Geochemistry of the Terrig River shale and the Bwlchgwyn-Minera-Ruabon siliceous shale units was studied in detail to gain precise knowledge of the chemical and mineralogical changes occurring during diagenesis. In the sandstones, early siderite formation is followed by dissolution of K-feldspar-carbonates and development of quartz overgrowth and kaolinite. Early acidic pore waters became more alkaline and the ionic concentration increased, resulting in precipitation of lath-like illite and partial dissolution of kaolinite. The final cement phase is a second, minor phase of blocky kaolinite formation, which may be related to post-Hercynian uplift. The sources of the secondary silica are: pressure solution; dissolution of feldspar; clay-mineral diagenesis; dewatering of siliceous shales and siltstones, and silica bearing Palaeozoic plants.

Key words: NAMURIAN, GEOCHEMISTRY, DIAGENESIS, PALYNOLOGY, PALYNOFACIES.

LIST OF CONTENTS

	<u>PAGE NO.</u>
<u>CHAPTER 1 INTRODUCTION</u>	1
1.1 THE NAMURIAN OF NORTH WALES	1
1.2 STRATIGRAPHICAL DIVISIONS	3
1.3 CORRELATION OF THE NAMURIAN	5
1.4 PREVIOUS WORK	8
1.5 PROJECT AIMS	10
1.6 MATERIAL STUDIED	11
1.6.1 Strata associated with the chert beds at Teilia and Pentre quarry, Prestatyn	11
1.6.2 Samples taken from Llanarmon-yn-ial cherty flags unit	12
1.6.3 Strata associated with the Terrig River Section	13
1.6.4 Strata associated with the Bwlchgwyn old quarry	14
1.6.5 Strata associated with the Minera old quarry	15
1.6.6 Strata associated with the Ruabon Mountain Section	15
1.6.7 Coal samples	16
1.7 METHODS AND TECHNIQUES	16
1.8 PLAN OF THE THESIS	20
 <u>CHAPTER 2 PREVIOUS PALYNOLOGICAL STUDIES</u>	 24
2.1 NAMURIAN PALYNOLOGY IN BRITAIN	24
2.1.1 Early Workers	24
2.1.2 Zonations	24
2.1.3 Correlations	26
2.1.4 Palaeoecological Studies	28
2.2 NAMURIAN PALYNOLOGY IN AREAS OUTSIDE BRITAIN	30
2.2.1 West Europe	30

	<u>PAGE NO.</u>
2.2.2 East Europe	31
2.2.3 Asia	32
2.2.4 North America	32
2.3 PALYNOLOGICAL STUDIES IN NORTH WALES	36
 <u>CHAPTER 3 SYSTEMATIC DESCRIPTION OF MIOSPORES</u>	 38
3.1 INTRODUCTION	38
3.1.1 <u>Anapiculatisporites</u> sp. A	38
3.1.2 <u>Convolutispora</u> cf. <u>cerebra</u>	40
3.1.3 <u>Lycospora</u> cf. <u>noctuina</u>	42
3.1.4 <u>Propriporites</u> <u>laevigatus</u>	44
3.1.5 <u>Laevigatosporites</u> cf. <u>minor</u>	46
 <u>CHAPTER 4 BIOSTRATIGRAPHICAL PALYNOLOGY</u>	 48
4.1 INTRODUCTION	48
4.2 ASSEMBLAGE I	49
4.2.1 Stratigraphical Comparison and Conclusions	50
4.3 ASSEMBLAGE II	51
4.3.1 Stratigraphical Comparison and Conclusions	52
4.4 ASSEMBLAGE III	54
4.4.1 Stratigraphical Comparison and Conclusions	55
4.5 ASSEMBLAGE IV	57
4.5.1 Stratigraphical Comparison and Conclusions	58
4.6 ASSEMBLAGE V	61
4.6.1 Stratigraphical Comparison and Conclusions	62
4.7 ASSEMBLAGE VI	63
4.7.1 Stratigraphical Comparison and Conclusions	64
4.8 ASSEMBLAGE VII	66
4.8.1 Assemblage VIIa	67
4.8.2 Assemblage VIIb	68

	<u>PAGE NO.</u>
4.8.3 Stratigraphical Comparison and Conclusions	69
4.9 PROBABLE REASONS FOR THE FAILURE OF MICROFLORAL RECOVERY IN THE GRONANT CHERT	71
4.10 COMPARISON WITH AREAS OTHER THAN BRITAIN	72
4.10.1 Western Europe	72
4.10.2 North America	74
4.11 CONCLUSIONS	78
 <u>CHAPTER 5 SEDIMENTOLOGY, PALYNOFACIES AND INTERPRETATION OF DEPOSITIONAL ENVIRONMENTS</u>	 99
5.1 INTRODUCTION	99
5.2 HISTORY OF PALYNOFACIES CLASSIFICATION	100
5.3 TECHNIQUES OF PALYNOFACIES ANALYSIS	102
5.4 STRATIGRAPHICAL SETTING	102
5.5 IDENTIFICATION OF DELTAIC SUB-ENVIRONMENTS IN THE PRESENT STUDIED SECTIONS	107
5.5.1 Interdistributary Bay shales/Shallow Marine Sandstones	107
5.5.2 Distributary Channel Sandstones	110
5.5.3 Natural Levee Sandstones	111
5.5.4 Abandoned Channel Sandstones	112
5.5.5 Swamp Shales	113
5.5.6 Coal Associations	115
5.6 DISCUSSION AND CONCLUSIONS	116
 <u>CHAPTER 6 GEOCHEMISTRY OF THE GRONANT CHERT AND THE LLANARMON-YN-IAL CHERTY FLAGS UNITS</u>	 132
6.1 INTRODUCTION	132
6.2 SELECTED MAJOR AND TRACE ELEMENT GEOCHEMISTRY	132
6.2.1 Silica	134

	<u>PAGE NO.</u>
6.2.2 Titanium	135
6.2.3 Relationship between the ratio Si/(Si+Al+Fe)	135
6.2.4 Variations of SiO ₂ and Al/Fe ratio	138
6.2.5 Manganese	141
6.3 ELEMENT (R-MODE) DENDROGRAMS FOR THE LLANARMON-YN-IAL CHERTY FLAGS	145
6.4 ELEMENT (R-MODE) DENDROGRAMS FOR THE GRONANT CHERT	149
6.5 CONCLUSIONS	152
 <u>CHAPTER 7 PETROLOGY</u>	 155
7.1 INTRODUCTION	155
7.2 MEGASCOPIC CHARACTERS OF THE GRONANT CHERT AND THE LLANARMON-YN-IAL CHERTY FLAGS	156
7.2.1 Colour	156
7.2.2 Texture	157
7.2.3 Banding	157
7.2.4 Bedding	158
7.2.5 Fractures	158
7.2.6 Cross-Cutting Relationship	159
7.3 CHERT FABRICS	159
7.4 VOID INFILLING FABRICS	159
7.4.1 Microdrusy Chalcedony	159
7.4.2 Drusy Quartz Mosaic	159
7.5 SIMPLE REPLACEMENT FABRICS	160
7.5.1 Quartz Euhedra	160
7.5.2 Quartz Laths	160
7.5.3 Microcrystalline Quartz	161
7.5.4 Spherulitic Chalcedony	161
7.5.5 Lutecite	162

7.6	COMPLEX REPLACEMENT AND RECRYSTALLIZATION FABRICS	162
7.6.1	Pseudodrusy Quartz Mosaic	162
7.6.2	Coarse Recrystallization Mosaics	162
7.6.3	Radial Quartz Aggregates	163
7.7	CATHODOLUMINESCENCE	163
7.8	SUMMARY	166
<u>CHAPTER 8</u>	<u>DIAGENESIS</u>	167
8.1	INTRODUCTION	167
8.2	SOURCE OF MAGNESIUM AND PROCESS OF DOLOMITIZATION IN THE GRONANT CHERT	167
8.3	CHERT-CARBONATE CARBONATE REPLACEMENT REVERSALS AND MACASITE-PYRITE RELATIONSHIP	172
8.4	INDEX OF CRYSTALLINITY FOR QUARTZ (68° QUINTUPLET)	173
8.5	VADOSE DIAGENESIS	176
8.6	DISCUSSION AND CONCLUSIONS	177
8.6.1	Sources of Silica	182
8.6.2	Time of Formation	183
8.6.3	Proposed Model for the Gronant Chert	184
<u>CHAPTER 9</u>	<u>GEOCHEMISTRY OF THE TERRIG RIVER SHALE AND THE BWLCHGWYN-MINERA SILICEOUS SHALE UNITS</u>	199
9.1	INTRODUCTION	199
9.2	ORGANIC GEOCHEMISTRY	199
9.3	VITRINITE REFLECTANCE	200
9.4	PREVIOUS WORK	201
9.5	INTERPRETATION OF THE PRESENT VITRINITE REFLECTANCE DATA	202

9.6	PETROLEUM GENERATION CAPABILITY OF THE SEDIMENTS UNDER CONSIDERATION	208
9.7	INORGANIC GEOCHEMISTRY	212
9.8	GRAIN SIZE MATURITY AND REDOX PARAMETERS OF THE TERRIG RIVER SHALE AND THE BWLCHGWYN AND MINERA SILICEOUS SHALE UNITS	214
9.9	MINERAL TRENDS RELATED TO SEDIMENTATION AND WEATHERING	217
9.10	ELEMENT (R-MODE) DENDROGRAM FOR THE 'TERRIG RIVER SHALE UNIT'	226
9.11	ELEMENT (R-MODE) DENDROGRAM FOR THE BWLCHGWYN MINERA SILICEOUS SHALE UNITS	228
9.12	ORGANIC CARBON AND TRACE ELEMENT RELATIONS	230
9.13	CONCLUSIONS	234

CHAPTER 10 PETROLOGY AND PROVENANCE OF THE BWLCHGWYN-
MINERA-RUABON SANDSTONE UNIT

10.1	INTRODUCTION	237
10.2	CLASSIFICATION	237
10.3	MINERALOGY	240
	10.3.1 Quartz	240
	10.3.2 Igneous Quartz	241
	10.3.3 Metamorphic Quartz	242
	10.3.4 Sedimentary Quartz	243
	10.3.5 Rock Fragments	243
10.4	UNDULOSE EXTINCTION AND POLYCRYSTALLINITY AS PROVENANCE INDICATORS	244
10.5	CATHODOLUMINESCENCE	246
10.6	CONCLUSIONS	249

	<u>PAGE NO.</u>
<u>CHAPTER 11 DIAGENESIS</u>	257
11.1 INTRODUCTION	257
11.2 PORE FLUID HISTORY	258
11.3 DISSOLUTION	260
11.4 DISSOLUTION OF FELDSPAR-CALCITE-QUARTZ	261
11.4.1 Kaolinization and Dissolution	262
11.5 CLAY REPLACEMENT	264
11.6 AUTHIGENIC MINERALS	264
11.6.1 Siderite	264
11.6.2 Quartz	266
11.6.3 Formation of Quartz	269
11.6.4 Clay Minerals	270
11.6.5 Semi-Quantitative XRD Analysis	270
11.6.6 Kaolinite	275
a) morphology	275
b) distribution	279
c) crystallinity	279
11.6.7 Formation of Kaolinite	280
11.6.8 Illite	285
a) morphology	286
b) textures and distribution	287
c) structures and crystallinity	288
11.6.9 Formation of Illite	289
11.6.10 Illite-Smectite	290
11.7 SOURCES OF SILICA	290
11.7.1 Pressure Solution	291
11.7.2 Dissolution of Feldspar	292
11.7.3 Clay Mineral Diagenesis	292
11.7.4 Dewatering of Siliceous Shales and Siltstones	294
11.7.5 Silica Bearing Palaeozoic Plants	296

	<u>PAGE NO.</u>
11.8 DISCUSSION AND CONCLUSIONS	296
11.8.1 Comparison with other Diagenetic Models	305

CHAPTER 12 CONCLUSIONS

APPENDICES	316
APPENDIX 1	316
APPENDIX 2	321
APPENDIX 3	322
APPENDIX 4	323
APPENDIX 5	324
APPENDIX 6	326
APPENDIX 7	328
APPENDIX 8	330
APPENDIX 9	331
APPENDIX 10	332
APPENDIX 11	333
APPENDIX 12	337
APPENDIX 13	341
APPENDIX 14	344
APPENDIX 15	347
APPENDIX 16	350
APPENDIX 17	353
REFERENCES	357

LIST OF FIGURES

PAGE NO.

Fig. 1.1	Map showing the extent of the Namurian outcrops in North Wales (after Ramsbottom, 1974b).	
	+ = Location of the present studied areas.	2
Fig. 1.2	Namurian palaeogeography (after Ziegler, 1982)	4
Fig. 3.1	Scatter diagram showing the distribution shape in <u>Laevigatosporites</u> cf. <u>minor</u> .	47
Fig. 5.1	Measured stratigraphic sections of the Namurian delta top sequences.	122
Fig. 5.2	Measured stratigraphic section of the Minera old quarry. (SJ 258530), North Wales.	123
Fig. 5.3	Measured stratigraphic section of the Ruabon Mountain. (SJ 25804580), North Wales.	123
Fig. 5.4	Palynofacies analysis of the Namurian delta top sequences, North Wales.	124
Fig. 5.5	Palynofacies analysis of the Namurian delta top sequences. (Minera old quarry), North Wales.	125
Fig. 5.6	Palynofacies analysis of the Namurian delta top sequences (Ruabon Mountain), North Wales.	126
Fig. 5.7	Mean kerogen distribution in the Namurian delta top palynofacies, North Wales.	127
Fig. 5.8	The sedimentation of organic material in a dynamic system is controlled by the energy level maintained in the system (after Fisher, 1980).	128
Fig. 6.1	Relation between the contents of TiO_2 and Al_2O_3 in the Llanarmon-yn-ial cherty flags, shale interbeds and the Gronant chert.	137
Fig. 6.2	Regression lines between Fe and Al.	137
Fig. 6.3	Variations of SiO_2 and Al/Fe from the Llanarmon-yn-ial cherty flags and shale interbeds. Location: SJ 2238 5617.	139

Fig. 6.4	Variations of SiO_2 and Al/Fe from the Gronant chert (SJ 094827).	140
Fig. 6.5	Correlation diagram between the contents of MnO and Al_2O_3 in the Gronant chert (after Lijima <i>et al.</i> 1985).	143
Fig. 6.6	The average rate of sedimentation of the Gronant chert is inferred from the average MnO/ Al_2O_3 ratio. (The original diagram is taken from Lijima <i>et al.</i> 1985).	144
Fig. 6.7	Element (R-mode) dendrogram for samples from the Llanarmon-yn-ial cherty flags and shale interbeds.	148
Fig. 6.8	Element (R-mode) dendrogram for samples from the Gronant chert.	151
Fig. 7.1	Summary of silica fabrics associated with Gronant chert. Similar fabrics were observed by Orme (1974) from the Visean limestones of Derbyshire.	166
Fig. 8.1	XRD tracings of the 68° quintuplet arranged in order of increasing crystallinity of quartz.	174
Fig. 8.2	A. Increase in silica solubility with increasing pH. Volosov (in Williams <i>et al.</i> 1985). B. Increase in silica solubility with increasing temperature for several silica polymorphs (after Williams <i>et al.</i> 1985).	180
Fig. 8.3	XRD patterns representing the diagenetic sequence of silica polymorphs.	181
Fig. 8.4	Schematic representation of the diagenetic sequence for development of the Gronant chert.	187
Fig. 9.1	Some scales of organic metamorphism (after Hood <i>et al.</i> 1975).	205
Fig. 9.2	Relation of LOM to maximum temperature and effective heating time (after Hood <i>et al.</i> 1975).	206
Fig. 9.3	Organic metamorphic stages of petroleum generation (after Vassoyevich <i>et al.</i> 1970).	211

Fig. 9.4	Some geochemical distributions through the Namurian in North Wales.	215
Fig. 9.5	Distribution of minerals and variations in Zirconium, sodium/potassium ratio through the Namurian sequence in North Wales.	218
Fig. 9.6	X-ray diffraction patterns of sample Min-3, using Ni filtered $\text{CuK}\alpha$ radiation showing the anatase main peak.	221
Fig. 9.7	Relation between the detrital quartz and detrital Zr in the Bwlchgwyn siliceous shale.	222
Fig. 9.8	Relation between the detrital quartz and detrital Zr in the Terrig River shale.	222
Fig. 9.9	Relation between the contents of Corg and quartz in the Bwlchgwyn siliceous shale.	222
Fig. 9.10	Relation between the contents of Corg and quartz in the Terrig River shale.	223
Fig. 9.11	Relation between the contents of Sr and illite in the Terrig River shale.	223
Fig. 9.12	Relation between K_2O and illite in the Terrig River shale.	223
Fig. 9.13	Negative correlation between Nb and illite in the Bwlchgwyn siliceous shale.	224
Fig. 9.14	Relation between Nb and illite in the Terrig River shale.	224
Fig. 9.15	Zn shows a positive correlation with illite in the Terrig River shale.	224
Fig. 9.16	Relation between the contents of Corg and Ni in the Terrig River shale.	225
Fig. 9.17	Negative correlation between Ti and illite in the Bwlchgwyn siliceous shale.	225
Fig. 9.18	Relation between the contents of Ti and illite in the Terrig River shale.	225

Fig. 9.19	Element (R-mode) dendrogram for samples from the 'Terrig River shales'.	229
Fig. 9.20	Element (R-mode) dendrogram for samples from the Bwlchgwyn and Minera siliceous shale.	229
Fig. 10.1	Classification of the Bwlchgwyn-Minera-Ruabon (Namurian) sandstones (after Folk, 1968).	238
Fig. 10.2	Geochemical classification of the Bwlchgwyn-Minera-Ruabon sandstone (after Moore and Dennen, 1970).	239
Fig. 10.3	Four variable plot of nature of quartz population in the Namurian sandstones. Dashed lined boundaries between source rock areas are taken from Basu <i>et al.</i> 1976.	245
Fig. 11.1	X-ray diffraction patterns of the clay fractions in the Bwlchgwyn-Minera-Ruabon sandstone, using Ni filtered CoK α radiation.	272
Fig. 11.2	X-ray diffraction patterns of the clay fractions in the Bwlchgwyn-Minera siliceous shale using Ni filtered CoK α radiation.	273
Fig. 11.3	X-ray diffraction patterns of the clay fractions in the Terrig River shale using Ni filtered CoK α radiation.	274
Fig. 11.4	Morphologic variations in kaolinite clay mineral (a), (b) and (c) (001) faces; (d) blocky kaolinite; (e) platy kaolinite.	277
Fig. 11.5	Total silica and relative amounts of silica species in solution in water at 25°C as a function of pH (after Blatt <i>et al.</i> 1980).	278
Fig. 11.6	Relationship between pH and the solubilities of calcite, quartz and amorphous silica (after Blatt <i>et al.</i> 1980).	278
Fig. 11.7	Activity diagram in the kaolinite-illite-K-feldspar system after Hutcheon (1981) whose data was calculated for 500 bars pressure.	283

Fig. 11.8 Variable thermal stability of kaolinite (after Dunoyer de Segonzac, 1970). 284

Fig. 11.9 A. Schematic representation of change in composition of pore water during initial compaction of a sandstone-shale sequence (after Wallace, 1976). 295

B. Schematic representation of change in composition of pore water in a sandstone-shale sequence during long term burial (after Wallace, 1976).

LIST OF TABLES

PAGES NO.

Table 1.1	Namurian stages used in Britain in relation to the bases of marine marker bands and Heerlen Conference (1935).	6
Table 1.2	Lithostratigraphical units used in the present thesis.	7
Table 4.1	The distribution of miospores in different localities of North Wales mentioned in the the text.	82
Table 4.2	The ranges of key spores illustrated are based upon the occurrence of spores in different localities of North Wales mentioned in the text.	89
Table 4.3	Summary of the present palynological study.	90
Table 5.1	Palynofacies characteristics of the main delta top sub-environments (after Denison and Fowler, 1980).	129
Table 6.1	Average compositions and standard deviations for major rock types.	133
Table 6.2	Ratios Si/(Si+Al+Fe) and correlation between Fe and Al in samples from the Gronant chert and the cherty flags and shale interbed.	136
Table 9.1	Thermal maturity and estimated maximum temperature for each sampling locality.	203
Table 9.2	Distribution of selected trace elements (ppm) against miospore assemblages.	236
Table 10.1	Electron probe microanalysis of quartz grains (core) and authigenic overgrowths from the Minera Sandstones.	251
Table 11.1	Diagenetic processes and the pore water conditions in the Namurian sandstones of North Wales.	260

Table 11.2	The minimum, maximum and average percentages of each of the clay minerals in the shales under survey.	271
Table 11.3	Comparison of the paragenetic sequence of the diagenetic events in the Namurian Sandstones of North Wales with those of some other deltaic sandstones.	307
Table A.5.1	Reflectance standards in common use.	324
Table A.9	Total organic carbon percentages in the studied sediments.	331
Table A.10	Quartz percentages in the studied sediments	332
Table A.11	Results of XRF analysis (major elements) of the present studied sediments.	333
Table A.12	Results of XRF analysis (trace elements) in ppm. of the present studied sediments.	337
Table A.13	The similarity matrices of the major and trace elements of the Gronant Chert.	341
Table A.14	The similarity matrices of the major and trace elements of the Llanarmon-yn-ial cherty flags.	344
Table A.15	The similarity matrices of the major and trace elements of the Terrig River shale.	347
Table A.16	The similarity matrices of the major and trace elements of the Bwlchgwyn-Minera siliceous shales.	350

LIST OF PLATES

CHAPTER 4

- Plate 4.1 Miospore species
- Plate 4.2 Miospore species
- Plate 4.3 Miospore species
- Plate 4.4 Miospore species
- Plate 4.5 Miospore species
- Plate 4.5 Miospore species
- Plate 4.6 Miospore species
- Plate 4.7 Miospore species
- Plate 4.8 Miospore species

CHAPTER 5

- Plate 5.1 Lateral accretion unit
- Plate 5.2 Llanarmon-yn-ial cherty flags unit and Maes-y-Droell quarry.
- Plate 5.3 Sedimentary organic matter
- Plate 5.4 Palynofacies distribution in different deltaic sub-environments.

CHAPTER 8

- Plate 8.1 Silica fabrics associated with the Gronant chert and the Llanarmon-yn-ial cherty flags units.
- Plate 8.2 Silica fabrics associated with the Gronant chert and the Llanarmon-yn-ial cherty flags units.
- Plate 8.3 Chert-carbonates-sulphides relationship and quartz overgrowth
- Plate 8.4 Biogenic constituents of the Gronant chert and the cherty flags.
- Plate 8.5 Subequant to polyhedral microquartz crystals and dissolved radiolarian test.

- Plate 8.6 Detrital illite clay coating on quartz overgrowth and replacement origin of microquartz.
- Plate 8.7 Dissolution of dolomite rhombs.
- Plate 8.8 Chert-carbonate replacement reversal features together with ? massive opal-CT and pyrite framboids.
- Plate 8.9 Megascopic characters of the Gronant chert.
- Plate 8.10 Cathodoluminescence photographs of the Gronant chert carbonates.
- Plate 8.11 Cathodoluminescence photographs of the Gronant chert carbonates.

CHAPTER 10

- Plate 10.1 Monocrystalline and polycrystalline quartz types.
- Plate 10.2 Rock fragments and authigenic quartz grains.
- Plate 10.3 Pressure solution features and quartz kaolinite relationship (Cathodoluminescence).
- Plate 10.4 Pressure solution features and quartz-kaolinite relationship (Cathodoluminescence).
- Plate 10.5 Complex fracturing and shallow etch pits in quartz overgrowths (Cathodoluminescence).
- Plate 10.6 Cathodoluminescence of quartz-chert rock fragment- calcite cement.

CHAPTER 11

- Plate 11.1 Dissolution of feldspar-carbonates-quartz. Sedimentary rock fragments. Authigenic illite.
- Plate 11.2 Siderite crystallization and formation of incipient quartz overgrowths.
- Plate 11.3 Stages of quartz overgrowth.
- Plate 11.4 Stage of quartz overgrowth.
- Plate 11.5 Stages of quartz overgrowth and quartz grain surface texture

- Plate 11.6 Authigenic platy and blocky kaolinite.
- Plate 11.7 Authigenic platy and blocky kaolinite.
- Plate 11.8 Authigenic tiny blocky kaolinite and dickite. Flaky morphology of detrital illite.

CHAPTER 1

INTRODUCTION

1.1 THE NAMURIAN OF NORTH WALES

In North Wales Namurian rocks are recorded in the area to the east of the Carboniferous Limestone outcrop from near Prestatyn in the north to Ruabon and Oswestry in the south (Ramsbottom, 1974b; see also Fig. 1.1). This distance covers about 56 km and is characterised by a major facies change from the thicker shaly succession of the northern area (the Holywell Shales) to the thinner predominantly sandy succession of the south, which is a part of the Cefn-y-Fedw Sandstone Group (Ramsbottom, 1974b). Deposition of the Cefn-y-Fedw Sandstone Group occurred in a shallow-marine to delta-swamp environment, while the Holywell Shales are mostly marine in origin.

North Wales lies on the south-western edge of the Central Province Namurian basin. The northern edge of St. Georges Land passes through the region (Fig. 1.2). It is believed that the sandy nature of the Namurian rocks of Denbighshire reflects its proximity to the coast-line. Basinal shaly deposits predominate in the north although according to Ramsbottom (1974b) there were a number of islands (as near Rhydymwyn) or an uneven coast-line.

The British Namurian comprises quartzitic and feldspathic types of sandstones. The sandstones derived from St. George's Land are of the quartzitic type and form a part of the Cefn-y-Fedw Sandstone Group (except for the Aqueduct Grit at the top). Ramsbottom (1969, 1970) advocated that the greatest influx of the Middle Cefn-y-Fedw Sandstone into the basin occurred during the early part of the Namurian and that, in areas to the south and east, denudation of St. George's Land ceased in the later Namurian.



Illustration removed for copyright restrictions

Fig.I.I. MAP SHOWING THE EXTENT OF THE NAMURIAN
OUTCROPS IN NORTH WALES.(after Ramsbottom,1974)

+ = Location of the present studied areas.

On the other hand, the source of the feldspathic sandstones was considered to be the north-east for the Central Province basin, but did not reach North Wales until R2 and G1 times. They also include the Lower Gwespys Sandstone and Aqueduct Grit.

Ramsbottom (1974b) considered that only in the basinal area (i.e. around Holywell and Flint), was deposition possibly continuous with the underlying Viséan rocks. However, the present palynological work indicates the presence of the lowest Namurian horizons further south around the Llanarmon-yn-ial area. Similarly, the palynological work also suggests the presence of other Namurian stages in the Terrig River, and the Bwlchgwyn and Minera quarry sections, which were previously thought to be missing (see Biostratigraphical Palynology Chapter 4). In other circumbasin areas the Namurian sea was transgressive, and thus it is in North Wales.

The basinal macrofossils of the Namurian mainly include non-benthonic goniatites and bivalves, while in contrast, the near coastal shallow water faunas are characterised by the presence of a benthonic fauna - usually of productoid, spiriferoid and other brachiopods and of benthonic mollusca.

The most north-westerly outcrop of Namurian beds in North Wales is at Prestatyn.

1.2 STRATIGRAPHICAL DIVISIONS

Major Carboniferous divisions were introduced early in the history of geology. The term Millstone Grit and Coal Measures were introduced in 1778 and 1811 by Whitehurst and Farey respectively. Conybeare and Phillips (1822) proposed the threefold division of the Carboniferous rock types into Carboniferous Limestone, Millstone Grit, and Coal Measures.



Aston University

Illustration removed for copyright restrictions

These latter divisions are still valid, and denoted in the three terms, Dinantian, Namurian and Westphalian.

However, Green *et al.* (1878) divided the Carboniferous into two, and referred the Millstone Grit and Coal Measures to the Upper Carboniferous and the Carboniferous Limestone and the Yoredale 'Series' to the Lower Carboniferous. These divisions were recognised by the Heerlen Conference in 1935. In 1960, the subcommission on Carboniferous Stratigraphy proposed the term 'Silesian' as a corresponding series name for the Upper Carboniferous of Western Europe (van Leckwijck, 1960, p.xxv). The Silesian is now accepted as a Subsystem and its constituent divisions the Namurian, Westphalian and Stephanian are considered to be Series (George and Wagner, 1972).

Jongmans and Gothan (1937) divided the Namurian into Namurian A, B, C, using goniatite horizons for the boundaries.

Bisat (1928) proposed a set of stages for the Namurian, including the Marsdenian and Kinderscoutian, and these through a process of evolution (Ramsbottom, 1969a), with the proposal of Yeadonian, Arnsbergian, and Pendleian by Hudson and Cotton (1943) and of Alportian and Chokierian by Hodson (1957), developed into the set of Stages used today. The limits and possible stratotypes of these stages have been discussed in detail by Ramsbottom (1969a).

A summary of the above observation can be seen in Table 1.1.

1.3 CORRELATION OF THE NAMURIAN

Goniatites are the primary means of correlation in the Namurian. The rate of evolution of goniatites being such that nearly every cyclothem contains its own distinctive and diagnostic species. The importance of goniatites in



Illustration removed for copyright restrictions

Table 1.1 Namurian stages used in Britain in relation to the bases of marine marker bands and Heerlen Conference (1935).

Series	Units
Basal Westphalian	Aqueduct + Chwarelau Coal
Namurian	Rhyd-y-ceirw Coal Bwlchgwyn-Minera-Siliceous Shale and Bwlchgwyn-Minera-Ruabon Sandstone Terrig River Shale
Viséan	Llanarmon-yn-ial Cherty Flags and Gronant Chert

Table 1.2 Lithostratigraphical Units used in the present thesis.

the Namurian stratigraphy has been described by Bisat (1924; 1928); Bisat and Hudson (1945); Hodson (1957) and Ramsbottom (1967; 1969b). The faunas of each individual goniatite band are given by Ramsbottom (1967). A combination of lithological correlation, based on cycles, and the recognition that new goniatite (and other faunas) enter after regressive periods enabled Ramsbottom (1977) to recognise a set of major cycles in the British Namurian. Each such major cycle (there are 11 in the Namurian) was termed a mesothem (see also Biostratigraphical Palynology Chapter 4).

Apart from goniatites, the Namurian has been biozoned using conodonts (Higgins, 1975) and miospores (Owens *et al.* 1977). In areas where goniatites are rare Namurian stages were recognised by means of miospores by Neves *et al.* (1965) and Owens (in Owens and Burgess, 1965).

Six miospore assemblages have been recognised from the Namurian sequences in North Wales during the present palynological study. These assemblages are dated for the first time by miospore evidence, compare fairly closely with the concurrent range zones defined by Owens *et al.* (1977) and Clayton *et al.* (1977). But because the sequences from which the samples are taken are not always continuous they are referred more loosely to assemblages. All these have been discussed more fully in Chapter 4.

1.4 PREVIOUS WORK

No detailed work on the geochemistry, sedimentology and palynology of the Namurian sediments in North Wales is reported so far. Early works were mostly concentrated on stratigraphy based on lithology and macro fossils.

Conybeare and Phillips (1822) noted that the Holywell Shales, corresponded in character and stratigraphical position to the similar shaly and sandy beds of the Millstone Grit of Derbyshire. But the same facies was later allocated to the Yoredale Series, of Lower Carboniferous age, by Green (1867). In the southern part of North Wales, Morton (1876) proposed the term Cefn-y-Fedw Sandstone, for all the beds between the top of the Carboniferous Limestone (which he took at the base of the Sandy Limestone) and the base of the Coal Measures. On Cefn-y-Fedw (the type section is Ruabon Mountain) he divided the Sandstone into Lower (comprising the Lower Sandstone and Cherty Shale), Middle (Middle Sandstone) and Upper (Lower Shale to top of Aqueduct Grit). The Geological Survey regarded the Cefn-y-Fedw Sandstone in this area as coincident with the Millstone Grit of the Pennines.

Goniatites made a revolutionary change in the Namurian stratigraphy of the British Isles. King (1913) reported the presence of goniatites in the Namurian sediments of North Wales. Jackson (1925) recorded the Namurian marker-goniatite Hudsonoceras proteus from the Holywell Shales, and later Sargent (1927) gave an almost complete zonal succession of goniatites in these shales. Jones and Lloyd (1930; 1942) recorded many goniatite localities from the Flintshire and south Denbighshire. Some of these recorded goniatites were from the Cefn-y-Fedw Sandstone Group, and these finally showed the contemporaneity of the Sandstone with the Holywell Shales.

Ramsbottom (1974b) gave a detailed review of the Namurian of North Wales based on the available published information and a re-interpretation and collation of information obtained from boreholes located mainly in the northern part of the district. It is now widely believed that (though not well established) the cherty beds above the Carboniferous Limestone in Flintshire are of Viséan age. Ramsbottom

(1974b) also excluded that part of the Cefn-y-Fedw Sandstone below the top of the Cherty Shale from the Namurian (see Table 1.2). However, the present palynological work suggests that in the Llanarmon-yn-ial area, the Llanarmon-yn-ial cherty flags unit has a long range (at an horizon spanning the P1 and the E1 goniatite zones of the upper most part of the Asbian to the Pendleian stage). Thus this unit can be considered convincingly as part of the Namurian. On the other hand, as the precise age of the Gronant chert is yet to be established, therefore, this unit may be regarded as part of the Namurian.

1.5 PROJECT AIMS

This thesis is fundamentally concerned with investigating the Viséan-Namurian chert beds and the Namurian sandstone succession (Cefn-y-Fedw Sandstone Group) in North Wales. Particular attention has been paid to the organic and inorganic geochemistry, sedimentology, mineralogy, diagenetic history, biostratigraphical palynology, and palynofacies content of the rocks with the aim of providing a comprehensive and detailed analysis of the sequence. It was not an original aim of this project to study the coal samples obtained from Dr. Mavis A. Butterworth. However, for a number of reasons, particularly to compare the vitrinite reflectance values of coals with adjacent shale beds and to know the overall palynostratigraphic position of the coals in the sequence, an investigation of three coal samples was initiated.

During fieldwork special precautions were taken to collect fresh exposed samples from quarries, road cuts and river sections. Before taking any sample the exposed and weathered surface was cleaned to about 10-15 cm. depth. This process avoids contamination by spores and pollen of living plants and recent soil horizons and removes surfaces which have undergone more oxidation than below. Samples were then cut to convenient sizes with the help of a hammer to ensure full representation

of the unit. They were first examined in the field and divided into separate layers wherever possible in accordance with the petrography of the unit. Later on, in the laboratory a detailed description of the petrography was made. Graphic logs were prepared for a number of representative sections. This system was followed for all rock types.

The term 'chert' will be used in this thesis in its widest sense to include all of the compact bedded and nodular deposits which consist essentially of crystalline, microcrystalline and/or cryptocrystalline silica together with varying proportions of impurities such as calcite, dolomite, carbonaceous matter, clay minerals, iron etc. The term 'cherty flags' will be used for hard, brittle rocks, friable in places, and white/creamy in colour with iron oxyhydroxides staining and containing substantial amount of clay minerals.

The terms 'sandstone and shale' will be used after Pettijohn (1975).

1.6 MATERIAL STUDIED

The area under present survey in North Wales crops out to the east of the Clwydian Range and includes the following localities:-

1.6.1 Strata associated with the chert beds at Teilia and Pentre quarry, Prestatyn.

All the cherts found at Teilia Farm disused quarry (SJ 079813) and at Pentre quarry (SJ 094827) during the present investigation will be referred to as 'Gronant Chert' (Figs. 1.1 and 6.4).

At Teilia, a distinctive lithology of papery laminated dark grey shales with interbedded black laminated argillaceous limestone which appears light grey on weathered surfaces and fractures conchoidally passes into black cherts towards the top of the sequence.

The old quarry at Teilia Farm is largely overgrown and infilled. An outcrop underneath tree roots in the north-east part of the quarry contains 1 metre of unfossiliferous black limestone, with parallel bedding planes about 15 cm. apart. At the Western edge of the quarry and about 5 metres below the level of the black limestone occurs a 30-40 cm. massive bedded limestone. At the northern edge of the quarry massive bedded black chert is seen.

Massive bedded chert, best seen in a 25 metres quarry section at Pentre quarry, is very well bedded with beds usually being 10-15 cm. thick and rarely much more. The chert here is black and breaks conchoidally except at the bedding planes where the rock is a cherty black limestone and has a platy fracture. The chert usually shows fine laminations in hand specimen and rarely very slight wave ripples.

The massive black chert beds pass up conformably into the black or dark grey shaly limestone with fine parallel laminations and which are usually very fissile. This happens in the top 8 metres of the quarry. However, the presence of substantial amounts of chert in them suggests that they are part of the Gronant chert.

Three samples were collected from Teilia quarry and twelve from Pentre quarry. All of them were studied geochemically and sedimentologically, but were found to be extremely unproductive for palynological investigation.

1.6.2 Samples taken from Llanarmon-yn-ial cherty flags unit

The Llanarmon-yn-ial cherty flag and shale interbed unit (Figs. 1.1 and 5.1) is best exposed in the Maes-y-Droell quarry (SJ 2180 5655), where it is about 15-20 metres thick and is underlain by another 15-20 metres thick of very fine to fine grained, friable and unconsolidated quartz rich

sandstones. This unit is characterised by creamy-white porcellanous quartzitic silts with alternating thin shale beds which are highly siliceous and pass into pure chert. This unit is also well exposed in the stream which runs from Graianrhyd (SJ 2188 5608) eastwards to the River Terrig, joining it at (SJ 2313 5623).

At (SJ 2238 5617), alternating creamy-white porcellanous quartzitic silts, which are iron oxyhydroxides stained and thin dark shales, which are sandy and friable are exposed in a small, disused quarry.

Further to the east from the above location, are more exposures of similar rocks, in the stream beds and banks.

Near Pant Terfyn at (SJ 2270 5550), more competent beds of porcellanous quartzitic silts are exposed in a small disused quarry. The rocks are creamy-white in colour, with iron oxyhydroxides staining and some badly preserved fossils.

A total of 65 samples were collected from all the localities mentioned above and will be termed in this thesis as Llanarmon-yn-ial cherty flags. Later on, these samples were studied in terms of geochemistry, sedimentology, palynology and palynofacies content.

1.6.3 Strata associated with the Terrig River Section

The River Terrig sections occur about 2 1/2 miles east of Llanarmon, and are typified by good exposures of a fine to medium grained sandstones interbedded with shales and siltstones (Figs. 1.1 and 5.1).

At location (SJ 2336 5688) a massive fine to medium grained sandstone is observed, interbedded with dark grey shales and siltstones, forming a small waterfall at the junction of a stream from Mynydd-du. The

interbedded shales and siltstones are occasionally highly siliceous. Three samples were collected at a vertical interval of 1 metre from this location.

At location (SJ 2335 5687), which is about 450-500 yds. lower down the river from the above location, there is a cliff section of about 15.24 metres thick, which consists essentially of weathered, light to dark grey, fissile and splintery shales/siltstones. The top most beds of this cliff were not accessible, but Wedd *et al.* (survey memoir, 1924; p.36) noted that the upper beds "consist of sandstones with brachiopod and plant remains and shales with black argillaceous limestones containing Posidoniella, Goniatites etc.". Four samples were collected at a vertical interval of 4 metres from this cliff section.

At (SJ 2329 5783), to the north-west of the above two locations the lithology is dominantly composed of fine to medium grained sandstones interbedded with dark grey shales. Two samples were collected from this location.

All the samples collected from the 'Terrig River Section' are shales and will be referred here as 'Terrig River Shale'.

The geochemistry, sedimentology, palynology and palynofacies content of these shales were studied in detail.

1.6.4 Strata associated with the Bwlchgwyn old quarry

Bwlchgwyn old quarry (SJ 2596 5311; Figs. 1.1 and 5.1) offers a fairly good section of fine to medium grained, tough quartzitic sandstones interbedded with dark grey to black extremely fine grained, vitreous, highly silicified thin siltstones/shales, which preserve a banded or laminated appearance with occasional flaky fracture. At the bottom of the quarry section thin fossiliferous fine to medium grained sandstone beds

are observed containing principally hinged brachiopods (Productids, Spiriferids, etc.). Near the top of the section a rather coarse grained sandstone bed with scattered pebbles and interstitial kaolinized and highly altered feldspar is seen directly overlying a lateral accretion unit and is very similar to the rock types recorded in the Aqueduct Grit Group.

A total of twenty samples (sandstones and siliceous shales) were collected from this quarry and their geochemistry, sedimentology, palynology and palynofacies content were investigated in detail.

1.6.5 Strata associated with the Minera old quarry

Minera old quarry (SJ 258 530; Figs. 1.1 and 5.2) is characterised by fine to medium grained highly quartzitic sandstones with intercalated thick dark grey, silicified siltstones/shales. The siltstone/shale intercalations are highly silicified at the bottom but lesser towards the top.

A total of eight samples (sandstones and siliceous shales) were collected and analyzed in detail.

1.6.6 Strata associated with the Ruabon Mountain section

Unfortunately, the location under consideration (SJ 2580 4580; Figs. 1.1 and 5.3) from the Ruabon Mountain consists mainly of arenaceous materials and hence no samples suitable for palynological studies were collected. A total of 10 samples, mostly sandstones were studied in terms of geochemistry, sedimentology and palynofacies content.

It would be wise to mention here that all the sandstone samples collected from the Bwlchgwyn-Minera-Ruabon area will be denoted here as 'Bwlchgwyn-Minera-Ruabon Sandstone Unit'. Similarly the interbedded siliceous shales/siltstones from the Bwlchgwyn and Minera quarry area will be referred to as 'Bwlchgwyn siliceous shale'/'Minera siliceous shale'.

Locations and Grid references of the present studied areas

LOCATIONS	GRID REFERENCES
Teilia Farm disused quarry, Prestatyn	SJ 079813
Pentre quarry, Prestatyn	SJ 094827
Maes-y-Droell quarry, Llanarmon- yn-ial area	SJ 2180 5655
From Graianrhyd eastwards to the River Terrig	SJ 2188 5608 SJ 2313 5623
Pant Terfyn, Llanarmon-y-ial area	SJ 2270 5550
Terrig River	SJ 2336 5688
Terrig River	SJ 2335 5687
Terrig River	SJ 2329 5783
Rhyd-y-Ceirw Coal Band, Terrig River	SJ 2336 5688
Bwlchgwyn old quarry	SJ 2596 5311
Minera old quarry	SJ 2580 5300
Ruabon Mountain Section	SJ 2580 4580
Aqueduct and Chwarelau Coal Seams	Australia, Marl pit, North Wales

1.6.7 Coal Samples

During the present investigation three coal samples were also studied palynologically and their vitrinite reflectance values and palynofacies content were also recorded.

One coal is from a 6" thick coal seam, in the 'Terrig River Section', locally known as the 'Rhyd-y-ceirw Coal Band'. Ramsbottom (1974b) has pointed out the stratigraphic position of this 'Coal Band' in between the Gastrioceras cumbriense and Gastrioceras cancellatum Marine Bands. The location of this sample is (SJ 2336 5688).

Two other coal samples, one each from the Aqueduct and Chwarelau Coal Seams, Australia, Marlpit, North Wales. The Aqueduct seam is situated below the Gastrioceras subcrenatum Marine Band at the base of the Westphalian series and the Chwarelau seam is from slightly higher in the sequence (Smith and Butterworth, 1967).

1.7 METHODS AND TECHNIQUES

A wide variety of methods and techniques have been used in the study which are briefly described below. More detailed analytical procedures are described in the appendices.

Palynological slides were prepared for each shale and coal sample. The shale samples were crushed to about 2-3 mm. in diameter, while the coals were crushed to pass through a B.S. 36 mesh (0.42 mm.). The mortar and the pestle was used repeatedly to crush harder grains of coals and clastics to avoid the whole sample from becoming powdered which causes the destruction of spore exines. For oxidation of coal samples about 1 gramme of coal was taken in each case and treated with different proportions of fuming and concentrated nitric acid, for periods ranging from 3-6 hours.

The separation of spores from clastic sediments was done by the treatment with dilute Hcl to get rid off any carbonate present, and then with 40% HF, to dissolve the silicates. Cellosize (aqueous solution of hydroxyethyl cellulose) and elvacite were used as mounting media for slides. Routine logging of the miospore species was done at a magnification of 400 times using a VICKERS MICROSCOPE. Fine details of morphology were examined at higher magnification using oil immersion. All photographs were taken using ZEISS PHOTO-MICROSCOPE II (66215).

Palynofacies slides were made of sandstone, shale, cherty flags and coal samples. The samples were crushed to pea-sized fragments and macerated in hydrochloric and subsequently hydrofluoric acid for a couple of weeks. Standard palynological slides were prepared using cellosize and elvacite. For coals normal palynological slide preparation technique was employed. One slide was made from each sample and a total of at least five traverses across the slides were point counted to establish the Kerogen components and the results were recalculated to 100%. and presented in different diagrams.

Dyed-resin impregnated thin sections were prepared for each chert, cherty flags and sandstone sample and some selected shales. Those containing carbonate cement were stained using the combined stain of potassium ferricyanide and Alizarine Red "S". One sandstone sample was also stained for feldspar using sodium cobaltinitrite and hydrofluoric acid (Chayes's Method). Petrographic studies included routine investigation of thin sections and modal analysis using conventional techniques (Carver, 1967).

Vitrinite reflectance values were measured for each coal and selected shale samples in order to know the diagenetic palaeotemperatures and hence to infer the thermal history of the sediments. The principle involved in this technique is light with a wavelength of 546 nm, reflected

at near normal incidence from a specified area of well polished vitrinite, measured under oil immersion using a photomultiplier (or similar device), is compared with light reflected under identical conditions from a number of standards of known reflectance. Sample preparation included washing, drying, mounting in cold-set resin and hand polishing through three grinding and three polishing stages. A detailed account of the equipment will be given in Appendix 5.

Chemical analysis of cherts, cherty flags, sandstones and shales for major and trace elements were made using X-ray fluorescence (XRF) technique. The analysis of the major and trace elements was made with the aim of defining the ultimate sources of the elements and mode of incorporation since this might indicate the primary composition of parent rocks. Interpreting these analyses were also important for understanding the inter-elemental relationship, their compositional variation and to understand some of the important factors that regulate the geochemistry of these sediments and their diagenetic changes.

Organic carbon was determined based by the ignition loss method as described by Dean (1974).

Quartz was determined following the method of Carver (1967).

The scanning electron microscope (SEM) was used especially to study authigenic minerals, dissolution features, time and textural relationships between the authigenic phases and to determine the silica sources. Cherts, cherty flags, sandstones and shales were prepared for SEM study. Samples with fresh fractured surfaces were fixed onto stubs and coated under vacuum by carbon or gold palladium. The associated energy dispersive analyser of X-rays (EDAX) was used for mineral identification by means of semi-quantitative chemical analysis.

The electron probe microanalyser (EPMA) was also used to study quantitatively the authigenic and detrital quartz. The analysis was carried out on carbon coated polished thin sections using 20 KV voltage. This technique was employed with a view to investigate any possible trace element variations with respect to the luminescence colour variations between the authigenic and detrital quartz core. However, the results were found to be inconclusive.

Cathodoluminescence was employed in order to distinguish between the different types of quartz grains and their possible source areas, to determine the pressure solution features, to establish the relationship between the quartz cementation and kaolinite precipitation and in the Gronant chert to obtain the different carbonate phases present. Cathodoluminescence was achieved using a Technosyn cold cathode luminescence model 8200 MK 2 instrument. An accelerating voltage of between 15-20 KV with a current of 0.2-0.4 mA and a beam area of approximately 100 mm² was applied to polished thin sections (see also Appendix 1).

Sixty-six oriented clay samples (less than 5 m fraction) were prepared by the dispersion of gently disaggregated cherty flags, chert, sandstone and shale samples followed by sedimentation onto glass slides or suction onto ceramic discs. For shales ultrasonic vibrator was also used. The oriented samples were dried at room temperature and analysed by X-ray diffraction (XRD) using Co K α radiation. The samples were then glycolated using ethylene glycol for about 12-14 hours by a vaporization method (Kunze, 1955) for the glass slides. The ceramic discs were glycolated by standing them in a shallow pool of ethylene glycol for 2-4 hours at 80°C. The samples were then re-run under the same diffractometer conditions in order to identify the presence of expandable clay minerals. To determine the existence of certain minerals (like Kaolinite) the samples were

subsequently heated up to 550°c for two hours (Carrol, 1970). At this temperature Kaolinite decomposes to amorphous meta-kaolin. A semi-quantitative analysis of all the clay mineral species was also performed.

Moreover, some bulk samples of cherts and shales were also X-rayed to have a comprehensive idea about their mineralogy.

X-ray diffraction technique was also used to identify different silica polymorphs and index of quartz crystallinity (CI) using CuK radiation.

Initially grain size analysis was also carried out on some selected sandstone samples. Later the author found that these sandstones are extremely affected by secondary silicification. Therefore, to avoid any possible error, no grain size data was used in this thesis.

Quartz grain surface texture study with the help of SEM was also avoided for the same reason.

1.8 PLAN OF THE THESIS

Chapters 2-4 are concerned with the study of the biostratigraphical palynology, while the results of the facies analysis is presented in Chapter 5. Geochemistry, petrology and diagenesis of the Gronant chert - Llanarmon-yn-ial cherty flags and the Bwlchgwyn-Minera-Ruabon sandstone/siliceous shale - Terrig River shale units are presented in Chapters 6-8 and Chapters 9-11. Chapter 11 is followed by appendices and a list of references cited.

Chapter 2 outlines a review of the previous Namurian palynology in Britain, West Europe, East Europe, Asia and North America with a particular emphasis in North Wales.

In Chapter 3, a brief systematic description of the miospores is given. Care has been taken to include mostly the newly described miospore species and to avoid those which are already well documented by different authors. A summary on the previous literature on spore classification and the classification adopted in the present work is also discussed.

Chapter 4 outlines a detailed description of different miospore assemblages proposed during the present investigation and their palynostratigraphical comparison and conclusions. A comparison with similar successions in West Europe and North America is also attempted. Probable reasons for the failure of microfloral recovery in the Gronant chert are also discussed.

In Chapter 5, the results of a facies analysis are presented, with particular reference to an integrated approach of the palynofacies content of the rock types and the conventional sedimentological facies interpretation. A brief review on the previous palynofacies classification and the classification favoured in the present work is also discussed.

In Chapter 6, selected major and trace element geochemistry of the Gronant chert - Llanarmon-yn-ial cherty flags units are presented. The values of the TiO_2/Al_2O_3 ; $Si/(Si+Al+Fe)$ and Al/Fe ratios have been computed from the results of chemical analysis in order to interpret the condition of deposition and diagenesis of these sediments. The inversely proportional relationship between the sedimentational rate and the MnO/Al_2O_3 ratio as proposed by several authors is also used to determine the rate of sedimentation of the Gronant chert. Element (R-mode) dendrograms have been constructed for both the units, which indicate that certain elements are to be associated with the minerals of a detrital origin, while others are associated with minerals of probable marine origin.

In Chapter 7, a detailed petrology of the Gronant chert- Llanarmon-yn-ial cherty flags units are presented. In Chapter 8, particular attention is given on the diagenetic history of the Gronant chert. An attempt has also been taken to determine the index of crystallinity for quartz (68° quintuplet). Results of the Cathodoluminescence study and the source of magnesium and the process of dolomitization in the Gronant chert are discussed. Chert-carbonate replacement reversals and marcasite-pyrite relationship in the Gronant chert is outlined. A detailed discussion of the chertification processes involved in the Gronant chert is given from analogy with the contemporaneous chertification processes of the limestone sequences in the United States and the processes thought to be occurring in oceanic sediments. A chertification model of the Gronant chert is then proposed using all available evidences.

In Chapter 9, selected major and trace element geochemistry of the Terrig River shale - Bwlchgwyn-Minera-Ruabon sandstone/siliceous shale units have been studied in detail and mineralogical distributions calculated. In order to fully understand chemical and mineralogical changes occurring during diagenesis an attempt is made to determine mineral trends related to sedimentation and weathering. The values of the ($\text{SiO}_2/\text{Al}_2\text{O}_3$), (M, Rb/K20) and (Cu/Zn) ratios have been computed from the results of the chemical analysis to interpret grain size variations, maturity and redox parameters. Element (R-mode) dendrograms have been constructed for those units, which indicate a change in the source area itself, rather than only a change in the weathering type. The relationship between the organic carbon and trace element is also discussed. Vitrinite reflectance results are interpreted in detail in order to know the diagenetic palaeotemperatures and petroleum generation capability of these sediments. A geochemical classification of the Bwlchgwyn-Minera-Ruabon sandstone unit is presented.

In Chapter 10, a detailed petrology and provenance study of the Bwlchgwyn-Minera-Ruabon sandstone unit is presented. Classification is done based on Folk's (1968) scheme.

In Chapter 11, particular emphasis is given on the diagenetic history of the Bwlchgwyn-Minera-Ruabon sandstone unit. Semi-quantitative analysis of the clay minerals is given. A paragenetic sequence of authigenic minerals is recognised. The formation of quartz overgrowth, Kaolinite-dickite, illite and siderite is shown to be an integral part of the diagenetic processes active within the sediments. From the data presented, speculations are made concerning the changing chemistry of interstitial solutions during the early diagenesis of these sediments. The possible sources of silica are discussed. Finally, the data presented in previous chapters are combined to discuss the overall diagenetic events which have affected the Bwlchgwyn-Minera-Ruabon sandstone/siliceous shale units.

It was intended to devote a chapter to comparing the Gronant chert and the Llanarmon-yn-ial cherty flags and shale interbed units. However, as this work progressed, it became apparent that the environment and processes responsible for these units have only a superficial resemblance, and a comparison has therefore not been made.

CHAPTER 2

PREVIOUS PALYNOLOGICAL STUDIES

2.1 NAMURIAN PALYNOLOGY IN BRITAIN

2.1.1 Early Workers

Raistrick continued his early works of 1934, 1937 and ultimately in 1938, published a paper where he examined in detail the miospore assemblages in some seams from the lower Carboniferous and Millstone Grit (Namurian) of the Northumberland Coalfield, listing many spore types which were different from those described from the Coal Measures of the same coalfield.

Millott (1939, 1945) described the vertical distribution of miospore assemblages in seams of Namurian and Westphalian age in the Cheadle and main North Staffordshire Coalfield.

In her (1948) paper on the Namurian Limestone Coal Group in Scotland, Knox had noted that the miospores from this Group were relatively greater in number and most of them different from those of her early works (1942, 1945) in the Productive Coal Measures.

2.1.2 Zonations

Balme and Butterworth (1951-2) were the pioneers, who studied the vertical distributions of fossil spores in the coal seams of Central England in order to utilise miospore assemblages in a zonal scheme. Later the work was continued in this direction by Butterworth and Millott when in 1960 they extended their earlier five assemblages (Butterworth and Millott 1954) into nine zones extending from the Upper Viséan to the Westphalian 'D' based on the evidence available from coal seams.

In 1967, Smith and Butterworth presented the most comprehensive account of British Carboniferous Palynology. They demonstrated the use of miospores extracted from coal seams in the problems of seam correlation and modified the zonation scheme of 1960. They were able to distinguish eleven stratigraphically distinctive miospore assemblages with reference to their occurrence in different coalfields. These assemblages have been numbered from I to XI in ascending order and embraced horizons from lower Viséan to Westphalian D.

Neves (1961) extended an earlier investigation to the miospores in both clastics and coals of Numurian age in the Southern Pennine region, and collated them to the standard sequence of goniatite stages. He did not erect an independent zonal scheme until 1969, when he studied the vertical distribution of miospore assemblages from twenty five horizons in the Woodland Borehole, County Durham, and subdivided the sequence into eight stratigraphical zones ranging from Upper Visean to Westphalian A in age.

Owens, in Owens and Burgess (1965), inspected the stratigraphical distributions of microflora in the Upper Carboniferous (Namurian- lower and middle Coal Measures) sediments of the Stainmore outlier, Westmorland, and correlated them with similar work done by Neves (1961) in the Southern Pennines. He concluded that though a close agreement between the distribution and composition of the microfloral assemblages does occur, the succession could not be positively correlated at all horizons with that in the Southern Pennines owing to the lack of a complete 'Goniatite' record at Stainmore. He also employed the assemblages to support the established goniatite stages and non-marine lam^el libranch zones.

Owens *et al.* (1976) noticed a distinctive group of zonate camerate miospores from the Namurian of Northern England and assigned them to the Mesozoic genus Kraeuselisporites. They claimed that this represents the first record of this genus in the Carboniferous.

Later, in 1977, Owens *et al.* introduced a broader palynological zonal scheme extending from the Upper Visean to the Westphalian A. They recognised in the Namurian deposits five assemblage zones based on data collected from coal seams and clastic sediments from Northern England and Scotland. These five assemblages substitute the three assemblages of Smith and Butterworth (1967), while the six Westphalian assemblages of the later authors were still accepted as standard for the British Westphalian.

In the meantime, Clayton *et al.* (1977) proposed a broad palynological zonal division for the whole of Western Europe, ranging from the Upper Devonian to the Lower Permian system. They replaced the earlier part of the zonal scheme based on coal seams, by an alternative scheme proposed by Loboziak (1974, 1976). Meanwhile, Owens *et al.* (1978), during the 1975 C.I.M.P. Meeting in Moscow, made an attempt at a comprehensive palynological subdivision of Carboniferous deposits based on a mixture of diverse zonal divisions designated by several authors in North-Western Europe and the Donetz Basin of the U.S.S.R.. This synthesis was later read to a meeting in Halifax, Nova Scotia.

2.1.3 Correlations

In 1958, Butterworth and Williams, had advocated in favour of a possibility of a regional correlation based on isolated miospores from Limestone Coal Group and Upper Limestone Group (Namurian A) Coals in the Midland Valley of Scotland, and noticed that the spore assemblages

were basically the same as assemblages of similar age in North America, Russia, and elsewhere.

Marshall and Williams (1970) inspected spore associations from 23 horizon of coals and clastics in the Yoredale Series of the Roman Wall area in Western Northumberland. They found no significant changes in miospore assemblages at the Viséan-Namurian boundary.

Neves *et al.* (1965) in a short communique investigated miospore assemblages from the Passage Group in Scotland and pointed out evidence for the presence of Upper Namurian Stages according to the spores and goniatite content.

In their work, Sabry and Neves (1970), presented miospore distributions in the sediments of the Sanquhar Coalfield, Dumfriesshire, Scotland, ranging in age from Upper Viséan to Westphalian C.

Whitaker and Butterworth (1978) described miospore assemblages from the Viséan and Namurian Series of the Ballycastle area, County Antrim, North-eastern part of Ireland and concluded that the miospore assemblages of the Upper Coal Group are more consistent with a Pendleian age than with the hitherto postulated Arnsbergian age. In 1979, the same authors described miospore assemblages from the Arnsbergian stage of the Namurian Series, around the type locality of Slieve Anierin, County Leitrim, Southern Ireland.

Recent work has been done by Butterworth and Mahdi (1982) on strata of middle Namurian and lowest Westphalian age in the Featherstone area of Northumberland, England, where they have described twelve new species including eight from the Namurian and four from the lower-most Westphalian.

2.1.4 Palaeoecological Studies:-

Neves (1958) isolated spore assemblages from a short sequence of coals, marine and non-marine shales, containing the Gastrioceras subcrenatum Marine Band of North Staffordshire. He noted that high frequencies of the saccate pollen genus florinites, which was borne by plants with Cordaitalean (Florin, 1936) and Coniferalean (Potonie and Kremp, 1955, p.22) affinities, occurred in the marine shale assemblages in contrast to the associated coal and non-marine shale, and he concluded that this was due to the surrounding of the basin of deposition with plants which yielded this pollen. Chaloner (1958) in his comment on Neves' paper concluded that the pollen was possibly dispersed from the upland flora outside the area of the swamp which was relatively undisturbed during transgression by the sea, in contrast to the Lycopods, Calamites and Pteridosperms on the swamp itself.

Pfefferkorn (1980) argued that instead of abusing the term 'upland flora' it should be restricted to floras which grow in elevated mountainous terrain.

Sullivan (1962) studied clastics and coals from about 45 horizons ranging from the upper part of the Communis zone (Upper Westphalian A) to the base of the Phillipsii zone (Upper Westphalian C) exposed at Wernddu Claypit, near Caerphilly, South Wales. He remarked that the assemblages yielded by the coals and shales have matching stratigraphical ranges to those used for zoning the coals of Great Britain and his results were in close agreement with the zonal scheme proposed by Butterworth and Millott, (1960). Hence he pleaded that miospore studies could be carried out on clastics in area previously neglected due to the high rank of the coal which precludes the preservation of the spores. He also showed the sediments in close juxtaposition to the coal would have closely identical assemblages to those extracted from coals; on the otherhand those assemblages isolated from sediments situated some distance from a coal seam yielded high

frequencies of Florinites - Potonieisporites complex; this 'make up' could serve as "marker-bands" for detailed correlation between coalfields.

The most comprehensive inquiry and research on the Carboniferous Coal Seams are those of Smith (1957, '62) who discussed the interrelationship between the sequence of miospore assemblages and the petrographic types in certain seams of the Lower and Middle Coal Measures in the Yorkshire coalfield. He found that certain seams included horizons of densospore rich crassidurain and he inferred that the peat forming crassidurain was deposited in aerobic conditions. Then he revealed a series of miospore "phases" which tend to occur in an explicit order in the British coal seams. These he named the "Lycospore", "Transition", "Densospore" and "incursion" phases. The "Lycospore" and "Densospore" phases were named after their respective dominant miospore genera; the "transition" phase because of its position in the phase sequence and the "incursion" phase he presumed to be associated with a period of flooding of the swamp by fresh water. He also pointed out that the "Lycospore" and "Densospore" phases are repulsive to one another in a vertically adjacent sequence - that is they never occur in contact with each other; the "Transition" phase always intervenes. The "Incursion" phase is an irregular component which might be found anywhere within a seam excepting within the "Densospore" phase. The Lycospore-Transition-Densospore- Transition-Lycospore sequence might be repeated any number of times with two or more "Lycospore or Densospore" phases repeated around a "Transition" and with "Incursion" phases randomly present. He then collated these "phases" with coal petrography and concluded that the "Lycospore" phase is associated with bright coal (vitrain), the "transition" phase is associated with coal intermediate between the bright and dull coal (clarain), the "Densospore" phase with black-dull coal (Crassidurain), and the "Incursion" phase with grey dull coal (tenuidurain).

This work was followed in 1965 by Marshall and Smith, who inspected miospore distributions in seat earth, coal and roof measures of Westphalian A, B and C age, and argued that the spore content of the seat earth is of value for the solution of correlation problems when the associated coal is lacking.

Muller (1959) in studies on recent shelf sediments, recorded that the quantity of spores and pollen decreases with increasing distance from the shoreline and place of vegetation, whereas hystrichospheres (including acanthomorph acritarchs) increase with increasing distance from the shore.

Later in 1978, Moore and Webb also supported Muller (1959), and argued that miospores relative to acritarchs gives an indication of the approximate distance from the shore line, aided by the influence of wind direction and rainfall.

2.2 NAMURIAN PALYNOLOGY IN AREAS OUTSIDE BRITAIN

2.2.1 West Europe

In France, Loboziak (1971) studied the miospores and megaspores derived from coal seams of Upper Namurian to Upper Westphalian 'C' horizons in the Western part of the Nord-pas-de-calais coalfield and proposed six zones subdivided into eighteen subzones. Later, Loboziak (1974), Coquel *et al.* (1976) and Loboziak *et al.* (1976) concentrated mostly on Westphalian and Stephanian deposits.

Neves (1964) examined miospores from 45 coal seams ranging in age from Upper Namurian A to Lower Westphalian B exposed in the La-Camocha Coal Mine, Gijon, North Spain. He divided the succession into 5 zones based on characteristic, well preserved microflora and argued that certain spore types have stratigraphic importance with restricted ranges and offer a good comparison with other Namurian-Westphalian sequences reported from

Europe and elsewhere. Later, Neves in Moore *et al.* (1971) worked on Namurian B to Westphalian C miospore assemblages in the Villamanin area of Northern Leon, north-western Spain, and proposed four miospore zones. These are

Zone 4 Triquitrites additus - Lower Westphalian C

Zone 3 Vestispora pseudoreticulatus - Westphalian B

Zone 2 Dictyotriletes bireticulatus - Lower Westphalian A

Zone 1 Raistrickia fulva - Namurian B-C

They also collated these sequences with coeval sequences in the United States and the U.S.S.R. and ultimately linked them to zonations based on plant fossils, cephalopoda and foraminifera.

Butterworth (1966) published a paper in India, in which she tried to show the 'distribution of Densospores' from the Devonian to the Permian systems of the northern hemisphere. She concluded that in general densospores were in abundance in more northerly regions and then migrated gradually southwards during the Carboniferous. According to her they are most common in areas of slow subsidence.

2.2.2 East Europe

Horst (1955) noted Namurian A and Westphalian A spore assemblages from Western Upper Silesia and Mährisch-Ostrian in Poland. The work continued in this direction and later in 1957, Dybova and Jachowicz examined miospores in 156 seams from Silesia ranging in age from Namurian A to Westphalian D. In 1970, they proposed three miospore phases and eleven subphases in an elaborate study of subsections of Upper Silesian Coals ranging in age from Namurian A to Westphalian D.

Jachowicz (1971) examined in detail spore assemblages of Namurian and Westphalian A age in North Poland and successfully established ten zones

in the Namurian and three in the Westphalian A. Later, he compared them with those in Britain and Western Europe; also in 1974, he described miospore distribution in Upper Silesian coal bearing strata of the same age.

Beju (1970) investigated miospore assemblages from the Moesian Platform of Romania and proposed three main zones (Cb1, Cb2, and Cb3) ranging from Viséan to lower most Westphalian in age.

2.2.3 Asia

Artuz (1957, 1959) examined spores from coal seams of Namurian to Lower Westphalian A age from the Zonguldak coalfield, Turkey. A further search was made by Agrali and Konyali (1969), who examined miospore distributions from Viséan to Westphalian D age in the Amasra Basin. Out of 18 boreholes Konyali inspected seven from the southern part, while Agrali did eleven from the north. They described ten new genera and listed the stratigraphical positions of 699 spore species belonging to 109 genera.

Teteriuk (1976) continued the early work of Ishchenko (1956 and 1958) in the Russian Donets Basin and studied miospores from strata of Tournaisian to Westphalian D age. He subdivided the Dinantian strata into three zones and the Namurian and Westphalian strata into five zones each and used Potonie and Kremp's spore classification. He later tied up the various palynological zonations in Europe and Russia.

Owens, Loboziak and Teteriuk (1978) and Clayton *et al.* (1977) have successfully attempted to link together sequences in North-Western Europe and the Russian Basins.

2.2.4 North America

Palynology was first used in the United States as a tool for correlation by Thiessen and Wilson (1923-24) with a view to correlate different coal seams. Earlier work of Schopf (1938), was later continued by Schopf,

Wilson and Bentall (1944) who erected a much used classification of the spore genera in Carboniferous coals of the United States.

In 1950, Kosanke concluded a detailed study in which he tried to show correlation of the important coals of Pennsylvanian age in Illinois. He described 100 new species in this report most of which have proved of lasting use.

Guennel (1952, 1958) described miospores of the same age from Indiana.

Hoffmeister, Staplin and Malloy (1955a) brought together all the available data of the stratigraphic distribution of miospores spanned from Pre-Devonian to Permian in age, in both North America and Eurasia. In their later paper of the same year (1955b), they tried to show the vertical distribution of miospores from both coal and clastic sediments in the Hardinsburg Formation of Upper Mississippian age, from Illinois and Kentucky. They used the system of classification proposed by Potonie and Kremp (1954) in this paper. They remarked that clastic sediments contain more diverse microfloras and are therefore better environment indicators compared with coals which represent a limited environment.

In 1956, Wilson and Hoffmeister examined microfloras isolated from the Croweburg Coal of Pennsylvanian age in the north-eastern part of Oklahoma. Then in 1976, Wilson, compiled all the data available since the 1950's to the present of the Desmoinesian Series (Pennsylvanian) of north-eastern Oklahoma; he described the nature of the distributions of fossil spores and pollen and their stratigraphical and palaeoecological significance.

Peppers (1964, 1970) studied the vertical variation of miospore assemblages from various lithological types in the Upper Pennsylvanian

cyclothems of the Illinois Basin from the McLeansboro Group and the Carbondale and Spoon Formations respectively.

Felix and Burbridge (1967) examined in detail the spores of the Springer Formation of South Oklahoma, to document its correct age. The three formations ranged from Lower Mississippian (Tournaisian) to Lower Pennsylvanian (Westphalian B) and they spotted that some of the spore species were restricted to either the Mississippian or the Pennsylvanian, whereas others were common to both systems. Ultimately, they concluded that the Springer Formation is a final transgressional facies ranging from the Mississippian Goddard formation to the Pennsylvanian Morrow Formation.

Urban (1971) noted miospore distributions in the Independence shale of eastern Iowa, which he concluded was of Upper Mississippian (Chesterian) age.

A detailed and notable research was carried out by Ettensohn and Peppers (1979), who studied miospore assemblages isolated from coals and clastics from the Pennington Formation (Chesterian) and Breathitt and Lee Formation (Morrowan) in north-eastern Kentucky, to determine their correct age. They judged on the basis of miospore and conodont distributions that the samples from the Pennington Formation appear to range in age from Middle Chesterian (Upper Viséan) to Upper Chesterian (Namurian A), while the samples from the Breathitt and Lee Formations are early Pennsylvanian (Namurian B- Westphalian A) in age.

Habib (1966) examined miospore assemblages in the Lower Kittanning Coal Seam (Lower Westphalian D) of Western Pennsylvania. He identified five associations starting with a Lycospora assemblage at the bottom and terminating with a Densosporites assemblage at the top. He argued that

the upward increase in abundance of the Densosporites assemblage coincided with a change from fresh to brackish water conditions, as marine water encroached upon the swamp during transgression. According to him, where a fresh water facies directly overlies the coal, the assemblage is dominated by Lycospora.

Ravn (1979) studied in detail the vertical variability of miospore assemblages in a thick coal designated CP-19-4 from the Cherokee Group of Iowa of Pennsylvanian age (Westphalian B). The author identified three major miospore associations, termed "intervals". The first occurring at the bottom of the seam, is the Florinites interval dominated by gymnosperm saccate taxa, Florinites, Pityosporites, Potonieisporites and Wilsonites. The middle portion of the seam is the Densosporites - Crassispora interval dominated by spores of herbaceous plants. The upper part of the seam is the Lycospora interval dominated by spores produced by arborescent lycopods such as Lepidodendron and is characterised by a low diversity of miospores which suggests a stable forest swamp.

Ravn and Fitzgerald (1982) investigated a diverse, well preserved miospore flora of Morrowan age from coals of a Pennsylvanian outlier (?Upper Namurian - Westphalian A) in Muscatine County, Iowa, U.S.A.. The diversity of the miospore population and the presence of numerous saccate and perisporate taxa in the assemblages helped them to come to a conclusion in favour of a mixture of miospores from contemporaneous peat swamp and "upland flora". They also noted "Disaccate" pollen grains which are the earliest examples recorded in these deposits.

Staplin (1960) examined the frequency distribution of miospores in coals, underclays and shales from the Mississippian Golata Formation, Alberta, Canada. He remarked that their frequencies differ markedly in the contrasting lithologies.

In 1967 Barss made a comprehensive review of thirteen Carboniferous and Permian miospore assemblages from the Yukon Territory, the North-West Territories and the Maritime Provinces of Canada.

Neves and Belt (1970) studied miospore associations from late Visean and Namurian A and B ages in the Antigonish and South-West Mabon Basin, Nova Scotia, Canada, and compared them with assemblages of similar ages from Britain and Spain.

Hacquebard and Donaldson (1969) and Hacquebard and Barss (1970) studied fossil spores with a view to interpreting the environments of deposition of coal measures in different areas of Canada.

2.3 PALYNOLOGICAL STUDIES IN NORTH WALES

Very little work has been done so far on the Carboniferous palynology of North Wales and perhaps not a single paper has been published on the Namurian palynology of this region.

A key work by Balme and Butterworth (1952) was extended later on by Butterworth and Millott (1954) to include Upper Carboniferous strata in the North Staffordshire, Cannock Chase and North Wales coalfields. In the subsequent years Butterworth and Millott (1955) and Butterworth (1956) brought together coal samples from different parts of North Wales such as: Llay Main, Gresford, and Point of Ayr collieries, the Whitegate A 5/1 borehole, Gardden Lodge, and the north-west Flintshire open cast sites and various outcrops. Ultimately in 1967 Smith and Butterworth presented their monograph of British Carboniferous palynology which will be discussed in the next chapter.

The Aqueduct and Chwarelau Coal Seams, Australia, Marl pit, have been studied in detail during the present investigation though their stratigraphic

positions were already placed by Smith and Butterworth (1967) in their Densosporites anulatus Assemblage V.

Hibbert and Lacey (1969) examined the distribution of miospores from the Basement Beds of the Lower Carboniferous in the Menai Straits of Caernarvonshire, North Wales and ultimately favoured a Viséan age for them.

More recently Watson (1979) from Sheffield University as part of his M.Sc project work attempted a study of the Carboniferous miospores from the Prestatyn District, North-East Wales.

The area under present palynological study in North Wales crops out to the east of the Clwydian Range and includes a number of localities such as: Teilia (S.J. 079813) and Pentre quarry (S.J. 094827) near Prestatyn; Maes Droell quarry (S.J. 2180 5655) and eastwards to the River Terrig, joining it at (S.J. 2313 5623), near Llanarmon-yn-ial (S.J. 190562) in the Alyn Valley; Bwlchgwyn old quarry (S.J. 25965311); Minera old quarry (S.J. 258530) near Minera, the Aqueduct and Chwarelau Coal Seams, Australia, Marlpit and the Rhyd-y-Ceirw Coal Band from the Terrig River Section. Unfortunately, samples from the Ruabon Mountain Section (S.J. 25804580) under consideration are mostly arenaceous and hence palynological work was not done.

CHAPTER 3

SYSTEMATIC DESCRIPTION OF MIOSPORES

3.1 INTRODUCTION

All the spores described in this chapter were recovered from the Rhyd-y-Ceirw Coal Band, Terrig River Section, and the Minera-Bwlchgwyn quarry areas, North Wales. The descriptive terminology and morphological classification used is that discussed by Grebe (1971) who reviewed and clarified terms employed in spore nomenclature by several workers including Potonié and Kremp (1955), Couper and Grebe (1961) and Kremp (1965).

The classification adopted during the present study is within the framework of Potonié and Kremp's (1954) system. The subturmae Acameratitriteles and Cameratitriteles proposed by Neves and Owens (1966) have been used to accommodate the appropriate genera.

3.1.1 Subinfraturma NODATI Dybová and Jachowicz 1957a
Genus ANAPICULATISPORITES (Potonié and Kremp) Smith and Butterworth 1967

Type species: A. isslbургensis Potonié and Kremp 1954.

Diagnosis. (Smith and Butterworth 1967, p.160 emended from Potonié and Kremp 1954, p.133).

Anapiculatisporites sp. A.

plate 4.2 figs. 12-17

Description:- spores radial, trilete; amb triangular, sides straight, convex or slightly concave; apices rounded or narrow. Laesurae distinct, simple, straight, two thirds to four fifths spore radius, occasionally not visible; sutures often open. Folding of gulaferous type is frequently present along the laesurae. Proximal surface laevigate, distal surface bearing about

25-40, fine, small, falcate spinae about $1.5\ \mu$ long, $1\ \mu$ in basal diameter and $1.5\ \mu$ to $2.5\ \mu$ apart. Spinae are generally sharply incurved from about halfway along their length. Exine thin; generally preserved in lateral compression.

Dimensions: (25 specimens). 15 (17) 23, fuming HNO_3 ; 6" coal from Rhyd-y-Ceirw, River Terrig, North Wales.

Comparison:- Anapiculatisporites sp. A differs from most described species in the falcate shape of its spines. A. hispidus Butterworth and Williams 1958 is larger ($30-39\ \mu\text{m}$) and has a greater number of spines (70-90) on its distal surface.

Occurrence:- Abundant in the present Assemblage VI.

3.1.2 Infraturma MURONATI Potonié and Kremp 1954

Genus CONVOLUTISPORA Hoffmeister, Staplin and Malloy 1955.

Type species. C. florida Hoffmeister, Staplin and Malloy 1955

Diagnosis. In Smith and Butterworth 1967, p.183 (from description in Hoffmeister, Staplin, and Malloy 1955, p.384).

Comparison. Distinguished from Camptotriletes (Naumova) Potonié and Kremp 1954 and Verrucosisporites (Ibrahim) Smith and Butterworth 1967 in its dominantly anastomosing ornament; Camptotriletes is characterised by the dominance of narrow rugulate ridges. Secarisporites Neves 1961 is distinguished by its characteristic discontinuous peripheral rim resulting from lateral fusion and overlapping of the lobate ornament in the region of the equator.

Convolutispora cerebra Butterworth and Williams 1958

Lectotype. Smith and Butterworth (1967), Plate 9, Fig.5. Preparation T48/3 in collection of National Coal Board Laboratories, Wath upon Dearne, Yorkshire (the holotype is missing).

Type locality. Shale Seam at 663 ft. 6in., Cawder Cuilb borehole, Central

Coalfield, Scotland; Namurian A.

Diagnosis. (In Smith and Butterworth 1967, p.184).

Size in micrometres:- (i) Lectotype 82; 55 (72) 83, fuming HNO_3 .

(ii) Measurements of another assemblage from the type locality extends the range to 92μ .

Convolutispora cf. cerebra

plate 4.2 fig. 30 and plate 4.3 figs. 1;4

Description:- Radial, trilete, circular. Laesurae indistinct, appear to be concealed by body ornamentation. The ornament is mostly characterised by closely spaced sinuose flat muri, separated by vermiculi and occasionally by enclosed small lumina. Muri range from $2-4\mu$ in width, rarely exceeding 5μ , and the width of lumina ranges from $1.5-2.5\mu$ and of vermiculi less than 1μ . Exine thick, $4-8\mu$, including muri.

Dimensions:- (11 specimens). Equatorial diameter 49(57) 66, fuming HNO_3 ; 6" coal from Rhyd-y-Ceirw, River Terrig, North Wales.

Comparison:- These specimens are almost similar to those Butterworth and Williams 1958 assigned to Convolutispora cerebra, but could be distinguished by their relatively smaller size, less thickened exine and the indistinct laesurae; they also resemble Convolutispora crassa Playford 1962, but C. crassa is essentially larger with a size range of 61(85) 115μ and has a thicker exine.

Occurrence:- Rare in the present Assemblage VI.

3.1.3 Supra subturma CAMERATITRILETES Neves and Owens 1966

This suprasubturma was proposed by Neves and Owens 1966 to accommodate those trilete, camerate miospores in which the intexine is completely enveloped by an exoexine of uniform or differentiated thickness. Separation of the two wall layers may be partial or more or less complete when attachment is restricted to the proximity of the trilete rays.

Subturma MEMBRANATITRILETES Neves and Owens 1966

Trilete, partially camerate miospores in which the sculptured or sculptureless exoexine show only partial separation from the intexine. In addition to proximal attachment, the two wall layers are in close contact over the whole, or polar region only, of the distal surface and/or along linear attachments which may be randomly or regularly oriented.

Infraturma CINGULICAMERATI Neves and Owens 1966

Trilete, cingulate miospores with a variable degree of chamber formation adjacent to the inner margin of the cingulum.

Genus LYCOSPORA (Schopf, Wilson and Bentall) Somers 1971.

Type species. *L. micropapillatus* (Wilson and Coe) Schopf, Wilson, and Bentall 1944.

Diagnosis. Emended in Somers 1971, p.55.

Remarks. This genus has a considerable number of species with small differences between them which makes identification difficult; several authors have tried to reduce the number of species by using different characters. The latest of these (Somers, 1971) reexamined a large number of types and other specimens. She grouped many published species into four broadly defined form species using type of ornament and the development of the cingulum as basic criteria. These species are:

- 1) *L. orbicula* (Potonié and Kremp) Smith and Butterworth 1967, with a very narrow cingulum.
- 2) *L. pusilla* (Ibrahim) Somers 1971, with clearly visible cingulum; she divided *L. pusilla* into two tendencies:- tendency A, with the zona reduced, (Cingulum & Zona)/Radius low, and tendency B, with the zona well developed, (Cingulum & Zona)/ Radius high; the tendency B she then divided into two groups according to the type of ornament. These are: tendency B1, smooth to punctate ornament and tendency B2, granulate.
- 3) *L. rotunda* (Bharadwaj) Somers 1971, with verrucate ornament

covering the whole exine including the flange.

4) L. noctuina var. noctuina Butterworth and Williams 1958, with verrucate and rugulate ornament arranged irregularly, zona smooth; and L. noctuina var. reticulata Kruszkewska with rugulae arranged in a pseudoreticulum.

This revision has been employed variously by subsequent authors, and the utility of certain synonyms has been questioned. Later, it is argued to recognise all the species separately in order to facilitate the possibility of using them for correlation and to a lesser extent for zonation.

Lycospora noctuina Butterworth and Williams 1958

Holotype. Smith and Butterworth (1967), Plate 20, fig.4. Preparation T54/1 in collection of National Coal Board Laboratories, Wath-upon-Deane, Yorkshire.

Type locality. 9" coal at 256 ft. 11 in., Darnley No.3 borehole, Central Coalfield, Scotland; Namurian A.

Diagnosis:- (In Smith and Butterworth 1967, p.248).

Size in micrometres:- (i) Holotype 36; 30-45, Schulze and 5% KOH (Butterworth and Williams 1958). (ii) 31 (35) 38, fuming HNO_3 ; seam at 419ft. 6in., Houghton Colliery borehole, Durham Coalfield, England; Westphalian A. (iii) 27 (36) 47, fuming HNO_3 ; seam at 31ft. 4in., Culross No.2 borehole, West Fife Coal field, Scotland; Namurian A.

Lycospora cf. noctuina

plate 4.5 figs. 14-18

Description:- spores trilete, Amb rounded triangular or rarely rounded. Laesurae distinct, straight, sometimes flexuose, extending to the inner thickened zone of the cingulum and occasionally to the flange; distinct sutural lips 1.5 to 2.5 μ in width. Cingulum 4.5 to 5.5 μ wide, two zones - the

inner zone more or less solid and the outer zone is essentially a flange or membrane, laevigate to slightly punctate and width generally greater than that of the inner zone. Exine of central area is thin and finely granulate and distally consists of a small number of large grana, verrucae or rarely rugulae 1-4 μ broad. Generally weathered, not well preserved.

Dimensions. (20 specimens) 18 (26) 32, fuming HNO_3 . 6" coal from the Rhyd-y-Ceirw, River Terrig, North Wales.

Comparison:- These specimens resemble those Butterworth and Williams 1958 assigned to L. noctuina, but can be distinguished on the basis of their relatively smaller size; from L. ?granulata Kosanke 1950 and L. pellucida (Wicher) Schopf, Wilson, and Bentall 1944, by their smaller size and the distribution of the characteristic ornamentation within the distal polar area; from L. pusilla (Ibrahim) Schopf, Wilson, and Bentall 1944, by their broader cingulum, prominent laesurae and the distribution of the characteristic wall ornamentation; from L. rotunda Bharadwaj 1957a, by their slightly smaller size and ornamentation and from L. subtriquetra Lubert and Waltz 1941, by their relatively smaller size. Lubert and Waltz 1941, gave a size range of 30-50 μ for L. subtriquetra.

Occurrence:- Abundant in the present Assemblage VI.

3.1.4 Infraturma MEMBRANATI (Neves) Neves and Owens 1966.

Trilete, camerate miospores in which the exoexine has partially separated from the intexine, and projects at the spore margin as a clear, thin membrane. The two exine layers may be attached to one another only in the region of the trilete mark, or the exoexine can be arranged as a series of folds which run over the surface of the spore body membrane.

Genus PROPRIOSPORITES Neves 1958.

Type species. P. rugosus Neves 1958

Diagnosis: In Neves 1958, p.10.

Comparison. The lobate and linear folding of the perisporal membrane is

characteristic of this genus.

Propriporites laevigatus Neves 1961.

1961 Propriporites laevigatus, Neves, p.269, pl. 33, fig.9.

Holotype. Neves 1961, pl.33, fig.9. Slide ref.5. 304770.

Type locality. Marine shales with Hudsonoceras proteum, Congleton Edge ganister quarry, Staffordshire (Loc.4) Sabdenian stage (H).

Diagnosis. In Neves 1961, p.269.

Size in micrometres:- (i) Holotype 77, 70-115 μ m (15 specimens), Schulze and KOH (Neves 1961). (ii) (7 specimens). 44(60)90 μ m, HF + fuming HNO_3 , dark shales/siltstones of different horizons in Bwlchgwyn and Minera old quarry, North Wales.

Description:- spores radial trilete, laevigate. Equatorial outline roughly oval to circular; laesurae straight, simple, length about three quarter radius of the spore body but occasionally indistinct. The laevigate perispore is strongly plicated by a number of long often sinuous lobes having a width of about 2.5-3.0 μ m., which traverse over the spore. The maximum and minimum number of lobes that encircles the spore is observed 12 and 3 respectively with an average number of 6.

Remarks. The size range given above differs from that cited by Neves 1961, but compares closely to the size ranges (45-90 μ m; 50 specimens) noted by Felix and Burbridge (1967).

Comparison. Differs from P. rugosa Neves 1958 in its laevigate exine.

Previous records. Neves 1961 Namurian A and B, Southern Pennines; Owens and Burgess 1965, Upper Namurian A, Stainmore Outlier, Westmorland; Felix and Burbridge, 1967, Upper Mississippian, Springer Formation, Oklahoma, U.S.A.; Clayton *et al.* 1977, Namurian A and B Western Europe.

Occurrence. Rare in the present Assemblage V, obtained from dark shales/siltstones, collected from Bwlchgwyn and Minera old quarry, North Wales. Sample numbers are: BG-7, BG-13, BG-16, Min-3 and Min 8.

(Pl. 4.7, figs. 4-6).

3.1.5 Turma MONOLETES Ibrahim 1933

Suprasubturma ACAVATOMONOLETES Dettmann 1963

Subturma AZONOMONOLETES Lubert 1935

Infraturma LAEVIGATOMONOLETES Dybova and Jachowicz 1957

Genus LAEVIGATOSPORITES Ibrahim 1933

Type species. *L. vulgaris* Ibrahim 1933

Diagnosis. (Smith and Butterworth 1967, p.281, translation from Potonié and Kremp 1954, p.165).

Remarks. Smith and Butterworth 1967, subdivided the species of *Laevigatosporites* on overall size into four species having a maximum length less than 100 μm . Spores between 16-35 μm were assigned to *L. minimus* (Wilson and Coe) Schopf, Wilson and Bentall 1944; spores between 35-65 μm were assigned to *L. minor* Loose 1934; and spores between 65-85 μm were assigned to *L. vulgaris* Ibrahim 1933, while those spores greater than 85 μm were assigned to *L. maximus* (Loose) Potonié and Kremp 1956. However several later authors have continued to use additional taxa.

Laevigatosporites minor Loose 1934.

1932 *Sporonites vulgaris* Ibrahim in Potonié, Ibrahim and Loose, in part.

1933 *Laevigatosporites vulgaris* Ibrahim, in part.

1934 *Laevigatosporites vulgaris minor* Loose, p.158, pl.7, fig.12.

1957a *Laevigatosporites minor* (Loose) Potonié and Kremp; Bharadwaj, p.109, pl.29, figs. 8,9.

1967 *Laevigatosporites minor* Loose; Smith and Butterworth, p.284, pl.24, fig.3.

Holotype. Loose 1934, pl.7, fig.12. Preparation v29, a.

Type locality. Bismarck Seam, Ruhr Coalfield, Germany; Upper Westphalian B.

Diagnosis. (Smith and Butterworth 1967, p.284, from Ibrahim 1933, p.39).

Size in micrometres. (i) Holotype 58.5, 40-70, Schulze and KOH (Loose 1934). (ii) 45-65, Schulze (Bharadwaj 1957a). (iii) 37(44)50, fuming HNO_3 ;

seam at 1,190 feet 11 inches, Daw Mill Colliery shaft, Warwickshire Coalfield, England; Westphalian D. (iv) 40 (56) 71, fuming HNO₃; seam at 1,758 feet 2 inches, Musselburgh No.1 borehole, Lothians Coalfield, Scotland; Westphalian B. (v) 36 (52) 67, fuming HNO₃; New Mine Seam at 33 feet 0 inch, Madeley Wood No.5 underground borehole, Coalbrookdale Coalfield, England; Westphalian B. (iii-v, Smith and Butterworth 1967).

Laevigatosporites cf. minor

plate 4.6, figs. 3-7

Description: Spores monolete, amb mainly subcircular but occasionally oval. Margin smooth, exine laevigate to rarely punctate, pale and about 1.0-1.5 μ thick. Usually with one or two small, sinuous compression folds. Laesurae straight, almost 1/2-3/4 of spore length with slightly raised lips. Sutures often open.

Dimensions. (24 specimens). 36(44)54, fuming HNO₃, 6" coal from Rhyd-y-Ceirw, River Terrig, North Wales.

Remarks. A scatter diagram of length against width Fig. (3.1) is drawn for this species from the Rhyd-y-Ceirw Coal Band; the diagram shows that it is possible to recognise only one species on the basis of shape, and that they are mainly subcircular to oval.

Comparison. These specimens are almost identical to those Loose (1934) assigned to L. minor, but differ in their subcircular shape and characteristic small sinuous compression folds. They differ from L. desmoinesensis (Wilson and Coe) Schopf, Wilson and Bentall 1944 (60-75 μ), L. maximus (Loose) Potonié and Kremp 1956 (>85 μ) and L. vulgaris (Ibrahim) Ibrahim 1933 (65-100 μ), in their much smaller size and subcircular shape and from L. minimus (Wilson and Coe) Schopf, Wilson and Bentall 1944 (20-30 μ), by their much bigger size.

Occurrence:- Abundant in the present Assemblage VI.

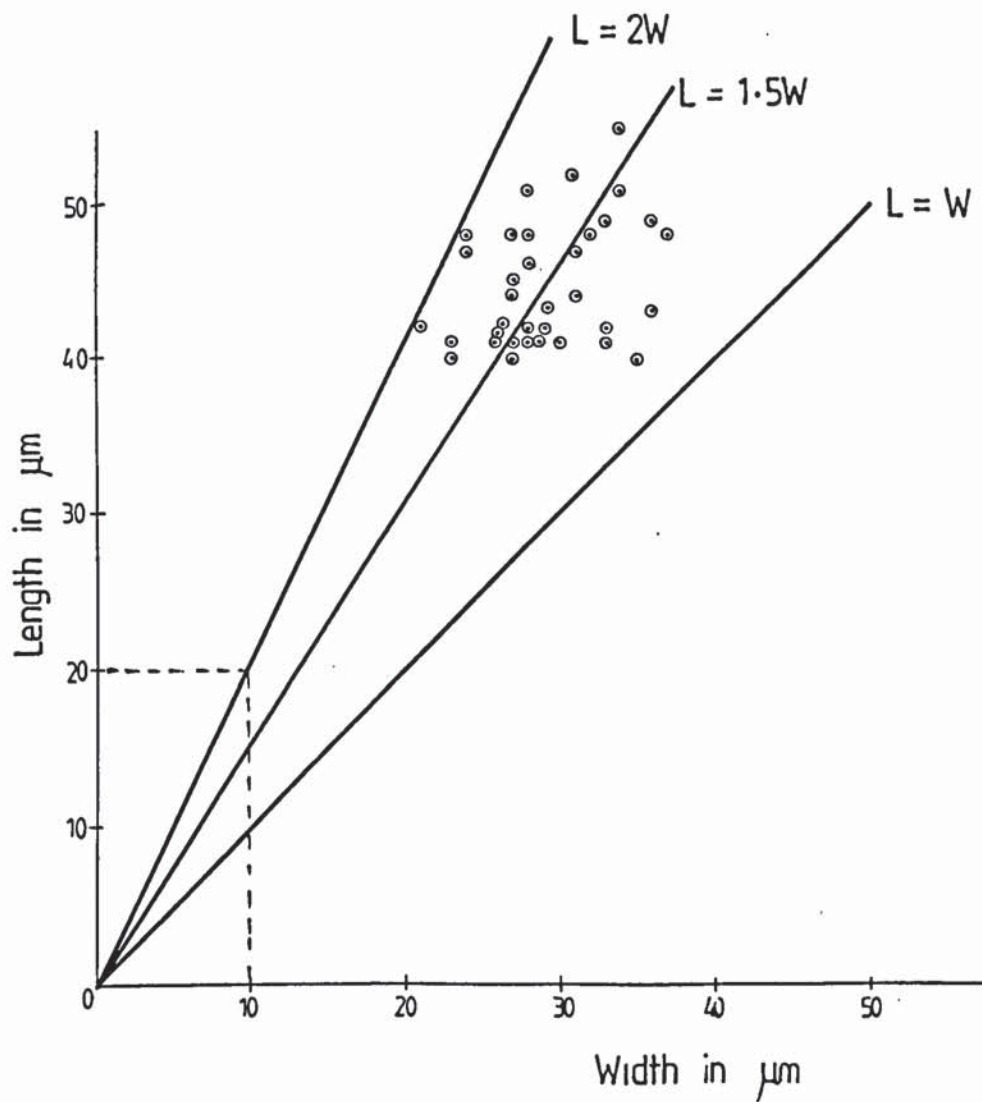


Fig. 3.I.
 Scatter diagram showing the distribution ^{of} shape in
Laevigatosporites cf. *minor*.

CHAPTER 4

BIOSTRATIGRAPHICAL PALYNOLOGY

4.1 INTRODUCTION

The main object of the present palynological study is the use of miospores for biostratigraphic zonation and the correlation of strata.

The miospores recovered from sediments and coals from different localities in North Wales (section 1.6) are moderately to well preserved, and the majority of the species noted in them could be assigned to previously documented Upper Carboniferous taxa.

The miospores isolated from Maes-y-Droell quarry and the adjoining stream section which runs from Graianrhyd eastwards to the River Terrig, Llanarmon-yn-ial area are weathered and badly preserved and accompanied by numerous debris. On the other hand, samples collected from other localities yield moderately to well preserved miospore assemblages.

The coal samples are found to be highly productive and contain a high variety of species. Among these four new species, one each of the genera Lycospora, Anapiculatisporites, Laevigatosporites and Convolutispora have been described from the Rhyd-y-Ceirw Coal Band and are dealt with in Chapter 3.

In general the assemblages are dominated throughout the sequence by spores of the genera Convolutispora, Lycospora, Densosporites and Calamospora; and also high frequencies of Punctatisporites, Knoxisporites, Crassispora and Apiculatisporis. The distribution of all species is shown in Table 4.1.

Quite a few of the miospore species recorded from the Bwlchgwyn and Minera old quarry area and the Rhyd-y-CVeirw Coal Band, are common to both Namurian and Westphalian strata. Others have stratigraphically significant distributions and are relatively common in certain parts of the sequence and uncommon in others as shown in Tables 4.1 and 4.2. These variations in distributions make possible the subdivision of the sequence into seven distinctive assemblages. They are similar to the concurrent range zones of other authors but because the sequences from which the samples are taken are not always continuous they are referred more loosely to assemblages.

In the following sections the assemblages are first described and then compared with the concurrent range zones defined by Owens *et al.* (1977) and Clayton *et al.* (1977), and with assemblages from strata of comparable age in Scotland, Northern England and Ireland described by earlier workers.

4.2 ASSEMBLAGE I

The oldest spore assemblages examined during the present investigation are obtained from samples 18P, 20P, 21P, 27P, 39P and 40P, from the Maes-y-Droell quarry and the stream which runs from Graianrhyd eastwards to the River Terrig, Llanarmon-yn-ial area, North Wales (Fig. 5.1) Most of the samples are weathered and the assemblages are characterised by little diversity in the spore types.

Convolutispora spp. are common constituents in this assemblage. Other species include Grandispora spinosa Hoffmeister, Staplin, and Malloy 1955, Crassispora maculosa (Knox) Sullivan 1964, Densosporites velatus Felix and Burbridge 1967, D. spinifer Hoffmeister, Staplin, and Malloy 1955, Convolutispora lepida Felix and Burbridge 1967 and Acanthotriletes sp.

The following species are recorded in this assemblage but have not been seen in the subsequent assemblages: Raistrickia nigra Love 1960, Ibrahimisporites sentus Felix and Burbridge 1967, Knoxisporites dissidius Neves 1961, Convolutispora superficialis Felix and Burbridge 1967, Tholisporites scoticus Butterworth and Williams 1958, Lophotriletes coniferus Hughes and Playford 1961, Cyclogranisporites cf. minutus Bharadwaj 1957, Spelaeotriletes arenaceous Neves and Owens 1966, and Acanthotriletes splendidus Neves.

In addition, species of zonal significance include Reticulatisporites carnosus (Knox) Neves 1964.

4.2.1 Stratigraphical comparison and conclusions

Sullivan and Marshall (1966) recorded Raistrickia nigra from the Blackbyre Limestone about 50m. below the Hurlet Limestone in Ayrshire; and also Neves *et al.* (1973) recorded it for the first time in their NM (R. nigra - Triquitrites marginatus) concurrent range zone which links up with the B and P1 zones of the Viséan series. Owens *et al.* (1977) noticed the disappearance of R. nigra at the upper boundary of their NC miospore zone.

Crassispora maculosa and Grandispora spinosa are first recorded by Neves *et al.* (1973) in their VF (Triquitrites vetustus - Rotaspora fracta) zone which covers the P1 and P2 zones of the Viséan. These two species are shown to be absent from the E2 and the lower H1 goniatite zones (Butterworth, 1984).

Tholisporites scoticus first appears in the Viséan and spans the middle of the E2 zone (Butterworth, 1984). T. scoticus is a species which is normally more common in the Pendleian stage (Whitaker and Butterworth, 1978). But in the present investigation T. scoticus occurs at very low frequencies.

The present assemblage has not many species in common with the Pendleian assemblages described by Neves (1961) from the Southern Pennines. This difference may be due to the fact that Neves' assemblages were isolated from the Southern Pennines, so that the assemblages may have different floral affinities from those in North Wales.

There are notable differences too between the present assemblage and those described by Smith and Butterworth (1967) from the Pendleian of Scotland and the North of England, notably in the absence of spores of the Genera Rotaspora and Tripartites. These were not described by Neves (loc. cit) from the Southern Pennines.

It is concluded especially from the presence of R. nigra, C. maculosa, T. scoticus and G. spinosa, that Assemblage I lies at an horizon between the uppermost part of NM zone of Neves *et al.* (1972) and the NC zone of Owens *et al.* (1977) and Clayton *et al.* (1977), at an horizon spanning the P1 and the E1 goniatite zones of the upper most part of the Asbian to the Pendleian stage, which roughly conforms to the lower and middle part of the N1 Mesothem of Ramsbottom (1977).

4.3 ASSEMBLAGE II

The assemblages are obtained from samples MAB1, MAB2 and MAB3, from the Terrig River Section (Fig. 5.1). They are productive and well preserved. Convolutispora spp., and thick-walled spores are common constituents in this assemblage.

The following is a list of species found in this assemblage: Convolutispora lepida, C. varicosa Butterworth and Williams 1958, C. crassa Playford 1962, C. mellita Hoffmeister, Staplin and Malloy 1955, Nexuosisporites comtus Felix and Burbridge 1967, Knoxisporites triradiatus Hoffmeister, Staplin and Malloy, 1955, Punctatisporites curviradiatus Peppers 1970, P.

pseudopunctatus Neves 1961, P. sinuatus (Artüz) Neves 1961, Auroraspora solisortus Hoffmeister, Staplin and Malloy 1955, Verrucosisporites cerosus (Hoffmeister, Staplin and Malloy) Butterworth and Williams 1958, Foveosporites futilis Felix and Burbridge 1967, Leiotriletes ornatus Ishchenko 1956, L. subintortus (Waltz) Ishchenko 1952, Lophotriletes labiatus Sullivan 1964, Kraeuselisporites echinatus Owens, Mishell, and Marshall 1976, Secarisporites remotus Neves 1961, Cyclogranisporites lasius (Waltz) Playford 1962, and Savitrissporites nux (Butterworth and Williams) Sullivan 1964.

The presence of the following species, which are not found in subsequent assemblages, have also stratigraphical significance:

Crassispora maculosa, Cingulizonates cf. capistratus (Hoffmeister, Staplin and Malloy) Staplin and Jansonius 1964, Densosporites hispidus Felix and Burbridge 1967, D. velatus, Knoxisporites inconspicuus Felix and Burbridge 1967, Reticulatasporites lacunosus Felix and Burbridge 1967, Convolutispora florida Hoffmeister, Staplin and Malloy 1955, C. sculptilis Felix and Burbridge 1967, Spelaeotriletes triangularis Neves and Owens 1966, Ibrahimispores cf. brevispinosus Neves 1961, Waltzispora planiangularata Sullivan 1964, Punctatisporites giganteus Neves 1961, P. aerarius Butterworth and Williams 1958, Leiotriletes labrum Urban 1971, Calamospora perrugosa (Loose) Schopf, Wilson and Bentall 1944, and Microreticulatisporites. sp. 1.

In addition, species of zonal significance include Reticulatisporites carnosus and Crassispora kosankei (Potonié and Kremp) Smith and Butterworth 1967.

4.3.1 Stratigraphical comparison and conclusions

Owens *et al.* (1977) in their comprehensive treatment described five palynological zones based on Namurian strata in Northern England and

Scotland. Their Stenozonotriletes triangulus - Rotaspora knoxi (TK) zone occurs from the base of the Arnsbergian stage to an horizon within the E2b zone of the stage and hence, therefore, includes the whole of the the E2a zone. The base of the 'TK' zone is characterised by the first appearances of Punctatisporites giganteus, P. pseudopunctatus, Verrucosisporites cerosus and Stenozonotriletes triangulus Neves 1961. The first three species are also recorded in the present Assemblage II. According to the above authors Reinschospora speciosa (Loose) Schopf, Wilson and Bentall 1944, Mooreisporites fustis Neves 1958 and Densosporites crassigranifer Artüz appear at an horizon close to the E2a-E2b limit; but none of these species is recorded from Assemblage II.

However, the miospore assemblages described by Whitaker and Butterworth (1978) from strata just above the basal lavas to the Upper Coal Group of possible Arnsbergian (Namurian, E2) age, from the Ballycastle area, County Antrim, Northern Ireland, have much in common with the present Assemblage II. Significant species present in both the assemblages are: Convolutispora varicosa, Crassispora maculosa, Grandispora spinosa, and Cingulizonates cf. capistratus; while Punctatisporites giganteus, P. pseudopunctatus, Verrucosisporites cerosus, Lophotriletes labiatus, Kraeuselisporites echinatus, Secarisporites remotus and Auroraspora solisortus are present in Assemblage II, but absent in the Antrim assemblage.

The present assemblage has not much in common with the Arnsbergian assemblages described by Neves (1961) from the Southern Pennines. The reason could be the same as mentioned earlier.

Neves *et al.* (1973) noted that Cingulizonates cf. capistratus first appears in the upper part of their VF concurrent range zone towards the top of the Viséan series and it also appears at the same stratigraphic position in the

Roman Wall District. Marshall and Williams (1970) also noted in the Roman Wall District an increase of this species at the base of their Namurian strata. Whitaker and Butterworth (1978) recorded the first appearance of C. cf. capistratus in strata below the Main Limestone at Ballycastle and an increase in abundance in assemblages immediately above the horizon of the Main Coal. The latest occurrence of C. cf. capistratus is recorded so far in the mid E2 zone (Butterworth, 1984).

Convolutispora varicosa was noted by Smith and Butterworth (1967) from their Namurian A assemblages. Marshall and Williams (1970) also recorded it from some horizons in the E1 strata of the Roman Wall District. It was recorded in addition by Neves *et al.* (1973) from uppermost Viséan strata.

Lophotriletes labiatus is recorded so far from the top of the E2 zone to the Westphalian A (Butterworth, 1984).

The ranges of C. maculosa and G. spinosa have already been mentioned in connection with Assemblage I.

It is concluded, from the presence of P. pseudopunctatus, V. cerosus, C. maculosa and especially from the presence of P. giganteus, L. labiatus and C. cf. capistratus, that Assemblage II lies at an horizon within the TK zones of Owens *et al.* (1977) and Clayton *et al.* (1977), at an horizon near the lower to middle part of the Arnsbergian stage, which corresponds to the upper part of the N1 and the middle part of the N2 Mesothems of Ramsbottom (1977).

4.4 ASSEMBLAGE III

The assemblages are obtained from samples 45P, 46P and 47P, from the Terrig River Section (Fig. 5.1). The samples are mostly weathered and

spores are moderately preserved and characterised by little diversity in the species present.

Like the previous assemblages, the present assemblage is also characterised by the genus Convolutispora. The common species which compose the assemblage under consideration are:

Convolutispora lepida, C. varicosa, C. ampla Hoffmeister, Staplin and Malloy 1955, Savitrisorites nux, Knoxisorites triradiatus, K. seniradiatus Neves 1961, Secarisorites remotus, Cyclogranisorites lasius, Hymenospora cf. caperata Felix and Burbridge 1967, Cingulizonates bialatus (Waltz) Smith and Butterworth 1967, Densosporites triangularis Kosanke 1950, Verrucosisporites cerosus, Leiotriletes densus Neves 1961, L. subintortus (Waltz) Ischenko 1952, Punctatisporites glaber (Naumova) Playford 1962, Grandispora spinosa, Acanthotriletes echinatus (Knox) Potonié and Kremp 1955, Spelaeotriletes minutus Butterworth and Mahdi 1982, and Stenozonotriletes lycosporoides (Butterworth and Williams) Smith and Butterworth 1967.

On the other hand, Crassispora kosankei is the only species of zonal significance recorded in this assemblage.

4.4.1 Stratigraphical comparison and conclusions

In fact, the present Assemblage III is not closely comparable with any assemblages previously described.

However, the miospore assemblage described by Butterworth and Mahdi (1982) from above the Brampton Lower Fell Top Limestone (from the middle or upper part of the E2b goniatite zone) which crops out in the Featherstone area of Northumberland, is comparable with Assemblage III. The significant species common to both the assemblages are:

Spelaeotriletes minutus, Grandispora spinosa, Cingulizonates bialatus,

Crassispora kosankei, Convolutispora spp., and Knoxisporites spp., while Densosporites intermedius Butterworth and Williams 1958, rare specimens of Tripartites spp., Rotaspora spp., Spinozonotriletes uncatus Hacquebard 1957, Kraeuselisporites ornatus (Neves) Owens, Mishell and Marshall 1976, Schulzospora rara Kosanke 1950, Bellisporites nitidus (Horst) Sullivan 1964, and Lycospora spp. are not recorded in the present study, but did occur in their assemblages. In the same paper, Butterworth and Madhi placed Spelaeotriletes minutus near the top of the E2 goniatite zone and later Butterworth (1984) did not show its further continuation in the subsequent zones.

On the otherhand, Acanthotriletes echinatus first appears at the base of the H1 goniatite zone and then continues upto Westphalian C (Butterworth, 1984).

The range of Grandispora spinosa has already been mentioned in Assemblage I.

Apart from a common presence of high frequencies of Convolutispora spp., the assemblages noted by Neves (1961) from two samples of marine shales from the Arnsbergian (E2) stage and from marine and non-marine shales and a coal from the H2a zone of the Staffordshire area of the Southern Pennines, are not consistent with the present Assemblage III.

The miospore assemblages of thin coals and associated sediments from the E2a-E2b zones around the type locality of Slieve Anierin, County Leitrim, Ireland by Whitaker and Butterworth (1978) are also not in close agreement with the present Assemblage III.

Moreover, the absence of C. cf. capistratus and C. maculosa in the present assemblage, indicates an horizon younger than Assemblage II.

Therefore, it is concluded, from the presence of G. spinosa, Spelaeotriletes minutus and Acanthotriletes echinatus, that Assemblage III is from the lowest part of the SO zone of Owens *et al.* (1977) and Clayton *et al.* (1977), at an horizon in between the uppermost limit of the E2 and the lowest limit of the H1 goniatite zones that is at the boundary between the Arnsbergian and the Chokierian stages, which also conforms with the boundary between the N3 and N4 Mesothems of Ramsbottom (1977).

4.5 ASSEMBLAGE IV

The assemblages are recorded from samples TA-1 and TA-2, from the Terrig River Section (Fig. 5.1). The spores are adequately preserved and identifiable and dominated by 'saccate' spores.

The assemblages are characterised by the high numbers of 'saccate' spores, mostly Potonieisporites elegans (Wilson and Kosanke) Habib 1966. Other species include Knoxisporites triradiatus, K. stephanephorus Love 1960, Convolutispora crassa, C. mellita, C. lepida, Lophotriletes labiatus, Secarisporites remotus, Savitrissporites nux, S. cf. obliquus Venkatachala and Bharadwaj 1964, Waltzisporea polita (Hoffmeister, Staplin and Malloy) Smith and Butterworth 1967, Tricidarissporites fasciculatus (Love) Gueinn, Neville and Williams 1960, Punctatissporites nitidus Hoffmeister, Staplin and Malloy 1955, P. solidus Hacquebard 1957, P. aerarius Butterworth and Williams 1958, P. validus Felix and Burbridge 1967, P. cf. incomptus Felix and Burbridge 1967, Calamospora microrugosa (Ibrahim) Schopf, Wilson and Bentall 1944, C. pedata Kosanke 1950, C. divergens Butterworth and Mahdi 1982, Dictyotriletes pactilis Sullivan and Marshall 1966, Ibrahimisporites brevispinosus Neves 1961, Diatomozonotriletes sp., Cristatissporites sp., Densosporites intermedius Butterworth and Williams 1958, D. aculeatus Playford 1962, D. spinifer, Rotaspora ergonulii (Agrali) Sullivan and Marshall 1966, Kraeuselisporites echinatus, Monoletes sp.,

Cingulizonates bialatus, Pilosisorites venustus Sullivan and Marshall 1966, Procoronaspora sp. 1, Nexuosisorites comtus, Foveosporites futilis, F. avcinii Ravn 1979, Trochospora mastospinosus Felix and Burbridge 1967, Gulisporites incomptus Felix and Burbridge 1967, Disphanospora parvigrecilis (Peppers) Ravn 1979, Costatacycclus crenatus (Felix and Burbridge) Urban 1971, Rugospora radiata Ravn 1979, Hymenospora cf. caperata Felix and Burbridge 1967, Tantillus triquetrus Felix and Burbridge 1967, Lycospora pusilla (Ibrahim) Schopf, Wilson and Bentall 1944, L. pellucida (Wicher) Schopf, Wilson and Bentall 1944, L. noctuina Butterworth and Williams 1958, Granulatisporites granulatus Ibrahim 1933, and Cyclogranisorites lasius.

In addition, species of zonal significance include Kraeuselisporites ornatus (Neves) Owens, Mishell and Marshall 1976, Lycospora subtriquetra (Luber) Potonié and Kremp 1955, Cirratriradites rarus (Ibrahim) Schopf, Wilson and Bentall 1944, Crassisporea kosankei and Cirratriradites saturni (Ibrahim) Schopf, Wilson and Bentall 1944.

4.5.1 Stratigraphical comparison and conclusions

Some characteristic species of Assemblage III are no longer present in Assemblage IV. These are: Grandispora spinosa, Spelaeotriletes minutus, Leiotriletes densus, L. subintortus, Densosporites triangularis, Stenozonotriletes lycosporoides, Convolutispora ampla and Verrucosisporites cerosus.

Owens, in Owens and Burgess (1965) has documented miospore assemblages from strata of mostly Arnsbergian age in the Stainmore outlier of the Northern Pennines. Samples examined from the lower part of the stage comprised, non-marine and marine shales, and contained a much stronger autochthonous element than Neves' assemblages. Strata studied from the 270 feet which extend from the High Wood Marine Beds

to the Mousegill Marine Bed (Stainmore, E2b-H2), yielded miospore assemblages which are rather badly preserved. The miospores obtained from the lower part of this section, from marine shales at 57 feet above the High Wood Marine Bed and from shales about 25 feet higher in the succession could be comparable with Assemblage IV, especially the common absence of Stenozonotriletes lycosporoides, Grandispora spinosa, Tripartites spp., and Rotaspora spp. (excepting only one species of R. ergonulii in Assemblage IV). Spores present at Stainmore but not recorded in Assemblage IV, are the species of Schulzospora elongata Hoffmeister, Staplin and Malloy 1955, S. ocellata (Horst) Potonié and Kremp 1955, Leiotriletes tumidus Butterworth and Williams 1958, Bellisporites nitidus (Horst) Sullivan 1964, and Remysporites magnificus (Horst) Butterworth and Williams 1958. Crassispora kosankei is present in both the assemblages. Owens suggests that the 'H' goniatite stage is characterised by the absence of many diagnostic E2 miospores and by the presence of Crassispora kosankei in small numbers.

Neves, Read and Wilson (1965) studied miospore assemblages from coal samples from the Passage Group of Scotland. They indicate that the lowest two coal samples (13 and 14) are of Upper Namurian A age and are differentiated from older horizons by the absence of Tripartites spp. and Rotaspora spp.

Neves (1969) investigated 7 samples from the Woodland Borehole, County Durham. He has dated his Group 5 assemblages from the base of the E2 to the base of the R1 goniatite stage and has indicated the absence of the Genera Tripartites spp. and Rotaspora spp. above 812 feet in the sequence.

The higher three samples (Neves loc. cit., plate III) are characterised by Spelaeotriletes arenaceus Neves and Owens 1966, Bellisporites nitidus, Chaetosphaerites pollenisimilis (Horst) Butterworth and Williams 1958,

Remysporites magnificus, Crassispora kosankei and Potonieisporites elegans. The last two species of Neves' Group 5 are also present in Assemblage IV.

Owens *et al.* (1977) and Clayton *et al.* (1977) described the composition of the higher assemblages in their Lycospora subtriquetra - Kraeuselisporites ornatus (SO) zone which collates closely with Assemblage IV, particularly in the absence of Punctatisporites giganteus, Tripartites spp., Rotaspora spp. (except one species of R. ergonulii), Remysporites magnificus and Grandispora spinosa and in the presence of Kraeuselisporites ornatus, Lycospora subtriquetra and Cirratriradites rarus. The above authors considered C. rarus as ~~sp.~~ indicative of a position slightly higher within the SO zone. Moreover, (Owens loc. cit.) and (Clayton loc.cit.) argued that the upper part of the 'SO' zone is equivalent to the 'H' goniatite stage, and they further established that the upper limit is equivalent to the boundary between the H2/R1 goniatite zones. This limit is marked by the gradual disappearance of the characteristic components of Upper Viséan and Namurian 'A' assemblages which are progressively replaced by species which become more characteristic of the Upper Namurian. Moreover, according to them this horizon is comparable with the boundary between the Mississippian-Pennsylvanian systems in North America.

One of the characteristic features of this assemblage is the presence of 'common large saccates'. Neves (1961, p.276) also recorded saccate genera like Florinites elegans, F. similis, and F. visendus from the Namurian A deposits of the Southern Pennines. Butterworth (personal communication 1986) has noted evidence of high occurrences of 'saccate spores' in the H2 zone.

Moreover, the presence of Acanthotriletes echinatus in this assemblage is also significant. The stratigraphic position of A. echinatus has already

been mentioned in connection with Assemblage III.

Therefore, by taking all the above mentioned information into consideration, it is concluded that, Assemblage IV is from the higher part of the 'SO' zone of Owens *et al.* (1977) and Clayton *et al.* (1977), at an horizon within the H2 Alportian stage, which corresponds with the N5 and the middle of the N6 Mesothems of Ramsbottom (1977).

4.6 ASSEMBLAGE V

The miospore assemblages obtained from these horizons include many species recorded in Assemblage IV and persisting into this assemblage but there are some significant features which made it possible to define the base and to divide the whole sequence into a separate Assemblage V.

The assemblages are recorded from samples BG-7, BG-13 and BG-16, from the Bwlchgwyn old quarry and Min-3 and Min-8, from the Minera old quarry (Figs. 5.1 and 5.2). The samples are productive and the spores well preserved.

The assemblage is characterised by the absence of 'saccate' spores and the rare occurrences of Convolutispora spp.. The dominant species include Propriporites laevigatus Neves 1961, Savitrisorites nux. Knoxisorites triradiatus. K. stephanephorus. Laevigatosporites minor Loose 1934, Secarisorites remotus. Leiotriletes ornatus. L. inermis (Waltz) Ishchenko 1952, Punctatisporites glaber. P. cf. incomptus. P. curviradiatus. P. pseudopunctatus. P. sinuatus. P. flexuosus Felix and Burbridge 1967, P. divaricatus Felix and Burbridge 1967, Calamospora microrugosa. C. straminea Wilson and Kosanke 1944, C. divergans. C. pallida (Loose) Schopf, Wilson and Bentall 1944, C. breviradiata Kosanke 1950, Savitrisorites cf. obliquus. Propriporites rugosus Neves 1961, Lophotriletes commissuralis (Kosanke) Potonie and Kremp 1955, L. cf. gibbosus (Ibrahim) Potonie and

Kremp 1954, Achanthotriletes echinatus, Granulatisporites granulatus, G. cf. piroformis Loose 1934, G. adnatoides (Potonie and Kremp) Butterworth and Williams 1958, Lycospora pusilla, L. pellucida, L. noctuina, Dictyotriletes cf. peltatus, Retusotriletes minutus Butterworth and Mahdi 1982, Convolutispora varicosa, C. crassa, Gulisporites incomptus Felix and Burbridge 1967, Hymenospora cf. caperata, H. palliolata Neves 1961, Camptotriletes triangularis Peppers 1970, Knoxisporites seniradiatus, Endosporites micromanifestus Hacquebard 1957, Schopfipollenites ellipsoides (Ibrahim) Potonie and Kremp 1954, Reticulatisporites polygonalis (Ibrahim) Potonie and Kremp 1954, Verrucosisporites verrucosus (Ibrahim) Ibrahim 1933, Apiculatasporites spinulistratus (Loose) Ibrahim 1933, Lophotriletes labiatus, and Auroraspora solisortus.

In addition, species of zonal significance include Kraeuselisporites ornatus, Lycospora subtriquetra, Cirratriradites rarus, Crassispora kosankei, Bellisporites nitidus and Schulzospora rara Kosanke 1950.

4.6.1 Stratigraphical comparison and conclusions

Assemblage V is more or less comparable with Neves' (1961) Kinderscoutian (R1) assemblage of the Southern Pennines. As Neves stated the species Crassispora kosankei and Knoxisporites seniradiatus are quite distinctive in the Kinderscoutian assemblage.

The Lycospora subtriquetra - Kraeuselisporites ornatus (SO) zone of Owens *et al.* (1977) and Clayton *et al.* (1977) compares closely with Assemblage V described above, except ~~for~~ for the absence of Apiculatisporis variocorneus Sullivan 1964 and Camptotriletes superbus Neves 1961, in the latter.

On the other hand Owens *et al.* (1977) and Clayton *et al.* (1977)

introduced the Crassispora kosankei - Grumosisporites varioreticulatus (KV) zone, which spans according to them from the base of the Kinderscoutian stage to an horizon within the middle of the R2 zone of the Marsdenian stage. The base of the KV zone is marked by the high frequency of Crassispora kosankei together with Ibrahimispores magnificus Neves 1961, Raistrickia fulva, Artuz 1957, Triquitrites bransonii Wilson and Hoffmeister, 1956 and Grumosisporites varioreticulatus (Neves) Smith and Butterworth 1967; none of these species excepting C. kosankei (at a very low frequency though) is recorded in Assemblage V.

In addition, the presence of L. minor, L. commissuralis and P. laevigatus in this assemblage are highly conclusive. Butterworth (1984) suggests that L. commissuralis and L. minor first appear in the middle of the R2 zone and then continues into the Westphalian D; while P. laevigatus has a range from Viséan to the middle R2 zone.

Therefore, it is concluded from the presence of P. laevigatus, L. minor and L. commissuralis, that Assemblage V lies at an horizon below the middle of the R2 zone of the middle Marsdenian stage, at an horizon near the top of the KV zone of Owens *et al.* (1977) and Clayton *et al.* (1977).

Hence, Assemblage V lies in the middle of the N9 Mesothem of Ramsbottom (1977).

4.7 ASSEMBLAGE VI

Assemblage VI, is derived from a coal sample (6" Rhyd-y-Ceirw Coal Band) from the Terrig River Section, North Wales (Fig. 5.4). The Rhyd-y-ceirw Coal Band is placed in between the Gastrioceras cumbriense and Gastrioceras cancellatum Marine Bands (G1, Yeadonian stage) by Ramsbottom (1974b).

The sample is productive and the spores are adequately preserved and identifiable. The Assemblage is characterised by its transitional nature between those of the Namurian B below and the Westphalian above. It is characterised by the absence of P. laevigatus, K. seniradiatus and Bellisporites nitidus.

Four new species, one each of the genera Lycospora, Laevigatosporites, Anapiculatisporites and Convolutispora have been described from this assemblage and are dealt with in the 'systematics' chapter.

The Assemblage also includes: Achanthotriletes echinatus, Convolutispora obliqua Neves 1961, C. jugosa Butterworth and Williams 1958, C. mellita, C. crassa, Anapiculatisporites minor (Butterworth and Williams) Smith and Butterworth 1967, Leiotriletes tumidus Butterworth and Williams 1958, Punctatisporites sinuatus, Calamospora pedata, Granulatisporites granulatus, G. adnatoides, G. minutus Potonié and Kremp 1955, Foveosporites avcinii, Waltzisporea polita, Laevigatosporites minor, Lycospora spp., Densosporites spp., Secarisporites sp., and Knoxisporites triradiatus.

In fact, species of Laevigatosporites spp., Lycospora spp., Densosporites spp., and Convolutispora spp. form the major part of this assemblage.

Species of zonal significance include Kraeuselisporites ornatus, Lycospora subtriquetra, ? Grumosporites varioreticulatus (Neves) Smith and Butterworth 1967, and Cirratriradites saturni (Ibrahim) Schopf, Wilson and Bentall 1944.

4.7.1 Stratigraphical comparison and conclusions

The assemblage described by Neves (1961) from the Yeadonian (G1) stage of the Southern Pennines, though not in accord with present Assemblage

VI, but is comparable in the presence of Lycospora spp., Densosporites spp., ?Grumosisporites varioreticulatus and Kraeuselisporites ornatus.

Owens (in Owens and Burgess 1965) studied assemblages from the 420 feet section between the Mousegill Marine Beds and the Swinstone Top Marine Band in Stainmore. Owens could not isolate any spores from a large number of samples of various lithologies from the sediments between the Swinstone Bottom and Top Marine Bands which Ramsbottom *et al.* (1978) indicate to be equivalent to the R2 and G1 goniatite stages. Owens and Burgess described a significant association of Grumosisporites varioreticulatus, Secarisporites remotus, Crassispora kosankei and Kraeuselisporites ornatus, with the absence of Ibrahimisporites brevispinosus, and Cirratiradites rarus, in a sample at 60 feet below the Swinstone Bottom Marine Band, which compares closely to the present Assemblage VI, excepting in the absence of C. kosankei. The above authors placed their assemblage in the upper part of the R2 or the lower G1 stage.

On the other hand, Owens *et al.* (1977) and Clayton *et al.* (1977) proposed their Raistrickia fulva - Reticulatisporites reticulatus (FR) zone, which extends according to them from the middle of the Marsdenian stage upto the base of the Westphalian. The base of the FR zone is marked by the appearance of Ahrensispores beeleeyensis Neves 1961, Dictyotriletes muricatus (Kosanke) Smith and Butterworth 1967, Bellisporites nitidus (reappearance after an appreciable absence), Cristatisporites indignabundus (Loose) Staplin and Jansonius 1964, and Reticulatisporites reticulatus (Ibrahim) Ibrahim 1933. Towards the top of the zone (at G1), Dictyotriletes bireticulatus (Ibrahim) Smith and Butterworth 1967 first appears. None of these species is recorded in the present Assemblage VI. This difference may be due to the fact that the 'FR' zone species were exclusive to Northern England, and hence have different stratigraphical ranges than in North Wales.

Moreover, the high frequency of Lycospora spp., Densosporites spp., Laevigatosporites spp., and Granulatisporites minutus, the absence of Propriporites laevigatus and the presence of four new species in this assemblage could be stratigraphically significant.

Butterworth (1984) indicates that G. minutus ranges from the middle G1 to Westphalian C. The ranges of P. laevigatus and L. minor have already been mentioned earlier in connection with Assemblage V.

Therefore, the absence of P. laevigatus in the present assemblage indicates an horizon above the middle of the R2 zone; the presence of G. minutus together with ?G. varioreticulatus indicate an horizon within the lower to middle G1 zone of the middle Yeadonian stage, at an horizon near the middle of the FR zone of Owens *et al.* (1977) and Clayton *et al.* (1977). This corresponds with the middle part of the N11 Mesothem of Ramsbottom (1977).

This is consistent with Ramsbottom's (1974b) conclusion that the Rhyd-y-Ceirw Coal Band is from in between the G. cumbriense and G. cancellatum Marine Bands.

4.8 ASSEMBLAGE VII

The highest assemblage examined in the present study is obtained from two coal samples, one each from the Aqueduct and Chwarelau Coal Seams, Australia, Marlpit, North Wales (Fig. 5.4). The Aqueduct seam is situated below the Gastrioceras subcrenatum Marine Band at the base of the Westphalian series and the Chwarelau seam is from slightly higher in the sequence.

The assemblages are characterised by the apparent absence of almost all the typical Namurian species and the presence of lower Westphalian species. Occasional morphological intergradation between Triquitrites cf. protensus and Ahrensisporites guerickei is also characteristic.

Higher frequencies of Lycospora pellucida and Apiculatisporis variocorneus Sullivan 1964, and lower frequencies of L. pusilla, Densosporites anulatus (Loose) Smith and Butterworth 1967, Crassispora kosankei and Grumosporites varioreticulatus (Neves) Smith and Butterworth 1967, in the Aqueduct coal sample compared to the Chwarelau one together with the restriction of certain species in the Chwarelau coal sample, allow Assemblage VII to be subdivided into Assemblage VIIa (Aqueduct coal seam) and Assemblage VIIb (Chwarelau coal seam).

4.8.1 Assemblage VIIa

The assemblages are well preserved and characterised by the absence of Westphalian species. The sample contains a wide variety of spore species and the assemblage is dominated by Lycospora spp., Apiculatisporis spp., Densosporites anulatus, Calamospora spp., and Granulatisporites spp.

The following is a complete list of all the species found in this assemblage. Leiotriletes cf. priddyi (Berry) Potonié and Kremp 1955, Punctatisporites sinuatus, Calamospora breviradiata, C. microrugosa, C. pallida, Granulatisporites granulatus, G. microgranifer Ibrahim 1933, Cyclogranisporites multigranus Smith and Butterworth 1967, Lophotiletes cf. gibbosus, Anapiculatisporites minor (Butterworth and Williams) Smith and Butterworth 1967, Apiculatisporis abditus (Loose) Potonié and Kremp 1955, A. cf. latigranifer (Loose) Potonié and Kremp 1955, A. variocorneus Sullivan 1964, Apiculatisporites spinulistratus (loose) Ibrahim 1933, Camptotriletes bucculentus (Loose) Potonié and Kremp 1955,



Ahrensisporites guerickei (Horst) Potonie and Kremp 1954, Triquitrites cf. protensus Kosanke 1950, Savitrissporites nux, Densosporites anulatus, Lycospora ? granulata, Kosanke 1950, L. noctuina, L. pellucida, L. pusilla, Spencerissporites radiatus (Ibrahim) Felix and Parks 1959, Florinites similis Kosanke 1950.

In addition, species of zonal significance include Raistrickia fulva Artuz 1957, Grumosisporites varioreticulatus, Crassispora kosankei, Cirratriradites saturni and schulzospora rara Kosanke 1950.

4.8.2 Assemblage VIIb

This includes well preserved miospores obtained from the Chwarelau Coal Seam. A total of 25 genera comprising 38 species are recorded here which vary considerably in their frequencies. The Assemblage VIIb shows a high degree of similarity to the Assemblage obtained from the Aqueduct Coal Seam, especially in the common occurrence of G. varioreticulatus, R. fulva, C. kosankei, C. bucculentus, T. cf. protensus, A. guerickei, L. pusilla and D. anulatus.

Assemblage VIIb differs from Assemblage VIIa in the presence of Punctatisporites punctatus Ibrahim 1932, Calamospora mutabilis (Loose) Schopf, Wilson and Bentall 1944, Verrucosisporites verrucosus (Ibrahim) Ibrahim 1933, Anaplanisporites baccatus (Hoffmeister, Staplin and Malloy) Smith and Butterworth 1967, Apiculatisporis irregularis (Alpern) Smith and Butterworth 1967, Dictyotriletes castaneaeformis (Horst) Sullivan 1964, Triquitrites tribullatus (Ibrahim) Schopf, Wilson and Bentall 1944, Reinschospora speciosa (Loose) Schopf, Wilson and Bentall 1944, Cirratriradites rarus, Radiizonates striatus (Knox) Staplin and Jansonius 1964, Potonieisporites elegans, Schopfipollenites ellipsoides var. corporeus Neves 1961, and in the apparent absence of Lophotrites cf. gibbosus, Apiculatisporis variocorneus and Cirratriradites saturni.

4.8.3 Stratigraphical comparison and conclusions

The species examined from Assemblage VII are of lower Westphalian A age (or perhaps just below the Lower Westphalian A). They match closely with assemblages of this age from well established stratigraphic successions recorded by Neves (1958, 1961), Owens in Owens and Burgess (1965), Neves, Read and Wilson (1965), Smith and Butterworth (1967), Neves (1968), Owens *et al.* (1977) and Clayton *et al.* (1977).

Assemblage VIIb differs from the slightly older Assemblage VIIa in the presence of lower percentages of L. pellucida and A. variocorneus, and higher frequencies of L. pusilla, D. anulatus, C. kosankei, and G. varioreticulatus together with the first appearance of certain significant species as mentioned earlier.

Neves (1958, 1961) studied several species from a short sequence associated with the Gastrioceras subcrenatum Horizon in the North Staffordshire coalfield and from a Namurian to lower Westphalian A sequence in the Southern Pennines. His species lists recorded from immediately below the G. subcrenatum Horizon and the lower Westphalian A have much in common with those recorded in Assemblage VII.

Smith and Butterworth (1967) established the Densosporites anulatus zone to include the uppermost Namurian and the lower most Westphalian A (lenisulcata zone); and they have already placed the present Assemblage VII (Aqueduct and Chwarelau Coal Seams) in their D. anulatus Assemblage zone V. The present findings compare closely with the species list recorded by the above authors.

One of the most significant features in Assemblage VII is the occasional morphological intergradation between the species of Triquitrites cf. protensus and Ahrensisorites guerickei. This feature is also indicated by

Neves *et al.* (1965) from their lowest (sample no.3) of three samples in the lowest part of the Westphalian sequence, in the Upper Passage Group, Scotland; and Neves (1968) in the Woodland Borehole, County Durham, from the lowest sample (at 336 feet) of three samples in his Group 2. These are characterised by a wide range of morphological variation in the Genus Ahrensisporites. Sabry and Neves (1970) noted the same significant complexity in species attributed to the genus Triquitrites, in both Polneil Burn and the Cat Cleuch area, Sanquhar Coalfield, Scotland. Owens *et al.* (1977) and Clayton *et al.* (1977) also mention this wide morphological intergradation between the genera Triquitrites and Ahrensisporites in their Triquitrites sinani and Cirratiradites saturni (SS) zone. All the above authors advocated that such a complexity is a diagnostic feature of the A. lenisulcata zone. Therefore, the present Assemblage VII (both VIIa and VIIb as they display the same feature) is most likely to be from the lowest part of the Westphalian A, and within the Anthraconia lenisulcata non-marine lamellibranch zone.

Moreover, the absence of Laevigatosporites spp. in Assemblage VIIa and VIIb, also strengthens the above conclusion as Clayton *et al.* (1977) state that the genus Laevigatosporites becomes quantitatively significant from the middle part of their 'ss' zone.

In addition, Neves *et al.* (1965) also described similar assemblages from the Namurian-Westphalian Boundary of Scottish Passage Group (coal seam 4-7), where they indicated that the assemblages show a progressive increase of species like Raistrickia fulva, Grumosporites varioreticulatus, Kraeuselisporites ornatus, Secarisporites sp., and Camptotriletes superbus Neves 1961.

Furthermore, Clayton *et al.* (1977) indicate that the lower limit of their RA zone (base of the Communis chronozone) is marked by the first

appearance of Radiizonates aligerens (Knox) Staplin and Jansonius 1964, and Punctatosporites minutus Ibrahim 1933. The absence of these species in the present Assemblage VII supports an horizon below the RA zone.

The presence of A. cf. latigranifer, C. bucculentus and T. cf. protensus in Assemblage VIIb, and the latter two species in the Assemblage VIIa, could also be stratigraphically important. Butterworth (1984) shows that the first appearance of A. cf. latigranifer and T. cf. protensus are just at the base of the Westphalian A, while C. bucculentus appears at a slightly lower horizon.

Therefore, the present investigation confirms with some certainty the position of Assemblage VII (both VIIa and VIIb) at the base of the Westphalian. This conclusion is in accord with Smith and Butterworth (1967) and conforms to the stratigraphic position of the Gastrioceras subcrenatum Marine Band (Ramsbottom, 1969).

4.9 PROBABLE REASONS FOR THE FAILURE OF MICROFLORAL RECOVERY IN THE GRONANT CHERT

An attempt to study miospore assemblages in the Gronant Chert was unsuccessful. These rocks are essentially silicified limestones (see Chapter 8). Therefore, extensive silicification is certainly the main reason for the absence of miospores in them. In addition to this, the absence of spores could also be due to the following factors:-

- i) The original shallow-marine environment may have precluded their preservation.
- ii) Pyrite framboid formation in these rocks during early stages of diagenesis might have destroyed at least some of the spores.
- iii) Limonitization of pyrite is the latest diagenetic event seen in these rocks, which is presumably still continuing. Conversion of pyrite to limonite (hydrated ferric iron oxides) requires extensive oxidation, which

in turn may destroy miospores.

4.10 COMPARISON WITH AREAS OTHER THAN BRITAIN

4.10.1 Western Europe

The assemblages recorded by Loboziak (1971) from the Westphalian A of the Nord-pas-de-Calais basin, North France, are more or less comparable with the present Assemblage VII. He recorded Lycospora spp., and Densosporites spp. as dominant species throughout the sequence; just above the base of the Westphalian A he noted the appearance of Verrucosisporites verrucosus, Cirratriradites saturni, Lophotriletes cf. gibbosus, Triquitrites tribullatus and Ahrensisporites guerickei, together with several other Westphalian A species.

Grebe (1971) established seven zonal assemblages in the Westphalian A to C of the Ruhr Coalfield, Germany. She divided the Westphalian A assemblages into zones I and IIa and b; these zones were dominated by high frequencies of D. anulatus, Schulzospora rara, Triquitrites spp., Ahrensisporites guerickei, Florinites sp., Radiizonates striatus, R. aligerens (appeared in her zone I and disappeared in her zone IIa), D. sphaerotriangularis, Cingulizonates loricatus and Dictyotriletes bireticulatus. The present Assemblage VII compares closely with the above assemblages excepting in the absence of last four species.

Van Wijhe and Bless (1974) divided the Westphalian strata of the Netherlands into six zones or assemblages. Their first zone or Apiculatisporis 1 zone is comparable more or less with the present Assemblage VII, in the common occurrence of Apiculatisporis spp., Crassispora kosankei, D. anulatus, C. saturni and Florinites spp. This zone was referred by them to the Lower Westphalian A of the Netherlands. They have also recorded L. minor and D. sphaerotriangularis in their

Apiculatisporis zone 1 (which are not present in Assemblage VII).

Neves (1964) examined miospore assemblages from Upper Carboniferous coals and shales from the La-Camocha Mine in North West Spain. He allocated the lowest assemblages to the Remysporites magnificus zone, which is characterised by the absence of Rotaspora spp., Tripartites spp., and Chaetosphaerites pollenisimilis. This feature together with the presence of Convolutispora spp., Savitrissporites nux, C. kosankei, D. anulatus, Lycospora spp., Laevigatosporites minor, Florinites sp., Schoofipollenites ellipsoides, S. rara and Hymenospora palliolata, compares closely to the present Assemblage V, from the Bwlchgwyn and Minera old quarry area. Other species recorded by Neves and not recorded in Assemblage V are Schulzospora campyloptera (Waltz) Potonié and Kremp 1955, Camptotriletes superbus Neves 1958, and Remysporites magnificus (Horst) Butterworth and Williams 1958. On the other hand species recorded in Assemblage V and not recorded from the R. magnificus zone are Bellisporites nitidus, Proprisporites laevigatus, Lycospora subtriquetra, Kraeuselisporites ornatus and Cirratriradites rarus. Neves argued that R. magnificus zone coincides with the Upper Namurian A.

The succeeding Dictyotriletes bireticulatus zone at La Camocha is characterised by increased numbers of Crassispora and Laevigatosporites together with Secarissporites remotus, Savitrissporites nux, Reinschospora speciosa, Dictyotriletes bireticulatus, D. castaneaeformis, Densosporites anulatus, D. sphaerotriangularis, Radiizonates striatus, Grumosissporites varioreticulatus, Camptotriletes superbus, Convolutispora spp., Schulzospora rara, Florinites spp., and many other Westphalian species. This assemblage was considered to span the Namurian B, C and the lower part of the Westphalian A. Most of these elements occur in the present Assemblage VI and particularly VII from the Rhyd-y-Ceirw and the Aqueduct and the Chwarelau Coal Seams respectively.

Moore *et al.* (1971) studied stratigraphically and palaeontologically the strata from the Villamanin area of Northern Leon, N.W. Spain. The palynology was carried out by R. Neves who divided the strata, which extends from Upper Namurian B to lower Westphalian C in age, into five assemblages. The Dictyotriletes bireticulatus and Florinites mediapudens assemblages have many species in common with those recorded in Assemblage VII; some of these species are Densosporites anulatus, Radiizonates striatus, Raistrickia fulva, Crassispora kosankei, Florinites spp., Schulzospora rara and other Westphalian species. These assemblages were deduced by Neves to be of Namurian C age and lower and middle Westphalian A age respectively.

4.10.2 North America

Felix and Burbridge (1967) recorded miospore assemblages from the Goddard, Springer and Morrow Formations (Mississippian/Pennsylvanian systems) in Southern Oklahoma. Sullivan and Mishell (1971) placed the base of the Goddard Formation at the Namurian/Viséan boundary on the basis of the first appearance of seven significant species at that horizon. Neves (1967) considered that four of those species are known to occur in the Viséan of Britain (see his table 3) and therefore, he placed the base of the Goddard Formation within the late Viséan.

Felix and Burbridge's range chart (table 2) and spore distribution chart for the Springer Formation (table 3), reveal significant elements on which comparisons can be made with the spores encountered in Assemblages I to V from Llanarmonyn-yn-ial, Terrig River and Bwlchgwyn and Minera old quarry sections respectively. Assemblage I, II and III are comparable to the lower part of the Springer Formation assemblage which includes all the samples from 03V16-1 to 03V17-2 and is illustrated in their table 3. It is characterised by the presence of the following genera: Ibrahimisporites,

Grandispora, Nexuosporites, Moorisporites Neves 1958 and Cincturasporites (Hacquebard and Barss) Bharadwaj and Venkatachala 1962. The last two species are not recorded in Assemblage I, II and III. On the otherhand, Assemblage IV and V are comparable to the upper part of the Springer Formation, which is characterised by the absence of the above named diagnostic species. However, the other elements which are significant in either two or all the three assemblages are: Convolutispora spp., Secarisporites remotus, Savitrissporites nux, Knoxisporites spp., Crassispora kosankei, Bellisporites nitidus, Tantillus triquetrus, Propriisporites laevigatus, Schulzospora rara and Potonieisporites elegans.

Ettensohn and Peppers (1979) examined four samples from the Pennington Formation in north-east Kentucky and their miospore distributions are shown in their table 1. The most significant species in what they considered to be late Chesterian (Namurian A) assemblages are: Leiotriletes tumidus, Granulatisporites tuberculatus Hoffmeister, Staplin and Malloy 1955, Acanthotriletes castanea Butterworth and Williams 1958, Grandispora echinata Hacquebard 1957, Reticulatisporites peltatus Playford 1962, Densosporites variabilis (Williams) Potonie and Kremp 1956, Schulzospora elongata Hoffmeister, Staplin and Malloy 1955, Pteroretis primum Felix and Burbridge 1961, Endosporites micromanifestus Hacquebard 1957, Grandispora spinosa, Crassispora maculosa, and Densosporites spinifer. The last three species are also recorded from the present Assemblage I and II and hence a slight comparison can be made with the above mentioned assemblage.

Ettensohn and Peppers (loc. cit.) also examined three samples from the younger Breathitt and Lee Formations, which are indicated by them to be of early Pennsylvanian (Namurian B to Westphalian A) age. Several species present in these samples such as: Leiotriletes cf. priddyi, Punctatisporites sinuatus, Calamospora mutabilis, Granulatisporites

granulatus, Anapiculatisporites minor, Savitrissporites nux, Lophotriletes commissuralis, Florinites similis, Crassispora kosankei, Spencerissporites radiatus, Cirratriadites saturni, Reinschospora speciosa and Radiizonates striatus, are also recorded either in Assemblage VI or in Assemblage VII or in both of them.

Kosanke (1950) noted the spore assemblages of coals of the Caseyville Formation, lowermost Pennsylvanian of Illinois and probably corresponding to the upper part of Namurian B and lower part of Namurian C of Europe, and the lower part of the Tradewater Group which probably corresponds to the upper half of the Namurian C and the Westphalian A. The Caseyville Formation contains a restricted microflora dominated by Lycospora spp. and Densosporites anulatus. Schulzospora rara is restricted to the middle coal and species of Laevigatosporites and Florinites appear for the first time and persist into the Tradewater Group. Moreover, Calamospora pedata occurs in the Caseyville Formation while Reinschospora spp. are recorded in the lower Tradewater Group. The Caseyville Formation assemblages seem to compare more or less with the present Assemblage VI (Rhyd-y-Ceirw Coal Band) while Assemblage VII (Aqueduct and Chwarelau Coal Seams) collates with the lower Tradewater Group.

Ravn and Fitzgerald (1982) examined six coals from Caseyville Formation outcrops in Muscatine County, Iowa, which are indicated by them to be of the KV (Namurian B), FR (Namurian C) and SS (lower Westphalian A) miospore zones of Clayton *et al.* (1977) in Europe. The broad assemblages described by the above authors compares partly with the present Assemblage VI and partly with VII. The significant species present in the Caseyville coals, Assemblage VI and Assemblage VII are: Punctatisporites sinuatus, Calamospora spp., Granulatisporites granulatus, Secarissporites sp., Savitrissporites nux, Grumosissporites varioreticulatus, Densosporites

anulatus, Lycospora pellucida, and Cirratriradites saturni. The absence of the following species are also common to them: Chaetosphaerites pollenisimilis (Horst) Butterworth and Williams 1958, Rotaspora spp., Tripartites spp., Grandispora spp., Proprisporites spp., and Auroraspora solisorta.

The following species are present in Caseyville coals and in Assemblage VI, but absent in Assemblage VII: Granulatisporites adnatus, G. minutus, Waltzispora polita, Convolutispora mellita, Laevigatosporites spp., and Foveosporites avcinii.

Similarly, the following is a list of species recorded only in Caseyville Coals and in Assemblage VII: Verrucosisporites verrucosus, Anaplanisporites baccatus, Apiculatisporis abditus, A. variocorneus, Camptotriletes bucculentus, Ahrensisporites guerickei, Reinschospora speciosa, Radiizonates striatus, Spencerisporites radiatus, Schulzospora rara, Florinites similis, Potonieisporites elegans, Schopfipollenites ellipsoides, Crassispora kosankei, Lycospora granulata and L. noctuina.

Barss (1967) has figured a wide variety of spores from the Westphalian A Riversdale Group of the Maritime Provinces of Canada. These include: Calamospora spp., Apiculatisporis spp., Laevigatosporites spp., Florinites spp., Schulzospora rara and Schopfipollenites ellipsoides var. corporeus. This assemblage can be compared closely with the present Assemblage VII, excepting in the absence of Laevigatosporites spp. in the latter.

Moreover, the present Assemblage VII also contains Densosporites anulatus, Cirratriradites saturni and Radiizonates spp., which are not listed in Barss's assemblage.

4.11 CONCLUSIONS

The miospore assemblages recorded during the present study confirm that the Namurian sequences of the Llanarmon-yn-ial area, Terrig River Section and the Bwlchgwyn and Minera old quarries, which have not previously been dated by miospore evidence, are from the Viséan-Namurian Boundary to Namurian C in age. The Aqueduct and the Chwarelau Coal Seams, Australia, Marl pit, which were also studied during the present investigation were already confirmed as basal Westphalian A in age, by Smith and Butterworth (1967).

Five species belonging to five genera are described in detail in Chapter 3. Four taxa from the Rhyd-y-Ceirw Coal Band are new; comparison and discussion of other species are given when needed and all taxa are figured in Plates 4.1-4.8.

Seven miospore assemblages have been recognised in the present palynological inquiry; one of them (Assemblage VII) has been divided into two sub-assemblages. The assemblages and sub-assemblages are based mainly either on the first appearances of new taxa or to some extent on variations in abundance.

The assemblages described in the present study are correlated with the assemblages in the Stainmore Outlier described by Owens in Owens and Burgess (1965); in the Woodland Borehole, County Durham, by Neves (1968); in the Passage Group of Scotland by Neves *et al.* (1965); in the Ballycastle area, County Antrim and the Slieve Anierin area, County Leitrim, by Whitaker and Butterworth (1978a and b); in the Featherstone area, Northern England by Butterworth and Mahdi (1982) and in the Northumberland and Durham and the Scottish coalfields described by Smith and Butterworth (1967). The assemblages compare fairly closely

with the concurrent range zones defined by Owens *et al.* (1977) and Clayton *et al.* (1977).

Detailed comparisons of the present assemblages with assemblages of the areas mentioned above indicate that the oldest Assemblage I spans the P1 and the E1 goniatite chronozones, at an horizon between the uppermost part of the NM Zone of Neves *et al.* (1972) and the NC zone of Clayton *et al.* (1977) which lie between the uppermost part of the Asbian stage to the Pendleian stage, and roughly conforms to the lower and middle part of the N1 Mesothem of Ramsbottom (1977).

Assemblages II, III and IV from the Terrig River Section span the E2 and the H2 goniatite chronozones, corresponding approximately to the limit of the TK and SO concurrent range zones of Clayton *et al.* (1977), which include the Arnsbergian and the Alportian stages. These three assemblages also span the upper part of the N1 and the middle of the N6 Mesothems of Ramsbottom (1977).

Wood (1936), Jones and Lloyd (1942) and Ramsbottom (1974) also recorded E2 beds from the Terrig River Section.

Assemblage V occurs in samples from the Bwlchgwyn and the Minera old quarry area. It lies at an horizon below the middle of the R2 zone of the middle Marsdenian stage, at an horizon near the top of the KV zone of Owens *et al.* (1977), and Clayton *et al.* (1977), which conforms to the middle of the N9 Mesothem of Ramsbottom (1977).

Bisat (1940) described Gastrioceras branneroides, which is the lowest characteristic fauna of the Gastrioceras cancellatum Marine Band, from the Minera Mill area and later Ramsbottom (1974b) recorded G. cancellatum from the same area. The present work concentrates mainly in the Minera

old quarry area where these immediately overlying beds have not been found.

Assemblage VI, is obtained from a coal sample (6" Rhyd-y-Ceirw Coal Band) from the Terrig River Section and occurs in the lower to middle G1 goniatite chronozone, at an horizon near the middle of the FR zone of Clayton *et al.* (1977) which corresponds to the middle of the Yeadonian stage. This accords with the correlations of Ramsbottom (1974b) who places the Rhyd-y-Ceirw Coal Band in between the Gastrioceras cumbriense and Gastrioceras cancellatum Marine Bands. Rhyd-y-Ceirw Coal Band corresponds with the middle part of the N11 Mesothem of Ramsbottom (1977).

Assemblage VII is recorded from two coal samples, namely the Aqueduct and the Chwarelau Coal Seams, Australia, Marlpit. Assemblage VIIa (Aqueduct Coal Seam) includes higher frequencies of L. pellucida and A. variocorneus and lower frequencies of L. pusilla, D. anulatus, C. kosankei and G. varioreticulatus, compared to Assemblage VIIb (Chwarelau Coal Seam). Assemblage VII as a whole corresponds to the base of the 'SS' miospore concurrent range zone of Clayton *et al.* (1977) which occurs at the base of the Westphalian A and is more or less equivalent to the A. lenisulcata non-marine bivalve chronozone of Ramsbottom *et al.* (1969) which is consistent with the stratigraphic position of the Gastrioceras subcrenatum Marine Band (Ramsbottom, 1969).

The present assemblages also compare closely with those published further afield from Western Europe and Northern America.

Probable reasons for the failure of microfloral recovery in the Gronant chert are discussed. Ramsbottom (1974b) noted that in the Abbey Mills borehole the cherts are overlain by low Namurian E zone beds and so, by

inference, these cherts are included in the Dinantian by the I.G.S. (Rhyl Map No.95, 1970) and by George *et al.* (1976).

SAMPLE No. MIOSPORE SPECIES	GRONANT CHERT	LLANARMON- YN-IAL CHERT	TERRIG MAB-3	TERRIG MAB-2	TERRIG MAB-1	TERRIG 46P	TERRIG 45P	TERRIG ARNOLD-2	TERRIG ARNOLD-1	BWLCHGWYN-16	BWLCHGWYN-13	BWLCHGWYN-7	MINERA-8	MINERA-3	RHYD-Y- CEIRW COAL	AQUEDUCT COAL	CHWARELAU COAL
Leiotrilletes densus																	
Leiotrilletes inermis																	
Leiotrilletes labrum																	
Leiotrilletes ornatus				+													
Leiotrilletes cf. priddyi																	
Leiotrilletes subintortus																	
Leiotrilletes tumidus																	
Punctatisporites aerarius																	
Punctatisporites curviradiatus																	
Punctatisporites divaricatus																	
Punctatisporites flexuosus																	
Punctatisporites glaber																	
Punctatisporites incomptus																	
Punctatisporites cf. incomptus																	
Punctatisporites mundus																	
Punctatisporites nitidus																	
Punctatisporites pseudopunctatus																	
Punctatisporites punctatus																	
Punctatisporites sinuatus																	
Punctatisporites solidus																	
Punctatisporites validus																	
Calamospora breviradiata																	
Calamospora divergens																	
Calamospora microrugosa																	
Calamospora mutabilis																	

Table: 4. 1 The distribution of miospores in different localities of North Wales mentioned in the text.
(Continued on next page)

SAMPLE No. MIOspore SPECIES	GRONANT CHERT														
	U N P R O D U C T I V E														
<i>Calamospora pallida</i>															
<i>Calamospora pedata</i>															
<i>Calamospora perrugosa</i>															
<i>Calamospora streminia</i>															
<i>Granulatisporites adnatoides</i>															
<i>Granulatisporites granulatus</i>															
<i>Granulatisporites microgranifer</i>															
<i>Granulatisporites cf. piroformis</i>															
<i>Cyclogranisporites lasius</i>															
<i>Cyclogranisporites cf. minutus</i>															
<i>Cyclogranisporites multigranus</i>															
<i>Verrucosisporites cerosus</i>															
<i>Verrucosisporites verrucosus</i>															
<i>Lophotriletes commissuralis</i>															
<i>Lophotriletes coniferus</i>															
<i>Lophotriletes cf. gibbosus</i>															
<i>Lophotriletes labiatus</i>															
<i>Waltzispore planiangularata</i>															
<i>Waltzispore polita</i>															
<i>Anapiculatisporites minor</i>															
<i>Anapiculatisporites sp. A</i>															
<i>Tricidarispore fasciculatus</i>															
<i>Anaplanisporites cf. beccatus</i>															
<i>Anaplanisporites globulus</i>															
<i>Apiculatisporis abditus</i>															

SAMPLE No. MIOPORE SPECIES	CHWARELAU COAL	AQUEDUCT COAL	RHYD-Y- CEIRW COAL	MINERA-3	MINERA-8	BWLCHGWYN	BWLCHGWYN	BWLCHGWYN	TERRIG ARNOLD-1	TERRIG ARNOLD-2	TERRIG 45P	TERRIG 46P	TERRIG MAB-1	TERRIG MAB-2	TERRIG MAB-3	LLANARMON- YN-IAL CHERT	GRONANT CHERT	
Dictyotrilletes pectilis																		
Dictyotrilletes cf. peltatus																		
Camptotrilletes bucculentus																		
Camptotrilletes triangularis																		
Ahrensia sporites guerickel																		
Triquitrites cf. protensus																		
Triquitrites cf. sculptilis																		
Triquitrites tribullatus																		
Reischospora speciosa																		
Diatomozonotrilletes sp.																		
Stenozonotrilletes lycosporides																		
Knoxisporites dissidus																		
Knoxisporites inconspicuus																		
Knoxisporites seniradiatus																		
Knoxisporites stephanephorous																		
Knoxisporites triradiatus																		
Reticulatisporites carnesus																		
Reticulatisporites polygonalis																		
Reticulatisporites lacunosus																		
Savitrissporites cf. obliquus																		
Savitrissporites nux																		
Bellisporites nitidus																		
Rotaspora ergonulii																		
Grumosporites varioreticulatus																		
Grassispora kosankei																		

SAMPLE No. MIOPORE SPECIES	GRONANT CHERT																			
	UNPRODUCTIVE																			
Crassipora maculosa																				
Densosporites anulatus																				
Densosporites intermedius																				
Densosporites hispidus																				
Densosporites spinifer																				
Densosporites triangularis																				
Densosporites velatus																				
Lycospora granulata																				
Lycospora noctuina																				
Lycospora cf. noctuina																				
Lycospora pellucida																				
Lycospora pusilla																				
Lycospora subtriquetra																				
Cristatisporites sp.																				
Cirratiradites rarus																				
Cirratiradites saturni																				
Cingulizonates bialatus																				
Cingulizonates cf. capistratus																				
Radiizonates striatus																				
Tholiosporites ? biannulatus																				
Endosporites micromanifestus																				
Spencerisporites radiatus																				
Schulzospora rara																				
Laevigatosporites minor																				
Laevigatosporites cf. minor																				

SAMPLE No. MIOPORE SPECIES															
	CHWARELAU COAL	AQUEDUCT COAL	RHYD-Y- CEIRW COAL	MINERA-3	MINERA-8	BWLCHGWYN	BWLCHGWYN	BWLCHGWYN	TERRIG ARNOLD-1	TERRIG ARNOLD-2	TERRIG 45P	TERRIG 46P	TERRIG MAB-1	TERRIG MAB-2	TERRIG MAB-3
Florinites similis	+														
Schepfipollenites ellipsoides															
Auroraspora solisortus															
Costatacyclus crenatus															
Disphanospora parigrecilis															
Foveosporites avcinii															
Foveosporites futilis															
Grandispora spinosa															
Gulispurites incomptus															
Hymenospora caperata															
Hymenospora caperata															
Hymenospora palliolata															
Ibrahimispores brevispinosus															
Ibrahimispores cf. brevispinosus															
Ibrahimispores magnificus															
Ibrahimispores sentus															
Kraeuselisporites echinatus															
Kraeuselisporites ornatus															
Nexuosisporites comtus															
Pilosporites venustus															
Potonielsporites elegans															
Procoronaspora sp.1															
Propriisporites laevigatus															
Propriisporites rugosus															
Retusotrilletes minutus															

<div> <div>MIOSPORE SPECIES</div> <div>SAMPLE No.</div> </div>							
	CHWARELAU COAL						
	AQUEDUCT COAL						
	RHYD-Y-CEIRW COAL						
	MINERA-3						
	MINERA-8		+				
	BWLCHGWYN		+				
	BWLCHGWYN		+				
	BWLCHGWYN		+				
	TERRIG ARNOLD-1		+				+
	TERRIG ARNOLD-2	+		+			
	TERRIG 45P		+		+		
	TERRIG 46P		+		+		
	TERRIG MAB-1					+	
	TERRIG MAB-2		+			+	
	TERRIG MAB-3						
	LLANARMON-YN-IAL CHERT				+		
	GRONANT CHERT						
	Rugospora radiata						
	Secarisorites remotus						
	Secarisorites ? sp. A						
	Spelaeotriletes arenaceous						
	Spelaeotriletes minutus						
	Spelaeotriletes triangulus						
	Trochospira mastospinosus						

VISEAN		NAMURIAN					WESTPH	GONIATITES	
P ₂	E ₁	E ₂	H ₁	H ₂	R ₁	R ₂	G ₁	MIOPORE ZONES	
Bellisporites nitidus Reticulatisporites carnosus		Stenozonotrilletes angulatus Rotaspora Knoxi	Lycospora subtriquetra Kraeuselisporites ornatus		Crassisporea Kosankei Grumosporites varioreticulatus		Raistrickia fulva Reticulatisporites reticulatus	Triquitrites sinani Cirratiradites saturni	
NC	TK	SO	KV	FR					
									SELECTED MIOPORE SPECIES
									Raistrickia nigra Ibrahimisporites sentus Tholisporites scoticus Lophotrilletes coniferus Convolutispora superficialis Spelaeotrilletes arenaceus Acanthotrilletes splendidus Reticulatisporites carnosus Densosporites velatus Crassisporea maculosa Grandispora spinosa Reticulatisporites lacunosus Waltzisporea planiangularata Cingulizonates cf. capistratus Punctatisporites giganteus Punctatisporites pseudopunctatus Nexuosporites comtus Spelaeotrilletes minutus Cingulizonates bialatus Knoxisporites seniradiatus Rotaspora ergonulii Ibrahimisporites brevispinosus Gulisporites incomptus Tricidarispores fasciculatus Costatacycclus crenatus Kraeuselisporites ornatus Cirratiradites saturni Knoxisporites stephanephorous Potonieisporites elegans Lycospora subtriquetra Bellisporites nitidus Propriisporites laevigatus Leiotrilletes tumidus Lycospora cf. noctuina Convolutispora cf. cerebra Anapiculatisporites sp. A Laevigatosporites cf. minor Raistrickia fulva Grumosporites varioreticulatus Triquitrites cf. protensus Ahrensisporites guerickei Apiculatisporis cf. latigranifer

Table 4.2 : The ranges of key spores illustrated are based upon the occurrence of spores in the different localities of North Wales mentioned in the text. R₁ probably absent (?). Miospore zones are after Owens et al. (1977). — zone of continuous presence
- - - - - zone of apparent absence

SER- IES	STAGES	GONIA- TITE INDEX	SPORES (Owens et al. 1977)	HER- LEEN 1935	MESO- THEMS RAMS- BOTTOM 1977	PRESENT STUDY	
						SAMPLES	ASSEMB- LAGES
WESTPHALIAN NAMURIAN	WESTPHALIAN A		SS Triquitrites sinani Cirratriaradites saturai	WESTPHALIAN A			VII
	YEADONIAN	G1	FR Raistrickia fulva Reticulatisporites reticulatus	NAMURIAN C	N11 N10	≡	VI V
	MARSDENIAN	R2	Crassisporea kosankei	NAMURIAN B	N9 N8	—	
	KINDERSCHOUTIAN	R1	KV Grumosporites varioreticulatus		N7	◆	6" Rhydy-Ceirw coal seam Terrig River
	ALPORTIAN	H2	SO Lycospora subtriquetra	NAMURIAN A	N6 N5 N4 N3	*	IV
	CHOKIERIAN	H1	TK Stenozonotriletes triangulus Rotaspora knoxi		N2	~	III
	ARNBERGIAN	E2	NC Bellisporites nitidus Reticulatisporites carnosus		N1	■	II
	PENDLEIAN	E1	VF Tripartites vetustus Rotaspora fracta			▲	I
	BRIGANTIAN	P2					
	VISEAN						

LEGEND:

- Samples
 ▲ 18P, 20P, 21P, 27P,
 ~ 39P and 40P
 ○ GRO-3 and GRO-4
- MAB1, MAB2 and MAB3
 * 45P, 46P and 47P } Terrig River
 * TA1 and TA2
- Min 3 and Min 8+
 — BG-7, BG-13 and BG-16 }
 ◆ 6" Rhydy-Ceirw coal seam } Terrig River
- ≡ Chwarelau Coal Seam
 ≡ Aqueduct Coal Seam
- Assemblages
 I. Upper most part of the Asbian and the
 Pendleian stages. 7 Upper Brigantian
 II. lower to middle of the Arnsbergian
 stage.
 III. at the boundary between the Arnsberg-
 ian and the Chokierian stages.
 IV. Within the Alportian stage.
 V. below the middle Marsdenian stage.
 VI. the middle Yeadonian stage.
 VII. at the base of the Westphalian.

Table 4.3 Summary of the present palynological study. Interpretation of different assemblages are discussed more fully in the text.

EXPLANATION OF PLATE 4.1All figures X500

- Fig. 1 Leiotriletes ornatus Ischenko 1956. Slide BG16 (1) 11.9 x 60.7
Fig. 2 L. tumidus Butterworth and Williams 1958. Rhyd-y-Ceirw Coal. Slide 662 6.9 x 68.0
Fig. 3 L. subintortus (Waltz) Ischenko 1952 var. rotundatus Waltz 1941. Slide M3. 21.0 x 73.8
Fig. 4 L. labrum Urban 1971. Slide M2. 9.8 x 71.2
Fig. 5 Punctatisporites pseudopunctatus Neves 1961. Slide M2. 19.9 x 71.2
Fig. 6 P. giganteus Neves 1961. Slide M3. 20.1 x 64.0
Fig. 7 P. pseudopunctatus Slide Min 8 (1)
Fig. 8 P. curviradiatus Peppers 1979. BG 16 (1). 16.8 x 73.8
Fig. 9 P. curviradiatus Peppers 1970. Slide M(1).
Fig. 10 Punctatisporites sp. Rhyd-y-Ceirw Coal. Slide 662. 20.2 x 78.7
Fig. 11 P. solidus Hacquebard 1957. Slide M8.
Fig. 12 P. sinuatus (Artuz) Neves 1961. Slide M3. 15.7 x 69.3
Fig. 13 Punctatisporites sp. Slide T1. 10.0 x 73.6
Fig. 14 P. aerarius Butterworth and Williams 1958. Slide M2. 8.1 x 71.5
Fig. 15 P. pseudopunctatus Neves 1961. Slide M2.
Fig. 16 cf. P. divaricatus Felix and Burbridge 1967. Slide Min.8 (1). 23.2 x 64.8
Fig. 17 P. sinuatus (Artuz) Neves 1961. Rhyd-y-Ceirw Coal. Slide 662.
Fig. 18 Calamospora pallida (Loose) Schopf, Wilson Bentall 1944. Slide Aq. 486 (1). 23.0 x 58.0
Fig. 19 C. microrugosa (Ibrahim) Schopf, Wilson and Bentall 1944. Slide Aq. 486 (1). 12.0 x 62.0
Fig. 20 C. breviradiata Kosanke 1950. Slide Ch. 485 (2) 14.6 x 57.2
Fig. 21 C. mutabilis (Loose) Schopf, Wilson and Bentall 1944. Slide Ch. 485 (2). 14.9 x 57.2
Fig. 22 Granulatisporites granulatus Ibrahim 1933. Slide Aq. 486 (1). 28.0 x 71.2
Fig. 23 G. microgranifer Ibrahim 1933. Slide Ch. 485 (2) 27.8 x 70.2

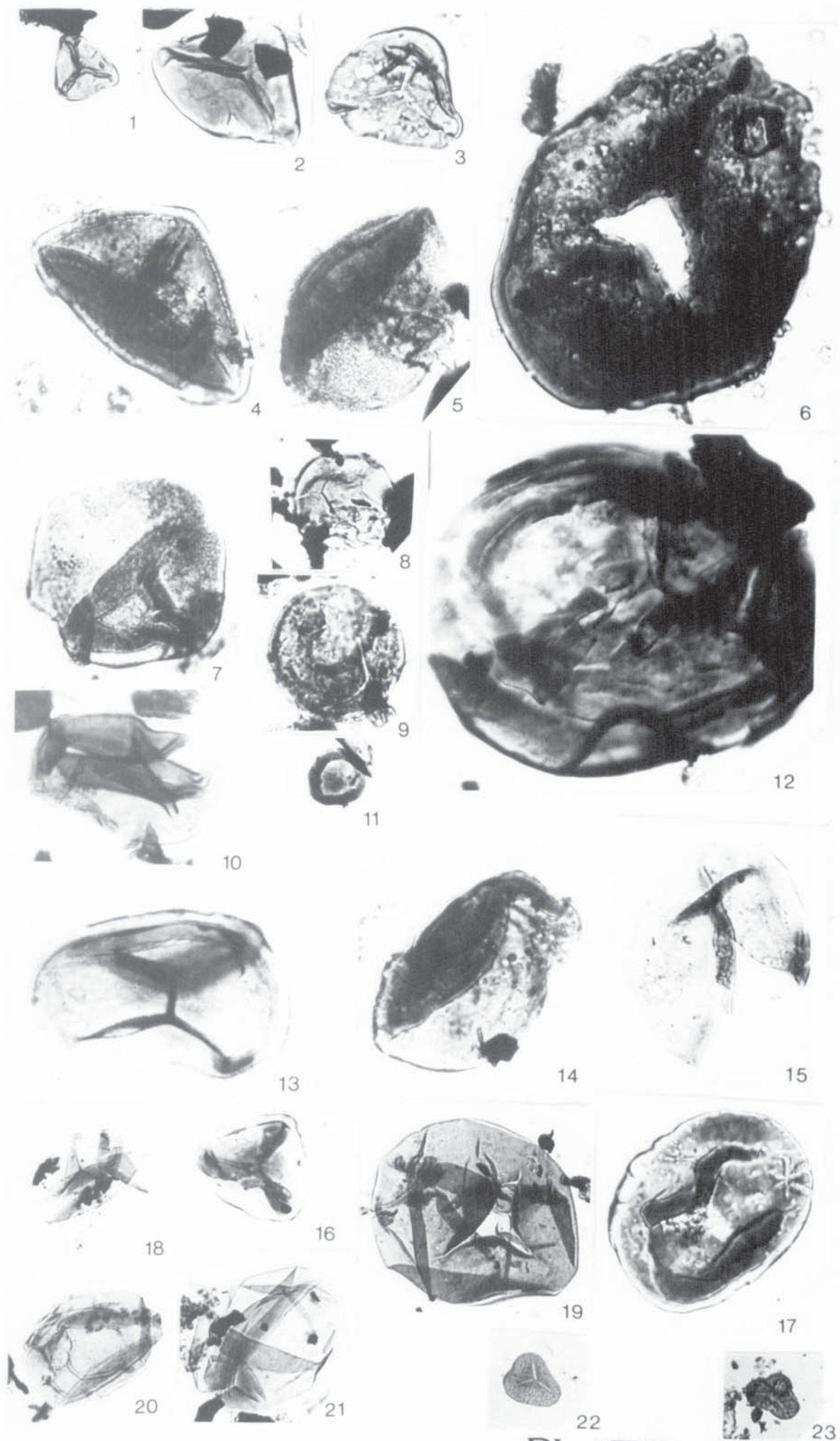


PLATE 4.1

EXPLANATION OF PLATE 4.2

All figures X500

- Fig. 1 Cyclogranisporites lasius (Waltz) Playford 1962. Slide T1. 21.9 x 79.6
- Fig. 2 Cyclogranisporites lasius (Waltz) Playford 1962. Slide M2.
- Fig. 3 Verrucosisporites cerosus Hoffmeister, Staplin and Malloy) Butterworth and Williams 1958. Slide T1. 29.6 x 65.1
- Fig. 4 V. cerosus (Hoffmeister, Staplin and Malloy) Butterworth and Williams 1958. Slide T1. 29.6 x 65.1
- Fig. 5 V. cerosus (Hoffmeister, Staplin and Malloy) Butterworth and Williams 1958. Slide M3.
- Fig. 6 Lophotriletes cf. gibbosus (Ibrahim) Potonie and Kremp 1954. Slide BG.16 (2). 10.7 x 59.0
- Fig. 7 L. cf. gibbosus (Ibrahim) Potonie and Kremp 1954. Slide BG.16 (2). 10.7 x 60.1
- Fig. 8 Lophotriletes sp. Slide M2
- Fig. 9 Waltzispora polita (Hoffmeister, Staplin and Malloy) Smith and Butterworth 1967. Rhyd-y-Ceirw Coal. Slide 662.
- Fig. 10 W. planiangulata Sullivan 1964. Slide M2. 0.7 x 69.0
- Fig. 11 Anapiculatisporites minor (Butterworth and Williams) Smith and Butterworth 1967. Rhyd-y-Ceirw Coal. Slide 662.
- Figs. A. spore A. sp. nov. Rhyd-y-Ceirw Coal. Slide 662. 26.0 x 57.9; 12-17 26.8 x 59.3; 26.5 x 60.0; 25.2 x 57.7; 25.8 x 57.2; 26.2 x 59.0.
- Fig. 18 Tricidarisorites sp. Slide 40P. 16.3 x 69.0
- Fig. 19 Tricidarisorites sp. Slide T1. 20.6 x 78.6
- Fig. 20 Apiculatisporis abditus (Loose) Potonie and Kremp 1955. Slide Aq. 486 (1). 6.0 x 73.0
- Fig. 21 A. abditus (Loose) Potonie and Kremp 1955. Slide Aq. 486 (1) 5.8 x 73.5
- Fig. 22 A. spinososaetosus (Loose) Smith and Butterworth 1967. Slide Ch. 485 (2). 26.8 x 57.8
- Fig. 23 A. variocorneus Sullivan 1964. Slide Ch. 485 (2). 18.9 x 74.6
- Fig. 24 Apiculatasporites spinulistratus (Loose) Ibrahim 1933. Slide Aq. 486 (1). 3.9 x 60.0
- Fig. 25 A. spinulistratus (Loose) Ibrahim 1933. Slide Aq. 486 (1). 0.3 x 68.0
- Fig. 26 A. spinulistratus (Loose) Ibrahim 1933. Slide Aq. 486 (2).
- Fig. 27 Acanthotriletes echinatus (Knox) Potonie and Kremp 1955. Slide 45P. 28.6 x 69.2
- Fig. 28 Raistrickia fulva Artuz 1957. Slide Aq. 486 (1). 21.5 x 62.0
- Fig. 29 Raistrickia nigra Love 1960. Slide 40P. 2.0 x 71.0
- Fig. 30 convolutispora cf. cerebra sp. nov. Rhyd-y-Ceirw Coal. Slide 662. 24.0 x 77.9. Also present Convolutispora sp.
- Fig. 31 See plate 4.5; Fig. 23

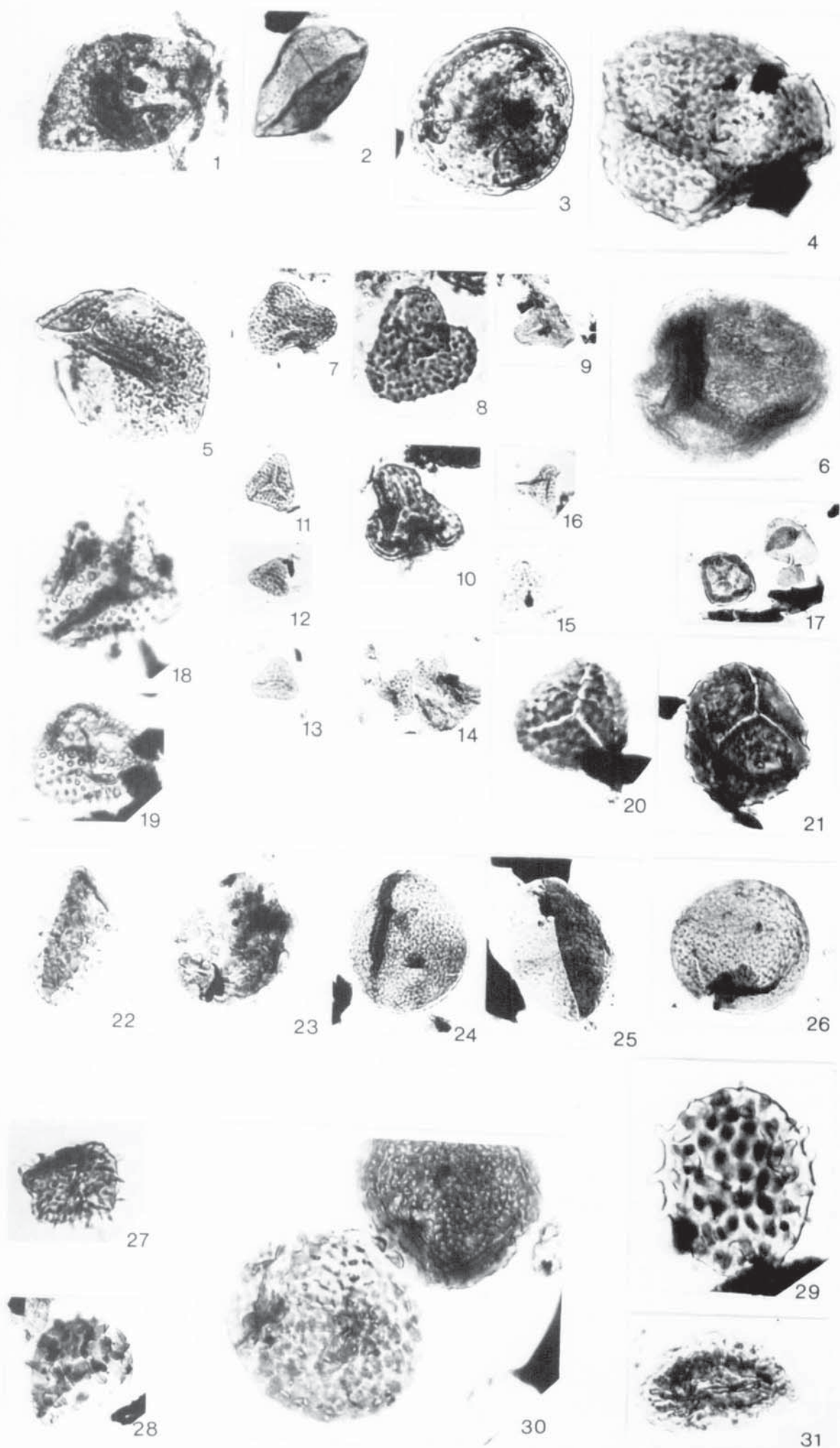
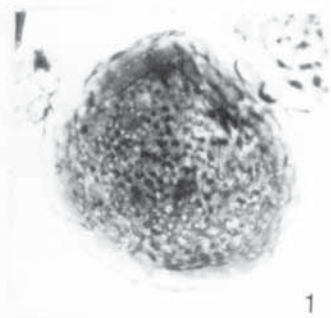
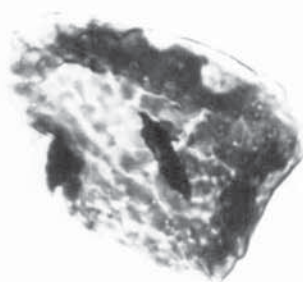


PLATE 4.2

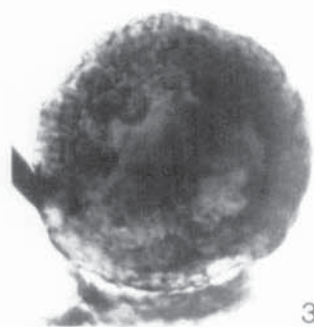
- Fig. 1 Convolutispora cf. cerebra sp. nov. Rhyd-y-Ceirw Coal. Slide 662. 22.4 x 78.7
- Fig. 2 C. crassa Playford 1962. Slide M3.
- Fig. 3 C. crassa Playford 1962. Slide T2. 3.2 x 71.3
- Fig. 4 C. cf. cerebra sp. nov. Rhyd-y-Ceirw Coal. Slide 662. 21.9 x 78.4
- Fig. 5 Convolutispora sp. Slide M3. 25.3 x 72.9
- Fig. 6 C. crassa Playford 1962. Slide T1.
- Fig. 7 C. florida Hoffmeister, Staplin and Malloy 1955. Slide M2. 25.0 x 71.8
- Fig. 8 Convolutispora sp. Rhyd-y-Ceirw Coal. Slide 662.
- Fig. 9 C. varicosa Butterworth and Williams 1958. Slide M2. 19.8 x 66.3
- Fig. 10 C. sculptilis Felix and Burbridge 1967. Slide M2. 8.8 x 80.8
- Fig. 11 C. lepida Felix and Burbridge 1967. Slide T1. 23.2 x 83.0
- Fig. 12 Microreticulatisporites sp. 1. Slide M2. 26.8 x 79.3
- Fig. 13 Microreticulatisporites sp. Slide 40P. 9.6 x 76.7
- Fig. 14 Dictyotrilletes peltatus Slide 13 (3). 7.7 x 65.0
- Fig. 15 Camptotrilletes bucculentus (Loose) Potonié and Kremp 1955. Slide Aq. 486 (3) 24.4 x 64.9
- Fig. 16 Ahrensisorites guerickei (Horst) Potonié and Kremp 1954. Slide Ch. 485 (2). 25.4 x 73.0
- Fig. 17 Ahrensisorites guerickei (Horst) Potonié and Kremp 1954. Slide Ch. 485 (2). 24.9 x 72.8
- Fig. 18 Triquitrites tribullatus (Ibrahim) Schopf, Wilson and Bentall 1944. Slide Ch. 485 (2) 22.2 x 61.7
- Fig. 19 T. cf. protensus Kosanke 1950. Slide Aq. 486 (3). 27.9 x 58.0
- Fig. 20 Reinschospora speciosa (Loose) Schopf, Wilson and Bentall 1944. Slide Aq. 486 (2).
- Fig. 21 Stenozonotrilletes lycosporoides (Butterworth and Williams) Smith and Butterworth 1967. Slide 47P. 26.5 x 76.2
- Fig. 22 S. lycosporoides (Butterworth and Williams) Smith and Butterworth 1967. Slide 47P. 17.6 x 75.0



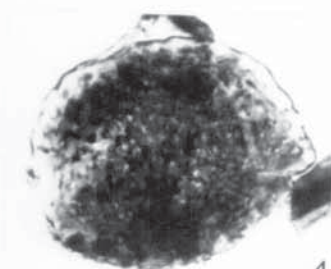
1



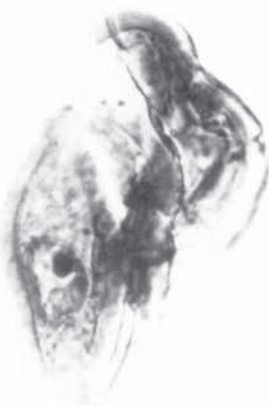
2



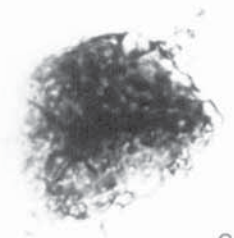
3



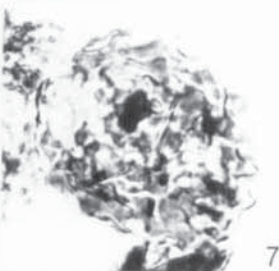
4



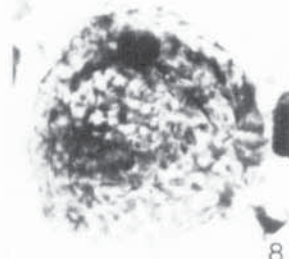
5



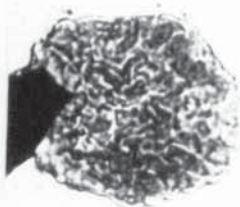
6



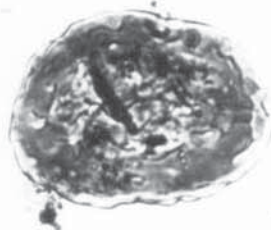
7



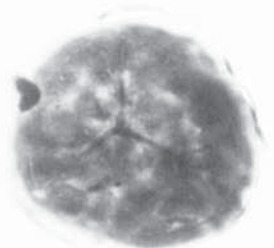
8



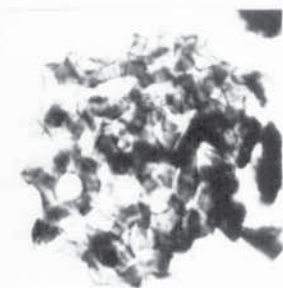
9



10



11



14



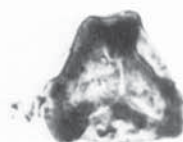
12



13



16



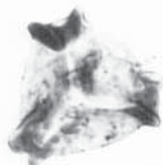
17



20



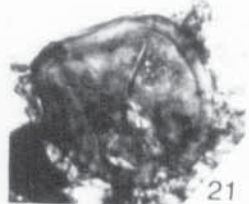
15



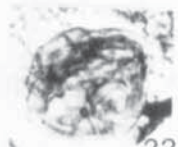
18



19



21



22

EXPLANATION OF PLATE 4.4All figures X500

- Fig. 1 Stenozonotriletes sp. Slide 45 P. 25.5 x 76.0
- Fig. 2 Knoxisporites stephanephorous Love 1960. Slide BG16 (1).
3.8 x 59.0
- Fig. 3 Knoxisporites sp. Slide m3. 5.6 x 68.9
- Fig. 4 Knoxisporites triradiatus Hoffmeister, Staplin and Malloy 1955.
Slide BG(1). 3.3 x 64.1
- Fig. 5 K. inconspicuus Felix and Burbridge 1967. Slide M2. 16.8 x 75.5
- Fig. 6 K. triradiatus Hoffmeister, Staplin and Malloy 1955. Slide M1
24.7 x 84.3
- Fig. 7 Knoxisporites sp. Slide M2.
- Fig. 8 Reticulatisporites carnosus (Knox) Neves 1964. Slide 40 p.
4.0 x 70.9
- Fig. 9 R. polygonalis (Ibrahim) Smith and Butterworth 1967. Slide
Min 8 (1). 24.8 x 74.9
- Fig. 10 Reticulatisporites lacunosus Felix and Burbridge 1967. Slide M2.
23.6 x 73.0
- Figs. Savitrissporites nux (Butterworth and Williams) Smith and
11-12 Butterworth 1967. Slides: Min 8 (1), 18.3 x 66.4; Aq. 486 (1),
23.0 x 59.0.
- Fig. 13 S. cf. obliquus Venkatachala and Bharadwaj 1964. Slide T1.
23.0 x 69.7
- Figs. Bellisporites nitidus (Horst) Sullivan 1964. Slides: BG 13 (1),
14-15 22.9 x 61.0 and 1.2 x 61.0.
- Fig. 16 Grumosissporites varioreticulatus (Neves) Smith and Butterworth
1967. Slide Ch. 485 (2) 30.1 x 64.4
- Figs. Crassispora kosankei (Potonie and Kremp) Smith and Butterworth
17-18 1967. Slide Min. 8 (1): 21.4 x 59.4 and 20.5 x 57.4
- Figs. C. maculosa (Knox) Sullivan 1964. Slides: Min 8 (1):
19-20 6.5 x 70.0 and M1: 16.6 x 84.9

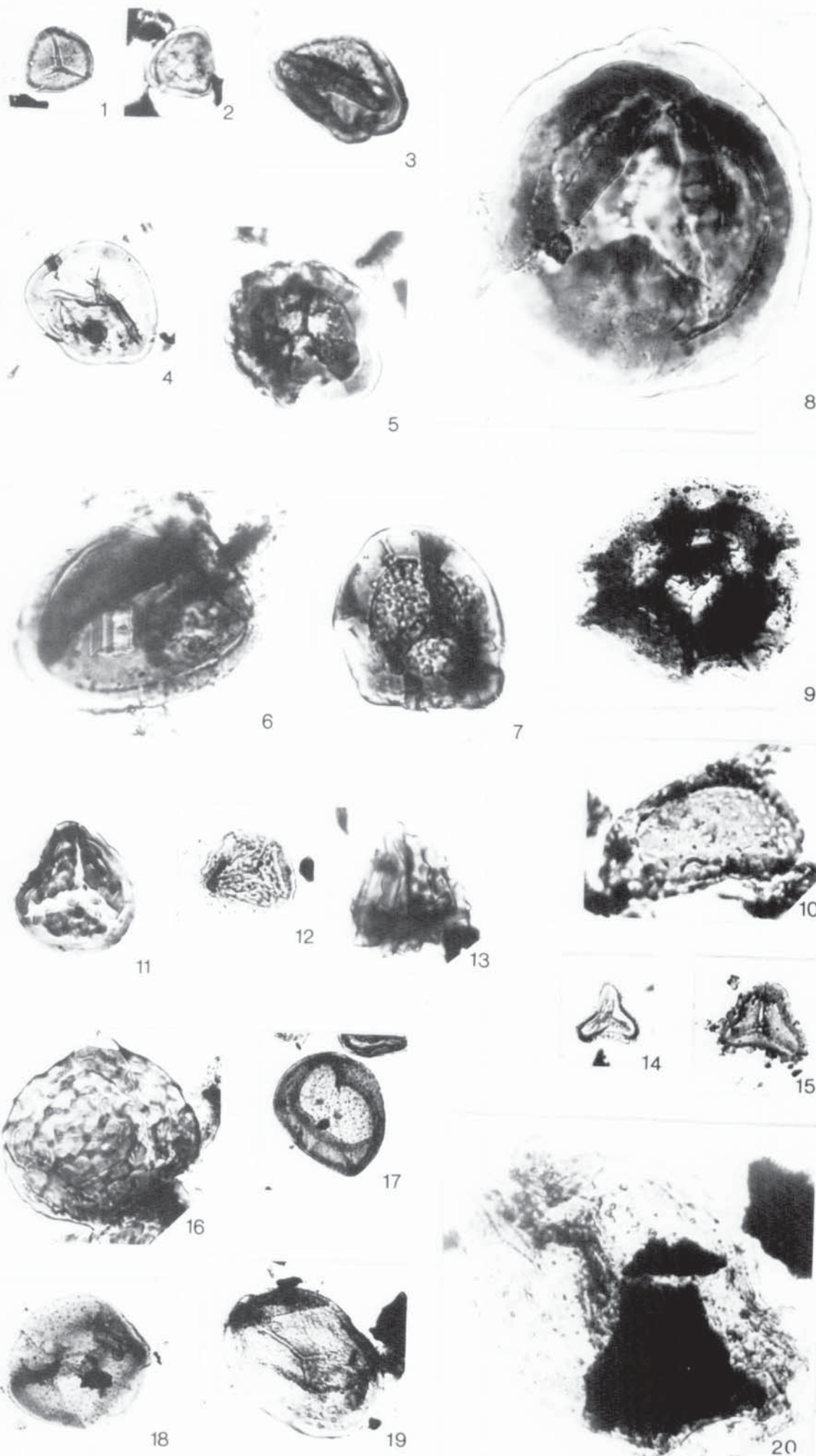


PLATE 4.4

EXPLANATION OF PLATE 4.5

All figures X500

- Fig. 1 Unidentified spore. Slide Aq. 486 (2). 21.4 x 59.4
- Figs. Densosporites anulatus (Loose) Smith and Butterworth 1967.
- 2-4 Slides: Aq. 486 (2): 22.8 x 71.2; Ch. 485 (2): 13.8 x 71.3 and Aq. 486 (1): 28.0 x 71.0
- Figs. Densosporites sp. Slides: Rhyd-y-Ceirw Coal (662): 25.0 x 59.8
- 5-6 and Min. 8 (1): 26.0 x 76.3
- Fig. 7 D. spinifer Hoffmeister, Staplin and Malloy 1955. Slide T2. 16.2 x 69.4
- Fig. 8 ? D. hispidus Felix and Burbridge 1967. Slide T1.
- Fig. 9 D. hispidus Felix and Burbridge 1967. Slide M1. 24.8 x 72.4
- Fig. 10 D. triangularis Kosanke 1959. Slide 47P. 26.3 x 71.3
- Fig. 11 Densosporites sp. Rhyd-y-Ceirw Coal. 662.
- Fig. 12 Lycospora pellucida (Wicher) Schopf, Wilson and Bentall 1944. Slide Aq. 486 (1). 21.5 x 68.0
- Fig. 13 L. ? granulata Kosanke 1959. Slide Ch. 485 (2). 14.0 x 71.1
- Figs. L. cf. noctuina sp. nov. Rhyd-y-Ceirw Coal. Slide 662. 60.0 x 63.2;
- 14-18 5.5 x 60.1; 5.8 x 62.5 and 4.9 x 63.8
- Fig. 19 L. subtriquetra Lubert and Waltz 1941. Slide T1. 25.9 x 68.8
- Fig. 20 Cristatisporites sp. Slide T2. 24.0 x 65.5
- Fig. 21 Cirratriradites saturni (Ibrahim) Schopf, Wilson and Bentall 1944. Rhyd-y-Ceirw Coal. Slide 662. 5.2 x 59.9
- Fig. 22 Cirratriradites sp. Rhyd-y-Ceirw Coal. Slide 662.
- Fig. 23 Cingulizonates cf. capistratus (Hoffmeister, Staplin and Malloy) Staplin and Jansonius 1964. Slide M1. 5.4 x 75.9
- Figs. Spencerisporites radiatus (Ibrahim) Felix and Parks 1959.
- 25-26 Slides: Ch. 485 (2) 21.3 x 65.0 and Aq. 486 (2) 1.1 x 75.0

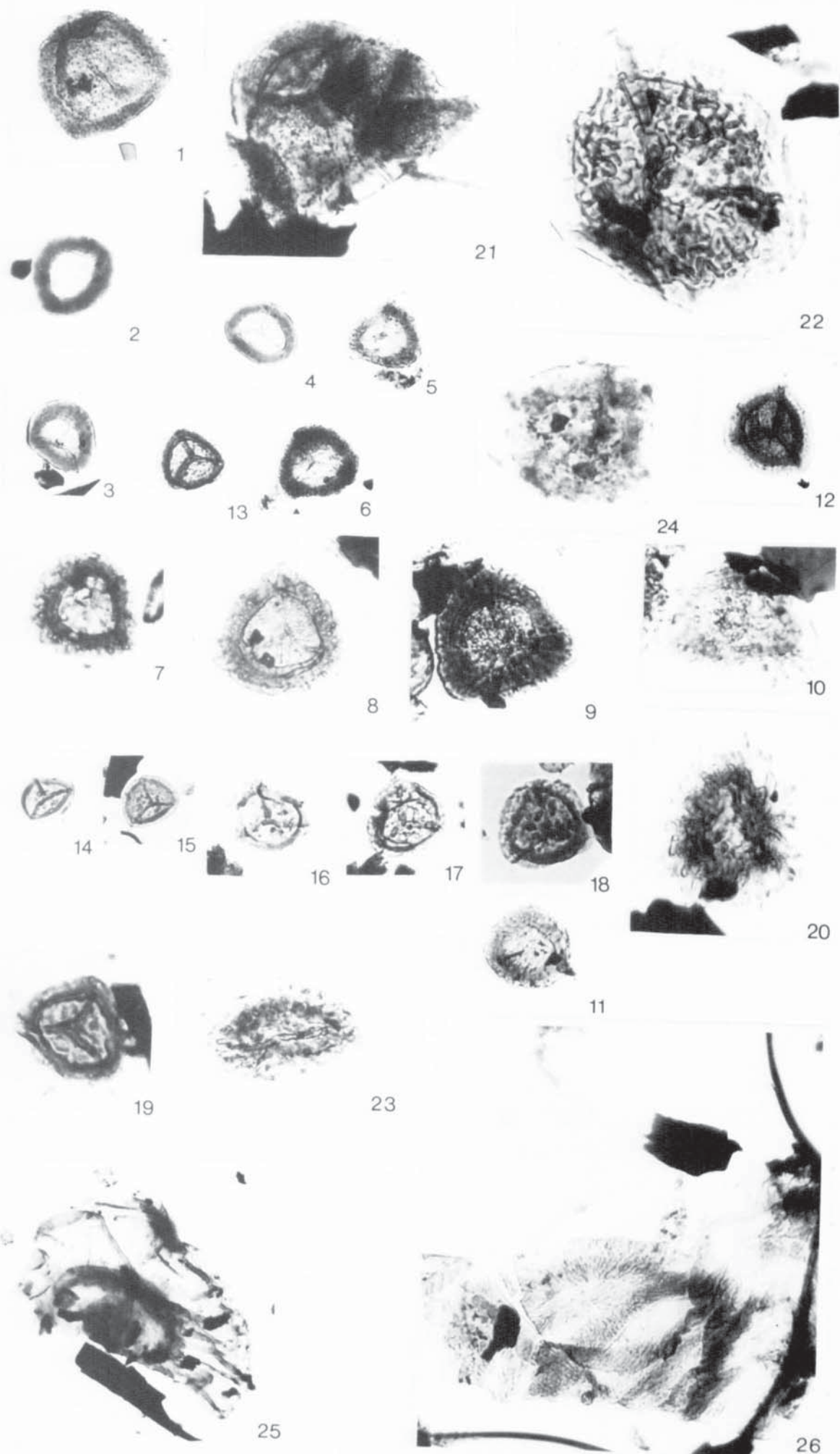


PLATE 4.5

- Fig. 1 Schulzospora rara Kosanke 1950. Slide Ch. 485 (2).
25.0 x 66.2
- Fig. 2 S. rara Kosanke 1950. Slide Ch. 485 (2). 26.9 x 68.7
- Figs. Laevigatosporites cf. minor sp. nov. Rhyd-y-Ceirw Coal. Slide 662.
3-7 9.7 x 59.4; 9.5 x 60.1; 8.5 x 58.2; 26.0 x 71.7 and 26.3 x 70.8
- Fig. 8 L. minor Loose 1934. Rhyd-y-Ceirw coal. Slide 662. 12.2 x 73.8
- Fig. 9 Florinites sp. Slide T1.
- Fig. 10 F. similis Kosanke 1950. Slide Aq. 486 (1). 11.9 x 72.7
- Fig. 11 Schopfipollenites ellopsoides (Ibrahim) Potonie and Kremp 1954.
Min. 8 (2). 19.5 x 72.5
- Fig. 12 Auroraspora solisortus Hoffmeister, Staplin and Malloy 1955.
Slide Min. 8 (2). 29.0 x 57.2
- Fig. 13 Diaphanospora parvigracila (Peppers) Ravn 1979. Slide T2.
29.0 x 70.0
- Fig. 14 Foveosporites avcinii Ravn and Fitzgerald 1982. Slide M2.
11.4 x 77.7
- Fig. 15 Foveosporites sp. Slide M1. 9.5 x 65.7
- Fig. 16 Gulisporites incomptus Felix and Burbridge 1967. Slide T1.
- Fig. 17 Grandispora spinosa Hoffmeister, Staplin and Malloy 1955.
Slide 40 P. 10.0 x 68.9

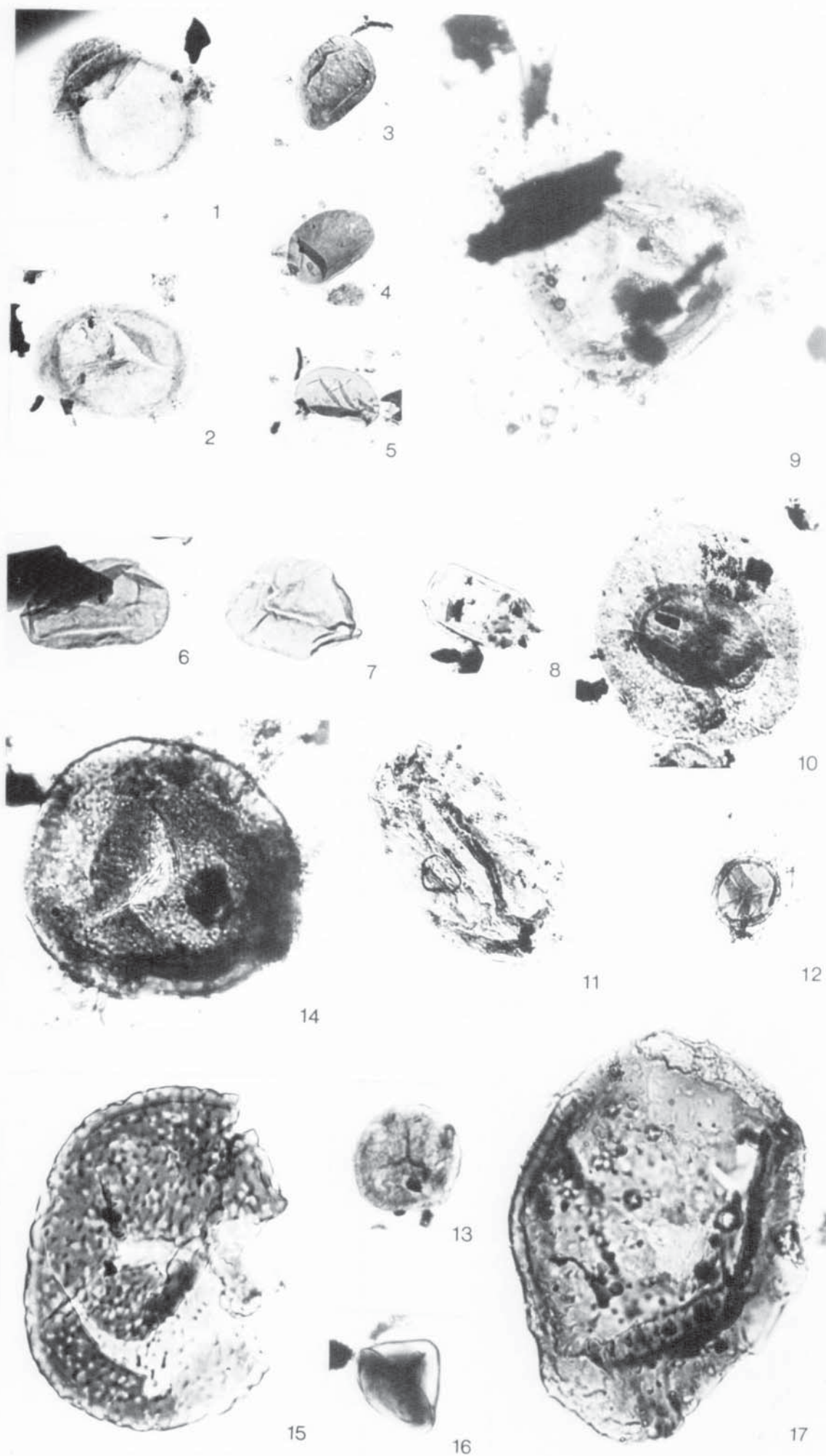
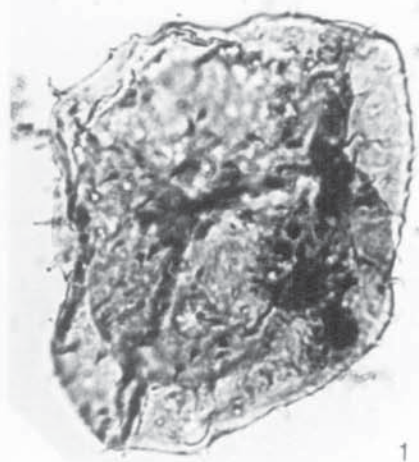


PLATE 4.6

- Fig. 1 Grandispora spinosa Hoffmeister, Staplin and Malloy 1955. Slide 47 P. 24.4 x 82.8
- Fig. 2 Grandispora spinosa Hoffmeister, Staplin and Malloy 1955. Slide 47 P. 22.8 x 80.1
- Fig. 3 Hymenospora cf. caperata Felix and Burbridge 1967. Slide Min. 8 (1). 5.0 x 63.9
- Figs. Propriisporites laevigatus Neves 1961. Slides: Min. 8 (2):
4-6 3.4 x 60.0; 2.8 x 59.5 and Min. 8 (1): 4.5 x 55.0
- Fig. 7 Kraeuselisporites ornatus (Neves) Owens, Mishell and Marshall 1976. Rhyd-y-Ceirw Coal. 662.
- Fig. 8 K. echinatus Owens, Mishell and Marshall 1976. T1. 23.4 x 82.0
- Fig. 9 Nexuosisporites comtus Felix and Burbridge 1967. M1. 24.3 x 70.2
- Fig. 10 Nexuosisporites comtus Felix and Burbridge 1967. M1. 20.2 x 74.0
- Fig. 11 Ibrahimisporites sentus Felix and Burbridge 1967. Slide 40 P.
- Fig. 12 Potonieisporites elegans (Wilson and Kosanke) Wilson and Venkatachala 1964. Slide T1. 15.8 x 68.3
- Fig. 13 Ibrahimisporites sp. Slide BG.16 (1). 25.0 x 72.2
- Fig. 14 Costatascyclus crenatus Felix and Burbridge 1967. Slide T2. 22.1 x 66.9
- Fig. 15 Ibrahimisporites brevispinosus Neves 1961. Slide T2. 29.0 x 69.0
- Fig. 16 Kraeuselisporites ornatus (Neves) Owens, Mishell and Marshall 1976. Slide T2. 28.9 x 69.0



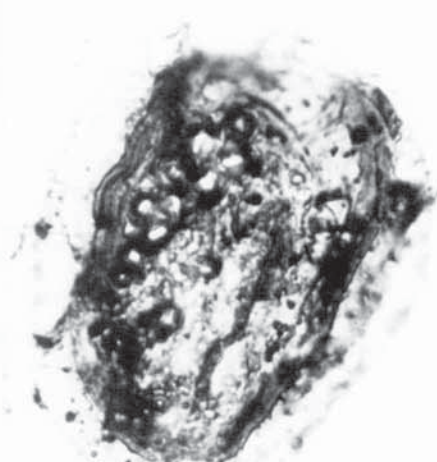
1



3



4



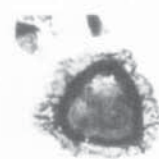
2



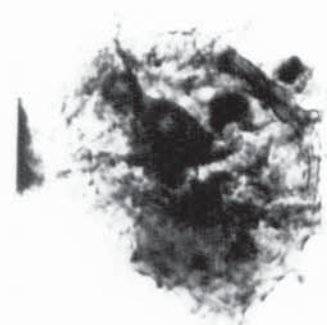
5



6



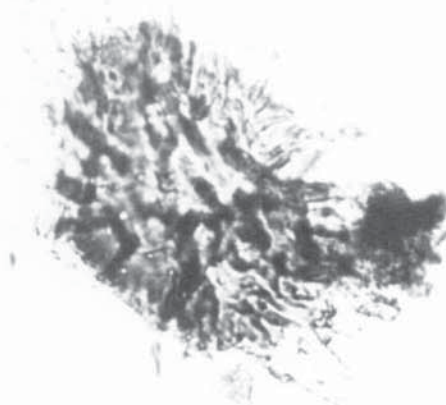
7



8



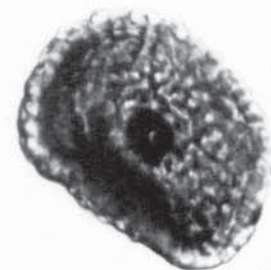
9



11



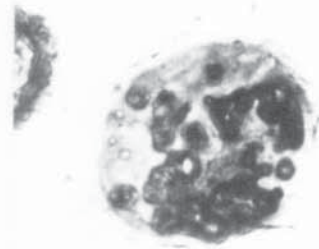
12



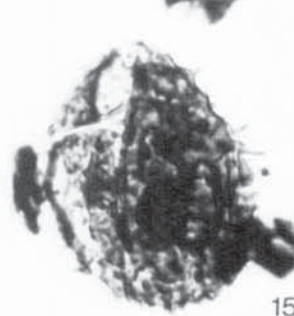
10



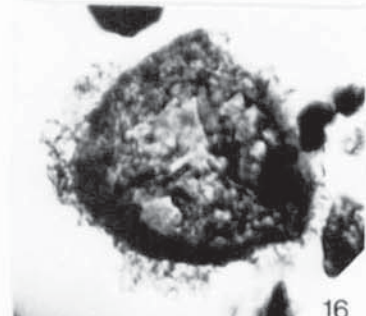
13



14



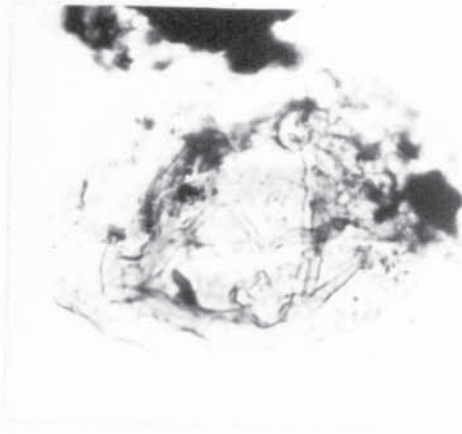
15



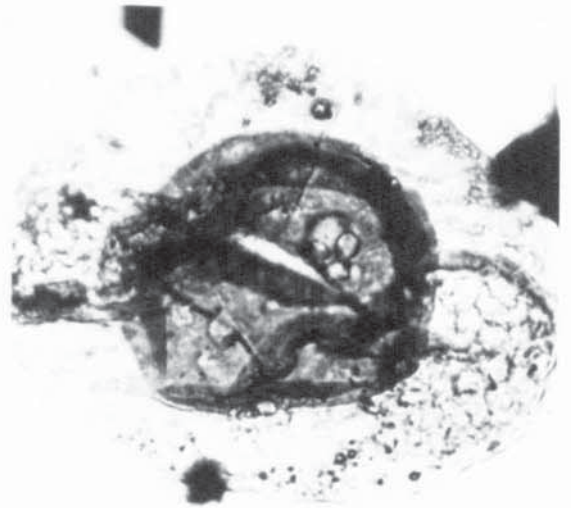
16

PLATE 4.7

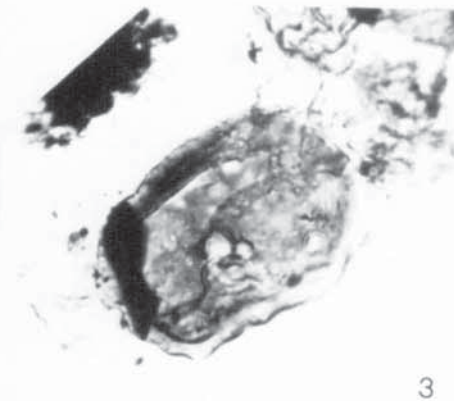
- Figs. 1-3 Potonieisporites elegans (Wilson and Kosanke) Wilson and Venkatachala 1964. Slides T2: 20.2 x 60.8; 17.1 x 59.0; and T1: 14.0 x 65.0.
- Fig. 4 Spelaeotriletes minutus Butterworth and Mahdi 1982. Slide 47 P. 19.3 x 75.5
- Fig. 5 S. triangularis Neves and Owens 1966. Slide M2. 4.9 x 69.0
- Fig. 6 Secarisporites remotus Neves 1961. Slide T2.
- Figs. 7-9 Thick walled spores. Slides M2 and M3. 21.0 x 73.8; 25.2 x 73.0 and 22.0 x 65.0
- Fig. 10 Unidentified spore. Slide M3.
- Fig. 11 Thick walled spore. Slide M1. 22.2 x 60.7
- Fig. 12 Secarisporites sp. Slide T1. 1.2 x 71.1
- Fig. 13 Secarisporites remotus Neves 1961. Slide T2. 1.8 x 65.0
- Fig. 14 Unidentified spore. Slide T2. 2.5 x 64.5.



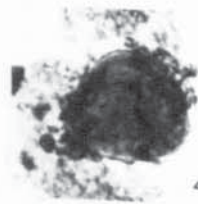
1



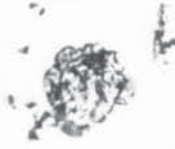
2



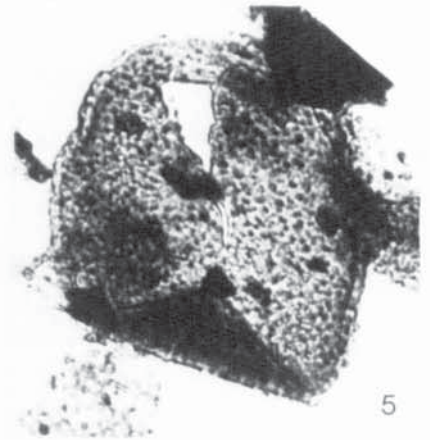
3



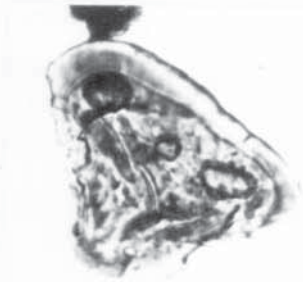
4



6



5



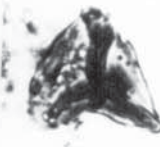
7



8



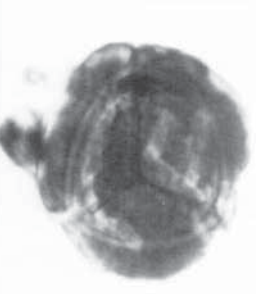
9



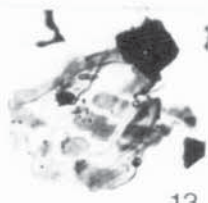
10



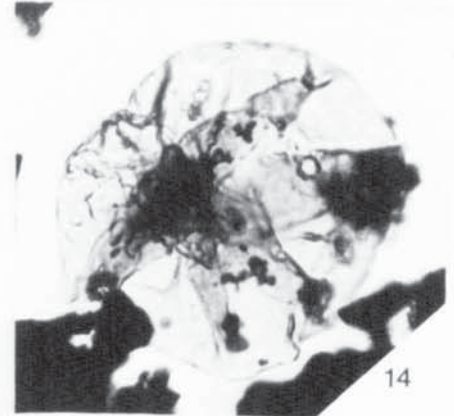
12



11



13



14

DI ΔΤΕ 4.8

CHAPTER 5

SEDIMENTOLOGY, PALYNOFACIES AND INTERPRETATION OF DEPOSITIONAL ENVIRONMENTS

5.1 INTRODUCTION

Palynofacies is a relatively new aspect of palynology which includes the qualitative and quantitative study of the kerogen content of sediments (Fisher, 1980) and thus aids sedimentological facies interpretation, particularly of delta top sands and shales (Denison and Fowler, 1980). The term was originally used by a number of palynologists including Combaz (1964), Hughes and Moody-Stuart (1967) and Batten (1973a) to refer to the general aspect of kerogen preparations. Its application in conjunction with conventional sedimentological techniques was chiefly directed towards palaeoenvironmental and biostratigraphical work but it is also a very common tool in maturation and source potential studies.

A complete knowledge of sandstone geometry and palaeoenvironments is essential in basin evaluation to improve petroleum exploration success and later during the production phase to optimise recovery. In both outcrop and subcrop, an integrated approach of sedimentological and palynofacies study is essential to make the most authentic reconstruction of ancient depositional environments. Over the past few years the development of palynofacies analysis has provided a further aspect to the integrated approach to sedimentology.

In this chapter palynofacies is used mainly in conjunction with conventional sedimentological techniques to give a more consistent and detailed identification of facies and to provide data on source, transport and depositional history of the sediments.

5.2 HISTORY OF PALYNOFACIES CLASSIFICATION

Increasing attention has been paid to kerogen classification by exploration palynologists in recent years. In view of the difficulties in determining precisely the origin of individual kerogen fragments, there have been several proposals for independent classifications of them.

The Van Krevelen diagram (1961) broadly visualised the principal types of sedimentary organic matter as sapropelic, mixed sapropelic/humic and ligneous (see also Combaz, 1975). Staplin (1969) attempted a detailed classification under primary and modified material. The work was going on in this direction and ultimately Staplin *et al.* (1973) successfully distinguished two important types of sapropel as sapropel A and B and defined it as "Sapropel A forms and accumulates in low energy, aqueous environments where the material can accumulate in masses on a still sea or lake bed, under conditions of little water circulation and reduced oxygenation"; "Sapropel B forms in high energy environments in the marine realm". Sapropel A is the principal organic component of oil shale.

Burgess (1974) classified the total sedimentary organic matter into amorphous, finely divided organic matter, herbaceous plant debris, woody plant debris, coaly fragments and algal debris.

Rogers (1979) proposed organic matter is essentially of two types: primary and secondary. The primary types included algal, herbaceous and woody types. The secondary types included amorphous and coaly types.

Combaz (1964, 1973, 1975) divided organic matter into organic debris like cutin and lignin; vitrinite; microfossils (spore, pollen, phytoplankton) and amorphous organic matter. Correia and Peniguel (1975) used a detailed classification which aimed to divide the organic matter into recognizable microorganisms, vegetative fragments and transformed organic matter.

According to Owens (1981) the most suitable of the schemes proposed so far appears to be that of Bujak, Barss and Williams (1977) in which four main categories of debris are shown: 'amorphogen' for unorganised structureless organic material which may be finely disseminated or coagulated into fluffy masses; 'phyrogen' which includes all non-opaque recognizable plant debris except that of woody origin, and includes spores, pollen, dinoflagellates and cuticles; 'hylogen', which accommodates non-opaque fibrous plant debris of woody origin and 'melanogen' for all opaque organic debris. But Venkatachala (1980) considered that this classification could not improve the understanding of the organic material. The latter author also recommended that classifications should be based upon morphological identification using transmitted light microscopy, whenever possible. He also proposed a detailed classification of amorphous organic matter. Parry *et al.* (1981) grouped kerogen into eight categories: black wood; brown wood; resin; cortex; cuticle; marine palynomorphs; terrestrial palynomorphs; and fresh water palynomorphs. Fisher (1980) proposed the primary division of the components of kerogen into humic and sapropelic types. His humic substances include: vitrinites and inertinites. On the other hand, sapropelic substances include: plant cuticles, plant spores, pollen, dinoflagellate cysts, acritarchs, algal bodies and dispersed amorphous or unstructured sapropel debris.

In the present investigation the classification proposed by Fisher (1980) is followed. However, it should be kept in mind that the present sediments are of Carboniferous age. Fisher (1980), however, studies sediments of Middle Jurassic age and a slight alteration in Fisher's 'sapropelic subdivision' is therefore necessary. In the present study the term 'sapropel' will include the following: miospores; plant cuticles; thin greenish-yellow algal matter; structured algal tissue; grey amorphous organic matter (see Venkatachala, 1980); and marine origin dark brown algal matter (see Venkatachala, 1980; see also Pl. 5.4 H).

To the author's knowledge very sporadic work has been done on the Carboniferous palynofacies and no well defined classification is proposed so far.

5.3 TECHNIQUES OF PALYNOFACIES ANALYSIS

The samples of sandstone, shale and cherty flags upon which this work is based were crushed to pea-sized fragments and macerated in hydrochloric and subsequently hydrofluoric acids for a couple of weeks. The organic residue was neutralized by repeated decanting and standard palynological slides were prepared using elvacite. During maceration the kerogen received no chemical oxidation or any deliberate physical separation. Careful examination of the slides revealed a number of different kerogen types such as among the humic substances: inertinites and vitrinites and among the sapropels: miospores, cuticles and different algal debris.

For coal samples the normal palynological slide preparation technique was employed (see Appendix 1).

The slides were logged in terms of the percentages of each of these kerogen types present. One slide was made from each sample and a total of at least five traverses across the slides were point counted to establish the kerogen components and the results were recalculated to 100% and plotted on the Figures 5.4-5.7).

Distribution plots of each kerogen type display associations which are common to different localities, and which apparently correlate with different depositional deltaic sub-environments.

5.4 STRATIGRAPHICAL SETTING

In North Wales the massive sandstones and grits of the 'Cefn-y-Fedw Sandstone Series' forms the highest elevations within the Carboniferous

area. They attain a maximum altitude of 1,648 feet above O.D on Ruabon Mountain (Wedd *et al.* 1927).

The Cefn-y-Fedw Series is not entirely arenaceous, the relatively finer grained sandstones especially are parted by subordinate silty shales, silts, and clayey shales, some of them silicified into chert, and occasional beds of limestone or highly calcareous sandstone.

Ruabon Mountain (Cefn-y-Fedw) and its neighbourhood constitutes the type area of the Cefn-y-Fedw Sandstone Series. From the southern part of Ruabon Mountain (Cefn-y-Fedw) Morton (in Wedd *et al.* 1927) instituted the following subdivisions:

	ft.
Aqueduct Grit	70
Upper Shale	30
Dee Bridge Sandstone	30
Lower Shale with Limestone	18-50
Middle Sandstone	200
Cherty Shale (Probably underestimated)	50
Lower Sandstone and Conglomerate	250

Total (Maximum) = 680	

Ramsbottom (1974b) noted that in North Wales deposition was possibly continuous with the underlying Viséan only in the basinal areas, that is around Holywell and Flint. However, the present palynological study suggests continuous deposition with the underlying Viséan even in the Llanarmon-yn-ial area (see later in this section). This has also been discussed in detail in Chapter 4.

The lithostratigraphical units used in this study are already presented in Table 1.2.

The Llanarmon-yn-ial cherty flags unit is a part of the Cefn-y-Fedw Sandstone Group (equivalents of the Millstone Grit Facies of the Pennines). This unit is about 10 m thick in the Maes-y-Droell quarry (SJ 2180 5655) where it directly overlies an approximately 15 m thick, white, soft, cross bedded, quartz rich sand unit. The cherty flags are too brittle and hard to be used economically. Some of these beds were not accessible to the author, as they occur high up on the quarry faces. The unit is stained in a variety of reds, oranges and browns, by iron oxyhydroxides. However, in a number of places waste material from the quarry processing plant has been dumped, and obscures the exposures.

The unit is also well exposed in the stream which runs from Graianrhyd (SJ 2188 5608) eastwards to the River Terrig, joining it at (SJ 2313 5623); in a small, disused quarry (SJ 2238 5617) and further east, near Pant Terfyn (SJ 2270 5550).

Goniatites and other marine fauna (apart from some unidentified brachiopods) are totally absent from this unit. Therefore, the age of this unit was determined palynologically. It is spanning the P1 and the E1 goniatite zones of the upper most part of the Asbian to the Pendleian stage (Table 4.3), which roughly conforms to the lower and middle part of the N1 Mesothem of Ramsbottom (1977).

Namurian rocks are well exposed in the Terrig River Section. E2 beds are recorded from near the base (Wood, 1936; Jones and Lloyd, 1942) and Ramsbottom (1974b) also noted benthonic fossils at the same horizon. On the east side of Hope Mountain *E. bisulcatum* of probably E2b age has been located, while E2 fossils are known from several places in the vicinity

(Jones and Lloyd, 1942). The quartzitic sandstones of the Cefn-y-Fedw Sandstone Group, which are probably several hundred feet thick are always overlie E2 beds and are overlain by a goniatite band Reticuloceras bilingue of R2b age. Unfortunately, these quartzitic sandstone beds were not studied in detail during the present survey.

The R1 shales containing R. reticulatum (Phillips) of R1c age generally overlie the Hope Mountain sandstones. This thick sandstone is the lateral correlative of the Dee Bridge sandstone farther south (Ramsbottom, 1974b). In the younger Namurian beds in the River Terrig marine bands are noted at about 2 km west of Tryddyn Church, with G. cancellatum Bisat (occurring in a limestone band) and G. cumbriense Bisat (associated with benthonic mollusca, both of them suggesting a near-shore facies). They are overlain by the sandstones which are the correlatives of the Aqueduct Grit of the Trevor section, and the Lower Gwespyr Sandstone of the north of the district. The most north-easterly extension of Cefn-y-Fedw Sandstone is around Hawarden, about 8 km north-east of the sections in the River Terrig (Fig. 1.1). In the northern part of Flintshire, no Cefn-y-Fedw Sandstone occurs, the rocks are mainly the representative of the Holywell shale facies (Ramsbottom, 1974b).

However, the present Terrig River shale consists mainly of shale/siltstone samples. Their palynological age determination is as follows:

SJ 2336 5688: lower to middle of the Arnsbergian

stage (i.e. lower to middle part of the E2).

SJ 2335 5687: at the boundary between the Arnsbergian and

the Chokierian stages (i.e. upper most limit
of the E2 and the lowest limit of the H1).

SJ 2329 5783: within the Alportian stage (H2).

These span the upper N1 to the middle of the N6 Mesothems of Ramsbottom (1977).

Near location SJ 2336 5688: 6" Rhyd-y-ceirw Coal Band:

Yeadonian stage (G1).

The samples of the Bwlchgwyn-Minera-Ruabon sandstone and the Bwlchgwyn-Minera siliceous shale unit were collected from the Bwlchgwyn old quarry (SJ 2596 5311); Minera old quarry (SJ 2580 5300) near Minera; and the Ruabon Mountain Section (SJ 2580 4580).

These sandstone and siliceous shale/siltstone samples are totally devoid of goniatites, though in the Bwlchgwyn quarry area the lower sandstone section contains marine fossils like brachiopods (hinged brachiopods such as Productids and Spiriferids) and crinoids. Palynological age determination of the interbedded siliceous shale/siltstone unit from both the Bwlchgwyn and the Minera quarry area was undertaken, which shows that this unit lies at an horizon below the middle of the R2 zone of the middle Marsdenian stage (Table 4.3). This unit also lies in the middle of the N9 Mesothem of Ramsbottom (1977). Near the top of the Bwlchgwyn quarry section a rather coarse grained sandstone bed with interstitial kaolinized and highly altered feldspar is seen directly overlying a large scale lateral accretion unit and is very similar to the rock types recorded in the Aqueduct Grit Group.

The highest samples inquired in the present study are taken from two coal samples, one each from the Aqueduct and Chwarelau Coal Seams, Australia, Marlpit, North Wales. The Aqueduct seam is situated below the Gastrioceras subcrenatum Marine Band at the base of the Westphalian series and the Chwarelau seam is from slightly higher in the sequence.

However, a detailed sedimentological summary based on field observations of the above mentioned sections is presented in Figs. 5.1, 5.2, and 5.3.

It should be wise to mention here that no attempt has been taken during the present investigation to study the Gronant chert palynofacies as it is well known that the Gronant cherts (originally limestones) are essentially a shallow-marine facies.

5.5 IDENTIFICATION OF DELTAIC SUB-ENVIRONMENTS IN THE PRESENT STUDIED SECTIONS

On the basis of sedimentological investigation and palynofacies study six deltaic sub-environments are distinguished. They are:

- i) interdistributary bay shales/shallow marine sandstones
- ii) distributary channel sandstones
- iii) natural levee sandstones
- iv) abandoned channel sandstones
- v) swamp shales
- vi) coal associations

For detailed discussion of the above sub-environments the following sections are referred.

5.5.1 Interdistributary Bay shales/Shallow Marine Sandstones

This palynofacies occurs in the Llanarmon-yn-ial area, the Terrig River and the Bwlchgwyn quarry section. In the Llanarmon-yn-ial the unit has a thickness of about 8 m and is well developed in the Maes-y-Droell quarry (SJ 2180 5655); in the stream which flows from Graianrhyd (SJ 2188 5608) eastwards to the River Terrig; in a small, disused quarry at (SJ 2238 5617); and near Pant Terfyn at (SJ 2270 5550). The facies here is mainly characterised by the creamy-white porcellanous quartzitized silts, which are iron oxyhydroxides stained and dark thin shales which are sandy and friable (Fig. 5.4 and Pl. 5.2 A). The individual beds of silts (cherty flags)

and shales vary in thickness from 5-10 cm and 2-5 cm respectively. The average quartz and organic carbon content of the shale interbeds are 48.5% and 1.5% respectively. Among the clay minerals detrital illite and kaolinite are noted in the silts and shales.

In the Terrig River the thickness of this unit is about 13.6 m (Fig. 5.4). The lithology is mainly characterised by light to dark grey, fissile and splintery and occasionally highly siliceous shale/siltstone. Most shales/siltstones show thin gradational lamination due to slight fluctuations in grain size. In some, thin laminae of cleaner sand are interlaminated, while in others ironstone nodules and laminae are noticed. Average quartz and organic carbon content of this unit are about 54.0% and 2.50% respectively. Detrital illite (about 43.0%) is the only clay mineral species present. A trace amount of pyrite is also noted.

In the Bwlichgwyn quarry, the unit becomes very thin (about 1 m) and mostly exposed at the lower part of the quarry area (Fig. 5.4). The lithology is characterised by greyish-white, fine to medium grained, massive to flat bedded, occasionally jointed siliceous pebbly sandstones with numerous brachiopods and crinoids marine fossils. The relatively coarser sandstones are laminated and well jointed but no pebbles noted. Palaeocurrents measurement from cross beds are impossible as most of the cross beds when present are deformed and distorted. Occasionally individual beds have sharp bases and much fine brachiopod and crinoid debris are concentrated at the base of each bed. Petrographically the sandstones are mostly fine to medium grained, and moderately sorted. Subangular to subrounded quartz grains are the dominant component, forming up to 95% of the rock. This reflects that the sandstones are fairly mature and contain only subordinate amount of authigenic kaolinite, illite and trace amounts of pyrite.

The ages of the 'interdistributary bay shale facies' in different localities of North Wales have already ^{been} mentioned in Section 5.4.

The palynofacies of these sediments is dominated by sapropels (e.g. greenish-yellow algal matter, dark-brown algal matter and miospores) and fine grained vitrinitic debris. Minor amounts of lath shaped inertinites are also recorded (Figs. 5.4; 5.7 A). Presumably these lath shaped inertinites were kept in suspension in higher energy conditions and not deposited earlier. Marine indicator dark brown algal matter (Venkatachala, 1980) is present in a very high frequency, but other marine indicator microplankton such as acritarchs, dinoflagellates and leiospheres are totally absent. However, fresh water alga Botryococcus is also not recorded in this facies. Miospore assemblages are most significant here, and rich in numbers and diverse in species (Chapter 4), suggesting deposition close to the margins of the open body of water (Denison and Fowler, 1980). Moreover, the presence of thick exined trilete miospores of larger and smaller size may indicate deposition nearer to the shore (Al-Ameri, 1983). Neves (1958) considered that saccate spores are generally dominant in marine shales. Thus the presence of a high frequency of saccate spores (Potamieisporites elegans) particularly in the Terrig River section strongly suggest a possible marine water influx in this facies type. This also supported by the geochemical facies analysis (Section 6.3; 9.10; 9.11). This facies also conforms with the N1 to the middle of the N6 mesothems of Ramsbottom (1977). See also Chapter 4.

The effects of physical degradation and biodegradation on the kerogen of this facies type is exhibited as partial corrosion of the fine structure of both the humic and sapropelic components (Pl. 5.4 C, D, H). Sorting ranges from moderate to poor.

The palynofacies assemblage described above is very similar to the 'Bay Shale' assemblage as described by Denison and Fowler (1980) from the Ness Formation in Brent Province, United Kingdom (Table 5.1). On the otherhand, the presence of marine fossils in the Bwlchgwyn sandstones suggest a shallow marine origin of them.

5.5.2 Distributary Channel Sandstones

This facies includes sandstones from the Bwlchgwyn old quarry (SJ 2596 5311), Minera old quarry (SJ 2580 5300), and the Ruabon Mountain (SJ 2580 4580) (see also Figs. 5.4; 5.5; 5.6). The unit is about 17 m, 9 m and 5 m thick in the Bwlchgwyn, Minera and the Ruabon sections respectively. The age of this unit was already given in Section 5.4.

The lithology consists mainly of greyish-white *thick to* lenticular bedded ~~medium to coarse grained~~ quartzitic sandstones interbedded with dark grey to black, extremely fine grained, vitreous, highly silicified thin siltstones/shales (swamp shale, see Section 5.5.5). Petrographically the sandstones are coarse to medium grained and moderately well sorted. Subrounded to rounded quartz grains are the dominant component, forming upto 90-95 percent of the rock. Subordinate amounts of authigenic kaolinite, altered illite and potash feldspar are invariably present. The sandstones are mature and authigenic quartz and authigenic kaolinite are the main cements present. Sedimentologically, the channels are marked by scoured bases with occasionally large lateral accretion units, with rare foresets (Pl. 5.1 A). Recently Fielding (1986) in a study of the fluvial channel and overbank deposits from the Westphalian of the Durham Coalfield, North-East England, also recorded lateral accretion units in distributary channel deposits.

The total kerogen content of these sandstones is extremely sparse (except a few inertinites) as in the highest energy regime, the majority of

materials remain in suspension and normally only the rare grains of the densest inertinitic kerogen can be deposited (Figs. 5.4; 5.5; 5.6; 5.7 B). On the other hand, some of these sandstone samples also contain minor amounts of vitrinite particles and rare cuticles and extremely rare miospores, suggesting a slower flow regime within the channel system allowing other lighter kerogens to fall out of suspension. Presumably the humic fraction of the palynoflora was generated elsewhere (such as in humic swamp associations), prior to its incorporation into the channels. Considerable transport is suggested by the fragmented nature of much of the palynofacies and the rounded nature of the quartz grains. No marine influence is present.

Sorting is moderate to good and physical degradation of the organic fragments is present.

The above findings are consistent with the distributary channel palynofacies assemblages as described by Fisher (1980) from the Middle Jurassic of Yorkshire and Denison and Fowler (1980) from the Ness Formation in the Brent Province (see also Table 5.1).

5.5.3 Natural Levee Sandstones

Natural levee sandstones (about 1.6 m thick) are only found at the top of the Minera old quarry interbedded with the swamp shale facies (Fig. 5.5). The sandstones are mainly light to dark grey in colour and fine or fine to medium grained containing thin interlamination of siltstones and carbonaceous debris. Occasionally some sand layers contain very faint crosslamination. A few sandstone beds are lenticular in profile. The unit is characterised by large drift wood fragments.

Petrographically these sandstones are mostly fine grained and moderately sorted. Angular to subangular quartz grains are the dominant component.

Quartz and both authigenic and detrital illite are the main cement, although authigenic kaolinite also occurs. A trace amount of siderite is also present. For the age of this unit Section 5.4 is referred.

The palynofacies are characterised by a considerable autochthonous element in the form of roots and thin rooted coals (Figs. 5.5; 5.7 D). They also contain fine oxidized vitrinitic and algal debris though most of the humic debris is inertinite. These deposits may also appear "bleached" when compared with the assemblages from the distributary channel sandstones and also contain extremely rare pteridophyte fern spores, probably originating from the "swamp shales" adjacent to the levee. No marine influence is present. The kerogens are moderately sorted and the effect of physical degradation is noticed. Biodegradation is absent.

Such palynofacies assemblages are typical of levee deposits in a delta top environment (Fisher, 1980; Parry *et al.* 1981; Denison and Fowler, 1980; see also Table 5.1).

5.5.4 Abandoned Channel Sandstones

Abandoned channel sandstones (about 1.9-2 m thick) are recorded only at the Ruabon Mountain section interbedded with the distributary channel sandstones (Fig. 5.6.) The lithology comprises laminated, thinly bedded sandstones and siltstones. The medium to fine grained sandstone laminae, about 20 mm thick, rarely have diffuse boundaries and grade, both upwards and downwards, into the adjacent siltstones.

Petrographically the sandstones are mostly yellowish-brown and medium to fine grained and contaminated by iron oxyhydroxide staining. They are poorly sorted. Subangular to subrounded quartz grains are the dominant component, forming up to 90 percent of the rock. Authigenic kaolinite and both detrital and authigenic illite are the main clay mineral species

present. Authigenic quartz is the dominant cement. A trace amount of siderite is also noticed.

The palynofacies is dominated by fine grained vitrinites and sapropelic materials (miospores + algal debris), reflecting the cessation of current activity (Figs. 5.6; 5.7 C). The larger fragments of inertinite are totally absent. This confirms a reduced energy environment where materials of saltation and suspension load (Fig. 5.8) of a higher energy system (for instance the interbedded distributary channel facies) have been deposited.

Miospores are rich in numbers and diverse in species having been derived from a variety of local and hinterland environments by aerial and aqueous transport. Most of them are less than 60μ m in size. Microplankton is absent, though occasionally thalloid algal material (dark brown algal matter, see Venkatachala, 1980) are noted.

There is less evidence of physical degradation in both the humic and sapropelic debris. Sorting is poor to moderate.

Such an assemblage fits well with the abandoned channel facies of Fisher (1980) and Denison and Fowler (1980; see also Table 5.1).

5.5.5 Swamp Shales

This is seen in the siliceous shales/siltstones from the Bwlchgwyn old quarry and the Minera old quarry sections.

In the Bwlchgwyn quarry the unit is seen at the top of the section alternating with the distributary channel sandstone facies. The overall thickness of the unit (the total thickness of individual shale beds) is about 1.5 m (Fig. 5.4).

In the Minera quarry the unit has a thickness of about 0.6 m and alternates with the distributary channel sandstone and natural levee sandstone facies (Fig. 5.5).

The age of the unit is described in Section 5.4.

The lithology comprises poorly bedded and weakly laminated shales and siltstones. The shales are generally black or dark grey in colour and of variable fissility. The siltstones are occasionally gradational to mudstone from which they are most readily distinguished by a lighter colour and by the presence of visible mica flakes. Carbonaceous plant debris are common particularly in the shale beds and fragments of ? Lepidodendron have been recognised. The average organic carbon and quartz content of this unit are about 3.40% and 59.65% respectively. Detrital and authigenic kaolinite/dickite (average about 21%) and detrital illite (average about 14%) are the main clay mineral species present. A trace amount of anatase is also noted.

Kerogen of this facies is dominated by vitrinitic material, the majority of which is fine grained, due to deposition in a low energy regime. Sapropels (miospores + algal debris) are another dominating palynofacies recorded here (Figs. 5.4; 5.5; 5.7 E). The presence of both non-marine and coal swamp miospores (Neves, 1958) in this facies may indicate a mixture of local swamp habitats and hinterland floras. However, inertinite is present in most of the samples suggesting localised increased current activity within a lower energy regime. Alternatively, higher energy conditions in shales may also be associated with syn-depositional structural highs (Denison and Fowler, 1980). Cuticles are seen in some samples.

Sorting is very poor and the effect of physical degradation is widespread, though biodegradation is also present.

The above mentioned palynofacies assemblages can be collated with the 'swamp shale' assemblages as described by Denison and Fowler (1980; see also Table 5.1).

5.5.6 COAL ASSOCIATIONS

Palynofacies content of three coal samples were also studied during the present investigation. One coal sample is derived from the 6" Rhyd-y-Ceirw Coal Band from the Terrig River section, which is situated between the Gastrioceras cumbriense and Gastrioceras cancellatum Marine Band (Ramsbottom, 1974b). Among the other two, one each from the Aqueduct and the Chwarelau Coal Seam, Australia, Marlpit, North Wales. Aqueduct Seam is situated below the Gastrioceras subcrenatum Marine Band and the Chwarelau is slightly higher in the sequence (Smith and Butterworth, 1967). However, during the present investigation these coals were also studied palynologically. For details, see Biostratigraphical Palynology (Chapter 4 and Table 4.3).

The Rhyd-y-Ceirw Coal Band is slightly higher in the fine grained humic vitrinitic component compared to the structured sapropels like miospores, while the reverse is true ^{the} in case of the Aqueduct and the Chwarelau Coal Seams (Fig. 5.4; 5.7 F; and Pl. 5.3 A, B). On the other hand Densosporites spp. are low in the Aqueduct Seam, suggest^{ing} that Smith's (1962) Densospore phase is barely reached here and which indicates a wetter environment for the plant communities in this part of the coal swamp. The high frequency of humic components (vitrinites) in these coals are also interesting. In a typical coal swamp, that is with a high water table, oxidising conditions may be maintained in the surface layers of the peats. However, gradual sinking and covering by younger peat layers produces conditions in which the dominant woody components of peat, leaf and root debris may be converted to vitrinites (Teichmuller, 1962; Kurbatov, 1963).

The low frequency of inertinite is expected as Carboniferous coals are vitrinitic (Fisher, 1980). Cuticles are rarely seen. The fine grained tendency of both the humic and sapropelic components strongly suggest deposition in a low energy regime.

Fresh water alga Botryococcus is not recorded.

Most of the palynofacies are affected by physical degradation and biodegradation. Sorting is poor.

5.6 DISCUSSION AND CONCLUSIONS

During the Namurian North Wales lay on the south-western edge of the Central Province basin (Ramsbottom, 1974b; see also Fig. 1.2). The northern coast of St. George's Land passes through the region and it is believed that the sandstones derived from St. George's Land are of the quartzitic type (i.e. Cefn-y-Fedw Sandstone Group). Feldspathic sandstones came from the north-east into the Central Province basin not before R2 and G1 times and they include the Lower Gwespyr Sandstone and Aqueduct Grit (Ramsbottom, 1974b).

Dinantian and Namurian sedimentation in the Central Province basin and in the Northern Pennines was dominated by the deposition of Yoredale type facies. Generally these consist of a limestone or marine band overlain by a coarsening upward sequence capped by a rootlet-bed and occasional thin coal. The coarsening upward sequence has generally been interpreted by different authors as forming by delta progradation.

Most of the clastic sequences in the Bwlchgywn-Minera-Ruabon area, which consist mostly of a large proportion of texturally mature sandstones (limestones in these sequences are fairly uncommon) were probably produced by constructive and destructive phases of fluvial dominated

deltas. A Mississippi type delta model can be applied here. But other areas such as the Llanarmon-yn-ial and the Terrig River, appear to have developed outside the main zone of fluvial dominated deltaic influence. Obviously the Gronant cherts near Prestatyn, are a shallow-marine facies - not a deltaic facies at all.

The formation of deltaic sequences in North Wales appears to have commenced close to the Dinantian-Namurian boundary. Above this deltaic sediments increase in abundance and at the same time limestones gradually die away. The fluvial influence within the delta gradually became more prominent at the beginning of R2 times. This reflects the increased terrigenous input in North Wales during the Namurian B time. Such an increase in sediment supply may result from a south-eastward shift in the major distributary channels or rejuvenation in the source area. The development of fluvial dominated deltaics thus heralded the complete end of limestone deposition and Yoredale cyclothem formation in North Wales.

Percival (1982) considered that storm deposition became a much more important factor in shallow-marine sedimentation on the Alston Block during the early Namurian. Therefore, the rare occurrence of shallow-marine conditions later in Namurian times in North Wales is consistent with the absence of storm deposits there. This may have been due to presumed rapid deltaic progradations across the North Wales only allowing limited time for shallow-marine reworking and deposition. From the foregoing, the broad pattern of sedimentation seen is closely comparable with that observed in present day deltas of the type classified by Fisher (1969) as elongated high constructive deltas. Examples of this type are the modern bird foot delta of the Mississippi (Fisk, 1961; Gould, 1970), the Colorado delta (Kanes, 1970) and the Guadalupe delta (Donaldson *et al.* 1970). All indicate that a prodelta sequence of muds and silts passes

gradationally upwards through delta slope silts into sands deposited around the distributary mouth bar as the system progrades. In deltas of this kind, sand deposition in the delta front area is limited to the vicinity of the distributary mouth (Collinson and Banks, 1975). According to these authors, as progradation continues, a linear sand body (bar finger sand of Fisk, 1952) is generated, which gradually thins away from the locus of the distributary and passes into finer grained interdistributary sediments (probably the interdistributary bay shale/shallow marine sandstone facies in the present case).

Obviously compared to the mouth bar, the energy condition of the distributary channel regime is higher. In the Bwlchgwyn-Minera-Ruabon area, the present study also indicates the upward passage from distributary channel sandstone into natural levee sandstone, abandonment sandstone and swamp shale facies comparable to commonly occurring fluvial fining upward sequences. Such sequences are generally held to be the product of lateral channel migration or abandonment. The repetition of the distributary channel facies towards the top of the Bwlchgwyn and Ruabon quarry area (Figs. 5.4; 5.6) may indicate periodic abandonment of distributary channels. Elliott (1974) and Fielding (1984a) considered that minor distributary channel deposits are formed by crevassing (channel bank breaching) of major distributaries, followed by long term maintenance of crevasse channels. However, more detailed work is needed to prove this in the present case which may be an interesting subject for future research.

From the foregoing it can be convincingly assumed that as the distributary channel sandstone facies occurs only in the Bwlchgwyn-Minera-Ruabon area and the more shaly/silty fine sand units of the proposed interdistributary bay shale/shallow marine sandstone occurs in the Llanarmon-yn-ial and the Terrig River area and gradually pinch out

towards Bwlchgwyn, it seems that the progradation of the distributary mouth gradually halted in and the around Bwlchgwyn area. However, it is not possible on the basis of present evidence to place the exact position of mouth bar arrest (though it seems more likely to be further south or south-west i.e. the Minera or the Ruabon area).

The features observed by Collinson and Banks (1975) from the Haslingden Flags (Namurian, G1) of south-east Lancashire and by Johnson (1981) from the (Arnsbergian, E2a) delta, in the western Bowland Fells, north Lancashire, have some similarity with the above observation.

Two distinct kerogen types can be seen from the present survey:

1. Humic particles such as vitrinites and lath shaped inertinites are dominated in anoxic conditions, such as in the swamp shales and coals.
2. Algal debris, terrestrial palynomorphs and cuticles (i.e. all sapropels) increasing distally from the sub-aerial delta.

The palynofacies distributions recorded in the different outcrops of the investigated area can be interpreted^{as} due to two principal causes: firstly, certain kerogens accumulated to sediments in a particular environment and secondly, energy of the depositional medium of that environment. In a dynamic system it is the energy of the depositional medium which controls the sedimentation of palynofacies. Consequently in the channel sands or winnowed marine sands, which are considered to be representative of high energy conditions - the least buoyant material will be deposited. On the other hand, more buoyant material will be deposited in progressively lower energy sediments such as in the distal delta front where the marine energy conditions decrease, more of the lighter kerogen begins to fall out of suspension. Present study also suggests thick-walled, large and small trilete fern spores may also be deposited in a lower energy regime. Integration of sedimentological and palynofacies study may,

therefore, reveal three distinct deltaic phases in these sediments: the coastal plain phase; the progradational phase; and the abandonment phase.

The coastal plain phase includes spiculitic cherty flags with greyish-white, fine grained fossiliferous pebbly sandstone and light to dark grey, fissile and splintery siliceous shale association deposited in a shallow marine condition or in a shallow, shoreline bay or interdistributary bay. The progradational phase consists of small scale coarsening upwards sequences which represent the infilling of an extensive interdistributary bay by distributary channel - natural levee - abandoned channel - repetition of distributary channel sandstones. A fluvial origin of the channels is suggested by the complete absence of features generally associated with tidal channels such as current reversals, mud drapes and marine fauna and marine palynofacies. The channels could be major fluvial distributaries which infilled interdistributary bay facies as progradation continues, and compare favourably with distributary channel sequences described from recent deltaic sediments (Oomkens, 1974). The Upper Carboniferous in the study area was therefore deposited in a moderately deep and subsiding basin which was repeatedly infilled by clastic sediments as progradation continued. Reading (1967) considered that Upper Carboniferous coarsening upwards cycles frequently attributed to delta progradation. Elliott (1975, 1976a) also observed similar features from the sedimentary history of a delta lobe from a Yoredale (Carboniferous) cyclothem, and the Upper Carboniferous sedimentary cycles produced by river dominated, elongate deltas.

During the abandonment phase, thin coal horizons and possibly swamp shales were deposited indicating localised marsh development following abandonment of the bay, channel and levees. However, localised repetitions of the progradational and abandonment phases may be

suggested by the interbedded occurrences of channel or levee sandstones with swamp shales in both the Bwlchgwyn and Minera sections.

In conclusion, the whole studied sequences may be regarded as an interaction between clear, shallow seas, in which carbonates were deposited (e.g. the Gronant chert), and clastic incursions by major river deltas.

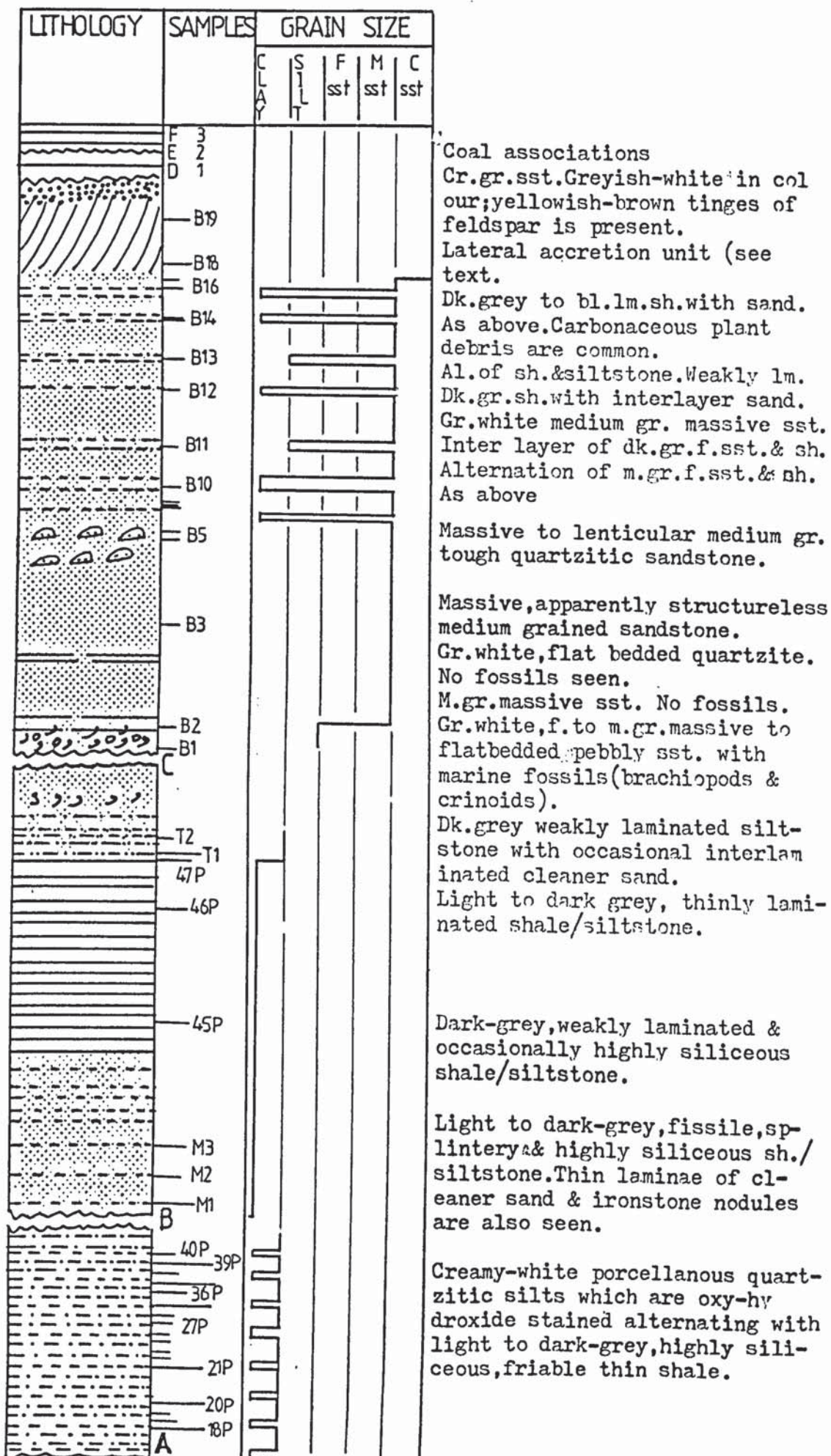


Fig. 5.1 • Measured stratigraphic sections of the Namurian delta top sequences. For legend see Fig. 5.4
Vertical scale: 1 cm. = 2 m.

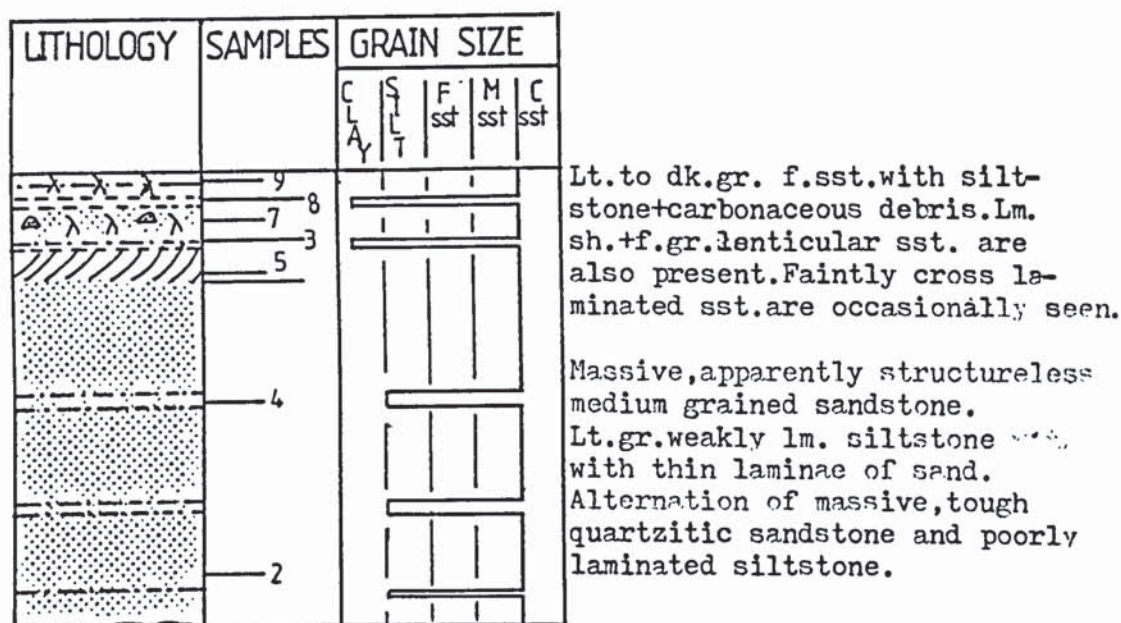


Fig. 5.2 Measured stratigraphic section of the Minera old quarry (SJ 2580 5300), North Wales. Vertical scale: 1 cm. = 2 m.

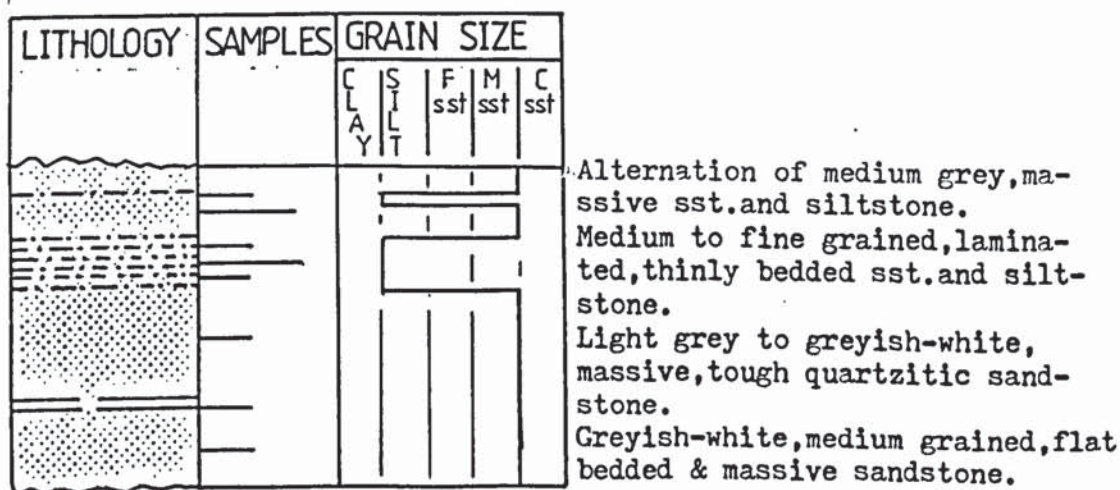


Fig. 5.3 Measured stratigraphic section of the Ruabon Mountain (SJ 2580 4580), North Wales. Vertical scale : 1 cm. = 2 m.

INTERPRETED ENVIRONMENT

KEROGEN COMPOSITION

- Inertinite
- Vitrinite
- Sapropel

SAPROPELIC COMPONENTS

- Miospores
- Cuticles
- Algal debris

HUMIC COMPONENT

- IBS — Interdistributary bay / Shallow marine
- CH — Distributary channel.
- LEV — Natural levee
- ACH — Abandoned channel
- SW — Swamp
- C — Coal

SORTING

- G — Good
- M — Moderate
- P — Poor
- VP — Very Poor

SCALE: 1cm = 3.1m

A: Llanammon-yn-ial church flags ; B: Terrig River Section ;
C: Bulchwynn old quarry ; D: Rhyd-y-ceirw coal band ;
E: Aqueeduct coal seam ; F: Chwarelau coal seam.

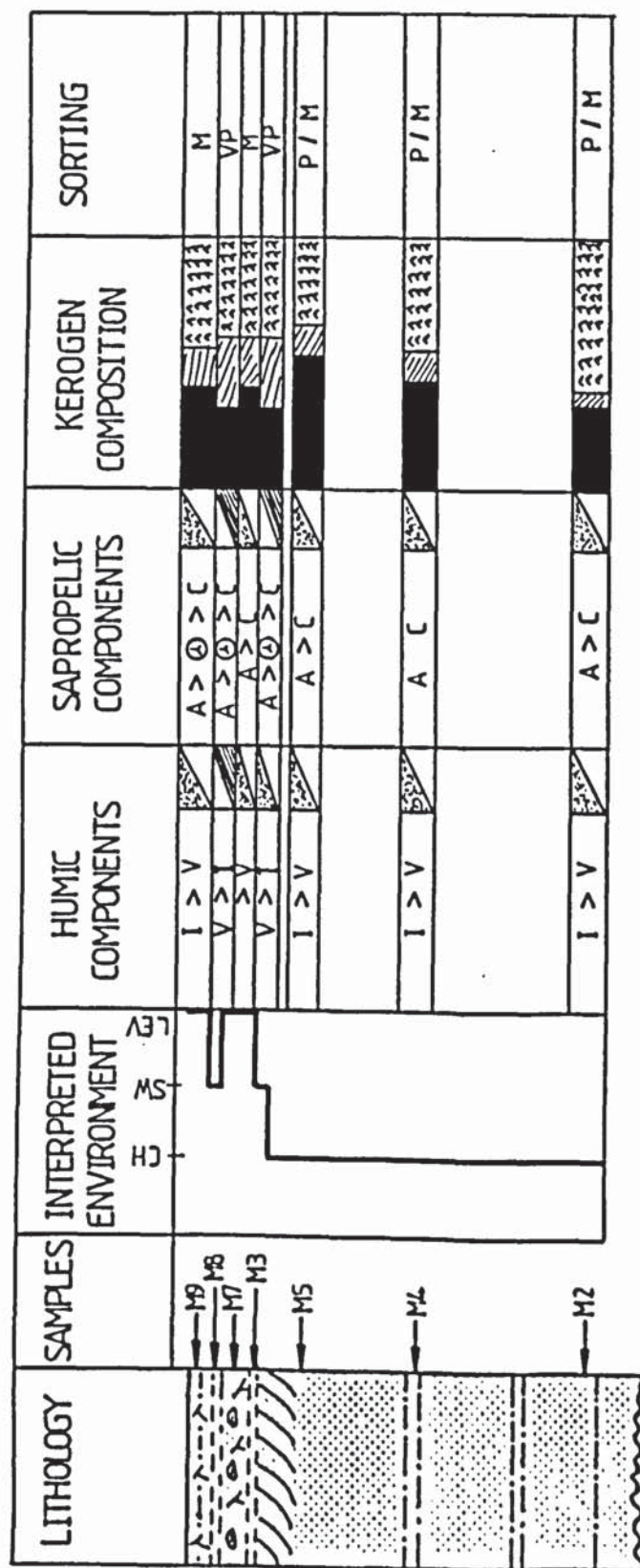


FIG.5.5. Palynofacies analysis of the Namurlan delta top sequences (Minera old quarry), North Wales. For legend see fig 5.4.

Vertical Scale: 1cm = 2m

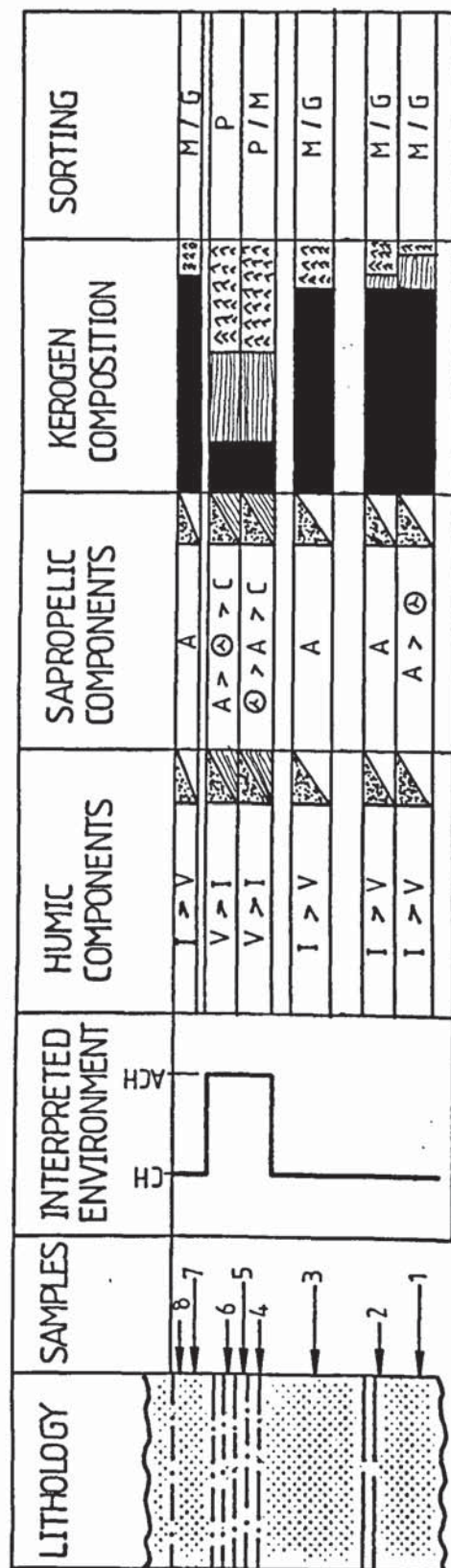
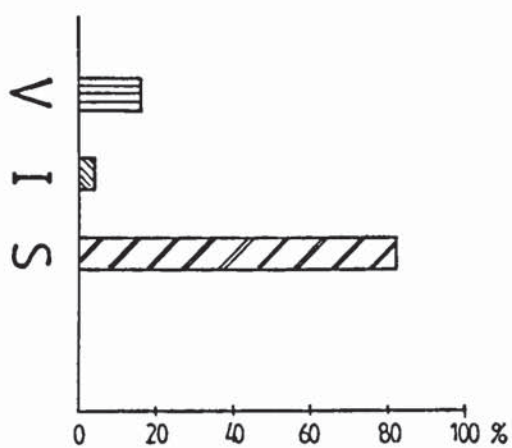
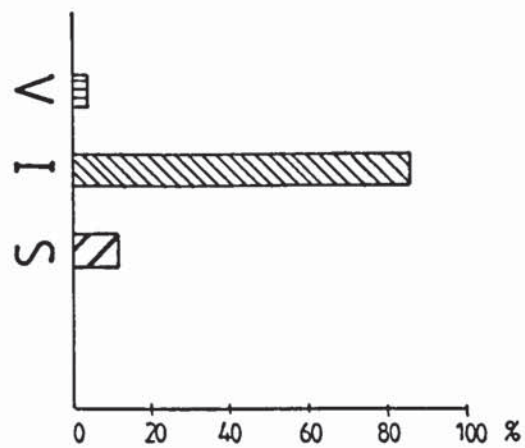


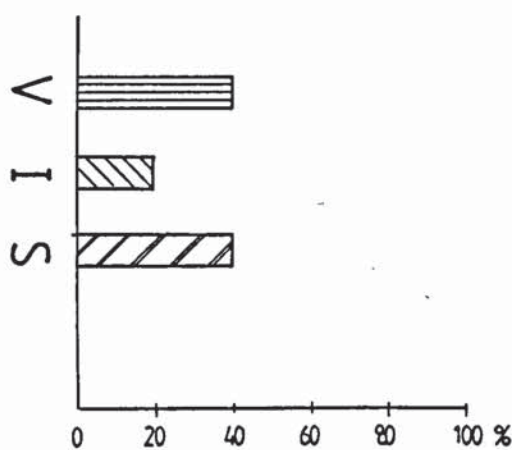
FIG.5.6. Palynofacies analysis of the Namurian delta top sequences (Ruabon Mountain), North Wales. For legend see fig 5.4. Vertical Scale : 1cm = 2m.



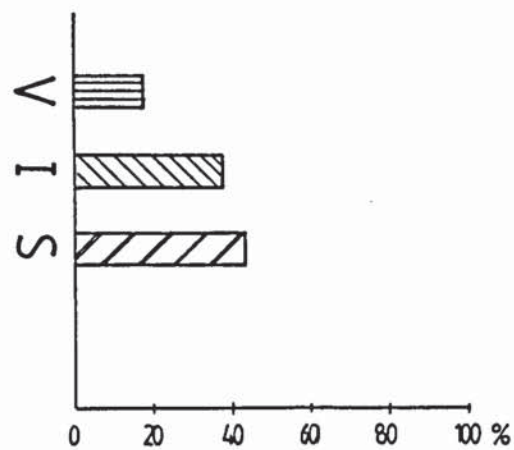
A. Interdistributary bay shale.



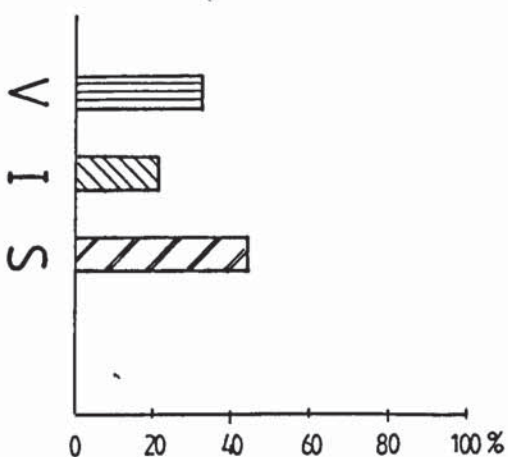
B. Distributary channel sandstone.



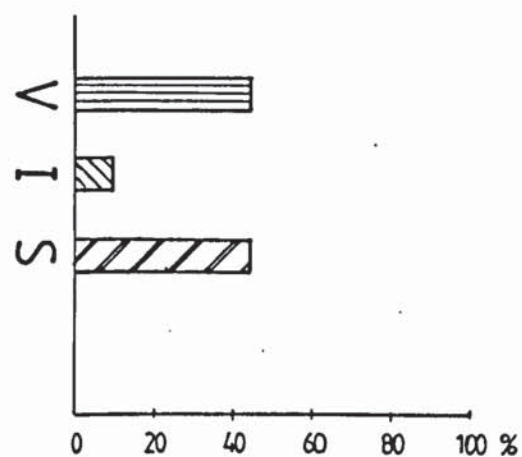
C. Abandoned channel sandstone.



D. Natural levee sandstone.



E. Swamp shale.



F. Coal associations.

Fig.5.7. Mean Kerogen distribution in the Namurian delta top palynofacies North Wales

V = Vitrinite , I = Inertinite , S = Sapropel.



Illustration removed for copyright restrictions

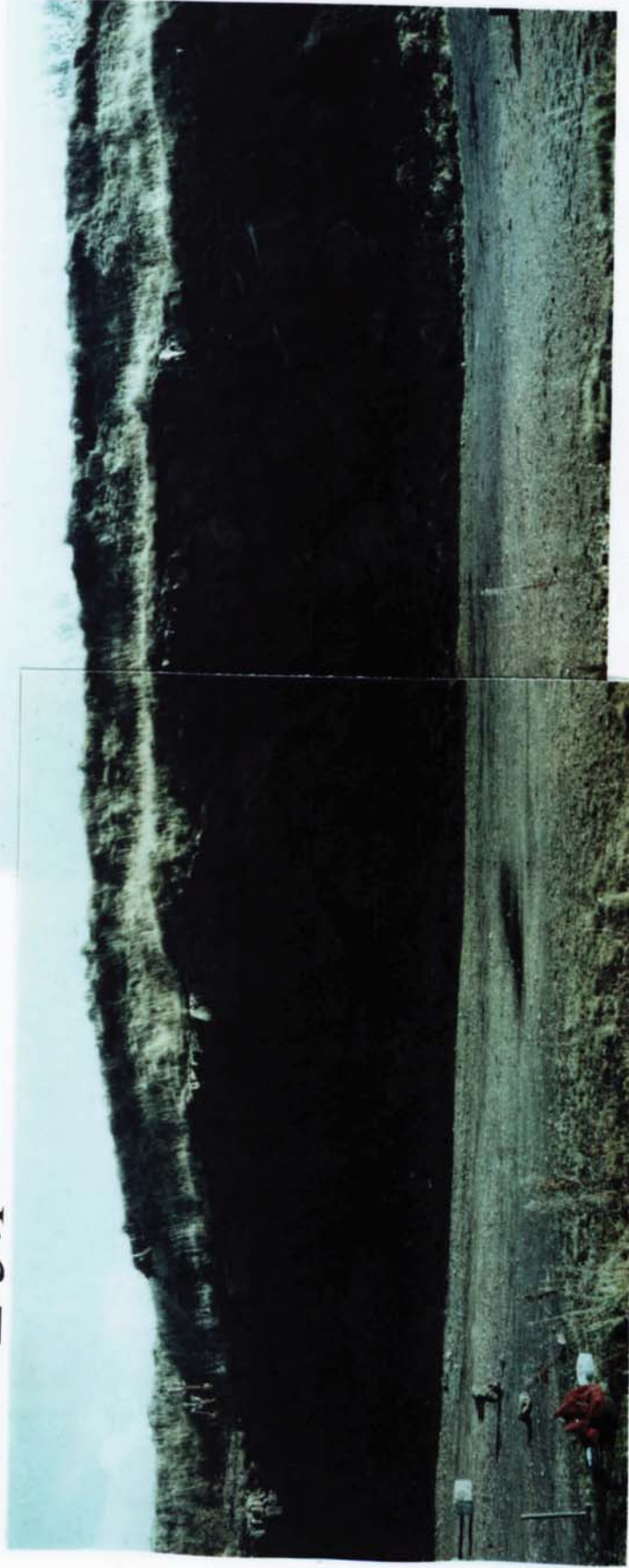
Fig. 5.3. The sedimentation of organic material in a dynamic system is controlled by the energy level maintained in the system. After Fisher (1980).



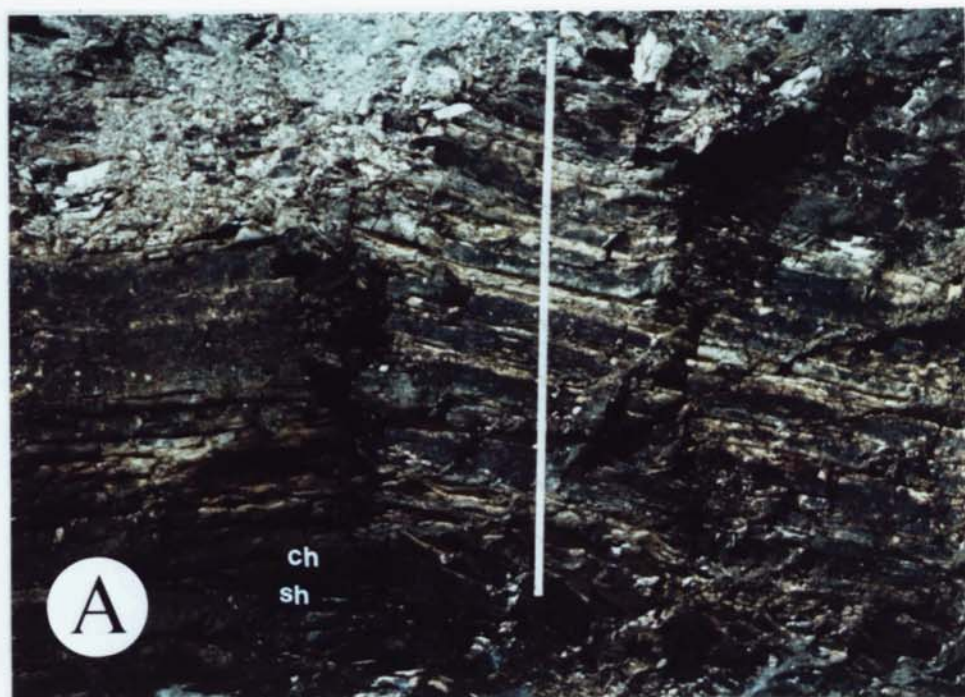
Illustration removed for copyright restrictions

Table 5.1 Palynofacies characteristics of the main delta top sub-environments (after Denison and Fowler, 1980).

PLATE 5.1



- A. Large scale lateral accretion unit in a sandstone body with channels marked by scoured bases. Note also the divergence between the inclined foreset bedding and the overlying horizontal topset beds. The beds to the left of the lateral accretion unit are massive.
Bwlchgwyn Quarry.



A. Alternating cherty flags (ch) and shales (sh), exposed in an old quarry at SJ 22386517. View facing N130. This unit is a part of the interdistributary bay shale facies.



B. The Maes-y-Dronell sand quarry SJ 21805655 viewed from Mynydd-Du, facing N160.

PLATE 5.2

PLATE 5.3

A. Sedimentary organic matter .

V = vitrinite (collinite); I = inertinite (macrinite); i = inertinite (semi-fusinite); and e = exinite (sporinite).

Scale:- 2 cm = 1 μ m. Polished block

Chwarelau Coal, Australia, Marlpit, North Wales.

B. Same features as shown above

Scale:- 2 cm = 1 μ m. Polished block

Aqueduct Coal, Australia, Marlpit, North Wales.

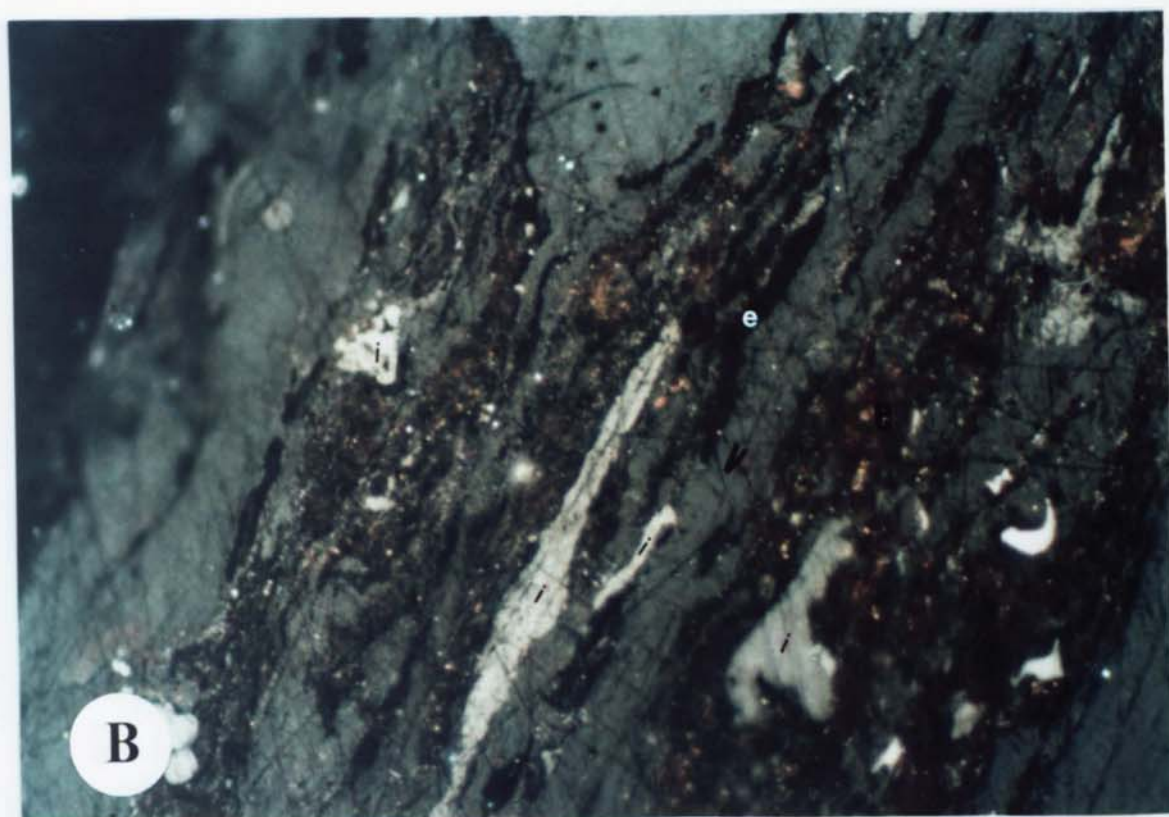
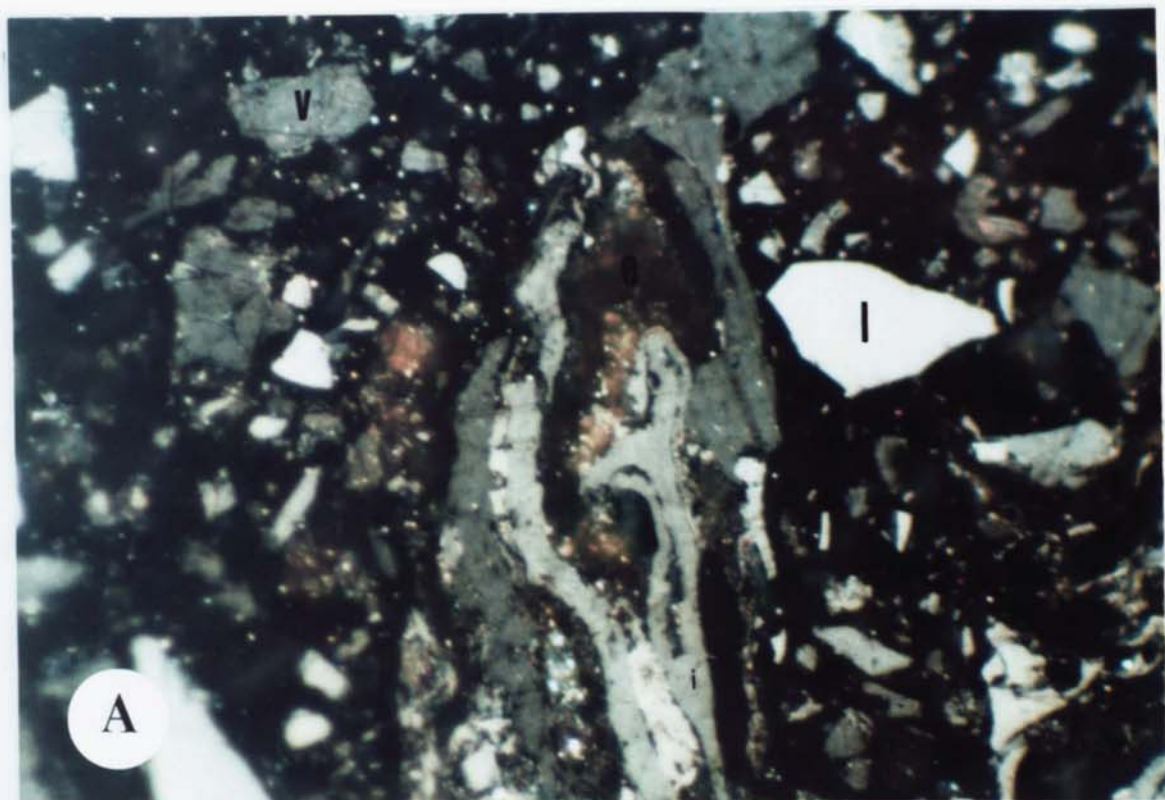


PLATE 5.3

PLATE 5.4

- A-B. Swamp shale palynofacies with lath shaped inertinitic (i) debris. Note also numerous fine grained, angular and occasionally rather gnarled vitrinitic debris (x) and greenish-yellow algal debris (a).
- C-D. Interdistributary bay shale palynofacies with angular pieces of fine grained vitrinitic debris (x). Note the effect of biodegradation (b) in an inertinitic debris at Fig. D, resulting as partial corrosion of the fine structures.
- E. Distributary channel palynofacies with rare presence of cuticle suggesting a lower energy regime within a higher energy environment.
- F. Abandoned channel palynofacies with woody tissue in the centre and scattered common vitrinite debris. Note the sign of physical degradation in the woody tissue.
- G. Natural levee palynofacies with abundant fine inertinitic and vitrinitic debris and "bleached" spore in the centre.
- H. Interdistributary bay shale palynofacies with dark-brown algal matter (thalloid algal matter), suggesting a possible marine water incursion within the facies. For explanation see text. Note the effects of physical degradation and biodegradation.

Width of field of photograph - 2.7 mm.

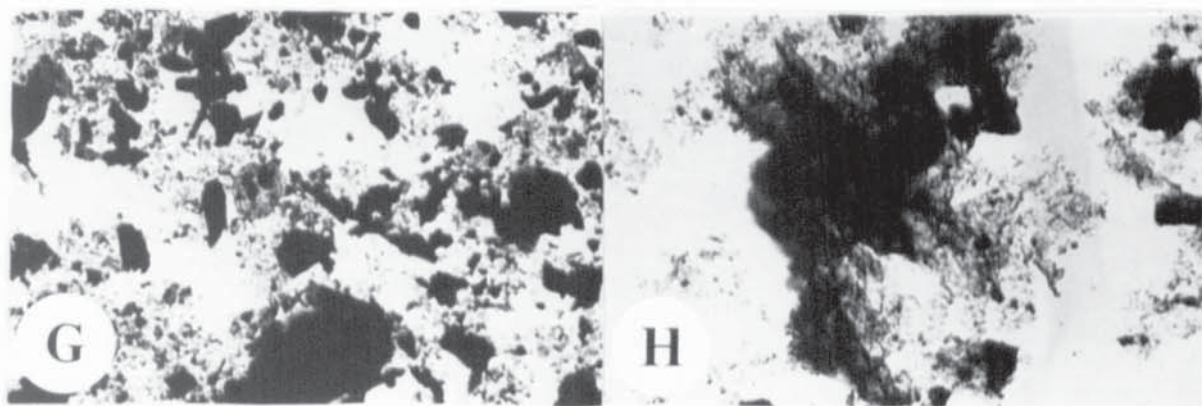
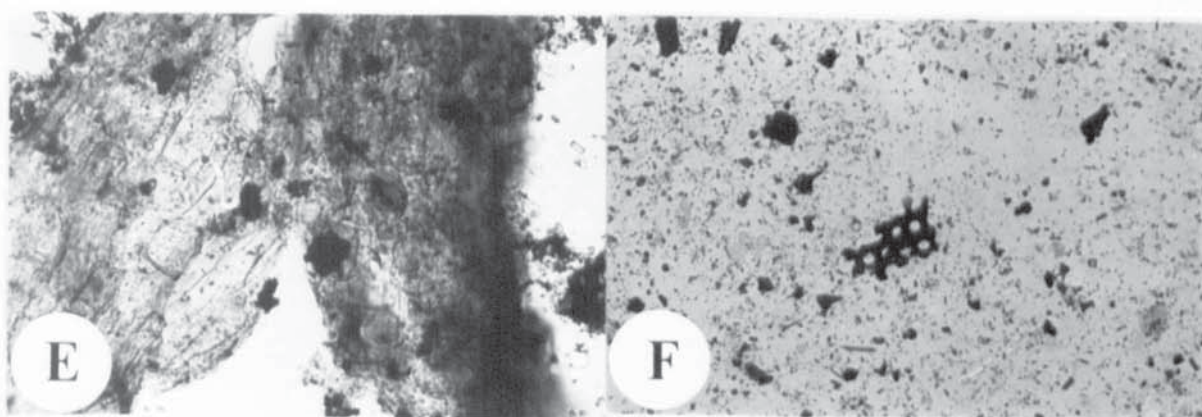
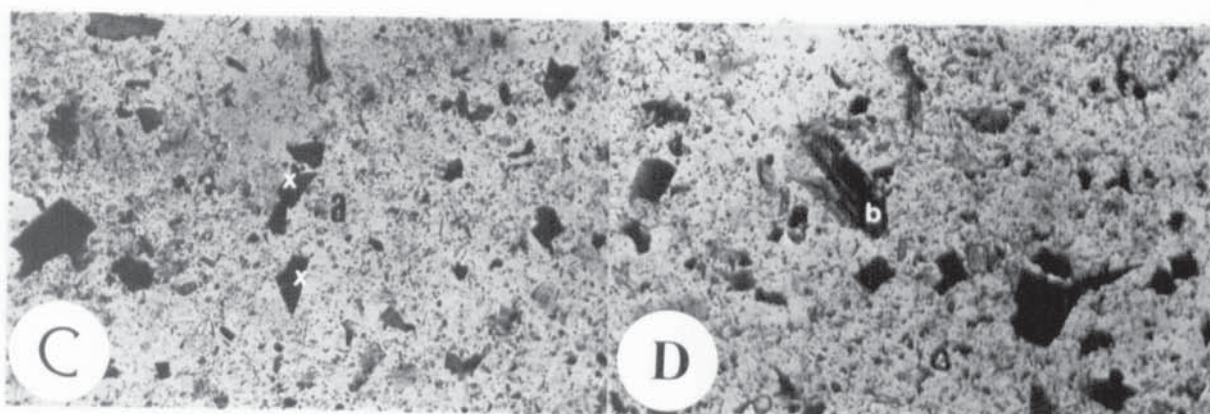
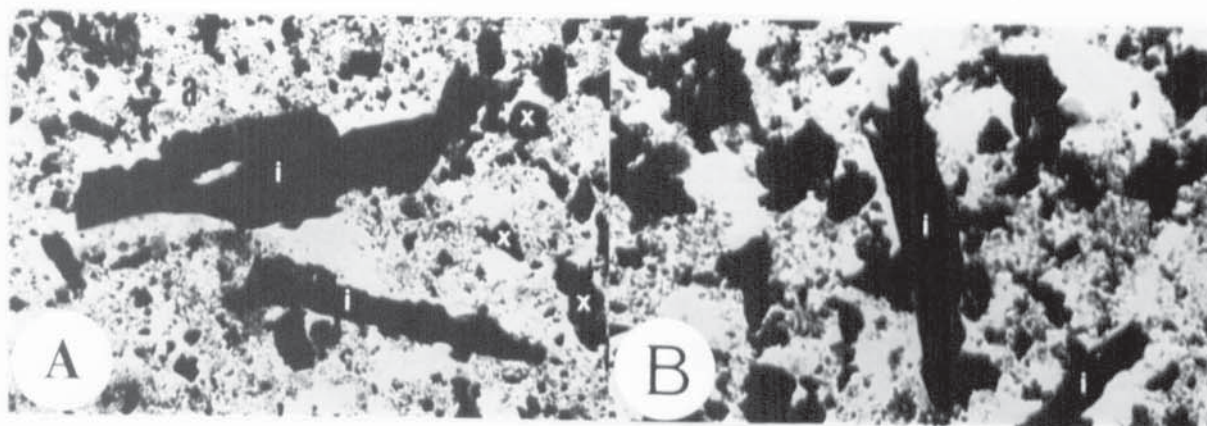


PLATE 5.4

CHAPTER 6
GEOCHEMISTRY OF THE GRONANT CHERT AND
THE LLANARMON-YN-IAL CHERTY FLAGS UNITS

6.1 INTRODUCTION

This chapter describes the geochemistry of the Gronant Chert and the Llanarmon-yn-ial Cherty Flags. The location of the sample analyzed is shown in Fig. 1.1. Analysis was mainly by X-ray fluorescence (XRF) and X-ray diffraction (XRD), samples being analyzed for both major and trace elements. Organic carbon was determined based by the ignition loss method as described by Dean (1974). The methodologies involved are given in Appendices 6 and 8. The results were statistically analyzed in order to ascertain the following:

- i) relationship of some selected major elements against Al₂O₃.
- ii) comparison of Al/Fe ratio of chert and shale interbeds.
- iii) interpretation of dendrograms (cluster analysis).
- and iv) to infer the rate and mechanism of sedimentation.

6.2 SELECTED MAJOR AND TRACE ELEMENT GEOCHEMISTRY

Dendrograms were constructed using parts per million values of each element. R-mode correlation matrices were made for all element pairs within the Gronant chert and the Llanarmon-yn-ial cherty flags (Tables A13.1 and A14.1). There are variations in significantly correlated elements between individual locations, but meaningful trends also become apparent.

Many elements in cherts and shale interbeds are related to major mineral components. The carbonate component of the Gronant chert is distinguished not only by high CaO and MgO contents, but also by high values of Mn and Sr. These elements are displaced when the carbonate is replaced by silica. On the contrary, Llanarmon-yn-ial cherty flags are

Component	Gronant chert	Cherty flags	Shale interbeds
SiO ₂ (%)	77.6	90.42	86.12
Al ₂ O ₃	3.09	6.11	8.48
TiO ₂	0.15	0.34	0.63
Fe ₂ O ₃	0.68	1.01	0.73
MgO	1.02	0.51	0.72
CaO	8.97	0.07	0.17
Na ₂ O	0.17	0.22	0.20
K ₂ O	0.64	1.41	2.16
P ₂ O ₅	0.15	0.07	0.06
Mn (ppm)	141 (106)	0.001	0.001
Cu	12 (20)	12 (7)	19 (21)
Ni	25 (24)	5 (1)	13 (19)
Zn	15 (6)	15 (4)	15 (5)
Zr	26 (22)	103 (17)	250 (154)
Y	26 (26)	20 (6)	23 (12)
Nb	7 (6)	7 (0.33)	15 (5)
Rb	16 (17)	49 (4)	72 (42)
Sr	363 (801)	57 (4)	62 (31)
Ba	135 (276)	101 (4)	146 (79)
No. of Samples	10	5	7

Table: 6.1 Average compositions and standard deviations* for major rock types.

* standard deviations are for trace elements only.

characterized by high Si, K and Al (Table 6.1). Generally speaking, shale interbeds (which are highly siliceous) are particularly richer in trace elements than are cherty flags, suggesting that most trace elements are rejected during the transformation from highly siliceous shale to cherty flags.

In addition, shale interbeds also contain more Al, K and Ca. Not surprisingly cherty flags are richer in Si content than the shale interbeds. However, Mn is almost totally depleted from the cherty flags and shale interbeds but is present in the Gronant chert. Chemical data supports the genesis of the Gronant chert by silica replacement of carbonates. Moreover, the general enrichment of trace elements in the Gronant chert together with high values of Ca; Sr; Mn; Ba, strongly suggest a silicified limestone origin.

6.2.1 Silica

The silica content of the cherty flags and shale interbeds ranges from 89 to 91% and 71 to 92%, averaging 90% and 86% respectively, while that of the Gronant chert falls mostly within the 26 to 93% range, averaging about 77.6% (see Table 6.1).

6.2.2 Titanium

Titanium is generally associated with terrigenous and volcanogenic components. It has an average value of 0.34% and 0.63% in the cherty flags and shale interbeds and about 0.15% in the Gronant chert (Table 6.1). The apparently higher percentages of TiO_2 in the cherty flags and shale interbeds than the Gronant chert are probably due to the presence of anatase in them. However, the average $\text{TiO}_2/\text{Al}_2\text{O}_3$ ratios of cherty flags and shale interbeds are 0.057 and 0.075 and that of the Gronant chert is 0.042, and all of them can be represented by the same regression line (Fig. 6.1), suggesting that the cherts formed by addition of biogenic silica to terrigenous clay (Matsumoto and Lijima, 1984). Forty six modern off-shore muds have an average $\text{TiO}_2/\text{Al}_2\text{O}_3$ ratio of 0.045 (Matsumoto and Lijima, 1984), the value of which is very close to the Gronant chert from North Wales.

6.2.3 Relationship between the ratio $\text{Si}/(\text{Si}+\text{Al}+\text{Fe})$

The ratio $\text{Si}/(\text{Si}+\text{Al}+\text{Fe})$ of the Gronant chert and the Llanarmon-yn-ial cherty flags has been computed from the results of chemical analysis. The chemical results are converted into ppm. following which the equation of regression lines between Fe and Al and coefficients of determination are computed (Table 6.2). Regression lines have been drawn on (Fig. 6.2).

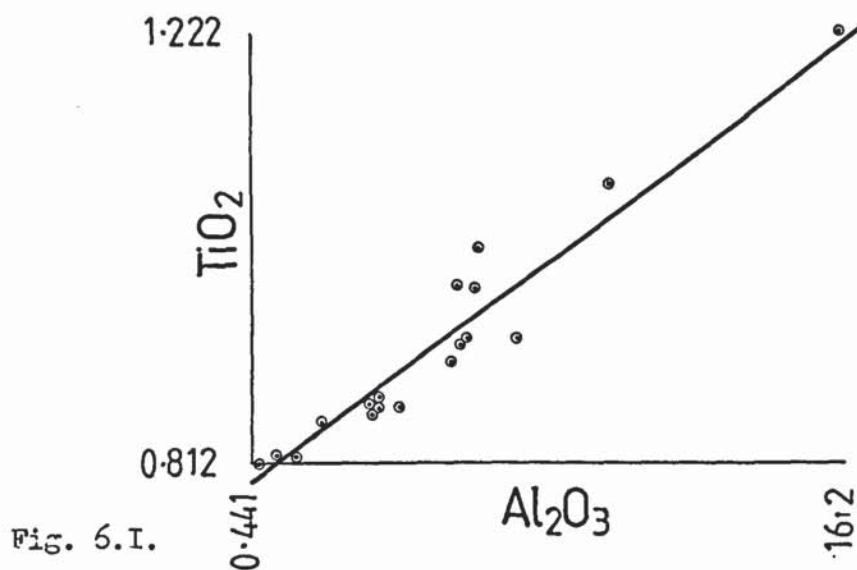
Location	N	Si/(Si+Al+Fe)	Correlation Fe - Al		
			r	y = ax+b	
				a	b
Gronant chert	9	0.95	0.58	0.15	+3060
Cherty flags	5	1.09	0.99	1.02	-52020
Shale interbed	6	1.13	0.92	0.08	+1190

Table: 6.2 Ratios Si/(Si+Al+Fe) and correlation between Fe and Al in samples from the Gronant chert and the cherty flags and shale interbed.

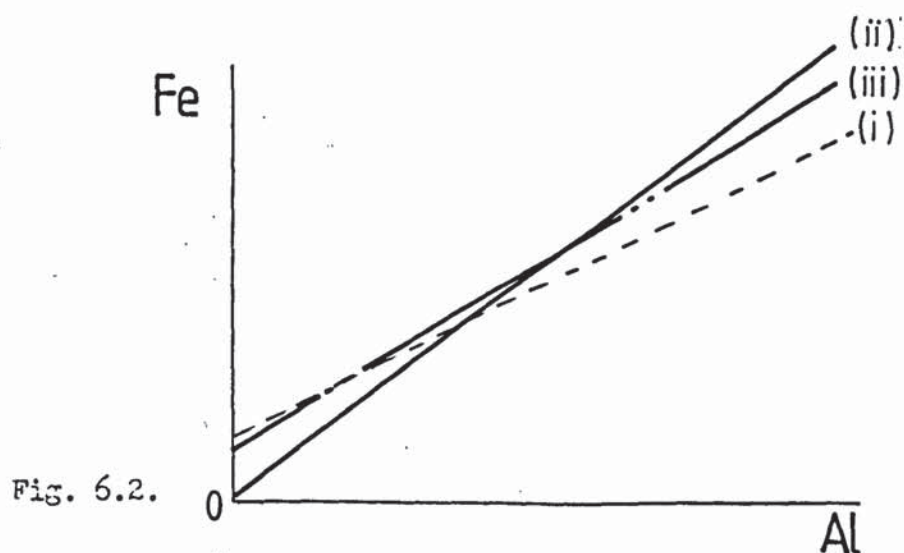
N: Number of samples analyzed; r- correlation matrix; y= ax+b: regression line equation where a= slope of lines drawn on Fig. 6.2 and b expressed in ppm.

The value of Si/(Si+Al+Fe) corresponding to samples of the Gronant chert is lower than that of the cherty flags and shale interbed. Moreover, the slope of the regression line Fe-Al (Fig. 6.2, parameter a in Table 6.2) for the Gronant chert although lower than that of the cherty flags, is somewhat closer to that for the shale interbeds. It has been noted previously by several authors that within a given basin the value of Si/(Si+Al+Fe) and the slope of the regression line Fe - Al increases with distance from detrital sources (Steinberg and Mpodozis, 1978; Rangin *et al.* 1981; Steinberg *et al.* 1984). Thus, according to the above authors with increasing distance from detrital sources, the ratio Fe/Al should increase and when these elements are correlated, the regression line slope increases.

However, in the present Carboniferous sediments, aluminium and iron (and manganese) may be considered as typically of detrital origin. Therefore, present results suggest that the Gronant chert section was probably



Relation between the contents of TiO_2 & Al_2O_3 in the Llanarmon-yn-ali cherty flags, shale interbeds and the Gronant chert.



- (i) Gronant Chert, $Y = 0.306 + 0.148(X)$
(ii) Cherty Flag, $Y = -5.202 + 1.016(X)$
(iii) Shale Interbed, $Y = 0.194 + 0.067(X)$

Regression lines between Fe and Al.

situated closer to detrital sources than the cherty flags and perhaps the shale interbeds.

6.2.4 Variations of SiO₂ and Al/Fe ratio

Variations of SiO₂ and the ratio of Al/Fe from the Gronant chert and the Llanarmon-yn-ial cherty flags have ^{been} studied in detail during the present investigation.

It should be mentioned here that the cherty flags and shale interbeds are almost devoid of carbonates (Table 6.1), while the Gronant cherts are not.

Eleven samples from the cherty flags and shale interbeds have been analyzed and their silica contents and values of the Al/Fe ratio reported on Fig. 6.3. The following conclusions can be drawn: (i) surprisingly, the silica content of the shale interbeds is almost similar to the cherty flags (apart from two exceptions in the lower most section); (ii) cherty flags are generally richer in Fe than shale interbeds; (iii) shale interbeds are generally richer in Al than adjacent cherty flags; (iv) fluctuations of SiO₂ and Al/Fe values are more or less systematically related in the cherty flags (with the exception of one sample in the lower most section). When the cherty flags composition remains more or less constant the corresponding Al/Fe ratio also remains constant. On the otherhand, the main modification concerns shale interbeds in which the Al/Fe ratio becomes very different (3.7 to 10.7) and shows no relationship with the corresponding slight silica variations; and finally, (v) Al/Fe ratios of shale interbeds vary widely from the adjacent cherty flags.

Similarly ten samples from the Gronant chert have been analyzed and their silica contents and values of the Al/Fe ratio given on Fig. 6.4. One may note that: (i) In the lower part of the section two samples are enriched in carbonate content corresponding to a decrease in silica content (e.g.

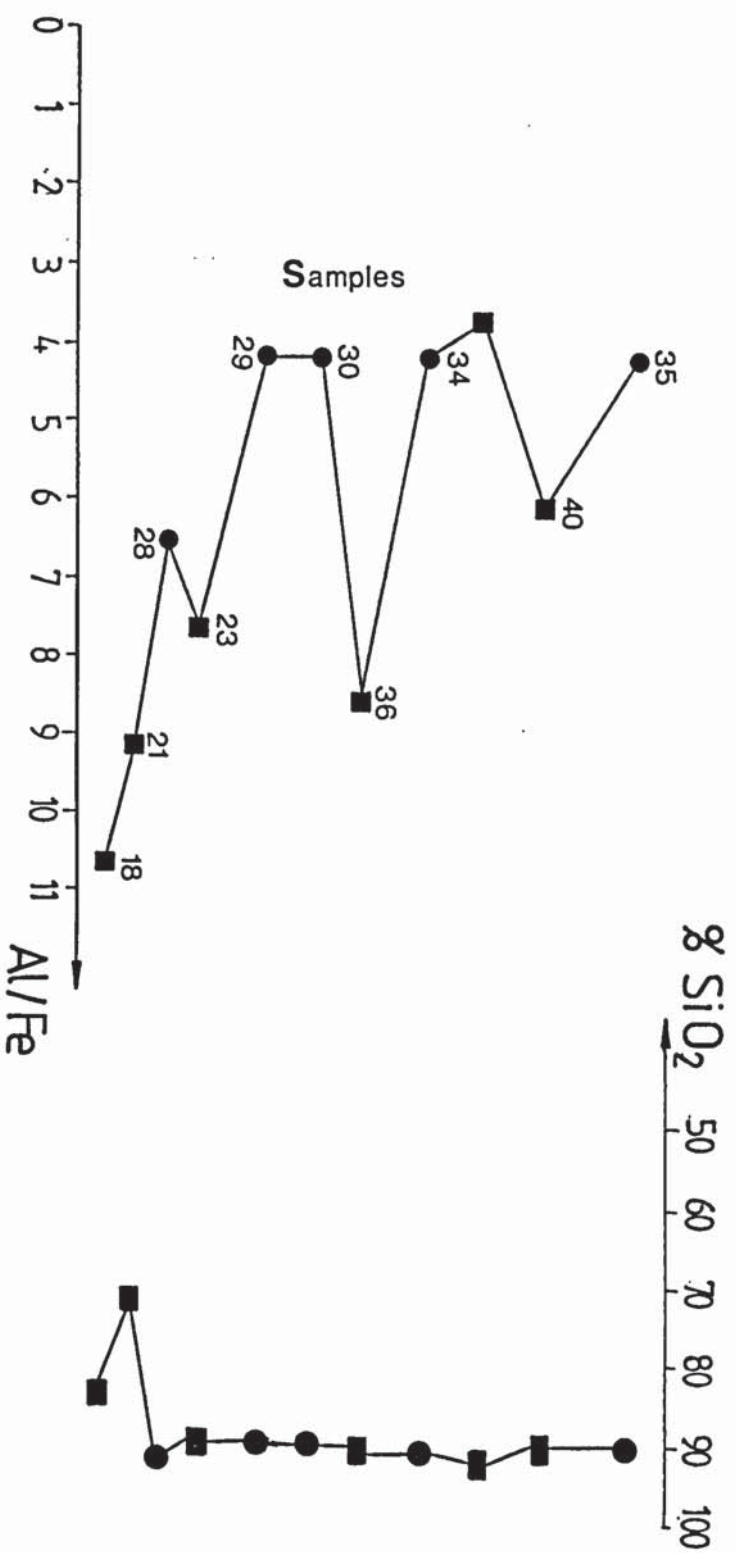


FIG.6.3

Variations of SiO₂ and Al/Fe from the Llanarmon-yn-ial cherty flags and shale interbeds.
 Cherty flags = circles; Shale interbeds = filled squares. Vertical Scale: 1cm = 2m.
 Location S. J. 2238 5617.

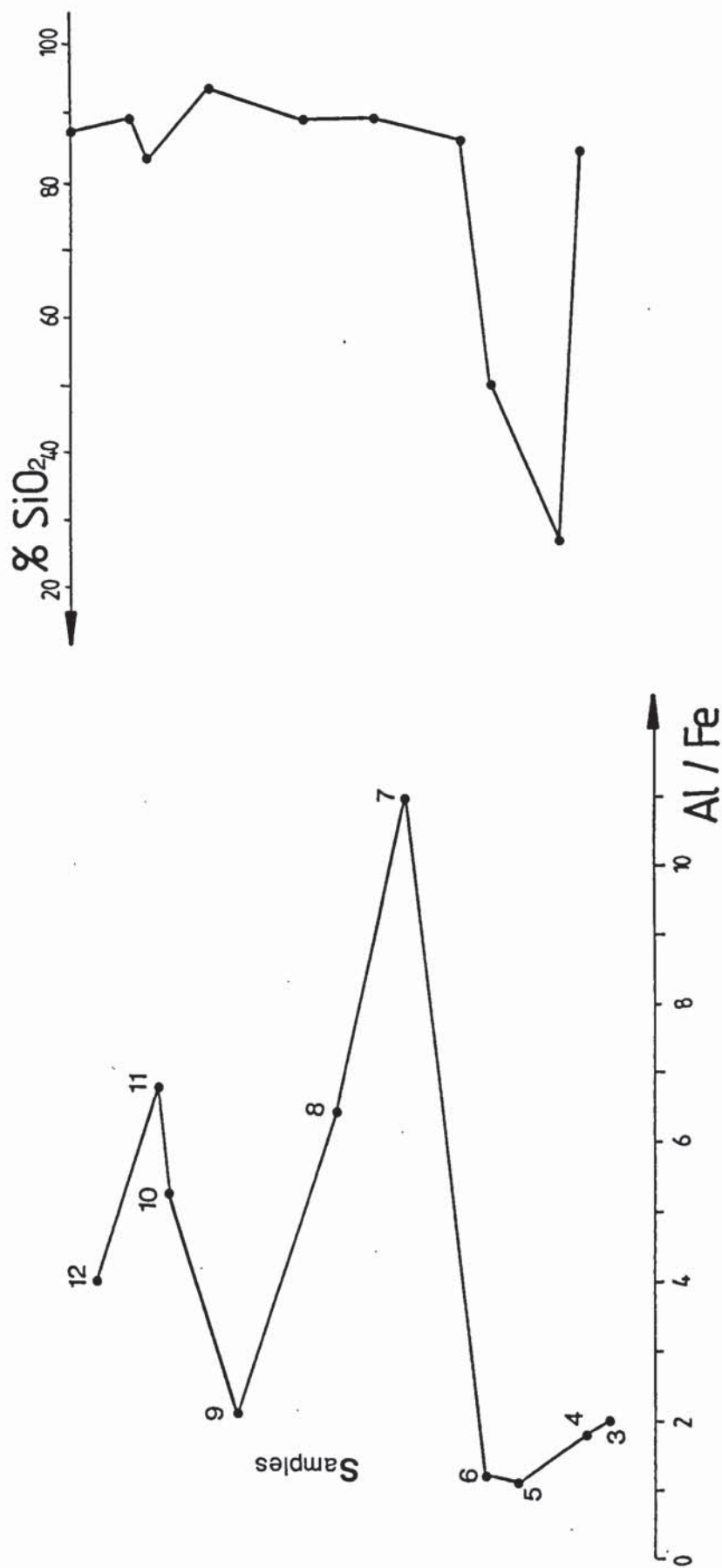


FIG.6.4. Variations of SiO₂ and Al / Fe from the Gronant chert (S. J. 094827)
chert beds = circles. Vertical Scale :- 1cm = 3m.

36.93 and 18.75 wt.% CaO; 0.61 and 5.69 wt.% MgO; Appendix 11); (ii) In the upper part of the section silica fluctuations weaken; (iii) fluctuations of Al/Fe values are wide in the middle than ⁱⁿ the upper and lower part of the section and their relation with minor silica variations is not clear. However, Fe generally increases when Si decreases especially in the lower part of the section; and finally, (iv) the composition of chert beds can fluctuate moderately (Gronant chert) or can be relatively constant (cherty flags).

From the foregoing, particularly from the Fig. 6.4 and section 6.2, it can be concluded convincingly that the Gronant chert is essentially a silicified limestone and that the silica is diagenetic in origin.

6.2.5 Manganese

The manganese content of the Gronant chert ranges from 0.001 to 300 ppm, averaging 141 ppm (Table 6.1). On the other hand, Llanarmon-yn-ial cherty flags are highly depleted in their manganese content. This may be due to a lack of a long contact with sea water or a leaching process may be responsible. The negative correlation of Mn with CaO in the Llanarmon-yn-ial area may also favour a leaching process at the time of deposition where the Eh is reducing and the pH is acidic. Under these conditions Mn and Fe will be easily removed (Mn^{2+} and Fe^{2+} are the mobile valencies in the two elements). Such conditions were prevailing in different parts of the British Isles during early E times because of the widespread coal seam deposition. This is consistent with the age of these sediments (see Biostratigraphical Palynology Chapter 4). The leaching process could also take place by means of percolating water after consolidation, and even the effect of the present day weathering processes can not be ignored.

Manganese is probably linked with CaO and MgO in the Gronant chert (see Section 6.4).

Fig. 6.5 displays the correlation diagram between the MnO and Al₂O₃ contents in the Gronant chert. Lijima *et al.* (1985) noted that when chert and shale is formed from a simple mixture of silica attributed from siliceous skeletons and terrigenous clay, the chert and shale should have the same MnO/Al₂O₃ ratio and plot on the solid dilution curves of the diagram (Fig. 6.5) on which the MnO/Al₂O₃ ratio is analogous to the mean value of shales of the bedded chert. However, the Gronant chert samples tend to concentrate on and around dilution curve II in Fig. 6.5 (though a few of them have some tendency to deviate upwards from dilution curve II). This possibly means that precipitation of manganese from ancient sea water could take place in the Gronant chert as in the case of the Upper Palaeozoic and Lower Mesozoic cherts of Japan (Lijima *et al.*, 1985).

Matsumoto and Lijima (1984) and Lijima *et al.* (1985) defined the inversely proportional relationship between the sedimentation rate and the MnO/Al₂O₃ ratio of modern marine sediments, as shown in Fig. 6.6. According to them the MnO/Al₂O₃ ratio decreases as the sedimentation rate increases from radiolarian ooze and brown clay to off-shore mud through calcareous ooze. The above authors also applied this relationship to ancient chert-shale sequences ranging in age from the Upper Palaeozoic to Tertiary Bedded Chert.

During the present investigation this diagram (Fig. 6.6) is also used in order to ascertain as precisely as possible the rate of sedimentation of the Gronant chert. However, it is seen that the Gronant chert has an average MnO/Al₂O₃ ratio of 0.019, which corresponds to a sedimentation rate of 7.5 m/m.y. (0.075 cm/100 yrs.).



Aston University

Illustration removed for copyright restrictions

Fig. 6.5 Correlation diagram between the contents of MnO and Al_2O_3 in the Gronant Chert. Curves I and II represent the average mixing trend of pure biogenic chert with parting shale in the Setogawa and Inner Chichibu terrain of Japan (Lijima et.al. 1985). The fields of the modern pelagic clays and the metaliferous clays of the East Pacific Rise are also taken from Lijima et.al. 1985.



Illustration removed for copyright restrictions

Fig. 6.6.

The average rate of sedimentation of the Gronant chert is inferred from the average $\text{MnO} / \text{Al}_2\text{O}_3$ ratio. The original diagram is taken from Ligima *et. al.*, 1985.

Matsumoto and Lijima (1984) used this diagram keeping in mind that the chemical compositions of sea water in their 'Setogawa Terrain' and the 'Chichibu Geosyncline', were the same as that of normal sea water, and also the MnO content in bedded chert did not change during diagenesis.

6.3 ELEMENT (R-MODE) DENDROGRAMS FOR THE LLANARMON-YN-IAL CHERTY FLAGS

Because of the large number of variables calculated in the chemical analysis of the whole number samples, an attempt has been made to reduce this large number into a few groups. These groups could facilitate the understanding of the behaviour of the associated elements. This was done using R-mode cluster analysis with the pair group method and arithmetic averages (Davies, 1973). The computer programme used for the analysis is included in Appendix 17.

From the Llanarmon-yn-ial cherty flags dendrograms (Fig. 6.7) it appears that the elements have been clustered into two groups indicating a change in the source material itself rather than only a change in the weathering type (Parker, 1974). On the right hand side Sr, Pb, Ca and Ba cluster together, but it also includes Corg, Th and S. Clemmey (1976) has used the strontium content to show the degree of marine influence in the orebody member of Kitwe, in Precambrian rocks of the Zambian Copperbelt. Sweeney (1985) proposed to use the high positive correlation between Sr and Mn as marine water influx indicator in the Permian Marl Slate. In the present case Sr is clearly calcite associated because of the highly significant correlation with CaO ($r = 0.99$ at the 99.9% level).

Moreover, the positive linkage of Sr with Pb ($r = 0.99$ at 99.9% level); Ba ($r = 0.74$ at 80% and 90% level); Corg ($r = 0.51$); Th ($r = 0.77$ at 80% and 90% level) and S ($r = 0.55$) indicates that these elements may be incorporated with a possible marine phase. On the contrary, Al, Rb and K are opposed

by Sr suggesting that Sr may not be linked with the clay mineral fraction (i.e. Sr does not follow clay minerals in its distribution). The association of Sr with Ba might also indicate a partial or total replacement of Ba in the extremely rare BaSO₄ traces in these sediments. The incorporation of Corg in the above mentioned possible marine phase may suggest a marine origin for them, but apparently the poorer concentration of trace elements in the Corg ruled out such a possibility. Tourtelot (1964) noted that sorption (because of long duration in the sea) was the reason for the enrichment of Corg in the trace elements. Sulaiman (1972) postulated that basinal Corg are of marine origin. Calvert (1976) argued that in anoxic marine black muds, deposited in near shore environment should be enriched in Pb, Cu, Zn, Ni and U. The present Corg correlates only with Pb among the above mentioned trace metals indicating an apparent poorer enrichment of trace metals. The positive correlation between S and Corg might suggest that while the Corg was deposited the environment was a reducing environment and syngenetic/diagenetic sulphides may be deposited. The positive correlation of Th with S and a very weak positive correlation of Th with Corg is not clearly understood. May be sorption onto the organic matter or precipitation by reducing conditions was responsible for this. Th does not correlate with the resistates or Al, suggesting that it is not associated with the clay minerals.

The left hand side of the dendrograms are comprised of Zn, Y, Cu, Fe, Ni, Zr, K, P, Al, Rb, Mg, Ti, Nb, U and Na. This association particularly the aluminosilicates represents a terrigenous and volcanogenic source for the sediments (Matsumoto and Lijima, 1984).

Al in this group is derived from the clay minerals: Kaolinite and illite, while K, Rb and Na are probably from illites. Ti, Zr, Y, Fe and Nb are all positively correlated and are amongst the elements most favourable for

the formation of resistates, thus denoting their detrital origin. Some Y may also be derived from Kaolinite (Sulaiman, 1972).

Uranium exhibits a positive correlation with P and Y, while all these elements show a negative correlation with Corg. A very high sedimentation rate may be assumed because of the opposing of Corg by them. The correlation of P with U could indicate a chemical precipitation of U in a ?Uranium-phosphate complex, while a negative correlation of P with Ca and CO₂ ruled out the presence of the carbonate-apatite in these sediments.

Goldschmidt (1954) and Mohr (1959) argued that Ni is usually left behind in the hydrolyzates after weathering. The same authors mentioned that Ni is stable in aqueous solutions, and thus it can migrate for a long distance, contrary to Fe, Mn and other elements, which precipitate readily. On the other hand, zinc goes into solution-acid solutions easily. Amongst the major elements which control the distribution of Ni and Zn are: Fe, Mg, Mn and S. Corg is also responsible to some extent. It is seen that Zn has a good correlation with Fe and Mg ($r = 0.99$ and 0.96 at the 99% and 99.9% level) while Ni correlates at 0.78 and 0.65 with the same elements at almost 80% and 99.9% level. On the contrary both Ni and Zn strongly oppose Corg and S. Thus the following two factors could play an important role in the distribution of Ni and Zn: Adsorption of Fe, Mg compound and replacing of Fe or/Mg in the clay minerals.

From the dendrograms it can be seen that Al and Fe show a clear linear relationship with Cu. Cu correlates with Fe and Al as high as 0.99 at the 99.9% level. This clearly means that Kaolinite and Fe-hydroxides have important role in the accumulation of Cu. The role of Corg and S is not clear in the distribution of Cu as both of them opposed by Cu. So, it is

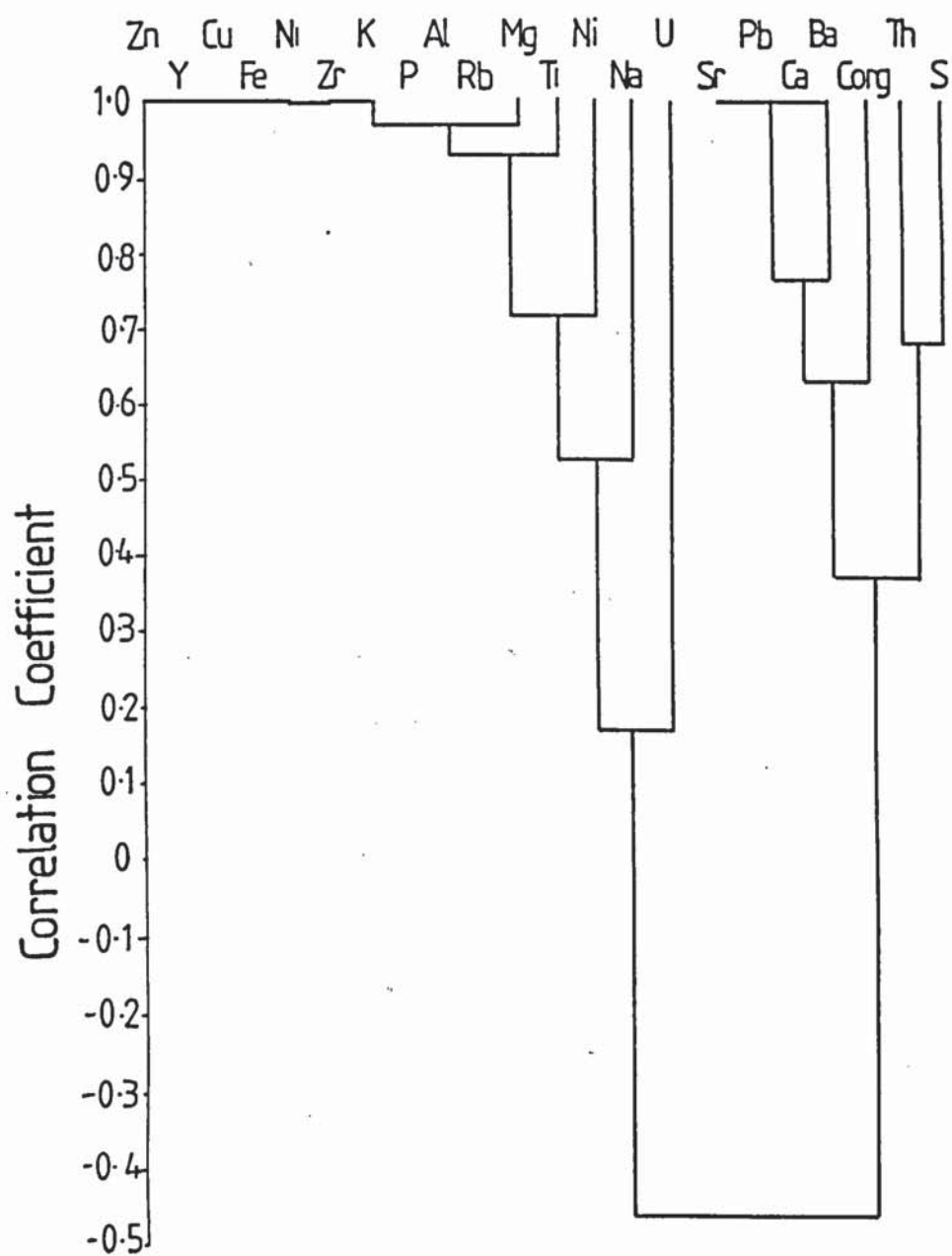


Fig. 6.7. Element (R-mode) Dendrogram for samples from the Llanarmon-yn-ial cherty-flags and shale interbeds.

obvious that Corg and S virtually has no role in the accumulation of Ni, Zn, and Cu in the Llanarmon-yn-ial area.

6.4 ELEMENT (R-MODE) DENDROGRAMS FOR THE GRONANT CHERT

Element dendrograms (Fig. 6.8) have also been produced from the samples obtained from the Gronant chert. In this case no significant separation of the elements into groups is noticed. Moreover, the relatively random distribution of the detrital trace elements (e.g. Zr, Ti, Y, Ni etc.) would tend to support the hypothesis of a change in the weathering type rather than in the source material itself (Parker, 1974).

In this instance once again Sr is showing a very good association with Ca ($r = 0.89$ exceeding 99.9% level). This is possibly a genetic relationship and could be an indicator of marine water influx in the original sediments. The incorporation of Ba, U, and S with Sr and Ca suggests that these elements are associated with the carbonate phase. In these sediments Ca is seen to occur as follows: (i) in carbonates as calcite and dolomite, (ii) in fossils (mainly shell fragments, crinoids and goniatites) and in (iii) in apatites. The strong positive correlation of U with Ca and Corg and a weak correlation with P suggests that U could be precipitated chemically with the carbonates, organics and sulphides or can be accumulated with the Corg. The strong positive linkage of S and Ca with Corg ($r = 0.71$ at the 95% and 99% limit and $r = 0.62$ at the 90% and 95% limit) indicates that Corg was deposited in a reducing alkali environment.

The remaining elements are grouped with Y, Zr, Ni, Rb, Ti, K and Al and possibly reflecting the detrital origin of these elements. On the other hand, excepting Nb, all the other resistates correlate positively with Corg suggesting that they may be adsorbed on Corg; similarly some of them (e.g. K, Al, Ti) may also be adsorbed by clay minerals (e.g. illite in the present case).

P shows a strong positive correlation with Fe ($r = 0.99$ at 99.9% limit) and Mg ($r = 0.97$ at 99% and 99.9% limit). Presumably the P was derived by two processes: (i) its attitude during chemical weathering and transportation to the sedimentation sites as well as weathering after deposition; and (ii) its precipitation. P, Mn and Fe may behave in a similar way during transportation (Strakhov, 1967). This probably indicates that P as PO_4^{3-} was brought to the basin in solution or as a suspension with the colloids of Mn and Fe or could also be in the form of adsorption on either these colloids or on the clays (Sulaiman, 1972). In the present case P is most likely to be incorporated either in the illite clay (as it correlates with K, $r = 0.98$ at the 99% and 99.9% level; and with Al, $r = 0.99$ at 99.9% level) or with the resistates. All the resistates present in these sediments such as Ti, Zr, Y and Nb display strong positive correlation with P. P also shows good linear relationship with Corg with $r = 0.64$. This association may arise either by precipitation from solution of phosphate derived locally from phosphatic organic compounds or by diagenetic replacement of calcareous material associated with organic matter (Pearson, 1979).

Manganese shows a significant positive correlation with Fe and to a lesser extent with Ca and Mg. These correlations indicate a similar behaviour for Mn, Fe and Carbonates. This might mean that these components were in the same condition at the time of transportation to the Visean-Namurian sea (i.e. partly in real solution as HCO_3^- of Mn, Fe, Ca and Mg and partly in the colloidal state as OH^- of these elements; Strakhov, 1967). Mn and Fe also might have been dissolved by percolating acid solution to form carbonates. According to Maynard (1983) at low Eh, Mn is largely controlled by carbonates, in contrast to Fe, which is controlled more by the sulphides.

Very strong positive correlation between Fe and Corg ($r = 0.97$ exceeding 99.9% level) is particularly important as it is indicating that Fe has



Element (R-mode) dendrogram for samples from the Gronant chert.

definitely been adsorbed by Corg. Fe also shows a good correlation with S ($r=0.78$ at the 99% and 99.9% level). It is generally noticed that whenever there is relatively high sulphur or high CO_2 in a sample, there is also high Fe_2O_3 in the chemical analysis. This observation is consistent with the presence of pyrite (Pl. 8.8D) and/or marcasite (Pl. 8.3D) in these samples.

The positive correlation ($r=0.59$) between Pb and S indicate that at least a portion of the Pb may be associated with the sulphide phase.

Generally speaking, sulphur increases towards north (i.e. towards Gronant and Prestatyn as compared to Llanarmon-yn-ial) suggesting that pyrite (and also marcasite) increases in the same direction. In the Llanarmon-yn-ial area sulphur is in the range of 0.01 to 0.10 wt.% and in the Gronant area 0.01 to 0.71 wt.%.

6.5 CONCLUSIONS

The rhythmic layering of cherty flags-shale sequences in the Llanarmon-yn-ial area is very marked.

McBride and Folk (1979) and Lijima *et al.* (1985) proposed four general mechanisms for the rhythmicity in the bedded cherts. They are: (1) diagenetic segregation of silica from initially sub-homogenous siliceous mud; (2) episodes of rapid and slow production of radiolaria/sponges in surface waters during a constant rate of mud deposition; (3) episodes of current deposition of radiolaria/sponges silt during constant mud deposition; and (4) episodes of current deposition of mud during constant radiolaria/sponges sedimentation. However, the following is a very brief discussion of the above four mechanisms in connection with the present investigation.

The shale partings intercalated with the biogenic cherty flags might be interpreted to be the product of the selective dissolution of siliceous skeletons from a mixture of radiolaria/sponges and clay during diagenesis, the dissolved silica migrating and precipitating as silica cement to form chert beds. When diagenesis includes only silica migration, then chert and shale interbeds should differ slightly in their 'Si' content (Steinberg *et al.* 1984). This is in accord with the present geochemical findings (see Table 6.1 and Fig. 6.3).

Model (2) and Model (3) emphasize that the chert beds and shale interbeds should differ only by their silica content, thus, according to Table 6.1 and Fig. 6.3, inadequate to explain the present sediments.

Model (4) emphasizes that the chert and shale interbeds will differ compositionally. Moreover, this model considers radiolarian/spicules ooze as the background sediment, thus chert bed composition should be nearly constant, while shale interbeds could be either constant or fluctuating, depending largely on the supply of muds from the source areas. The cherty flags are characterised by a nearly constant composition of silica and Al/Fe ratio while, in the shale interbeds, particularly the Al/Fe ratio fluctuates widely (Fig. 6.3) and a minor variation of silica is concentrated mostly in the lower section. Thus this mechanism fits well with the Llanarmon-yn-ial cherty flags.

Therefore, from the above observation it can be concluded that the mechanisms of diagenesis and the episodes of current deposition of mud during constant radiolaria/sponge sedimentation are consistent with the Llanarmon-yn-ial cherty flags unit.

The present geochemical findings strongly suggest that the Gronant chert is essentially a silicified limestone and that the silica is diagenetic in origin.

Moreover, it also indicates slow rates of sedimentation (about 0.075 cm/100 yrs.) of this unit. However, the basic elements of a chertification model for the Gronant Chert are discussed more fully in Chapter 8.

CHAPTER 7

PETROLOGY

7.1 INTRODUCTION

Gronant cherts are generally black to dark grey, massive to well bedded cherts; beds being usually 5-10 cm. thick. Chert beds usually show fine laminations and rarely wave ripples of argillaceous materials. Occasionally organic materials are aligned in fairly continuous laminae set in a micritic matrix. The rocks are poorly bioclastic containing mainly fragmented ooids, calci-spheres, broken crinoid fragments and rarely fragments of fenestrate bryozoan.

Llanarmon-yn-ial cherty flags are characterised by creamy-white porcellanous quartzitic silts with alternating thin shale beds which are highly siliceous and pass into pure chert. The cherty flags are stained in a variety of reds, oranges and browns, by iron oxyhydroxides.

Quartz, chalcedony and lutecite are the principal types of silica encountered in both the Gronant chert and the Llanarmon-yn-ial cherty flags. Sosman (1927) defined chalcedony as optically microfibrinous, occurring as colloform bands or spherulites, with concentric or parallel bands of brown or yellow colouration under transmitted light. Later, several other workers such as Folk and Weaver (1952) and Deer *et al.* (1963), suggested that chalcedony is essentially composed of minute crystals of quartz with submicroscopic, about $0.1\mu\text{m}$ diameter, water filled pores, which Folk and Weaver (loc. cit.) believed due to the brown or yellow colouration bands and the low refractive indices and densities with respect to quartz. Chalcedony has lower refractive indices (1.534-1.539) than quartz and the component fibres are usually length fast although some variation may occur.

Wilson (1966) used the term lutecite to denote a specific form of replacement silica. Lutecite though has concentric bands of inclusions like spherulitic chalcedony and may contain vestiges of replaced material but actually like quartz, it is length slow. However, it could be applied to an intermediate stage, which still shows evidence of a fibrous habit but is length slow, perhaps in the recrystallization of spherulitic chalcedony to a radial quartz aggregate.

During the present investigation XRD failed to trace any particular silica polymorph in these sediments. However, siliceous oozes (Pl. 8.4 A-H; Pl. 8.5 A-B) and very occasionally ?massive opal-CT (Pl. 8.4 B-C; Pl. 8.7 D) is observed with the SEM. The possibility that some of these ? opal-CT may form more recently rather than early in the diagenesis can not be ruled out. The definition and nomenclature of the common silica polymorphs will be given in Section 8.6.

7.2 MEGASCOPIC CHARACTERS OF THE GRONANT CHERT AND THE LLANARMON-YN-IAL CHERTY FLAGS

Megascopic characters which describe genesis of the cherts and the cherty flags are only discussed here. These are:-

7.2.1 Colour

Gronant chert is essentially black to dark grey in colour. Sargent (1921) and Stevenson and Gaunt (1971) noted that the colour of the chert normally resembles that of the associated limestone. Thus dark grey limestone generally contain dark grey or black chert and light grey limestone frequently contain grey, cream or white chert. On the other hand, Llanarmon-yn-ial cherty flags generally are white/creamy in colour with iron oxyhydroxide staining.

7.2.2 Texture

Dense, unfossiliferous Gronant cherts generally have a conchoidal or subconchoidal fracture and are associated with unfossiliferous, thinly bedded limestones. On the contrary, cherts in the poorly fossiliferous limestones (containing brachiopods, broken crinoid fragments, fragmented ooids and rarely fragments of fenestrate bryozoan) mostly enclose shell fragments and crinoid plates which often show only peripheral silicification. The cherty flags of the Llanarmon-yn-ial area occasionally contain very badly preserved brachiopod shell fragments.

7.2.3 Banding

Gronant chert is essentially a nodular chert which has occasional, internal light and dark coloured layers either nearly conformable with the outer surface of nodules nor parallel with the margins of more elongate bodies. This phenomenon was also observed by Sargent (1921), Jessop (1931) and by Orme (1974) from cherts of a number of localities at different levels in the D2 limestones. Sargent considered this banding as a result of "Liesegang effect" (described by R. E. Liesegang, 1898) in chert. However, recent work by Decelles and Gutschick (1983) from the 'Mississippian Wood Grained Chert in the Western Interior United States' proved that Ostwald-Prager theory (that explains Liesegang banding) can only be applied in case of concentric banding.

Generally the shapes and dimensions of the nodules, and the width of individual bands vary considerably (Pl. 8.9 A). Usually the nodules are larger, less regular in shape, and often possess only three or four well defined bands. The limestones in which such cherts may occur are fine grained, being micrite or poorly fossiliferous micrite. These bands (Pl. 8.9A) which have some concentric nature may be explained in terms of Ostwald-Prager theory (for details of this theory, see Decelles and Gutschick, 1983).

Microcrystalline quartz, microcrystalline calcite, and finely divided carbonaceous material are the basic constituents of the banded cherts. Dolomite rhombs are also present in most of the bands. Interpenetration and deformation of adjacent bands resulting from compaction have been observed (Pl. 8.9 A).

In fact, some bandings in the Gronant chert (e.g. those which are nearly concentric) are not a primary sedimentary feature, but presumably developed during diagenesis. This is illustrated by the following observations: the nearly concentric geometry of the banding and the authigenic nature of the dolomite.

7.2.4 Bedding

Bedding is present in the Gronant chert, generally as laminae and thin beds up to 1 cm. thick (Pl. 8.9 B). Porcellanite inclusions are rarely associated with the bedding planes (Pl. 8.9 B). Keene (1975) considered that such inclusions may form where the growth of the chert encloses the area and cuts off the supply of silica, trapping the partly silicified original minerals.

Bedding is not obvious in the Llanarmon-yn-ial cherty flags.

7.2.5 Fractures

Fractures are rarely seen in the Gronant chert which are characterised by fracturing with little or no displacement of fragments. The nearly conchoidal nature of the fracturing across undisturbed bedding indicates that it occurred after the silicification of the beds. The fragments are now silicified with megaquartz or chalcedony (Pl. 8.9 B).

7.2.6 Cross- Cutting Relationship

Stylolites as well as bituminous bedding plane laminae pass directly from limestone into and through many chert nodules (Pl. 8.9 D), suggesting that the chert has replaced limestone which already contained these structures.

7.3 CHERT FABRICS

A variety of names for different chert fabrics have been applied by different workers, but in the present study the classification proposed by Orme (1974) will be followed:-

7.4 VOID INFILLING FABRICS

7.4.1 Microdrusy Chalcedony

Microdrusy chalcedony generally occurs as veins filling fine fractures and grades into microcrystalline quartz, (pl. 8.1 B) and rarely into megaquartz mosaic (Pl. 8.1 A, C). However, almost all of the microdrusy chalcedony was seen to be length fast. Generally in the coarse textured chert this type of chalcedony is common.

7.4.2 Drusy Quartz Mosaic

Drusy quartz mosaic as defined by Folk (1959) is a mosaic of equant anhedral grains of quartz which shows a regular grain size increase away from cavity walls and the outer edges of allochems (Pl. 8.1 D, E, F). Orme (1974) argued that drusy quartz mosaic fabric is assigned to void infilling processes and is analogous to the mosaic quartz of Walker (1962) and drusy quartz of Sosman (1927). Generally speaking, microdrusy chalcedony and drusy quartz mosaic are common primary void infilling fabrics occupying areas between clastic grains in the coarse textured cherts and cherty flags.

7.5 SIMPLE REPLACEMENT FABRICS

7.5.1 Quartz Euhedra

In the Gronant chert and in the Llanarmon-yn-ial cherty flags, euhedral crystals of quartz are usually of fine sand and silt grade and most commonly occur as small clusters (Pl. 8.5 A, C, D, E, F and Pl. 8.6 A-C) and rarely as large scattered single crystals (Pl. 8.6 E). The euhedral crystals of quartz in the Gronant chert commonly shows cross-cutting relationships with skeletal fragments. Usually the quartz crystals occur at widely spaced and randomly distributed centres, outward growth from a seed point appearing to take place along a spired junction which advances at the expense of the calcite of the host rock (in the case of the Gronant chert), and continues until the euhedral form is attained. Some idiomorphic faces may be formed before others. Presumably the size of each quartz crystal is governed by the silica available at a particular seed point. In the Llanarmon-yn-ial cherty flags the growth of the small quartz euhedra was eventually inhibited in some places by detrital illite clay coatings which covered up many of the quartz nucleation sites reducing quartz development. However, at gaps in the clay coatings, some quartz continued to develop, forming large euhedral overgrowths (Pl. 8.6 A-C). Some of the distinct quartz growth stages in the Llanarmon-yn-ial cherty flags can be correlated with those described by Waugh (1970), Pittman (1972), Marzolf (1976) and Wilson (1978).

Section 8.4 shows that the Gronant chert index of crystallinity (CI) for quartz is lower than the cherty flags. This is consistent with the SEM micrographs which show better euhedral quartz crystals in the cherty flags than the Gronant chert.

7.5.2 Quartz Laths

Quartz crystals elongated along the c-axis to form laths are common in the Llanarmon-yn-ial cherty flags and rare in the Gronant chert. The laths

seen in the Gronant chert show some idiomorphic faces (Pl. 8.1 G) but those found in the cherty flags tend to show serrated boundaries (Pl. 8.1 H).

7.5.3 Microcrystalline Quartz

This is the commonest fabric in the cherts and the cherty flags. It is composed of aggregates of small quartz grains of about $10\mu\text{m}$ or less (Meyers, 1977) which commonly show undulatory extinction (Folk and Weaver, 1952) (Pl. 8.1 B). In the Gronant chert microquartz pseudomorphs shell fragments (Pl. 8.6 F) and trilete miospore (Pl. 8.6 F) proves it is a replacement and not a cement. SEM examination shows that microquartz is a fabric of distinct polyhedral equant to subequant quartz grains (Pl. 8.5 A, C-H). Blatt *et al.* (1980) noted that euhedral quartz crystals are absent in microquartz because of mutual interference of crystals during growth. Mega quartz consists of mosaics of quartz crystals that are $30\text{--}250\mu\text{m}$ across (Meyers, 1974).

7.5.4 Spherulitic Chalcedony

Spherulitic chalcedony is rare in both the Gronant chert (Pl. 8.2 A) and in the Llanarmon-yn-ial cherty flags. From Plate 8.2 A it is clear that although concentric rings are evident a fibrous habit is not well developed. Also overgrowths (og) on segments which have lost their fibrous habit totally have unit extinction (Pl. 8.2 A). Orme (1974) noted that the early stages of chalcedony or quartz replacement of crinoid fragments take place either near the outer margin or begins as a zone of replacement silica progressing outwards from the central canal. He further observed a cross-cutting relationship between spherulitic chalcedony and calcite fabric and suggested that spherulitic chalcedony is of a replacement origin. However, the extreme rarity of such features in the present sediments may indicate that they are more diagenetic than the sediments observed by Orme (1974).

7.5.5 Lutecite

Lutecite is relatively more common in the Gronant chert and in the Llanarmon-yn-ial cherty flags than the spherulitic chalcedony. The definition of lutecite has already^{been} mentioned earlier. From (Pl. 8.2 B-C) the fibrous fabric is still evident in parts of the chalcedony spherulites but do not radiate from a single well defined focus. Like spherulitic chalcedony above, overgrowths on the fibrous areas have fibrous to undulose extinction but overgrowths on segments without fibrous habit have unit extinction. Generally lutecite occurs as aggregates with subcircular or hexagonal outline. It occurs in association with spherulitic chalcedony. Orme (1974) considered lutecite as a partial shell replacement feature. Folk and Pittman (1971) considered lutecite to be an indicator of silicification in highly basic or sulphate rich environments, and hence a close association with evaporites was postulated. However, generally speaking, lutecite is not abundant in these sediments. Moreover, the absence of length slow chalcedony and the abundance of length fast chalcedony ruled out such a possibility in the present instance.

7.6 COMPLEX REPLACEMENT AND RECRYSTALLIZATION FABRICS

7.6.1 Pseudodrusy Quartz Mosaic

Pseudodrusy quartz mosaic can form by replacement, with calcite ghost fabrics sometimes preserved as inclusions (Pl. 8.1 F). Orme (1974) and several other workers mentioned some difficulty in deducing the origin of this chert fabric i.e. whether void infiller or replacement origin.

7.6.2 Coarse Recrystallization Mosaics

Recrystallization resulting in grain enlargement is a common feature in both the Gronant chert and the Llanarmon-yn-ial cherty flags. Such fabrics have a much coarser texture than the microcrystalline quartz, and unlike drusy quartz mosaics, there is no regular directional size increase in the component grains, rather an irregular size distribution is characteristic.

The grain boundaries may be straight, curved or crenulated (Pl. 8.2 D). Undulose extinction is common and this fabric is normally associated with spherulitic chalcedony.

7.6.3 Radial Quartz Aggregates

Radial quartz aggregates is essentially an aggregate of quartz grains which radiate from well defined centres. Generally they display wavy extinction. Occasionally in some radial aggregates spherulitic chalcedonic features such as concentric bands can be seen without any fibrous fabric, which may indicate that the radial quartz aggregates have developed from spherulitic chalcedony (Orme, 1974). On the contrary, radial quartz aggregates with no concentric bands of inclusions may indicate an advance stage in the diagenetic events. This latter type of radial quartz aggregate is present in both the Gronant chert and the Llanarmon-yn-ial cherty flags (Pl. 8.2 E-G).

Figure 7.1 represents a summary of the observed silica fabrics during the present investigation.

7.7 CATHODOLUMINESCENCE

During this investigation different types of carbonates were distinguished using cathodoluminescence. The methodology involved in this technique is discussed in detail in Appendix 2.

In carbonate minerals it results from substitution of manganese for calcium, which activates cathodoluminescence to produce brightly luminescent cements, and iron, which quenches cathodoluminescence to produce dull luminescent cements (Sippel and Glover, 1965; Pierson, 1978; Grover and Read, 1983). It has been suggested that a minimal amount of 1,000 ppm manganese is necessary to produce a detectable luminescence, but Bernard (1978) noted that a highly luminescent sample may contain

manganese not more than 100 ppm. The latter author also noted that iron and manganese concentrations in dolomite increase and decrease together with greater variations in the iron content. According to Bernard (1978) iron (Fe II) inhibits the luminescence in dolomite when its concentration reaches 10 ppm or 1 weight % MnII. This relation suggests that iron, in concentrations higher than 1 weight %, is the major control of cathodoluminescence in dolomite. Carpenter and Oglesby (1976), Oglesby (1976) and Frank *et al.* (1982) have presented a model which suggests the cathodoluminescent cement zonation related largely to changes in redox potential of pore fluids. In the model proposed by Grover and Read (1983), the major CL zones (which reflect abundance of MnCO_3 and FeCO_3 in calcite/dolomite) relate to redox potentials, sulfide content, and to a lesser extent the pH of pore fluids from which the cement precipitate. The low manganese content (av. 95 ppm) in the Middle Ordovician non-luminescent carbonate, Virginia, suggests it probably formed from waters that had high redox potentials and that were oxidizing (Garrels and Christ, 1965; Oglesby, 1976; Krauskopf, 1979). Manganese in such waters would have been in an oxidized (Mn^{4+} , Mn^{3+}) state that would have inhibited its substitution for calcium in calcite (Meyers, 1974; Oglesby, 1976).

Bright cement results from reduction of manganese, due to a decrease in redox potentials of pore fluids (Garrels and Christ, 1965; Oglesby, 1976; Krauskopf, 1979). Under these conditions, manganese readily substitutes for calcium in the calcite lattice. Dull cement contains both manganese and iron. From the foregoing it can be concluded that iron and manganese bearing calcites form under more reducing conditions than bright cement, because lower redox potentials allow iron, in addition to manganese to be incorporated into calcites.

In the Gronant chert carbonates, two distinct luminescence colours could be discerned: (i) a bright red-orange luminescence in non-ferroan dolomite and dolomitized shell fragments and cherts and (ii) bright yellow luminescence ferroan dolomite. In addition to these, occasional dull red-orange luminescence in dolomitized shell fragments (particularly calci-spheres) can be seen (Pl. 8.10 A, B; Pl 8.11 A, B). The non-luminescent areas in the photographs are chert.

The dominating bright red-orange and bright yellow luminescent carbonates in the Gronant chert may indicate that most of the carbonates were formed under relatively weaker reducing condition as bright carbonates result from reduction of manganese. The average manganese concentration in the Gronant chert is about 180 ppm (Appendix 12). Such an average may well explain the general bright luminescing tendency of carbonates in the Gronant chert.

Thin section study reveals that occasionally dolomite rhombs have a cloudy centre (Pl. 8.3 G, H). Presumably the cloudy centre resulted from dolomite replacement of calcite allochems, probably at a time when opal-CT was inverted to quartz (see Section 8.6.3). However, CL colours for such dolomite rhombs remain the same (throughout the crystal). CL also reveals that apart from well formed dolomite rhombs, minor amounts of rounded and irregular forms of dolomite can also be traced.











NAME	MORPHOLOGY	PROCESS
MICRODRUSY CHALCEDONY		VOID INFILLING.
DRUSY QUARTZ MOSAIC		
PSEUDO DRUSY QUARTZ MOSAIC		
QUARTZ EUHEDRA		REPLACEMENT
QUARTZ LATHS		
MICROCRYSTALLINE QUARTZ		
SPHERULITIC CHALCEDONY		
LUTECITE		REPLACEMENT and RECRYSTALLIZATION MOSAIC
RADIAL QUARTZ AGGREGATE		
COARSE RECRYSTALLIZATION MOSAIC		

Fig. 7.I.

Summary of Silica Fabrics Associated with Gronant chert. Similar Fabrics were observed by Orme (1974) from the Viséan limestones of Derbyshire

CHAPTER 8

DIAGENESIS

8.1 INTRODUCTION

The definition of the term 'diagenesis' is given in Chapter 11 and a detailed discussion of the processes involved in chert diagenesis is referred to Section 8.6. However, the following is a brief description of different diagenetic features observed in the Gronant chert.

8.2 SOURCE OF MAGNESIUM AND PROCESS OF DOLOMITIZATION IN THE GRONANT CHERT

Dolomite is the thermodynamically stable carbonate phase in sea water, but it is not common in recent deep sea calcareous sediments (Baker and Kastner, 1981). On the contrary, dolomite is an abundant constituent of ancient carbonate bearing rocks now exposed on land such as the Gronant chert.

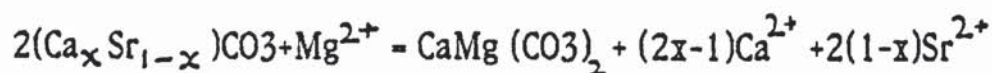
In the Gronant chert the individual dolomite grains can be clearly seen in the thin sections, in the CL and in the SEM using EDAX spot analysis. SEM shows mostly well formed rhombs of dolomite, while CL indicates in addition to rhombs the occasional presence of more rounded and irregular forms. CL also reveals that almost all the grains (particularly the rhombs) contain compositional zonation, with a bright red-orange luminescent non-ferroan dolomite core surrounded by a thin rim of yellow luminescent ferroan dolomite, which is again surrounded by bright red-orange luminescence non-ferroan dolomite. Individual minerals were identified using stained thin sections and EDAX spot analysis. Semi-quantitative analyses using the EDAX system reveal that the centres and the edges of the rhombs contain a high Mg/Ca ratio and low in Fe, while the thin rims are relatively higher in Fe.

The fact that dolomite is more abundant to the chert samples which contain relatively more organic carbon suggests that its presence is related to diagenetic reactions in organic rich sediments. The association of dolomite, chert and organic matter is quite common in deep sea sediments recovered by the Deep Sea Drilling Project (DSDP) (Davies and Supko, 1973; Baker and Kastner, 1981; Kelts and Mckenzie, 1982), but the opinions about its formation are divided. Several other workers like Irwin, Curtis and Coleman (1977), suggested mainly from isotopic evidence, that ferroan dolomite in the Kimmeridge Ledges of Dorset formed relatively soon after burial (at depths of 10-915 m and temperatures of 16-41°C) as a product of bacterial fermentation of organic matter. Pyrite framboids were found enclosed by, and hence possibly pre-dated the dolomite (Irwin, 1980). Friedman and Murata (1979) suggested that dolomitic nodules and concretionary layers in the Miocene Monterey shale formed principally at shallow depths in the sulphate reduction zone. Pisciotta and Mahoney (1981) and Kelts and Mckenzie (1982) noted that in the late Cenozoic diatomaceous sediments of the Gulf of California, dolomite appears to have formed in both the sulphate reduction and fermentation zones. Authigenic dolomite is also known to occur at very shallow depths in the recent sediments of some fresh water lakes (Muller *et al.* 1972). Therefore, it can be convincingly concluded that dolomite can form at any stage during diagenesis provided suitable geochemical conditions exist. Katz (1971) suggested that zoned dolomite rhombs in the Middle Jurassic Mahmal Formation of Israel formed due to early diagenetic replacement of calcium carbonate under shallow water evaporitic conditions. However, such conditions were not experienced during deposition of the Gronant chert as is evidenced by the abundance of length fast chalcedony (Pl. 8.1 A-B) and the lack of evidence of any evaporite minerals. Occasionally, ghost textures or dolomitized calci-spheres or other shell fragments and dolomitized siliceous oozes were observed by CL (Pl. 8.10 A, B; Pl. 8.11 A, B).

Dolomite rhombs in the Gronant chert are frequently associated and occasionally intergrown with aggregates of framboidal pyrite (Pl. 8.3 E, F), indicating that growth of both may have been related to bacterial degradation of organic matter in the sulphate reduction zone. This also suggests that dolomite precipitation preceded, or was contemporaneous with pyrite formation, while ferroan dolomite/calcite possibly slightly post dated pyrite formation.

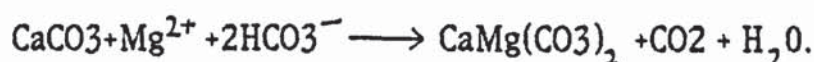
Baker and Kastner (1981) have shown that SO_4^{2-} in sea water inhibits dolomite formation, but that dolomite can form at shallow depth in organic rich marine sediments where SO_4^{2-} is removed from the pore waters by bacterial reduction. According to them sulphate reduction promotes dolomitization in three ways: (i) by removal of the dissolved sulphate inhibitor; (ii) by production of alkaline conditions; and (iii) by production of NH_4^+ , which exchanges for absorbed Mg^{2+} on clays. However, the Mg/Ca ratio of the pore waters may also control which carbonate phase will form under these circumstances. In their experiments conducted at 200°C and sea water ionic strengths, Baker and Kastner established a calcite/dolomite phase boundary at an Mg/Ca ratio of 0.57-1.06, and a dolomite/magnesite boundary at a ratio of 2.11-3.41. However, the relevance of these conditions to low temperature dolomite formation is not yet clear (Pye, 1985).

In the pore waters of near surface marine sediments sources of Mg include sea water, ionic exchange processes involving clays and, to a lesser extent, breakdown of chlorophyll and dissolution of biogenic calcite or Mg-calcite (Sayles and Manheim, 1975). Sayles and Manheim also observed some distinctive trends in deep sea calcareous sediments especially Mg^{2+} is exchanged for Ca^{2+} , Sr^{2+} is slightly enriched and minor SO_4^{2-} depletion takes place as dolomite is precipitated.



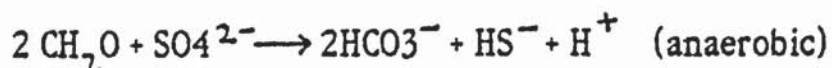
Gronant chert is characterised by slow rates of sedimentation (7.5 m/m.y., i.e. 0.075 cm/100 yrs) see Section 6.2.5). Sayles and Manheim (1975) also noted that in more rapidly deposited sediments (>1 cm/100 years) Mg^{2+} depletion exceeds Ca^{2+} enrichment, a feature that requires reactions which remove Mg^{2+} and HCO_3^- instead of normal substitution of Mg for Ca. Direct precipitation of Mg^{2+} and SO_4^{2-} is not possible and because SO_4^{2-} reduction occurs only through:

$2\text{CH}_2\text{O} + \text{SO}_4^{2-} \longrightarrow \text{HS}^- + 2\text{HCO}_3^- + \text{H}^+$ then the required loss of both Mg^{2+} and HCO_3^- can be compensated by:

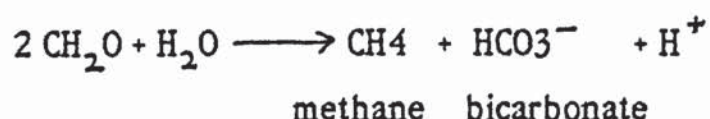


The supply of Mg from the sea water and from the clay mineral will be expected to decline with depth, while the supply of Ca ions to pore water normally increases with depth as shell debris is dissolved. The zone of maximum dissolution of shell debris in organic rich argillaceous sediments probably occurs at a depth of a few metres below the surface, where pH may fall to 6.5 or lower (Morris, 1980). The presence of marcasite in the Gronant chert (Pl. 8.3 D) clearly indicates that during the course of diagenesis pH certainly falls to 6.5 and this may coincide with the increase of Ca ions in the pore water. Based on Mg/Ca ratio, therefore, the surface few metres of sediment should provide very favourable conditions for dolomite formations during early diagenesis (Pye, 1985). This zone of dolomitization, which corresponds with the zone of sulphate reduction is not supposed to be ferroan, since virtually all the available Fe^{2+} is rapidly combined with H_2S and precipitated as pyrite framboids (Pl. 8.8 D) (Goldhaber and Kaplan, 1975; Berner, 1984). However, below the zone of sulphate reduction, where sulphide ions are no longer available to combine with ferrous iron, Fe^{2+} may be incorporated in carbonate phases to form ferroan dolomite/ferroan calcite rim.

Presley and Kaplan (1968) considered that the levels of HCO_3^- obtained from the metabolic sulphate reduction equation:



were much higher than expected from sulphate reduction with depth alone and inferred that other metabolic processes must be active e.g. fermentation:



The occurrence of fermentation and methane production in shallow marine cores was also reported by Nissenbaum *et al.* (1972) in a study of Saanich inlet, British Columbia, Canada. Kastner and Geiskes (1976) and Geiskes *et al.* (1981) noted from deep sea sediments that concomitant with SO_4^{2-} reduction there occurs an increase in HCO_3^- and NH_4 due to methanogenesis and fermentation (Baker and Kastner, 1981). Hence the process of methanogenesis and fermentation could also be important for the Gronant chert dolomitization.

Kastner *et al.* (1977) and Baker and Kastner (1981) also noted experimental results which indicate the transformation of opal-A to opal-CT retards dolomitization of calcite by incorporating Mg^{2+} . Apparently, Mg^{2+} is released for dolomite formation when opal-CT inverts to quartz. During the present investigation the presence of relicts of massive opal-CT in the Gronant chert is seen with the SEM (Pl. 8.4 B, C; Pl. 8.7 D). This means, of course, that most of the opal-CT has already been inverted to quartz. Presumably during the above reaction some Mg^{2+} was released to the pore water for dolomite formation.

From the foregoing it can be concluded that a number of processes were active for the dolomite formation in the Gronant chert and that the dolomitization is certainly an early diagenetic phenomenon.

However, the possibility of some dolomites being inherited from the original limestones can not be justified, because of the subsequent chert-carbonate replacement reversals and multiple reversals reactions.

8.3 CHERT-CARBONATE REPLACEMENT REVERSALS AND MARCASITE-PYRITE RELATIONSHIP

There is evidence in the Gronant chert that silicification of a carbonate deposit is not the only direction of replacement. Reversals have occurred as shown by discrete dolomite rhombs (Pl. 8.3 G; Pl. 8.8 A, B) and more massive non-ferroan calcite replacement of chert in the veinlets (Pl. 8.3 A, B; Pl. 8.7 H; Pl. 8.8 F, G). Pseudomorphs of ferroan calcite after non-ferroan calcite also exist in the veinlets. Formation of non-ferroan calcite beyond the borders of the veinlet by replacement of chert is indicated by i) well crystalline non-ferroan calcite crystals centred on the veinlets; ii) the failure of the outer edges of the carbonate veinlet to match; and iii) the occurrence of relict inclusions of undigested silica with non-ferroan calcite. Further, dissolution of dolomite rhombs (Pl. 8.7 A-G; Pl. 8.8 C) and pseudomorphs of silica after dolomite rhombs exist (Pl. 8.7 D, G) and suggest multiple replacement reversals.

Walker (1962), Swett (1964) and Orme (1974) recorded similar features in other limestones. Walker (1962) suggested that on the basis of what is known concerning the relative solubilities of amorphous silica and calcium carbonate in water of varying pH, such reversals may be partly pH controlled. Varying pH conditions during diagenesis of the Gronant chert is confirmed by the presence of marcasite-pyrite phases (Pl. 8.3 D-F).

Geological field data indicates that marcasite is wide spread in fresh water, brown coal, peat, and swamp environments which, for the most part, are acid in nature (pH 6.5; Degens, 1965; Maynard, 1983). In contrast, pyrite is abundant in marine sediments that provide a neutral or alkaline environment (Degens, 1965; Maynard, 1983). Low temperature experiments in the Fe-S system show that marcasite forms from acid solutions whereas pyrite requires neutral to alkaline conditions. In view of the close agreement in the pH requirements between natural and experimental iron sulfide formation, one may suspect that pH is the major factor in determining the mode of crystallization.

In organic rich sediments (like the Gronant chert) decaying organic matter just beneath the surface reduces pH to as low as 6.5 for marcasite precipitation. There is evidence in the Gronant chert that silica is precipitated from solutions characterized by low pH (Pl. 8.3 D). Therefore, the combined effect of organic matter and pH variation, produced conditions necessary for silica precipitation, carbonate dissolution, and their reversals and multiple reversals in the Gronant chert. The petrographic evidence presented here supports the idea that silica can be highly mobile in carbonate environments. Undoubtedly, processes of solution and redistribution of silica and carbonates have been important aspects of diagenesis in the Gronant chert (see also Section 8.6.3).

8.4 INDEX OF CRYSTALLINITY FOR QUARTZ (68° QUINTUPLET)

Klug and Alexander (1954) noted that the deterioration of the X-ray traces of quartz at high angles of 2θ are indicative of smaller crystallites (generally about 1 to $5\mu\text{m}$ in diameter). The wide range in crystallinity of quartzose cherts from deep sea sediments were first discussed by Hathaway (1972) from a set of five X-ray diffraction peaks at 2θ of 67° to 69° , $\text{CuK}\alpha$ radiation. Later, these peaks were referred to as the 68° quintuplet by Murata and Norman (1976). The latter authors considered a

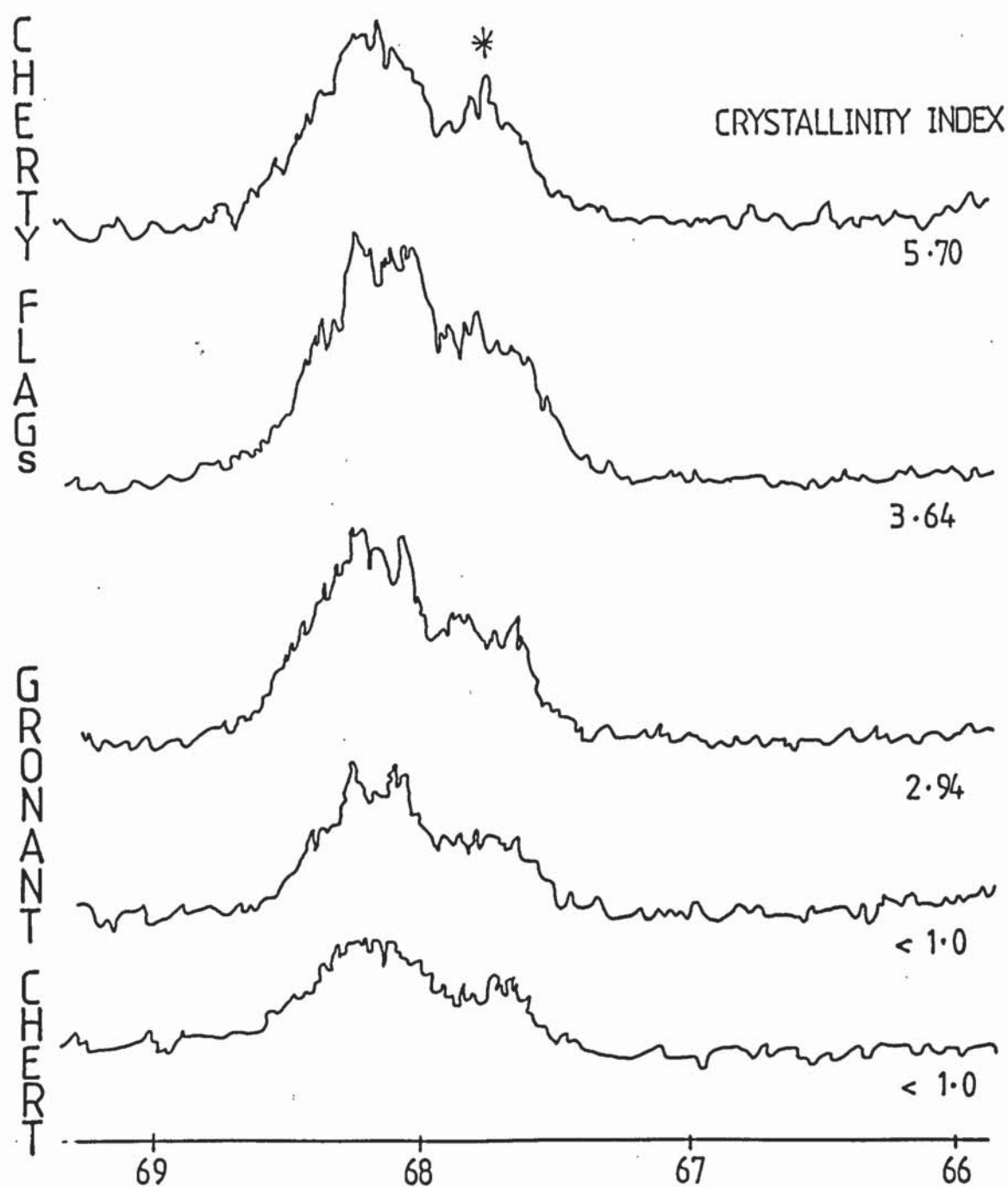


Fig. 8.I. XRD tracings of the 68° quintuplet arranged in order of increasing crystallinity of quartz. (*) marks the (212) peak at 2θ of 67.75° which is measured to obtain the crystallinity index given to the right of the tracings.

crystallinity index of <1.0-3.0, are examples of poorly crystallized quartz, while CI of 8.0-10.0 indicate well crystallized metamorphosed quartz. They further noted that CI depends on crystalline size (up to about $1\ \mu\text{m}$ in diameter) and sometimes could also be affected by lattice distortions due to mechanical stress but nevertheless time factor alone can not improve crystallization.

During the present investigation the 2θ interval of 66° to 69° was scanned at $1/4^\circ/\text{min}$, with nickel filtered Cu radiation. The profile of the 68° quintuplet (Figure 8.1) ranges from a simple broad hump (in the Gronant chert) to a series of profiles of relatively better resolution (in the Llanarmon-yn-ial cherty flags). The index of crystallinity was derived from the intensity of the (212) peak at 2θ of 67.74° (asterisk sign) using the formula:

$$\text{CI} = 10aF/b \text{ (see Murata and Norman, 1976).}$$

where a = Height of this (*) peak

b = Total height above background

and scaling factor $F = 1.67$.

The result shows that the Gronant chert index of crystallinity for quartz (<1.0-2.94) is lower than the Llanarmon-yn-ial cherty flags (3.64-5.70). This may indicate that the Llanarmon-yn-ial cherty flags are better crystallized than the Gronant chert. This is in agreement with the SEM micrographs which display better euhedral quartz crystals in the cherty flags compared to the Gronant chert (Pl. 8.5 A, C, E, F and Pl. 8.6 B, C, E). It should be noted here that the Gronant chert and the Llanarmon-yn-ial cherty flags are almost contemporaneous in age (see Chapter 4). Presumably the difference in the CI of the cherty flags from the Gronant chert is mostly a reflection of the difference in average size of their constituent crystallites.

Quartz with poor CI is extensively reported in the literature. A very low value of CI (<1.0) was noticed by Murata and Norman (1976) from the Chalk of England. Poor crystallinity of 1.3 of the Pliocene chert from magadiite, Oregon, U.S.A. is due to the rapid precipitation from a silica-rich solution at near surface temperatures (Hay, 1968; Sheppard and Gude, 1974). Crystallinity of the biogenic chert from the 'Miocene Monterey Shale' of California, varies randomly between 2.0-3.2. Murata and Larson (1975) considered their poor crystallinity may be characteristic of such diagenetic microquartz (biogenic opal-A → opal-CT → microquartz), which would be metastable relative to better crystallized macroquartz. Such hypothesis fits well with the Gronant chert where a similar sequence of diagenetic microquartz is proposed (Section 8.6.3). Several other authors like McBride and Thompson (1970) linked the low crystallinity (2.2) of Caballos Novaculite of Texas (Devonian and Mississippian) to its mild diagenetic history and the higher crystallinity of the Arkansas Navaculite (5.7-9.8) with the more intense metamorphism imposed by the Ouachita orogeny (Goldstein and Hendricks, 1953). Similarly, Bailey *et al.* (1964) argued that the higher crystallinity (6.2-9.0) of the cherts from the late Mesozoic Franciscan Formation of California probably resulted from the intense metamorphism to which they were later subjected. Alternatively, the moderate crystallinity (6.5-7.0) of the Huronian cherts of Michigan suggest that age may not be a major controlling factor of better crystallinity for quartz (Murata and Norman, 1976).

From the foregoing, it is obvious that neither the Gronant chert nor the Llanarmon-yn-ial cherty flags were subjected to intense metamorphism.

8.5 VADOSE DIAGENESIS

In the Gronant chert a mosaic of detrital silt-size calcite crystals or microcrystalline calcite crystals and rare pellets, small ^{ec}unrecognizable skeletal debris are found fill^{ing} many pore spaces. Generally they have dull

to bright red-orange luminescence colour. They rest on host sediment and on different chert fabric and commonly about other carbonates (pl. 8.10; A-B. Pl. 8.11; A-B).

Dunham (1969) considered that silt-size calcite crystals and pellets are characteristic of vadose diagenesis. It happens when silt-size calcite particles attributed from the internal erosion of the host limestone are carried by the meteoric waters in the vadose zone. Some silt-size calcite crystals may have also formed as fine, suspended particles within pore fluids, which subsequently settled on cement (Grover and Read, 1983). However, Moore *et al.* (1976) argued against a vadose-meteoric diagenesis of the silt-size calcite crystals as according to them superficially similar internal sediments may be formed by boring sponges in subtidal environments. However, textural evidence favours a vadose diagenesis origin for the Gronant chert microcrystalline calcites.

8.6 DISCUSSION AND CONCLUSIONS

The basic elements of a chertification model for the Gronant chert is derived from analogy with the contemporaneous chertification processes of the limestone sequences in the United States and the processes thought to be occurring in oceanic sediments.

Silica generally precipitates from natural aqueous solution as amorphous silica (opal-A) in many low temperature environments. Siliceous microorganisms, such as sponge spicules, radiolarians and diatoms, precipitate opal-A to form siliceous tests. These tests accumulate on the sea floor to form siliceous oozes. A number of reports are now available on the progressive burial diagenesis of these opal-A deposits (Siever, 1962; Mizutani, 1970; Calvert, 1983; Murata and Larsen, 1975; Keene, 1976; Kastner *et al.* 1977; Hein *et al.* 1978; Isaacs, 1980; Williams *et al.* 1985 etc.).

First, siliceous tests are fragmented, partially dissolve (Pl. 8.4 A-H; Pl. 8.5 A, B) and silica overgrowths may precipitate (Williams *et al.*, 1985). These overgrowths are known to be as opal-A' (Hein *et al.* 1978; Williams *et al.* 1985). As the amorphous silica polymorphs (opal-A and opal-A') are buried deeper in the sedimentary basin, a less soluble disordered cristobalite-tridymite phase (opal-CT) forms (Pl. 8.4 A-C; Pl. 8.7 D and Jones and Segnit, 1971). The opal-CT then recrystallizes to quartz (Pl. 8.5 A, C-H). Crystallinity of the quartz progressively increases as a result of crystal growth, until it equals that of quartz crystals of igneous or metamorphic origin (seen in the Llanarmon-yn-Ial cherty flags; Pl. 8.6 A-B, E; Fig 8.1 and 8.3; also see Section 8.4). This sequence (i.e. opal-A - opal-CT - quartz) of transformations is largely controlled by a dissolution - reprecipitation pathway as evidenced by Williams *et al.* (1985). Several workers considered that sedimentary fabrics of quartz cherts and porcellanites are often not appreciably different from those of opal-CT cherts and porcellanites. Sometimes opal-CT can be pseudomorphed in quartz cherts (Pl. 8.4 A-C; Pl. 8.7 D). Retention of fabric has been used as evidence of solid-state opal-CT - quartz transformation.

Evidence of dissolution - reprecipitation theory is also seen in $^{18}\text{O}/^{16}\text{O}$ ratios of the three diagenetic zones of the Miocene Monterey Formation of California. $\delta^{18}\text{O}$ decreases abruptly at the opal-A/opal-CT and opal-CT/quartz boundaries but remains relatively constant within each zone (Murata *et al.* 1977; Pisciotta, 1981). This indicates dissolution - reprecipitation and isotopic fractionation between each silica phase and interstitial water at ambient temperatures (Williams *et al.* 1985). Finally, according to Williams *et al.* (1985), dissolution-reprecipitation in opal-A - opal-CT and opal-CT - quartz transformations is the strength of the Si-O bond itself, where both transformations must break Si-O bonds, and, in the solid state, this would entail activation energies at least equal to the bond strength of 89 kcal/mole.

The generalized silica diagenetic sequence can be modified after Williams *et al.* (1985): opal-A (siliceous biogenic ooze) - opal-A' (non-biogenic amorphous silica) - opal-CT - better ordered opal-CT - cryptocrystalline quartz or chalcedony - microcrystalline quartz. From a chemical point of view thermodynamic and kinetic controls dictate this diagenetic sequence. Therefore, the diagenetic sequence of silica is controlled largely by aqueous solubility of phases, which is primarily a function of crystal structure and particle size and shape (Williams *et al.* 1985). The other factors involved in concentration of silica in sediment pore waters are:

(i) pH of the water (Fig. 8.2 A); (ii) temperature (and pressure to a much lesser extent, Fig. 8.2 B); (iii) type and concentration of other dissolved silica species, such as polymers and complexes, in the water; (iv) additional minerals in the sediment; and (v) pore water diffusion rates.

The retarding effects of clays on the opal-A - opal-CT transformation are widely reported in the geological literature. On the contrary, carbonates increase the rate of reaction (Keene, 1976; Land, 1979). Kastner *et al.* (1977) suggested that, in the alkaline, Mg-enriched environment of the carbonates, a compound nucleates with $\text{Mg}/\text{OH} \sim 1/2$. This compound provides nucleation sites for opal-CT lepispheres by attracting silanol groups.

However, while clays retard the opal-A - opal-CT reaction, they appear to enhance the opal-CT - quartz reaction (Isaacs, 1982; Williams *et al.* 1985). Water acts as a catalyst in the opal-CT to quartz transformation. The temperature of transformation of opal-CT - quartz in the sedimentary realm occurring within a range of 31°-165°C (Murata *et al.* 1977; Mizutani, 1977; Pisciotto, 1981). However, the present vitrinite reflectance result suggests a temperature range of 62°-65°C in the Llanarmon-yn-ial cherty flags and thus consistent with the temperatures range mentioned above (see also Table 9.1). Quartz precipitates from solutions

Fig. 8.2A.



A. Increase in silica solubility with increasing pH;
Volosov (in Williams *et al.*, 1985)

B.



B. Increase in silica solubility with increasing temperature
for several silica polymorphs. Williams *et al.* (1985)

- ① AMORPHOUS SILICA , ② β -CRISTOBALITE , ③ α -CRISTOBALITE ,
④ CHALCEDONY, ⑤ α -QUARTZ .

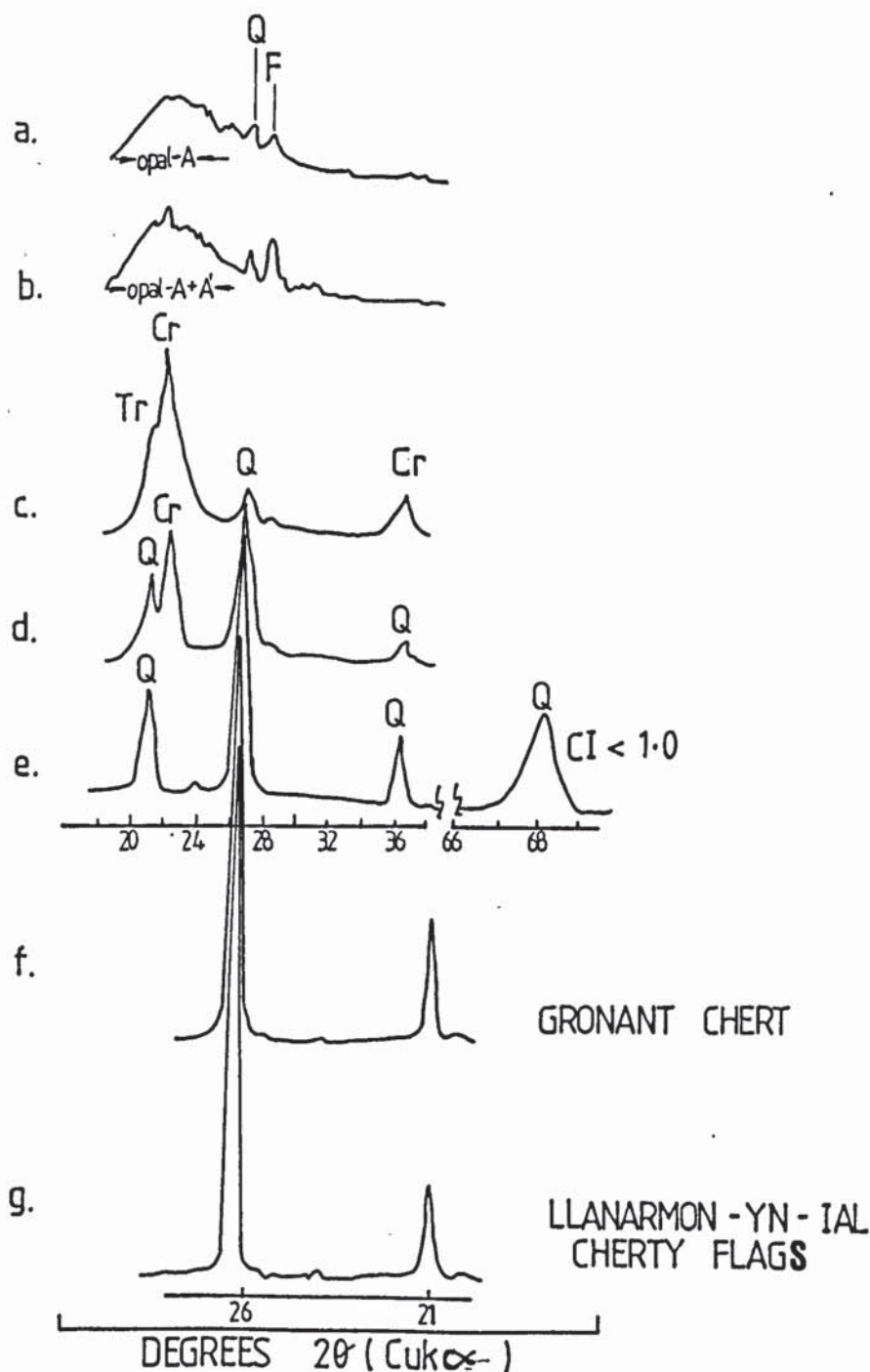


Fig. 8.3 XRD patterns representing the diagenetic sequence. Q= quartz(a-c,detrital;d-g,diagenetic). F=feldspar (detrital). C_r=cristobalite. T_r=tridymite. a-e modified from different authors(in Williams et.al. 1985). a)diffuse hump between approximately 19° and 25° 2θ representing opal-A. b) opal-A hump showing development of small peaks in the 19-25° 2θ range, reflecting early precipitation of opal-A. c) XRD pattern for opal-CT, with d(101) spacing=4.097Å. d) XRD pattern for opal-CT showing increasing crystallinity and decreasing d-spacing with depth. d(101) spacing=4.040Å.e) Transformation of biogenic silica from opal-CT to poorly crystalline quartz. C.I measured= (I.O.f see text for detail). f-g; Present study. f= Gronant Chert; g= Llanarmon-yn-ial cherty flags. Note; the better crystallinity of quartz compared to d-e.

undersaturated with respect to opal-A or opal-CT (Mackenzie and Gees, 1971; Bhattacharyya, 1983).

The final stage in the diagenetic sequence includes slow recrystallization from cryptocrystalline to microcrystalline quartz, which can be measured by the crystallinity index of Murata and Norman, 1976 and see also Section 8.4.

Therefore, in the words of Williams *et al.* (1985) the whole diagenetic sequence can be summarized as follows:

"Amorphous silica phases (opal-A) precipitate in nature due to the formation of dense colloids in supersaturated alkaline aqueous solutions with low relative concentrations of other ions. Opal-A dissolves and yields solutions of still relatively high silica content. In pore waters containing abundant cations, open framework polymers form which flocculate to yield opal-CT. Opal-CT becomes increasingly ordered, primarily due to preferential growth of cristobalite relative to tridymite and crystal size increase. Opal-CT dissolves to yield pore waters of low silica concentration, which allows slow growth of quartz crystals from monomeric solution. The quartz crystals then slowly increase in size and crystallinity. Carbonates appear to enhance opal-CT formation, possibly due to the activity of positively charged hydroxyl complexes. Hence, polymerization in relatively pure systems is involved in opal-CT formation, and slow growth from monomeric (low silica concentration) solutions is involved in precipitation of quartz in sedimentary realms".

8.6.1 SOURCES OF SILICA

Siliceous fossils such as sponge spicules (Pl. 8.4 A-F) and radiolaria (Pl. 8.4 G, H; Pl. 8.5 A, B) are found in most of the chert samples examined and it is the biogenous materials that supply most of the silica for the chertification of the Gronant chert. Keene (1975) argued that generally most silica

dissolves and migrates to the site of chertification and hence the radiolarians and spicules preserved in the cherts do not necessarily contribute their silica to the chertification of the sediments until and unless they are replaced by a mineral other than silica. Preservation of spicules and particularly the radiolarians are very poor in the Gronant chert indicating that the dissolved siliceous fossils could have provided the silica for its formation. This is also proved by examining two samples with the SEM from the adjacent limestones, where spicules and radiolarians have been dissolved, providing silica for the chert. The rare and highly dissolved radiolarians present in the Gronant chert range in size from 4 to 15 μm , suggesting that dissolution has affected both the smaller and larger radiolarians; while the complete absence of diatoms may indicate that they have already dissolved and contributed their silica for the chertification.

Apart from biogenous materials, a small amount of silica of the cherts and small-scale shell replacements may come from the Visean-Namurian sedimentary environments, diagenetic redistribution may have played a major role. Small changes of pH would be a basic control in this process as they would also be in subsequent chert-carbonate reversals and multiple reversals.

Additional silica may be released by the diagenetic alteration of volcanically derived clays as proposed by Keene and Kastner (1974). However, the release of silica by illitization of detrital smectite or desorption from Kaolinite cannot be ruled out as possible sources.

8.6.2 Time of Formation

The early formation of the Gronant chert is indicated by the compaction of beds around nodules (Pl. 8.9A) and the formation of stylolites (Pl. 8.9 D). Compaction of beds may happen after a considerable time, when the

over-burden became significant and lithification occurred in the surrounding sediments.

The nature of the source of silica may also indicate when silicification occurs. Generally, in the diagenetic history of the rock the supply of silica from volcanic glass and clays may become available later than biogenous silica (Keene, 1976). However, the major silica donor of these sediments is the biogenous silica, suggesting silicification in the early stage of diagenesis.

8.6.3 Proposed Model for the Gronant Chert

The present geochemical work strongly suggests that the Gronant chert is essentially a silicified limestone and that the silica is diagenetic in origin. This is also supported by the petrological data. The advance stage of silicification and the ghosts of calcite fabrics included in the silica testify to late stage replacement of a limestone (Pl. 8.1 A-F). However, a detailed knowledge of the palaeohydrology, aqueous chemistry, host lithologies, burial history, sources of silica, and sources of magnesium for dolomite formation is necessary in order to understand more fully the origin and diagenesis of the Gronant chert. Unfortunately, detailed information about the palaeohydrology and aqueous chemistry cannot be retrieved. Reasonable assumption may be that advective fluxes of silica, magnesium, and calcium were primarily vertical within the host sediments (Heath, 1974), although shale interbeds may have promoted horizontal advective flux (Chilingar *et al.* 1979). Recent studies from modern deep sea sediments indicate that abundant dissolved amorphous silica (about 60 ppm) is present in near bottom sea water and interstitial water (Siever *et al.* 1965; Manheim *et al.* 1970; Lerman, 1978) providing a favourable chemical environment for chert production.

In fine grained marine sediments as observed by Berner (1980), the rate of molecular diffusion within pore waters, rather than pore water flow, controls diagenetic chemical redistribution over distances on the order of 1 m. Thus it can be convincingly suggested that the origin of the Gronant chert is linked to diffusive processes rather than advective processes.

Heath and Moberly (1971) and Lancelot (1973) have shown the significance of host sediment during chert diagenesis. Kastner *et al.* (1977) and Williams *et al.* (1985) noted that the rate of opal-A to opal-CT transformation is greatly inhibited by the presence of reactive clay minerals.

It is now well known that chert forms during burial diagenesis. Keene (1975) considered that high porosity and permeability in the host sediments encourage the rate and extent of chert formation. The host sediments for the Gronant chert were limestones. It may be very difficult to assume a high porosity in a consolidated limestone. Therefore, the rate and extent of chert formation may not be very fast. However, based on evidence obtained from geochemical and petrological data, the following interpretation can be made for the diagenetic sequence in the development of the Gronant chert (Fig. 8.4).

- (1) Sponge spicules and radiolarians in the host limestones dissolved, releasing abundant silica to interstitial fluids.
- (2) The dissolved silica locally migrated to sites of eventual Gronant chert nodules and began to precipitate and nucleate as opal-CT. At the same time microbial reduction of SO_4^{2-} , methanogenesis, and fermentation in the surrounding organic rich sediments caused increased alkalinity and NH_4^+ concentration in interstitial fluids, which in turn may have led to incipient dolomitization and pyritization.

- (3) Transformation of opal-CT to quartz. Magnesium was released during the transformation and dolomitization process may be promoted. Coeval diffusion of CaCO_3 into the opal-CT.
- (4) Decaying organic matter just beneath the surface may have led to increased acidity to precipitate silica and marcasite and to dissolve carbonates.
- (5) Nevertheless, local replacements of carbonate by silica and subsequent reversals and multiple reversals may have continued.
- (6) Microcrystalline calcite crystals may be due to vadose diagenesis and of relatively late events.

Limonitization of pyrite framboids is considered to be the latest diagenetic event in the Gronant chert, which is presumed to be still continuing.

Several lines of evidence corroborate the above diagenetic sequence for the Gronant chert. Diagenetic sequence (biogenic opal-A → opal-CT → microquartz) is consistent with the quartz crystallinity index of the Gronant chert (68° quintuplet, see Section 8.4). Relatively better preservation of siliceous fossils (e.g. sponge spicules) in the Gronant chert than in the enclosing carbonate rocks may suggest that the silica for the Gronant chert was derived from the dissolution of siliceous fossils in the host sediments, similar to the process reported by Keene (1975) and others for cherts recovered by the DSDP. The association of chert, organic matter, and dolomite in the Gronant chert suggests that sulfate reduction in the associated limestones was the primary cause of dolomitization.

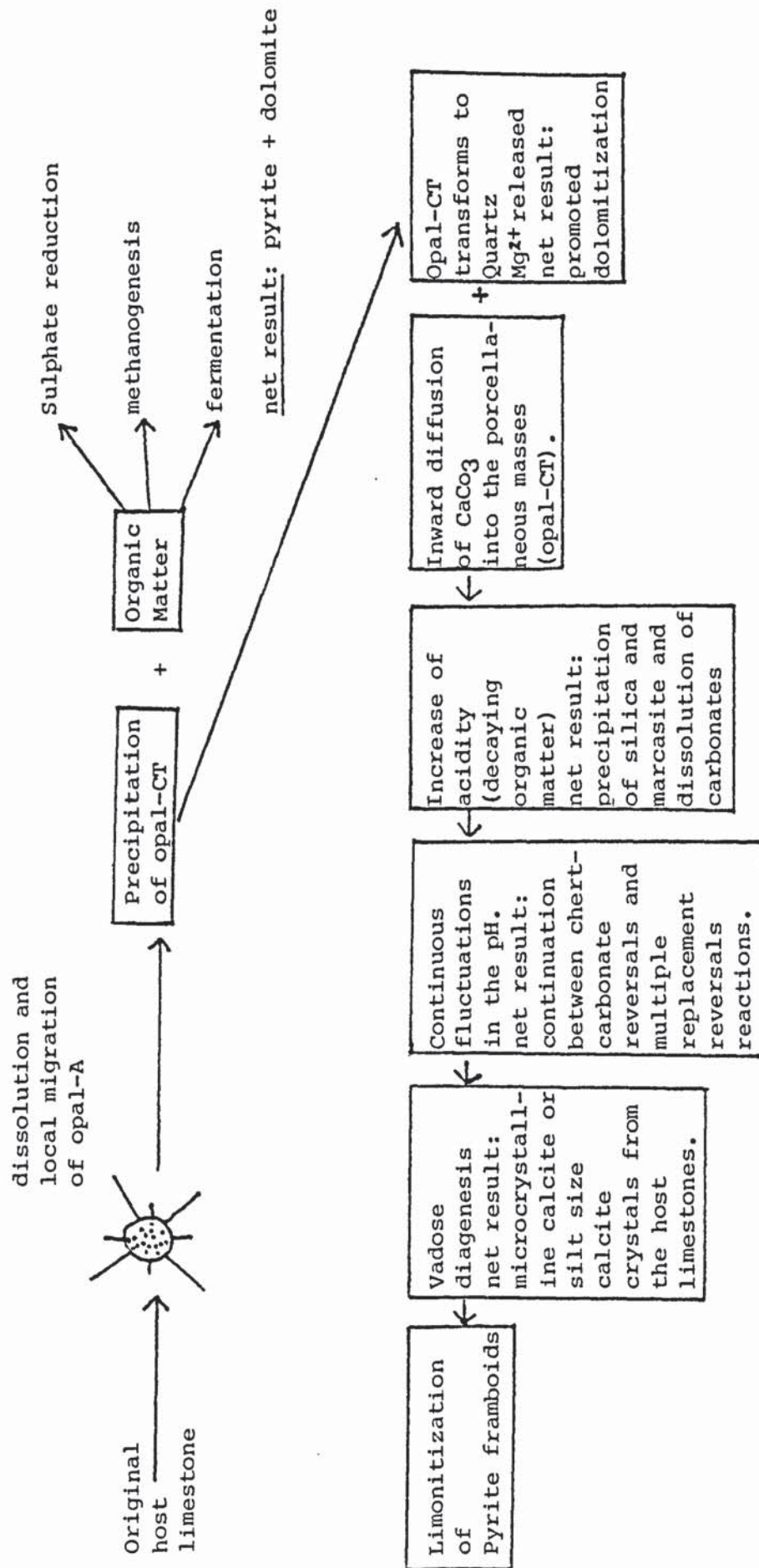


Figure 8.4: Schematic representation of the diagenetic sequence for development of the Gronant chert. See text for explanation.

PLATE 8.1

All thin section photomicrographs

- A. Ghost of brachiopod shell fragment (b) is surrounded by microdrusy chalcedony. Note. Carbonaceous matter (O). Gronant chert. Width of field of photograph = 0.23 mm; XN
- B. Length fast (lf) microdrusy chalcedony filling fine fractures and grades into microcrystalline quartz (mq). Llanarmon-yn-ial cherty flags. Width of field of photograph = 0.23 mm; XN
- C. Calci-spheres fragment (c) completely replaced by microcrystalline quartz and surrounded by microdrusy chalcedony. Gronant chert. Width of field of photograph = 0.23 mm; XN
- D-F. Shell fragments have been completely replaced by drusy quartz mosaic (see shaded area). This is reflecting an advance stage of silicification of an original host limestone. Note 'F' contains tiny remnant of the original calcite (ca) and thus resembles pseudo-drusy quartz mosaic.
q = drusy quartz mosaic. Gronant chert.
Width of field of photograph = 0.23 mm; XN
- G. Numerous quartz laths (l) with idiomorphic faces. Note the presence of dolomite rhombs (d). Gronant chert.
Width of field of photograph = 0.23 mm; XN
- H. Numerous quartz laths (l) with occasional idiomorphic faces and serrated boundaries. Llanarmon-yn-ial cherty flags
Width of field of photograph = 0.23 mm; XN.

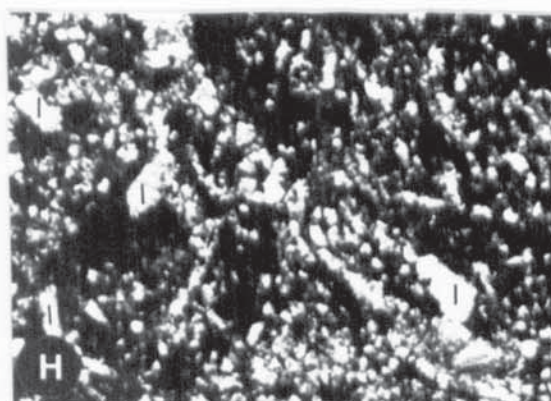
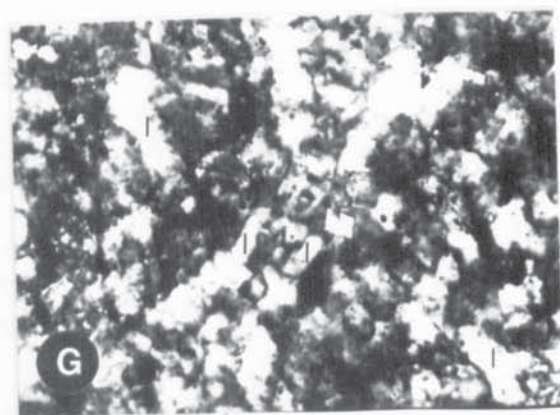
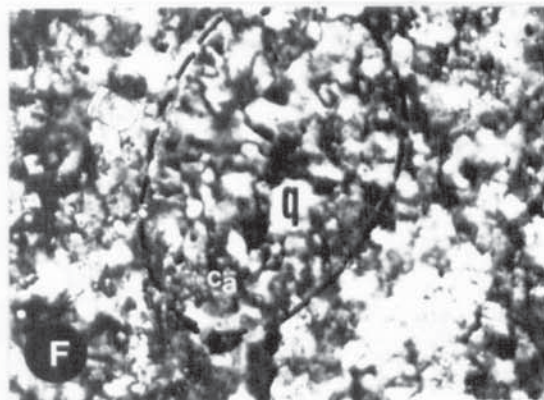
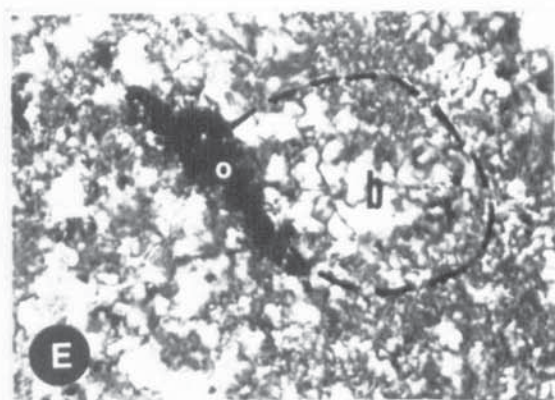
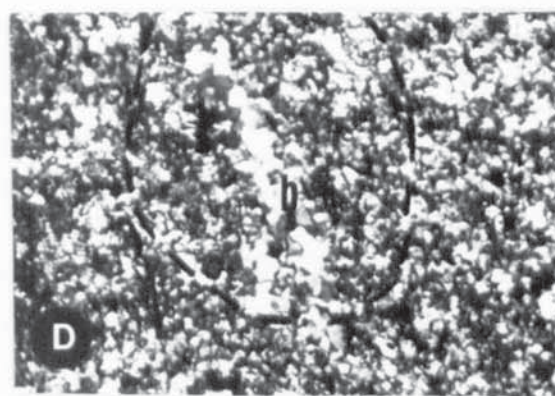
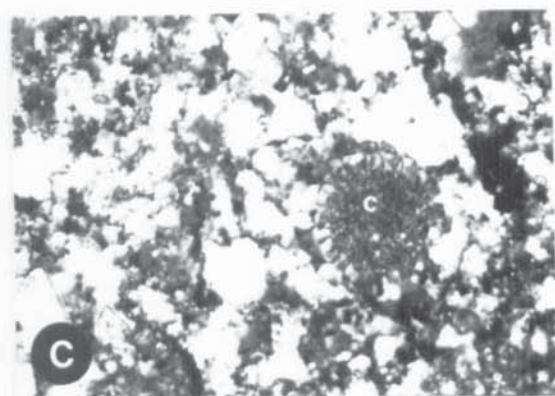
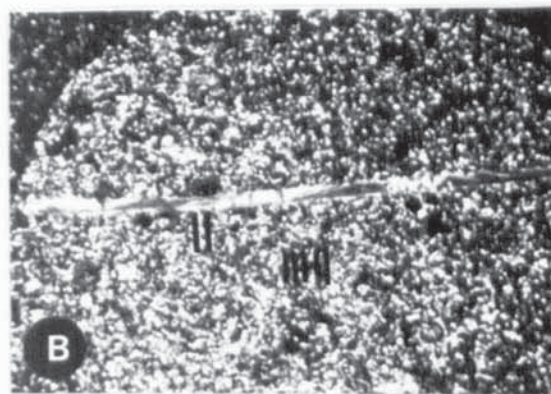
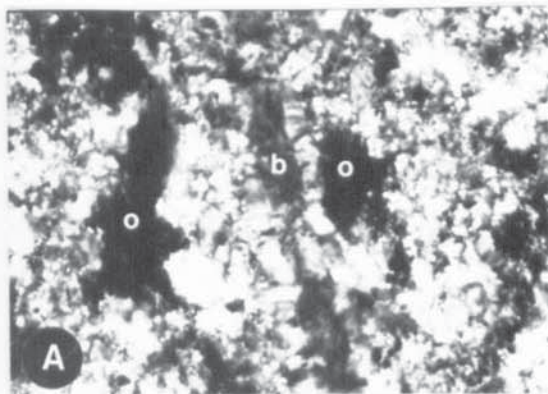


Plate 8.1

PLATE 8.2

All thin section photomicrographs

- A. Spherulitic chalcedony. The fine radiating fibres are dominantly length fast. Note the overgrowth (og) has unit extinction.
Gronant chert.
Width of field of photograph = 0.23 mm; XN
- B-C. Spherulite developed in the Llanarmon-yn-ial cherty flags. Concentric nature is evident but fibrous fabric is not well developed and do not radiate from a single well defined focus. The fabric is mostly length slow and the term lutecite could be applied.
Width of field of photograph = 0.23 mm; XN
- D. Coarse recrystallization mosaics in the Gronant chert. Such mosaics have a much coarser texture than microcrystalline quartz. Note the presence of dolomoldic cavity (d) in the centre of the picture. There is evidence of silica-carbonate reversal.
Width of field of photograph = 0.23 mm; XN
- E-G. Radial quartz aggregate in the Gronant chert (E) and in the cherty flags (F-G). Probably the aggregate has developed through the recrystallization and enlargement of an original replacement spherulite of chalcedony.
Width of field of photograph = 0.23 mm; ppl.
- H. Probable brachiopod shell fragment partly replaced by quartz. Idiomorphic faces of quartz (i) are present where they are in contact with the remnant calcite (ca) of the shell. Gronant chert.
Width of field of photograph = 0.23 mm; ppl.

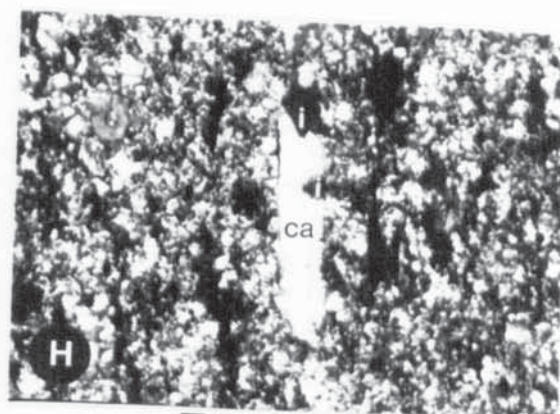
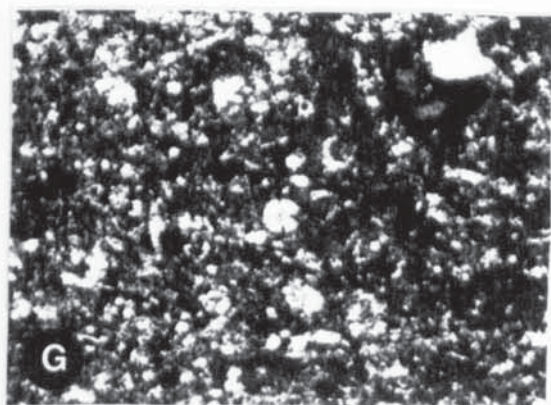
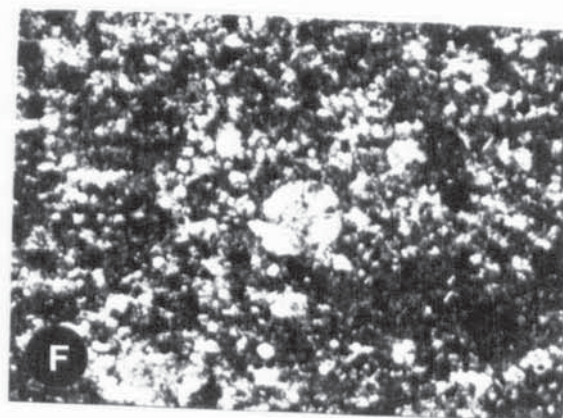
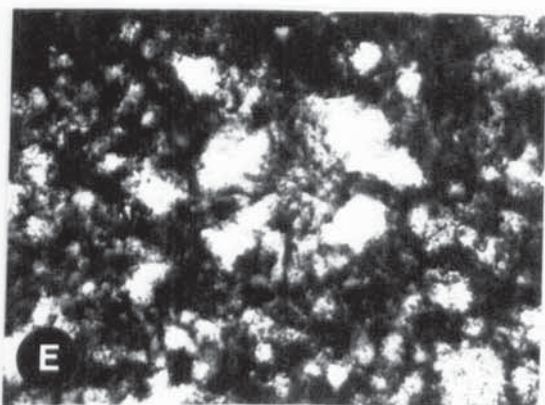
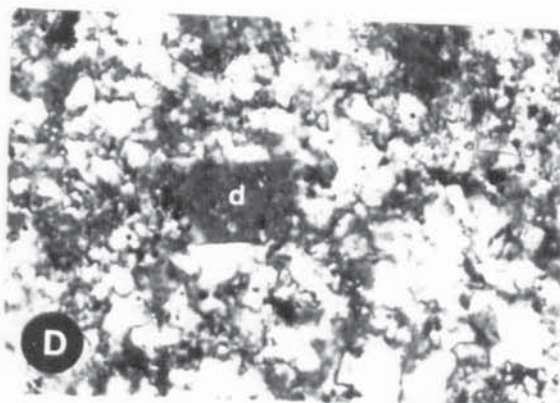
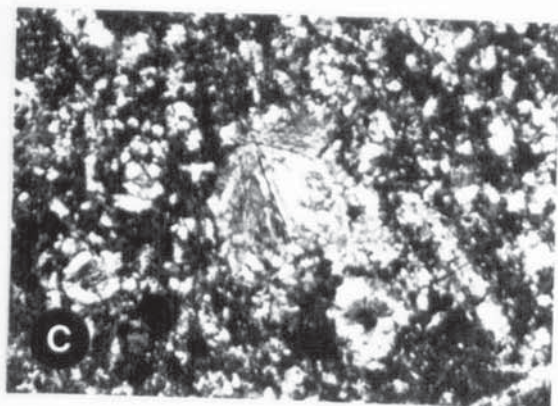
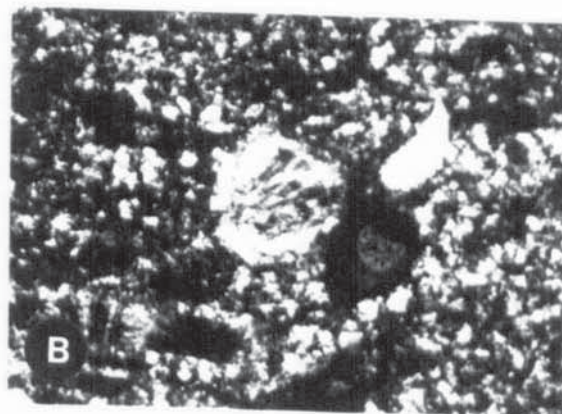
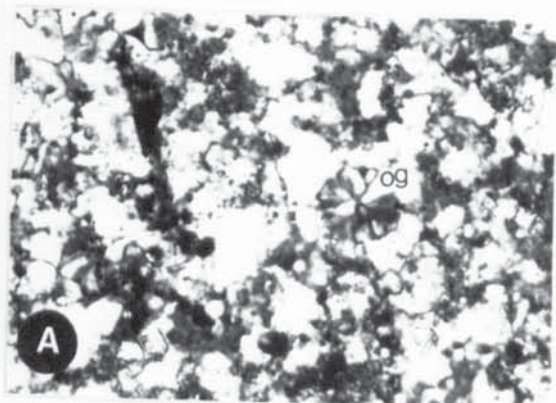


Plate 8.2

PLATE 8.3

All thin section photomicrographs

- A-B. Dolomite rhombs (d) and well crystalline non-ferroan calcites (ca) replacing chert (ch) along a fracture in the Gronant chert. Note also the occasional pseudomorphs of ferroan calcite (fe) after non ferroan calcite, which indicate that ferroan calcite post dates non ferroan calcite.
Width of field of photograph - 0.23 mm; XN
- C. Quartz overgrowth developed in a detrital quartz grain; Llanarmon-yn-ial cherty flags.
Width of field of photograph - 0.23 mm; XN
- D. Marcasite crystal (m) is floating on a chert fabric (ch). Gronant chert. polished thin section. ppl.
Width of field of photograph - 0.23 mm.
- E-F. Dolomite grains (d) appear to be intergrown with aggregates of framboidal pyrite (p). For explanation see text. polished thin section. ppl.
Width of field of photograph - 0.23 mm
Gronant chert.
- G-H. Cloudy centred dolomite rhombs. Presumably the cloudy centre is resulted from dolomite replacement of carbonate allochems. For details, see text. Gronant chert.
Width of field of photograph - 0.23 mm; XN.

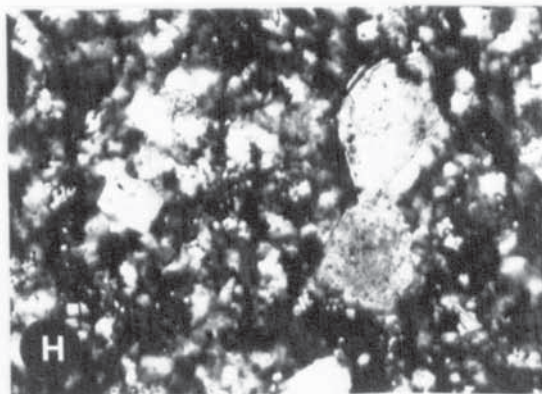
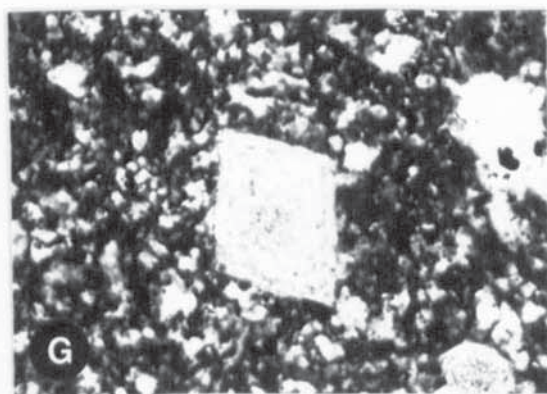
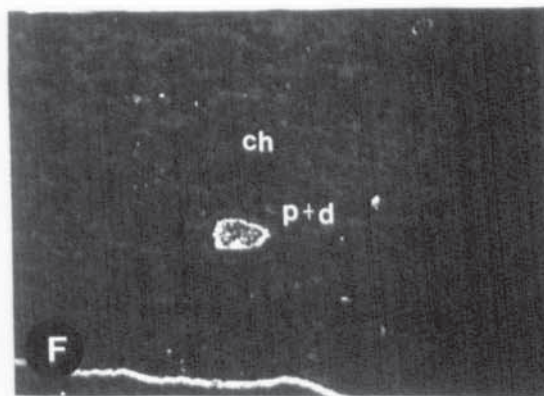
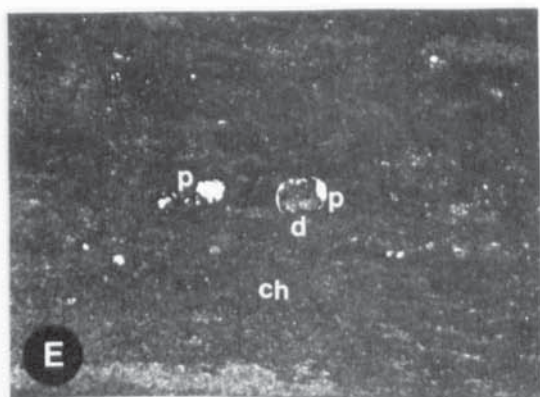
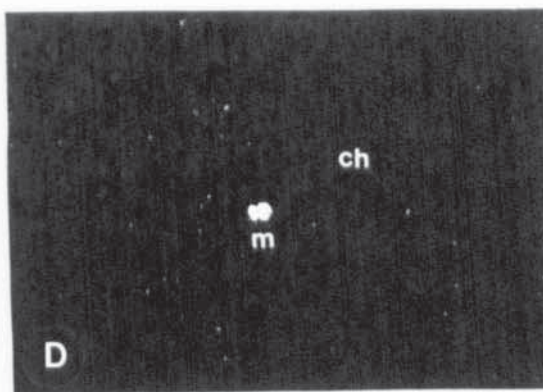
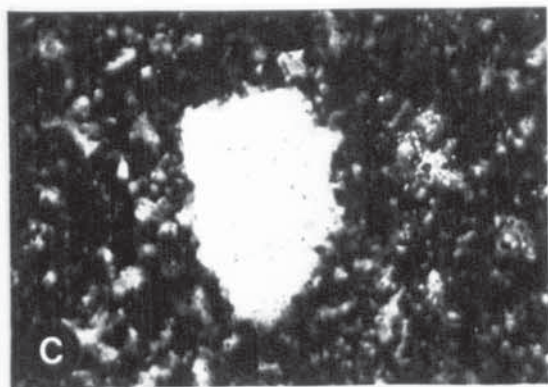
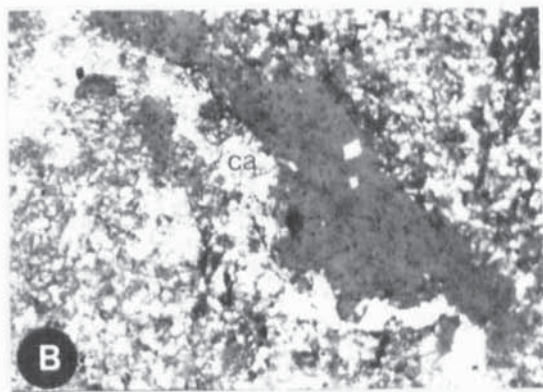
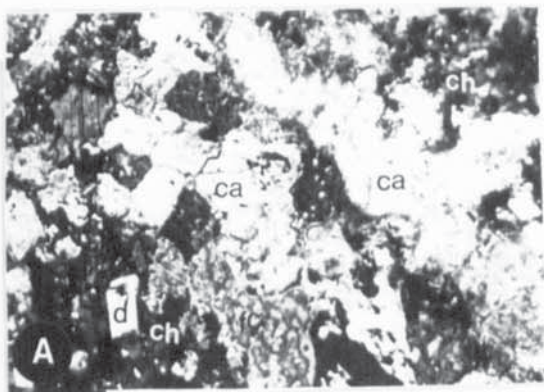


Plate 8.3

PLATE 8.4

All SEM photomicrographs (Gold coating)

A-H. SEM photomicrographs of biogenic constituents of the Gronant chert and the cherty flags.

A-F: showing slightly to highly dissoluted abundant longitudinal sponge spicules. Note the presence of massive opal-CT (T) on and around the spicule molds. os = unknown bivalve ostracod shell fragment.

A-E = Gronant chert. F= Llanarmon-yn-ial cherty flags.

G-H = Highly dissoluted radiolarian test (R) found in the Gronant chert.

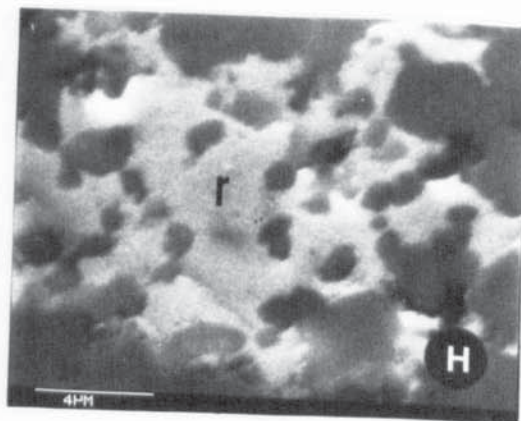
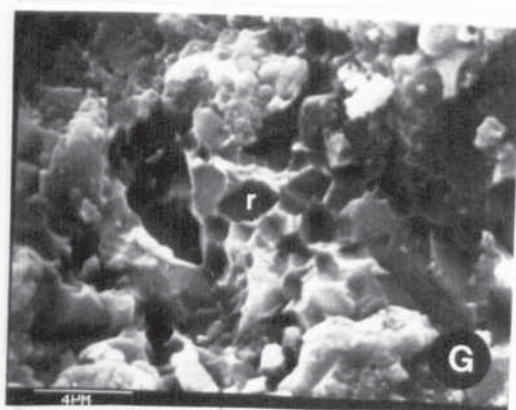
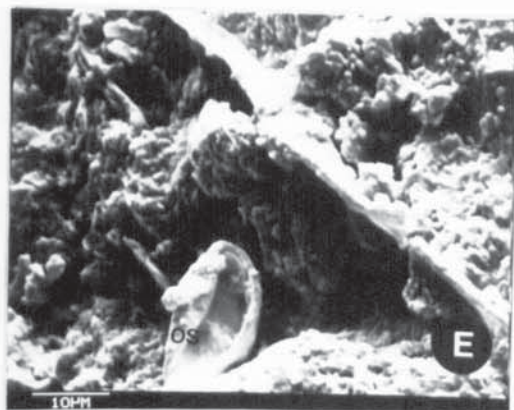
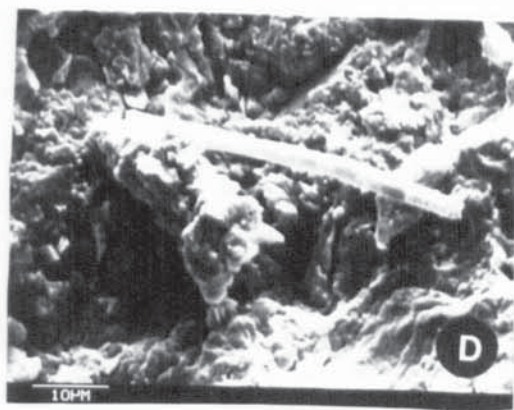
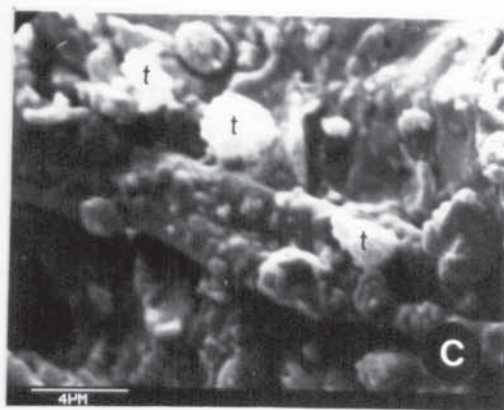
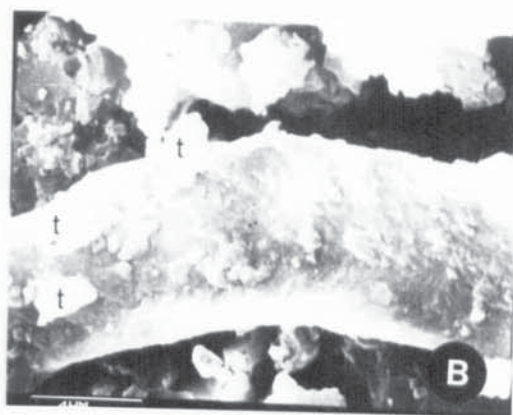


Plate 8.4

PLATE 8.5

All SEM photomicrographs (Grönant chert) (Gold coating)

- A. Subequant to polyhedral microquartz crystals are associated with highly *corroded* radiolarian test (r). These radiolarians together with sponge spicules and diatoms are presumed to be the main source of silica in these sediments.
For details see text.
- B. Highly *corroded* radiolarian test (r).
- C. Isolated occurrence of subequant to polyhedral microquartz crystals - resulting from replacement of shell fragments.
Crystallinity index of such quartz crystals is low.
For explanation see text.
- D. Enlargement of above.
- E. Similar features to 'c' above.
- F. Calcite shell fragment (cs) is being replaced by microquartz (mg).
The net result is elongate crystal shape.
- G-H. Enlargement of 'F'.

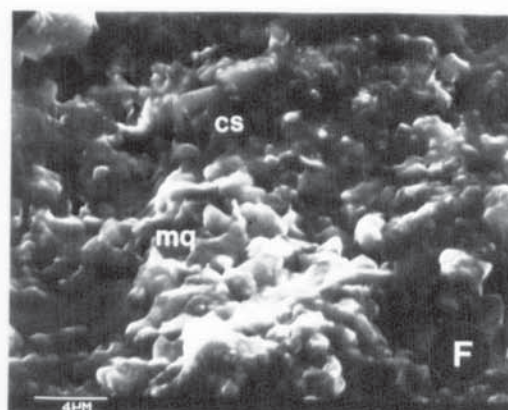
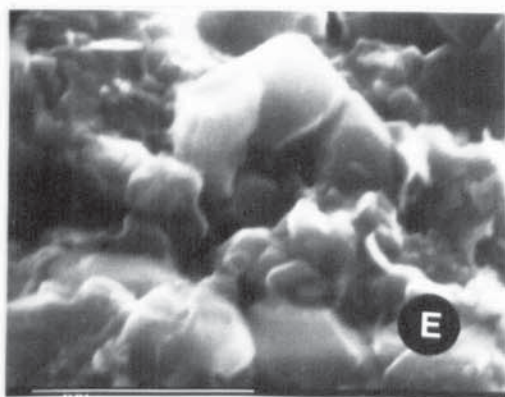
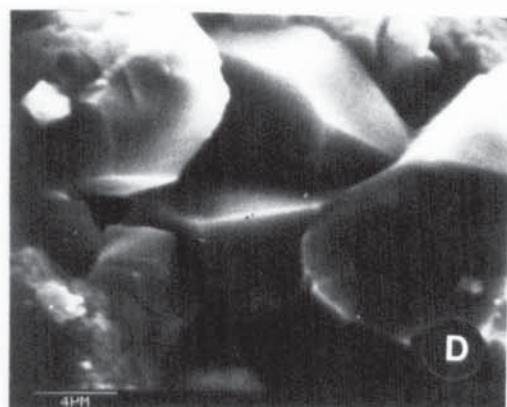
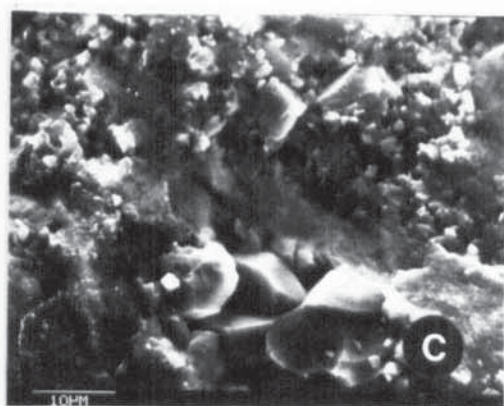
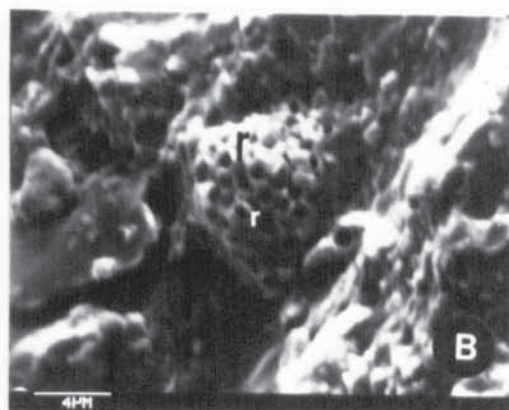
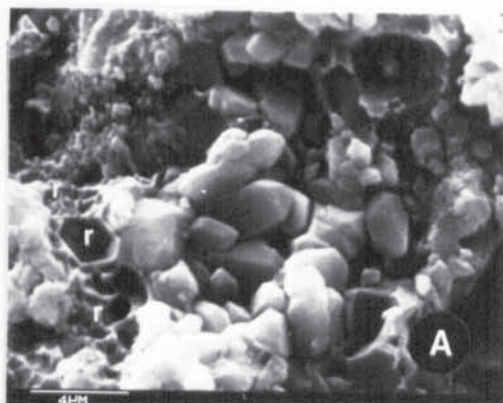


Plate 8.5

PLATE 8.6

All SEM photomicrographs (Gold coating)

- A. Coating of detrital illite clay (di) has prevented quartz overgrowth formation (o) in places. Note also in illite free areas quartz overgrowth is well developed.
Llanarmon-yn-ial cherty flags.
- B. Enlargement of above.
- C. Representing similar feature as mentioned in 'A'.
Llanarmon-yn-ial cherty flags.
- D. Illite of detrital origin (di). Llanarmon-yn-ial cherty flags.
- E. Isolated euhedral quartz crystal.
Llanarmon-yn-ial cherty flags.
- F. Microquartz (Mq) is replacing trilete miospore (ts).
Gronant chert.
- G. Microquartz (Mq) is replacing calcite shell fragment (Cs).
Gronant chert.
- H. Highly dissoluted dolomite rhomb (d). Note. replacement origin of microquartz.
Gronant chert.

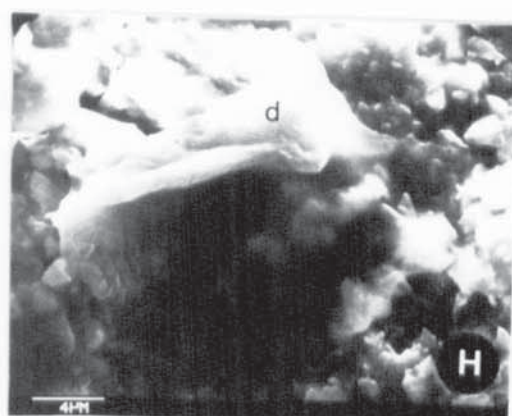
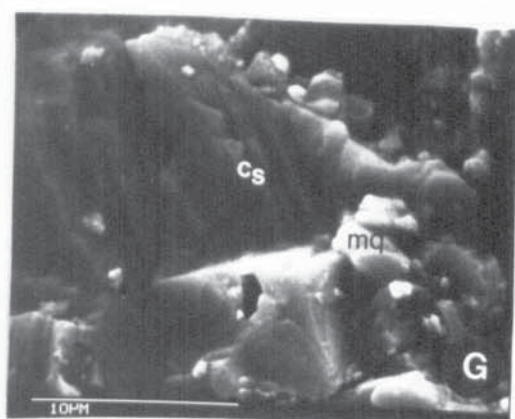
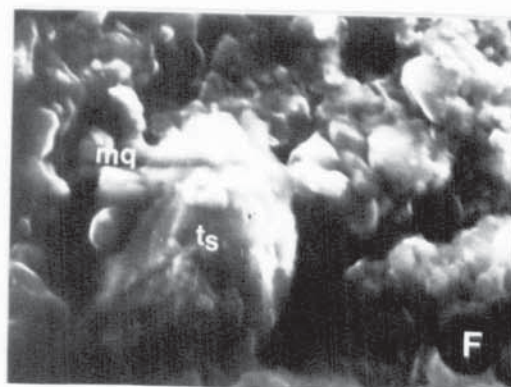
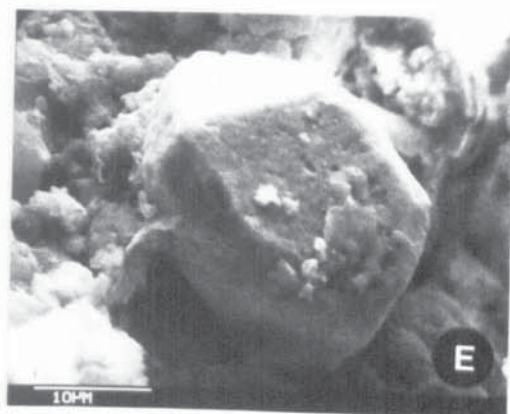
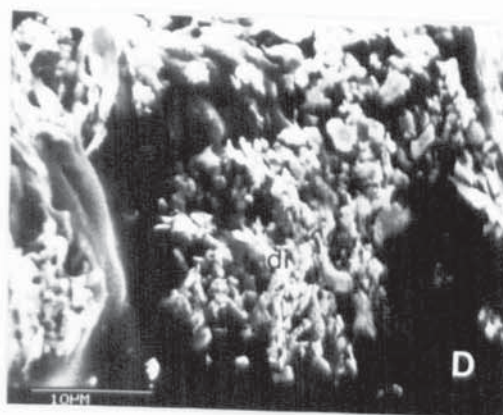
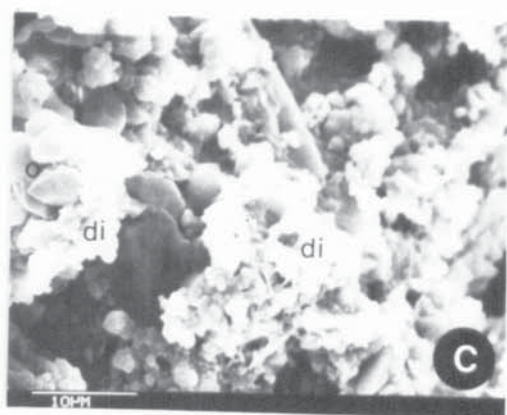
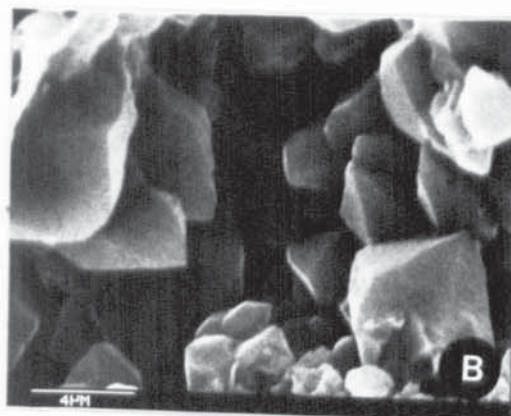
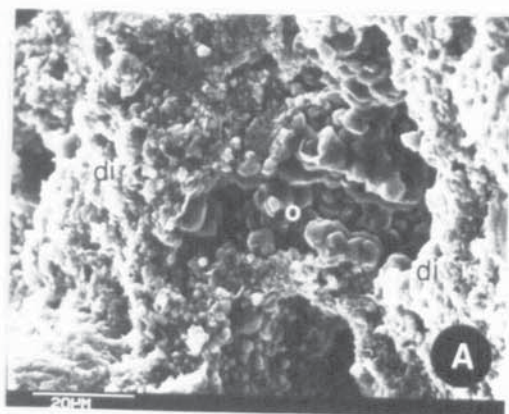


Plate 8.6

PLATE 8.7

All SEM photomicrographs (Gold coating)

- A-G. Dissolution of dolomite rhombs. Note: there is evidence of chert-carbonate replacement reversals. Note also massive opal-CT (t) is associated with the dissolved dolomite.
Ch. = chert fabric.
Gronant chert.
- H. Dolomite rhomb (d) replacing chert (Ch) along a vein in the Gronant chert.

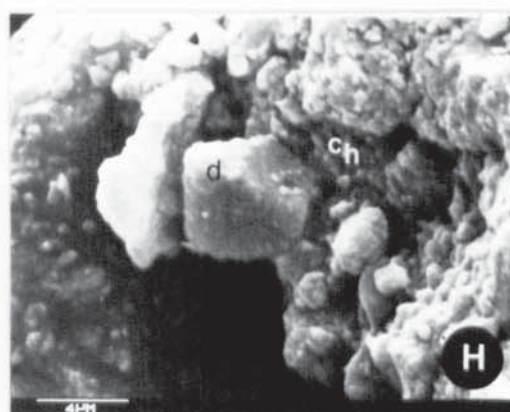
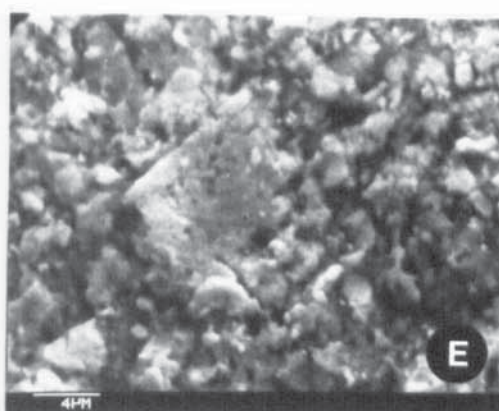
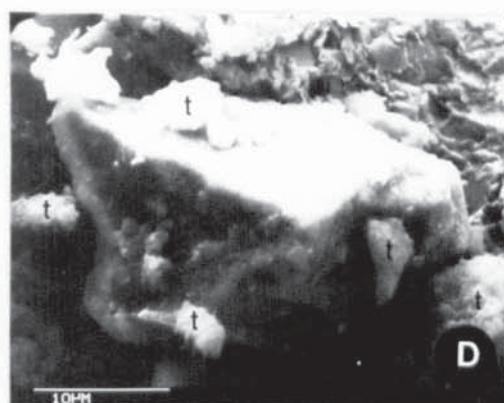
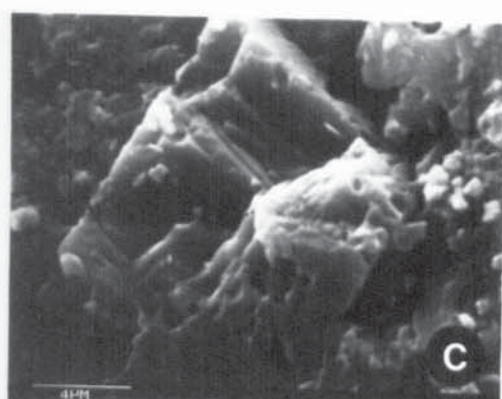
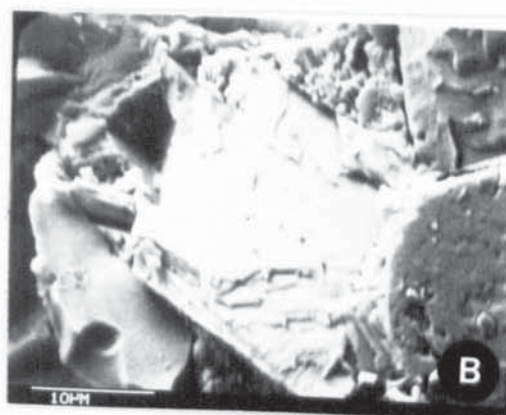
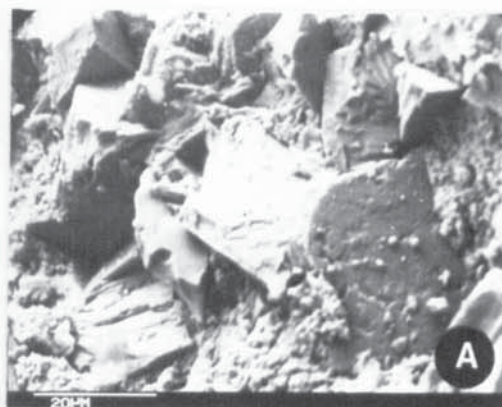


Plate 8.7

PLATE 8.8

All SEM photomicrographs (Gold coating)

- A. Pseudomorphs of rhombic dolomite after chert fabric.
Gronant chert.
- B. Enlargement of above.
- C. Dissolution of dolomite rhombs (d). Note: microquartz (mq) is replacing dolomite rhombs.
Gronant chert.
- D. Spherical shaped pyrite framboids on the cherty groundmass.
Polished rock chip.
Gronant chert.
- E. Possible massive, rounded opal-CT.
Gronant chert.
- F. Secondary porosity is resulted from the dissolution of calcite crystal. EDAX spot analysis reveals that the white areas of the photograph are calcite (c) and the dark areas are chert fabric (Ch).
Polished rock chip.
Gronant chert.
- G. Veinlet cut across the chert fabric (Ch). Note the dolomite rhombs (d) are pseudomorphous after chert fabric near the veinlet.
Gronant chert.
- H. Silt size microcrystalline calcite pseudomorphous after chert fabric. A vadose diagenetic origin is proposed for them. See text for explanation.
Gronant chert.

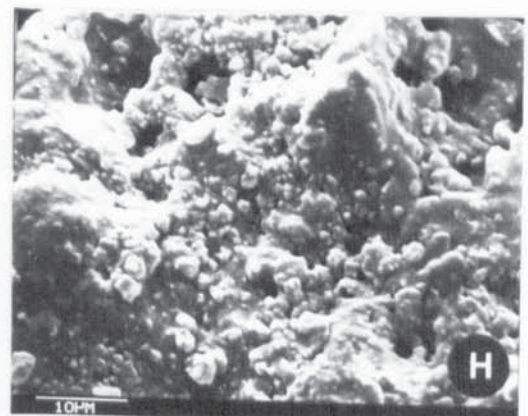
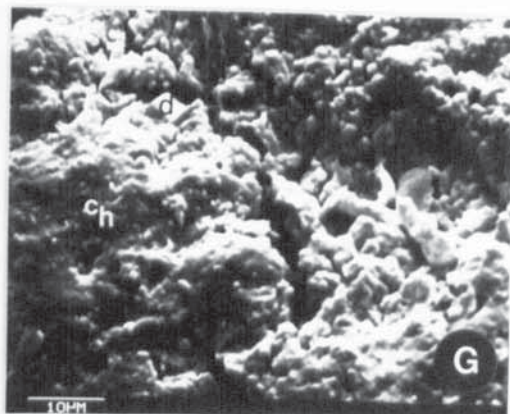
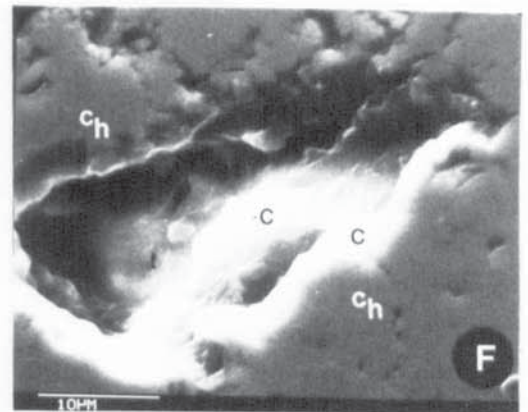
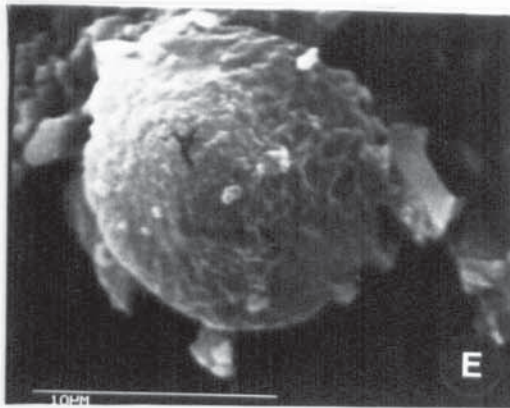
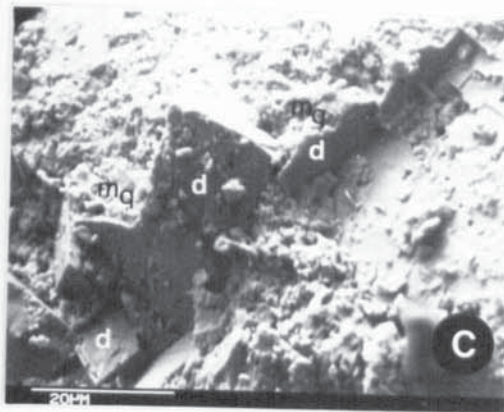
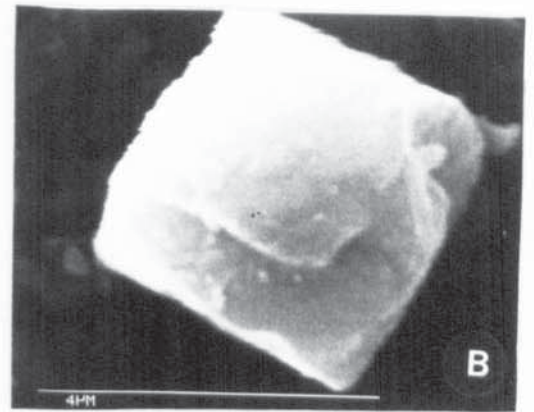
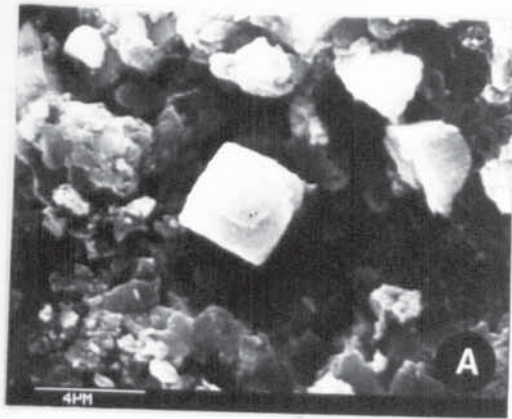


Plate 8.8

PLATE 8.9

- A. A possible "Liesegang rings" in the Gronant chert.
- B. Generally bedding occurs as laminae and thin beds upto 1 cm thick in the Gronant chert. Note the presence of porcellanite inclusions (Pc) with the bedding planes. Note also the presence of fractures (b). For explanation see text.
- C. Plant fossil ? Adinities machaneki. Note the presence of one goniatite species ? Posidoniella sulcata in the shaded area. Gronant chert.
- D. Organic material is aligned in fairly continuous laminae set in a finely crystalline non ferroan calcite matrix. There are conspicuous jagged stylolites in these layers which are black lined due to the concentration of organics during ? pressure solution of the calcite. One smaller vertical stylolite is also present. Chert fabric (Ch) is obvious towards the top of the photograph. The quartz here is a microcrystalline replacement and encloses clusters of micrite particles. Note: pyrite framboids are also present. Gronant chert. Thin section photomicrograph. ppl. Scale: x 50.

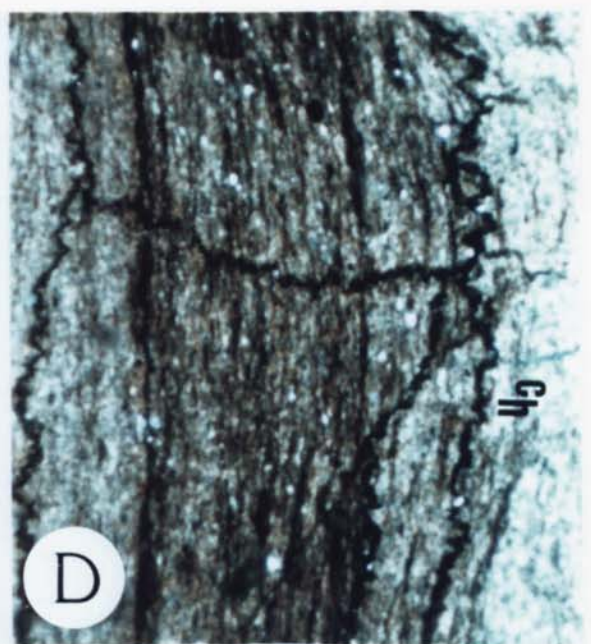
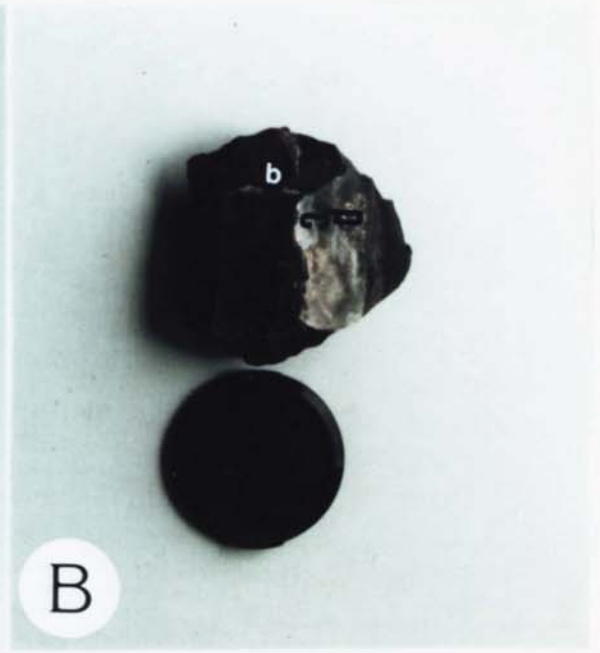


Plate 8.9

PLATE 8.10

All Cathodoluminescence photographs

- A. Two distinct luminescence colours are obvious:
(i) a bright red-orange luminescence non-ferroan dolomite and dolomitized shell fragments and
(ii) bright-yellow luminescence ferroan dolomite. Note the dark areas are chert fabric. Note also a vadose diagenesis origin is considered for the tiny, red-orange microdolomite crystals (for detailed explanation see text).
Field of view (approximately) 1.8 mm.
- B. Note in the middle of the photograph a bright red-orange luminescence dolomite rhomb is surrounded by a thin, bright-yellow luminescence ferroan dolomite rim.
Field of view (approximately) 1.8 mm.

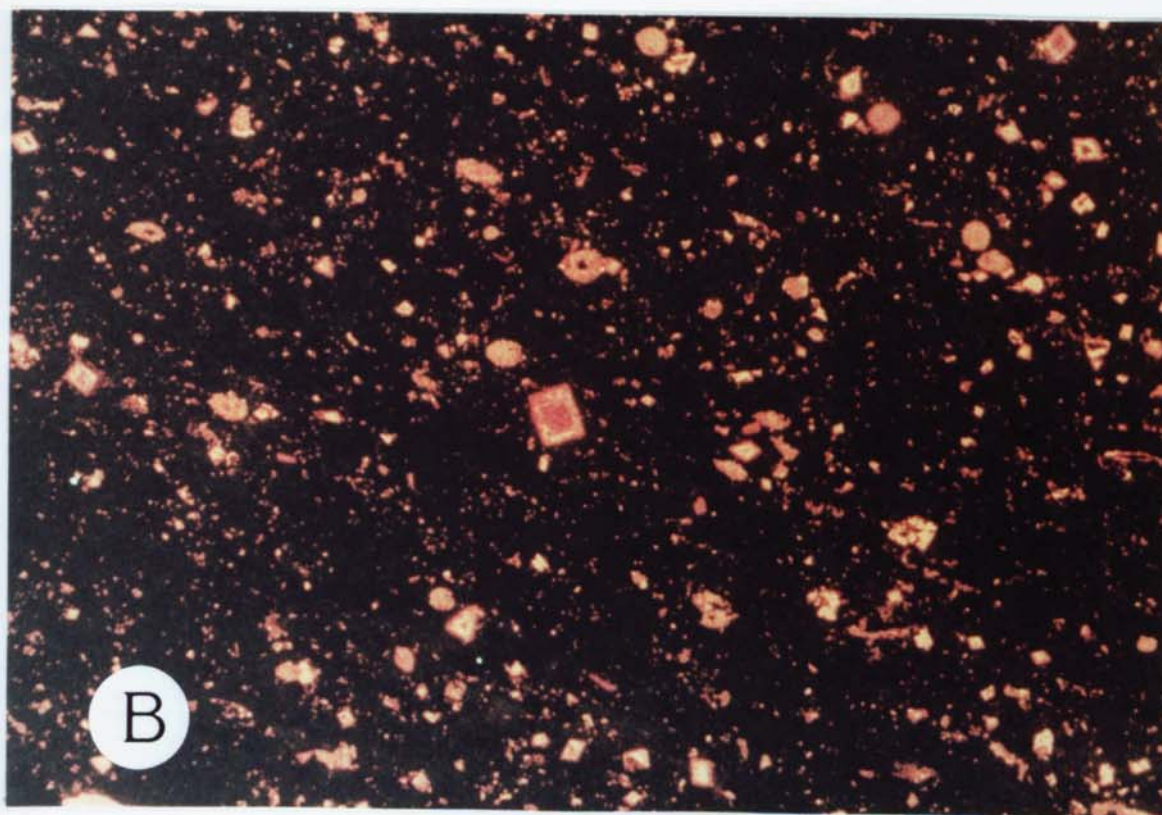
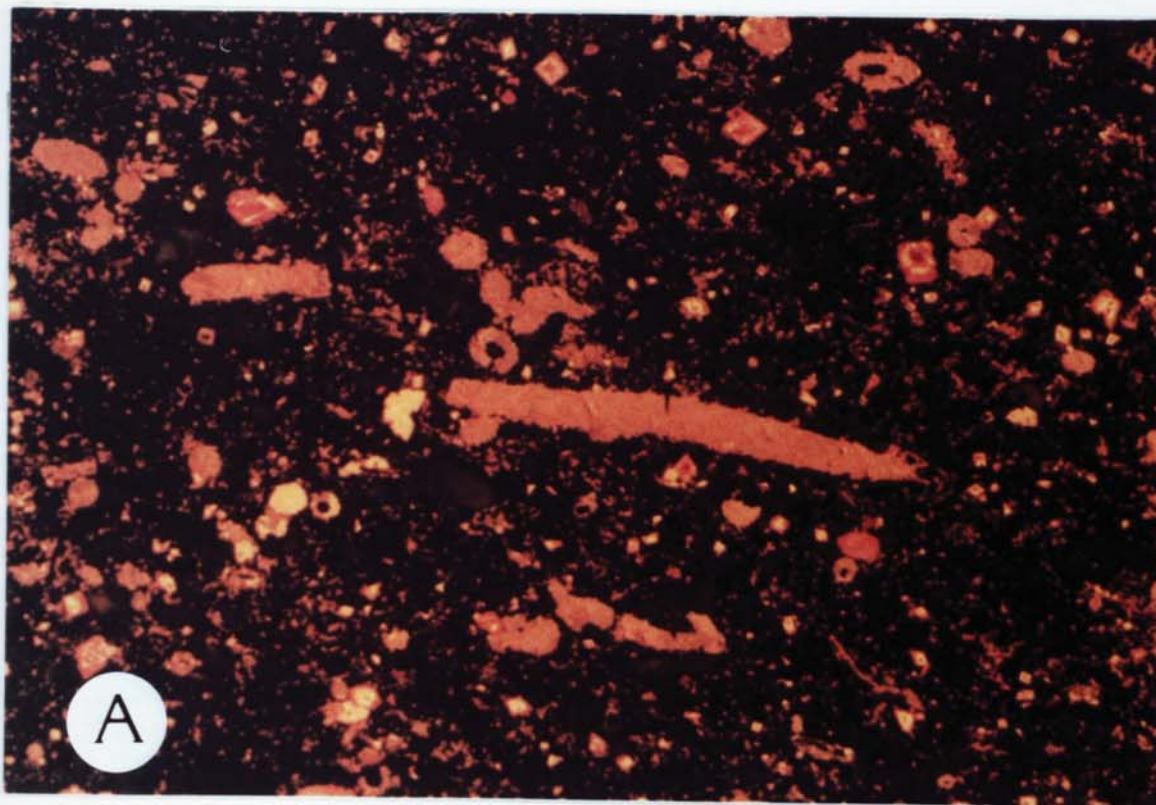


Plate 8.10

PLATE 8.11

- A. Note carbonate cements (ferroan dolomite) on calci-spheres. Note also dolomitized shell fragments.
Field of view (approximately) 1.8 mm.
- B. Note dull red-orange luminescence dolomitized calci-spheres and other shell fragments.
For details see Pl. 8.10 A; B.
Field of view (approximately) 1.8 mm.

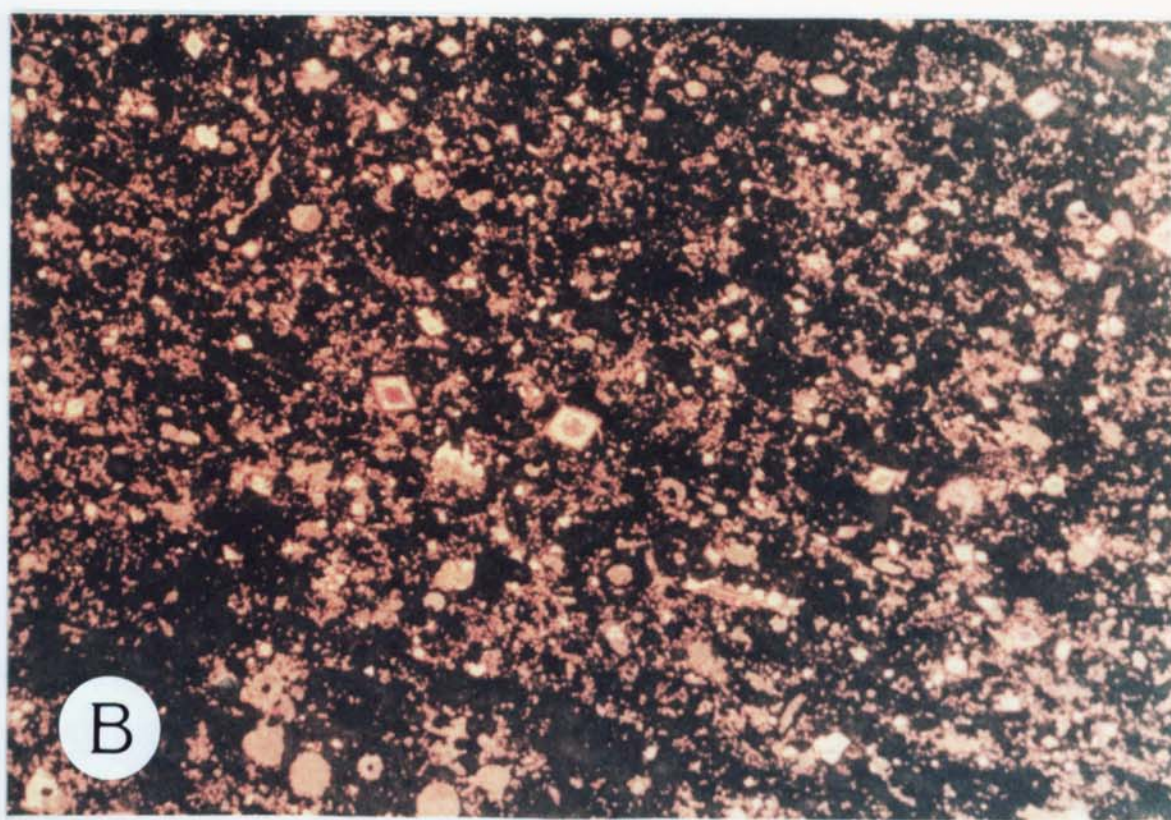
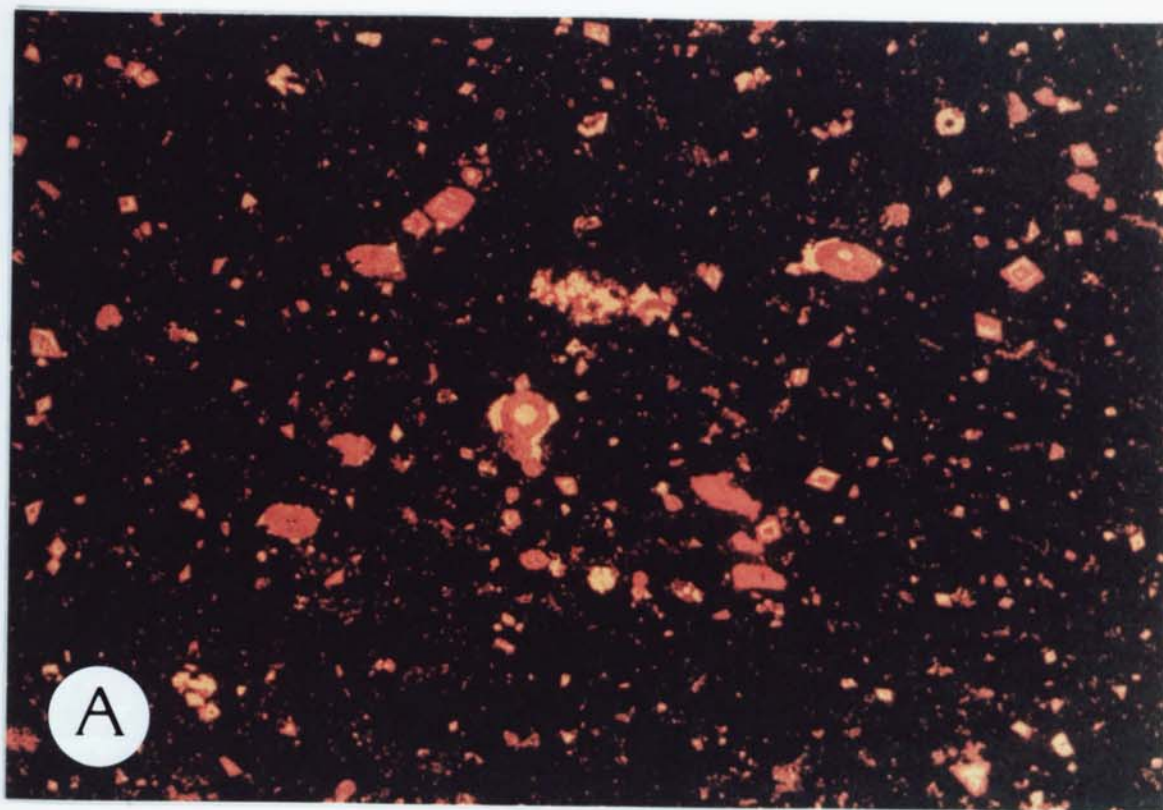


Plate 8.11

CHAPTER 9

GEOCHEMISTRY OF THE TERRIG RIVER SHALE AND THE BWLCHGWYN MINERA SILICEOUS SHALE UNITS

9.1 INTRODUCTION

This chapter deals with the organic and inorganic geochemistry of the 'Terrig River Shale and the Bwlchgwyn-Minera Siliceous Shale Units'. The location of the samples is shown in Fig. 1.1.

The results were statistically analysed and an attempt made to link the geochemical data with petrographic, mineralogical, palynofacies and palynological observations in order to build up a clear picture of diagenesis of the sediments under survey.

9.2 ORGANIC GEOCHEMISTRY

This section describes the examination of solid organic matter particularly vitrinite, in selected shale and coal samples encountered during the present investigation and links relations between their vitrinite reflectance values and the level of thermal metamorphism (LOM) using the nomogram of Hood *et al.* (1975), in order to deduce diagenetic temperatures for quartz cementation and illitization of the associated sandstones and shales. In addition, an attempt has also been taken to infer the petroleum generation capability of the sediments under consideration using the nomogram of Hood *et al.* (1975) and Vassoyevich *et al.* (1970). The results obtained are consistent with those obtained from the clay mineral diagenesis of these sediments.

All together ten samples (seven shales + three coals) were selected to determine their vitrinite reflectance values. Out of seven shale samples, two each were taken from the Bwlchgwyn quarry area (SJ 2596 5311),

Minera old quarry (SJ 258 530) and the Terrig River Section (SJ 2313 5623). One each from the Llanarmon-yn-ial cherty flags unit (SJ 2180 5655) and the Rhyd-y-Ceirw Coal Band (Terrig River Section) and the other two (Aqueduct + Chwarelau Coal Seam) were taken from the Australia Marl pit area. The age and stratigraphic positions of all these samples were determined palynologically during the present investigation and are given in detail in the 'Biostratigraphical Palynology Chapter 4'. The Gronant chert samples were not included in this study mainly because of their calcareous nature.

Random reflectance measurement was undertaken in order to avoid rotation of the microscopic stage. Details of the sample preparation and other methodologies involved are given in Appendix

9.3 VITRINITE REFLECTANCE

Vitrinites have low hydrogen content and high oxygen content. They consist mainly of aromatic structures, with short aliphatic chains connected by oxygen containing functions. Vitrinite is mostly derived from structured woody (lignified) materials and has limited potential for oil, but high potential for gas (Brooks, 1981). The vitrinite group includes tellinite, the cell wall material of land plants, and collinite, the substance that fills the cell cavities. The reflectance and the rate of maturation of these two submacerals are about the same. The reflectance of light on a polished surface of vitrinite increases with maturation because of a change in molecular structure of the maceral. Vitrinite is composed of clusters of condensed aromatic rings linked with chains and stacked on top of each other. With increasing maturity, the clusters fuse into larger, condensed aromatic ring structures. Eventually they form sheets of condensed rings that assume an orderly structure. The increase in the size of these sheets and their orientation causes increased reflectivity. Where anisotropy is greatest the maximum and minimum reflectivity of vitrinite differ

considerably in the higher maturity ranges. That is why it is important to state whether the random or the maximum reflectivity is used. Either method is valid and the distinction is noteworthy mainly in the higher maturity range, i.e., $>1.0 R_o$ (the mean reflectivity of vitrinite is denoted by the symbols R_o or R_m oil). Most source rock maturity involves the R_o range from 0.2 to 2 percent.

Vitrinite maturation is not effected by pressure, only by temperature. Vitrinite histograms tend to broaden as rank increases. The mode with the higher reflectance represents recycled vitrinite, while that with the lower reflectance is primary vitrinite.

9.4 PREVIOUS WORK

The use of vitrinite reflectance as a technique for determining the maturation of sedimentary rocks was first described by Teichmüller (1958) in her study of the Wealden Basin, Germany. In 1961, studies of Ammosov and Tan were significant in showing the application of vitrinite reflectance in defining the limits of oil occurrence in several petroliferous basins of the U.S.S.R. Ting (1975) demonstrated from laboratory experiments that, reflectance, which measures maturation changes in sediments, will increase exponentially with a linear increase in temperature. Hood *et al.* (1975) proposed a model for predicting levels of organic maturation in source rocks in which the combined maximum temperature (T_{max}) and "effective heating time" (T_{eff}) were derived from their level of Organic Metamorphism (LOM) scale. This work together with Bostick's (1973) work could be regarded as a modification of Karweil's (1955) nomogram. Dow (1977) noted that vitrinite maturation is not effected by pressure, only by temperature and he further suggested that recycled vitrinite is very common in sediments. The same author successfully prepared vitrinite reflectance profiles for Cretaceous through Pliocene and Pleistocene sediments of the Louisiana Gulf coast using data

from 12 wells. Several other authors like Castaño and Sparks (1974), Houseknecht (1984), used vitrinite reflectance values in order to interpret burial history and palaeotemperatures of diagenesis. Unfortunately, no previous reflectance data is seen by the present author on the Namurian shales of North Wales. However, Creaney (1980) described petrographic texture and vitrinite reflectance variation on the Alston Block, north-east England. The same author in 1982 determined vitrinite reflectance values from the Beckermonds Scar and Raydale Boreholes, Yorkshire. But the Geology of these areas is quite different from those localities in North Wales under present consideration.

9.5 INTERPRETATION OF THE PRESENT VITRINITE REFLECTANCE DATA

In the present survey the results are expressed in terms of mean random vitrinite reflectance (Ro%) measured at 546 nm under oil immersion (Zeiss immersion oil N = 1.518 at 546 nm) and presented in Table 9.1. The reflectance standards used were 0.306 and 0.904 (Ro random).

Vitrinite was identified as those particles appearing grey in reflected light which had reflectivities intermediate to inertinite and liptinite (Pl. 5.3 A, B).

It is rather difficult to reconstruct the absolute temperatures to which the samples under investigation were heated, but reasonable estimates can be made by using the relationships among thermal maturity, maximum temperature and effective heating time (i.e. the time elapsed during which a specific rock was within 15°C (27°F) of its maximum temperature) as discussed by Hood *et al.* (1975). See Figures 9.1 and 9.2. Table 9.1 summarises the thermal maturity and maximum temperature experienced by each sampling locality under consideration.

In the light of the tectonics and palynostratigraphy of the studied region, it is critical to clarify the sequence of events that could have influenced diagenesis of the Bwlchgwyn-Minera (and perhaps Ruabon) sandstone unit:-

Table 9.1: Thermal maturity and estimated maximum temperature for each sampling locality

Locations	Minera	Bwlchgwyn	Terrig River	Llanarmon-yn-ial Cherty flags	Rhyd-y-Ceirw Coal	Aqueduct Coal	Chwarelau Coal
Vitrinite reflectance Ro(%)	0.69	0.69	0.28	0.70	0.69	0.74	0.7
LOM ¹	9.0	9.0	<7.3	9.1	9.0	9.5	9.5
Tmax 280 my ² (°c)	56	56		62	56	72	72
Tmax 230 my ³ (°c)	60	60		65	60	78	78

¹ Level of organic metamorphism, estimated using conversion charts of Hood *et al.* (1975).

² Estimated using nomogram of Hood *et al.* (1975) and assuming an effective heating time of 280 million years.

³ Estimated using nomogram of Hood *et al.* (1975) and assuming an effective heating time of 230 million years.

- (i) deposition below the Middle Marsdenian stage (see Biostratigraphical Palynology Chapter 4).
- (ii) structural deformation as a result of late Armorican (or Hercynian) orogenic movements which took place at the end of the Carboniferous period.
- (iii) wide spread unconformity between the Carboniferous and the Triassic rocks (Wedd *et al.* 1927).
- (iv) gradual cooling and erosion to present configuration.

The Bwlchgwyn-Minera-Ruabon sandstone/siliceous shale units attained maximum depth of burial perhaps at the Middle Marsdenian stage, but did not reach maximum temperatures firstly until the end of Carboniferous and secondly in Lower Triassic times.

The assumed burial and thermal history can be used to predict the absolute temperatures by using the nomogram of Hood *et al.* (1975). Effective heating time mentioned above can be assumed to be about 280 million years on the basis of Hercynian orogenic movement and around 230 million years on the basis of regional unconformity between the Carboniferous and the Triassic rocks. Application of these constraining values to the temperature-time-thermal maturity nomogram of Hood *et al.* (1975) results in the estimates of maximum temperatures listed in Table 9.1.

Assuming the longer effective heating time (280 my), the rocks of the Llanarmon-yn-ial cherty flags; Bwlchgwyn-Minera-Ruabon sandstone/siliceous shale units; Rhyd-y-Ceirw Coal Band; and the Aqueduct and the Chwarelau coal seams would have been exposed to maximum temperatures



Illustration removed for copyright restrictions

Fig. 9.I. Some scales of organic metamorphism.
After Hood et. al. (1975).



Illustration removed for copyright restrictions

Fig. 9.2. Relation of LOM to maximum temperature and effective heating time. (After Hood et al. 1975)

of 62°, 56°, 56°, 56°, 72° and 72°c respectively. Similarly, assuming the relatively shorter effective heating time (230 my), the same rocks would have been exposed to maximum temperatures of 65°, 60°, 60°, 60°, 78° and 78°c respectively. The above temperature ranges for the Bwlchgwyn-Minera-Ruabon sandstone/siliceous shale units explain well the quartz cementation and the conversion of illite-smectite to illite in these sediments which will be discussed more fully in Chapter 11.

Table 9.1 and Fig. 9.1 further indicate that the studied shales and coals (except Terrig River Shale) can be correlated with the 'High Volatile Bitumen Coal Rank'. Similarly, the miospore colours encountered during the present investigation ranges from yellow and yellow to dark brown, which fits well with the proposed Coal Rank (Fig. 9.1).

From Table 9.1 it is also clear that the average reflectance value of the Terrig River Shale is much lower compared to the other average values, the reasons of which will be discussed here.

The present palynofacies data (Chapter 5) suggests that the majority of the organic matter in the Terrig River Shale is amorphous and is considered to be biodegraded algal material. The average organic carbon content of these samples is 2.57% (Appendix 9). Palynofacies data also suggest that the Terrig River Shale belongs to the 'Interdistributary bay shale facies' (Chapter 5).

Walker *et al.* (1983) noted that organic matter dominated by amorphous algal material matures at a significantly faster rate and thus at lower TTI values (time-temperature index of Lopatin, 1971), than structured organic debris. According to them vitrinite dispersed in dominantly amorphous sapropelic organic matter fails to develop the reflectance reached under equal conditions in vitrinite-rich kerogen. Similarly, Hutton and Cook

(1980) and Hutton and others (1980) indicate that algal material matures more rapidly than vitrinite and provide data suggesting that the degree of vitrinite reflectance in Australian coal having similar time-temperature histories is inversely proportional to the concentrations of algal material in the coals. They argued that "algal material, in response to increasing burial temperature, releases aliphatic rich compounds which are diffused onto the vitrinite while its reflectance is still quite low ($<0.6\% R$), thus depressing the reflectance values relative to the true thermal history of the sediment".

Thus, the high amount of amorphous, algal material of the Terrig River shale could be acting in a similar way in order to reduce the reflectances of the incorporated vitrinites. Hence, it would be wise to conclude that vitrinite reflectance is less definitive as an indicator of thermal maturation, at least, for the alginite-rich source rocks such as the present Terrig River shale.

On the other hand, maturation estimates based on spore colouration (yellow to dark brown) of the Terrig River shale suggest High Volatile Bitumen to Medium Volatile Bitumen, Coal Rank, corresponding to equivalent reflectance values $>0.78\% R_o$ (Figure 9.1). This value is significantly higher than the measured reflectance of only $0.28\% R_o$ (Table 9.1).

9.6 PETROLEUM GENERATION CAPABILITY OF THE SEDIMENTS UNDER CONSIDERATION

Vitrinite reflectance values can only suggest the level of maturation of the samples examined. They cannot predict the presence of oil and gas, because these frequently migrate updip along permeable beds or through fracture or fault systems to shallower reservoirs at lower levels of maturation. However, no major oil accumulations are associated with

reflectivities above about 1.3 percent and the larger gas fields are found in the Ro range from 1.3 to 3 percent.

The liptinite and vitrinite maceral group of coal are capable of yielding petroleum, while inertinite maceral has virtually no convertibility to hydrocarbons (Dow, 1977). Inertinite is generally regarded as 'dead carbon' because they are essentially unaffected by heat and their convertibility to Petroleum may approach zero (Erdman, 1975).

In the following the application of the LOM scale as proposed by Hood *et al* (1975) was used in conjunction with the principal stages of petroleum generation as introduced by Vassoyevich *et al* (1970), to infer the petroleum generation capability of the sediments under consideration. The correlation of Vassoyevich's stages with the LOM scale via percent volatile matter is shown in Figure 9.3. The correlation nomogram suggests that the stage of formation of diagenetic methane and the three principal stages of generation of oil, condensate plus wet gas, and high temperature katagenetic methane fall in LOM ranges of <7.8, 7.8-11.6 (mainly 9-10), 11.6-13.5, and >13.5 respectively. Figure 9.3 also suggests that the maturation of source rock hydrocarbons can make oil generation possibility. Hood *et al* (1975) from laboratory experiments suggest that the compositions of source rock hydrocarbons first become crude oil like (mature) in the LOM range of about 9 to 11.5. It is clear from the Figure 9.3, that the zone of initial maturity occupies essentially the high LOM (two thirds of Vassoyevich's oil stage) typically represents oil generation. This indicates that at least the low LOM (one third of Vassoyevich's oil stage) is from oil generation without reaching maturity - therefore without effective oil expulsion from the source rock.

From Table 9.1 it is seen that apart from the Terrig River shale, the LOM values of the rest of the samples including coals fall near the boundary

1

between the immature zone and the zone of initial maturity. This suggests that all these samples belong to Vassoyevich's 'oil stage' without reaching maturity (Fig. 9.3), - therefore without effective oil expulsion from the source rock. The above conclusion is in close agreement with the clay mineral diagenesis of these sediments which will be discussed now.

The clay mineralogy of these siliceous shales (Terrig River shale and coals are not included) is dominated by illite and dickite; a trace amount of mixed layer illite-smectite is also present in a few samples, while smectite and chlorite are totally absent (see Chapter 11). Though some of the illites are detrital in the shales, the associated sandstones contain mainly authigenic kaolinite, authigenic illite and very rare dickite and mixed layer illite-smectite (see Chapter 11). It is well known that smectite dehydration occurs in the temperature range of the liquid hydrocarbon generation and the conversion of smectite to illite through mixed layer illite-smectite is important in flushing oil from its source rocks (Powers, 1967; Burst, 1969). Smectite-illite transition is associated with the release of water and according to Powers (1967) this begins at a depth of about 1800 m in the Gulf Coast corresponding to a temperature of about 90°C (Perry and Hower, 1972). On the other hand, Lahann (1980) concluded that extensive secondary silicification may be an indication that the illitization reaction has taken place at low temperature

(~ 50°C). Lahann's (1980) conclusion is in close agreement with the sediments under consideration and also the temperature range given by Lahann (1980) is consistent with the temperatures obtained from vitrinite reflectance technique in this investigation (see Table 9.1). Details of the clay mineral diagenesis are referred to in Chapter 11.

It is certain that the temperatures obtained during the present survey are much lower than the temperature range needed (90°-120°C) for the generation of liquid hydrocarbon. Moreover, the process of illitization in



Aston University

Illustration removed for copyright restrictions

Fig. 9.3.

ORGANIC METAMORPHIC STAGES OF PETROLEUM
GENERATION AFTER VASSOYEVICH ET AL (1970)

these samples is much lower compared to the extensive quartz cementation (particularly in the sandstones) which might indicate, according to Lahann (1980) that the temperature of the shales never rose rapidly to 100-120°C during the course of diagenesis. Hence, no effective flushing of hydrocarbon from the source rocks can be expected (but time can play a significant role in this case). However, this result is in accord with the results obtained from Vassoyevich *et al.* (1970) principal stages of oil generation as shown in Fig. 9.3.

The results are consistent with the absence of hydrocarbon inclusions in these sediments.

As mentioned earlier the Terrig River shale is essentially alginite rich and hence gives anomalously low reflectance of vitrinite. Thus the reflectance values obtained are definitely an unreliable indicator of the maturity of these intertributary bay shales. However, Walker *et al.* (1983) also noted low reflectance of vitrinite (0.13% to 0.41% Ro) from the Miocene Modelo Formation in the Los Angeles Basin, California and remarked by saying, "the low vitrinite reflectance values measured in this study confirm that commercial quantities of oil can be associated with Ro and TTI values below the range considered indicative of significant petroleum generation". It should be noted here that the above authors also dealt with alginite-rich shales.

9.7 INORGANIC GEOCHEMISTRY

In this section the major and trace element geochemistry of the 'Terrig River shale' and the Bwlchgwyn-Minera siliceous shale units were studied in detail and mineralogical distributions calculated.

Analysis was mainly by X-ray fluorescence (XRF) and X-ray diffraction (XRD). Mineralogical calculations were done using a computer technique as proposed by Ashby and Pearson (1979). Quartz was determined after

Raish (in Carver, 1967). The determination of organic carbon is described in Chapter 6. Detailed methodologies involved are given in Appendix 6 and Appendix 8. The results were statistically analysed in order to ascertain the following:-

- i) redox parameters by using Cu/Zn ratio as put forward by Hallberg (1976)
- ii) grain size: $\text{SiO}_2 / \text{Al}_2\text{O}_3$ (Bjorlykke, 1974)
maturity: $M = (\text{K}_2\text{O} + \text{Al}_2\text{O}_3) / (\text{Na}_2\text{O} + \text{MgO})$; $\text{K}_2\text{O} / \text{Na}_2\text{O}$ (Bjorlykke, 1974); $\text{Rb} / \text{K}_2\text{O}$ (Wedepohl, 1969; Bjorlykke, 1974; Dypvik, 1977).
- iii) the relations between quartz and Zr; quartz and Corg; quartz with Na and K in order to determine the energy of the depositional environment
- iv) to relate the clay minerals with the different geochemical ratios in order to have a better picture of the conditions of deposition and the diagenetic changes there of.
- v) element (R-mode) dendrograms were done to obtain a better understanding on the distributional trend of the major and trace elements of the sediments under survey.
- vi) to find out the organic carbon and trace element relationship in the Bwlchgwyn-Minera siliceous shale and the Terrig Rivershale. In doing so, palynological and palynofacies results were used to support the geochemical data.
- vii) a table was constructed to show the distribution of important major and trace elements against miospore assemblages as proposed in Chapter 4.
- viii) correlation was done whenever possible with the 'Geochemistry of Irish Namurian argillites' after Sulaiman (1972) and the 'Geochemistry of the Namurian Marine and Non-Marine Shales' Derbyshire, England (Spears and Amin, 1981).

It would be wise to mention here the following:-

firstly, the stratigraphical position of the Terrig River shale and the

Bwlchgwyn siliceous shale as shown in Figures (9.4 and 9.5) is based on their biostratigraphy as proposed in Chapter 4, and secondly, as the Bwlchgwyn and Minera siliceous shale belong to the same age (Chapter 4) and have very similar geochemical properties, Minera siliceous shale is not included in the above figures for the sake of simplicity.

9.8 GRAIN SIZE, MATURITY AND REDOX PARAMETERS OF THE TERRIG RIVER SHALE AND THE BWLCHGWYN AND MINERA SILICEOUS SHALE UNITS

The Terrig River shale is made up of quartz (about 52.0%); 10Å clay mineral, illite (about 41.0%); siderite (about 3.0%) and organic carbon (about 3.0%). In addition, trace amounts of feldspar, pyrite and apatite were also detected (Fig. 9.5). On the other hand, the Bwlchgwyn and Minera siliceous shale is dominated by quartz (about 59.0%) together with 7Å clay mineral, dickite (about 20.0%) and 10Å clay mineral, illite (about 13.0%); siderite (about 4.0%) and organic carbon (about 4.0%). Moreover, trace amounts of kaolinite, feldspar, pyrite, apatite and anatase were also noticed (Fig. 9.5). It should be noted here that kaolinite is the only 7Å clay mineral in the interbedded sandstones.

The grain size parameters studied show the relatively coarse grained Terrig River shale to have a very weak upwards coarsening tendency. Similarly, all the maturity parameters (M , Rb/K_2O) show an upwards increasing maturity. Cu/Zn ratio of the Terrig River shale indicates that the lower part of the shale experienced reducing conditions (Fig. 9.4; this is also consistent with the trace amount of pyrite in the lower part - see Fig. 9.5), while the upward decreasing Cu/Zn values suggest increasing oxidizing conditions.

The average organic carbon and P_2O_5 contents of these shales are about 3.0 and 0.25 wt.% respectively. The measured concentrations of Ni, Cu, Rb

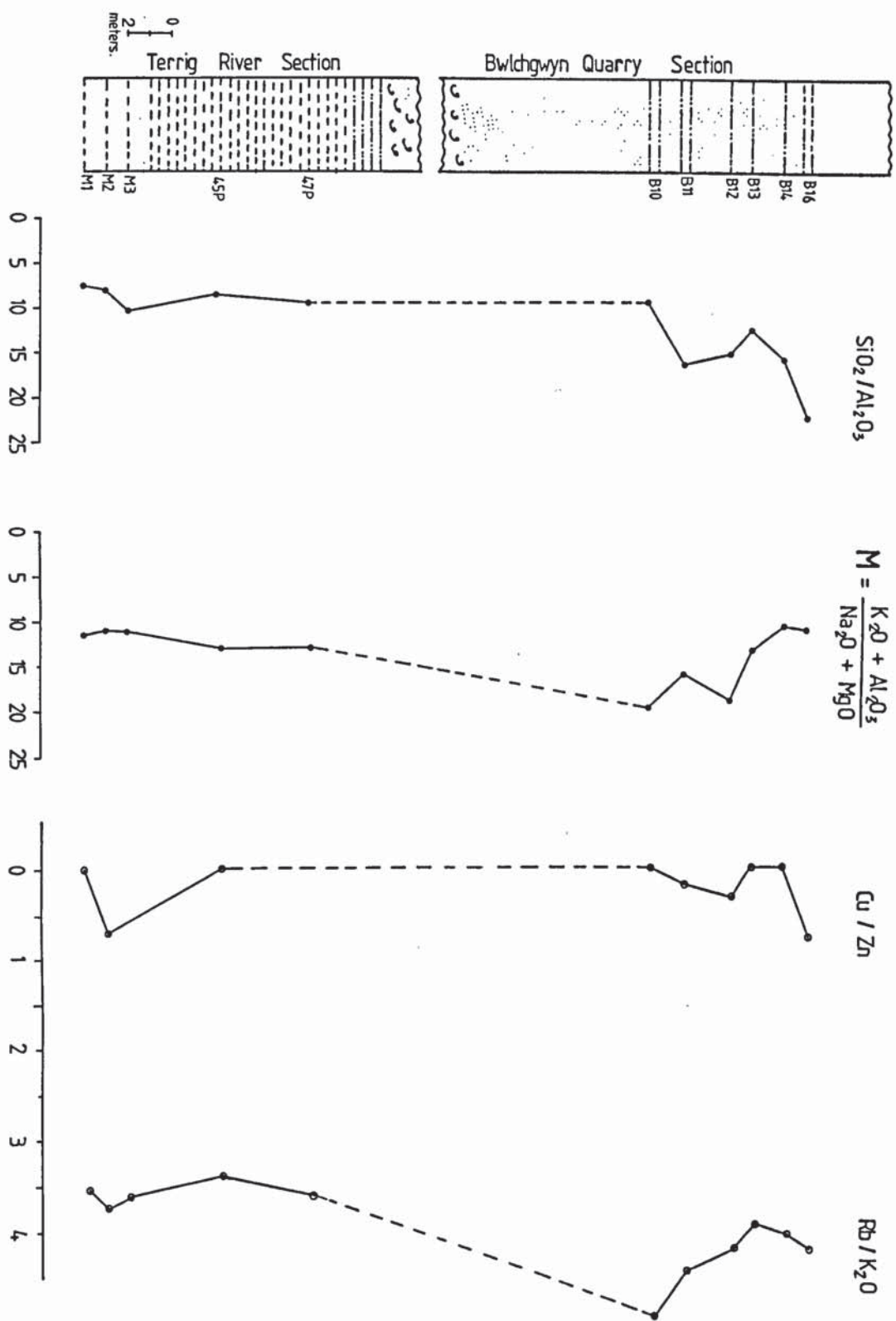


FIG.9.4.

Some geochemical distributions through the Namurian in North Wales. The SiO_2/Al_2O_3 ratio is a grain size parameter. The $M = (K_2O + Al_2O_3) / (Na_2O + MgO)$ and Rb/K_2O ratios give information on the maturity of the sediments. Cu/Zn ratio is redox parameter indicator.

and Sr vary only slightly and Mn is virtually absent in these shales (Appendix 12).

The overall coarsening and increasing maturity tendency^{upwards} in the Terrig River shale probably reflects a shallowing of the depositional basin and the deposition of more altered material. Geochemical studies show increasing oxidation conditions, which match rather well the shallowing conditions shown.

On the other hand, slightly fluctuating grain size parameters of the Bwlchgwyn siliceous shale (and also Minera) are noticed with a coarsening tendency at the bottom, relative fining at the middle and an upward coarsening again. However, the Bwlchgwyn siliceous shale (and also Minera) is coarser than the underlying Terrig River shale. The different maturity parameters studied in these shales display complicated development with an increasing maturity at the lower most part, from where it decreases. These shales are also characterised by fluctuating oxidizing - reducing conditions (Fig. 9.4). The Cu/Zn ratio increases slightly in the lower part, suggesting more reducing depositional conditions there, while in the middle oxidizing condition may prevail. However, the highest Cu/Zn ratio is seen in the top most sample (BG-16), where consequently the most reducing conditions may have existed (this is also featured by the presence of siderite and trace amounts of pyrite together with the higher Ni and Cu concentration in this sample). The organic carbon content in BG-16 sample is about 7.67 wt.%, though minor amounts of P_2O_5 (0.028 wt.%) are detected.

The average TiO_2 , Rb and Ni are rather constant in these shales; though the values of TiO_2 and Rb are comparatively lower than the Terrig River shale (Appendix 11 and Appendix 12). Like the Terrig River shale Mn is totally absent again, and the value of Cu fluctuates only slightly, while the Zn

remains rather constant. TiO_2 may be associated with non-clay residual minerals like anatase. Anatase is seen present in quite a few samples which is also proved by XRD (Fig. 9.6). Sr content increases downward in the columnar section (i.e. in the Terrig River shale). Extremely low Ca/Sr ratios in both the Terrig River shale and the Bwlchgwyn and Minera siliceous shale may indicate lower original calcite contents in these sediments.

Geochemical data suggests that like the underlying Terrig River shale the Bwlchgwyn and Minera siliceous shale also represent an upwards coarsening development and hence reflect shallowing of the depositional basin. The maturity increases at the lower most part, from where it decreases, indicating renewed deposition, new weathering conditions and particularly source area variations.

9.9 MINERAL TRENDS RELATED TO SEDIMENTATION AND WEATHERING

To understand the chemical and mineralogical changes occurring during diagenesis it is important to distinguish first those variations which are due to weathering and/or sedimentation effects. In Figure 9.5 the recalculated mineralogical analyses using different methodologies as mentioned earlier have been plotted against stratigraphic level. One of the most striking features is the positive correlation of quartz and zircon in the Terrig River shale ($r = 0.85$, see also Fig. 9.8) and in the Bwlchgwyn and Minera siliceous shale ($r = 0.45$, see also Fig. 9.7). Pearson (1979) also noted such a feature from the Hepworth Carboniferous sequence in Yorkshire, and concluded that both quartz and Zircon are detrital minerals whose hydrodynamic properties are such that particles of both respond similarly to changes of energy of the depositional environment. The overall increase in abundance of both minerals in the Terrig River shale indicates an active area of sedimentation and mirrored by the conclusion made in Section 9.8; though the minima of quartz distribution at samples

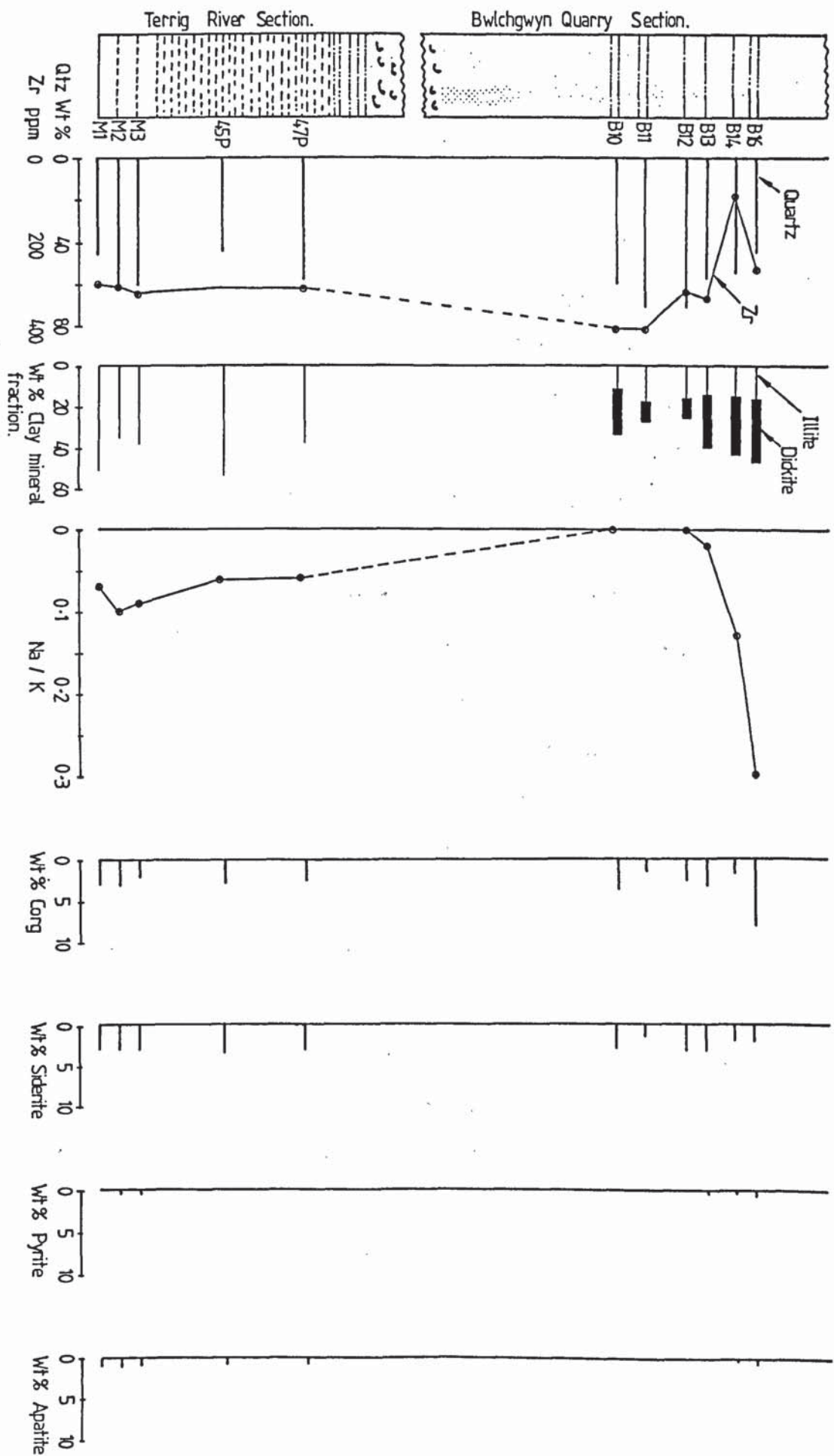


FIG.9.5. Distribution of minerals and variations in Zirconium, Sodium / Potassium ratio through the Namurian sequence in North Wales. Scale: See Fig.9.4

M1 and 45P might suggest a relatively lower energy condition within an active sedimentation unit (Fig. 9.5). These assumed lower energy conditions could be tentatively equated with the marine transgressions as is seen in the Biostratigraphical Palynology Chapter 4.

On the other hand, in the Bwlchgwyn siliceous shale the lower part is featured by relatively high abundance of Zircon and quartz, implying an active area of sedimentation, from where the Zircon decreases and fluctuates widely throughout the section, while near the top quartz also shows a decreasing tendency; to suggest renewed deposition, new weathering conditions and more precisely source area variation. This conclusion fits well with Section 9.8. Moreover, the higher part of this section is characterised by subsidiary minima of quartz and Zircon, coupled with high organic carbon content and the presence of relatively higher amount of pyrite (though siderite is the dominant carbonate mineral - Fig. 9.5). This may be tentatively interpreted as a possible marine or perhaps brackish water influx in the relatively fresh water swamp shale (see Chapter 5). Here pyrite has formed diagenetically by bacterial reduction of sulphate. Trace amounts of apatite are also present at this horizon. Disseminated siderite is present throughout the section.

Several authors^{have} noted a positive relation between quartz and organic carbon distribution and related it to the rate of sedimentation. In this study the correlation between quartz and Corg is negative both in the Terrig River shale and the Bwlchgwyn and Minera siliceous shale (Figs. 9.9 and 9.10). Figure 9.5 also shows no definite relationship between quartz and organic carbon distribution. Sulaiman (1972) reported both positive and negative correlation between quartz and Corg from the Irish Namurian sediments.

The quartz-Zircon trend in the Terrig River shale is in accord with the clay mineral composition. Mica content increases with energy of the depositional environment and kaolinite decreases. Two important conclusions may be drawn. Firstly, the dominant control on the distribution of clay lattice in the Terrig River shale is sedimentational: they are detrital clays derived from the weathering of soils. Secondly, their differentiation or distribution may reasonably be interpreted as a grain size effect. SEM photographs (Pl. 11.8 H) and XRD traces (Fig. 11.3) are also in accord with the detrital origin of illites. However, the clay mineral distribution in the Bwlchgwyn siliceous shale is ambiguous. It is seen that dickite increases with a corresponding increase in grain size (Figs. 9.4 and 9.5), despite the fact that it is finer material than illite.

Again two conclusion can be drawn: firstly, dickite is almost certainly authigenic (as kaolinite in the interbedded sandstones is totally authigenic) and secondly, source area variation and a change in the weathering condition (perhaps cessation of weathering) could be responsible.

The trend of Na/K ratio in Figure (9.5) is interesting and is consistent with the grain size analysis (Fig. 9.4). Na and K in the studied shales are mostly confined in the detrital illites. Deer *et al.* (1962) noted that fresh muscovite contains more K and Na than average illite. Micas are often degraded to illite during weathering by loss of K (also Na), uptake of H_2O and partial opening of the lattice. Coarser fractions of the sediment will tend to include fresher micas, alternatively, finer fractions ^{carry} more degraded illites and more smectites (Pearson, 1979). An increase in sodium and potassium with coarseness of the sediment may thus arise naturally (see Figs. 9.4 and 9.5).

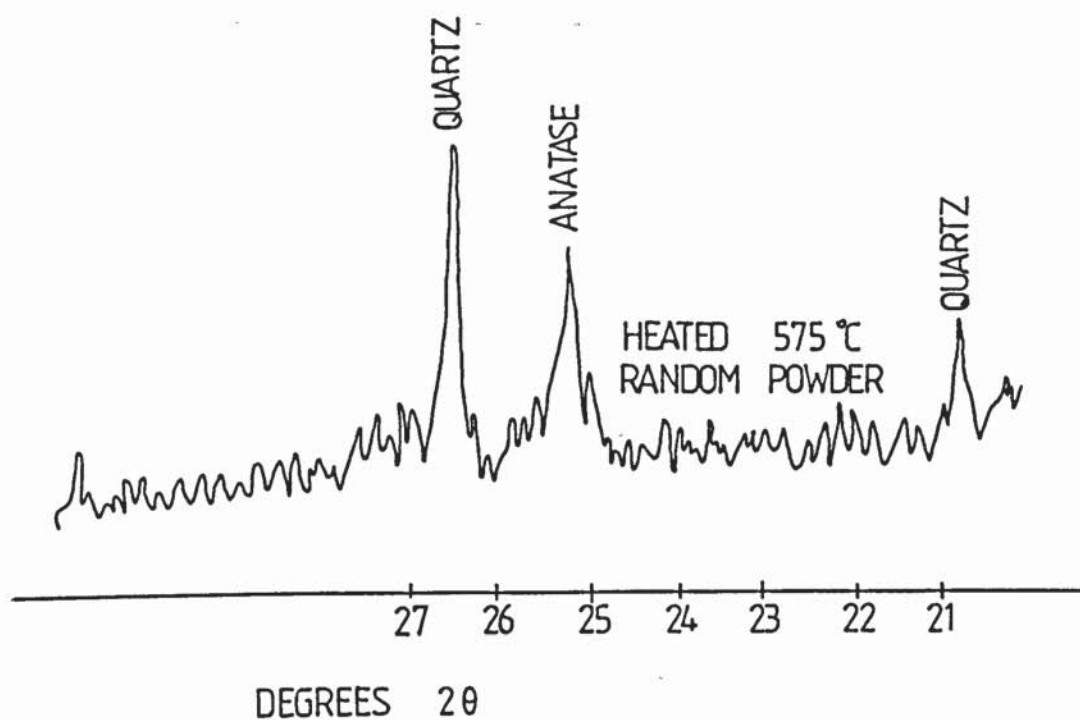


Fig. 9.6.

X-ray diffraction patterns of sample Min 3, using Ni filtered $\text{CuK}\alpha$ radiation showing the anatase main peak.

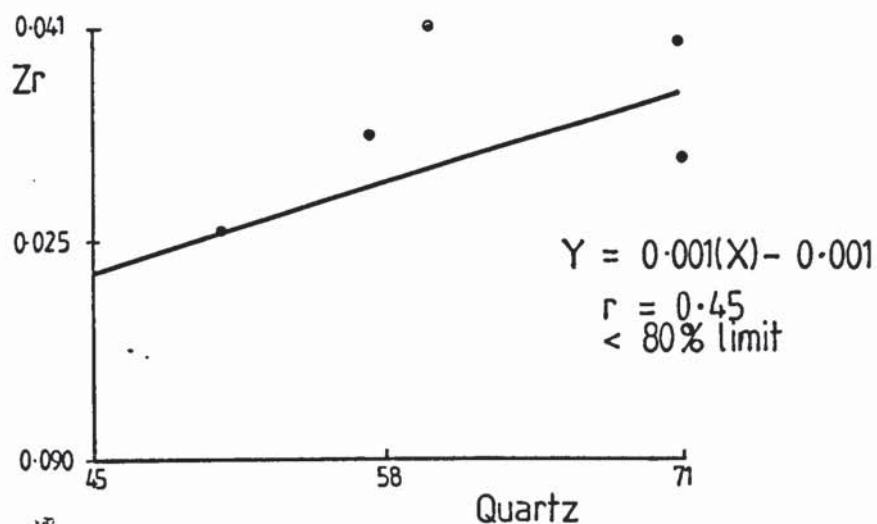


Fig. 9.7 Relation between the detrital quartz and detrital Zr in the Bwlchgwyn siliceous shale. The diagonal line indicates the regression for all of them

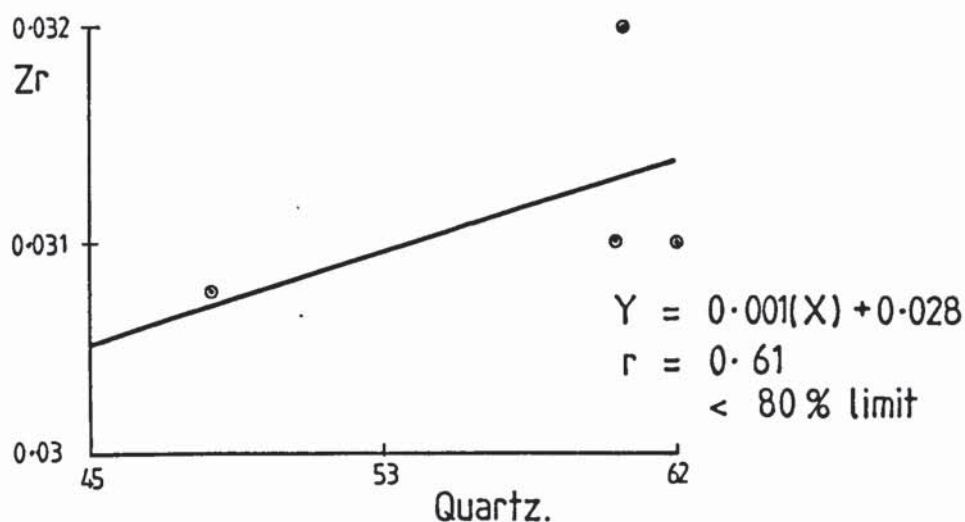


Fig. 9.8 Relation between the detrital quartz and detrital Zr in the Terrig River shale

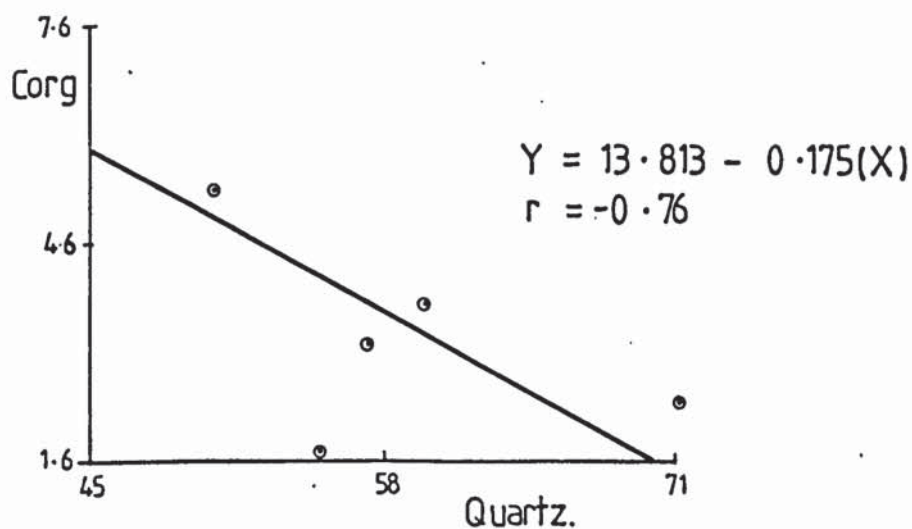


Fig. 9.9 Relation between the contents of C_{org} and quartz in the Bwlchgwyn siliceous shale

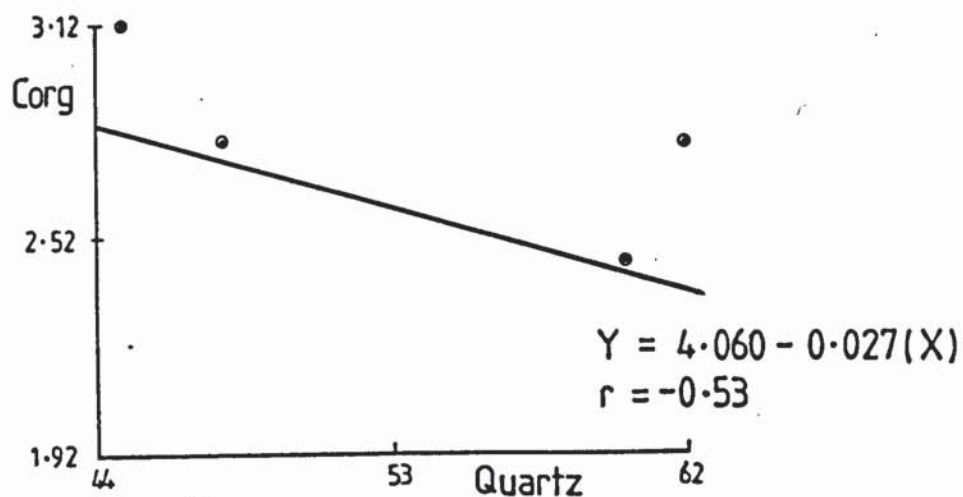


Fig. 9.I0 Relation between the contents of Corg and quartz in the Terrig River shale

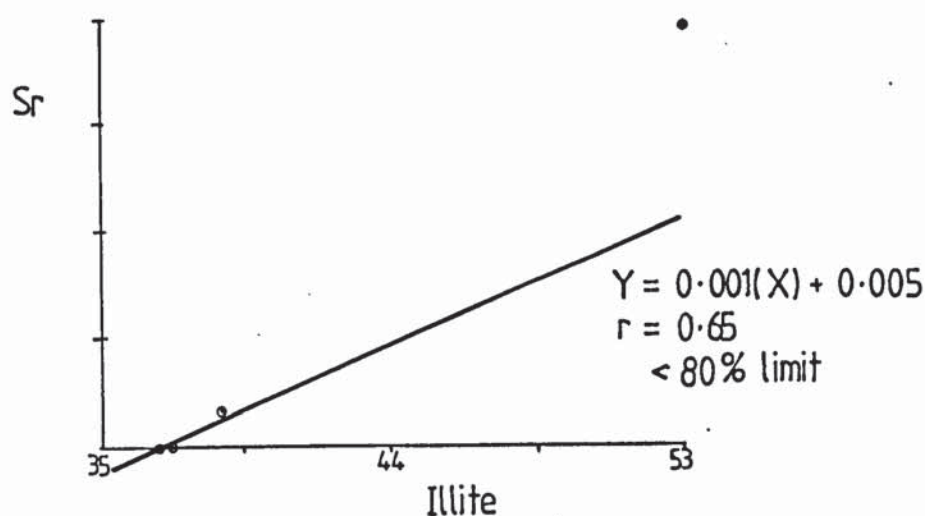


Fig. 9.II Relation between the contents of Sr and illite in the Terrig River shale

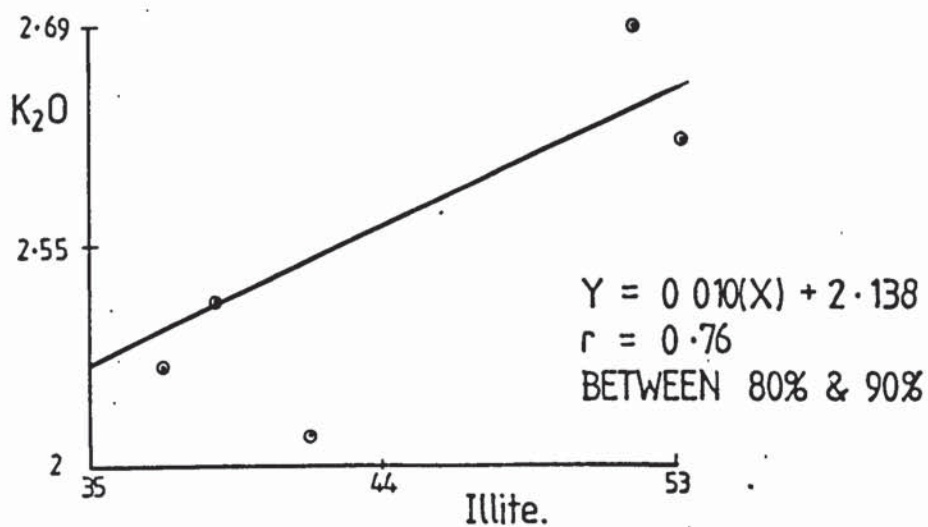


Fig. 9.I2 Relation between K_2O and illite in the Terrig River shale

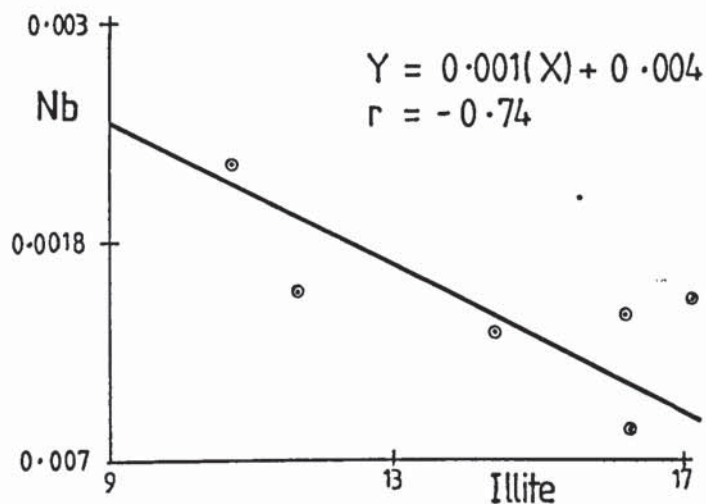


Fig. 9.13 Negative correlation between N_b and illite in the Bwlchgwyn siliceous shale

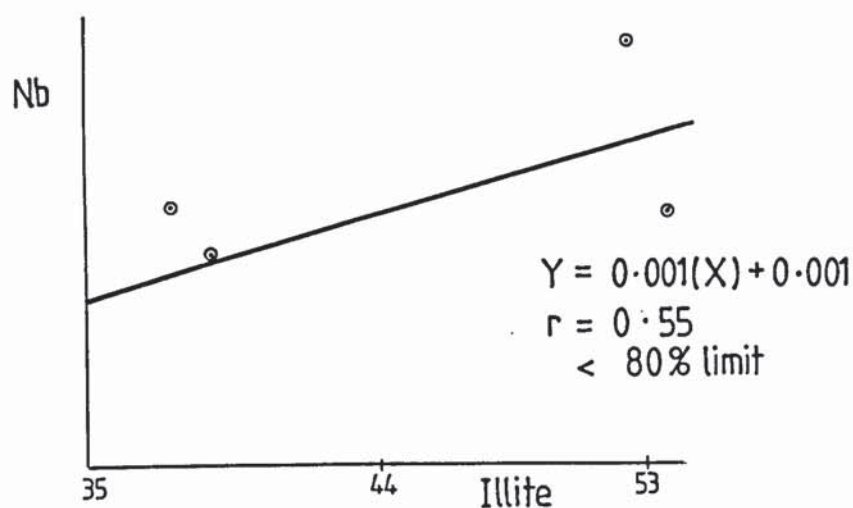


Fig. 9.14 Relation between N_b and illite in the Terrig River shale

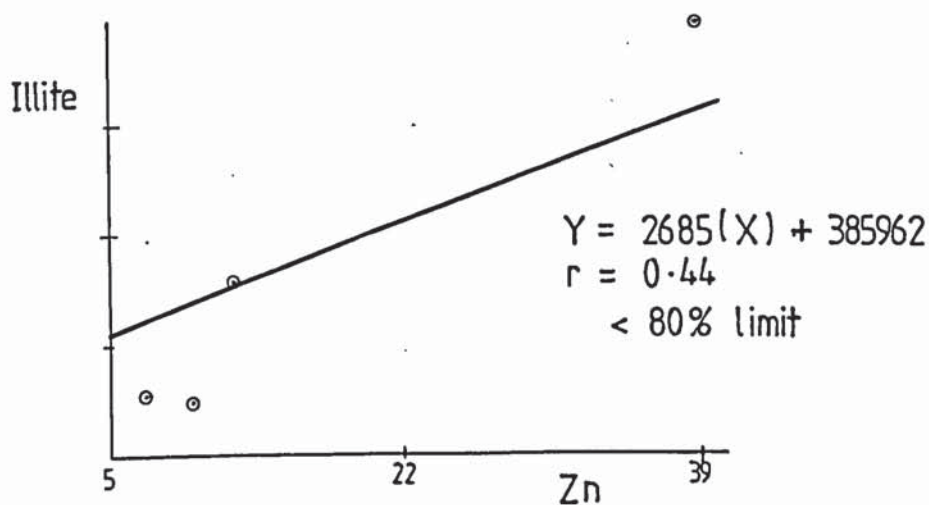


Fig. 9.15 Zn shows a positive correlation with illite in the Terrig River shale

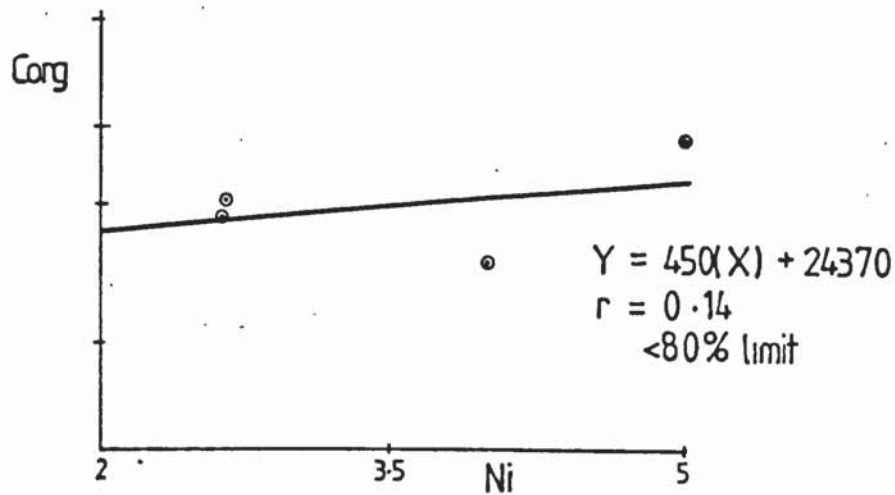


Fig. 9.I6 Relation between the contents of Corg and Ni in the Terrig River shale

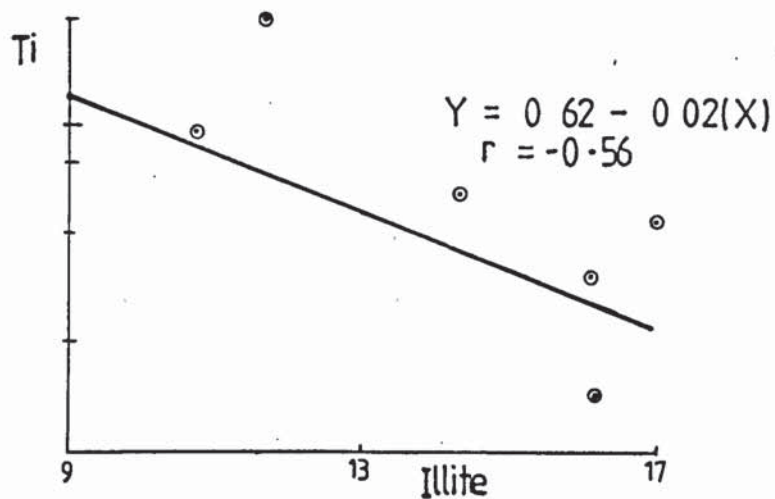


Fig. 9.I7 Negative correlation between Ti and illite in the Bwlchgwyn siliceous shale

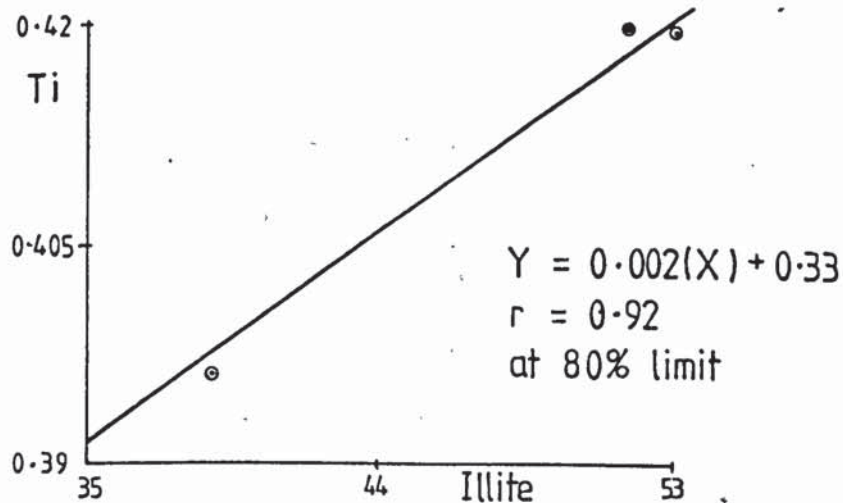


Fig 9.I8 Relation between the contents of Ti and illite in the Terrig River shale

9.10 ELEMENT (R-MODE) DENDROGRAM FOR THE TERRIG RIVER SHALE UNIT

Element dendrograms have been produced from the samples obtained from the Terrig River shale (Fig. 9.19). A brief synopsis of the technique of cluster analysis has already been given in Chapter 6 and the computer program is included in Appendix 17.

On the right hand side of the dendrogram the elements like Al, Mg, Ti, Rb, Th, Zr, Nb, Ba and Ca have been grouped together. Such an association especially the alumino-silicates represent a terrigenous and volcanogenic source (see Chapter 6). This means that such an association (particularly detrital index elements) indicates a change in the source area, rather than only a change in the weathering type (Parker, 1974).

Al, K, Rb and Na are probably derived from illite (Fig. 9.12), where illite correlates positively with K O at $r=0.76$ at the 80% and 90% level). All the resistates like Ti, Zr, Y, Fe and Nb are positively correlated and hence denoting their detrital origin. Nb also correlates positively with illite ($r=0.55$, Fig. 9.14). The positive correlation of Th with the resistates suggest that it is also associated with illite. Similarly, Mg collates with Al ($r=0.99$, exceeding 99.9% level), K ($r=0.97$, exceeding 99.9% level), Rb ($r=0.96$, exceeding 99.9% level) and Ti ($r=0.93$, exceeding 99.9% level), hence indicates its linkage with illite. Deer *et al.* (1962) noted that Mg could replace Al in the octahedral layer of illite. Those authors also reported about 2% MgO associated with illites of Illinois. The strong positive correlation of Ca and Ba ($r=0.82$ exceeding 99.9% level) and their association with the clastic elements and resistates, may suggest a possible marine water influx in the original clastics.

On the left hand side of the dendrogram, the close association of Fe, Corg, P and S indicates the presence of a strong reducing environment. This is

consistent with Section 9.8 and 9.9. Strong mutual correlation between Fe and Corg ($r = 0.83$, exceeding 99.9% level) suggests that Fe has been adsorbed by Corg and hence denoting its detrital origin. Fe also shows a weak positive correlation with S and P. All these relations are in close agreement with the presence of siderite in these shales. Moreover, the weak positive correlation of P with K and Al cannot be ignored as a possibility of its being incorporated with illite. Y also has a correlation coefficient of 0.61 at the 95% and 99% level with Fe and 0.65 at the 95% and 99% level with P. This indicates that Y is linked (through transportation, or due to leaching) more with the dissolved phase rather than the clay particles themselves (Sulaiman, 1972).

Both Ni and Pb show positive correlation with K and Al suggest that they are also incorporated with illite. On the contrary their negative correlation with S negate the possibility of their being associated with sulphides. But the positive correlation between Ni and Corg could be important (Fig. 9.16). The weak positive correlation of Ni with Mg signifies that adsorption on Mg compound and replacing of Mg in the clay mineral (in this case illite). Ti also correlates positively with illite (Fig. 9.18).

The correlation coefficient between Sr and U is high ($r = 0.85$, exceeding 99.9% limit). On the other hand, both Sr and U correlate with Fe, Corg, P and S indicating their possible incorporation with sulphides. U can also be accumulated with Corg. The role of Corg in the accumulation of U is very extensively examined in the literature (e.g. Bloxam, 1964; Bloxam and Thomas, 1969, etc.). Generally speaking, the reason for this accumulation is due to the reduction of U^{+6} soluble to U^{+4} insoluble compounds in reducing environments. But many authors reported that the leaching of most U from the sediment above the Ph (2.2) was necessary to remove U^{+4} compounds. Thus Corg acts sometimes, as a trap to adsorb U from percolating solutions or sea water and then complexing with some of it

after reducing it to the U^{+4} state. However, as U possesses better correlation with P it is believed that Corg did not play an important epigenetic role in accumulating U, and that most of the U existing now in the sediments is that precipitated or adsorbed syngenetically. The presence of carbonate-apatite may not be expected as U possesses a negative correlation with Ca.

Sr is seen correlating with illite ($r = 0.65$, Fig. 9.11), but opposing Ca. The negative correlation between Sr and Ca may be due to the low concentration of Sr compared to the Gronant chert (Chapter 6). The average value of Sr in the Terrig River shale is 62 ppm. These values are lower than the values reported by Nicholls and Loring (1962) for the shales from Bersam, North Wales. Those authors found that Sr does not follow calcium in the carbonates. They postulated that Sr is incorporated in the clay fraction. The present investigation is in close agreement with the above conclusion. But this is contrary to the findings of Spears and Amin (1981). Spears and Amin (1981) from a study of marine Namurian shales from Derbyshire, concluded that the association of Sr and calcium is clear because of the highly significant correlation coefficient between them.

Zn shows a weak positive correlation with Fe, Corg and P suggesting it might be associated with the reducing environment of deposition.

9.11 ELEMENT (R-MODE) DENDROGRAM FOR THE BWLCHGWYN-MINERA SILICEOUS SHALE UNITS

The dendrograms of the Bwlchgwyn-Minera siliceous shale are almost similar to the Terrig River shale and hence to avoid repetition individual elements and their distribution will not be discussed in detail here. One remarkable difference in the clay mineralogy between these shales is the presence of dickite in addition to illite in the Bwlchgwyn-Minera siliceous shale.

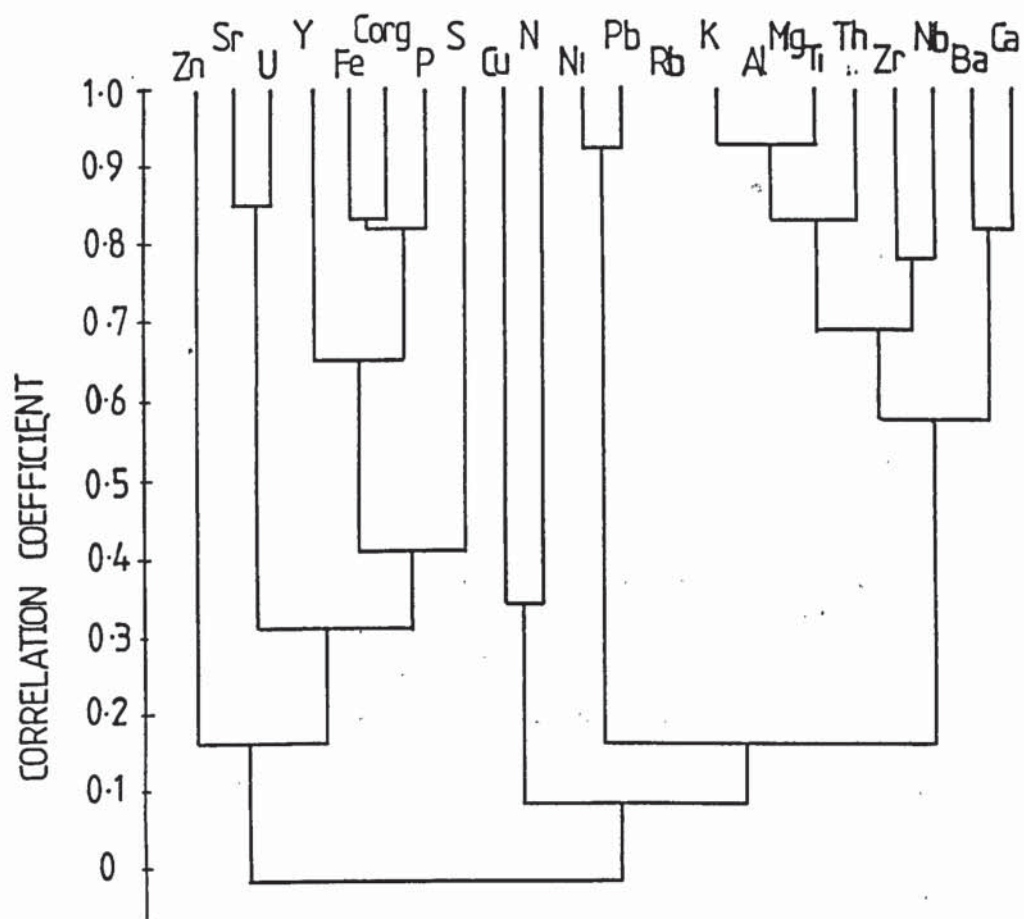


Fig. 9.19. Element (R-mode) dendrogram for samples from the 'Terrig River Shales'.

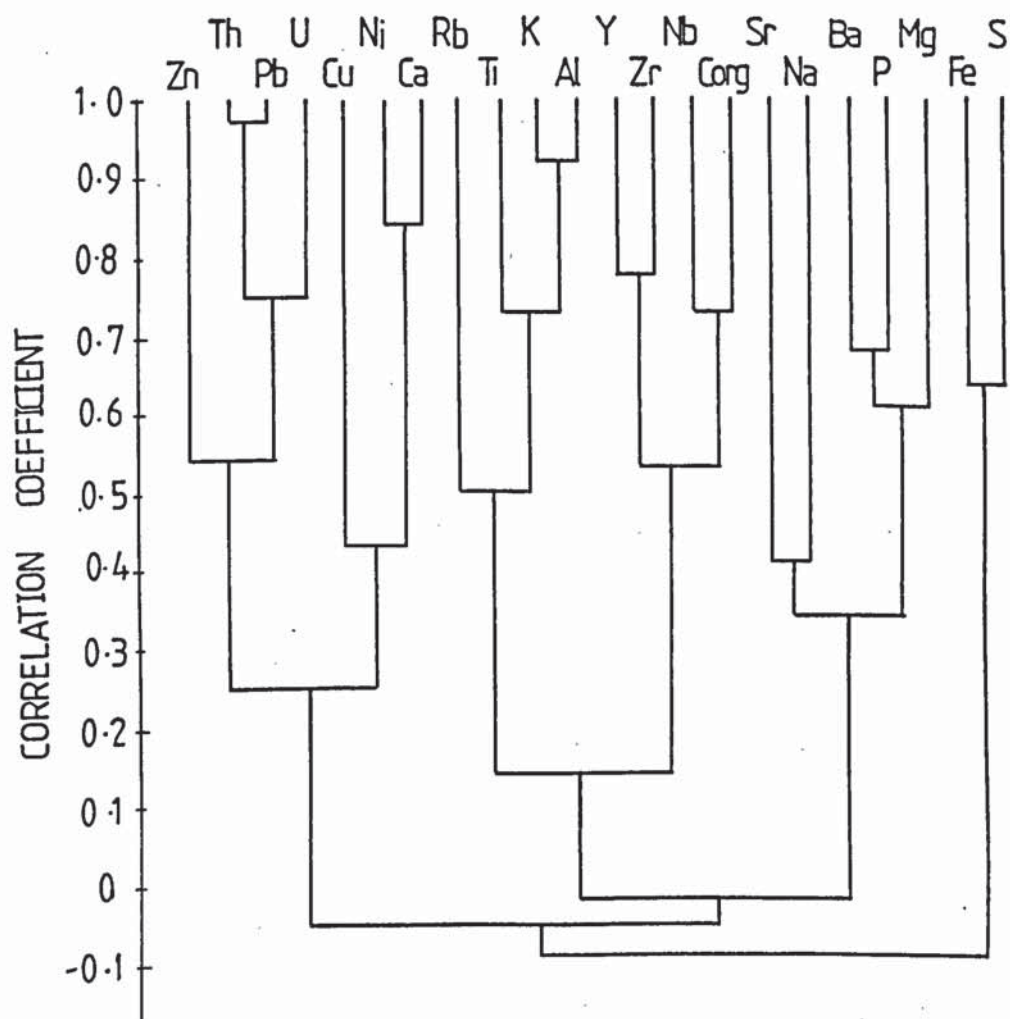


Fig. 9.20. Element (R-mode) dendrogram for samples from the 'Bwlchgwyn and Minera Siliceous Shales'. -229-

There could be an obvious separation of the detrital index elements (e.g. Ti, Y, Zr, Nb) in Fig. 9.20, like Fig. 9.19. The significance of such a grouping has already been mentioned in Chapter 6 and in Section 9.10, and it correlates well with Section 9.8 and 9.9. The ultimate linkage of the elements like Sr and Ba with the detrital suite may reflect the influence of a fresh water influx (Sweeney, 1985). This is also consistent with the palynofacies study (Chapter 5).

9.12 ORGANIC CARBON AND TRACE ELEMENT RELATIONS

The organic matter in sedimentary rocks may consist largely of vegetal substances. An important variable is the proportion of marine to terrestrial organic matter (Philippi, 1974). It must be noted, however, that organic substances of plants differ from those of planktonic organic matter (Degens, 1965; Philippi, 1974).

Vegetal organic matter forms lignite and carbonaceous plant remains which consist of lignin and cellulose with small amounts of protein, while marine organic matter is rich in protein, amino acid, lipid and fatty constituents with minor amounts of lignin and cellulose. Moreover, the composition of organic matter also depends on its environment of deposition (Philippi, 1974; Powell *et al.* 1976).

It follows, therefore, that organic matter of different origins will vary in composition and the content of the various decomposition products. Hence, the type of organic matter and the depositional environment in which it is accumulated and underwent diagenesis are the most important factors in controlling the enrichment of elements (Spears and Amin, 1981).

It might be suitable now to have a look at the reasons behind the depletion of Corg in trace elements in the Bwlchgwyn-Minera siliceous shale, while it has an important role in the Terrig River shale.

Recalling what was mentioned about the nature of the Corg in the studied sediments, it was found that it was mostly detrital in its origin and dominated by plant fragments in the Bwlchgwyn-Minera siliceous shale and of marine algae in the Terrig River shale.

Amongst the elements which are adsorbed onto or associated partly with the organic carbon in the Terrig River shale are Zn, Cu, Ni, Pb, U, Sr etc. (see Figs. 9.19; 9.20 and Appendices 15, 16), while none of these elements are linked with the organic carbon of the Bwlchgwyn-Minera siliceous shale (see Fig. 9.20 and Appendix 16). Sulaiman (1972) also noted that the depletion of Corg in trace elements from the 'near shore facies' of the Irish Namurian and an enrichment of Corg in trace elements from the 'basinal area' of the Irish Namurian.

As far as palynostratigraphy is concerned (see Chapter 4 and Table 4.3) the Terrig River shale ranges from the lower to middle of the Arnsbergian Stage to within the Alportian Stage (i.e. E₂-H₂) and lies from the upper N1 to the middle N6 mesothems of Ramsbottom (1977). On the other hand, the Bwlchgwyn-Minera siliceous shale lies below the Middle Marsdenian stage (i.e. middle R₂) and coincides with only the middle of the N9 mesothem of Ramsbottom (1977).

Miospore assemblages listed from the E2 to the lowest part of the H1 in the Terrig River shale, are not consistent with the assemblages recorded by different authors from the Southern Pennines, or the North of England or Scotland. This may suggest a different floral affinity and a source area variation for these sediments. On the contrary, the assemblages recorded from the H2 to the middle of the R2, correlate closely with the assemblages recorded from the Southern Pennines, North of England and Scotland, suggesting a northerly source of vegetation.

In addition, palynological study further confirms the presence of near shore miospore species in the Terrig River shale assemblages (e.g. high percentages of thick walled miospores and the presence of saccate spores), while these species are not common in the Bwlchgwyn-Minera siliceous shale assemblages.

Palynofacies study also indicates the abundance of marine algal material in the Terrig River shale, while in the Bwlchgwyn-Minera siliceous shale and ^{sandstones} derived plant materials (e.g. coal macerals: vitrinite, inertinite) are dominant. Integration of sedimentological investigation and palynofacies study indicates that the Terrig River shale belongs to 'interdistributary bay shale facies', while the Bwlchgwyn- Minera siliceous shale ^{is} a 'swamp facies' (Chapter 5).

Moreover, element dendrograms also suggest a possible marine water influx in the Terrig River shale (Fig. 9.19).

Terrig River shale also shares some common geochemical features as noted by Spears and Amin (1981) from their Namurian marine shales from Derbyshire, England.

From the foregoing the differences between the Corg from the Terrig River shale and the Bwlchgwyn-Minera siliceous shale can be summarised in the following two points:

1. In the Bwlchgwyn-Minera area the Corg is overwhelmingly plant fragments, and it was deposited not far from the land.
2. In the Terrig River Section the Corg is more marine and the detrital plant fragments would have travelled for long distances and been in contact with the marine-brackish environment for a longer time.

A survey of the literature on the importance of Corg in the distribution and accumulation of the trace elements is related to this study. It is well known that marine Corg has more amino acid and proteins than the non-marine Corg, which, in turn, has more lignin and cellulose. Thus elements like Ni, Y are necessary for marine algae. As far as trace elements are concerned, the elements necessary for the biochemical life will not contribute much to the trace elements now found in the Corg. (Tourtelot, 1964). The latter author also noted that marine Corg is much more abundant than the non-marine Corg, and its role in accumulating trace elements could be more important. He then postulated that since the marine and non-marine Corg, are of the same origin, sorption (because of long duration in the sea) was the reason for the enrichment of the marine Corg. Works of the following authors like Goldschmidt (1954), Bloxam (1964), emphasised the enrichments of trace elements by marine and non-marine Corg.

From the foregoing, it could be concluded that, there would be no difference between the marine and non-marine organic matter in accumulating trace elements if subjected to the same environment.

Sulaiman (1972) proposed a leaching process was responsible for the depletion of Corg in trace elements from his 'near shore facies' of the Irish Namurian. Such a leaching process is certainly responsible for the high depletion of Mn from the Terrig River shale and the Bwlchgwyn-Minera siliceous shale. This is also evidenced by the negative correlation of Mn with CaO and MgO.

So, if this leaching process is also invoked for the depletion of Corg in trace elements in the Bwlchgwyn-Minera area, then why is the Terrig River Corg enriched by trace elements? Thus Sulaiman's (1972) proposal is rejected in favour of the Tourtelot (1964) hypothesis, that the lack of a long contact

with the sea water did not give this Corg (in this instance Corg of the Bwlchgwyn-Minera siliceous shale) the opportunity to adsorb much of the trace elements.

The widespread silicification of these shales could also be another reason (see Chapter 11).

9.13 CONCLUSIONS

The geochemistry of the Naumrian shale sequences has been studied in detail.

The grain size parameter ($\text{SiO}_2 / \text{Al}_2\text{O}_3$) indicates that the Bwlchgwyn siliceous shale is coarser than the underlying Terrig River shale. Similarly the maturity parameters of the Terrig River shale are characterised by slightly lower $\text{Rb}/\text{K}_2\text{O}$ and M ratios, suggesting lower maturity than the overlying Bwlchgwyn siliceous shale. On the other hand, fluctuating Cu/Zn ratio in both the Terrig River shale and the Bwlchgwyn siliceous shale may indicate fluctuating oxidizing-reducing conditions in the environment of deposition.

Quartz and Zirconium trends probably reflect the energy of the depositional environment. The general increase in abundance of both minerals in the Terrig River shale may indicate a more active sedimentation, while in the upper part of the Bwlchgwyn siliceous shale the minor fluctuations in the content of Zr is probably due to its relative paucity in the source area.

Illite in the Terrig River shale and dickite and illite in the Bwlchgwyn siliceous shale dominate the clay mineralogy. Illite is certainly detrital and the high crystallinity of dickite confirms it is authigenic in origin.

Siderite formed when sulphide activity was sufficiently low and organic matter was available to maintain a low Eh and provide a source of carbonate ions. It is assumed that siderite and trace amounts of pyrite account for most of the iron now present. Ti is mostly present as anatase. The increase in Na/K ratio at the top of the sequence (i.e. towards Bwlchgwyn shale) perhaps reflects an increased contribution of relatively coarser grained sediments.

Element dendrograms of the Terrig River shale and the Bwlchgwyn-Minera siliceous shale show the clustering of different elements into two main groups, suggesting a change in the source material itself rather than only a change in the weathering type.

The depletion of Corg in trace elements in the Bwlchgwyn-Minera siliceous shale compared to the Terrig River shale may be due to their (Bwlchgwyn-Minera siliceous shale) lack of a long contact with sea water.

LOCATIONS	Zn	Cu	Ni	Pb	Sr	ASSEM- BLAGES	AGE
Chwarelau and Aquaduct Coal	COALS					VII	at the base of the Westphalian
Rhyd-y-ceirw Coal (Terrig River)						VI	the middle Yeadonian stage
Bwlchgwyn and Minera Shale	15	3	6	56	32	V	below the Middle Meridenian stage
Terrig River Shale (3)	NO CHEMICAL DATA					IV	within the Alportian stage
Terrig River Shale (2)	25	0.001	3	28	64	III	at the boundary between the Arnsbergian and the Chokierian stages
Terrig River Shale (1)	10	102	3	24	61	II	lower to middle of the Arnsbergian stage
Llanarmon-yn- ial cherty flags	15	19	13	142	62	I	Upper most part of the Asbian and the Pendleian stages
Gronant Chert	16	12	25	22	363	-	Upper most part of the Asbian and the Pendleian stages

Table 9.2 Distribution of selected trace elements (ppm) against
miospore assemblages.

CHAPTER 10

PETROLOGY AND PROVENANCE OF THE BWLCHGWYN-MINERA-RUABON SANDSTONE UNIT

10.1 INTRODUCTION

This chapter deals with the mineralogy, petrography and provenance of the Bwlchgwyn-Minera-Ruabon Sandstone Unit.

All the sandstone samples were studied in thin sections, grain mounts, and polished grain mounts. Point counting using the line method (Carver, 1967), with 500 counts per thin section was carried out on most of the specimens. Cathodoluminescence and electron probe microanalysis techniques were also employed in this study (for methodologies see Appendix 2 and Appendix 4).

10.2 CLASSIFICATION

According to Folk's (1968) classification these Namurian sandstones are mainly quartz arenite, while a few are considered to be sublitharenites (Fig. 10.1).

During the present investigation an attempt was also taken to classify these sandstones geochemically as proposed by Moore and Dennen (1970). Average compositions of the sandstones were recalculated to atomic weight percent and SI-AL-FE plotted on a ternary diagram of Moore and Dennen (1970) as shown in Fig. 10.2. The Figure indicates that the sandstones under survey are mainly 'orthoquartzites', while a few samples can be considered as 'sandstones'.

This classification fits well with the petrographical classification mentioned above.



Fig. 10.1.

Classification of the Bwlchgwyn–Minera–Ruabon (Namurian)
sandstones (after Folk, 1968)

FIG10.2. Geochemical classification of the Bwlchgwyn - Minera - Ruabon Sandstone (after Moore and Dennen, 1970) -239-

10.3 MINERALOGY

The exposures of the Bwlchgwyn-Minera-Ruabon sandstones tend to occur particularly in quarry areas. They exhibit a comparatively simple mineralogy as all thin sections examined indicate an approximate composition of quartz 93-95%, feldspar 0.2-0.5%, clay minerals 2-3% and rock fragments (including chert) 3-4%.

The following is a brief description of the main detrital components:-

10.3.1 Quartz

Quartz is the predominant mineral in these sandstones as it is one of the most stable minerals in sedimentary environments. It forms about 93-95% and includes many varieties which reflect the type of rocks in the source area. The grains are moderately sorted, subrounded to rounded and prolate to oblate, equant aligned in shape and often show a slight elongation parallel to the c-axis and orientation parallel to the bedding. Folk (1968) considered such an elongation as due to preferred abrasion and the weak tendency of quartz to fracture parallel to the c-axis rather than perpendicular to it. An attempt to study the quartz surface textures using the SEM was unsuccessful due to the fact that the grain surfaces are covered with authigenic quartz overgrowths which mask the original surface textures.

Monocrystalline quartz makes up the bulk of these Namurian sandstones. It usually has undulose extinction, though straight extinctions also do occur. Undulose quartz is thermodynamically less stable than non-undulose quartz and tends to break into small grains (Blatt *et al.* 1980). The origin of undulose quartz is still debateable. Undulosity may increase when the sediments have subsequently been folded and faulted in tectonically active area (Conolly, 1965; Fuchtbauer, 1974; Basu *et al.* 1975). Deep burial may produce undulose extinction but lithostatic

pressure alone has only a minor effect on the percentage of undulose quartz grains (Fuchtbauer, 1974). Metamorphic quartz shows a marked undulosity but large plutonic quartz was also found to have a high degree of undulosity (Pettijohn, 1975). Thus, the presence of undulose quartz cannot be considered a reliable indicator of provenance (Blatt and Christie, 1963). Polycrystalline grains are present in a very minor amount in these sandstones compared to the monocrystalline grains. It seems likely therefore, that the fine and medium size fractions contain a large amount of disaggregated polycrystalline quartz grains and broken undulose grains.

10.3.2 Igneous Quartz

A high proportion of the quartz in these sandstones is slightly to strongly undulose monocrystalline quartz. But it is not possible to assign its origin unless they have got some other diagnostic features inherited from its common source rocks (Folk, 1974). On the other hand, monocrystalline quartz with undulose extinction, few vacuoles and no inclusions is present (Pl. 10.1A). This type of quartz may represent a plutonic source area, but it can be produced from other source areas (Blatt, 1967; Folk, 1968). Similarly, monocrystalline quartz grains which have straight extinction, no inclusions and water clear colour are not uncommon in these sandstones. According to Folk (1974) this quartz may be of volcanic origin.

Polycrystalline quartz is a grain which forms of two or more than two crystal units of different optical orientation. This type of quartz is seen particularly in the medium grained sandstones. Polycrystalline quartz composed of two crystals with straight to slightly curved intercrystal boundaries may be from a plutonic source (Pl. 10.1 B). A plutonic source may also be indicated by undulose quartz where the undulosity was produced due to different c-axis orientations when the different zones are separated by lines of vacuoles or bubbles which suggest traces of healed

fractures (Blatt, 1967, Folk, 1968). This type of quartz is represented by Pl. 10.1 C.

Quartz with different types of mineral inclusions are not rare. Oriented acicular rutile inclusions may indicate a granitic source; needle shaped or elongated tourmaline may originate in either igneous or metamorphic rocks (Blatt *et al.* 1980). The above two types of inclusions are shown in plates 10.1 D and 10.1 E.

10.3.3 Metamorphic Quartz

Polycrystalline quartz of metamorphic origin is most common in the sandstones under consideration. Scholle (1979) noted that polycrystalline quartz with ten or more individual crystals is an excellent indicator of metamorphic source. According to Blatt *et al.* (1980) sand size polycrystalline quartz with five or more crystals is usually derived from gneisses. This type of gneissic quartz is abundant in the studied sandstones and represented by polycrystalline grains with elongated individual crystals and crenulated (Pl. 10.1 F) or sutured (Pl. 10.1 G) crystal boundaries. This includes stretched metamorphic quartz, formed when quartz bearing rocks such as sandstones, granites, schists, or vein quartz are sheared or strained in the absence of recrystallization (Folk, 1968).

Other types of metamorphic quartz were recognized in these sandstones. These include, polycrystalline quartz with elongate individual crystals having straight intercrystalline boundaries with slightly undulose extinction, and oriented mica inclusions indicating a schistose origin (Folk, 1968), and polycrystalline quartz with silt size individual crystals (Pl. 10.2 A) derived from fine schists (Folk, 1968; Blatt *et al.* 1980).

10.3.4 Sedimentary Quartz

Quartz grains with rounded overgrowths indicate reworked sandstones (Pl. 10.2. B). This type of quartz is abundant in these Namurian sandstones. Cathodoluminescence study also shows the presence of rounded overgrowths and detrital grains.

10.3.5 Rock Fragments

Rock fragments constitute up to 3 to 4 % in these Namurian sandstones.

Igneous rock fragments are mainly volcanic fragments consisting of very fine crystalline matrix and small lath-like plagioclase crystals (Pl. 10.1 A). Plutonic rock fragments are less common and usually represented by fragments of graphic granite showing quartz and feldspar intergrowth (Pl. 10.2 C).

Metamorphic and sedimentary rock fragments are more abundant than igneous rock fragments. They are characterised by their distinctive texture, and usually consist mainly of mica with lens-like elongate quartz crystals and probably represent mica schists (Pl. 10.2 D). Fragments of sheared metaquartzites are represented by large grains consisting of many elongate quartz crystals (Pl. 10.2 E).

Sedimentary rock fragments include sandstone, siltstone and carbonate rock fragments. Sandstone and siltstone rock fragments are more abundant. They are subangular to subrounded and may indicate an intraformational origin since they do not have the durability to survive long transportation (Pl. 10.2 F). Another type of sandstone rock fragment, which are well rounded and cemented by iron oxide (Pl. 10. 2G).

Carbonate rock fragments mostly include shell fragments (Pl. 10.2 H).

Chert is present mostly as a microcrystalline quartz and rarely with chalcedony (Pl. 11.1A). Chalcedony is found occasionally and usually shows a zebraic texture (Pl. 11.1 B). Chert and chalcedony may originate from underlying nodular and bedded chert (see Chapter 8).

10.4 UNDULOSE EXTINCTION AND POLYCRYSTALLINITY AS PROVENANCE INDICATORS

Basu *et al.* (1975) used undulose extinction and polycrystallinity for provenance interpretation. They proposed the following variables: the amount of monocrystalline quartz, the amount of undulose quartz, and the amount of polycrystalline quartz which was divided into the ones with 2-3 crystals per grain and the type with more than three crystals per grain.

These divisions were based on the fact that low rank metamorphic rocks contain a larger amount of quartz with more than three crystals per grain and contain both undulose and nonundulose quartz, whereas plutonic quartz is predominantly non-undulose. Large populations of undulose quartz (apparent undulosity $>5^\circ$) are more diagnostic than a large population of non-undulose quartz. Also according to above authors, high rank metamorphic rocks give rise to polycrystalline quartz with a number of crystals similar to that of plutonic rocks.

The limitations of this technique are:

1. Degree of undulosity is a function of tectonic activity and hence sandstones deposited in tectonically active areas may have a higher proportion of undulosity induced by folding and faulting.
2. A higher proportion of polycrystalline grains can be expected in texturally immature sandstones, while in more mature sandstones polycrystalline quartz breakage produces more monocrystalline quartz.

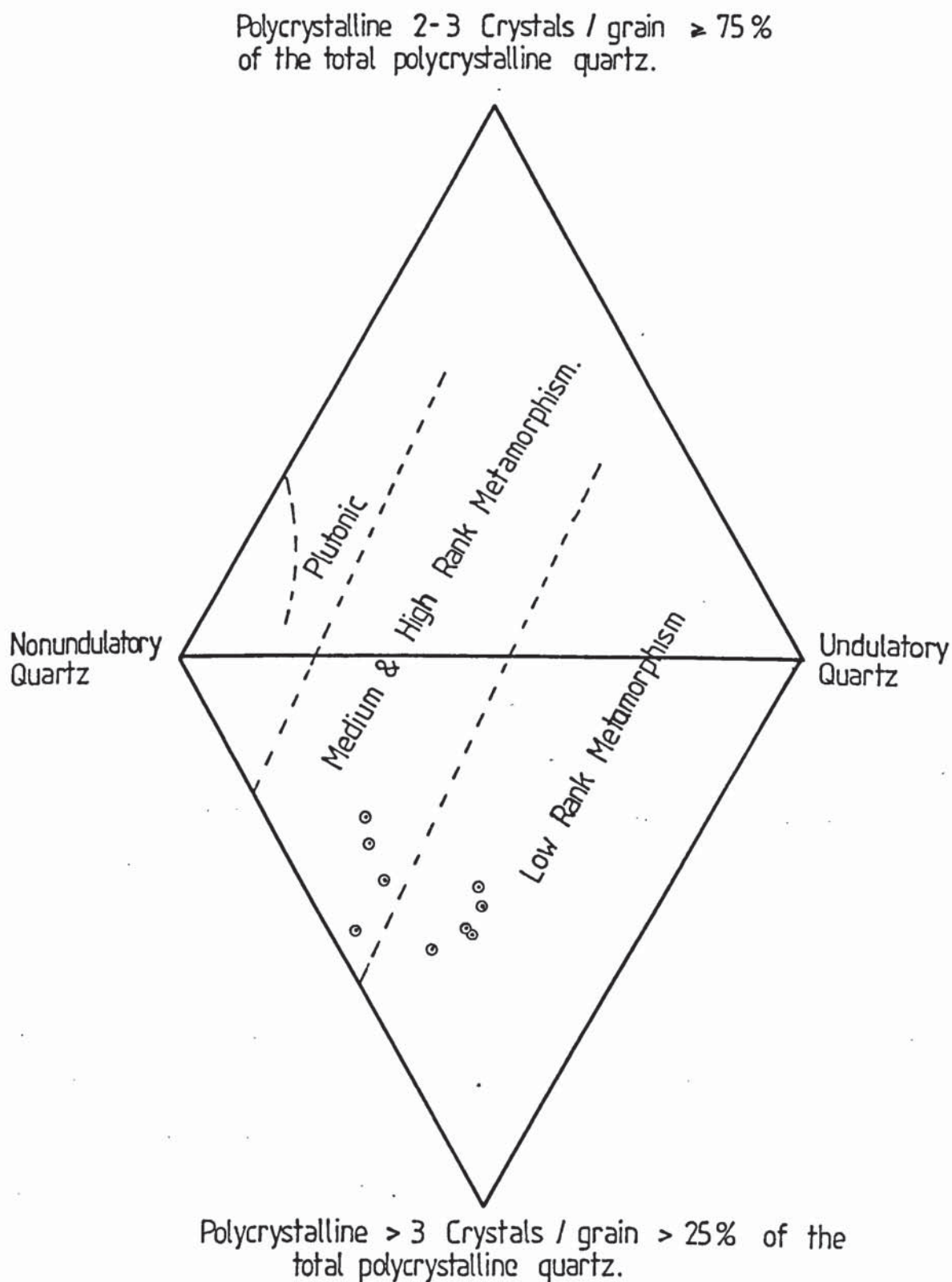


Fig.10.3. Four variable plot of nature of quartz population in the Namurian Sandstones. Dashed lined boundaries between source rock areas are taken from Basu *et al.* (1976, Fig.6).

To minimize these effects Basu *et al.* (1975) limited their studies to the medium sand fraction.

In the present study point counting for the above mentioned variables was carried out on thin sections of mostly the medium size fraction of selected sandstone samples from the Bwlchgwyn-Minera-Ruabon sandstones. Plotting the results on the four variable diagram (Figure 10.3) indicates that the source area of these Namurian sandstones in NW North Wales falls near the boundary between the middle-upper rank metamorphic and low rank metamorphic rocks.

10.5 CATHODOLUMINESCENCE

Cathodoluminescence in minerals derives from the presence of extraneous ions or other lattice distortions in the crystal structure (Nickel, 1978). Sprunt (1981) examined 17 high-temperature quartz samples and found that titanium in the absence of iron made blue luminescence and ferric iron in the absence of titanium produced red luminescence. The latter author also noted that CL is quenched by iron in carbonates, and ferrous iron may serve to quench luminescence in quartz.

CL has been effectively used in sandstone petrography to differentiate between detrital quartz cores and authigenic quartz overgrowths (Smith and Stenstrom, 1965; Sipple, 1968; Sibley and Blatt, 1976). This distinction can be made as detrital quartz luminesces in the visible range (blue and red or orange), whereas authigenic quartz does not.

Zinkernagel (1978) gave the comprehensive CL characteristics of igneous, metamorphic and authigenic quartz in rocks ranging in age from Precambrian to Tertiary. He identified three distinct types of luminescence in quartz that are dependent on the temperature of crystallization: 1) 'violet' or blue luminescing quartz derived from igneous

or fast cooled high grade metamorphic sources ($>573^{\circ}\text{C}$); 2) 'brown' or 'orange' luminescing quartz derived from slow-cooled, high grade metamorphic or low grade metamorphic sources ($<573^{\circ}\text{C}$); and 3) non-luminescing quartz, which formed at temperatures less than 300°C . The above author also noted that authigenic quartz that has been subjected to low grade metamorphism will exhibit low intensity orange CL where the induced luminescence is probably the result of lattice oscillations.

Sipple (1968); Pettijohn *et al.* (1973); Zinkernagel (1978) concluded that authigenic quartz formed at low temperatures does not usually exhibit CL because extraneous ions are not easily incorporated into the crystal lattice.

In the present investigation the cathodoluminescence (CL) technique was found extremely useful because of the following reasons:-

- i) to establish the paragenetic sequence between quartz-kaolinite-dickite. CL reveals that two phases of quartz overgrowth cementation are separated by a phase of kaolinite precipitation.
- ii) to show the pressure solution evidences as a source of silica in these sandstones.
- iii) for provenance study.

However, in this chapter emphasis will be given on provenance study.

The most abundant type of quartz in these Namurian sandstones is the one with extremely faint orange/badly definable dull grey-brown colour (Pl. 10.3 A, B; Pl. 10.4 A, B; Pl. 10.5 A, B) to brown luminescence (Pl. 10.6 A). Extremely faint orange luminescence is characteristic of low temperature quartz (Ruppert *et al.*, (1985) which is consistent with the vitrinite reflectance result (Section 9.5), while brown or orange luminescing quartz is derived from slow-cooled, high grade or low grade metamorphic sources (Zinkernagel, 1978).

Quartz with red-violet to red luminescence is also abundant. Red luminescence may also be a characteristic of quartz subjected to low temperature deformation or low temperature secondary quartz (Sprunt *et al.* 1978) and hence in accord with the vitrinite reflectance result. Sprunt (1981) examined 17 high temperature quartz samples and concluded that ferric iron in the absence of titanium produced red luminescence. As mentioned earlier, the quartz under investigation is considered to be low temperature origin, hence Sprunt's (1981) conclusion may not be applicable here. However, electron probe microanalysis technique was employed during the present investigation in order to know the distributional trend of the major and particularly the trace elements in the quartz detrital core and in the authigenic overgrowth (Table 10.1).

Table 10.1 shows the average elements distributions recorded from different red and brown luminescing quartz. Careful observation of the Table shows a little MgO in the core. The presence of MgO possibly indicates an igneous source rock. Similarly red luminescing detrital quartz grains (Pl. 10.3 A; Pl. 10.4 A, B) may indicate an igneous source (Zinkernagel, 1978). Some of the quartz shows a heterogenous blue luminescence (mostly faint blue) which indicates a source from contact metamorphic rocks (Zinkernagel, 1978) but studies by Sprunt *et al.* (1978) suggested that metamorphic quartz may also show homogenous blue luminescence (Pl. 10.5 A; Pl. 10.6 A). Traces of healed fractures were also revealed by cathodoluminescence in this type of quartz and also in other luminescence varieties of quartz. The fractures are generally healed by secondary quartz growth. It is difficult to ascertain whether fracturing occurs in source rocks or in sandstones. These features have been described by Sippel (1968).

Quartz of hydrothermal origin is extremely rare in these sandstones (Pl. 10.4 B). They are characterised by intensive zoning and bottle green luminescence colour (Zinkernagel, 1978).

Sedimentary quartz with rounded overgrowth which is abundant in these sandstones, and was difficult to recognise due to the lack of a clear dust line, is easily recognised by the non-luminescence of the overgrowths (Pl. 10.3 A, B; Pl. 10.4 A, B; Pl. 10.5 A, B).

Chert rock fragments which can easily be detected in transmitted light show brown luminescence (Pl. 10.6 B).

Cathodoluminescence study shows that the most predominant quartz type in these Namurian sandstones is of low temperature origin; sedimentary and metamorphic origin with subordinate igneous quartz. This is consistent with the petrographic evidences which indicate an abundance of metamorphic and sedimentary rock fragments and also in accord with the provenance studies based on polycrystallinity and undulose extinction (Figure 10.3).

10.6 CONCLUSIONS

The quartzitic nature of the studied sandstones indicate that they came from St. George's Land in the early Namurian (i.e. the southern part of Welsh massif; see also Fig. 1.2 and Ramsbottom, 1969; 1970; 1974b). The main source of these Namurian sandstones seem to be from medium to high rank metamorphic rocks and low rank metamorphic rocks, with additional supplies from ^{reworked metamorphic,} igneous and sedimentary sources.

This conclusion is reflected by the abundance of metamorphic quartz and rock fragments and supported by the study of undulose extinction and polycrystallinity which have indicated that the detrital quartz is mainly

from a medium to high rank metamorphic rocks and low rank metamorphic rocks. This ~~was~~ also confirmed by the abundance of brown-orange luminescent quartz.

Detrital grains of sedimentary origin are of two folds: quartz with reworked overgrowths (reworked sandstones) and intraformational sedimentary rock fragments. Detrital grains of igneous origin are represented by quartz of hydrothermal origin, volcanic and plutonic rock fragments and euhedral zircon grains.

CORE			OVERGROWTH	
OXIDES	%	TOTAL	%	TOTAL
SiO ₂	98.23	98.64	99.96	100.06
BaO	0.003		0.001	
TiO ₂	0.006		0.004	
Nb ₂ O ₅	0.002		0.016	
ZrO ₂	0.014		0.007	
Y ₂ O ₃	0.002		0.002	
Cr ₂ O ₃	0.002		0.025	
K ₂ O	0.030		0.020	
MgO	0.352		0.002	
UO ₂	0.002		0.002	
ThO ₂	0.002		0.024	

Table 10.1 Electron probe microanalysis of quartz grains (core) and authigenic overgrowths from the Minera Sandstones.

PLATE 10.1

All thin section photomicrographs (except E)

- A. Strongly undulose monocrystalline quartz with numerous small vacuoles. XN. Note also the presence of volcanic rock fragment (r) consisting of very fine crystalline matrix and lath like plagioclase crystals.
Width of field of photograph = 2.7 mm,
Bwlchgwyn sandstone.
- B. Polycrystalline quartz (p) composed of two crystals with straight to slightly curved intercrystal boundaries. Note also concavo-convex grain boundaries
Width of field of photograph = 2.7 mm, XN
Ruabon Sandstone.
- C. Traces of healed fractures may indicate a plutonic source rock. ppl.
Width of field of photograph = 2.7 mm.
Bwlchgwyn sandstone.
- D. Oriented acicular rutile inclusions on the detrital quartz grains. XN.
Width of field of photograph = 2.7 mm.
Minera Sandstone.
- E. Tourmaline inclusion on the detrital quartz grain (d). SEM photomicrograph.
Scale bar = 20 μ m,
Minera Sandstone.
- F. Polycrystalline grains with elongated individual crystals and crenulated crystals boundaries. XN.
Width of field of photograph = 2.7 mm.
Bwlchgwyn Sandstone.
- G. Polycrystalline grains with elongated individual crystals and sutured crystal boundaries. XN.
Width of field of photograph = 2.7 mm.
Bwlchgwyn Sandstone.
- H. Highly compacted kaolinite in between the quartz grains. Note also concavo-convex and sutured grain boundaries. XN.
Width of field of photograph = 2.7 mm,
Bwlchgwyn Sandstone.

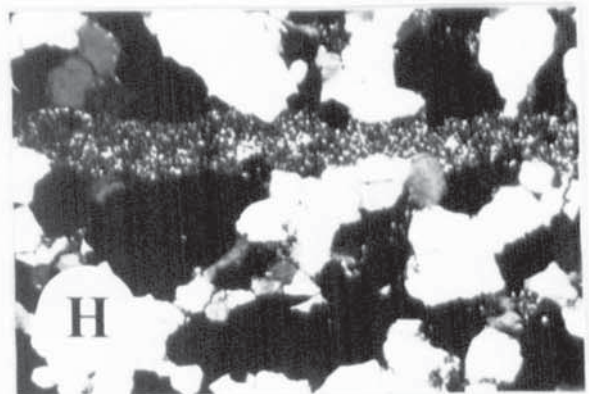
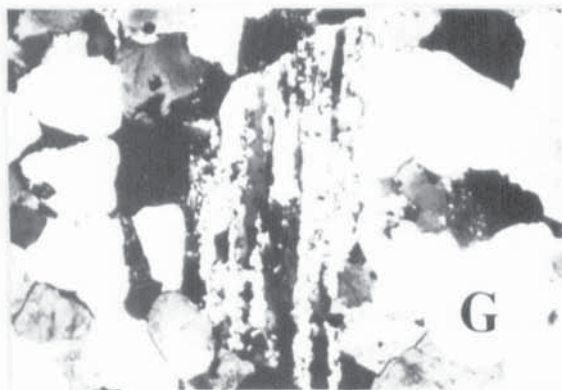
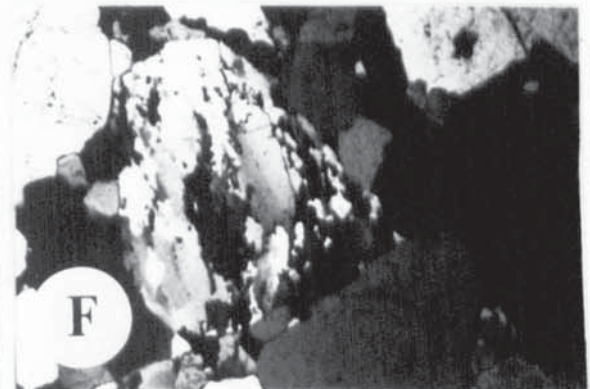
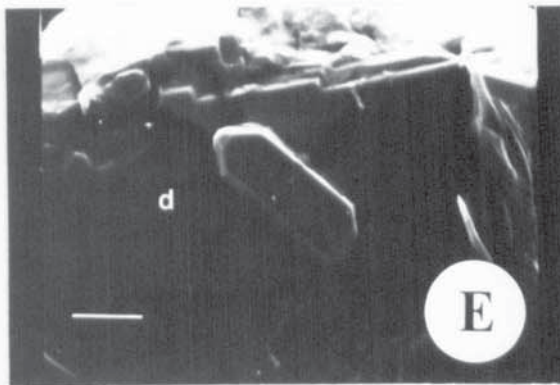
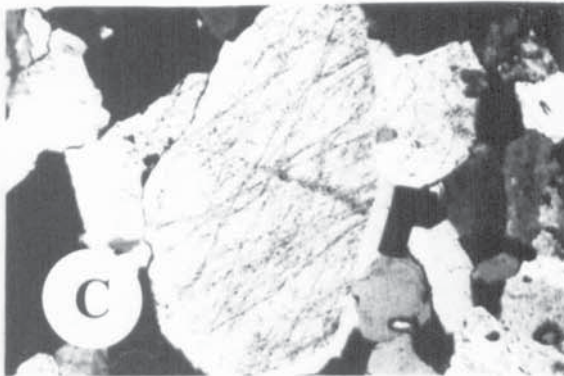


PLATE 10.1

PLATE 10.2

All thin section photomicrographs

- A. Polycrystalline quartz with silt size individual crystals. XN
Width of field of photograph = 2.7 mm,
Minera Sandstone.
- B. Quartz grain with rounded overgrowth. XN.
Width of field of photograph = 2.7 mm,
Minera Sandstone.
- C. Fragments of Graphic granite showing quartz (white) and feldspar (grey) intergrowth, XN. 2.7 mm.
Minera Sandstone.
- D. Metamorphic rock fragment consist of mica with lens like elongate quartz crystals. XN.
Width of field of photograph = 2.7 mm,
Bwychgwyn Sandstone.
- E. Sheared metaquartzites are represented by large grains consisting of many elongate quartz crystals. XN.
Width of field of photograph = 2.7 mm,
Ruabon Sandstone.
- F. Subangular to subrounded sedimentary rock fragments. XN.
Width of field of photograph = 2.7 mm,
Ruabon Sandstone.
- G. Sandstone rock fragments which are rounded and cemented by iron oxide. XN.
Width of field of photograph = 2.7 mm,
Bwlchgwyn Sandstone.
- H. Carbonate rock fragments are normally represented by shell fragments (? brachiopod). XN.
Width of field of photograph = 3.4 mm,
Bwlchgwyn Sandstone.

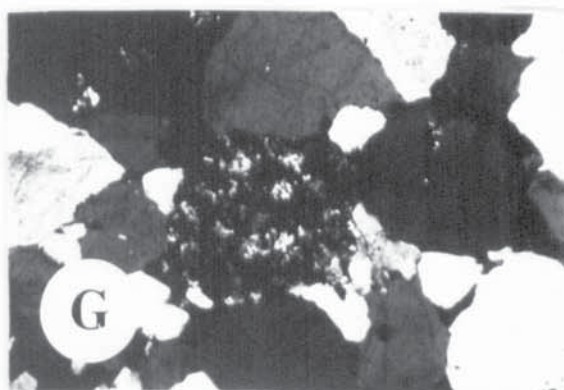
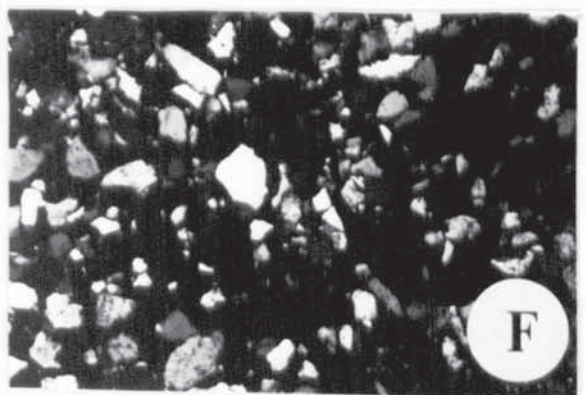
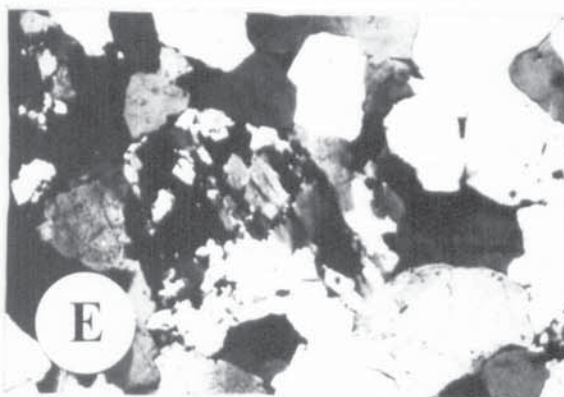
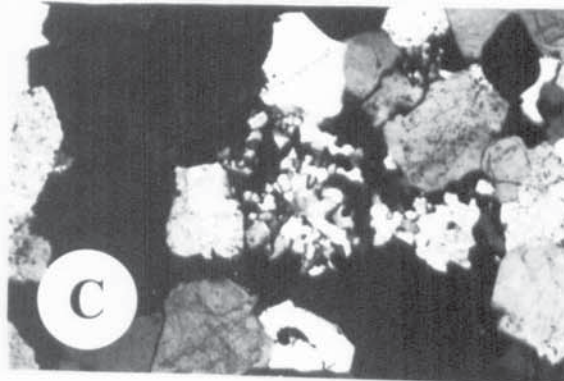
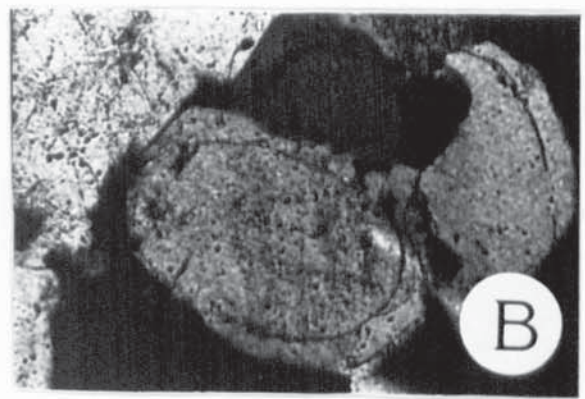
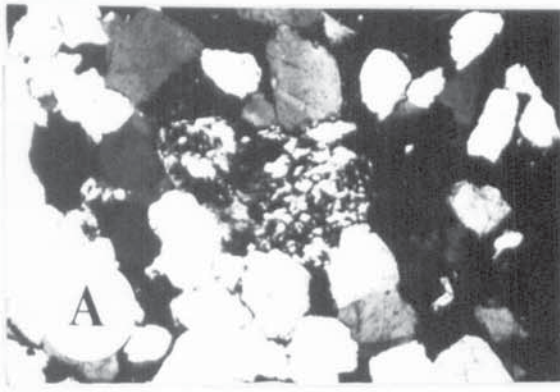


PLATE 10.2

PLATE 10.3 and PLATE 10.4

Cathodoluminescence photographs showing the most abundant type of quartz is the one with extremely faint orange/badly definable dull grey-brown to brown luminescence. Red luminescence quartz is also present. For explanation see text.

Note the characteristic pressure solution features (arrowed) which are only discernable with the help of CL in these sandstones. Note also the two phases of quartz overgrowth development separated by a phase of kaolinite precipitation.

d = detrital grain surface; o= overgrowth; I and (i) = altered illite clays which are now pseudomorphed kaolinite; k = kaolinite.

Note also the presence of hydrothermal origin quartz (h) in Pl. 10.4 B.

Field of view (approximately) 2.8 mm,
Bwlchgwyn sandstone.

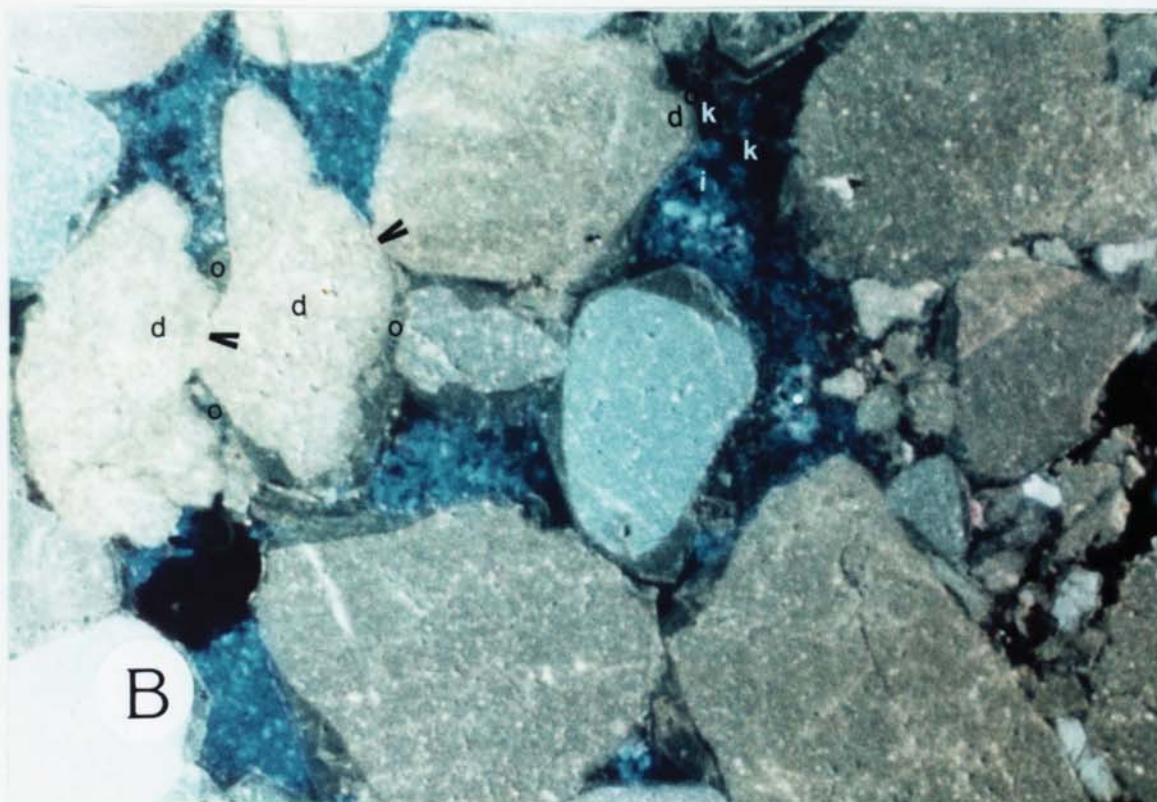
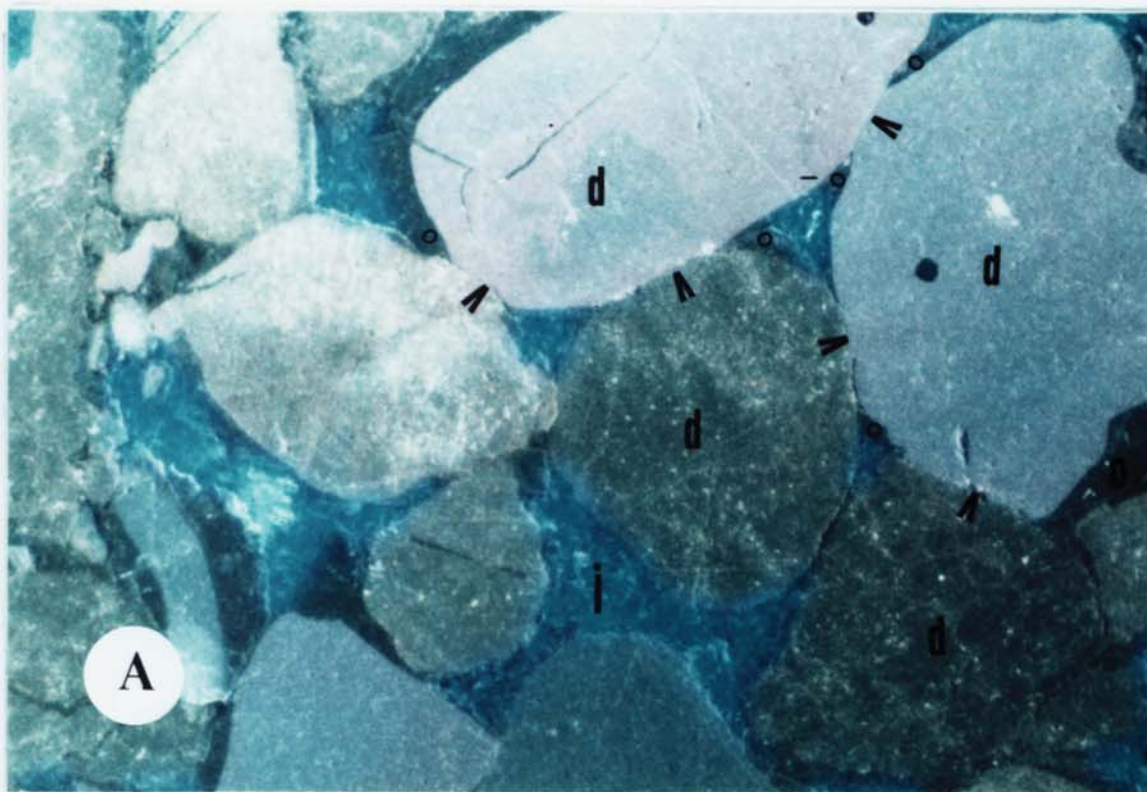


PLATE 10.3

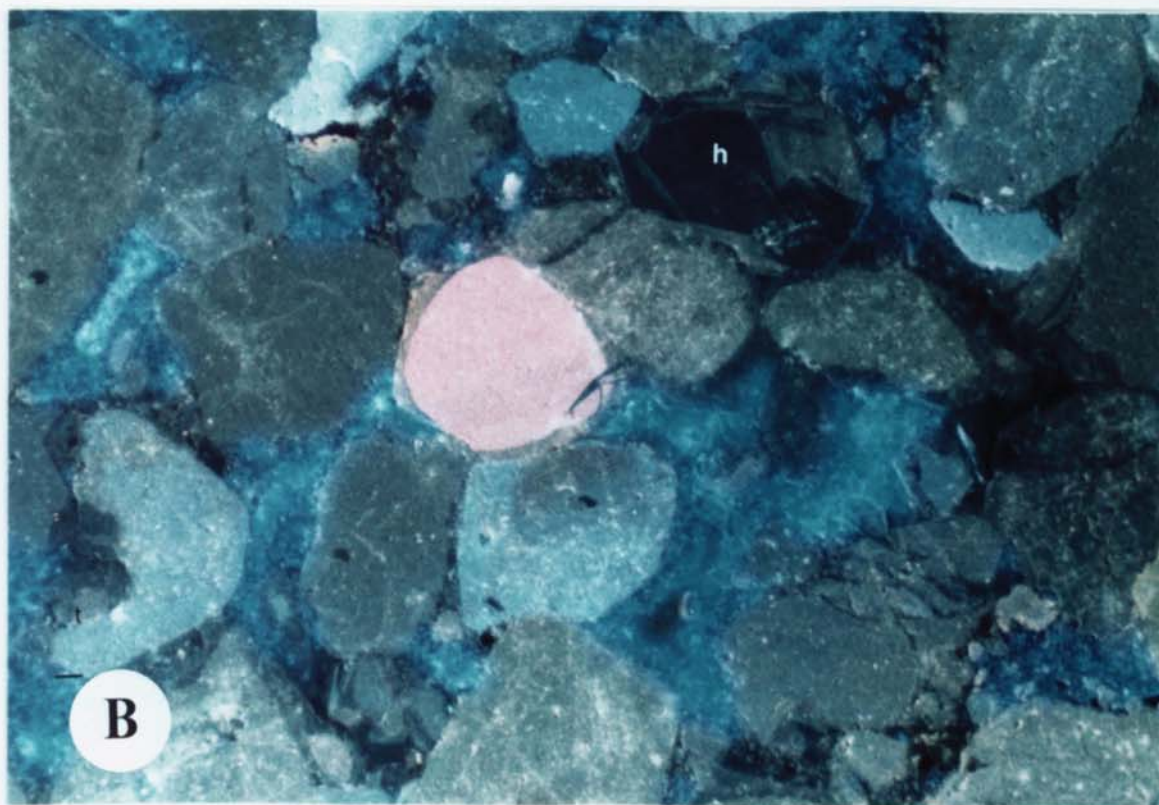
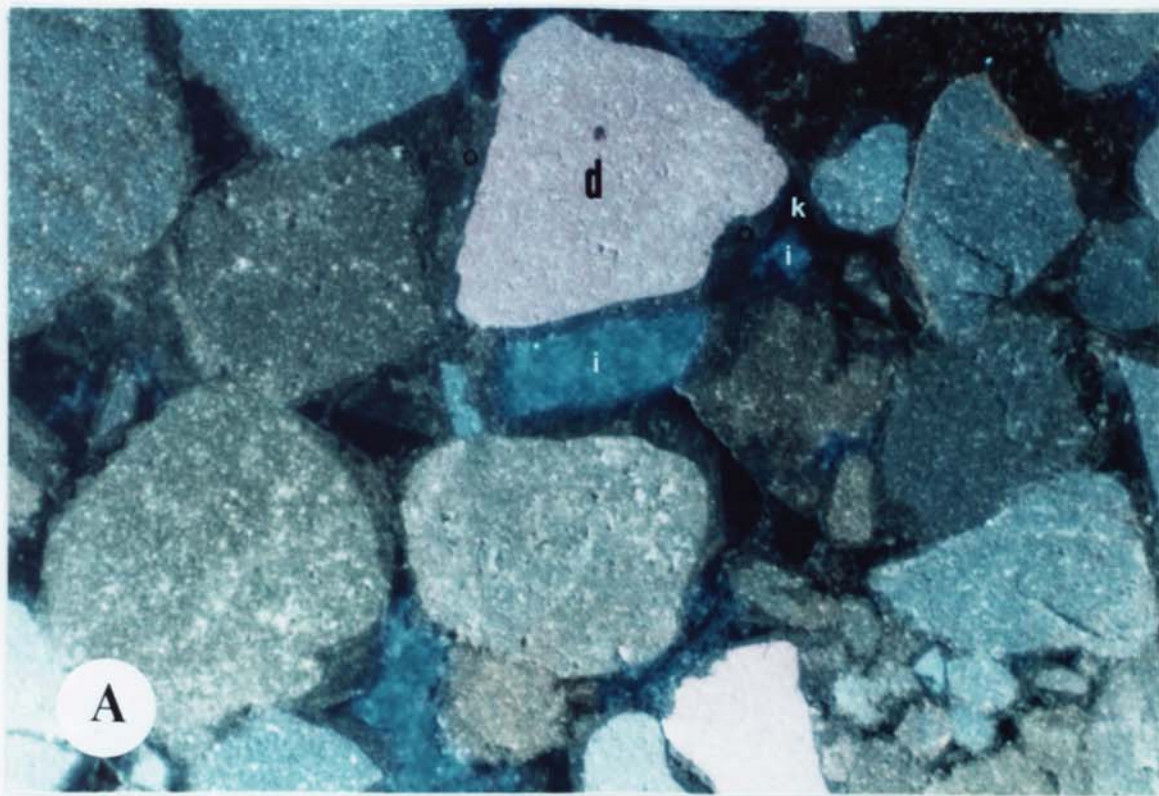


PLATE 10.4

PLATE 10.5

CL photographs showing the well developed quartz overgrowths (o) and detrital grain surface (d). The important feature is the presence of shallow etch pits (e) in quartz overgrowths (Pl. 10.5 A). For explanation of these shallow etch pits see Chapter 11. Note also an example of complex fracturing (f) on the left hand side of Pl. 10.5 B.
Field of view (approximately) 2.8 mm,
Minera sandstone.

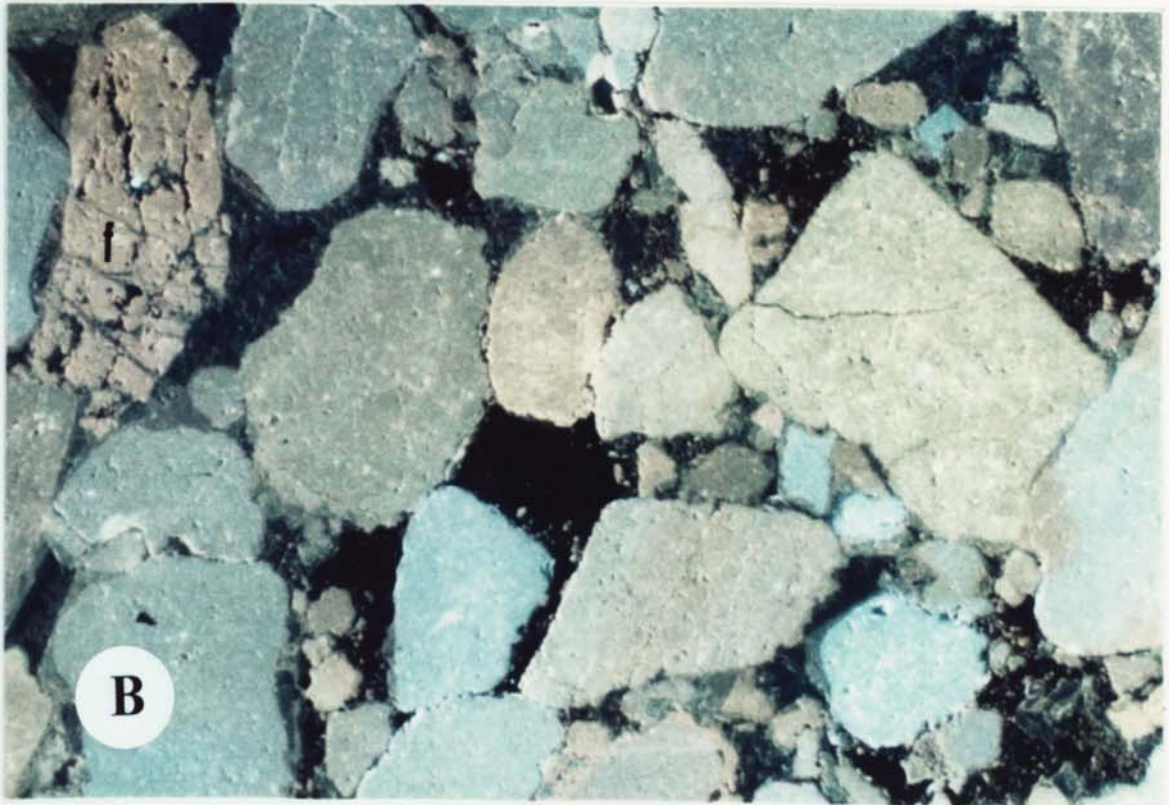
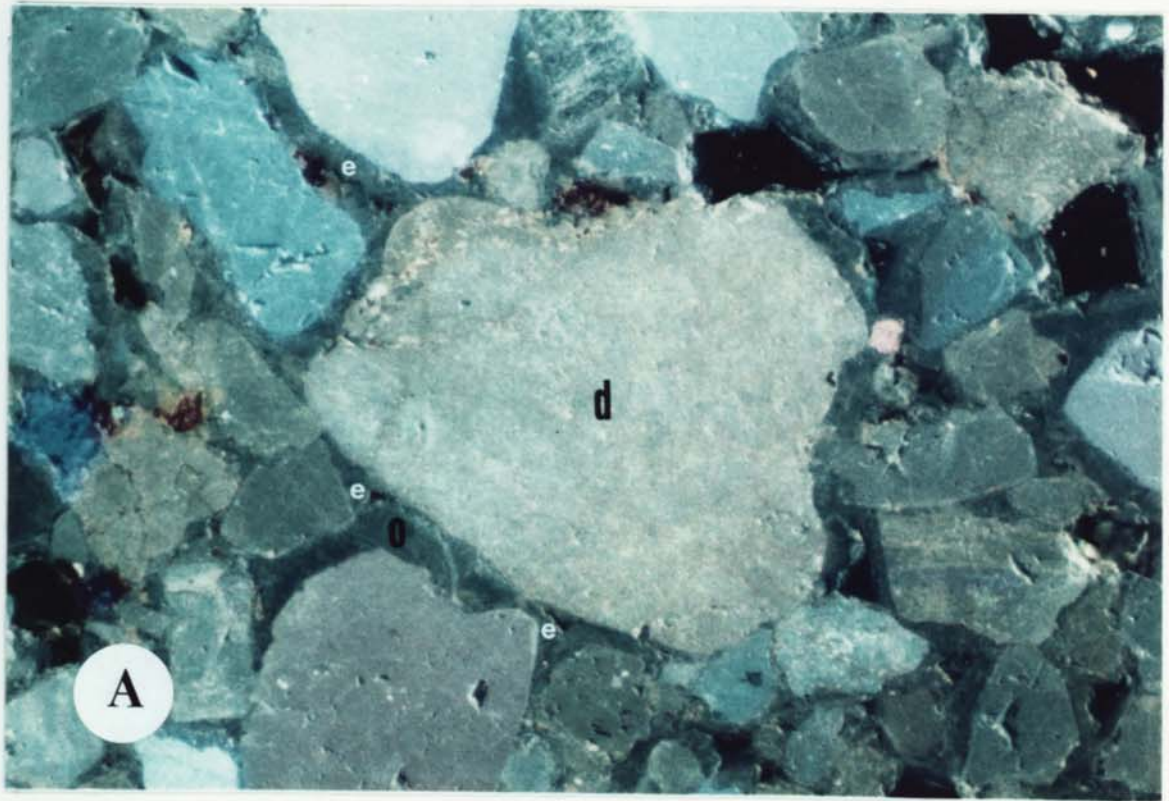


PLATE 10.5

PLATE 10.6

- A. Illustrating the characteristic blue-violet luminescence detrital core and red luminescence overgrowth. For explanation see text. See also the presence of brown luminescence quartz.
Scale bar = 150 μ m; i = kaolinite pseudomorphed by illite.
Bwlchgwyn sandstone.
- B. Characteristic brown luminescent chert rock fragment (Ch)
Scale bar = 150 μ m
Bwlchgwyn sandstone.
- C. Red luminescent carbonate cement. Carbonate cement is extremely rare in these sandstones. Note quartz luminescent is absent.
Scale bar = 150 μ m
Ruabon Sandstone.

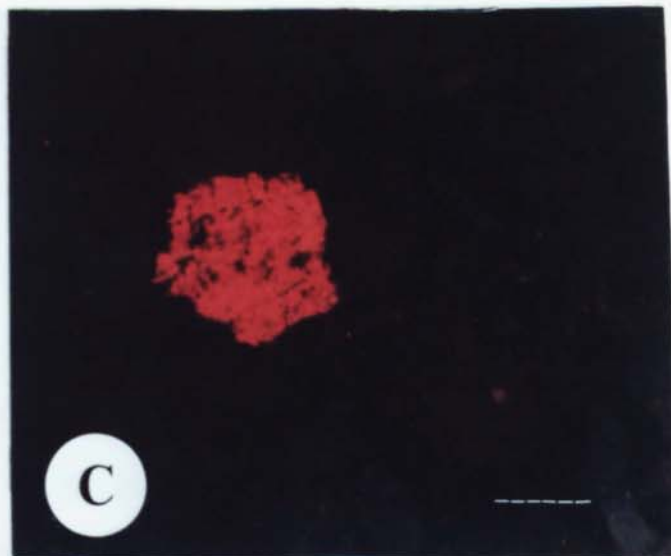
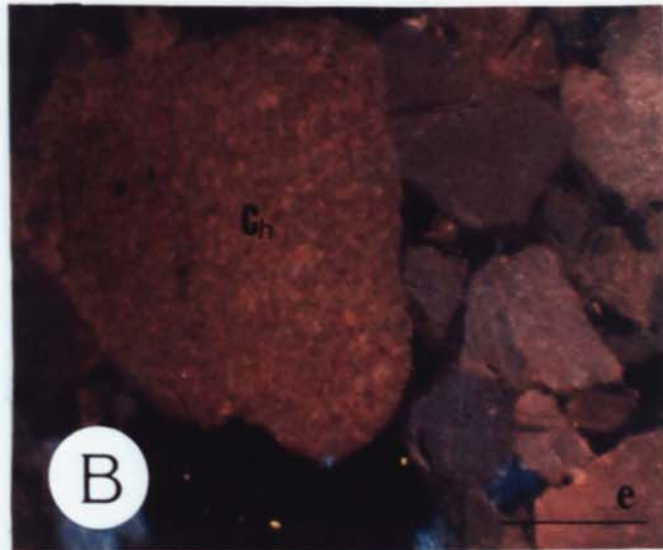


PLATE 10.6

CHAPTER 11

DIAGENESIS

11.1 INTRODUCTION

The term diagenesis is derived from Greek dia. meaning through and Greek genesis meaning formation or origin. Basically, it is the process involving all physical and chemical changes which take place in sediments after deposition but before metamorphism and sub-aerial weathering and which result in secondary porosity.

Since early diagenetic processes take place in an aqueous setting near the depositional interface the depositional environment exercises considerable influence on diagenetic reactions including the resultant authigenic mineral assemblages (Turner, 1980).

The Namurian sandstones in the Bwlchgwyn-Minera-Ruabon area of North Wales were subjected to two different diagenetic processes, such as:

a) Physical process:- this process is characterised by microcrystalline siderite which are frequently plastically deformed between more competent grains of quartz. Their final shape ranges from oval (slight compaction) to particularly thin laminae (extensive compaction). Extensive compaction is also featured by the highly compacted kaolinite in between the quartz grains (Pl. 10.1 H); and the concavo-convex and sutured grain boundaries (Pl. 10.1 B).

b) chemical processes:- diagenetic chemical processes occur in response to changes in pressure, temperature and formation water chemistry. Authigenic minerals can be resulted from solution (neoformation) and interaction between a solid phase and the pore water causing replacement or alteration. Alteration includes degradation and aggradation of clay minerals (Millot, 1970). The effects of the chemical processes in these sandstones can be summarised as follows:

- (1) dissolution of feldspar and quartz
- (2) kaolinite replacement of quartz
- (3) formation of an authigenic mineral suite which includes in paragenetic sequence:
 - (a) siderite crystallization
 - (b) quartz overgrowth
 - (c) kaolinite-dickite precipitation
 - (d) second generation quartz overgrowth
 - (e) illite-smectite (this mixed layer clay mineral is present as only trace amount and has no definite position in the sequence)
 - (f) illite lath growth
 - (g) blocky kaolinite precipitation
 - (h) oxidation of siderite
 - (i) kaolinite precipitation

Before describing in detail the above diagenetic features, it would be wise to have a look very briefly the pore fluid history of the area under survey.

11.2 PORE FLUID HISTORY

The sandstones under investigation belong to the delta top sub-environments with little salinity (see Chapter 5). Therefore, these delta top sandstones would have had fresh connate water. Generally speaking, the assumed connate water would have become increasingly saline and alkaline during burial diagenetic reactions releasing ions into solution. On the otherhand, local reversals of the trend may occur as a result of chemical reactions which release H⁺ ions. Again a regional reversal of the trend towards increased salinity and alkalinity may be favoured firstly, because of the N9 marine transgression (mesothem) of Ramsbottom (1977; see also Biostratigraphical Palynology Chapter 4) during the middle Marsdenian stage; and secondly, structural deformation as a result of late Armorican (or Hercynian) orogenic movements at the

end of Carboniferous; fresh meteoric waters may have penetrated into the sandstones, especially in the structural highs. At this stage quartz cementation took place (Section 11.6.2) and pore fluid evolution was greatly arrested. Some freshening of the pore waters in the sandstones may have occurred after the Carboniferous-Triassic unconformity (Section 9.5).

Data is not available to the author on the present day pore fluid composition of the sandstones used in this study. However, data on the compositions of pore fluids from the Millstone Grit and Coal Measures Sandstones from East Midlands indicate that fresh water has penetrated some, at least the shallower, sandstones, e.g. the Mexborough Rock at Glentworth with salinity of 23, 532 mg/1.^{*} However, it should be borne in mind that the regional geology of the East Midlands and North Wales is quite different.

Table 11.1 summarises the diagenetic processes and the pore water conditions observed in the study.

^{*} (Huggett, 1982)

Diagenetic Processes	Pore water condition
Siderite crystallization	ALKALINE
Quartz overgrowth	
cementation	
Second generation quartz	
overgrowth cementation	
Illite lath	ACIDIC
Dissolution of rock	
components	
Platy and blocky	
Kaolinite crystallization	

Table 11.1: Diagenetic processes and the pore water conditions in the Namurian sandstones of North Wales.

11.3 DISSOLUTION

The detrital silicate grains and carbonates underwent different degrees of alteration due to their reaction with the interstitial pore water with which they were not in equilibrium. This alteration process includes the dissolution and the *in situ* replacement by clay. The degree of alteration depends on the fundamental principles of mineral stability (Keller, 1969) in which minerals are stable only in their formation environment. The lowest members of Bowen's reaction series (olivine, pyroxene, amphibole and ca-plagioclase) tend to be the most unstable phase in the new sedimentary (or depositional) environment.

Dissolution which is a crucial diagenetic feature in these sandstones includes not only the detrital grains but also some of the authigenic minerals and carbonates as well. Dissolution is important for the following reasons: 1) As the dissolution takes place by hydrolysis (Walker *et al.* 1978; Turner, 1980), it supplies a vital source of differentions to the pore water including K, Na, Al, Si, Ca, Mg and Fe. Most of these ions are precipitated later as authigenic minerals. 2) It provides a fundamental source of secondary porosity in the form of dissolution voids. 3) It increases mineralogical maturity of the sediments as a result of increasing the quartz/feldspar ratio due to the abundance of feldspar dissolution and 4) Incomplete dissolution and the clay replacement of the silicate mineral grains increase the clay size fraction and so decrease the textural maturity (Folk, 1951).

11.4 DISSOLUTION OF FELDSPAR - CALCITE - QUARTZ

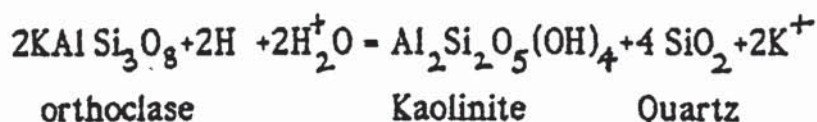
The studied sandstones show that feldspar and calcite are the most common minerals to suffer dissolution. Rare relicts of them in these sandstones indicate their former existence and dissolution voids are picked out in thin section by dyed araldite resin.

The feldspars suffer various degrees of intrastratal dissolution. Potassium feldspar is rarely present and plagioclase feldspar (as it is more chemically unstable than potassium feldspar) is completely dissolved. Dissolution of orthoclase has been observed with the SEM (Pl. 11.1 C-F). The feldspar is preferentially etched along the cleavage planes (Pl. 11.1C). Etching may penetrate deeply into the grain, which gives the feldspar the appearance of a bundle of rods (Pl. 11.1D). Sometimes dissolution has been so intense that all that remains of many feldspars are randomly scattered needles (Pl. 11.1E). In all the above mentioned cases kaolinite was seen associated with the dissolved feldspar. SEM photograph also reveals the association of illite laths with the dissolved feldspar (Pl. 11.1 F).

These dissolution features are very rare as they have not been detected in thin section.

11.4.1 Kaolinization and dissolution

Dissolution of feldspar and kaolinite formation took place in acidic pore waters:



Phase diagram (Figure 11.7), which is taken from Hutcheon (1981), suggests that this will occur below pH5 in the temperature range anticipated for early diagenesis (and is consistent with vitrinite reflectance result). Hutcheon's data was calculated for 500 bars. Wollast (1967) showed experimentally that if $a\text{K}^+/a\text{H}^+$ goes much below 5 or 6, and the silicic acid concentration in solution is below 10^{-3} g/litre, feldspar will kaolinize. Eberl and Hower (1975) noted that feldspar kaolinization is favoured by a low Si/Al ratio. These conditions could be available for delta top diagenesis or relatively fresh water diagenesis. Several authors noted that dissolution and kaolinization of alkali feldspar are important processes, during fresh water diagenesis, yet the solubilities of feldspars are very low (3×10^{-7} mole/litre for K-feldspar and 6×10^{-7} mole/litre for Na feldspar) (Berner, 1978), so that pore water saturation is reached with a very small amount of dissolution. The reaction is most advanced in the thick (>20m) sandstones where down flushing of meteoric water would have been most effective (Huggett, 1982).

During the present investigation it is seen that the relatively medium to coarse grained sandstones display feldspar dissolution most effectively than the fine grained sandstones. This should be the case because from the thick coarse grained sandstones dissolved constituents can most rapidly be removed from the feldspar solution interface and least in the sandstones

with a high detrital matrix content. This feldspar dissolution phase is assumed to be related to post-Hercynian penetration by meteoric water (Section 11.2).

Dissolution of feldspar and carbonate has been an important means of early secondary porosity formation in these sandstones though the formation of secondary porosity does not necessitate a net increase in total porosity as kaolinite (+ dickite) formation as suggested above follows with the feldspar dissolution.

The dissolution effect on carbonate is very considerable in producing large amounts of the secondary dissolution pores. Dissolution is most of the time so extensive that no remnants of the original material were left as a clue to indicate its previous presence. This type of secondary pore can sometimes be detected by their larger size than the surrounding detrital grains (Pl. 11.1 G). These oversized pores (Schmidt and McDonald, 1979b) are occasionally seen in these sandstones, and the original pore filling was more likely to have been carbonate (Pittman, 1979) than any detrital component.

The decrease in pH brought about by the release of H during the kaolinization would have favoured carbonate dissolution (Figure 11.7; see also Section 11.8). This can also be explained by the pH solubility curves of quartz, calcite, and amorphous silica (Blatt *et al.* 1980). Figure 11.6 clearly indicates that near neutral pH both silica and calcite precipitate, but towards acid solutions calcite is highly unstable and dissolves readily, when silica precipitation may continue. This can also explain the presence of a huge amount of silica cementation in these sandstones. This carbonate dissolution is probably also related to the Hercynian orogenic movement. Using the cathodoluminescence technique (Section 11.7.1) it was observed that in some instances prior to quartz overgrowth occurring pressure

dissolution or pressure solution took place between adjacent quartz grains (Pl. 10.3 A, B). This feature will be discussed more fully later.

However, the occasional replacement of quartz by kaolinite (Pl. 11.1 H) may indicate that quartz is slightly unstable under kaolinite forming conditions (Ross and Kerr, 1930).

11.5 CLAY REPLACEMENT

Clay replacement is generally not as common as dissolution in these Namurian sandstones. However, the replacement clay, which is considered authigenic (Wilson and Pittman, 1977) also effects the chemistry of sediments.

In SEM studies feldspar is sometimes shown to be partially replaced by kaolinite associated with dissolution (Pl. 11.1 C-E), and in thin section quartz is also seen to be partially replaced by kaolinite (Pl. 11.1 H). Very occasionally rock fragments have also been partially replaced by clay minerals.

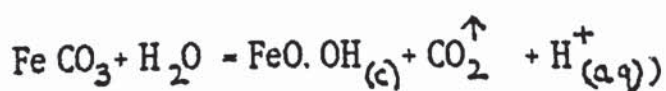
11.6 AUTHIGENIC MINERALS

11.6.1 Siderite

Microcrystalline siderite cement was found very occasionally as a pore rimming cement together with some rounded reworked grains. Siderite cementation was found as thin crust around the detrital quartz grains (Pl. 11.2 A, B). Compaction of siderite cement and its presence at grain contacts (Pl. 11.2 C) and being overgrown by quartz overgrowths (Pl. 11.2 D) suggest an early cement origin. This is consistent with the observation of Berner (1980) that siderite can form at depths as shallow as 0.5 m in nearshore and fresh water muds. Siderite formation needs sufficient organic material to be incorporated into the cement in order to keep the iron in the reduced state aided by a low CO_2 concentration that is necessary to maintain the Fe^{2+} in solution as $\text{Fe}(\text{HCO}_3)_2$. Strong reducing condition is

necessary for siderite formation in which all sulphate is reduced by bacterial decomposition of organic material to H_2S . Berner (1981) concluded that when all the S has precipitated out as iron sulphides (pyrite), the Fe^{2+} concentration may build up to saturation with siderite. A low sulphate concentration increases the likelihood of siderite formation. The sandstones under consideration are characterised by low S (Appendix 11) and low organic matter. Low sulphate is characteristic of fresh water thus the predominance of authigenic siderite in non-marine sediments.

Some of the microcrystalline form siderite (Pl. 11.2 D) has been oxidised to goethite. With the SEM goethite needles were observed overlying siderite and all other diagenetic minerals (particularly authigenic quartz Pl. 11.2 D). However, the X-ray diffraction of the fine clay fraction separated from some of the studied sandstones, shows no evidence of goethite peaks despite their brown colour. This indicates that the amount of goethite present is below the XRD detection limits. Goethite, as seen with the SEM may have occurred during the Hercynian uplift and folding, or during more recent penetration of the sandstones by meteoric water or fresh water. However, the goethite needles were observed overlying siderite and quartz, indicating that oxidation of siderite occurred after the main phase of diagenesis. Assuming a closed system, the important results of this reaction are the increase in acidity and porosity (Huggett, 1982).



In some samples kaolinite occurs having precipitated in the secondary porosity created by siderite dissolution via oxidation to goethite. It could be expected as the local decrease in pH brought about by the release of H^+ during the oxidation of siderite to goethite would have favoured kaolinite (and perhaps dickite) formation.

11.6.2 Quartz

Examination of detrital quartz grains from the Bwlchgwyn-Minera-Ruabon sandstones using cathodoluminescence and scanning electron microscopy, reveals the existence of euhedral quartz overgrowths. Distinct growth stages are visible and correspond to those described by Waugh (1970a), Pittman (1972), Marzolf (1976) and Wilson (1978). Overgrowths in these sandstones are well known but this is the first study in which they are examined by cathodoluminescence and scanning electron microscopy.

Cathodoluminescence (CL) of polished thin sections indicated that as much as 95% of the quartz is overgrowth in the arenites. Grain to grain contacts are occasionally observed, which suggests that some compaction of the sediments occurred prior to the onset of quartz cementation. SEM reveals quartz overgrowing authigenic siderite (Pl. 11.2 A, B, D) and illite (Pl. 11.5 E), while CL reveals two phases of quartz overgrowth cementation are separated by a phase of kaolinite precipitation (Pl. 10.3 B; Pl. 10.4 A). These phases suggest that quartz formation continued throughout the time that other authigenic minerals were forming.

The evidence from SEM examination suggests that the processes leading to the formation of large well developed overgrowths are complex. Pittman (1972) identified two types of incipient overgrowths and these have been observed in the sandstones studied here. Firstly, development commences with the appearance of numerous oriented crystalline projections (2-20 μ m). See (Pl. 11.2 D-H). Some of these are larger than the initial growth features described by Pittman (1972) and Marzolf (1976) but are nearer to those observed by Waugh (1970) and Wilson (1978). Some specimens display two stages of overgrowth development as shown by Pittman (1972). Pl. 11.3 A A shows that the smallest forms are 'bloblike' to euhedral discrete crystals while the larger overgrowths have well developed crystal faces. These two varieties of overgrowths are connected in places.

Marzolf (1976) also noted that the smallest forms could be euhedral shaped. This feature was not observed by Wilson (1978) from the Namurian sandstones of the Southern Pennines. Secondly, there are isolated overgrowths with well defined crystal faces which commonly grow until contact is made with an overgrowth that nucleated elsewhere on the surface of the host grain (Pl. 11.3 B-D). The orientation and relative facial development of the small quartz euhedra are governed by the crystal lattice of the detrital grain. The most rapid growth takes place in the direction of the c-axis (Van Praagh, 1947; 1949) and this axis can be determined from the orientation displayed by the quartz euhedra. Divergent orientations indicating polycrystalline or composite grains have not been found. Similar observation was also done by Wilson (1978) from the Namurian sandstones of the Southern Pennines.

Normally the tendency of overgrowth is to grow into a pore space until and unless an adjacent grain or overgrowth is encountered (Pl. 11.2 D; Pl. 11.3 E). Continued growth leads to enlargement of the quartz euhedra aided by merging and overlap of the crystal faces. This results in the formation of larger faces which continue to grow at the expense of the initial oriented euhedra (Pl. 11.3 F-H). For this to happen similar crystallographic orientations of the small euhedra is essential. At this stage boundaries between euhedra gradually cease to exist and growth continues as a single crystal. Whether prism or rhombohedral faces predominate is a function of the initial growth location with respect to the detrital grain axes (Wilson, 1978). Presumably it is at this stage incompletely developed crystal faces may appear (Pl. 11.4 A-H). Pittman (1972) noted that such a crystal face could develop due to merging of irregular overgrowths and eventually the holes in the crystal face would have been infilled providing growth of authigenic quartz continued. Given sufficient space overgrowth development may be completed by masking the whole of the detrital grain surface. Waugh (1970) noted such features from the 'Penrith Sandstone'.

However, this final stage has not been recorded in the sandstones under survey with the exception of a few small grains not bigger than $120\ \mu\text{m}$. Similar features were also noted by Wilson (1978) from the Southern Pennines. In general, growth has proceeded to the stage where large areas of the detrital grains are masked by either well-defined prism or rhombohedral faces or both, with considerable areas of the detrital grain still unmasked (Pl. 11.3 B, D; Pl. 11.4 A; Pl. 11.5 A-D). Obviously the lack of total enclosure of the detrital grains is due to the lack of available space for complete crystal growth within the host rock. This could be due to the presence of grain to grain contacts (pressure solution) in these sandstones as revealed by cathodoluminescence.

Riezebos (1974) was unable to establish from SEM observations whether or not the boundaries between quartz overgrowths and the detrital grains are continuous or interrupted by voids. However, Pittman (1972) concluded that the 'dust line' was composed of voids, he postulated that the 'dust' enters into the voids after overgrowth formation.

Huggett (1982) using a high voltage electron microscope (HVEM) confirmed that the contact between a host grain and its overgrowth is punctuated by numerous voids. The latter author also noted that the 'dust' is essentially of iron oxides. However, the present study is inconclusive.

Coatings on quartz grains are considered to be important in controlling quartz cementation in a number of sandstones. Heald (1965); Pittman and Lumsden (1968) and Tillman and Almon (1979) suggested that clay coats inhibit overgrowth. Pittman (1972) observed overgrowths which had grown over thin clay rims. He also suggested that overgrowths will form on quartz grains which are only partly covered with a clay coat or on a thin microscopically discontinuous clay coat. However, in this study it was observed that a quartz overgrowth was able to nucleate where a gap in a

clay coat occurs, and may spread, either over the clay coat or form small prismatic growths between the clay particles (Pl. 11.5 E). Generally tangential (Pl. 11.5 E) and radial rims of illite laths are better quartz overgrowth inhibitors than kaolinite. Kaolinite has normally few points of contact with the quartz grains on which it rests, thereby leaving much of the grain surface available for overgrowth.

"Gullying" a high relief surface texture that was first described by Higgs (1979) is illustrated by the Pl. 11.5 F. This sort of texture where all gradations between slightly modified, youthful, immature overgrowth could be discerned, is thought to be originated from marine abrasion/dissolution of pedologically formed overgrowths (Higgs, 1979).

11.6.3 Formation of Quartz

Conditions favourable to quartz precipitation are low temperatures (Garrels and Christ, 1965; Fournier, 1973) and $\text{pH} < 9$ (Krauskopf, 1979; Blatt *et al.* 1980). In unsaturated solutions at ordinary temperature (25°C) and pH values of less than 9 silica in true solution is predominantly in the form of orthosilicic acid (H_4SiO_4 ; See Figure 11.5). It is understood from laboratory experiments that the solubility of silica is a function of temperature, pressure and the crystalline state of the solid phase. Normal procedure is amorphous silica > opal-CT > chalcedony > quartz. The solubility of quartz at 25°C and 1 bar is $\sim 6\text{ppm}$ (Morey *et al.* 1962). With increasing temperature the solubility of quartz rises only slowly such as 21 ppm at 50°C ; 62 ppm at 100°C and 140 ppm at 150°C . From Figure 11.6 the pH range necessary for silica precipitation (and calcite) is also obvious i.e. $\text{pH} < 9$. Krauskopf (1979) also demonstrated that the solubility of quartz rises abruptly above pH 9. Quartz cementation is, therefore, likely in the same chemical and physical environment as feldspar and mica alteration to kaolinite, because these reactions require H^+ ions and therefore a low pH.

11.6.4 Clay Minerals

This is not the place to give a text book on clay mineralogy the basis of which is now well established (Brindley and Brown, 1980). However, morphology, crystallinity, distribution and the outlines of a system of identification will be discussed here only of those clay minerals which were found in the present survey.

The morphological descriptions are mostly based on observations made with the SEM attached with EDAX spot analysis system. Qualitative data on their crystallinity have been obtained using X-ray diffraction (XRD). The clays were identified in thin section by reference to Deer *et al.* (1966) and from X-ray diffractograms by reference to Brown (1961) and Brindley and Brown (1980). The clays identified were kaolinite, dickite, illite and rarely trace amounts of mixed layer illite-smectite.

11.6.5 Semi-Quantitative XRD Analysis

Semiquantitative XRD analyses of the clay fraction of the Bwlchgwyn-Minera siliceous shales were obtained partly following the method of Carver (1967). But Carver's method calculates the clay minerals as 100% of the sample, which is not the case actually. To get rid of this problem and also to get the absolute percentages of each clay mineral species a quantity called "clay", which equals the weight percentage of the clay in the sample was calculated as follows:-

$$\text{clay \%} = 100 - (\text{quartz \%} + \text{organic carbon \%} + \text{carbonate \%})$$

The above equation is in agreement with the simple mineralogy of these siliceous shales (Section 9.8). The clay percentages obtained from Carver's (1967) method were then computed with the "clay" percentages obtained from the above equation to get the absolute percentages of individual clay mineral species. In doing so the rare occurrences of trace amounts of mixed

layer illite-smectite was totally ignored. However, the accuracy of the whole method ranks only as semiquantitative analysis.

'Terrig River Shales' contain only one clay mineral species (i.e. illite), hence the above equation could easily be used to find out their absolute percentages on a semiquantitative rank.

The minimum, maximum and average percentages of each of the clay minerals in the 'Bwlchgwyn- Minera Siliceous Shale' and the 'Terrig River Shale' are given in Table 11.2. The X-ray diffraction results of the sandstones and the interbedded siliceous shales of the Bwlchgwyn-Minera-Ruabon area are shown in Figures 11.1; 11.2 and that of the 'Terrig River Shale' is in Figure 11.3.

Location	Terrig River n=7			Bwlchgwyn Quarry n=7			Minera Quarry n=7		
	Mini- mum %	Maxi- mum %	Average %	Mini- mum %	Maxi- mum %	Average %	Mini- mum %	Maxi- mum %	Aver- age %
Dickite	-	-	-	10.0	31.0	21.60	trace	16.81	16.81
Illite	35.0	53.0	43.0	11.35	17.0	15.0	9.0	40.0	24.0
Illite- Smectite	-	-	-			trace amount			

Table: 11.2 The minimum, maximum and average percentages of each of the clay minerals in the shales under survey.

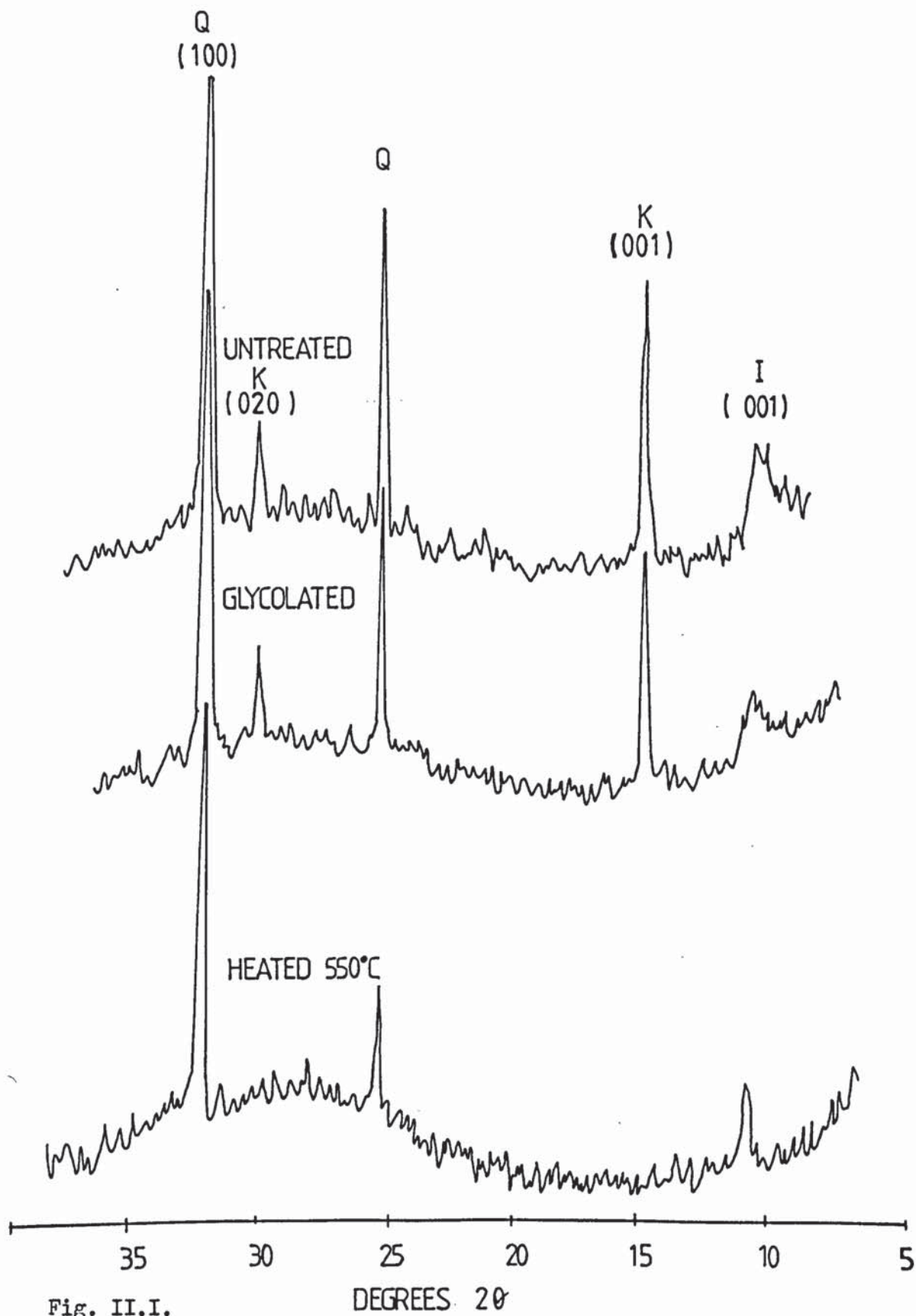


Fig. II.I.

X-ray diffraction patterns of the clay fractions in the 'Bwlchgwyn - Minera Ruabon Sandstone', using Ni filtered $\text{CoK}\alpha$ radiation. K = Kaolinite, I = Illite, Q = Quartz.

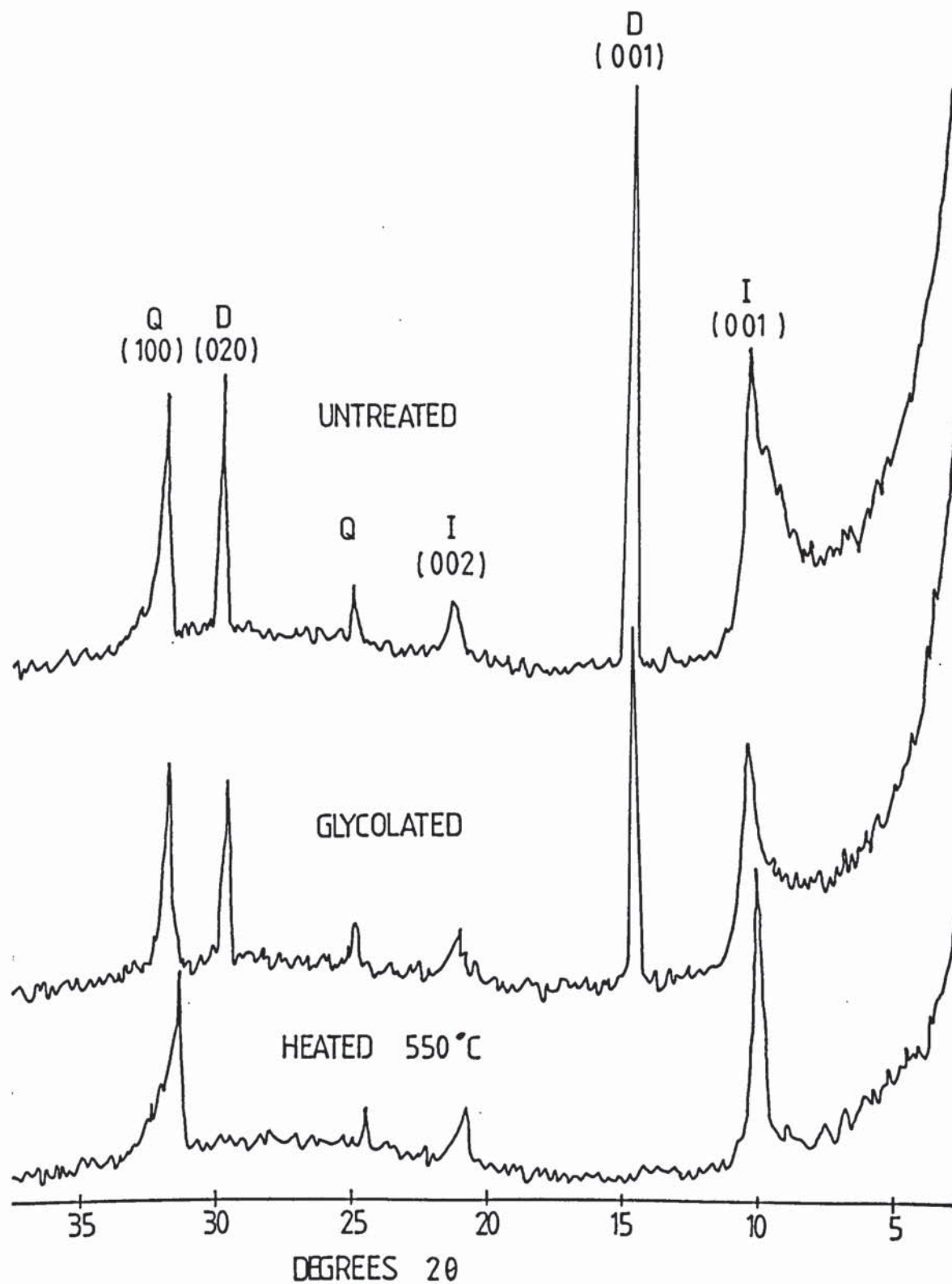


Fig. II.2.

X-ray diffraction patterns of the clay fractions in the Bwlchgwyn-Minera Siliceous Shale using Ni filtered $\text{CoK}\alpha$ radiation. D = Dickite, I = Illite Q = Quartz.

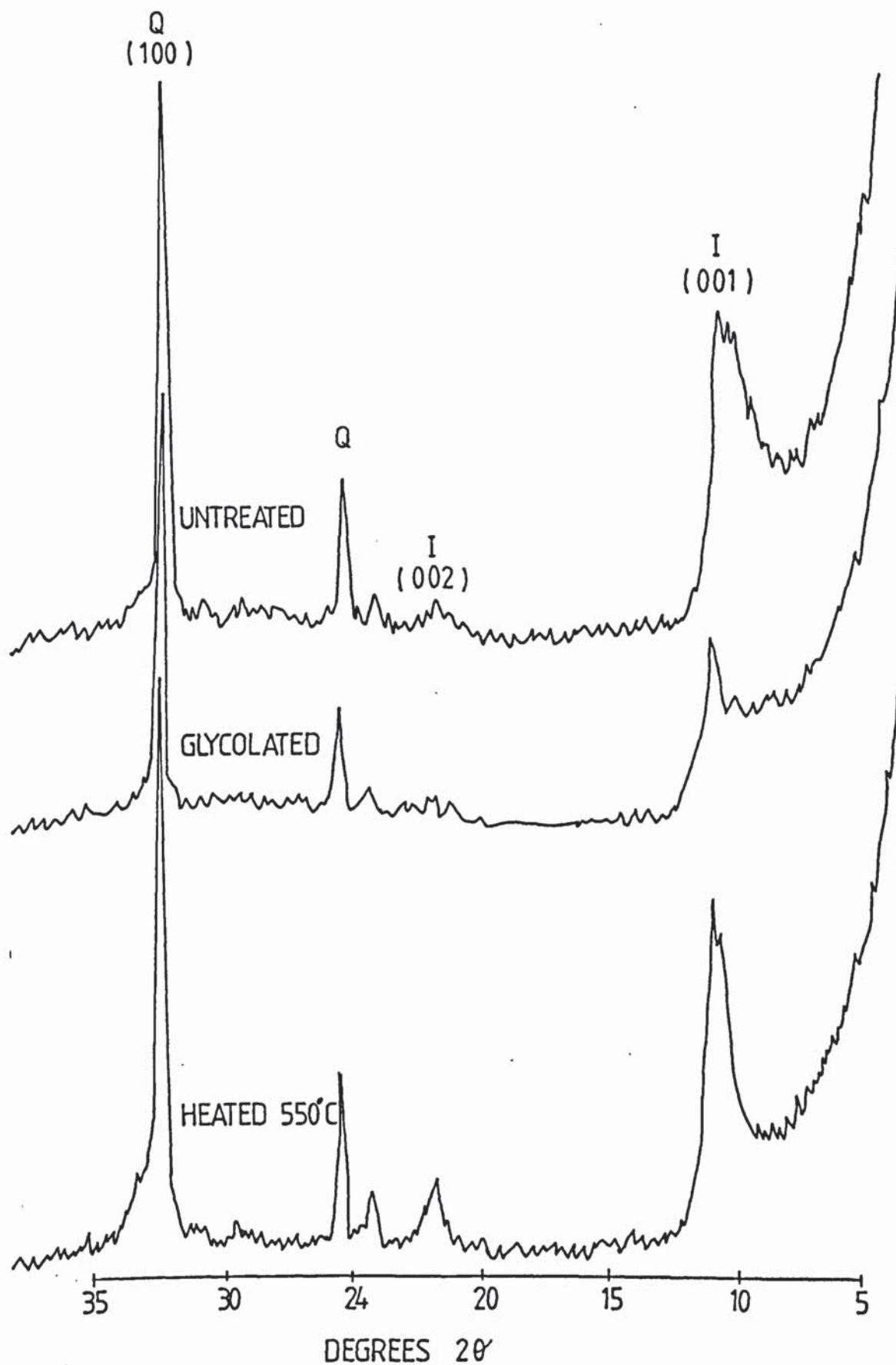


Fig. II.3.

X ray diffraction patterns of the clay fractions in the Terrig River Shale using Ni filtered $\text{CoK}\alpha$ radiation. I = Illite, Q = Quartz.

11.6.6 Kaolinite

7Å clay mineral, Kaolinite will be discussed in detail in this section. In doing so passing reference of another 7Å clay mineral, dickite, will be made whenever necessary.

It is difficult to distinguish between kaolinite and dickite by using SEM only but they can be readily identified using X-ray diffraction.

Judging from Brindley and Robinson (1946a) the author believes that most of the kaolinite encountered in the siliceous shale samples are dickite rather than kaolinite minerals. This may be supported by the suggestions of Hanson *et al.* (1981) that dickite is the more stable polymorph of this group. The kaolinite group minerals which formed during early stages of diagenesis were probably transformed to a high stable polymorph (dickite) in the shales.

Some authors prefer to use the term kandites to include both kaolinite and dickite due to the confusion which may arise out of using the term kaolinite.

However, the following is a detailed description of morphology, distribution and crystallinity of kaolinite observed in the sandstones.

(a) Morphology

Kaolinite, the dominant 7Å clay mineral in the sandstone generally forms 6 sided polygonal plates about $6\mu\text{m}$ - $10\mu\text{m}$ across the (001) face (with respect of width). The 6 faces of the {001} form may be equi-dimensional or 2 (or 3) of the faces may develop to the detriment of the other 4 (or 3) faces (Figure 11.4). Interfacial angles are usually around 120° . Growth steps and growth spirals are common features of the (001) face (Pl. 11.6 A-C). Growth steps are possibly the cause of the wedge shaped crystals

which were occasionally noticed (Pl. 11.6 D). Crystals which have a c-axis elongation are termed 'blocky' (b) Kaolinite (Pl. 11.6 E, G, H; Pl. 11.7 G; Pl. 11.8 A), and those which are short in their c-axis direction are called 'platy' kaolinite (Pl. 11.6 F, H; Pl. 11.7 A, B, D).

Blocky kaolinite mostly occurs as randomly arranged and loosely packed with a high proportion of face to edge contacts (Pl. 11.6 E, G, H; Pl. 11.7 G), while platy kaolinite mostly forms books stacked parallel to the C-axis (Pl. 11.6 F, H; Pl. 11.7 A, B, D). Loosely packed platy kaolinite with a high proportion of face to edge contacts were extremely rare. The books are referred to as vermicules if the C-axis length is more than double the width of the plates and the plates in books and vermicules may all have approximately the same thickness, or they may vary by more than $1\mu\text{m}$ in thickness (Huggett, 1982). Crescent shaped vermicules are not rare (Pl. 11.7E). The curvaturae in this case is probably due to the presence of wedge shaped plates in the book rather than random stacking of them. In cases, where the plate thickness varies only slightly the plates are often closely spaced and arranged in crystallographic continuity (Pl. 11.7 A-C). Sometimes closely spaced plates appear to have slipped over one another (Pl. 11.6 H; Pl. 11.7 A). When the plate thickness varies widely the plates usually show a random arrangement in the stack and the plate width may also vary along the length of a stack (Pl. 11.6F). Books with a crystallographic continuity sometimes appear to be fused along a seam parallel to the C-axis (Pl. 11.6H; Pl. 11.7 A). Thin plates are sometimes bent around large kaolinite crystals (Pl. 11.7 B) or around a plate which is at an angle to the rest of the book. Occasionally plates with ragged or rounded faces were observed (Pl. 11.7 H). These may be dissolution features. Mansfield and Bailey (1972) noted that grooves or notches in kaolinite flakes and books may be indications of twinning (Pl. 11.7 F).

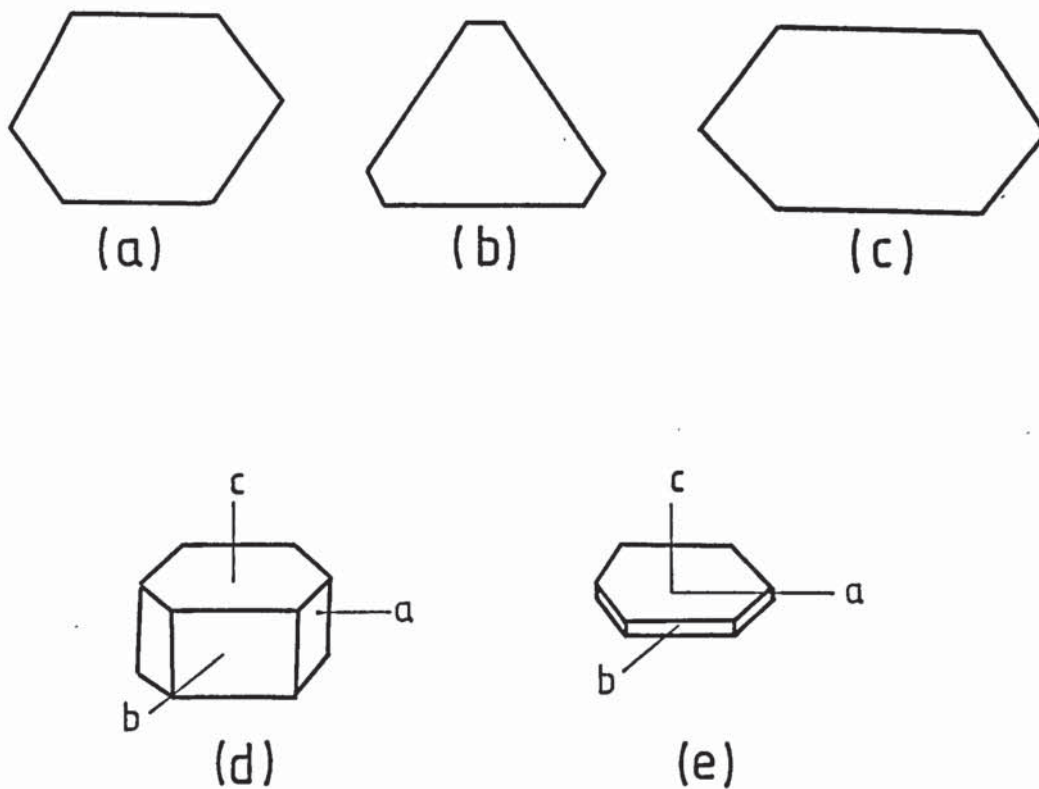


Fig. II.4.

Morphologic variations in Kaolinite clay mineral (a),(b) &(c) (001) faces;(d) blocky Kaolinite;(e) platy Kaolinite.



Fig. II.5.

Total silica and relative amounts of silica species in solution in water at 25°C as a function of pH. (after Blatt et al., 1980)



Fig. II.6.

Relationship between pH and the solubilities of calcite, quartz and amorphous silica. (after Blatt et al., 1980)

(b) Distribution

Kaolinite is abundant in the sandstones while dickite is the main 7Å clay mineral in the interbedded siliceous shales. Platy kaolinite is more common than the blocky kaolinite in the sandstones. Thin section study reveals that kaolinite is fresh and uncontaminated by any other minerals. Blocky kaolinite generally forms pore fills and very small (<20 μm) blocky kaolinite crystals occasionally enveloped by quartz overgrowth (Pl. 11.8 C, D) or occur either singly and resting on larger kaolinite plates (Pl. 11.8 B) or in clusters (Pl. 11.8 C, D). Huggett (1982) noted that kaolinite books and vermicules mostly occur lining pore spaces between grains. However, during the present investigation it was noted that 'books' may occur both as 'pore filling' and 'pore lining'. Cathodoluminescence (CL) study reveals that two phases of quartz overgrowth cementation are separated by a phase of kaolinite precipitation.

(c) Crystallinity

With the help of XRD and SEM, dickite is the most dominating kaolin mineral detected in the siliceous shale interbeds of the Bwlchgwyn-Minera-Ruabon sandstone unit. According to Brindley (1980), dickite is a better crystallised material than kaolinite though it is the less common form of the kaolin minerals.

Sulaiman (1972) reported halloysite, in addition to kaolinite from the Irish Namurian. However, halloysite was not detected during the present investigation. This may suggest that the clay mineralogy of the Irish Namurian and the North Wales Namurian differ slightly.

The dickite (001) spacing measured from XRD traces varies between 7.11Å-7.12Å. The peak is invariably sharp indicating a high degree of crystallinity. All dickites are unaffected by glycolation and heating to 550°C (and a little higher) destroys their crystal structure (Figure 11.2).

Kaolinite is the dominating kaolin mineral detected in the sandstones. There is a transition from well crystalline to poorly crystalline kaolinite which is reflected in the diffraction patterns by the broadening and weakening of the peaks and a tendency for adjacent reflections to fuse. This is accompanied by an increase in spacing of the basal reflections from 7.12 Å to 7.14 Å. Examples of the complete range of diffraction patterns are given by Brindley (in Brown, 1980).

The general absence of the 021 reflection on the XRD traces (seen only very rarely) is indicative of b-axis disorder (Barrios *et al.* 1977).

All kaolinites, similar to dickites, are unaffected by glycolation and heating to 550°C destroys their crystal structure (Figure 11.1).

It should be remembered that these are averaged observations from all the kaolinites and dickites present and may represent a mixture of well crystallised and b-axis disordered varieties.

11.6.7 Formation of Kaolinite

The kaolinite occurs as a neoformational authigenic cement which formed in fresh, acid pore waters with a low aK^+ / aH^+ (see Section 11.4 and the Figure 11.7, the activity diagram in the kaolinite-illite-K-feldspar system) and a high Al_2O_3 concentration. Huang and Keller (1970) noted that the formation of kaolinite at low temperatures may be catalysed by organic compounds which enhance the solubility of Al_2O_3 and SiO_2 by complexing with them, thus making available the otherwise highly insoluble Al. This may have been an important process for the large scale kaolinization in these sandstones as the interbedded siliceous shales contain high amount of Corg (average about 4.5 wt%; see Appendix 9).

On the other hand, the low aK^+/aH^+ required for kaolinite formation may also have been maintained by degraded illite absorbing K^+ . But the illites found in these sandstones contain irregular 'blob-like' (gel-like) cores (Pl. 11.1 F), suggests that the illites form by chemical precipitation rather than from the degradation of micas (Güven *et al.* 1980). Moreover, compared to kaolinite, authigenic illite is rare in these sandstones.

On the contrary, the illites of the siliceous shale interbeds are structurally disordered presumably caused by the presence of hydrated cations in the interlayer sites and contain high K^+ (see Section 11.6.8 (c)).

Thus, it seems likely that the illites and the Corg of the interbedded siliceous shales played an important role for the kaolinization and dickitization of the sediments under consideration. Certainly some of the kaolinite formed late in the diagenetic history as a result of meteoric waters penetrating the sandstones, probably after the Hercynian orogenic movement. The small, blocky uncleaved kaolinite crystals, resting on books of thin kaolinite plates (Pl. 11.8 B) may be of just such a late diagenetic origin. In some samples kaolinite infills porosity created by siderite dissolution, hence these kaolinites must post-date oxidation of siderite.

The abundant pore filling euhedral crystals of kaolinite which are not contaminated with any precursor mineral must be neoformational.

Millot (1970) noted that the preparation of synthetic kaolinite from solution requires the Al^{3+} to be in hexacoordination. Siffert and Wey (1961) induced hexacoordination of Al^{3+} by complexing with oxalate ions. An analogous role under natural conditions may be played by some organic constituents of soils or sedimentary organic matter in rocks such as acetate ions. Ca^{2+} and Mg^{2+} may inhibit hexa-coordination of Al^{3+} , thus these two

cations inhibits kaolinite formation. But a low pH and a high Al to cations ratio favour the formation of $\text{Al}(\text{OH})_4^{3-}$ (Milot, 1970).

In this study it was noted that kaolinite has a random crystallographic orientation within, and adjacent to feldspar (Pl. 11.1 C-E). Such a feature indicates a solution phase in the transformation of feldspar to kaolinite (Huggett, 1982) and thus the kaolinite is neoformational. Tchoubar (1965) found that following feldspar dissolution the initial kaolin mineral to precipitate was usually halloysite, which within hours transformed to bohemite. In a few weeks time the bohemite recrystallized into disordered kaolinite sheets which ultimately broke up into laths or ordered kaolinite. Rarely kaolinite^{is} the first phase to precipitate. The necessary conditions of the above experiments were: total pressure 23 bars and partial pressure of CO_2 of 7 bars, temperature of 200°C and an initial pH of 4 which rose to 5.5 during the experiments. However, one should be skeptical about the same sequence of transformations during natural diagenesis. In this study the kaolin minerals were recrystallized from precursor phases.

Keller *et al.* (1981) noted that feldspars (which are virtually devoid of vanadium (Rankama and Sahama, 1950) generally alter to well crystallised kaolinite (i.e. Kaolinite with sharp XRD reflections). Kaolinites of the present investigation also give sharp XRD traces suggest a possible deficiency in vanadium.

Hurst and Irwin (1982) noted that books of thin kaolinite dominates freshwater sandstones, while blocky kaolinite predominates in marine sandstones. They argued that the books of platy kaolinite grow in an environment where there is a rapid input of nutrient ions, (Al^{3+} , Si^{4+} etc), such as a flux of meteoric water through a fluvial aquifer.



Aston University

Illustration removed for copyright restrictions

Fig. II.7.

Activity diagram in the Kaolinite - illite-K-Feldspar system after Hutcheon, 1981 whose data was calculated for 500 bars pressure.



Aston University

Illustration removed for copyright restrictions

Fig.II.8.

Variable thermal stability of Kaolinite (After Dunoyer de Segonzac 1970)

↓ = Limit,  = Persistence.

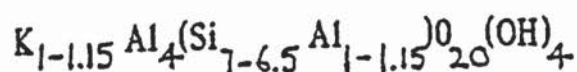
Huggett (1982) noted that thin plates (and perhaps seams) of kaolinite are formed by cleaving and twinning along {001} planes of blocky kaolinite under pressure. The latter author also argued that kaolinite would not be expected to form in marine sandstones unless the pore water was diluted by fresh water flushing; it is thus a later cement in marine sandstones than in fresh water sandstones.

The following is a compilation of authigenic clay sequences after Hurst and Irwin (1982):-

5 marine sandstones	1 contains no kaolinite
	1 contains early kaolinite
	1 contains middle stage kaolinite
	1 contains late kaolinite
	1 contains very late kaolinite
7 brackish sandstones	1 contains no kaolinite
	6 contain middle stage kaolinite
4 fluvial sandstones	4 contain early kaolinite
	1 contains late kaolinite

11.6.8 Illite

Illite was defined by Grim (1953) as the aluminous, K-deficient mica fraction of clay size materials. It usually covers a range of clay compositions which may be represented by the general formula:-



The following is a detailed description of morphology, textures - distribution and structure - crystallinity of illite encountered in this study.

(a) Morphology

Generally the morphology of illite is quite varied. In the simplest of terms, illite occurs as plates, blades and laths (Huggett, 1982). Sometimes it forms composite particles.

Unfortunately, authigenic illite in the sandstones under survey is rare. Whenever present it occurs only as laths (Pl. 11.1 F; Pl. 11.5 E).

Laths are 'hairy' or ribbon like projections of illite. They are frequently wavy and sometimes curled parallel to the short axis of the lath to form loops (Pl. 11.5 E). Occasionally laths are bifurcated and the terminations of the laths may be pyramidal or straight (Pl. 11.1 F). Güven *et al.* (1980) identified the lath elongation direction as the a-axis, while Huggett (1982) noted that some laths appeared to be growing from illite plates without any unique orientation, suggest that the a-axis is not the only lath elongation direction. Güven *et al.* (1980) also observed the presence of irregular 'blob-like' (gel-like) cores which have a chemistry very similar to the laths. According to them illites having a blob like core seem to form by chemical precipitation, and not from the degradation of micas. Such 'blob like' cores in a illite lath were also detected during the present investigation (Pl. 11.1 F). The presence of illite laths in sandstone pores greatly increases microporosity and pore tortuosity while decreases the permeability (Güven *et al.* 1980). The fragile nature of the illite lath can result in a migration of fines (Pl. 11.1 F) problem during hydrocarbon production (Güven *et al.* 1980).

The lath observed in this study was about 50 μm long and 0.7-1.5 μm in width (Pl. 11.1 F). To the author's knowledge this could be the longest and widest lath reported so far. Laths up to 30 μm long, 200 Å thick and 0.1-0.3 μm wide were recorded by Güven *et al.* (1980) from the Norphlet Formation (Jurassic, Mississippi), the Wilcox Formation (Eocene, Texas) and

the Fort Union Formation (Palaeocene-Wyoming). Long laths were also reported by Colter and Ebborn (1978) from Triassic Sands of the North Irish Sea; Glennie *et al.* (1978) from the Rotliegendes Sands (Permian, North Sea) and McHardy *et al.* (1982) from Sands of the Magnus Field (North Sea). The laths upto 6 μ m long were observed by Blanche and Whitaker (1978) from the Brent Sand Formation (Jurassic, North Sea); Taylor (1978) from the Triassic Sands of the Viking Graben (North Sea); and by Huggett (1982) from the Westphalian Coal Measure Sandstones, West Midlands. In this study no facility was available for measuring lath thickness.

(b) Textures and Distribution

It is not very clear from the present investigation whether illite occurs as a pore filling or pore rimming clay. It was observed that illite laths appeared to be present on quartz overgrowths (Pl. 11.5 E) and in holes in corroded feldspar (mostly illite fines - Pl. 11.1 F) and as inclusions in feldspar (Pl. 11.1 F). Relationship between illite and kaolinite is not well understood. Virtually compared to kaolinite, illite is rare in these sandstones; Huggett (1982) also noted an inverse relationship between illite and kaolinite from the Westphalian Coal Measure Sandstones, West Midlands.

With the SEM grain lining (tangential to the grains) illite lath was found very occasionally. Where an illite grain coating is discontinuous, quartz overgrowth has often nucleated on the exposed quartz and spread over the illite (Pl. 11.5 E).

The origins of the illite, which is both authigenic and detrital, are diverse. In thin section, detrital illite grains and clay rims were recognised, the latter were tentatively identified from their presence at grain contacts. With the SEM it was possible to distinguish between the ragged detrital

illites (Pl. 11.8 H) and the delicate authigenic illites (Pl. 11.1 F; Pl. 11.5 E). Detrital illites generally have a ragged appearance with stubby projections unlike the spine like edges that develop in authigenic illite/smectite and illite (Pittman and Wilson, 1977).

In thin sections very occasionally highly birefringent plates were noted within kaolinite books, which could be an indicator of relict muscovite or pseudomorphous illite.

(c) Structure and Crystallinity

Illite is generally identified by an integral series of basal peaks founded on a 10\AA c-axis spacing. Non basal reflections are weak.

On glycolation, illite is essentially non-expanding. Small amounts of expandable material will go undetected.

On heating to 550°C the (001) peak of illite may show a slight collapse, although if this is very marked it suggests that expandable layers are present.

During the present investigation the illite (001) spacing (measured from XRD traces) ranges from 10.1\AA to 10.2\AA (using quartz as an internal standard) in the sandstones and from 9.9\AA to 10.5\AA in the siliceous shales of the Bwlchgwyn-Minera-Ruabon area. On the other hand, the 'Terrig River Shale' has an average value of about 10.1\AA (Figure 11.3).

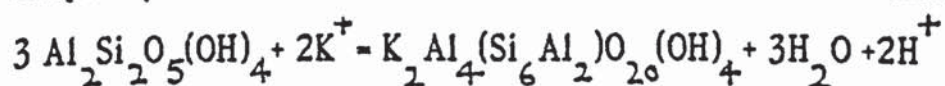
Values less than 10\AA may be due to K^+ deficiency or substitution of Fe^{2+} or Mg^{2+} for $[\text{Al}^{3+}]^{\text{IV}}$ (Güven, 1972). Values in excess of 10\AA are probably due to structural disorder caused by the presence of hydrated cations in the inter layer sites (Huggett, 1982).

It was not possible to identify the illite as either 1M or 2M by the method of Sulaiman (1972). Sulaiman (1972) reported three peaks of 2M illite polymorphs at 3.00 Å, 2.87 Å and 2.80 Å respectively, from the Irish Namurian argillites. He concluded that the presence of illite polymorphs may reflect a detrital origin of the illite.

11.6.9 Formation of Illite

Authigenic illite is rare in these sandstones. In one sample it is noticed pseudomorphing kaolinite (Pl. 10.3 A, B; Pl. 10.4 A, B) while in another sample it is seen pseudomorphing potash feldspar (Pl. 11.1 F). Some kaolinite has been slightly dissolved (Pl. 11.7 H) but most remains quite fresh with no sign of being replaced by illite. However, in thin sections very occasionally highly birefringent plates were noted within kaolinite books which could be an indicator of pseudomorphous illite or perhaps relict muscovite. From Figure 11.7 it can be seen that the kaolinite-illite stability field boundary will shift to a still lower temperature if the aK^+/aH^+ is increased. It would, therefore, be expected that early formed kaolinite should be dissolved or replaced by illite with increased burial as a result of increased pore water aK^+/aH^+ or increased temperature. Vitrinite reflectance result suggests that temperature did not rise more than 60°C (Table 9.1). So the explanation is that aK^+/aH^+ was increased to dissolve kaolinite and to pseudomorph kaolinite by illite.

The following equation is taken from Huggett (1982) where for the sake of simplicity the formula of muscovite was used instead of illite.



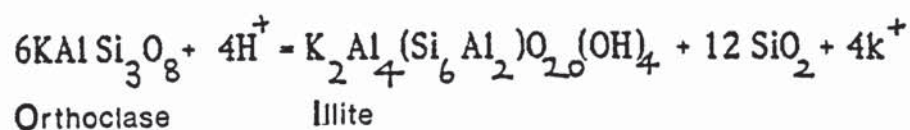
Kaolinite

Illite

The increase in aK^+/aH^+ required for this reaction in the present case may have been brought about by the following reaction:

dissolution and kaolinization of orthoclase (see Section 11.4.1).

The illitization of kaolinite releases H^+ ions which may be neutralised by dissolving feldspars to form illite and quartz (Bj  klykke, 1981),:



However, the process of transformation of smectite to illite in the mixed layer illite/smectite clay will be discussed in detail in Section 11.8.

The average crystallinity of the illite present in a sedimentary rock may be used as a measure of the diagenetic grade. The crystallinity was first quantified by Weaver (1960), which he called the sharpness ratio (S/R). Kubler (1968) measured the total peak width at the half peak height, which he called the illite crystallinity index (CI). However, during the present investigation illite crystallinity was not measured due to paucity of authigenic illite in these sandstones.

11.6.10 Illite - Smectite

In some samples, ^a trace amount of illite - smectite was found during the present investigation. The K^+ ions required to illitize the smectite layers may be supplied by the reaction of orthoclase to form kaolinite in the sandstones (see Section 11.4.1).

11.7 SOURCES OF SILICA

The sources of the secondary silica are numerous and have been extensively discussed (Phillip *et al.* 1963; F  chtbauer, 1967; Sippel, 1968; Waugh, 1970b; Hower *et al.* 1976; Sibley and Blatt, 1976 and Hawkins, 1978).

However, the following sources of silica are most important for the sandstones under consideration:-

- i) pressure solution

- ii) dissolution of feldspar
- iii) clay mineral diagenesis
- iv) dewatering of siliceous shales and siltstones
- and v) silica bearing Palaeozoic plants.

11.7.1 Pressure Solution

Thin section study of the sandstones under investigation reveals that there was very little compaction prior to quartz overgrowth formation. Most of the concavo-convex grain boundaries (Pl. 10.1 B) are composed of overgrowth, rather than detrital grain surfaces. But using the cathodoluminescence technique the evidences of the detrital quartz dissolution (pressure solution) before overgrowth formation were observed occasionally (Pl. 10.3 A, B).

Turner (personal communication, 1986) noted that pressure solution is important particularly in the orthoquartzites, deeply buried sandstones and in the metamorphic quartzites. It may also reduce secondary porosity (Schmidt and McDonald, 1979). Some authors have also argued against the very existence of pressure solution (Deelman, 1975), but later these arguments were rejected on theoretical (Athkinson and Rutter, 1975) and experimental (Sprunt and Nur, 1976; de Boer *et al.* 1977) verification. Thermodynamic analyses of pressure solution (de Boer, 1977; Robin, 1978) support the idea of Weyl (1959). Rutter (1976) concluded that the pressure solution process comprises three sequential steps:-

- 1) dissolution of the quartz grain at the point of stress
- 2) diffusion of silica through a fluid film away from the stressed point
- and 3) precipitation of quartz in adjacent pore spaces.

Pettijohn *et al.* (1972) argued that high effective pressures develop at point contacts and increase the solubility of quartz at these points such that they dissolve; the solution process is perhaps most advanced where

clay coats are present between grains. The dissolved silica is added to the pore water which becomes supersaturated with respect to quartz and reprecipitates the SiO_2 as quartz overgrowth on clay free quartz (Pettijohn *et al.* 1972). Sometimes high supersaturation of SiO_2 with pore water may give rise to concentric rims of amorphous silica as is evidenced by De Boer *et al.* (1977). Such concentric rims of amorphous silica were occasionally encountered in thin sections during the present study. However, if the clay rim were not present the quartz could precipitate as overgrowth in the area immediately adjacent to the point of dissolution (Pl. 10.3 A, B). Under such conditions the stress would then be spread over a larger area and consequently less pressure dissolution would occur and less SiO_2 would be available for overgrowth (Huggett, 1982).

Houseknecht (1984) studied the Hartshorne Sandstone (Carboniferous) of the USA and concluded that intergranular pressure solution increases with decreasing grain size in any sandstone and increases regionally with thermal maturity, while quartz cement increases with increasing grain size and decreasing thermal maturity. The studied sandstones are on average medium grained (though a few coarse and fine grained varieties are also present) and are characterised by high quartz cementation which was formed at a relatively lower temperature (see Section 9.5); thus consistent with Houseknecht's (1984) observation.

11.7.2 Dissolution of Feldspar

Dissolution of feldspar is one of the most important sources of silica for the sandstones under investigation. This process has already been described in detail in Section 11.3.

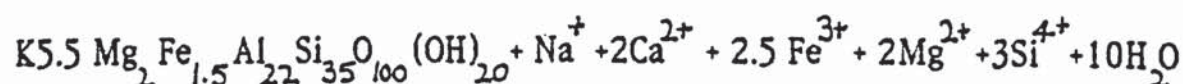
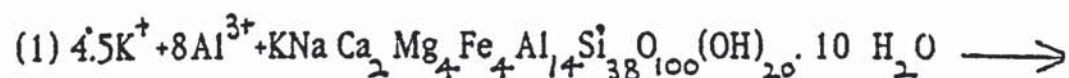
11.7.3 Clay Mineral Diagenesis

An additional source of silica is certainly the clay mineral diagenesis, i.e. the smectite, to illite transformation. Towe (1962) calculated for this

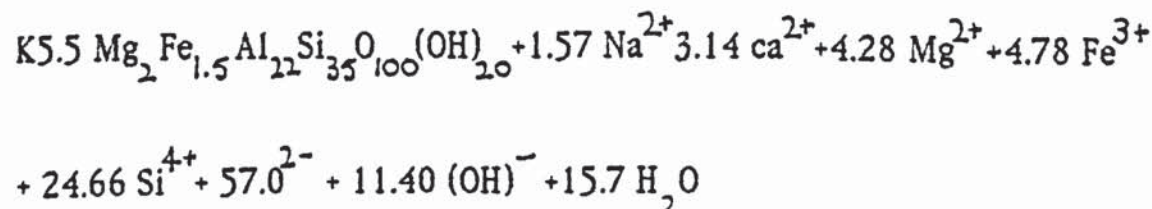
transformation 3 wt.% Si to be released, as Si^{4+} must be substituted by Al^{3+} to fix additional K^+ in the illite lattice (see also Perry and Hower, 1970; and Section 11.8).

According to Hower *et al.* (1976) such mineralogical changes in argillaceous sediments of the Gulf Coast take place over the interval 2000 to 3700 m of burial. The latter authors also regarded shales as closed chemical systems with respect to Mg^{2+} , Al^{3+} and Si^{4+} and did not discuss their significance in relation to cementation of associated sand units.

However, Boles and Franks (1979) showed that potentially large amounts of silica can be generated by the conversion of smectite to illite in accordance with the following two reactions:-



1 = constant oxygen



2 = constant aluminium

The completion of reaction (1) would mean 500g of smectite in 1 litre of sediment would produce 45g of SiO_2 .

On the otherhand, Lahann (1980) suggested that extensive quartz cementation may indicate illitization reaction took place at low temperature ($\sim 50^{\circ}\text{C}$). The latter author also noted that rapid increase of temperature in shales to $100-120^{\circ}\text{C}$ would result an end of silica migration, while at the same time rate of illitization may increase. However, in 1989 ³ the present investigation high quartz cementation and minor amounts of authigenic illite indicate that temperature never rose rapidly to $100-200^{\circ}\text{C}$ during diagenesis (see also Section 9.5). This is also evidenced by the absence of hydrocarbon inclusions in the sediments.

11.7.4 Dewatering of Siliceous Shales and Siltstones

Dewatering of the siliceous shales and siltstones by compaction may have contributed some dissolved SiO_2 to the sandstones under survey. In fact the stratigraphic distribution and the huge thickness of delta top sandstone beds in and around the studied region having high pre-cement porosity (about 40%; pre-cement porosity is the sum of the present primary porosity + the total amount of cement) suggest that fluids expelled from shale would have moved easily through sandstone beds. Füchtbauer (1967) and Wallace (1976) demonstrated on the basis of textural evidence that dissolved SiO_2 moved from shale units to adjacent sandstone beds, where it was precipitated as quartz cement. Wallace (1976) suggested that silica mobility is a prominent feature of diagenesis in the sand-shale sequence. In addition, considering the effects of compaction on shales, he further suggested that during progressive burial diagenesis of the interbedded shales and sandstones, Na^+ and H_4SiO_4 concentrations in the sandstones increase relative to shales where as K^+ , Al^{3+} , Mg^{2+} and Ca^{2+} are held in shales (Figure 11.9 A, B). Therefore, from Figure 11.9 A, B it can be seen that diagenesis may take place within a sand-shale pair acting as a closed system and ions such as Si, Al, Na and K may have been rearranged *in situ* without long distance transport.

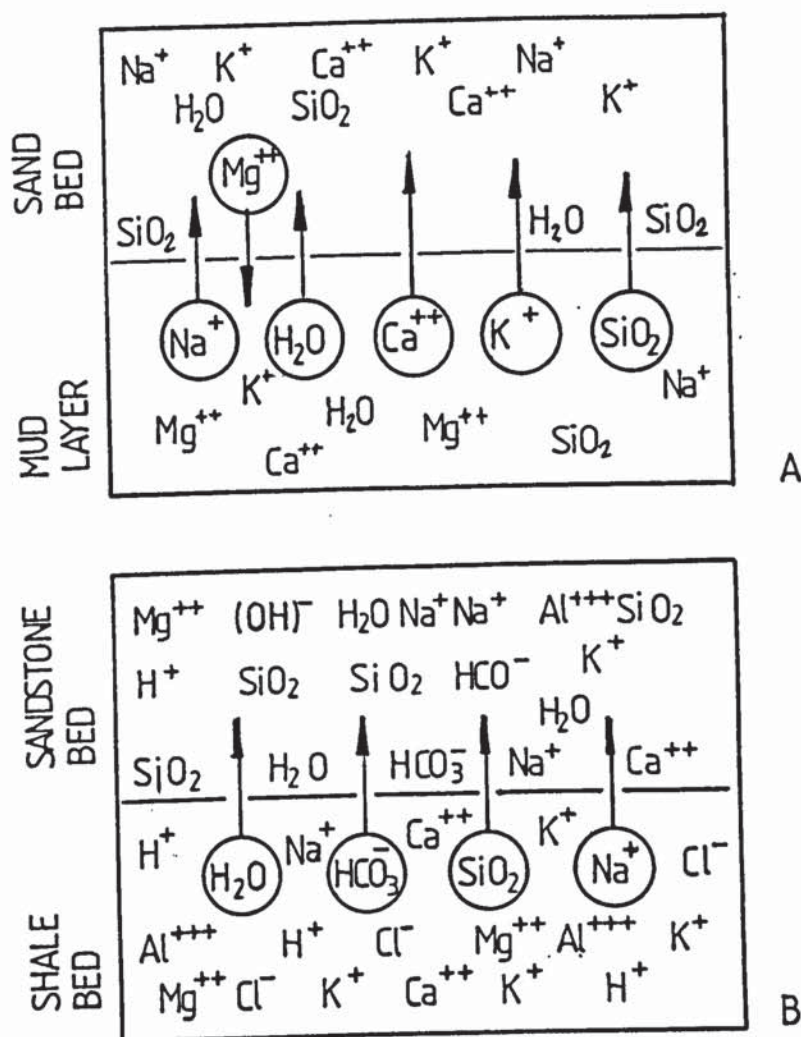


Fig. II.9 Schematic representation of change in composition of pore water during initial compaction of a sandstone-shale sequence. Na^+ , H_2O , Ca^{++} , K^+ , and SiO_2 is expelled from mud into adjacent sand beds before compaction destroys avenues of escape around clay particles in the mud. Mg is concentrated in the mud unit. Temperature below 60°C

1:B. Schematic representation of change in composition of pore water in a sandstone-shale sequence during long term burial. H_2O , HCO_3^- , Na^+ , and SiO_2 concentration in sandstone increases relative to shale. K^+ , Cl^- , Al^{+++} , Mg^{++} , Ca^{++} and H^+ are held in shale units, which result in a relative dilution of these cations in pore water expelled into adjacent sandstone beds. The temperature range was probably between 60°C and 200°C . Quartz would have been stable and microcline unstable at the lower part of this temperature range, whereas quartz and quartz+microcline would have been stable in the upper part of the temperature range. (after Wallace, 1976).

However, Huggett, (1982) did not consider dewatering of shales as an important silica donor for the lower and middle Coal Measure Sandstones of the East Midlands.

11.7.5 Silica Bearing Palaeozoic Plants

Present palynological study indicates the presence of abundant silica bearing palaeozoic plants such as lycopods, Calamites etc, in the interbedded siliceous shales. Certainly these plants may have contributed some dissolved SiO_2 to the overlying sandstones.

Silica bearing siliceous oozes like radiolaria, sponge spicules etc. were not observed in these sediments, though these siliceous oozes are the major silica donor to the underlying chert beds (see Chapter 8).

11.8 DISCUSSION AND CONCLUSIONS

The diagenetic history within the Namurian sandstone-shale sequences from different localities in North Wales has been studied in detail.

In these sandstones the process of intrastratal dissolution of framework silicates together with pressure solution, clay mineral diagenesis and dewatering of shales and siltstones provided the interstitial environment with the necessary Si, Al, K and Fe ions which are required for the precipitation of authigenic minerals.

During this study in addition to kaolinite and illite, a trace amount of illite/smectite was also noted in a few samples. It is thought (though there is no distinct indication) that as a result of deep burial diagenesis conversion of smectite to illite by way of a mixed-layer illite/smectite has led to a complete illitization of these sediments.

However, there is substantial evidence in the literature of the diagenetic transformation of expanding clay minerals (Burst, 1969; Perry and Hower, 1970; Dunoyer de Segonzac, 1970; Perry and Hower 1972; Hower *et al.* 1976; Boles and Franks, 1979; Hower, 1981b; Imam, 1983; Pollastro, 1985). Perry and Hower (1970) showed a gradual decrease in expandability in illite/smectite clay from about 80% to 20% smectite layer with increasing depth in U.S. Gulf Coast Tertiary sequence.

Hower (1981A) and Schultz (1978) postulated that the most distinctive character of the diffraction profile of the randomly interstratified illite/smectite (smectite layer more than 40%) is that the 17 Å peak intensity decreases progressively until it completely disappears (as in the present case).

Imam (1983) studying the Neogene sediments of the Bengal Basin, Bangladesh, noted a gradual decrease in 17 Å peak intensity (18 Å for glycerated ones) of the illite/smectite clays followed by a complete disappearance between 3,532 m (Begumganj - 1 well section) to 4100 m (BODC-2 well section) of burial.

Pollastro (1985) in a study of the lower Tertiary and upper Cretaceous sediments of Wyoming and the upper Cretaceous Niobrara Formation, Denver basin, Colorado, observed that the conversion of smectite to illite through a mixed-layer illite/smectite was the major depth related reaction in clay mineral assemblages of these sediments. Such a reaction may take place in both interbedded sandstone and shale. According to Pollastro in deeply buried rocks rigid laths of illite may be formed diagenetically from the wall surfaces of I/S honeycombs. He further pointed out that such reactions are late diagenetic in origin and may take place in restricted or relatively closed geochemical systems, as in early cemented rocks having extremely low permeability and little or no potassium feldspar and

detrital mica. However, well developed, rigid illite laths are also observed during this study (Pl. 11.1 F and Pl. 11.5 E), though I/S honeycombs could not be seen. This may indicate that the studied sediments have been affected by intense deep burial diagenesis where most of the I/S layers have been transformed to illite.

The transformation of smectite to illite would cause important changes in chemical composition among which fixation of K^+ in interlayer spaces of smectite could be significant. Hower *et al.* (1976) introduced the following general reaction for such conversion: $\text{Smectite} + \text{Al}^{3+} + K^+ = \text{illite} + \text{Si}^{2+}$. However, the actual reaction is considered to be more complicated involving loss of H_2O , Ca^{2+} , Na^+ , Mg^{2+} , and Fe^{2+} (Hower *et al.* 1976; Boles and Franks, 1979; Boles, 1981).

Pollastro (1985) and also Boles and Franks (1979) considered that some I/S clay is destroyed by cannibalization of smectite layers to give the necessary chemical components needed to make I/S with a relatively higher illite content. According to the latter authors additional K^+ and Al^{3+} may be derived from K-feldspar and K-micas, if they are available.

Temperature is the main factor controlling smectite to illite/smectite transformation; pressure and geological age are less important (Perry and Hower, 1972). Shaw (1980) noted that pore water chemistry is at least equally important for clay mineral diagenesis. The conversion of smectite to illite appears to begin at about 60°C-80°C (Boles, 1981) and complete illitization of the illite/smectite may take place at temperatures between 130°C and 180°C (Shaw, 1980). The present vitrinite reflectance results suggest that the shale samples have experienced a temperature of about 56°C (see Chapter 9). This temperature is fairly close to the temperature range mentioned by Boles (1981) necessary to begin the conversion of smectite to illite, but it is much lower than the temperature needed for

complete illitization (see above). However, in the present case complete illitization has already taken place in both shales and sandstones. This may indicate that temperature together with geological age (reaction time) and pressure should be considered in the case of ancient sediments.

From the foregoing, one reasonable assumption can be made: the apparent absence of 17\AA peak intensity in the diffraction profiles of the clay fractions of the Namurian sandstones and shales is due to the transformation of illite/smectite to illite during burial diagenesis.

However, the possibility of a decrease in abundance or absence of smectite clay in the original detrital input during deposition cannot be totally ruled out. According to the well established differential settling model (Gibbs, 1977) a variation in composition of the original detrital clay minerals deposited in various sub-environments of a prograding delta (see also Chapter 5) could be possible due to a physical sorting of clay minerals by size. That is to say, a differential sedimentation process could have caused a lateral change in clay minerals composition during deposition (Gibbs, 1977). This may also well explain the absence of kaolinite in the 'Terrig River shale' (see also Section 9.8).

The temperatures at which kaolinite becomes unstable are variable (Dunoyer de Segonzac, 1970; see also Fig. 11.8). The stability of kaolinite is also a function of geochemical environment; with an increase of pH the stability of kaolinite decreases (Shaw, 1980).

Phase equilibria calculated from thermodynamic data suggest that dissolution of feldspar and formation of kaolinite will occur below pH 5 in the temperature range anticipated for early diagenesis (Fig. 11.7).

Quartz precipitation requires low temperatures (Garrels and Christ, 1965; Fournier, 1973) and $\text{pH} < 9$ (Krauskopf, 1959; Blatt *et al.* 1972). Quartz cementation is therefore likely to be in the same chemical and physical environment as feldspar alteration to kaolinite. Temperatures required for the precipitation of quartz and kaolinite as suggested by the activity diagrams mentioned above are consistent with the diagenetic temperatures obtained from vitrinite reflectance data in the present investigation.

Cathodoluminescence study reveals that two phases of quartz overgrowth cementation are separated by a phase of kaolinite precipitation. This may suggest that quartz cementation was continuing while other authigenic minerals were being precipitated.

Shallow etch pits in quartz overgrowths were observed occasionally by CL (Pl. 10.5 A). The cause of the etching is uncertain. An increase in alkalinity may be a possible explanation because of the rapid increase in quartz solubility above pH 9. However, the absence of calcite or dolomite cement in these sandstones may rule out this possibility.

Kaolinite mostly forms pore filling cements which have generally few points of contact with grain surfaces, thus leaving much of the quartz grain surfaces available for overgrowth. Discontinuous clay coatings also encourage overgrowth. According to Pettijohn *et al.* (1972) high effective pressures develop at point of contacts and increase the solubility of quartz at these points such that they dissolve. The solution process is presumably most advanced where clay coats are present between grains. The dissolved SiO_2 is added to the pore water which becomes supersaturated with respect to quartz and reprecipitates the SiO_2 as quartz overgrowth on clay free quartz. On the contrary, if the clay rims were not present the quartz could precipitate as overgrowth in the area immediately adjacent to

the point of solution (Pl. 10.4 A, B).

Clay minerals are significant in the process of sandstone diagenesis. They are important porosity filling and permeability reducing cements, and important releasers and absorbers of ions into and from the pore fluid.

There are three mechanisms by which authigenic clays may form (Huggett, 1982): aggradation, degradation, and neoformation. Recrystallization of pre-existing phases results from the first two mechanisms, whilst the third is due to direct precipitation from solution. The present study suggests that neoformation and to a minor extent replacement are the predominant mechanisms of clay formation in the sandstones (and to some extent in the siliceous shale interbeds). In this study both blocky and platy kaolinite were seen to be common. This is not in accord with the published scanning electron micrographs which show that blocky kaolinite is rare. Authigenic illite when present was found as laths.

Presumably early diagenesis occurred under open conditions. A high fluid flow rate in the original very porous, unconsolidated sands would have ensured an open system. Early fresh water diagenesis produced siderite in reducing conditions, quartz and kaolinite formed from carbonate, feldspar (and perhaps muscovite) dissolution. Also carbonate and feldspar leaching produced early secondary porosity.

Gradually pore water alkalinity increased and decreased again as diagenesis advanced. This reversal reaction is evidenced by the presence of well crystallised illite lath in the dissolved feldspar ? overgrowth (Pl. 11.1 F). The increase in alkalinity may be related to the clay producing reaction (Section 11.4.1) which uses up the H⁺ ions. Dissolution of kaolinite (Pl. 11.7 H) may also indicate an increase in alkalinity. From the kaolinite-illite-K-feldspar phase diagram (Fig. 11.7) it may be seen that

this indicates that the pH and/or the temperature have fluctuated. Vitrinite reflectance results suggest that temperature did not rise above 60°C in the interbedded siliceous shales. Thus it may be wise to assume that alkalinity rose during the course of diagenesis and resulted illite lath and feldspar ? overgrowth. Subsequent lowering of the alkalinity could be assumed by the dissolution of feldspar ? overgrowths, paucity of authigenic illite and the presence of quartz-kaolinite as a stable phase in these sandstones. However, quartz and kaolinite may precipitate at lower pH but this could also be a result of an increase in alkalinity. Curtis (1983) noted that kaolinite precipitation is favoured under acid condition where cations (Na^+ , K^+ , Ca^{2+} , and Mg^{2+}) are not present in sufficient quantity to produce cation aluminosilicates. Under deep burial condition such acid pore waters may generate as a result of kerogen maturation and destabilize carbonates and aluminosilicates and take metals, including aluminum into solution (Curtis, 1983). He further pointed out that the isolation of these solutions from the principal source of maturity, would cause an increase of pH as further mineral dissolution occurs and the net result would be the precipitation of kaolinite. This may also well explain the paucity of carbonates in these sediments.

Sims (1970) also considered that very low cation concentrations at relatively moderate silica values favour crystallization of kaolinite.

However, oxidation of siderite and a second phase of kaolinite precipitation (tiny blocky kaolinite) may have happened late in the diagenesis. All the above mentioned diagenetic events may be related to periods of folding (Hercynian) and uplift (Hercynian and post Cretaceous) during which fresh pore waters migrated into the sandstones. However, oxidation of siderite may also have occurred during more recent penetration of the sandstones by fresh water.

The factors controlling diagenesis of the sandstones under investigation are primarily composition, environment of deposition, pore fluid chemistry and migration, pressure and temperature. Sediments with a high proportion of stable grains like quartz and quartzose rock fragments may retain a higher proportion of their primary porosity. As such, neoformed, diagenetic minerals may be more important because their formation is not obstructed by reduced pore fluid movement or any other grain contact caused by earlier cements. Composition of the sediment is therefore a fundamental control of diagenesis particularly for the sandstones under survey. Similarly, environment of deposition is another fundamental and significant control of diagenesis for the present sediments as it determines the geometry of the sandstones, their sorting, porosity and the connate pore water composition. Nature of the authigenic cements which formed during early diagenesis may be determined by this environment of deposition factor. Mineralogy may be a more important factor of diagenesis during increasing burial and can in turn change the pore fluid composition. With burial, temperature and pressure also increase and may have been responsible for the pressure changes in the phases in equilibrium with the pore fluid, and hence changes in the phases which precipitated. However, in the present 'Bwlchgwyn-Minera-Ruabon Sandstone' fresh water diagenesis has predominated, producing relatively large volumes of quartz and kaolinite cement.

The diagenetic processes in these sandstones can be classified into two types with respect to their influence on reservoir properties. These are:

(1) Porosity reducing processes:

- i) Quartz overgrowth cementation
- ii) Kaolinite cement crystallization
- iii) illite lath and illite fines
- iv) compaction

(2) Porosity enhancing process:

Complete dissolution of some rock components and development of secondary porosity.

Early quartz overgrowth cementation is the most effective in destroying porosity and permeability. It affects almost every sample and reduces porosity and permeability to zero.

Kaolinite also reduces porosity but to a lesser extent. It probably reduces a significant, if not identical, volume of porosity that had been secondarily produced by feldspar and carbonate dissolution.

Illite laths and illite fines increase microporosity and pore tortuosity but decreases the permeability.

The effect of compaction in porosity reduction principally by grain deformation and pressure solution increases with burial depth. The presence of pressure solution in these sandstones is confirmed by the cathodoluminescence technique (Section 11.7.1).

Complete dissolution of detrital feldspars, carbonates and lithic fragments leads to the development of secondary porosity, thus increasing the total porosity of the sandstones.

The diagenetic processes identified in this study are relevant to the diagenetic stages recognised by Schmidt and McDonald (1979a). These stages are:

1) eodiagenesis stage, 2) mesodiagenesis (mechanical compaction or immature), 3) mesodiagenesis (mature) and 4) telodiagenesis (after burial).

It is seen that most of the diagenetic changes in the studied sandstones have taken place during the mature mesodiagenetic stage. The net result of this stage is the reduction of primary porosity and the formation of secondary porosity by dissolution of carbonates and feldspars. The majority of secondary porosity is produced in this stage by the effect of mesogenetic decarbonatization. During mesodiagenesis most of the CO₂ required to form carbonic acid originates from organic matter undergoing thermomaturation (Schmidt and McDonald, 1979a). Savkevic (1971) suggested that the CO₂ originated from the organic matter oxidation and released interlayer water from smectite-illite conversion; both could form the acidic water required to dissolve the carbonates. Dissolution of feldspar would also take place at this stage.

Therefore this stage is characterised by the active role of chemical diagenetic processes in the lithification of sandstones under investigation. Though physical processes of compaction may continue during this stage, chemical processes of diagenesis (quartz + kaolinite + illite precipitation and carbonate + feldspar dissolution) become the major controlling factors in determining the reservoir properties of these sandstones. The physico-chemical process of pressure solution also becomes important in this stage. Pressure solution together with smectite-illite conversion and feldspar dissolution increased lithification of sandstones both by overly tight compaction and by acting as a source of silica for quartz overgrowths.

Oxidation of siderite may have taken place during the eodiagenetic or telodiagenetic stage.

11.8.1 COMPARISON WITH OTHER DIAGENETIC MODELS

In the geological literature several accounts of the diagenesis of deltaic clastic rock sequences are available. The U.S Gulf Coast Tertiary sequence is probably the most studied area in this respect.

In Table 11.3, a comparison is shown of the sandstone diagenetic model (paragenetic sequence) of the presently studied Namurian sandstones of North Wales with those of the Tertiary deltaic sandstones of the Gulf coast Basin, U.S.A. (Loucks *et al.* 1977; Stanton, 1977), the Tertiary deltaic sandstone of Niger delta (Lambert, 1981), the Neogene deltaic sandstone of Bengal Basin, Bangladesh (Imam, 1983); the Cretaceous shelf sandstones which accumulated south of a delta in the Denver Basin, Colorado, U.S.A. (Porter and Weimer, 1982) and the Pennsylvanian deltaic sandstone of North Central Texas, U.S.A. (Land and Dutton, 1978).

However, Table 11.3 indicates that the diagenetic model of the deltaic Namurian sandstone of North Wales has some features in common with other models listed there.

Namurian SSt. North Wales (Present Study)	Bengal Basin (Bangladesh) Neogene deltaic Sst. (Imam, 1983)	Tertiary deltaic Sst. Wilcox fm: Gulf Coast Basin U.S. (Stanton, 1977)	Tertiary deltaic Sst. Frio fm: Gulf Coast Basin U.S. (Loucks et. al. 1977)	Cretaceous Shelf Sst. Denver Basin Colorado, U.S. (Potter and Weimer, 1982)	Pennsylvanian deltaic sst. Texas, U.S. (Land and Dutton, 1978)	Tertiary deltaic Sst. Niger delta (Lambert, 1981)
Siderite cryst.	Compaction	Compaction	Feld. leaching	Compaction	Compaction	Kaol. precip.
Dissol. of felds. and carb.	chlorite rims siderite cryst.	Qtz. overgrowth calcite cementn.	Poik. calcite cementation	chlorite rims Qtz overgrowth	chlorite rims Qtz. overgrowth	Kaol. unstable Smectite form.
Qtz overgrowth	Poik. calcite	and replacement	compaction	calcite cementn.	calcite cementn.	Calc. precip.
Compaction	cementation	Dissol. of calcite	clay rims	and replacement	Dissol. of calcite	Dissol. of
Kaolinite	Illite coat	Precip. of kaol.	Feld. overgrowth	Soln. of calcite	Kaol. precip.	calcite
precip.	Qtz overgrowth	Precip. of	Qtz overgrowth	Kaol. precip.	Barite precip.	Qtz overgrowth
2nd generation	Late calcite	Fe-calc.	calcite cementn.			Siderite cryst.
Qtz overgrowth	cementation	Precip. of	Dissol. of calcite			Pyrite precip.
Illite lath	and repl.	minor dolomite	cements, feld. and lithics.			
Blocky kaolinite	Dissol. of calc.		Kaol. cryst.			
precip.	cement, feld., etc,		Fe calc. cementn.			
Oxidation of siderite Kaol. Precip.	Kaol. cryst.					

Table 11.3: Comparison of the paragenetic sequence of the diagenetic events in the Namurian Sandstones of North Wales with those of some other deltaic sandstones.

PLATE 11.1

- A. Thin section photomicrograph of chert rock fragment.
Width of field of photograph = 2.7 mm; XN
Bwlchgwyn Sandstone
- B. Zebraic texture chalcedony is associated with microcrystalline chert (Ch). Width of field of photograph = 2.7 mm
Thin section photomicrograph. XN
Bwlchgwyn Sandstone
- C. Etching of feldspar (f) along the cleavage plane. K = kaolinite.
SEM photomicrograph (carbon coating).
Scale bar = 40 μm
Bwlchgwyn sandstone
- D. Etching may penetrate deeply into the grain, which gives the feldspar (f) the appearance of a bundle of rods. K = kaolinite; q = quartz overgrowth. Scale bar = 100 μm . SEM photomicrograph (carbon coating).
Bwlchgwyn sandstone
- E. Randomly scattered needles (arrowed) of highly dissolved feldspar. q = quartz overgrowth. Scale bar = 100 μm . SEM photomicrograph (carbon coating).
Bwlchgwyn sandstone.
- F. Dissolution of feldspar. Note the dissolved feldspar is pseudo-morphed by illite lath (il) and the presence of irregular blob like or gel like cores (g) as observed by Güven *et al.* (1980). Note also the fragile nature of illite laths may result in illite fines (if). Scale bar = 20 μm . SEM photomicrograph (Gold coating).
Minera sandstone.
- G. Oversized pore (p) probably resulted from the dissolution of carbonates. Note kaolinite (k) is filling the pore space.
Scale bar = 2.7 mm; XN. Thin section photomicrograph.
Minera sandstone.
- H. Dissolution of detrital quartz (d) and its overgrowth (o) by authigenic kaolinite (k). Width of field of photograph = 2.7 mm;
Thin section photomicrograph. XN
Bwlchgwyn sandstone.

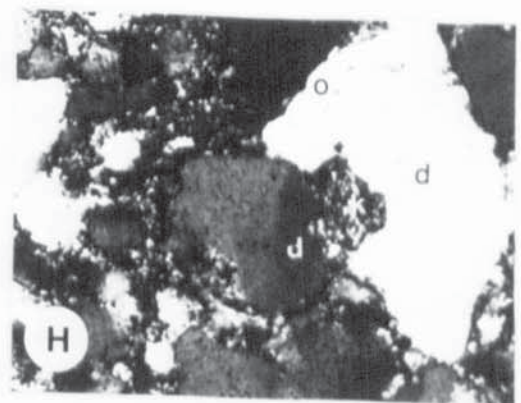
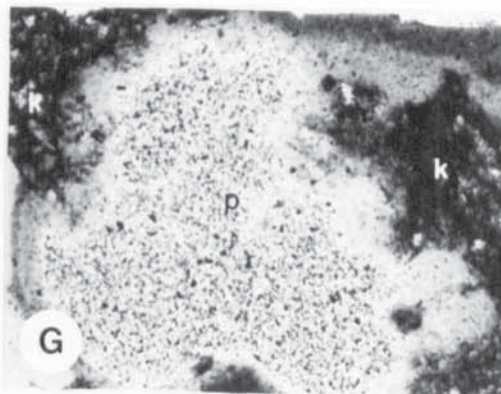
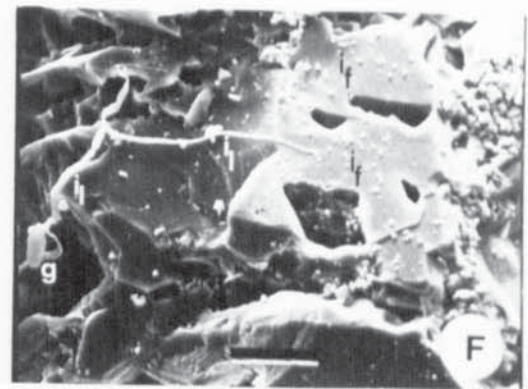
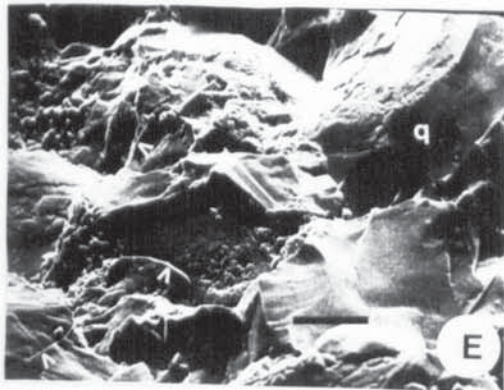
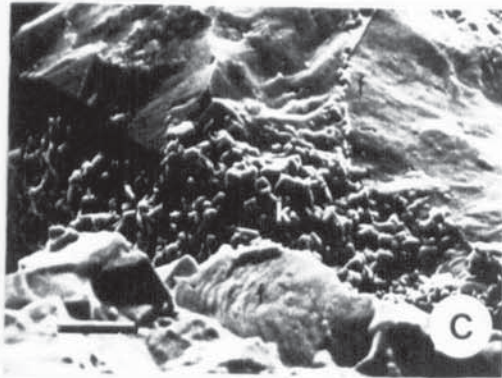
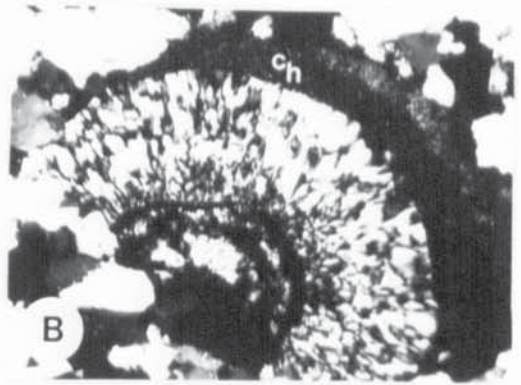
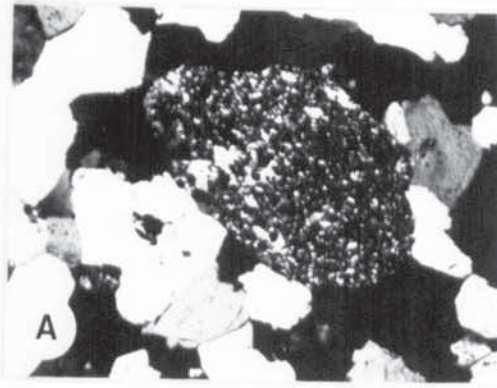


Plate 11.1

PLATE 11.2

- A. Siderite (s) forms a thin crust around the detrital quartz grain (q). Note the honeycomb pattern of the siderite crust.
Scale bar = 20 μ m. Bwlchgwyn sandstone. SEM photomicrograph (Gold coating)
- B. Enlargement of above. Scale bar = 10 μ m.
- C. In thin section siderite (s) is seen to cement completely detrital quartz grains (q). Note also the compaction of siderite cement and its presence at grain contacts. XN. Bwlchgwyn sandstone.
Width of field of photograph = 2.7 mm.
- D. Formation of incipient quartz overgrowths (o) on detrital quartz surface. Note also rounded reworked siderite grain (s) being overgrown by quartz overgrowths and delicate goethite needles (arrowed).
Scale bar = 4 μ m. Bwlchgwyn Sandstone.
SEM photomicrograph (Gold coating).
- E-H. Anastomosing system of relatively small, interconnected overgrowths (o). d = detrital grain surface, SEM photomicrographs (Gold coating).
Scale bar = 100 μ m (E); 20 μ m (F-H). Figures (E-G) from Bwlchgwyn sandstone and Figure H from Ruabon sandstone.

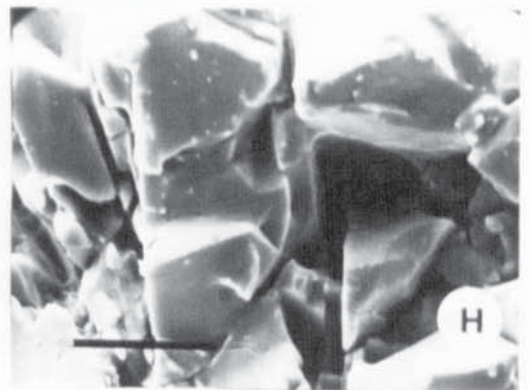
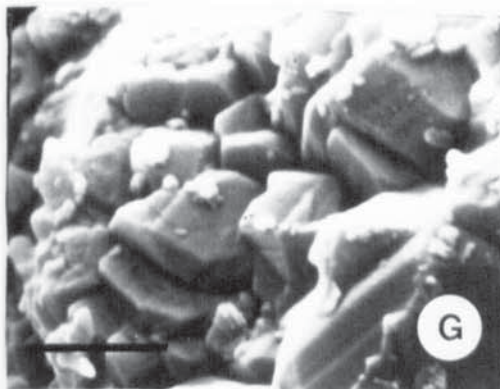
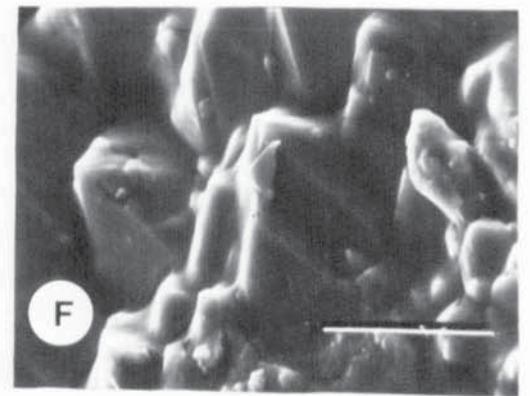
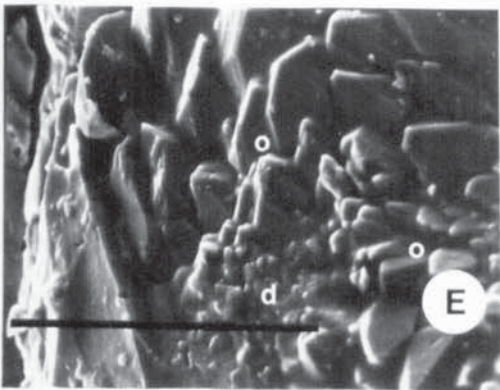
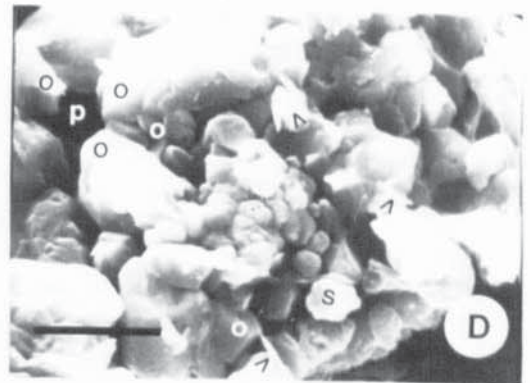
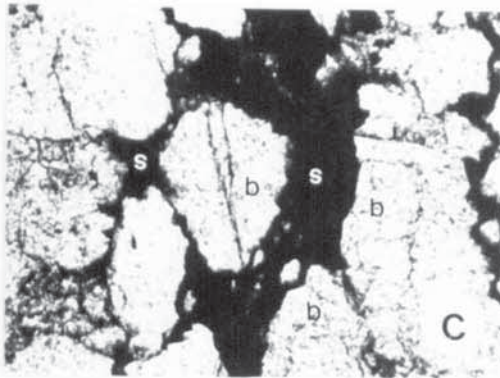
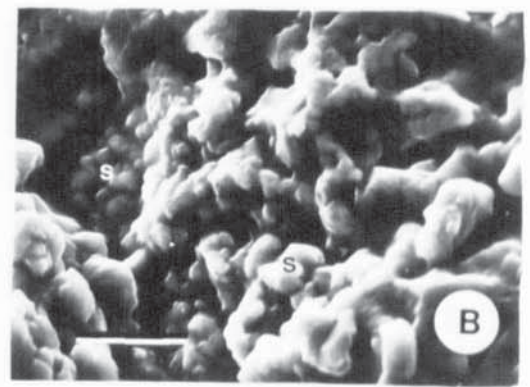
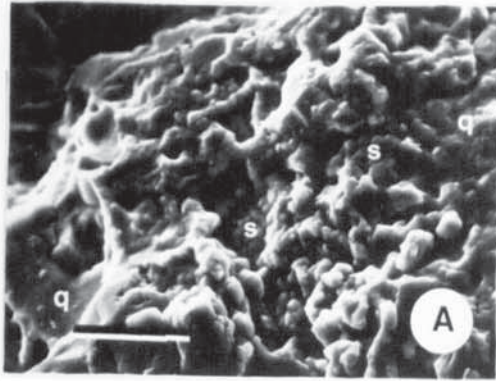


Plate 11.2

PLATE 11.3

All SEM photomicrographs (Gold coating)

- A. Two generations of overgrowths development (arrowed). Larger have well defined crystal faces and the smaller crystals have well defined to blob like crystal faces.
Scale bar = 10 μm .
Bwlchgwyn Sandstone.
- B-D. Illustrating how overgrowths with well defined crystal faces (o) grow and meet adjacent overgrowths (arrowed). Note the presence of detrital grain surface (d).
Scale bar = 100 μm .
Bwlchgwyn Sandstone.
- C. Enlargement of B. Scale bar = 20 μm .
- E. Quartz overgrowths grow into pores in a sandstone until an obstruction is encountered such as an adjacent detrital grain or another overgrowth. Note the presence of pore spaces (P).
Scale bar = 20 μm .
Bwlchgwyn Sandstone.
- F-H. Illustrating the tight fitting that is possible as overgrowth subunits grow to meet and overlap (arrowed). Note the presence of pore spaces (P).
Scale bar = 20 μm (F-G; Ruabon Sandstone); 40 μm (H; Mineral Sandstone).

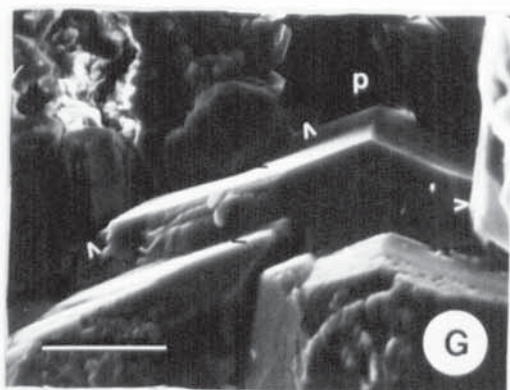
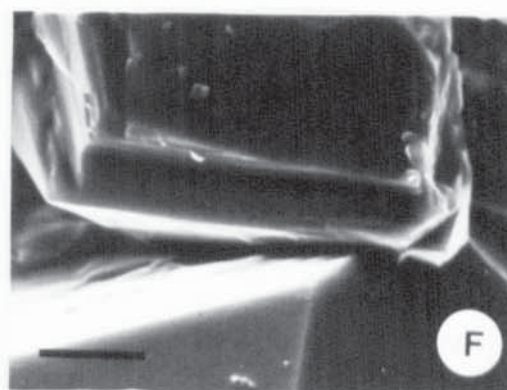
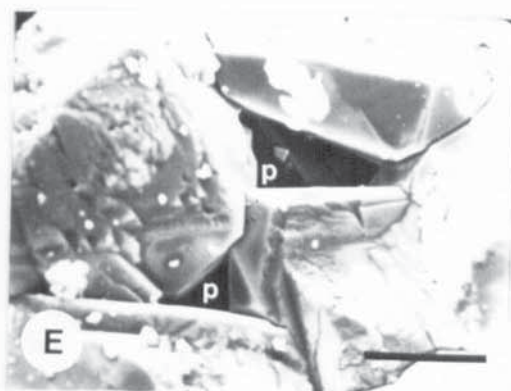
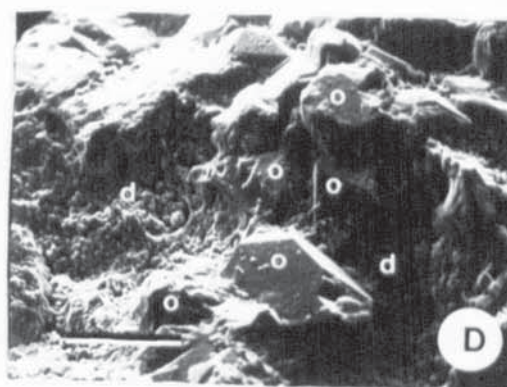
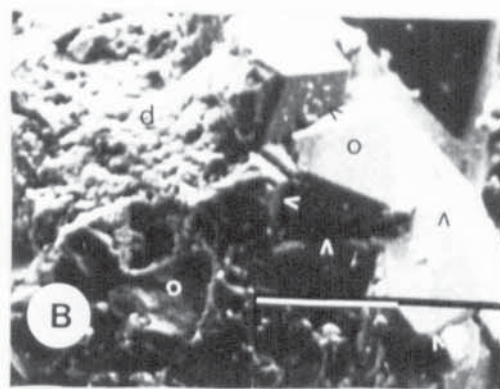
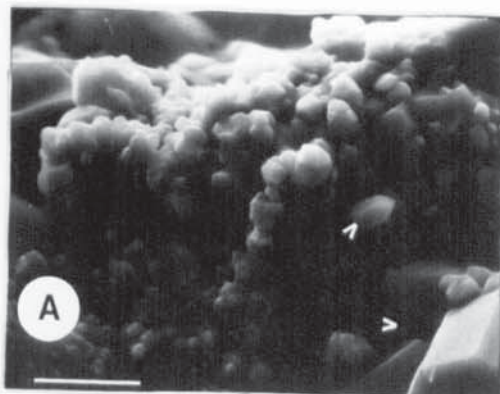


Plate 11.3

PLATE 11.4

All SEM photomicrographs (Gold coating)

A-H. Showing holes in overgrowth resulting from incomplete infill after merging of irregular overgrowths.

Scale bar = 200 μm (A); 100 μm (B); 40 μm (C-G); 10 μm (H).

Figures (A-F) from Bwlchgwyn sandstone. Figure (G) from Ruabon sandstone and Figure (H) from Minera sandstone

O = overgrowth; d = detrital grain surface.

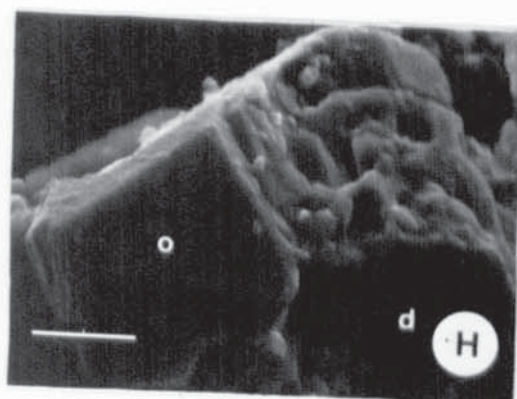
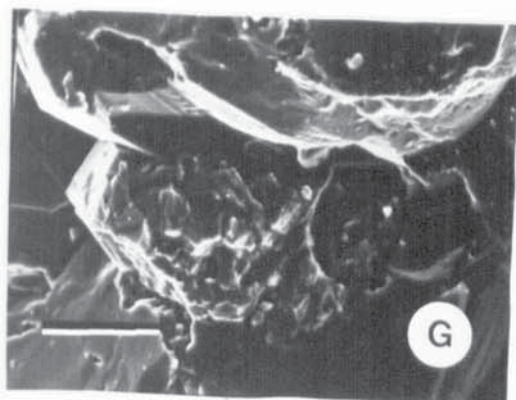
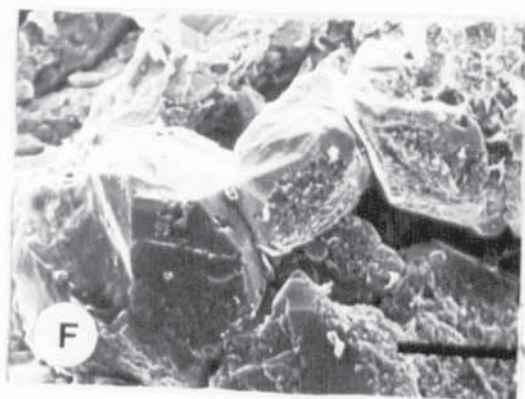
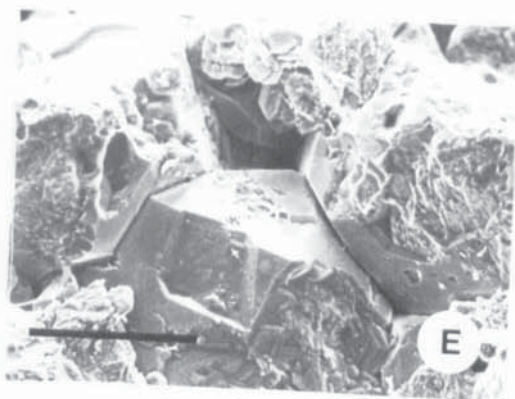
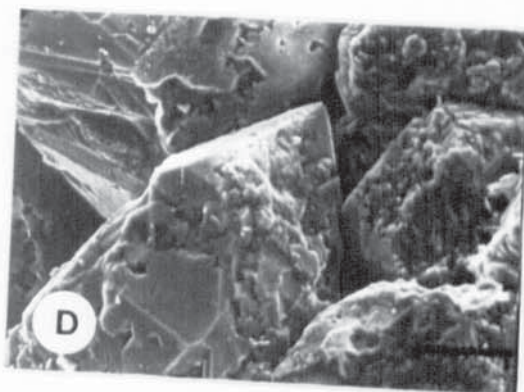
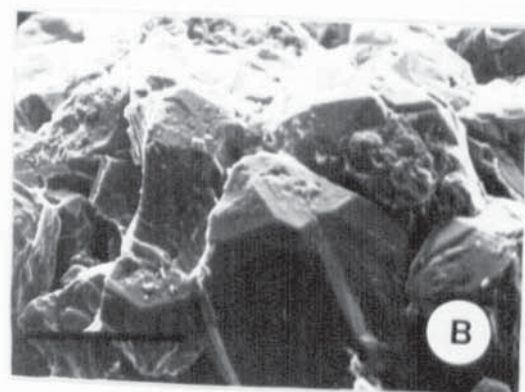
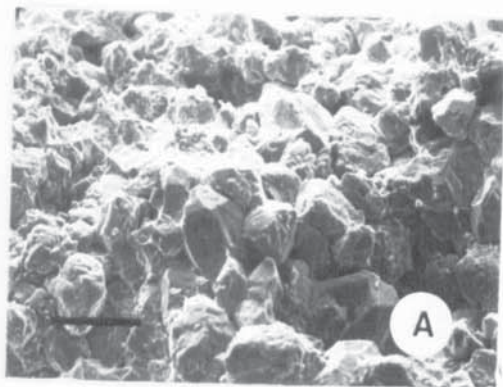


Plate 11.4

PLATE 11.5

All SEM photomicrographs (Gold coating)

- A-D. Unusually well developed prism faces of quartz overgrowths, showing pyramidal terminations.
Scale bar = $40\text{ }\mu\text{m}$ (A); $20\text{ }\mu\text{m}$ (B-D).
Bwlchgwyn Sandstone.
O = overgrowth; d = detrital grain.
- E. Coating of illite laths(i) has prevented quartz overgrowth formation (o) in places. Note also in illite free areas quartz overgrowth is well developed and the growth of overgrowth (o) in the pore spaces (p).
d = detrital grain surface.
Scale bar = $40\text{ }\mu\text{m}$.
Bwlchgwyn Sandstone.
- F. Gullying - a high relief surface texture
Scale bar = $10\text{ }\mu\text{m}$.
Minera Sandstone.
- G. Presolved area (a) where grain now removed, was in contact.
Scale bar = $40\text{ }\mu\text{m}$.
Minera Sandstone
- H. Rounded flaky aggregates typical of iron oxide (?) grains.
Scale bar = $10\text{ }\mu\text{m}$.
Ruabon Sandstone.

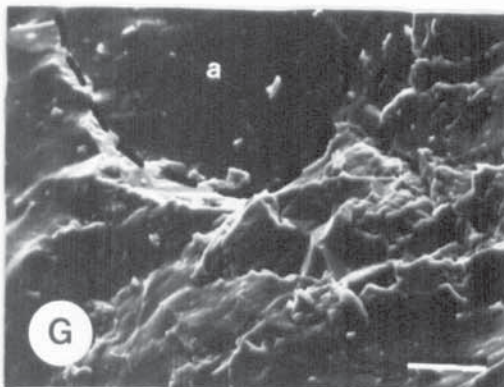
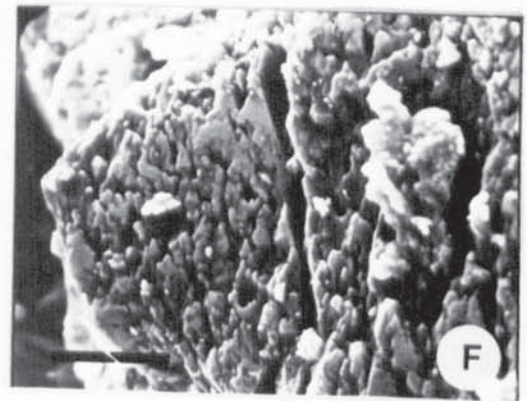
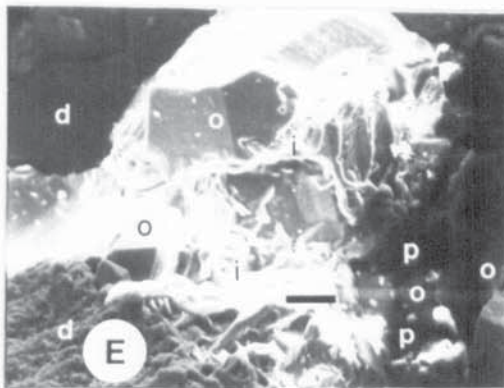
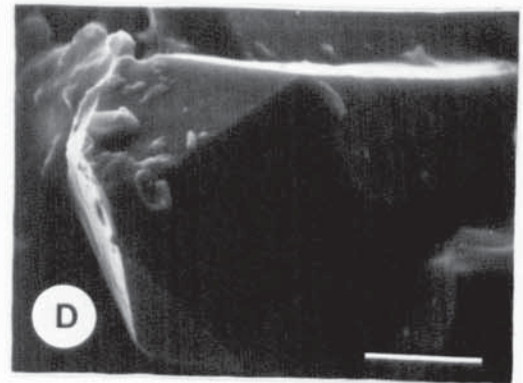
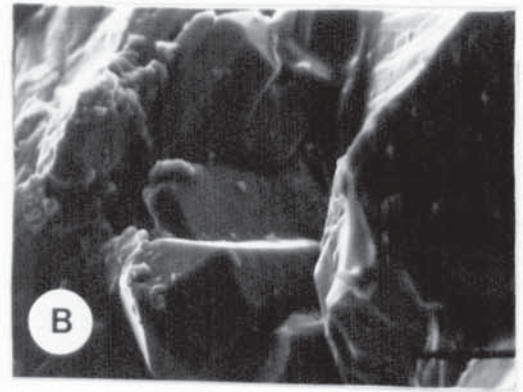
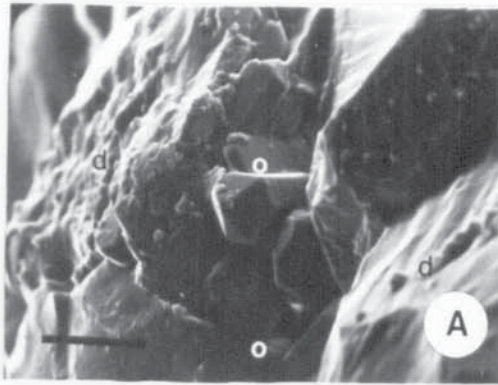


Plate 11.5

PLATE 11.6

All SEM photomicrographs (Gold coating)

- A. Growth steps (arrowed) on platy kaolinites (P). Note presence of cleaved blocky kaolinite (b).
Scale bar = 10 μm .
Bwlchgwyn sandstone.
- B-C. Growth steps on platy kaolinite (arrowed).
Scale bar = 10 μm (B; Bwlchgwyn sandstone); 4 μm (C; Minera sandstone).
- D. Kaolinite book with wedge shaped crystals (w).
Scale bar = 10 μm .
Minera sandstone.
- E. Blocky kaolinite crystals (b); also present kaolinite plates (p).
Scale bar = 4 μm .
Bwlchgwyn sandstone.
- F. Book of kaolinite plates in approximate crystallographic continuity.
Scale bar = 10 μm .
Bwlchgwyn sandstone.
- G. Blocky kaolinite crystals (b).
Scale bar = 10 μm .
Bwlchgwyn sandstone.
- H. Book of platy kaolinite (P) with a seam. Note also the presence of blocky kaolinite (b).
Scale bar = 4 μm .
Minera sandstone.

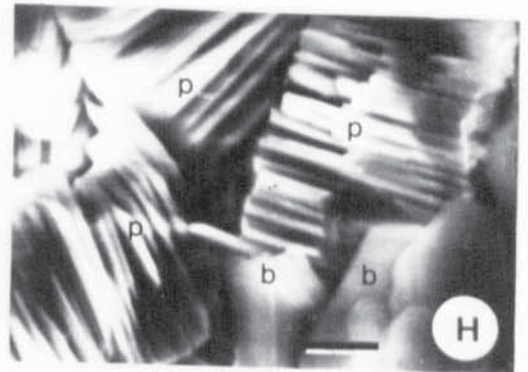
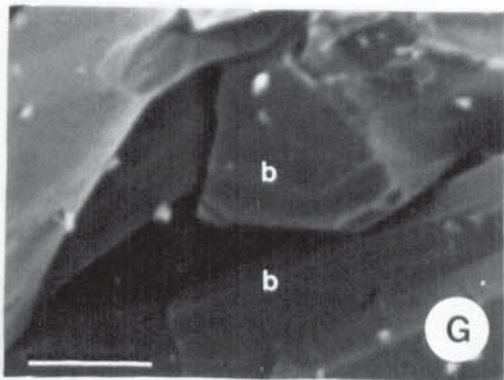
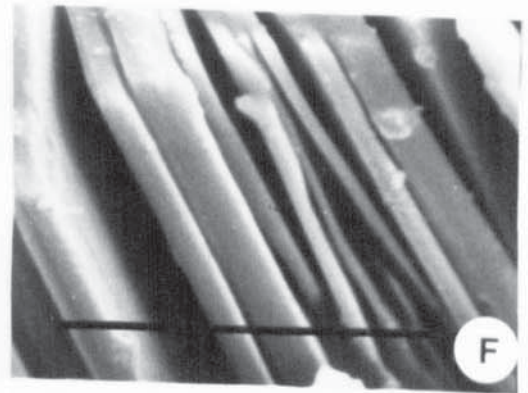
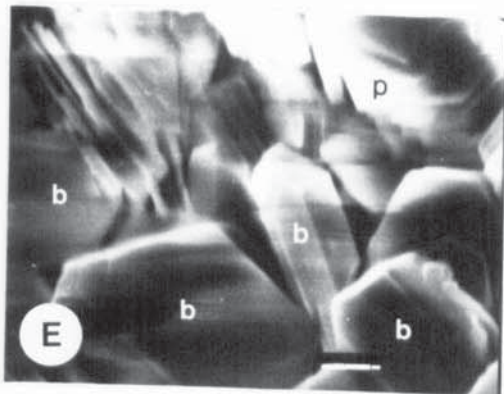
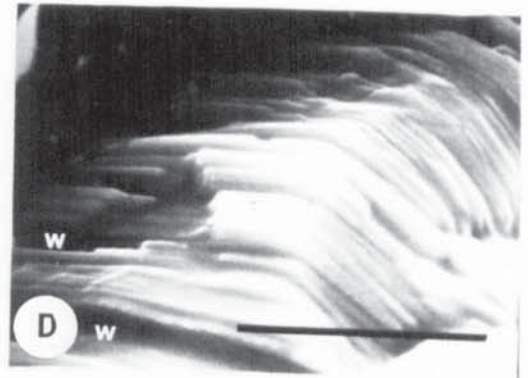
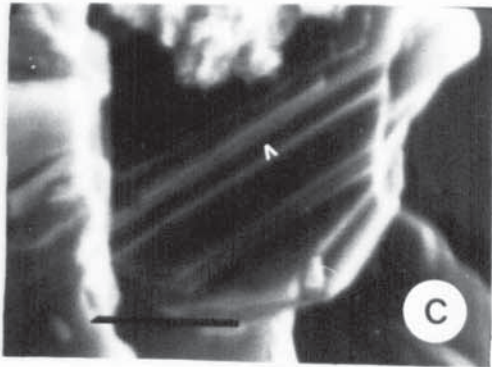
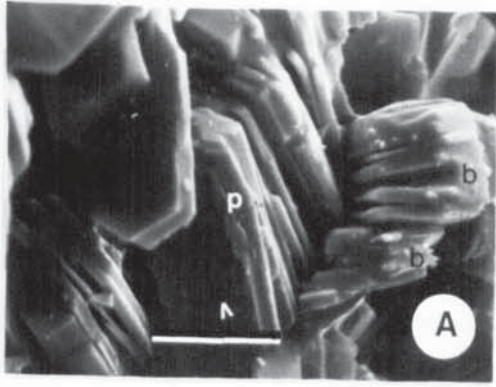


Plate 11.6

PLATE 11.7

All SEM photomicrographs (Gold coating)

- A. Book of closely spaced thin kaolinite plates which appear to have slipped over one another.
Scale bar = 10 μ m.
Minera sandstone.
- B. Thin plates are sometimes bent (arrowed) around large and thick kaolinite crystals. Note also the well developed blocky kaolinite (b).
p = platy kaolinite.
Scale bar = 10 μ m.
Bwlchgwyn sandstone.
- C-D. Book of kaolinite plates in approximate crystallographic continuity. Note also the well developed (001) faces.
Scale bar = 4 μ m.
Bwlchgwyn sandstone.
- E. Vermicular kaolinite of thin plates.
Scale bar = 10 μ m.
Minera sandstone.
- F. Grooves or notches in kaolinite flakes may be indications of twinning.
Scale bar = 4 μ m.
Bwlchgwyn sandstone.
- G. Books of kaolinite plates from Ruabon sandstone
Scale bar = 4 μ m.
- H. Ragged or rounded faces of kaolinite may indicate dissolution feature.
Scale bar = 10 μ m.
Minera sandstone.

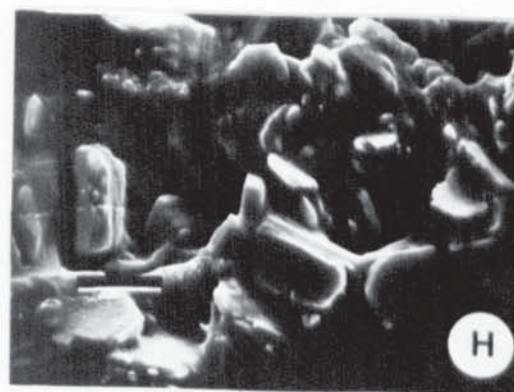
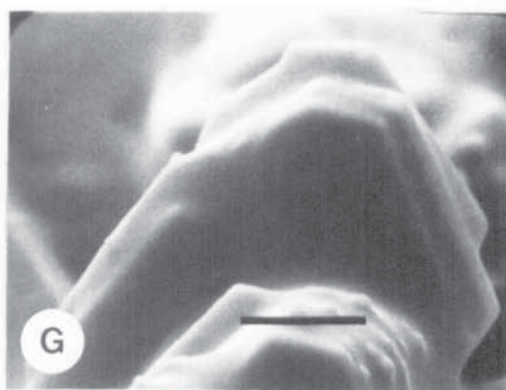
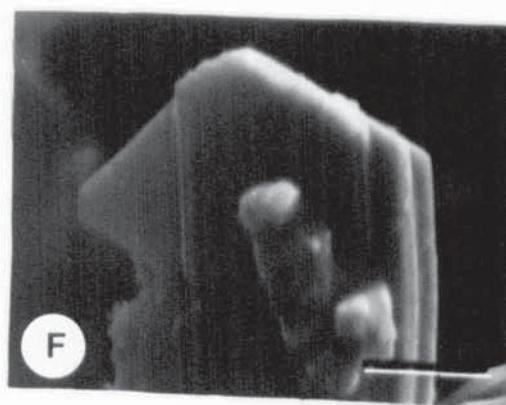
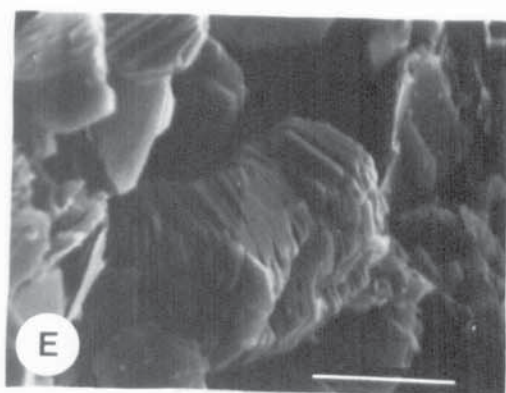
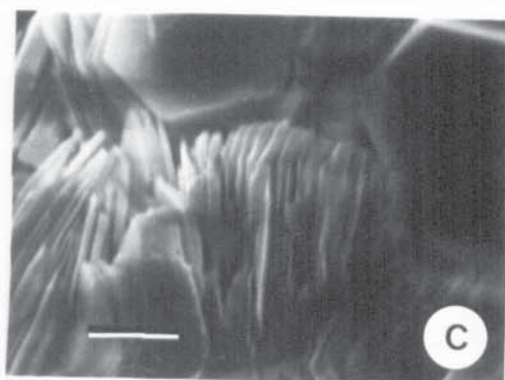
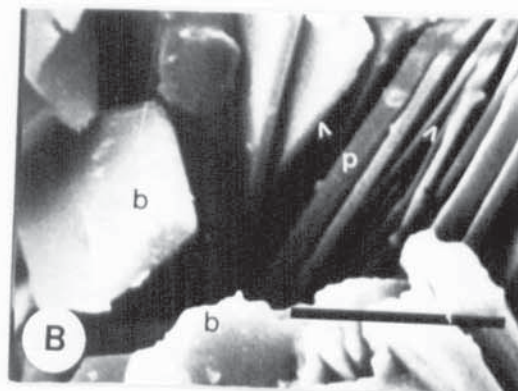
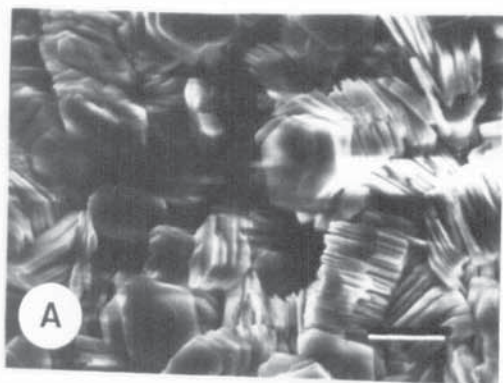


Plate 11.7

PLATE 11.8

All SEM photomicrographs (except G). Gold coating

- A. Tiny blocky kaolinite crystals occasionally occur in a group on larger kaolinite blocks (b).
Scale bar = 4 μm .
Minera sandstone.
- B. Small blocky kaolinite crystals may also occur singly on a relatively larger kaolinite block (b).
Scale bar = 2 μm .
Bwlchgwyn sandstone.
- C. Occasionally tiny blocky kaolinite crystals may also occur as clusters.
Scale bar = 10 μm .
Bwlchgwyn sandstone.
- D. Enlargement of above. Scale bar = 4 μm .
- E. Dickite blocks (d) are pseudomorphed by detrital illite (I).
Scale bar = 100 μm .
Minera siliceous shale
- F. Enlargement of above. d = dickite
Scale bar = 40 μm .
- G. Thin section photomicrograph of stylolite (s) which cuts overgrowth. Note also the presence of concavo-convex grain contact (c). ppl.
Width of field of photograph = 2.7 mm
Bwlchgwyn sandstone.
- H. The flaky morphology of detrital illite (id).
Scale bar = 4 μm .
Bwlchgwyn sandstone.

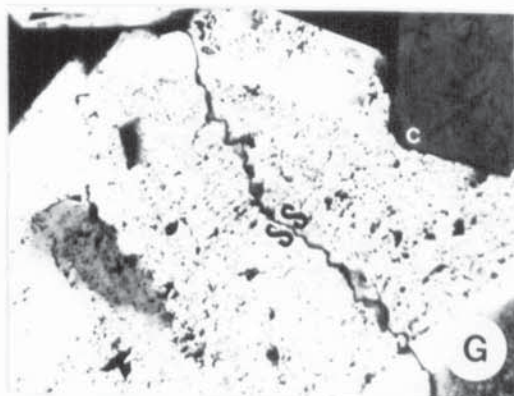
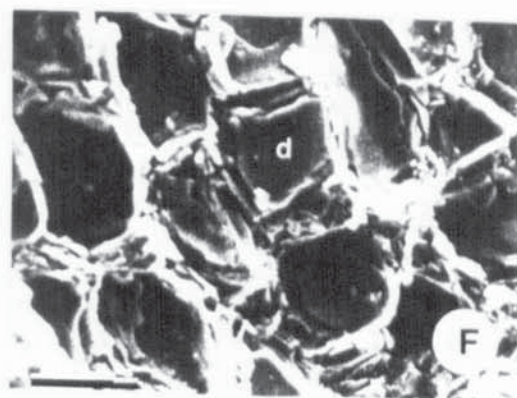
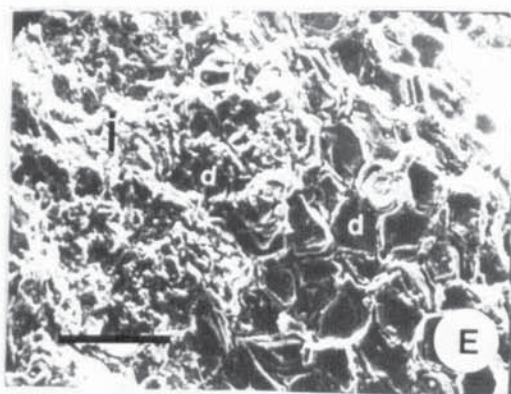
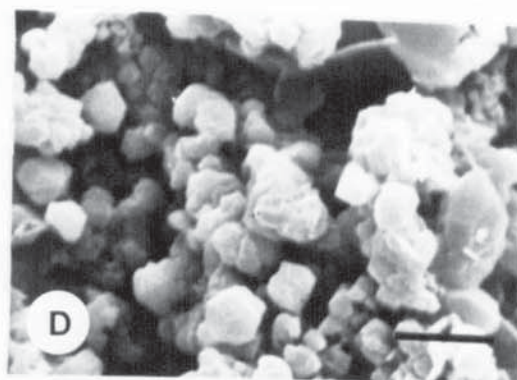
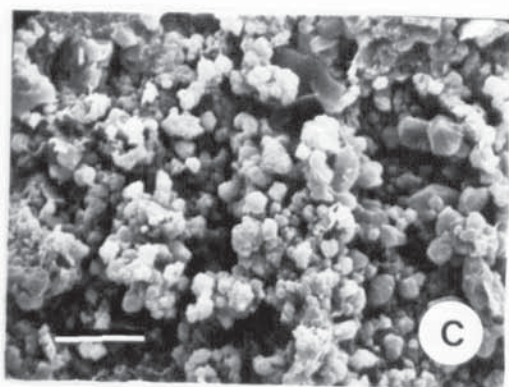
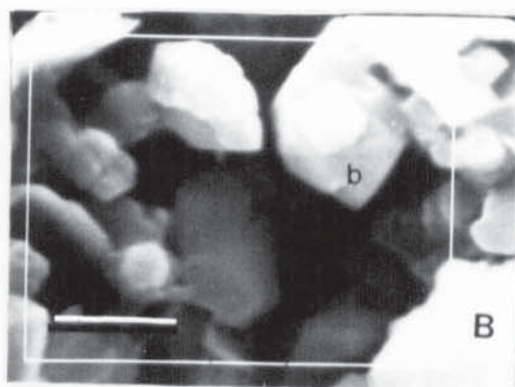
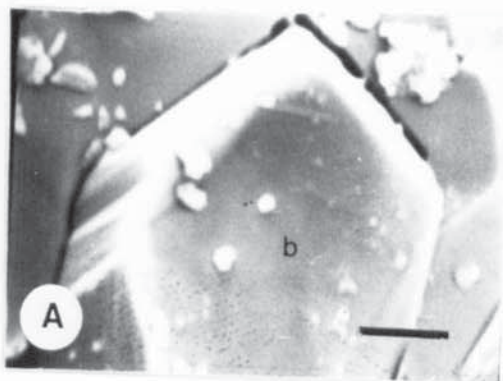


Plate 11.8

CHAPTER 12

CONCLUSIONS

A variety of sedimentological, diagenetic and palynological studies have been employed during the present investigation with the aim of providing a comprehensive and detailed analysis of the Viséan - Namurian chert beds and the Namurian clastic succession (Cefn-y-Fedw Sandstone Group) in North Wales.

The miospore contents of sediments and associated thin coals are attributed to the E1 to middle G1 zones of the Namurian Pendleian-middle Yeadonian stages (apart from the Aqueduct and the Chwarelau Coal Seams which were found to be basal Westphalian A in age). The miospore assemblages compare fairly closely with the concurrent range zones defined by Owens et. al. (1977) and Clayton et. al. (1977). Tentative comparisons are also made with assemblages of similar ages described from Western Europe and Northern America.

The sedimentary and palynofacies descriptions and consequent facies interpretation suggest that the clastic sequences in the Bwlchgwyn-Minera-Ruabon areas, were probably produced by fluvial dominated deltas where a Mississippi type delta model can be applied. But the Llanarmon-yn-ial and the Terrig River areas, appear to have developed outside the main zone of fluvial dominated deltaic influence. The deposition of the Gronant chert near Prestatyn, took place under shallow-marine conditions.

In the Gronant chert and in the Llanarmon-yn-ial cherty flags the most common variety of silica is quartz, which is occasionally associated with chalcedony and or/lutecite. Where the three

varieties occur together there is fabric evidence of a transition from chalcedony, through lutecite to quartz.

Geochemical study suggests that the rhythmic layering of the Llanarmon-yn-ial cherty flags - shale sequences are largely due to two mechanisms as proposed by McBride and Folk (1979) and Lijima et. al. (1985). These are: diagenesis and the episodes of current deposition of mud during constant radiolaria/sponge sedimentation. Similarly, geochemical and petrological studies indicate that the Gronant chert is essentially a silicified limestone and that the silica is diagenetic in origin. The major sources of diagenetic silica in the Gronant chert are considered to be organic (sponge spicules + radiolarians). The following interpretations can be made for the diagenetic sequences in the development of the Gronant chert:

- 1) The organic contents of the host limestones dissolved, releasing abundant silica which ultimately migrated to sites of Gronant chert nodules and began to precipitate and nucleate as opal-CT. Simultaneously microbial reduction of SO_4^{2-} , methanogenesis and fermentation caused increased alkalinity and NH_4^+ concentration in interstitial fluids; this led to incipient dolomitization and pyritization.
- 2) Magnesium was released during opal-CT to quartz transformation and also promoted dolomitization.
- 3) Local replacements of carbonate by silica and subsequent reversals and multiple replacement reversals may have continued throughout the Gronant chertification processes.

Petrological, geochemical and diagenetic studies of the Terrig River shale and the Bwlchgwyn-Minera-Ruabon sandstone/siliceous shale units reveal that these Namurian clastic sediments have undergone

a relatively deep burial history. Diagenesis in the sandstones involves a dissolution phase creating secondary porosity via the dissolution of carbonates and feldspars and this was accompanied by the generation of various types of cements in the following order: siderite crystallization, quartz overgrowths, kaolinite - dickite precipitation, a second generation of quartz overgrowths, illite-lath growth, blocky kaolinite precipitation and oxidation of siderite. Unlike other studies, notably of the Tertiary Gulf Coast sediments, there is no direct evidence of smectite to illite conversion by way of a mixed - layer illite/smectite in sandstones or shales. The sources of the secondary silica are: pressure solution, dissolution of feldspars, clay mineral diagenesis, dewatering of siliceous shales and siltstones and silica-bearing Palaeozoic plants.

APPENDIX 1

PALYNOLOGICAL SLIDE PREPARATION

Sample preparation

The samples were thoroughly cleaned and were left to dry at room temperature. Before crushing the samples, the equipment was washed and cleaned to avoid any contamination between samples.

The shale samples were crushed to about 2-3 mm. in diameter, while the coals were crushed to pass through a B. S. 36 mesh (0.42 mm.). The mortar and the pestle were cleaned thoroughly with a brush and hot water immediately after each sample was crushed and then dried properly. Compressed air was also used to clean the sieve. The mortar and the pestle was used repeatedly to crush harder grains of coal and clastics to avoid the whole sample from becoming powdered which causes the destruction of spore exines.

A jaw crusher was employed for very hard and compact shales.

Representative samples for chemical treatment (maceration processes) were obtained by the 'cone and quarter' method as described by Twenhofel and Tyler (1941).

Oxidation

Oxidation of the organic matter to remove ulmins and humic substances is called maceration. There are a number of methods of oxidation and among them the most noteworthy are the use of Schulze reagent (potassium chlorate and concentrated nitric acid) followed by alkali solution, and the Zetzsche and Kälin (1932) method utilizing fuming nitric acid. In the present work the Schulze method was not used since it is more lengthy and the use of alkali has been shown to increase the size of spores exines

and in some cases destroy them.

Zetzsche and Kälén (1932) used fuming nitric acid saturated with bromine which they thought protected the spore exines but later authors including Shaw and Yeadon (1964) considered the bromine unnecessary. They observed that sporopollenin contains cellulose, a xylan fraction and high percentage of a lipid fraction. Zetzsche and Kälén had thought erroneously that the sporopollenin might be of a polymeric terpenoid nature and that their mixture with fuming nitric acid and bromine would protect the wall of fossil spores during the process of oxidation.

Kosanke (1950), Staplin (1960) and other authors, all noticed that the type and time of oxidation, may have varying effects on spore exines, as it is well known that certain spores oxidise more quickly than others. So considerable experience is needed in order to determine the length of time and type of oxidation required for a certain sample.

The following methods were used for the present investigation:-

About 1 gramme of coal was taken in each case and treated with different proportions of fuming and concentrated nitric acid, for periods ranging from 3-6 hours.

- i) 40-50 ml. fuming nitric acid (S.G. 1.5).
- ii) 20 ml. conc. HNO_3 with 40 ml. fuming HNO_3 .

The second type of oxidation tends to take a slightly longer period than the first, but gives satisfactory results.

After oxidation the residues were filtered by a Buchner funnel containing a sintered glass disc (porosity grade 3), and cleaned with the original mixture two or three times to make certain that the residue was totally oxidized, and then washed with conc. nitric acid for at least three to four

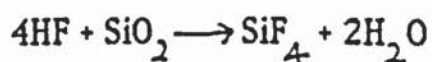
times, until the drops from the funnel glass became colourless. In this way the filter plate would be rid of the ulmins and humic matters, leaving the organic residue containing unoxidized plant cuticle and miospores. The residues were then washed with dilute nitric acid four to five times, and finally with distilled water several times to remove the fine material which tends to become aggregated during oxidation. The microspores of the filter plate become blocked, while continuously cleaning, so blowing air many times from the pressure flash helps to keep the filtration process going (Neves and Dale 1963).

Residual organic compounds may be removed by treatment with a weak solution of KOH and NaOH. But during the present study no alkali was used for either coal or shale sample maceration.

Actually, the strength of oxidation and also the time of oxidation vary from sample to sample depending on a) the carbon content of the coal and b) the degree of weathering. Therefore, care was taken at short intervals to see whether the samples were ready for dilution or not.

Removal of silicates

The separation of spores from clastic sediments was done by the treatment of shales and siltstones with dilute HCl to get rid of any carbonate present, and then with 40% HF, to dissolve the silicates. After testing for effervescence with dilute HCl about 10-15 grammes of a representative shale/siltstone sample was mixed with 250 ml. hydrofluoric acid (HF) in a polythene jar and left at room temperature for about 7 days. Each day the sample was stirred in order to speed the reaction. The products of the reaction are:



The residue was then decanted carefully and the jar filled with distilled

water, stirred, left to settle for several hours, and then decanted again. This process was repeated for six or seven times, until the residue became neutral. The residue was then transferred into a filter glass funnel and oxidized by the addition of $1/3$ conc. HNO_3 + $2/3$ fuming HNO_3 for almost 2 hours and then the same procedure was gone through as described above for coal.

Ultrasonic vibration

During the present study ultrasonic vibration technique was employed several times, especially for sediments, in order to disperse or breakdown the aggregates of insoluble organic particles, which enclosed and obscured the spores. For sediments it was used for about 10 seconds before and after the treatment with HNO_3 , while for coals immediately after the oxidation for about 15 seconds.

After ultrasonics it was necessary to filter the maceration again and clean it with distilled water to remove minute particles.

Mounting of spore residue

In the present investigation cellosize (aqueous solution of hydro-xyethyl cellulose) and elvacite were used as mounting media. The following procedures were adopted:-

- i) A few drops of the organic residue were drawn off by means of a slender pipette (dropper) and with almost double the amount of 2% cellosize solution were placed in a small jar and thoroughly mixed using a pipette.
- ii) One or two drops of the mixture were then spread evenly and carefully over the entire surface of a cover slip. The moisture was allowed to dry off slowly in a low temperature hot plate (slightly above the room temperature) where upon the cellosize dried as a hard thin film.

iii) When the cover slips were dried off, one drop of elvacite was used in order to mount them on a cleaned glass slide.

After labelling the slides were ready for use.

The advantages of this method over those involving the use of other mounting media are firstly, collosize is a dispersal agent so that flocculation does not occur on the slide and secondly, since collosize dries as a thin film the spores are all in the same plane of focus. Moreover, such slide appear to be permanent as they are not liable to dry up as those made of glycerine jelly do. Cellosize was first recommended by Jeffords and Jones (1959). Elvacite has the advantage over canada balsam that it does not require the use of a hot plate.

Microscopy

Routine logging of the miospores species was done at a magnification of 400 times using a VICKERS MICROSCOPE. Fine details of morphology were examined at higher magnification using oil immersion. All photographs were taken with the ZEISS PHOTOMICROSCOPE II (66215) and the stage coordinates for photographed specimens linked to that microscope.

APPENDIX 2

CATHODOLUMINESCENCE TECHNIQUES

Cathodoluminescence was achieved using a Technosyn cold cathode luminescence model 8200 MK 2 instrument. An accelerating voltage of between 15-20 KV with a current of 0.2-0.4 mA and a beam area of approximately 100 mm² was applied to polished thin sections. Non-polished sections were used during preliminary investigation, but lacked the detail of well polished sections. To reduce exposure time while recording observations, and thus reduce problems associated with vibrations and drifting 'standard' conditions, 1000 ASA Kodacolour VR colour slide film was used. Exposure times were variable, being typically 8-30 seconds for red-orange carbonates and 5-15 minutes for poorly luminescing silicates.

APPENDIX 3

SEM TECHNIQUE

Scanning Electron Microscopy

The scanning electron microscope (SEM, Cambridge stereoscan 150) with energy dispersive analysis of x-rays (EDAX) was used to study most of the sandstone, chert, cherty flags and shale samples as small chips, individual grains and as oriented grain mounts of clay fraction. Polished sections were also studied using SEM in order to identify authigenic overgrowths which were difficult to identify with certainty using optical microscopy. SEM was used with success to study authigenic minerals, dissolution features and paragenetic relation between mineral constituents. The attached EDAX was very helpful in identifying different clay minerals.

The samples were prepared by mounting the fresh chips onto aluminium stubs and coated either by carbon if semi-quantitative analysis was to be carried out or gold palladium if better resolution was required.

APPENDIX 4
ELECTRON MICROPROBE ANALYSIS

Cambridge Microscane MK5 microprobe was used to analyse quartz samples. An accelerating voltage of 20 KV, current of approximately 5nA and a count time of 100 seconds was used during all analyses. Peak and back ground counts were corrected for dead time before calculation of the unknown value by comparison with the standard counts. The uncorrected value was then corrected for atomic number, absorption and fluorescence effects using the program devised by Sweatman and Long (1969).

APPENDIX 5

METHOD OF DETERMINING MICROSCOPICALLY THE REFLECTANCE OF VITRINITE

Principle

Light with a wave length of 546 nm, reflected at near normal incidence from a specified area of well polished vitrinite, measured under oil immersion using a photomultiplier (or similar device), is compared with light reflected under identical conditions from a number of standards (in the present case standards 0.306 and 0.904 (Ro random) were used) of known reflectance.

Materials

Immersion oil of a non-drying, non-corrosive type, with a refractive index of 1.5180 ± 0.0004 at 23°C at a wavelength of 546 nm, and with a temperature coefficient ($-dn/dt$) of less than $0.0005/\text{K}$.

Table A5.1 Reflectance standards in common use

Designation	Refractive Index	Reflectance in immersion oil %
optical glasses	1.70-1.97	0.32-1.66
Spinel	1.73	0.42
Leucosapphire	1.77	0.59
Yttrium aluminium garnet (YAG)	1.84	0.92
Diamond	2.42	5.28
Silicon carbide	2.66	7.50

Apparatus

Binocular polarizing reflected light microscope with photometer. Microscope stage capable of being rotated through 360° perpendicular to the optical axis and which can be centred by adjusting either the stage or the objective. Random reflectance measurements (as in the present case)

required removal of the microscope polarizer. The room temperature should be within the range of $23 \pm 3^{\circ}\text{C}$.

Sample preparation

Sample preparation in this study was standardised and involved washing, drying, mounting in cold-set resin and hand polishing through three grinding and three polishing stages.

A detailed account of the methodology of this technique is given by Mackowsky (1975).

APPENDIX 6

MAJOR AND TRACE ELEMENTS DETERMINATION BY X-RAY FLUORESCENCE

Sample Preparation

The analyses were carried out using a Philips 1400 X-ray fluorescence spectrometer.

Samples were first washed to remove any extraneous material, and were then crushed in a jaw crusher and finally ground in a TEMA mill for a total of three minutes. Ground samples were then dried overnight at a temperature of 110°C.

Pressed Powder Pellets

To 8.5g of a sample was added 1.5g of Bakelite (R0214/1) binding agent. This was then placed on a shaking table for 30 minutes to ensure homogenisation. The homogenised material was then placed in a steel mould and pressed to a pressure of 20 tons/in² for 10 seconds. The pellets produced were then cured overnight in an oven at a temperature of 120°C.

Fused Glass Discs

To prepare fused glass discs, samples were crushed, ground and dried as above. To 0.75g of a carefully weighed sample was added 5.3333 times the measured weight of Johnson and Matthey Spectroflux 105. This was then placed in an oven at 1100°C for 30 minutes. When completely cooled the weight loss (loss on ignition) was made up with spectroflux. A meker burner was then used to remelt and homogenise this.

A preheated (220°C) disc-shaped graphite mould was used to form the fused glass disc. Gentle hand pressure was applied via a steel rod to ensure an even spread of the melt.

Cooled fused discs were stored in individual plastic envelopes in a dessicator.

Analysis

Calculation of results were compared with the recommended concentrations for elements in the standards where they averaged and compiled using USGS world standards (Abbey, 1980). Thirty six standards using known and fixed percentages of the different elements analysed were used.

APPENDIX 7

Checklist for Petrographic Description of the present Sandstones (modified after Blatt, 1982)

- I. Name of formation or member, geographic and stratigraphic location, geologic age
- II. Texture
 - A. Mean grain size and sorting
 - B. Textural name
 - C. Grain shape
 - D. Stage of textural maturity
 - E. Fabric
- III. Mineral composition
 - A. Percentage of quartz
 - 1. Monocrystalline vs. polycrystalline
 - 2. Undulatory vs. nonundulatory
 - 3. Size and texture of crystals in polycrystalline grains, e.g., sutured, elongated
 - B. Percentage of chert
 - C. Percentage of feldspar
 - D. Percentage of lithic fragments
 - 1. Types of fragments and relative abundances, describing fragment mineralogy accurately, e.g., sillimanite schist rather than metamorphic rock fragment; basalt and biomicrite rather than volcanic rock fragment and limestone fragment.
 - 2. Relation between fragment type and grain size
 - E. Micas
 - F. Other terrigenous minerals, such as tourmaline and zircon

- G. Clay matrix: most abundant clay based on optical properties (an X-ray diffractogram is essential as a supplement to the rock description)

IV. Classification

V. Interpretation and paragenesis

- A. Probable major source areas, e.g., mostly granite with minor older sandstones
- B. Kinetic energy of depositional environment, based on grain size and sorting
- C. Permissible depositional environments
- D. Diagenetic changes
 - 1. Age relations of authigenic constituents
 - 2. Effects of intrastratal solution
 - 3. Effects of compaction

APPENDIX 8
METHOD OF DETERMINATION OF ORGANIC CARBON

The ignition loss procedure described below is taken from Dean (1974).

(a) A powdered sample is dried in an oven at 90°-100°c in a pre-weighed ceramic crucible for one hour. After cooling to room temperature in a desiccator, the sample and crucible are weighed. This gives the dry weight of the sample which is the basis for all weight loss calculations

(b) The sample and crucible are then placed in a muffle furnace and heated to 550°c for one hour. After cooling to room temperature, the sample is again weighed. The difference between this weight and the dry weight is the amount of organic carbon ignited.

(c) The sample is returned to the muffle furnace and heated to 1,000°c for one hour. The weight loss between 550-1,000°c is the amount of CO₂ evolved from carbonate minerals.

APPENDIX 9 TOTAL ORGANIC CARBON PERCENTAGES IN THE STUDIED SEDIMENTS

GRONANT CHERT

<u>Sample No.</u>	<u>Percentage organic carbon</u>
3	1.42
4	4.86
5	4.9
6	1.57
7	1.90
8	1.80
9	1.78
10	4.26
11	1.73
12	2.87

LLANARMON-YN-IAL CHERTY FLAGS

18	1.23
21	1.64
23	1.44
26	1.06
27	1.50
28	1.03
29	1.0
30	1.20
34	1.0
35	1.0
36	1.08
39	1.09
40	1.63

TERRIG RIVER SHALE

1	3.12
2	2.78
3	1.92
45	2.60
47	2.44

BWLCHGWYN-MINERA SILICEOUS SHALE

7	4.56
10	3.73
11	1.59
12	2.40
13	3.20
14	1.68
15	3.49
16	7.67

APPENDIX 10 QUARTZ PERCENTAGES IN THE STUDIED SEDIMENTS

LLANARMON-YN-IAL CHERTY FLAGS

Sample No.	Percentage Quartz
18	51.30
21	52.60
23	43.40
27	38.0
36	38.10
39	38.40
40	57.0

TERRIG RIVER SHALE

1	45.20
2	61.80
3	60.20
45	44.45
47	59.90

BWLCHGWYN-MINERA SILICEOUS SHALE

MINERA QUARRY	3	62.0
	8	49.45
BWLCHGWYN QUARRY	7	61.30
	10	59.70
	11	70.50
	12	70.60
	13	57.0
	14	54.90
	15	54.90
	16	44.90

APPENDIX 11 RESULTS OF XRF ANALYSIS (MAJOR ELEMENTS) OF THE PRESENT STUDIED SEDIMENTS

UNIT	Sp. No.	Fe ₂ O ₃	MnO	TiO ₂	CaO	K ₂ O	So ₃	P ₂ O ₅	SiO ₂	Al ₂ O ₃	MgO	Na ₂ O
GRONANT CHERT	3	0.24	0.007	0.015	8.53	0.07	0.09	0.08	84.08	0.63	0.83	0.24
	4	1.68	0.02	0.11	36.93	0.85	0.71	0.09	26.41	4.13	0.61	0.04
	5	1.55	0.04	0.13	18.75	0.53	0.30	0.31	48.89	2.35	5.70	0.13
	6	0.27	0.01	0.01	7.61	0.05	0.09	0.10	86.01	0.44	0.77	0.18
	7	0.41	0.02	0.52	0.14	1.14	0.03	0.03	89.39	5.98	0.44	0.14
	8	0.14	0.01	0.02	6.51	0.20	0.009	0.06	88.86	1.16	0.12	0.21
	9	0.21	0.03	0.02	3.72	0.07	0.03	0.07	93.26	0.57	0.43	0.17
	10	1.09	0.03	0.36	0.73	1.76	0.06	0.42	83.52	7.56	0.62	0.27
	11	0.42	0.17	0.16	3.62	0.84	0.01	0.19	88.87	3.71	0.34	0.24
	12	0.83	0.03	0.17	3.16	0.94	0.03	0.15	87.37	4.38	0.35	0.27
	18	0.72	0.009	0.80	0.22	2.50	0.02	0.11	83.73	10.09	0.83	0.20
	21	1.34	0.01	1.22	0.40	4.30	0.03	0.10	71.30	16.20	1.39	0.27
LLANARMON-YN-IAL CHERTY FLAQS	22	0.17	0.01	0.08	0.03	0.42	0.03	0.03	99.22	1.96	0.18	0.19
	23	0.64	0.003	0.64	0.15	1.75	0.03	0.06	89.72	6.56	0.62	0.16
	26	0.26	-0.002	0.06	0.09	0.46	0.07	0.03	98.77	2.09	0.18	0.19
	27	0.41	0.005	0.30	0.20	1.37	0.02	0.03	91.82	5.65	0.50	0.22

APPENDIX 11 (continued)

UNIT	Sp. No.	Fe ₂ O ₃	Mno	TiO ₂	CaO	K ₂ O	So ₃	P ₂ O ₅	SiO ₂	Al ₂ O ₃	Mgo	Na ₂ O
LLANARMON-YN-IAL CHERTY FLAGS	28	0.66	0.003	0.30	0.30	1.32	0.08	0.06	91.76	5.77	0.47	0.17
	29	1.10	0.003	0.35	0.06	1.44	0.04	0.09	89.97	6.20	0.54	0.30
	30	1.11	0.003	0.35	0.06	1.45	0.02	0.09	89.97	6.18	0.53	0.24
	31	0.28	-0.004	0.07	0.08	0.45	0.04	0.05	98.48	2.13	0.17	0.18
	34	1.11	0.004	0.36	0.06	1.45	0.09	0.09	90.36	6.23	0.53	0.17
	35	1.09	0.01	0.35	0.05	1.44	0.04	0.09	90.07	6.21	0.54	0.25
	36	0.53	0.003	0.35	0.07	1.43	0.04	0.04	90.49	6.04	0.54	0.21
	38	0.18	0.003	0.07	0.04	0.43	0.08	0.03	99.35	1.97	0.19	0.21
	39	1.03	-0.003	0.30	0.19	1.20	0.02	0.14	91.80	5.05	0.42	0.33
	40	0.78	-0.002	0.51	0.04	1.63	0.04	0.04	89.73	6.40	0.53	0.22
TERRIG RIVER SHALE	1	2.96	0.009	0.71	0.38	2.69	0.05	0.26	78.87	10.34	0.92	0.22
	2	2.03	0.01	0.66	0.28	2.57	0.03	0.25	76.61	9.28	0.80	0.29
	3	1.35	0.03	0.65	0.30	2.42	0.05	0.21	84.69	8.20	0.68	0.26
	45	2.18	-0.004	0.69	0.29	2.62	0.05	0.26	80.74	9.58	0.76	0.19
	47	2.49	0.012	0.66	0.24	2.48	0.04	0.29	82.04	8.75	0.72	0.17

APPENDIX 11 _____ (continued)

UNIT	Sp. No.	Fe ₂ O ₃	Mno	TiO ₂	CaO	K ₂ O	SO ₃	P ₂ O ₅	SiO ₂	Al ₂ O ₃	Mgo	Na ₂ O
BWLCHGWYN-MINERA-SANDSTONE (RUABON MOUNTAIN)	1	0.14	0.002	0.03	0.006	0.012	0.09	0.02	99.78	0.21	0.04	0.22
	2	1.12	0.01	0.42	0.04	0.61	0.09	0.03	94.88	3.84	0.31	0.20
	3	0.52	0.01	0.18	0.02	0.20	0.07	0.03	99.37	1.23	0.11	0.18
	5	0.10	0.01	0.09	0.01	0.10	0.06	0.02	99.62	0.76	0.07	0.18
	6	0.09	0.002	0.09	0.005	0.02	0.06	0.02	99.36	0.48	0.03	0.16
BWLCHGWYN-MINERA-RUABON SANDSTONE (MINERA QUARRY)	1	0.19	-0.003	0.11	0.01	0.13	0.09	0.02	99.93	1.20	0.08	0.14
	3	0.27	-0.002	0.66	0.25	0.87	0.09	0.03	76.28	3.96	0.31	0.22
	4	0.17	0.004	0.21	0.14	0.41	0.06	0.02	96.18	2.25	0.16	0.18
	5	0.15	-0.004	0.08	0.03	0.06	0.09	0.07	99.52	0.83	0.05	0.17
	6	0.16	0.01	0.11	0.007	0.09	0.09	0.03	99.13	0.85	0.05	0.32
	7	0.29	0.002	0.35	0.03	0.57	0.09	0.02	96.69	2.60	0.23	0.12
	8	0.75	-0.001	0.60	0.21	1.92	0.12	0.25	76.49	8.32	0.76	0.26

APPENDIX 11 _____ (continued)

UNIT	Sp..No.	Fe ₂ O ₃	Mno	TiO ₂	CaO	K ₂ O	So ₃	P ₂ O ₅	SiO ₂	Al ₂ O ₃	Mgo	Na ₂ O
BWLCHGWYN-MINERA-RUABON SANDSTONE (BWLCHGWYN QUARRY)	2	0.13	0.001	0.10	0.02	0.04	0.02	0.04	99.88	0.67	0.04	0.19
	3	0.29	-0.001	0.08	0.008	0.07	0.01	0.17	99.53	0.88	0.05	0.13
	5	0.55	-0.004	0.08	0.006	0.12	0.02	0.07	99.27	0.99	0.05	0.15
	6	0.45	0.004	0.35	0.05	0.32	0.04	0.03	97.07	3.22	0.14	-0.04
	7	0.40	0.005	0.74	0.15	1.22	0.01	0.04	85.46	7.46	0.43	0.12
	9	1.30	0.007	0.28	0.03	0.43	0.06	0.05	97.35	1.99	0.17	0.19
	10	0.82	0.005	0.83	0.07	1.60	0.05	0.03	83.51	9.02	0.53	0.02
	11	0.55	-0.002	0.61	0.07	1.09	0.04	0.03	92.63	5.07	0.40	-0.04
	12	2.14	0.001	0.53	0.10	1.01	0.50	0.03	88.03	5.87	0.37	0.009
	13	0.67	-0.002	0.64	0.02	1.33	0.06	0.03	87.52	7.11	0.49	0.17
	14	1.90	-0.014	0.33	0.09	1.36	0.08	0.08	88.72	5.66	0.49	0.21
	15	0.30	0.01	0.006	6.62	0.12	0.14	0.05	83.05	0.80	0.70	0.09
	16	0.19	-0.003	0.41	0.10	0.61	0.12	0.03	88.05	4.05	0.24	0.20
	18	0.32	-0.006	0.04	0.01	0.07	0.02	0.02	99.24	0.59	0.05	0.23
	19	0.13	-0.008	0.09	0.01	0.16	0.03	0.02	99.57	1.64	0.08	0.19

APPENDIX 12 RESULTS OF XRF ANALYSIS (TRACE ELEMENTS) IN PPM OF THE PRESENT STUDIED SEDIMENTS

UNIT	Sp. No.	Cu	Ni	Zn	Rb	Sr	Y	Zr	Nb	Th	U	Pb	Ba
GRONANT CHERT	3	1	6	13	2	167	9	9	2	2	-2	8	27
	4	28	34	13	34	2638	25	20	4	-9	23	10	917
	5	63	56	21	18	204	25	35	5	4	6	40	87
	6	-1	7	14	1	111	8	9	2	3	-2	9	19
	7	3	6	17	2	166	9	11	20	1	-1	13	36
	8	-2	4	15	4	128	11	12	14	1	-2	6	30
	9	-2	3	5	1	42	8	9	2	3	-2	10	17
	10	13	60	25	48	67	92	78	8	11	5	80	63
	11	1	20	13	25	56	25	34	9	4	2	17	68
	12	15	56	21	27	53	46	38	5	6	1	27	80
LLANARMON-YN-IAL CHERTY FLATS	18	9	10	27	81	44	34	439	18	21	-0.009	671	159
	21	23	14	21	163	82	45	330	22	20	0.001	202	297
	23	1	8	17	56	37	24	428	21	10	-0.001	27	145
	26	-2	2	7	11	41	5	21	3	5	-0.002	136	46
	27	6	2	8	43	60	9	74	11	6	2	20	46

APPENDIX 12 (continued)

UNIT	Sp. No.	Cu	Ni	Zn	Rb	Sr	Y	Zr	Nb	Th	U	Pb	Ba
LLANARMON-VN-IAL CHERTY FLATS	28	0	3	8	41	63	9	72	7	9	-0.001	153	107
	29	15	5	18	50	56	24	109	8	8	0.001	19	97
	30	16	5	17	52	55	23	111	7	7	2	21	104
	31	-1	2	7	10	58	6	21	3	3	-0.001	26	36
	34	5	7	10	50	55	22	110	8	8	0.001	20	100
	35	15	5	17	52	55	23	111	7	6	0.001	22	100
	36	6	4	8	53	49	16	99	12	6	5	11	121
	38	-5	2	7	12	31	5	31	3	3	-0.001	22	6
	39	8	4	12	44	123	15	129	13	8	7	44	166
	40	3	6	11	62	38	21	252	10	8	0.001	20	90
	41	29	6	11	56	41	21	327	16	10	0.001	32	117
TERRIG RIVER SHALE	1	-5	2	5	96	62	47	301	18	11	2	31	229
	2	303	5	17	96	58	32	305	16	13	0.001	20	221
	3	4	2	7	88	62	25	321	16	11	2	21	291
	46	-4	2	39	99	69	42	309	16	11	3	28	238
	47	-3	4	10	89	59	27	309	13	11	2	28	234

APPENDIX 12 (continued)

UNIT	Sp. No.	Cu	Ni	Zn	Rb	Sr	Y	Zr	Nb	Th	U	Pb	Ba
BWLCHGWYN-MINERA- RUABON SANDSTONE (RUABON MOUNTAIN)	1	-1	7	16	60	37	22	252	10	7	1	19	83
	2	-2	3	8	58	42	22	326	16	12	1	31	119
	3	15	56	20	11	31	6	30	2	2	-0.001	24	46
	5	3	4	12	9	48	5	27	3	4	-0.001	8	32
	6	-7	3	11	36	32	11	343	9	9	-0.001	91	54
BWLCHGWYN-MINERA-RUABON SANDSTONE (MINERA QUARRY)	1	60	17	29	3	10	6	114	69	4	-0.001	28	-0.001
	3	-5	2	12	34	39	23	462	31	18	-0.001	707	1
	4	-1	9	23	14	18	9	171	5	12	-0.001	533	-0.001
	5	-5	9	21	1	8	8	90	4	16	-0.001	796	5
	6	-7	1	11	0	11	7	96	3	4	-0.001	51	-0.001
	7	-6	2	20	23	19	12	302	8	9	-0.001	261	-0.001
	8	8	5	8	57	37	23	425	21	10	0	25	132

APPENDIX 12 (continued)

UNIT	Sp. No.	Cu	Ni	Zn	Rb	Sr	Y	Zr	Nb	Th	U	Pb	Ba
BWLCHGWYN-MINERA-RUABON SANDSTONE (BWLCHGWYN QUARRY)	2	-3	2	8	-0.001	7	5	61	79	7	-0.001	312	-0.001
	3	5	2	52	5	4	5	60	4	42	-0.001	2819	-0.001
	5	5	2	94	6	7	5	120	3	12	-0.001	753	-0.001
	6	-1	1	36	11	15	10	336	34	12	-0.001	553	-0.001
	7	14	5	24	58	37	20	483	15	32	-0.001	1443	7
	9	9	3	72	18	13	8	279	6	22	-0.001	1178	-0.001
	10	4	6	23	78	37	30	407	16	21	-0.001	738	7
	11	3	4	18	48	23	23	404	16	17	-0.001	584	-0.001
	12	6	7	18	42	24	25	314	15	15	-0.001	524	23
	13	-6	2	5	52	30	20	332	14	14	-0.001	416	5
	14	-1	3	17	54	46	11	98	7	17	-0.001	756	129
	15	10	34	23	48	47	15	291	13	17	-0.001	664	47
	16	11	18	15	25	27	17	278	9	9	-0.001	246	-0.001
	18	0	13	12	1	6	5	47	2	4	-0.001	55	-0.001
	19	26	45	149	3	7	7	64	40	4	-0.001	77	-0.001

APPENDIX 13 Table A13.1 THE SIMILARITY MATRICES OF MAJOR AND TRACE
ELEMENTS OF THE GRONANT CHERT

	Zn	Cu	Ni	Rb	Sr	Y	Zr
Zn	1.0000	0.4508	0.7803	0.6027	-0.1542	0.7369	0.7529
Cu	0.4508	1.0000	0.6943	0.3730	0.3048	0.2206	0.3159
Ni	0.7803	0.6943	1.0000	0.8294	0.1217	0.8065	0.8331
Rb	0.6027	0.3730	0.8294	1.0000	0.3420	0.8880	0.8826
Sr	-0.1542	0.3048	0.1217	0.3420	1.0000	-0.0338	-0.1053
Y	0.7369	0.2206	0.8065	0.8880	-0.0338	1.0000	0.9745
Zr	0.7529	0.3159	0.8331	0.8826	-0.1053	0.9745	1.0000
Nb	0.2445	-0.1967	-0.1932	-0.0960	-0.1600	-0.0431	-0.0193
Th	0.6366	0.0561	0.6584	0.6584	-0.4234	0.8958	0.9059
U	0.0445	0.4954	0.3746	0.5655	0.9498	0.2040	0.1689
Pb	0.7699	0.3806	0.7920	0.7510	-0.1893	0.9269	0.9511
Ba	-0.1042	0.3354	0.2082	0.4297	0.9933	0.0459	-0.0199
Fe	0.4874	0.8548	0.7921	0.7061	0.6223	0.4759	0.4992
Mn	0.4764	0.5996	0.7892	0.6045	-0.1206	0.6759	0.7388
Ti	0.5493	0.0539	0.3013	0.3558	-0.0825	0.4444	0.4477
Ca	-0.1180	0.5821	0.1989	0.2352	0.8990	-0.1388	-0.1493
K	0.6963	0.1822	0.6489	0.8000	0.1149	0.8106	0.7988
S	-0.0289	0.5881	0.2847	0.3518	0.9367	-0.0067	-0.0332
P	0.6942	0.5090	0.7900	0.7369	-0.1530	0.8316	0.9099
Al	0.6648	0.1497	0.5870	0.7384	0.1356	0.7435	0.7235
Mg	0.3280	0.8870	0.4478	0.0380	-0.0425	-0.0003	0.1438
Na	0.1978	-0.2707	0.2188	0.2197	-0.5564	0.4280	0.4331
Corg	0.5389	0.8439	0.8170	0.7299	0.5423	0.5659	0.5844

APPENDIX 13 (continued)

	Nb	Th	U	Pb	Ba	Fe	Mn	Ti
Zn	0.2445	0.6366	0.0445	0.7699	-0.1042	0.4874	0.4764	0.5493
Cu	-0.1967	0.0561	0.4954	0.3806	0.3354	0.8548	0.5996	0.0539
Ni	-0.1932	0.6584	0.3736	0.7920	0.2082	0.7892	0.7892	0.3013
Rb	-0.0960	0.6584	0.5655	0.7510	0.4297	0.7061	0.6045	0.3558
Sr	-0.1600	-0.4234	0.9498	-0.1893	0.9933	0.6223	-0.1206	-0.0825
Y	-0.0431	0.8958	0.2040	0.9269	0.0459	0.4759	0.6759	0.4444
Zr	-0.0193	0.9059	0.1689	0.9511	-0.0199	0.4992	0.7388	0.4477
Nb	1.0000	-0.1372	-0.1995	-0.0196	-0.1746	-0.2003	-0.2916	0.6708
Th	-0.1372	1.0000	-0.1849	0.8928	-0.3471	0.1683	0.6778	0.3358
U	-0.1995	-0.1849	1.0000	0.0894	0.9668	0.8057	0.1550	0.0071
Pb	-0.0196	0.8928	0.0894	1.0000	-0.1252	0.4852	0.7689	0.4837
Ba	-0.1746	-0.3471	0.9668	-0.1252	1.0000	0.6696	-0.0436	-0.0581
Fe	-0.2003	0.1683	0.8057	0.4852	0.6696	1.0000	0.5553	0.2115
Mn	-0.2916	0.6778	0.1550	0.7689	-0.0436	0.5553	1.0000	0.0539
Ti	0.6708	0.3358	0.0071	0.4837	-0.0581	0.2115	0.0539	1.0000
Ca	-0.3386	-0.4612	0.8943	-0.1861	0.8876	0.7056	0.0345	-0.3096
K	0.3925	0.6146	0.2914	0.7370	0.1817	0.4881	0.3629	0.8394
S	-0.2895	-0.3611	0.9522	-0.0595	0.9316	0.7855	0.0721	-0.1232
P	-0.1760	0.8264	0.1525	0.9357	-0.0876	0.5407	0.8121	0.2611
Al	0.4580	0.5355	0.2847	0.6675	0.1952	0.4579	0.2751	0.8836
Mg	-0.2041	0.0188	0.1337	0.2832	-0.0380	0.5494	0.5018	-0.0536
Na	-0.3461	0.6501	-0.4608	0.3382	-0.5050	-0.3083	0.3242	-0.3313
Corg	-0.1617	0.2679	0.7512	0.5999	0.5892	0.9756	0.6653	0.2261

APPENDIX 13 (continued)

	Ca	K	S	P	Al	Mg	Na	Corg
Zn	-0.1180	0.6963	-0.0289	0.6942	0.6648	0.3280	0.1978	0.5389
Cu	0.5861	0.1822	0.5881	0.5090	0.1497	0.8870	-0.2707	0.8439
Ni	0.1989	0.6489	0.2847	0.7900	0.5870	0.4478	0.2188	0.8170
Rb	0.2352	0.8000	0.3518	0.7369	0.7384	0.0380	0.2197	0.7299
Sr	0.8990	0.1149	0.9367	-0.1530	0.1356	-0.0425	-0.5564	0.5423
Y	-0.1388	0.8106	-0.0067	0.8316	0.7435	-0.0003	0.4280	0.5659
Zr	-0.1493	0.7988	-0.0332	0.9099	0.7235	0.1438	0.4331	0.5844
Nb	-0.3386	0.3925	-0.2895	-0.1760	0.4580	-0.2041	-0.3461	-0.1617
Th	-0.4612	0.6146	-0.3611	0.8264	0.5355	0.0188	0.6501	0.2679
U	0.8943	0.2914	0.9522	0.1525	0.2847	0.1337	-0.4608	0.7512
Pb	-0.1861	0.7370	-0.0595	0.9357	0.6675	0.2832	0.3382	0.5999
Ba	0.8876	0.1817	0.9316	-0.0876	0.1952	-0.0380	-0.5050	0.5892
Fe	0.7056	0.4881	0.7855	0.5407	0.4579	0.5494	-0.3083	0.9756
Mn	0.0345	0.3629	0.0721	0.8121	0.2751	0.5018	0.3242	0.6653
Ti	-0.3096	0.8394	-0.1232	0.2611	0.8836	-0.0536	-0.3313	0.2261
Ca	1.0000	-0.1127	0.9742	-0.0350	-0.1148	0.3381	-0.4938	0.6277
K	-0.1127	1.0000	0.0721	0.5718	0.9928	-0.0824	-0.0348	0.5178
S	0.9742	0.0721	1.0000	0.0374	0.0756	0.2990	-0.5589	0.7105
P	-0.0350	0.5718	0.0374	1.0000	0.4800	0.4617	0.3944	0.6344
Al	-0.1148	0.9928	0.0756	0.4800	1.0000	-0.1167	-0.1194	0.4775
Mg	0.3381	-0.0824	0.2990	0.4617	-0.1167	1.0000	-0.1806	0.5517
Na	-0.4938	-0.0348	-0.5589	0.3944	-0.1194	-0.1806	1.0000	-0.2387
Corg	0.6277	0.5178	0.7105	0.6344	0.4775	0.5517	-0.2387	1.0000

APPENDIX 14 Table A 14.1 THE SIMILARITY MATRICES OF THE MAJOR AND TRACE
ELEMENTS OF THE LLANARMON-YN-IAL CHERTY FLAGS

	Zn	Cu	Ni	Rb	Sr	Y	Zr
Zn	1.0000	0.9877	0.9946	0.9486	-0.9765	0.9980	0.9904
Cu	0.9877	1.0000	0.9974	0.9733	-0.9962	0.9852	0.9974
Ni	0.9946	0.9974	1.0000	0.9717	-0.9935	0.9935	0.9990
Rb	0.9486	0.9733	0.9717	1.0000	-0.9811	0.9587	0.9812
Sr	-0.9765	-0.9962	-0.9935	-0.9811	1.0000	-0.9773	-0.9954
Y	0.9980	0.9852	0.9945	0.9587	-0.9773	1.0000	0.9920
Zr	0.9904	0.9974	0.9990	0.9812	-0.9954	0.9920	1.0000
Nb	0.8189	0.7576	0.7650	0.6158	-0.7029	0.7892	0.7418
Th	-0.7351	-0.7390	-0.7642	-0.8430	0.7762	-0.7755	-0.7804
U	0.3790	0.4785	0.4331	0.5774	-0.4792	0.3811	0.4644
Pb	-0.9961	-0.9973	-0.9997	-0.9669	0.9916	-0.9947	-0.9980
Ba	-0.8448	-0.7676	-0.8001	-0.6568	0.7464	-0.8372	-0.7758
Fe	0.9933	0.9987	0.9987	0.9643	-0.9932	0.9901	0.9967
Ti	0.9433	0.9677	0.9584	0.9049	-0.9686	0.9312	0.9424
Ca	-0.9957	-0.9968	-0.9999	-0.9696	0.9921	-0.9954	-0.9986
K	0.9933	0.9968	0.9954	0.9571	-0.9863	0.9877	0.9929
S	-0.6108	-0.5761	-0.5964	-0.6774	0.5572	-0.6393	-0.6152
P	0.9794	0.9966	0.9951	0.9840	-0.9997	0.9811	0.9972
Al	0.9855	0.9913	0.9939	0.9556	-0.9924	0.9842	0.9907
Mg	0.9620	0.9633	0.9750	0.9709	-0.9747	0.9746	0.9776
Na	0.6259	0.5208	0.5680	0.5388	-0.4863	0.6471	0.5652
Corg	-0.6537	-0.5867	-0.5882	-0.4342	0.5157	-0.6162	-0.5643

APPENDIX 14 (continued)

	Nb	Th	U	Pb	Ba	Fe	Ti
Zn	0.8189	-0.7351	0.3790	-0.9961	-0.8448	0.9933	0.9433
Cu	0.7576	-0.7390	0.4785	-0.9973	-0.7676	0.9987	0.9677
Ni	0.7650	-0.7642	0.4331	-0.9997	-0.8001	0.9987	0.9584
Rb	0.6158	-0.8430	0.5774	-0.9669	-0.6568	0.9643	0.9049
Sr	-0.7029	0.7762	-0.4792	0.9916	0.7464	-0.9932	-0.9686
Y	0.7892	-0.7755	0.3811	-0.9947	-0.8372	0.9901	0.9312
Zr	0.7418	-0.7804	0.4644	-0.9980	-0.7758	0.9967	0.9524
Nb	1.0000	-0.2583	0.1230	-0.7795	-0.8523	0.7800	0.7454
Th	-0.2583	1.0000	-0.3211	0.7505	0.5405	-0.7333	-0.6334
U	0.1230	-0.3211	1.0000	-0.4276	0.1656	0.4364	0.3796
Pb	-0.7795	0.7505	-0.4276	1.0000	0.8070	-0.9992	-0.9597
Ba	-0.8523	0.5405	0.1656	0.8070	1.0000	-0.7991	-0.7720
Fe	0.7800	-0.7333	0.4364	-0.9992	-0.7991	1.0000	0.9690
Ti	0.7454	-0.6334	0.3796	-0.9597	-0.7720	0.9690	1.0000
Ca	-0.7716	0.7613	-0.4271	0.9999	0.8057	-0.9986	-0.9572
K	0.8067	-0.7019	0.4550	-0.9970	-0.7947	0.9981	0.9631
S	-0.4103	0.6766	-0.5492	0.5921	0.3495	-0.5675	-0.3517
P	0.7061	-0.7842	0.4802	-0.9931	-0.7497	0.9938	0.9631
Al	0.7493	-0.7573	0.3719	-0.9934	-0.8193	0.9944	0.9769
Mg	0.6409	-0.8814	0.3670	-0.9704	-0.7842	0.9645	0.9133
Na	0.6045	-0.5866	0.0681	-0.5702	-0.6535	0.5398	0.3350
Corg	-0.9603	0.0269	-0.1316	0.6064	0.6948	-0.6080	-0.5637

APPENDIX 14 (continued)

	Ca	K	S	P	Al	Mg	Na	Corg
Zn	-0.9957	0.9933	-0.6108	0.9794	0.9855	0.9620	0.6259	-0.6537
Cu	-0.9968	0.9968	-0.5761	0.9966	0.9913	0.9633	0.5208	-0.5867
Ni	-0.9999	0.9954	-0.5964	0.9951	0.9939	0.9750	0.5680	-0.5882
Rb	-0.9696	0.9571	-0.6774	0.9849	0.9556	0.9709	0.5388	-0.4342
Sr	0.9921	-0.9863	0.5572	-0.9997	-0.9924	-0.9747	-0.4863	0.5157
Y	-0.9954	0.9877	-0.6393	0.9811	0.9842	0.9746	0.6471	-0.6162
Zr	-0.9986	0.9929	-0.6152	0.9972	0.9907	0.9776	0.5652	-0.5643
Nb	-0.7716	0.8067	-0.4103	0.7061	0.7493	0.6409	0.6045	-0.9603
Th	0.7613	-0.7019	0.6766	-0.7842	-0.7573	-0.8814	-0.5866	0.0269
U	0.4271	0.4550	-0.5492	0.4802	0.3719	0.3670	0.0681	-0.1316
Pb	0.9999	-0.9970	0.5921	-0.9931	-0.9934	-0.9704	-0.5702	0.6064
Ba	0.8057	-0.7947	0.3495	-0.7497	-0.8193	-0.8742	-0.6535	0.6948
Fe	-0.9986	0.9981	-0.5675	0.9938	0.9944	0.9645	0.5398	-0.6080
Ti	-0.9572	0.9631	-0.3517	0.9631	0.9769	0.9133	0.3350	-0.5637
Ca	1.0000	-0.9957	0.5984	-0.9938	-0.9935	-0.9741	-0.5750	0.5961
K	-0.9957	1.0000	-0.5810	0.9874	0.9866	0.9492	0.5513	-0.6488
S	0.5984	-0.5810	1.0000	-0.5768	-0.5124	-0.6107	-0.8510	0.3694
P	-0.9938	0.9874	-0.5768	1.0000	0.9918	0.9776	0.5080	-0.5201
Al	-0.9935	0.9866	-0.5124	0.9918	1.0000	0.9754	0.5080	-0.5564
Mg	-0.9741	0.9492	-0.6107	0.9776	0.9754	1.0000	0.5863	-0.4268
Na	-0.5750	0.5513	-0.8510	0.5072	0.5080	0.5863	1.0000	-0.5519
Corg	-0.5961	-0.6488	0.3694	-0.5201	-0.5564	-0.4268	-0.5519	1.0000

APPENDIX 15 TABLE A 15.1 THE SIMILARITY MATRICES OF MAJOR AND TRACE ELEMENTS OF THE TERRIG RIVER SHALE

	Zn	Cu	Ni	Rb	Sr	Y	Zr
Zn	1.0000	0.0590	0.1278	0.1146	0.2508	0.3304	-0.0210
Cu	0.0590	1.0000	0.1275	0.1502	-0.1485	0.0250	0.1751
Ni	0.1278	0.1275	1.0000	-0.0549	-0.2379	-0.0242	0.3158
Rb	0.1146	0.1502	-0.0549	1.0000	-0.0493	0.6171	0.4850
Sr	0.2508	-0.1485	-0.2379	-0.0493	1.0000	0.3745	-0.5623
Y	0.3304	0.0250	-0.0242	0.6171	0.3745	1.0000	0.2706
Zr	-0.0210	0.1751	0.3158	0.4850	-0.5623	0.2706	1.0000
Nb	0.0263	0.1293	0.1246	0.6318	-0.3248	0.3550	0.7773
Th	0.1372	0.2399	0.5530	0.7499	-0.1350	0.5015	0.6972
U	0.2133	-0.2484	-0.2159	-0.3231	0.8543	0.3331	-0.6405
Pb	0.1583	0.0635	0.9225	0.2146	-0.0554	0.2657	0.4056
Ba	-0.0304	0.1034	-0.2220	0.8213	0.0949	0.5389	0.4734
Fe	0.0006	0.1424	-0.3368	0.5056	0.1480	0.6170	0.2169
Ti	0.0647	0.1238	0.1533	0.9171	-0.2951	0.5073	0.7489
Ca	0.0751	0.1562	-0.0658	0.7870	0.0447	0.4825	0.3836
K	0.0967	0.1572	0.0476	0.9885	-0.1369	0.5836	0.5653
S	-0.0278	-0.1654	-0.5260	-0.0385	0.1654	0.3516	-0.0956
P	0.1731	0.1661	-0.2378	0.2683	0.4780	0.6521	0.0420
Al	0.1167	0.1312	0.1172	0.9755	-0.1013	0.6042	0.5202
Mg	0.0713	0.1413	0.0938	0.9608	-0.1283	0.5860	0.5131
Na	-0.1286	0.3216	-0.1229	0.2181	0.4908	-0.0155	-0.2870
Corg	0.0184	0.2818	-0.3360	0.3083	0.2587	0.6601	0.0305

APPENDIX 15 (continued)

	Nb	Th	U	Pb	Ba	Fe	Ti
Zn	0.0263	0.1372	0.2133	0.1583	-0.0304	0.0006	0.0647
Cu	0.1293	0.2399	-0.2484	0.0635	0.1034	0.1424	0.1238
Ni	0.1246	0.5530	-0.2159	0.9225	-0.2220	-0.3368	0.1533
Rb	0.6318	0.7499	-0.3231	0.2146	0.8213	0.5056	0.9171
Sr	-0.3248	-0.1350	0.8543	-0.0554	0.0949	0.1480	-0.2951
Y	0.3550	0.5015	0.3331	0.2657	0.5389	0.6170	0.5073
Zr	0.7773	0.6972	-0.6405	0.4056	0.4734	0.2169	0.7489
Nb	1.0000	0.6962	-0.5328	0.3011	0.5682	0.1695	0.8102
Th	0.6962	1.0000	-0.3696	0.7612	0.5515	0.1615	0.8674
U	-0.5328	-0.3696	1.0000	-0.1032	-0.1934	0.0112	-0.5270
Pb	0.3011	0.7612	-0.1032	1.0000	0.0385	-0.2092	0.3874
Ba	0.5682	0.5515	-0.1934	0.0385	1.0000	0.6568	0.7048
Fe	0.1695	0.1615	0.0112	-0.2092	0.6568	1.0000	0.3194
Ti	0.8102	0.8674	-0.5270	0.3874	0.7048	0.3194	1.0000
Ca	0.6251	0.5622	-0.3307	0.0968	0.8235	0.6427	0.6791
K	0.6994	0.8048	-0.4100	0.2927	0.8028	0.4792	0.9490
S	-0.2209	-0.3383	0.4019	-0.4613	0.1326	0.3831	-0.1489
P	-0.0689	0.0776	0.4319	-0.0973	0.5465	0.8242	0.0530
Al	0.6912	0.8308	-0.3727	0.3704	0.7380	0.4251	0.9401
Mg	0.7256	0.8062	-0.3902	0.3416	0.7148	0.4036	0.9322
Na	-0.0535	0.1203	0.1027	-0.0230	0.3207	0.0580	0.0175
Corg	-0.0215	0.0136	0.2741	-0.3856	0.3836	0.8315	0.1073

APPENDIX 15 (continued)

	Ca	K	S	P	Al	Mg	Na	Corg
Zn	0.0751	0.0967	-0.0278	0.1731	0.1167	0.0713	-0.1286	0.0184
Cu	0.1562	0.1572	-0.1654	0.1661	0.1312	0.1413	0.3416	0.2818
Ni	-0.0658	0.0476	-0.5260	-0.2378	0.1172	0.0938	-0.1229	-0.3360
Rb	0.7870	0.9885	-0.0385	0.2683	0.9755	0.9608	0.2181	0.3083
Sr	0.0447	-0.1369	0.1654	0.4780	-0.1013	-0.1283	0.4908	0.2587
Y	0.4825	0.5836	0.3516	0.6521	0.6042	0.5860	-0.0155	0.6601
Zr	0.3836	0.5653	-0.0956	0.0420	0.5202	0.5131	-0.2870	0.0305
Nb	0.6251	0.6994	-0.2209	-0.0689	0.6912	0.7256	-0.0535	-0.0215
Th	0.5622	0.8048	-0.3383	0.0776	0.8308	0.8062	0.1203	0.0136
U	-0.3307	-0.4100	0.4019	0.4319	-0.3727	-0.3902	0.1027	0.2741
Pb	0.0968	0.2927	-0.4613	-0.0973	0.3704	0.3416	-0.0230	-0.2495
Ba	0.8235	0.8028	0.1326	0.5465	0.7380	0.7148	0.3207	0.3856
Fe	0.6427	0.4792	0.3831	0.8242	0.4251	0.4036	0.0580	0.8315
Ti	0.6791	0.9490	-0.1489	0.0530	0.9401	0.9322	0.0175	0.1073
Ca	1.0000	0.8112	-0.0915	0.3976	0.7800	0.7773	0.3507	0.4087
K	0.8112	1.0000	-0.1126	0.2228	0.9886	0.9782	0.1621	0.2725
S	-0.0915	-0.1126	1.0000	0.4750	-0.1773	-0.2075	-0.2926	0.5187
P	0.3976	0.2228	0.4750	1.0000	0.1656	0.1232	0.0971	0.8252
Al	0.7800	0.9886	-0.1773	0.1656	1.0000	0.9930	0.1732	0.2264
Mg	0.7773	0.9782	-0.2075	0.1232	0.9930	1.0000	0.1687	0.2252
Na	0.3507	0.1621	-0.2926	0.0971	0.1732	0.1687	1.0000	0.0138
Corg	0.4087	0.2725	0.5187	0.8252	0.2264	0.2252	0.0138	1.0000

APPENDIX 16 Table A16.1: THE SIMILARITY MATRICES OF THE MAJOR AND TRACE ELEMENTS OF THE BWLCHGWYN-MINERA SILICEOUS SHALES

	Zn	Cu	Ni	Rb	Sr	Y	Zr
Zn	1.0000	0.4446	0.3671	0.2589	0.0819	0.0866	0.0595
Cu	0.4446	1.0000	0.5935	-0.0291	0.2886	-0.2786	-0.0344
Ni	0.3671	0.5935	1.0000	-0.2054	0.3654	-0.4305	-0.3186
Rb	0.2589	-0.0291	-0.2054	1.0000	0.3159	0.2486	0.0691
Sr	0.0819	0.2886	0.3654	0.3159	1.0000	-0.6289	-0.5131
Y	0.0866	-0.2786	-0.4305	0.2486	-0.6289	1.0000	0.7818
Zr	0.0595	-0.0344	-0.3186	0.0691	-0.5131	0.7818	1.0000
Nb	-0.2272	-0.3565	-0.3645	-0.1144	-0.2072	0.5997	0.7546
Th	0.6145	0.0298	-0.2585	0.3150	-0.2077	0.3405	0.5471
U	0.4381	0.5175	-0.1448	0.1878	-0.0052	0.0102	0.4045
Pb	0.6643	0.0561	-0.1818	0.2058	-0.1231	0.1647	0.3782
Ba	-0.2173	0.0513	0.0756	0.2643	0.6422	-0.5406	-0.5795
Fe	0.1001	-0.3364	-0.3333	0.1585	-0.1157	0.0204	-0.4115
Ti	-0.1379	-0.2591	-0.8098	0.3548	-0.3974	0.7285	0.6358
Ca	0.3827	0.2661	0.8359	-0.0600	0.2925	-0.2698	-0.0909
K	-0.3576	-0.2584	-0.7123	0.6317	0.0494	0.2849	0.0978
S	0.1241	-0.0206	0.0719	-0.3366	-0.3837	0.2439	-0.0612
P	-0.3180	-0.0297	-0.1395	0.2053	0.0990	0.0041	0.0978
Al	-0.1681	-0.1283	-0.7054	0.6498	-0.1441	0.4717	0.2664
Mg	-0.0253	0.0545	0.2742	0.5834	0.3910	-0.0491	-0.0056
Na	-0.5882	0.0081	-0.0437	-0.2729	0.4080	-0.5032	-0.2128
Corg	-0.3250	-0.0555	-0.1216	-0.3911	-0.0918	0.2652	0.5136

APPENDIX 16 (continued)

	Nb	Th	U	Pb	Ba	Fe	Ti
Zn	-0.2272	0.6145	0.4381	0.6643	-0.2173	0.1001	-0.1379
Cu	-0.3565	0.0298	0.5175	0.0561	0.0513	-0.3364	-0.2591
Ni	-0.3645	-0.2585	-0.1448	-0.1818	0.0756	-0.3333	-0.8098
Rb	-0.1144	0.3150	0.1878	0.2058	0.2643	0.1585	0.3548
Sr	-0.2072	-0.2077	-0.0052	-0.1231	0.6422	-0.1157	-0.3974
Y	0.5997	0.3405	0.0102	0.1647	-0.5406	0.0204	0.7285
Zr	0.7546	0.5471	0.4045	0.3782	-0.5795	-0.4115	0.6358
Nb	1.0000	0.2192	-0.0046	0.1041	-0.2873	-0.2718	0.4684
Th	0.2192	1.0000	0.7556	0.9708	-0.4405	-0.0217	0.3761
U	-0.0046	0.7556	1.0000	0.7429	-0.2126	-0.1925	0.3070
Pb	0.1041	0.9708	0.7429	1.0000	-0.4277	0.0160	0.2402
Ba	-0.2873	-0.4405	-0.2126	-0.4277	1.0000	0.3436	-0.3768
Fe	-0.2718	-0.0217	-0.1925	0.0160	0.3436	1.0000	-0.0162
Ti	0.4684	0.3761	0.3070	0.2402	-0.3768	-0.0162	1.0000
Ca	-0.0823	0.0531	-0.0940	0.0894	0.0370	-0.2516	-0.7521
K	0.0858	-0.0381	0.0559	-0.1727	0.4138	0.2922	0.6528
S	0.0416	-0.1437	-0.2394	-0.1308	-0.0599	0.6419	-0.1588
P	0.1645	-0.1818	-0.0401	-0.3159	0.6807	0.1116	-0.0123
Al	0.0580	0.1706	0.2474	0.0248	0.1151	0.2498	0.8002
Mg	-0.0142	-0.0606	-0.0904	-0.1805	0.5674	-0.0114	-0.2588
Na	0.0875	-0.3791	-0.0434	-0.3539	0.4999	-0.2587	-0.1557
Corg	0.7338	-0.0619	-0.0169	-0.1366	-0.0896	-0.4443	0.2301

APPENDIX 16 (continued)

	.Ca	K	S	P	Al	Mg	Na	Corg
Zn	0.3827	-0.3576	0.1241	-0.3180	-0.1681	-0.0253	-0.5882	-0.3250
Cu	0.2661	-0.2584	-0.0206	-0.0297	-0.1283	0.0545	0.0081	-0.0555
Ni	0.8359	-0.7123	0.0719	-0.1395	-0.7054	0.2742	-0.0437	-0.1216
Rb	-0.0600	0.6317	-0.3366	0.2053	0.6498	0.5834	-0.2729	-0.3911
Sr	0.2925	0.0494	-0.3837	0.0990	-0.1441	0.3910	0.4080	-0.0918
Y	-0.2698	0.2849	0.2439	0.0041	0.4717	-0.0491	-0.5032	0.2652
Zr	-0.0909	0.0978	-0.0612	0.0978	0.2664	-0.0056	-0.2128	0.5136
Nb	-0.0823	0.0858	0.0416	0.1645	0.0580	-0.0142	0.0875	0.7338
Th	0.0531	-0.0381	-0.1437	-0.1818	0.1706	-0.0606	-0.3791	-0.0619
U	-0.0940	0.0559	-0.2394	-0.0401	0.2474	-0.0904	-0.0434	-0.0169
Pb	0.0894	-0.1727	-0.1308	-0.3159	0.0248	-0.1805	-0.3539	-0.1366
Ba	0.0370	0.4138	-0.0599	0.6807	0.1151	0.5674	0.4999	-0.0896
Fe	-0.2516	0.2922	0.6419	0.1116	0.2498	-0.0114	-0.2587	-0.4443
Ti	-0.7521	0.6528	-0.1588	-0.0123	0.8002	-0.2588	-0.1557	0.2301
Ca	1.0000	-0.6893	0.0670	-0.0250	-0.7139	0.5012	-0.1223	-0.0909
K	-0.6893	1.0000	-0.2171	0.5155	0.9213	0.2700	0.1691	-0.0044
S	0.0670	-0.2171	1.0000	-0.0225	-0.1473	-0.1463	-0.3398	-0.0558
P	-0.0250	0.5155	-0.0225	1.0000	0.3235	0.6576	0.4895	0.3652
Al	-0.7139	0.9213	-0.1473	0.3235	1.0000	0.1294	-0.0182	-0.0343
Mg	0.5012	0.2700	-0.1463	0.6576	0.1294	1.0000	0.1174	-0.0753
Na	-0.1223	0.1691	-0.3398	0.4895	-0.0182	0.1174	1.0000	0.5728
Corg	-0.0909	-0.0558	0.3652	-0.3652	-0.0343	-0.0753	1.0000	0.5728

Appendix I7.

List of the Cluster Analysis Programme produced by Davies, 1973. The Correlation Coefficient is used as a similarity measure.

```

0000      LIST (LP)
0001      PROGRAM (FXXX)
0002      INPUT 1 = CRT
0003      INPUT 3 = TRN
0004      INPUT 5 = CR1
0005      OUTPUT 2 = LPC/132
0006      OUTPUT 3 = LP1/132
0007      COMPRESS INTEGER AND LOGICAL
0008      COMPACT PROGRAM
0009      EXTENDED DATA
0010      TRACE 2
0011      END

0012      TRACE 1
0000      MASTER CLUS42
0001      DIMENSION X(50,50),IPAIR(2,50),XLEV(50),I(50,50)
0002      MD=50
0003      ND=50
0004      MM=50
0005      1 READ(3,1000) ITYPE,ISI*
0006      IF (ITYPE .LE. 0) GO TO 4
0007      IF (ITYPE .NE. 3) GO TO 2
0008      CALL READN(A,N,M,MM,MM)
0009      GO TO 4
0010      2. CALL READN(X,M,N,ND,ND)
0011      CALL PRINTN(X,M,N,ND,ND)
0012      * WRITE(2,2001)
0013      IF (ITYPE .NE. 2) GO TO 3
0014      MT=M
0015      IF (N .GT. M) MT=N
0016      DO 110 I=1,MT
0017      DO 110 J=I,MT
0018      XS=X(I,J)
0019      X(I,J)=X(J,I)
0020      X(J,I)=XS
0021      110 CONTINUE

0022      MT=M
0023      M=N
0024      N=MT
0025      3 IF (ISIM .EQ. 1) CALL RCOEF(X,N,M,ND,ND,A,MM)
0026      IF (ISIM .EQ. 2) CALL DIST(X,N,M,ND,ND,A,MM)
0027      4 CALL PRINTN(A,M,M,MM,MM)
0028      WRITE (2,2002)
0029      CALL WPGA(A,M,MM,IPAIR,XLEV,ISIM)
0030      CALL DENDRO(IPAIR,XLEV,M,M,ISI)
0031      GO TO 1
0032      1000 FORMAT (2IG)
0033      2001 FORMAT(1H0,4X,19HINPUT DATA MATRIX -,1X,
0034      140HCOLUMNS = VARIABLES, ROWS = OBSERVATIONS)
0035      2002 FORMAT (1H0,4X,17HSIMILARITY MATRIX)
0036      6 CONTINUE
0037      STOP
0038      END

```

continued

```

0039      C*****
0040      SUBROUTINE WPGA(X,M,M1,IPAIR,XLEV,ISIM)
0041      DIMENSION X(M1,M1),IPAIR(2,M1),XLEV(M1)
0042      DIMENSION I1(100),I2(100),XSIM(100)
0043      WRITE(2,2001)
0044      DO 110 I=1,M
0045      I1(I)=I
0046      110 CONTINUE
0047      XXXX=-9.0E+35
0048      IF (ISIM.NE.1) XXXX=+9.0E+35
0049      M3=M-1
0050      IC=0
0051      1 DO 100 I=1,M
0052      IF (I1(I).LE.0) GO TO 100
0053      IX=0
0054      XX=XXXX
0055      DO 101 J=1,M
0056      IF (I.EQ.J) GO TO 101
0057      IF (I1(J).LE.0) GO TO 101
0058      GO TO (11,12),ISIM
0059      11 IF (X(J,I)-XX) 101,101,12
0060      12 IF (X(J,I)-YX) 13,101,101
0061      13 XX=X(J,I)
0062      IX=J
0063      101 CONTINUE
0064      I2(I)=IX
0065      XSIM(I)=XX
0066      100 CONTINUE
0067      DO 102 I=1,M3
0068      IF (I1(I).LE.0) GO TO 102
0069      J=I2(I)
0070      IF (I1(J).LE.0) GO TO 102
0071      IF (J.LE.I) GO TO 102
0072      IF (I1(J).EQ.I) GO TO 14
0073      IF (ABS(XSIM(I)-XSIM(J)).GT.0.0001) GO TO 102
0074      14 IC=IC+1
0075      IPAIR(1,IC)=I
0076      IPAIR(2,IC)=J
0077      XLEV(IC)=XSIM(I)
0078      WRITE(2,2002) I,J,XSIM(I)
0079      I1(I)=J
0080      I1(J)=0
0081      DO 103 K=1,M
0082      X(K,I)=(X(K,I)+X(K,J))/2.0
0083      103 CONTINUE
0084      102 CONTINUE
0085      DO 105 I=1,M3
0086      IF (I1(I).LE.0) GO TO 105
0087      IF (I1(I).EQ.I) GO TO 105
0088      J=I1(I)
0089      DO 106 K=1,M
0090      IF (I1(K).LE.0) GO TO 106
0091      X(K,I)=(X(K,I)+X(K,J))/2.0
0092      106 CONTINUE
0093      I1(I)=I
0094      105 CONTINUE
0095      IF (IC.LT.M3) GO TO 1
0096      WRITE(2,2003)
0097      RETURN
0098      2001 FORMAT(1H1)
0099      2002 FORMAT(6X,2I5,F15.5)
0100      2003 FORMAT(1H0,4X,17HCOLUMNS 1 AND 2 - IX,
0101      135H OBSERVATIONS COMBINED INTO CLUSTERS /
0102      25X,41HCOLUMN 3 - SIMILARITY LEVEL OF CLUSTERING)
0103      END

```

END OF SEGMENT, LENGTH 336, NAME WPGA

```

0104      C*****
0105      SUBROUTINE DENDRO(IPAIR,XLEV,M,M1,ISIM)
0106      DIMENSION IPAIR(2,M1),XLEV(M1)
0107      DIMENSION IOUT(51),XX(13)
0108      DIMENSION I1(100),I2(100)
0109      DATA ISLNK,ICI,ICP,ICM/1H,1H1,1H.,1H-/
0110      M2=M-1
0111      DO 100 I=1,M
0112      I1(I)=0
0113      I2(I)=0

```



```

0114 100 CONTINUE
0115 DO 101 I=1,M2
0116 J=I-1
0117 11 IF (J .LE. 0) GO TO 12
0118 IF (IPAIR(1,I) .EQ. IPAIR(1,J)) GO TO 13
0119 J=J-1
0120 GO TO 11
0121 12 I2(I)=1
0122 GO TO 15
0123 13 K=I(J)
0124 IF (K .EQ. 0) GO TO 14
0125 J=K
0126 GO TO 13
0127 14 I1(J)=I
0128 DO 102 J=1,I
0129 K=J
0130 IF (IPAIR(2,I) .EQ. IPAIR(1,J)) GO TO 16
0131 102 CONTINUE
0132 GO TO 101
0133 16 I2(K)=0
0134 I1(I)=K
0135 101 CONTINUE
0136 DO 103 I=1,M2
0137 JS=I
0138 IF (I2(I) .NE. 0) GO TO 20
0139 103 CONTINUE
0140 GOTO 97
0141 20 NODE=IPAIR(1,JS)

0142 XMIN=XLEV(1)
0143 XMAX=XMIN
0144 DO 104 I=1,M2
0145 IF (XLEV(I) .LT. XMIN) XMIN=XLEV(I)
0146 IF (XLEV(I) .GT. XMAX) XMAX=XLEV(I)
0147 104 CONTINUE
0148 DX=(XMAX-XMIN)/25.0
0149 XMIN=XMIN-DX
0150 XMAX=XMAX+DX
0151 DX=(XMAX-XMIN)/60.0
0152 IF (ISIM .NE. 2) GO TO 21
0153 DX=-DX
0154 XMIN=XMAX
0155 21 DO 105 I=1,51
0156 ICUT(I)=ISLAK
0157 105 CONTINUE
0158 X=XMIN
0159 DO 106 I=1,13
0160 XX(I)=X
0161 X=X+DX*5.0
0162 106 CONTINUE
0163 WRITE (2,2000)
0164 WRITE (2,2001) (XX(I),I=1,12,2)
0165 WRITE (2,2002) (XX(I),I=1,13,2)
0166 WRITE (2,2003)
0167 22 X=XMIN
0168 IF (JS .NE. 0) X=XLEV(JS)
0169 IS=IFIX((X-XMIN)/DX)+1
0170 DO 110 I=IS,51
0171 ICUT(I)=ICM
0172 110 CONTINUE
0173 ICUT(IS)=IC0
0174 IF (JS .NE. 0) WRITE (2,2004) ICUT,NODE,X
0175 IF (JS .EQ. 0) WRITE (2,2004) ICUT,NODE
0176 IF (JS .EQ. 0) GOTO 31
0177 DO 111 I=IS,51
0178 ICUT(I)=ISLAK
0179 111 CONTINUE
0180 ICUT(IS)=ICI
0181 WRITE (2,2004) (ICUT(I),I=1,13)
0182 NODE=IPAIR(2,JS)
0183 JS=I1(JS)
0184 GO TO 22
0185 31 WRITE(2,2003)
0186 WRITE (2,2002) (XX(I),I=1,13,2)
0187 WRITE (2,2001) (XX(I),I=2,12,2)
0188 WRITE (2,2005)
0189 GOTO 96
0190 97 CONTINUE
0191 WRITE(2,9)
0192 9 FORMAT(10HFAILED AT )
0193 96 CONTINUE
0194 RETURN
0195 2000 FORMAT (1H1)
0196 2001 FORMAT (6X,OF10.4)
0197 2002 FORMAT (1X,7F10.4)
0198 2003 FORMAT(6X,14+,12(5H-----))
0199 2004 FORMAT (6X,61A1,1X,I3,F10.4)
0200 2005 FORMAT(1H0,4X,15HORDER OF CORRECTION = ,1X,
0201 15HVALUES ALONG X-AXIS ARE SIMILARITIES)
0202 END

```

continued

```

0203      C*****
0204      SUBROUTINE DIST(X,N,M,N1,M1,A,M2)
0205      DIMENSION X(N1,M1),A(M2,M2)
0206      AN=M
0207      DO 100 I=1,M
0208      DO 100 J=1,M
0209      DISTX=0.0
0210      9 FORMAT(10HFAILED AT )
0211      DO 101 K=1,N
0212      DISTX=DISTX+(X(K,I)-X(K,J))**2
0213      101 CONTINUE
0214      A(I,J)=SQRT(DISTX/AN)
0215      A(J,I)=A(I,J)
0216      100 CONTINUE
0217      RETURN
0218      END

```

END OF SEGMENT, LENGTH 113, NAME DIST

```

0219      C*****
0220      SUBROUTINE READM(A,N,M,N1,M1)
0221      DIMENSION A(N1,M1)
0222      READ (3,1000) A,M
0223      DO 100 I=1,N
0224      READ (3,1001) (A(I,J),J=1,M)
0225      100 CONTINUE
0226      RETURN
0227      1000 FORMAT (2I0)
0228      1001 FORMAT(37F0.0)
0229      END

```

END OF SEGMENT, LENGTH 68, NAME READM

```

0230      C*****
0231      SUBROUTINE PRINTM(A,N,M,N1,M1)
0232      DIMENSION A(N1,M1)
0233      DO 100 IS=1,M,10
0234      IE=IS+9
0235      IF(IE-M) 2,2,1
0236      1 IE=M
0237      2 WRITE (2,2003) (I,I=IS,IE)
0238      DO 101 J=1,N
0239      WRITE (2,2001) J,(A(J,K),K=IE,IE)
0240      101 CONTINUE
0241      100 CONTINUE
0242      RETURN
0243      2000 FORMAT (1H1,1X,10I12)
0244      2001 FORMAT (1H0,IE,10F12.4)
0245      END

```

END OF SEGMENT, LENGTH 91, NAME PRINTM

```

0246      C*****
0247      SUBROUTINE COSEP(X,N,M,N1,M1,A,M1)
0248      DIMENSION X(N1,M1),A(M1,M1)
0249      AN=M
0250      DO 100 I=1,M
0251      DO 100 J=1,M
0252      SX1=0.0
0253      SX2=0.0
0254      SX11=0.0
0255      SX22=0.0
0256      SX1X2=0.0
0257      DO 101 K=1,N
0258      SX1=SX1+X(K,I)
0259      SX2=SX2+X(K,J)
0260      SX1X1=SX1X1+X(K,I)**2
0261      SX2X2=SX2X2+X(K,J)**2
0262      SX1X2=SX1X2+X(K,I)*X(K,J)
0263      101 CONTINUE
0264      T1=(SX1X1-SX1**2/AN)
0265      T2=(SX2X2-SX2**2/AN)
0266      T3=(SX1X2-SX1*SX2/AN)
0267      R=1/SQRT(T2+T3)
0268      A(I,J)=R
0269      A(J,I)=R
0270      100 CONTINUE
0271      RETURN
0272      END

```


REFERENCES

- Abby, S., 1980. Studies in "Standard Samples" for use in the general analysis of silicate rocks and minerals. *Geostandards Newsletter*, 4, 163-190.
- Agrali, B. and Konyali, Y., 1969. Etude des microspores du Bassin Carbonifere de Asmara. *Bull. Min. Res. Expl. Turkey*. 73, 45-132.
- Al-Ameri, T.K., 1983. Acid-resistant microfossils used in the determination of Palaeozoic palaeoenvironments in Libya. *Palaeogeography, Palaeoclimatology, Palaeoecology*, 44, 103-116.
- Ammosov, I.I. and Tan, S.I., 1961. Stages of alteration of coals and the paragenetic relation of fossil fuels. Moscow: Izd. Akad. Nauk SSSR, 117 P.
- Artüz, S., 1957. Die Spora dispersae der Türkischen Steinkohle vom Zonguldak-Gebiet. *Istanb. Univ. Fen Fak. Mecm.*, B22, 4, 239-63.
- Artüz, S., 1959. Zonguldak bölgesindeki Alimolla, Suluve Büyük Kömür damarlarının sporolojik etudu. *Istanb. Univ. Fen Fak. Mon.*, 15, 1-73.
- Ashby, D.A. and Pearson, M.J., 1979. Mineral distribution in sediments associated with the Alton Marine Band nr. Penistone, South Yorkshire. International clay conference 1978. *Developments in Sedimentology*, 27 (eds. M.M. Mortland and V.C. Farmer), 311-321.
- Athkinson, B.K. and Rutter, E.H., 1975. Pressure solution or indentation? Comment and reply, *Geology*, 3, 477-478.
- Bailey, E.H., Irwin, W.P. and Jones, D.L., 1964. Franciscan and related rocks, and their significance in the geology of Western California. *California Div. Mines and Geology Bull.*, 183, 177 P.
- Baker, P.A. and Kastner, M., 1981. Constraints on the Formation of Sedimentary Dolomite. *Science*, 213, 214-216.
- Balme, B.E. and Butterworth, M.A., 1951-2. The stratigraphical significance of certain fossil spores in the central group of British coalfields. *Trans. Inst. Min. Engrs., Lond.*, 111, 870-85.
- Barrios, J., Plancon, A., Cruz, M.I. and Tchoubar, C., 1977. Qualitative and Quantitative study of stacking faults in a hydrazine treated Kaolinite-Relationship with the infrared spectra. *Clays and Clay Minerals*. 25, No.6, 422-429.

- Barss, M.S., 1967. Carboniferous and Permian spores of Canada. Can. Geol. Surv. pap., 67, 1-94.
- Basu, A., Young, S.W. and Suttner, L.D., 1975. Reevaluation of the use of undulatory extinction and polycrystallinity in detrital quartz for provenance interpretation. Jour. Sedim. Petrol., 45, 873-882.
- Batten, D.J., 1973a. Palaeontology, 16, 1-40.
- Beju, D., 1970. New contributions to the palynology of Carboniferous strata from Romania. Congr. Avan. Etudes stratigraph. Geol. Carbonifere, Compt. Rend., 6, Sheffield 1967, 2, 459-486.
- Bernard, P.J., 1978. Control of Cathodoluminescence of Dolomite by iron and manganese. Am. Assoc. Petrol. Geol. (abs.), 553-554.
- Berner, R.A., 1978. Sulphate reduction and the rate of deposition of marine sediments. Earth Planet. Sci. Lett., 37, 492-8.
- Berner, R.A., 1980. Early Diagenesis. A Theoretical Approach, Princeton Univ. Press, 241 P.
- Berner, R.A., 1981. Kinetics of weathering and diagenesis. In: Lasaga, A.C. and Kirkpatrick, R.J. (eds.) Kinetics of Geochemical Processes. Reviews in Mineralogy, 8, 111-34, Mineralogical Society of America.
- Berner, R.A., 1984. Sedimentary pyrite formation an up date. Geochimica et Cosmochimica Acta, 48, 605-15.
- Bharadwaj, D.C., 1957a. The palynological investigations of the Saar coals. Palaeontographica, Abt. B, 101, 73-125.
- Bharadwaj, D.C. and Venkatachala, B.S., 1962. Spore assemblage out of a lower Carboniferous shale from Spitsbergen. The palaeobotanist, 10, 18-47.
- Bhattacharyya, D.P., 1983. Origin of berthierine in ironstones. Clays and Clay Minerals, 31, 173-182.
- Bisat, W.S., 1924. The Carboniferous goniatites of the North of England and their zones. Proc. Yorks. Geol. Soc., 20, 40-124.
- Bisat, W.S., 1928. The Carboniferous goniatite zones of England and their continental equivalents. C.R. Cong. Strat. Carb. (Heerlen), 117-33.

- Bisat, W.S. and Hudson, R.G.S., 1945. The lower Reticuloceras (R1) goniatite succession in the Namurian of the North of England. *Proc. Yorks. Geol. Soc.*, 24, 383-440.
- Bjørlykke, K., 1974. Depositional history and geochemical composition of lower Paleozoic epicontinental sediments from the Oslo region. *Norges Geologiske undersøkelse*, 305, 1-81.
- Blanche, J.B. and Whitaker, J.H. McD., 1978. Diagenesis of part of the Brent sand Formation (Middle Jurassic) of the northern North Sea Basin. *J. Geol. Soc. London*, 135, 73-82.
- Blatt, H., 1967. Original characteristics of clastic quartz grains. *J. Sedim. Petrol.*, 37, 401-424.
- Blatt, H. and Christie, J.M., 1963. Undulatory extinction in quartz of igneous and metamorphic rocks and its significance in provenance studies of sedimentary rocks. *J. Sedim. Petrol.*, 33, 1326-1339.
- Blatt, H., Middleton, G. and Murray, R., 1980. *Origin of sedimentary rocks*. 2nd Ed., Prentice-Hall, New Jersey, 782 p.
- Bloxam, T.W., 1964. Uranium, thorium, potassium and carbon in some black shales from the South Wales coalfield. *Geochim. Cosmochim. Acta*, 28, 1177-85.
- Bloxam, T.W. and Thomas, R.L., 1969. Palaeontological and geochemical facies in the *Gastrioceras subcrenatum* marine band and associated rocks from the north crop of the South Wales coalfield. *Quart. Jl. Geol. Soc. Lond.*, 124, 239-281.
- Boles, J.R., 1981. Clay diagenesis and effects on sandstone cementation (case histories from the Gulf Coast Tertiary). In: *Clays and resource geologists* (F.S. Longstaffe, ed.). Toronto: Mineralogical Association of Canada. 199 p.
- Boles, J.R. and Franks, S.G., 1979. Clay diagenesis in the Wilcox Formation sandstones of south-west Texas: implications of smectite diagenesis on sandstone cementation. *Jour. Sed. Pet.*, 49, 55-70.
- Bostick, N.H., 1973. Time as a factor in thermal metamorphism of phytoclasts (coaly particles): *Cong. Internat. Strat. Geol. Carbonif.*, 7th, Krefeld, 1971, *Compte Rendu*, 2, 183-193.

- Brindley, G.W. and Brown, C. (eds.), 1980. Crystal structures of clay minerals and their x-ray identification. Mineralogical Society Monograph, 5, Mineralogical Society, London, 455P.
- Brindley, G.W. and Robinson, K., 1946a. Structure of Kaolinite. *Miner. Mag.*, 27, 242-253.
- Brooks, J., 1981. Organic maturation of sedimentary organic matter and petroleum exploration - A review. In *Organic Maturation Studies and Fossil Fuel Exploration*, (ed.) by J. Brooks. Academic Press, 441 P.
- Brown, G., (Ed.), 1961. The x-ray identification and crystal structures of clay minerals. *Miner. Soc. London*, 544 P.
- Bujak, J.P., Barss, M.S. and Williams, G.L., 1977. Offshore Eastern Canada's organic type and colour and hydrocarbon potential. *Oil Gas Jour.*, 4 April, 198-201; 11 April, 96-100.
- Burgess, J., 1974. *Geol. Soc. Am. Spl. paper*, 153, 19-30.
- Burst, J.F., 1969. Diagenesis of Gulf Coast clayey sediments and its possible relation to petroleum migration. *Am. Assoc. Petrol. Geologists Bull.*, 53, 73-93.
- Butterworth, M.A., 1956. The distribution of microspores in the coalfields lying to the West of the Pennines. Thesis, Univ. of Edinburgh.
- Butterworth, M.A., 1966. The distribution of Densospores. *The Palaeo-Botanist*, 15, No. 1-2, 16-28.
- Butterworth, M.A., 1984. Pollen and Spore Biostratigraphy of the Phanerozoic in North-West Europe-Upper Carboniferous. B.M.S. Palynology Group Meeting, 17-19 Dec., 1984, Univ. of Cambridge.
- Butterworth, M.A., 1982-1986. Personal Communication.
- Butterworth, M.A. and Millott, J. O'N., 1954-5. Microspore distribution in the seams of North Staffordshire, Cannock Chase and North Wales coalfields. *Trans. Inst. Min. Engrs. Lond.*, 114, 501-20.
- Butterworth, M.A. and Williams, R.W., 1958. The small spore floras of coals in the Limestone Group of the Lower Carboniferous of Scotland. *Trans. Roy. Soc. Edinb.*, 63, 353-92.
- Butterworth, M.A. and Millott, J.O'N., 1960. Microspore distribution in the coalfields of Britain. *Proc. Inst. Committee for coal petrol.* 3, 157-63.

- Butterworth, M.A. and Mahdi, S.A., 1982. Namurian and Basal Westphalian A miospore assemblages from the Featherstone area, Northern England. *Pollen et Spores*, Vol. XXIV, no.3-4, 481-510.
- Calvert, S.E., 1976. The mineralogy and chemistry of near shore sediment. In *Chemical Oceanography* (eds. J.P. Riley and R. Chester), 2nd Edn. 6, Academic Press.
- Calvert, S.E., 1983. Sedimentary Geochemistry of silicon, in Aston, S., ed., *Silicon Geochemistry and Bio-geochemistry*, New York, Academic Press.
- Carroll, D., 1970. Clay minerals: a guide to their x-ray identification. *Spec. pap. Geol. Soc. Am.*, 126, 80 P.
- Carpenter, A.B. and Oglesby, T.W., 1976. A model for the formation of luminescently zoned calcite cements and its implications. *Geol. Soc. America Abstracts with Programs*, 8, 469-470.
- Carver, R.E., 1967. *Procedures in Sedimentary Petrology*. Wiley. Interscience, New York.
- Castanó, J.R. and Sparks, D.M., 1974. Interpretation of vitrinite reflectance measurements in sedimentary rocks and determination of burial history using vitrinite reflectance and authigenic minerals. *Geol. Soc. Am. Spec. pap.*, 153, 31-51.
- Chaloner, W.G., 1958. The Carboniferous upland flora. *Geol. Mag.*, 95, 261-2.
- Chilingar, G.V., Bissell, H.J. and Wolf, K.H., 1979. Diagenesis of carbonate sediments and epigenesis (or catagenesis) of limestones, in Larsen, G., and Chilingar, G.V., eds., *Diagenesis in sediments and Sedimentary Rocks. Developments in Sedimentology 25A*, 247-422.
- Clayton, G., Coquel, R., Doubinger, J., Gueinn, K.J., Loboziak, S., Owens, B. and Streel, M., 1977. Carboniferous Miospores of Western Europe: illustration and zonation. *Meded. Rijks Geol. Dienst*, 29, 1-71.
- Clemmey, H., 1976. Aspects of stratigraphy, sedimentology and ore genesis in the Zambian copper belt with special reference to Rokana mines. Unpublished Ph.D. Thesis, Univ. of Leeds.
- Collinson, J.D. and Banks, N.L., 1975. The Haslingden Flags (Namurian G1) of South-East Lancashire: Bar Finger Sands in the Pennine Basin. *Proc. Yorks. Geol. Soc.*, 40, part 3, No.26, 431-458.

- Colter, V.S. and Ebber, J., 1978. The petrography and reservoir properties of some Triassic sandstones of the Northern Irish Sea Basin. *Jour. Geol. Soc. Lond.*, 135, 57-62.
- Combaz, A., 1964. *Revue Micropaléont.*, 7, 205-218.
- Combaz, A., 1973. 6 cong. de géochimie organique, Paris (Ed. Technip.).
- Combaz, A., 1975. *Coll. Int. Mat. Org. Sed.*, Paris, 90-101.
- Connolly, J.R., 1965. The occurrence of polycrystallinity and undulatory extinction in quartz in sandstone. *Jour. Sedim. Petrol.*, 35, 116-135.
- Conybeare, W.D. and Phillips, W., 1822. *Outlines of the geology of England and Wales.* London.
- Coquel, R., Doubinger, J. and Loboziak, S., 1976. Les microspores - guides du Westphalien à l'Autunien d'Europe occidentale. *Rev. Micropaléont.*, 18, 4, 200-212.
- Correia, M. and Peniguel, G., 1975. *Bull. Centre Rech. Pau SNPA*, 9 (1), 99-127.
- Creaney, S., 1980. Petrographic texture and vitrinite reflectance variation of the Alston Block, North-East England. *Proc. Yorks. Geol. Soc.*, 42, part 4, no. 32, 553-580.
- Creaney, S., 1982. Vitrinite reflectance determinations from the Beckermunds Scar and Raydale Boreholes, Yorkshire. *Proc. Yorks. Geol. Soc.*, 44, part 1 no.7, 99-102.
- Curtis, C.D., 1983. Link between Aluminium mobility and destruction of secondary porosity. *Am. Assoc. Petrol. Geol.*, 67, no.3, 380-384.
- Davies, J.C., 1973. *Statistics and data analysis in Geology.* Wiley, New York, 550 P.
- Davies, T.A. and Supko, P.R., 1973. Oceanic sediments and their diagenesis: some examples from deep sea drilling. *Jour. Sed. Pet.*, 43, 381-390.
- Dean, W.E., 1974. Determination of carbonate and organic matter in calcareous sediments and sedimentary rocks by loss on ignition: comparison with other methods. *Jour. Sed. Pet.*, 44, no.1, 242-248.
- DeBoer, R.B., 1977. On the thermodynamics of pressure solution - interaction between chemical and mechanical forces. *Geochim. Cosmochim. Acta*, 41, 249-256. -362-

- DeBoer, R.B., Nagtegaal, P.J.C. and Duyvis, E.M., 1977. Pressure solution experiments on quartz sand. *Geochim. Cosmochim. Acta*, 41, 257-264.
- DeCelles, P.G. and Gutschick, R.C., 1983. Mississippian Wood grained chert and its significance in the Western interior United States. *Jour. Sed. Pet.*, 53, no.4, 1175-1192.
- Degens, E.T., 1965. *Geochemistry of sediments*. Prentice Hall Inc., New Jersey, 342 P.
- Deelman, J.C., 1975. Pressure solution or indentation? *Geology*, 3, 23-24.
- Denison, C. and Fowler, R.M., 1980. Palynological identification of facies in a deltaic environment. *Proceedings of a conference on Sedimentation of the North Sea Reservoir Rocks Geilo*, XII, 1-22.
- Deer, W.A., Howie, R.A. and Zussman, J., 1963. *Rock forming minerals*. 4. Framework silicates, Longmans, Green and Co., London, 435 P.
- Dettmann, M.E., 1963. Upper Mesozoic microfloras from south-eastern Australia. *Proc. Roy. Soc. vict.*, 77, 1-148.
- Donaldson, A.C., Martin, R.H. and Kanes, W.H., 1970. Holocene Guadalupe delta of Texas Gulf Coast. In J.P. Morgan (ed.), *q.v.*, 107-137.
- Dow, W.G., 1977. Kerogen studies and Geological interpretations. *Jour. Geochem. Expl.*, 7, 79-99.
- Dunham, R.J., 1969. Early vadose silt in Townsend mound (reef), New Mexico, in *Depositional environments in carbonate rocks: SEPM Spec. publ.* 14, 139-181.
- Dunoyer de Segonzac, G., 1970. The transformation of clay minerals during diagenesis and low grade metamorphism. A review. *Sedimentology*, 15, 181-346.
- Dybova, S. and Jachowicz, A., 1957. Microspores of the Upper Silesian Coal Measures. *Prace Inst. geol.*, 23, 1-328.
- Dybova, S. and Jachowicz, A., 1970. Mikrosporen-phasen in Densteinkohlenflozen des oberschlesischen steinkohlenbeckens. *C.R. 6th cong. Intr. Strat. Geol. Carb.*, Sheffield, 1967, 2, 665-678.
- Dypvik, H., 1977. Mineralogical and geochemical studies of Lower Paleozoic rocks from the Trondheim and Oslo Regions, Norway. *Norsk Geologisk Tidsskrift*, 57, 205-241.

- Eberl, D.D. and Hower, J., 1975. Kaolinite synthesis: the role of the Si/Al and (alkali)/H⁺ ratio in hydrothermal systems. *Clays and Clay Minerals*, 23, 301-309.
- Elliott, T., 1974. Interdistributary bay sequences and their genesis. *Sedimentology*, 21, 611-622.
- Elliott, T., 1975. The sedimentary history of a delta lobe from a Yoredale (Carboniferous) sedimentary cycles produced by river dominated, elongate deltas. *Jour. Geol. Soc.*, 132, 199-208.
- Elliott, T., 1976a. Upper Carboniferous sedimentary cycles produced by river dominated, elongate deltas. *Jour. Geol. Soc.*, 132, 199-208.
- Erdman, J.G., 1975. Geochemical formation of oil; in Fischer, A.G. and Judson, S. (ed.) *Petroleum and Global Tectonics*, Princeton University Press; Princeton, New Jersey.
- Ernst, W.G. and Calvert, S.E., 1969. An experimental study of the recrystallization of porcelanite and its bearing on the origin of some bedded cherts. *Am. Jour. Sci.*, 267 A, 114-133.
- Ettensohn, F.R. and Peppers, R.A., 1979. Palynology and biostratigraphy of Pennington shales and coals (Chesterian) at selected sites in northeastern Kentucky. *Jour. Paleont.*, 53, 453-474.
- Farey, J., 1811. General view of the agriculture and minerals of Derbyshire. London.
- Felix, C.F. and Parks, P., 1959. An American occurrence of Spencerisporites. *Micropalaeontology*, 5, 359-366.
- Felix, C.J. and Burbridge, P.P., 1967. Palynology of the Springer Formation of Southern Oklahoma, U.S.A. *Palaeontology*, 10, 349-425.
- Fielding, C.R., 1984a. Upper delta plain lacustrine and fluviolacustrine facies from the Westphalian of the Durham coalfield, NE England. *Sedimentology*, 31, 547-567.
- Fielding, C.R., 1986. Fluvial channel and overbank deposits from the Westphalian of the Durham coalfield, NE England. *Sedimentology*, 33, 119-140.
- Fisher, M.J., 1980. Kerogen distribution and depositional environments in the Middle Jurassic of Yorkshire, U.K. *Int. Palynol. Conf.*, Lucknow (1976-77), 2, 574-580.

- Fisher, W.L., 1969. Facies characterization of Gulf Coast delta systems with some Holocene analogues. *Trans. Gulf-Cst. Ass. Geol. Socs.*, 239-261.
- Fisk, H.N., 1952. Geological investigations of the Atchatalaya basin and the problem of Mississippi River diversion. U.S. Army Corps. Engineers. Mississippi River Committee, Vicksburg, 145 P.
- Fisk, H.N., 1961. Bar-finger sands of Mississippi Delta. In J.A. Peterson and J.C. Osmond (Editors). *Geometry of Sandstone Bodies*. Am. Assoc. Petrol. Geol., Tulsa, 29-52.
- Florin, R., 1936. On the structure of the pollen grains in the Cordaitales. *Svensk bot. Tidskr.*, 30, 624-651.
- Folk, R.L., 1951. Stages of textural maturity in sedimentary rocks. *Jour. Sedim. Petrol.*, 21, 127-130.
- Folk, R.L., 1959. Practical petrographic classification of limestones. *Am. Assoc. Petrol. Geol.*, 43, 1-38.
- Folk, R.L., 1968. *Petrology of sedimentary rocks*. Hamphills, Austin, Texas, 170 P.
- Folk, R.L., 1974. *Petrology of sedimentary rocks*. Austin, Texas, Hamphills, 182 P.
- Folk, R.L. and Weaver, C.E., 1952. A study of the texture and composition of chert. *Am. Jour. Sci.*, 250, 498-510.
- Folk, R.L. and Pittman, J.S., 1971. Length slow chalcedony: a new testament for vanished evaporites. *Jour. Sedim. Petrol.* 41, 1045-58.
- Fournier, R.O., 1973. Silica in thermal waters: laboratory and field investigations. *Proc. Symp. Hyrogeoch. Biogeochem.*, Tokyo, 1, 122-139.
- Frank, J.R., Carpenter, A.B. and Oglesby, T.W., 1982. Cathodoluminescence and composition of calcite cement in the Taum Sank Limestone (Upper Cambrian), south east Missouri. *Jour. Sed. Petrol.*, 52, 631-638.
- Friedman, I., and Murata, K.J., 1979. Origin of dolomite in Miocene Monterey shale and related formations of the Tremblor Range, California. *Geochim. Cosmochim Acta*, 43, 1357-65.
- Fuchtbauer, H., 1967. Influence of different types of diagenesis on sandstone porosity. 7th World Petroleum Congr., Proc., 2, 353-369.

- Fuchtbauer, H., 1974. Sediments and Sedimentary rocks 1.2nd Ed., Schweizerbart, Stuttgart, 464 P.
- Garrels, R.M. and Christ, C.L., 1965. Solutions, Minerals and Equilibria. Harper and Row, New York, 450 P.
- Geiskes, J.M., Nevsky, B. and Chain, A., 1981. Interstitial water studies, Leg 63, in Yeats, R.S., *et al.*, eds., Init. Repts. DSDP, 63, 623-629. U.S. Govt. Printing off.
- George, T.N., Johnson, G.A., Mitchell, M., Prentice, J.E., Ramsbottom, W.H.C., Sevastopulo, G.D. and Wilson, R.B., 1976. A correlation of Dinantian rocks in the British Isles. Spec. Report No. 7. Geol. Soc. London, 87 p.
- Gibbs, R.J., 1977. Clay mineral segregation in the marine environment. Jour. Sed. Petrol., 47, 237-243.
- Glennie, K.W., Mudd, G.C. and Nagtegaal, P.J.C., 1978. Depositional environment and diagenesis of Permian Rotliegendes sandstones in Leman Bank and Sole Pit areas of the U.K. Southern North Sea. Jour. Geol. Soc. London, 135, 25-34.
- Goldhaber, M.B. and Kaplan, I.R., 1975. Controls and consequences of sulfate reduction rates in marine sediments. Soil Science, 119, 42-55.
- Goldschmidt, V.M., 1954. Geochemistry. Clarendon Press.
- Gould, H.R., 1970. The Mississippi Delta complex. In J.P. Morgan (ed.), q.v., 3-30.
- Goldstein, A. Jr. and Hendricks, J.A., 1953. Siliceous sediments of ouachita facies in Oklahoma. Geol. Soc. America Bull., 64, 421-442.
- Grebe, H., 1971. Die Verbreitung der Mikrosporen im Ruhrkarbon von den Bochumer Schichten bis zu den Dorstener Schichten (Westfal A-C). Palaeontographica, Abt B, 140, (1-3), 27-115.
- Green, A.H., Russell, R., Dakyns, J.R., Ward, J.C., Fox-strangways, C., Dalton, W.H. and Holmes, T.V., 1878. The geology of the Yorkshire coalfield. Mem. Geol. Surv. U.K.
- Grim, R.E., 1953. Clay Mineralogy. McGraw Hill, New York, 384 P.
- Grover, G., Jr and Read, J.F., 1983. Paleoaquifer and Deep Burial related cements defined by regional cathodoluminescent patterns, Middle Ordovician carbonates, Virginia. Am. Assoc. Petrol. Geol., 67, no.8, 1275-1303.

- Guennel, G.K., 1952. Fossil spores of the Alleghenian coals in Indiana. Rep. Progr. Indiana Dep. conserv. geol. surv., 4, 1-40.
- Guennel, G.K., 1958. Miospore analysis of the Pottsville coals of Indiana. Bull. Indiana Dep. conserv. geol. Surv., 13, 1-101.
- Güven, N., 1972. Electron optical observations on marblehead illite. Clays and Clay Minerals. 20, no.2, 83-88.
- Güven, N., Hower, W.E. and Davies, D.K., 1980. Nature of authigenic illites in sandstone reservoirs. Jour. Sed. Pet., 50, 761-766.
- Habib, D., 1966. Distribution of spore and pollen assemblages in the Lower Kittanning coal of Western Pennsylvania. Palaeontology, 9, 629-666.
- Hacquebard, P.A., 1957. Blant spores in coal from the Horton Group (Mississippian) of Nova Scotia. Micropaleontology, 3, 301-324.
- Hacquebard, P.A. and Donaldson, 1969. Paleogeography and facies aspect of the Minto Coal Seam, New Brunswick, Canada. C.R. 6th Congr. Int. Strat. Geol. Carb. Sheffield, 1967, 3, 861-872.
- Hallberg, R.O., 1976. A geochemical method for investigation of paleoredox conditions in sediments. Ambio Spec. report, 4, 139-147.
- Hancock, N.J. and Taylor, A.M., 1978. Clay mineral diagenesis and oil migration in the Middle Jurassic Brent sand formation. Jour. Geol. Soc. London, 135, 69-72.
- Hathaway, J.C., 1972. X-ray mineralogy studies- Leg 11, pt.2, in Hollister, C.D., Ewing, J.I., and others, 1972. Initial Reports Deep Sea Drilling Project, 11, Washington, U.S. Govt. Printing Office, 772-789.
- Hay, R.L., 1968. Chert and its sodium-silicate precursors in sodium-carbonate lakes of East Africa. Contr. Mineralogy Petrology, 17, 255-274.
- Hawkins, P.J., 1978. Relationship between diagenesis, porosity reduction and oil emplacement in Late Carboniferous sandstone reservoirs, Bothamsall oilfield, E. Midlands. Jour. Geol. Soc. London, 135, 7-24.
- Heald, M.T., 1956. Cementation of Simpson and St. Peter sandstones in parts of Oklahoma, Arkansas, and Missouri. Jour. Geol., 64, 16-30.

- Heath, G.R., 1974. Dissolved silica and deep sea sediments. SEPM, Spec. Pub. 20, 77-93.
- Heath, G.R. and Moberly, Jr., R., 1971. Cherts from the western Pacific, Leg 7, DSDP, in Winterer, E.L., *et al.* eds., Init. Repts. DSDP, 7, 991-1007, U.S. Govt. Printing Office.
- Hein, J.R., Scholl, D.W., Barron, J.A., Jones, M.G. and Miller, J., 1978. Diagenesis of late Cenozoic diatomaceous deposits and formation of the bottom simulating reflector in the Southern Bering Sea. *Sedimentology*, 25, 144-181.
- Hibbert, F.A., and Lacey, W.S., 1969. Miospores from the Lower Carboniferous Basement Beds in the Menai Straits region of Caernarvonshire, North Wales. *Palaeontology*, 12, 420-440.
- Higgins, A.C., 1975. Conodont zonation of the late Viséan-early Westphalian strata of the south and central Pennines of Northern England. *Bull. Geol. Surv. Gt. Br.*, 53, 1-90.
- Higgs, R., 1979. Quartz grain surface features of Mesozoic-Cenozoic sands from the Labrador and Western Greenland continental margins. *Jour. Sed. Pet.*, 49, no.2, 599-610.
- Hood, A., Gutjahr, C.C.M. and Heacock, R.L., 1975. Organic metamorphism and the generation of petroleum. *Am. Assoc. Petrol. Geol. Bull.*, 59, no.6, 986-996.
- Hodson, F., 1957. Marker horizons in the Namurian of Britain, Ireland, Belgium and Western Germany. *Pub. Assoc. Etud. Paleont. Strat. Houill.*, 24, 1-26.
- Hoffmeister, W.S., Staplin, F.L. and Malloy, R.E., 1955b. Mississippian plant spores from the Hardinsburg Formation of Illinois and Kentucky. *Jour. Paleont.*, 29, 272-339.
- Horst, U., 1955. Die sporal dispersae des Namurs von Westoberschlesien und Mährisch-ostrau. *Palaeontographica*, B98, 137-236.
- Houseknecht, D.W., 1984. Influence of grain size and temperature on intergranular pressure solution, quartz cementation, and porosity in a quartzose sandstone. *Jour. Sed. Pet.*, 54, 348-361.
- Hower, J., 1981A. X-ray diffraction identification of mixed layer clay minerals. In: *Clays and the resource geologist* (F.J. Longstaffe, ed.). Toronto: Mineralogical Association of Canada, 199 P.

- Hower, J., 1981B. Shale diagenesis. In: Clays and the resource geologist (F.J. Longstaffe, ed.). Toronto: Mineralogical Association of Canada, 199 P.
- Hower, J., Eslinger, E.V., Hower, M. and Perry, E.D., 1976. Mechanisms of burial metamorphism of argillite sediments. *Geol. Soc. Am. Bull.*, 87, 725-737.
- Huang, W.H. and Keller, W.D., 1970. Dissolution of rock forming silicate minerals in organic acids: Simulated first stage weathering of fresh mineral surfaces. *Am. Mineralogist*, 55, 2076-2094.
- Hudson, R.G.S. and Cotton, G., 1943. The Namurian of Alport Dale, Derbyshire. *Proc. Yorks. Geol. Soc.*, 25, 141-173.
- Huggett, J.M., 1982. The growth and origin of authigenic clay minerals in sandstones. Ph.D. Thesis. Univ. of London (unpublished).
- Hughes, N.F. and Playford, G., 1961. Palynological reconnaissance of the lower Carboniferous of Spitsbergen. *Micropaleontology*, 7, 27-44.
- Hughes, N.F. and Moody-Stuart, J.C., 1967. *Rev. Palaeobot. Palynol.*, 1, 259-268.
- Hurst, A.R. and Irwin, H., 1982. Geological modelling of clay diagenesis in sandstones. *Clays and Clay Minerals*, 17, 5-22.
- Hutcheon, I., 1981. Application of thermodynamics to clay minerals and authigenic mineral equilibria. In: Longstaffe, F.K. (ed.) *Clays and the resource geologists*, Min. Ass. Can., Short Course Hdbk, 7, 169-192.
- Hutton, A.C. and Cook, A.C., 1980. Influence of alginite on the reflectance of vitrinite from Joadja, N.S.W., and some other coals and shales containing alginite. *Fuel*, 59, 711-714.
- Hutton, A.C., Kantsler, A.J., Cook, A.C. and Mckirdy, D.M., 1980. Organic matter in oil shales. *Australian Pet. Explor. Assoc. Jour.*, 20, 44-67.
- Ibrahim, A.C., 1932. Beschreibung von Sporentormer aus Floz Agir. In *Potonie sporenform aus den Flozen Agir und Bismarck des Ruhrgebietes*. *Neues Jb. Miner. Geol. Palaeont. BeilBd.*, 67, 447-449.
- Ibrahim, A.C., 1933. Sporenformen des Agirhorizonts des Ruhr-Reviers. *Konrad Triltsch, Wurzburg*, 1-47.
- Imam, M.B., 1983. Diagenesis in the Neogene clastic sediments of the Bengal Basin, Bangladesh. Unpubl. Ph.D. Thesis. Univ. of London, 221P.

- Irwin, H., 1980. Early diagenetic carbonate precipitation and pore fluid migration in the Kimmeridge clay of Dorset, England. *Sedimentology*, 27, 577-591.
- Irwin, H., Curtis, C.D. and Coleman, M., 1977. Isotopic evidence for source of diagenetic carbonates formed during burial of organic rich sediments. *Nature* 269, 209-213.
- Isaacs, C.M., 1980. Diagenesis in the Monterey Formation examined laterally along the coast near Santa Barbara, California, U.S. Geol. Surv. Open file Rept. No.80-606, 329 P.
- Isaacs, C.M., 1982. Influence of rock composition on kinetics of silica phase changes in the Monterey Formation, Santa Barbara area, California. *Geology*, 10, 304-308.
- Ishchenko, A.M., 1952. Atlas of the microspores and pollen of the Middle Carboniferous of the Western part of the Donets Basin. *Izd. Akad. Nauk Ukr. S.S.R.*, 1-83. (In Russian).
- Ishchenko, A.M., 1956. Spores and pollen of the Lower Carboniferous deposits of the Western extension of the Donets Basin and their stratigraphical importance. *Akad. Nauk Ukr. S.S.R. Trudy Inst. Geol. Nauk, Ser. Strat. Palaeont.*, 11, 1-185 (in Russian).
- Ishchenko, A.M., 1958. Spore-pollen analysis of the Lower Carboniferous sediments of the Dnieper-Donets Basin. *Ibid.* 17, 1-188 (in Russian).
- Jachowicz, A., 1971. A microfloristic description and stratigraphy of the productive Carboniferous of the Upper Silesian Coal Basin. *Inst. Geol. Prace. (Warsaw)*, 61, 185-277.
- Jachowicz, A., 1974. Die stratigraphische Gliederung der Namurablagerungen im oberschieischen Steinkohlenbecken auf Grund von Miosporenuntersuchungen. *Congr. Avan. Etudes Stratigraph. Geol. Carbinifere, Compt. Rend.*, 7, Krefeld 1971, 3, 227-241.
- Jackson, J.W., 1925. Sabden Shale fossils near Holywell, Flintshire. *Naturalist*, No.821, 183.
- Jefford, R.M. and Jones, D.H., 1959. Preparation of slides for spores and other microfossils. *Jour. Palaeont.*, 33, 355-357.
- Jessop, P., 1931. Agate and the cherts of Derbyshire. *Proc. Geol. Ass.*, 42, 29-43.

- Johnson, E.W., 1981. A tunnel section through a prograding Namurian (Arnsbergian, E2a) delta, in the Western Bowland Fells, North Lancashire. *Geol. Jour.*, 16, 93-110.
- Jones, J.B. and Segnit, E.R., 1971. The nature of opal. I. Nomenclature and constituent phases. *Jour. Geol. Soc. Australia*, 18, 57-68.
- Jones, R.C.B. and Lloyd, W., 1942. The stratigraphy of the Millstone Grit of Flintshire. *Jour. Manchr. Geol. Ass.*, 1, 247-262.
- Jongmans, W.J. and Gothan, W., 1937. Betrachtungen uber die Ergebnisse des zweiten kongresses fur karbonstratigraphie. *C.R. 2me Cong. Strat. Carb.* (Heerlen, 1935), 1, 1-40.
- Kanes, W.H., 1970. Facies and development of the Colorado River delta in Texas. In J.P. Morgan (ed.), *q.v.*, 78-106.
- Karweil, J., 1955. Die metamorphose der Kohlen vom standpunkt der physikalischen chemie: *Deutsch. Geol. Gesell. Zeitschr.*, 107, 132-139 (in German).
- Kastner, M. and Geiskes, J.M., 1976. Interstitial water profiles and sites of diagenetic reactions, Leg 35, DSDP, Bellingshausen abyssal plain, Earth Planet. *Sci. Lett.*, 33, 11-20.
- Kastner, M., Keene, J.B. and Geiskes, J.M., 1977. Diagenesis of siliceous oozes: I. Chemical controls on the rate of opal-A to opal-CT transformation - an experimental study. *Geochim. Cosmochim. Acta*, 41, 1041-1059.
- Katz, A., 1971. Zoned dolomite crystals. *Jour. Geology*, 79, 38-51.
- Keller, W.D., 1969. Chemistry in Introductory Geology. *Bros. Pub.*, Columbia, Missouri, 108 p.
- Keller, W.D., Reichelt, M. and Neuzil, J., 1981. Morphology of kaolinite weathered from a non-feldspathic micaphyllite. *Clay and Clay Minerals*, 16, 289-295.
- Kelts, K. and Mackenzie, J., 1982. Diagenetic dolomite formation in Quarternary anoxic diatomaceous muds of Deep Sea Drilling Project. Leg 64, Gulf of California, in Blakeslee, J. *et al.* eds. *Init. Repts. DSDP*, 64, 553-569.
- Keene, J.B., 1975. Cherts and porcellanites from the North Pacific, in Larsen, R.L., *et al.* eds., *Init. Repts. DSDP*, v.32, 429-507, U.S. Govt. Printing Office.

- Keene, J.B., 1976. Distribution, mineralogy and petrography of biogenic and authigenic silica in the Pacific Basin. Unpub. Ph.D. Thesis, University of California at San Diego.
- Keene, J.B. and Kastner, M., 1974. Clays and formation of deep sea chert. *Nature*, 249, 754-755.
- King, W.B.R., 1914. Summ. Prog. Geol. Surv. Gt. Br. for 1913, 12-14.
- Klug, H.P. and Alexander, L.E., 1954. X-ray Diffraction procedures. New York (John Wiley), 716 P.
- Knox, E.M., 1941-2. The microspores in some coals of the productive coal measures in Fife. *Trans. Inst. Min. Engrs.*, London, 101, 98-112.
- Knox, E.M., 1945-6. Microspores in the Productive Coal Measures of the Central Coalfield of Scotland. *Trans. Inst. Min. Engrs.*, London, 105, 137-142 and 268-270.
- Knox, E.M., 1947-8. The microspores in coals of the Limestone Coal Group in Scotland. *Trans. Inst. Min. Engrs.*, London, 107, 155-163.
- Kosanke, R.M., 1950. Pennsylvanian spores of Illinois and their use in correlation. *Bull. Ill. Geol. Surv.*, 74, 1-128.
- Krauskopf, K.B., 1979. Introduction to geochemistry: New York, McGraw-Hill, 617 P.
- Kübler, B., 1968. Evaluation quantitative du métamorphisme par la cristallinité de l'illite. *Bull. Centre Rech. Pau*, 2, 385-397.
- Kunze, G.W., 1955. Ethylene glycol solvation technique used in x-ray diffraction. *Clays clay Miner.* In: W.O. Milligan (Ed.) Publication 395, Nat. Acad. Sci. - Nat. Res. Count. Washington, 88-93.
- Kurbatov, J.M., 1963. On the question of the genesis of peats and humic acids (in Russian). *Intern. Peat Cong.*, Leningrad.
- Lahann, R.W., 1980. Smectite diagenesis and sandstone cement: the effect of reaction temperature. *Jour. Sed. Pet.*, 50, 755-760.
- Lambert-Aikhionbare, D.O., 1981. Sandstone diagenesis and its relation to petroleum generation and migration in Niger Delta. Unpublished Ph.D. thesis, London University, 298 p.

- Lancelot, Y., 1973. Chert and silica diagenesis in sediments from the Central Pacific, in Winterer, E.L., *et al.* eds. Init. Repts. DSDP, 17, 377-405, U.S. Govt. Printing Office.
- Land, L.S., 1979. Chert-Chalk diagenesis: the Miocene Island Slope of North Jamaica. *Jour. Sed. Pet.*, 49, 223-232.
- Land, L.S. and Dutton, S.P., 1978. Cementation of a Pennsylvanian deltaic sandstone: Isotope data. *Jour. Sed. petrol.*, 48, 1167-1176.
- Lerman, A., 1978. Chemical exchange across sediment-water interface. *Annual Rev. Earth Planet Sci.*, 6, 281-303.
- Liesegang, R.E., 1898. *Chemische Reaktionen in Gallerton*, Düsseldorf.
- Llajima, A., Matsumoto, R. and Tada, R., 1985. Mechanism of sedimentation of rhythmically bedded chert. *Sed. Geol.*, 41, 221-233.
- Lloyd, W. and Jones, R.C.B., 1930. The Upper Carboniferous of Flintshire (abstract). *Geol. Mag.*, 67, 45 p.
- Loboziak, S., 1971. Les micro-et mégaspores de la partie occidentale du bassin houiller du Nord de la France. *Palaeontographica*, Abt. B, 132, 1-127.
- Loboziak, S., 1974. Considérations palynologiques sur le Westphalien d'Europe occidentale. *Rev. Palaeobot. Palyn.*, 18, 271-289.
- Loboziak, S., Coquel, R. and Jachowicz, A., 1976. Stratigraphie du Westphalien d'Europe occidentale et de Pologne a la lumière des études palynologiques (microspores). *Ann. Soc. Géol. Nord*, 96, 2, 157-172.
- Lopatin, N.V., 1971. Temperature and geologic time as factors in coalification. *Akad. Nauk SSSR Izv. Ser. Geol.*, no.3, 95-106 (in Russian).
- Loose, F., 1934. Sporenformen aus dem Flöz Bismarck des Ruhrgebietes. *Arb. Inst. Palaobot. Berl.*, 4, 127-164.
- Loucks, R.G., Bebout, D.G., and Galloway, W.E., 1977. Relationship of porosity formation and preservation to sandstone consolidation history, Gulf Coast Lower Tertiary Frio Formation. *Trans. Gulf Coast Assoc. Geol. Soc.*, 27, 109-120.
- Love, L.G., 1960. Assemblages of small spores from the Lower oil-shale Group of Scotland. *Proc. Roy. Soc. Edinb.*, 67, 99-126.

- Luber, A.A., 1935. Les types petrographiques de charbons fossiles du Spiksbergen. *Chimie combustible solide*, 6, 186-195 (in Russian).
- Luber, A.A. and Waltz, I.E., 1941. Atlas of microspores and pollen grains of the Palaeozoic of the U.S.S.R. *Trans. All-Un. Sci. Res. Inst. Geol. (VSEGEI)*, 139, 1-107 (in Russian).
- Mackenzie, F.T. and Gees, R., 1971. Quartz: synthesis at earth surface conditions. *Science*, 73, 533-535.
- Mackowsky, M.T.H., 1975. Coke microscopy. P. 298-302 in STACH, E. (Ed.) *stach's textbook of coal petrology*. Gerbruder Borntraeger, Berlin-Stuttgart, 428 p.
- Manheim, F.T., Chan, K.M. and Sayles, F.L., 1970. Interstitial water studies on small core samples, DSDP, Leg 5, in McManus, D.A., *et al*/eds. *Init. Repts. DSDP.*, 5, 501-511. U.S. Govt Printing Office.
- Mansfield, C.F. and Bailey, S.W., 1972. Twin and pseudo-twin intergrowths in kaolinite. *Am. Min.*, 57, 411-425.
- Marshall, A.E. and Smith, A.H.V., 1965. Assemblages of miospores from some Upper Carboniferous coals and their associated sediments in the Yorkshire coalfield. *Palaeontology*, 7, 656-673.
- Marshall, A.E. and Williams, J.E., 1970. Palynology of the Yoredale "Series" in the Roman Wall district of Western Northumberland, Northern England. *Congr. Avan. Etudes Stratigraph Geol. Carbonifere compte. Rend.* 6, Sheffield 1967, 3, 1147-1148.
- Marzolf, J.E., 1976. Sand grain frosting and quartz overgrowth examined by scanning electron microscopy-the Navajo Sandstone, (Jurassic?), Utah. *Jour Sed. Pet.*, 46, 906-912.
- Matsumoto, R. and Lljima, A., 1984. Chemical Sedimentology of some Permo-Jurassic and Tertiary bedded cherts in Central Honshu, Japan. *Sed. Geol.*, 175-192.
- Maynard, J.B., 1983. *Geochemistry of Sedimentary Ore Deposits*. Berlin, xi + 305 p.
- McBride, E.F. and Folk, R.L., 1979. Features and origin of Italian Jurassic radiolarites deposited on continental crust. *Jour. Sedim. Petrol.*, 49, 837-868.

- McBride, E.F. and Thomson, A., 1970. The Caballos Novaculite, Marathon Region, Texas. *Geol. Soc. Am. Spec. Pap.*, 122, 129 P.
- McHardy, W.J., Wilson, M.J. and Tait, J.M., 1982. Electron microscope and x-ray diffraction studies of filamentous illite clay from sandstones of the Magnus Field. *Clay Miner.* 17f, 23-29.
- Meyers, W.J., 1974. Carbonate cement stratigraphy of the Lake Valley Formation (Mississippian) Sacramento Mountains, New Mexico. *Jour. Sed. Pet.*, 44, 837-861.
- Meyers, W.J., 1977. Chertification in the Mississippian Lake Valley Formation, Sacramento Mountains, New Mexico. *Sedimentology*, 24, 75-105.
- Miller, J., 1978. Diagenesis of late Cenozoic diatomaceous deposits and formation of the bottom simulating reflector in the Southern Bering Sea. *Sedimentology*, 25, 144-181.
- Millot, G., 1970. *Geology of Clays*. Springer-Verlag, Heidelberg.
- Millott, J. O'N., 1945-6. The microspores in the coal seams of North Staffordshire. pt. II. The seams of the Cheadle coalfield. *Ibid.* 105, 91-102.
- Mizutani, S., 1970. Silica minerals in the early stage of diagenesis. *Sedimentology*, 15, 419-436.
- Mohr, P.A., 1959. A geochemical study of the Lower Cambrian Manganese Shale Group of the Harlech Dome, North Wales. *Geochim. Cosmochim. Acta*, 17, 186-200.
- Moore, B.R. and Dennen, W.H., 1970. A geochemical trend in silicon-aluminium-iron ratios and the classification of clastic sediments. *Jour. Sed. Pet.*, 40, 1147-1152.
- Moore, C.H., Graham, E.A. and Land, L.S., 1976. Sediment transport and dispersal across the deep fore-reef and Island slope (-55m to -305 m), Discovery Bay, Jamaica. *Jour. Sed. Pet.*, 46, 174-187.
- Moore, L. R., Neves, R., Wagner, R.H. and Wagner Gentis, C.H.T., 1971. The stratigraphy of Namurian and Westphalian rocks in the Villamanin area of Northern Leon, N.W. Spain. *Trabajos de geologica*, 3, Fas. Ci. Univ. Oviedo, 307-363.

- Moore, P.D. and Webb, J.A., 1978. An illustration guide to pollen analysis. Hodder and Stoughton, London, 133 p.
- Morey, G.W., Fournier, R.O. and Rowe, J.J., 1962. The solubility of quartz in water in the temperature interval 25 to 300°C. *Geochim. Cosmochim. Acta*, 26, 1029-1043.
- Morris, K.A., 1980. Comparison of major sequences of organic rich mud deposition in the British Jurassic. *Jour. Geol. Soc. London*, 137, 157-170.
- Morton, G.H., 1876-8. The Carboniferous Limestone and Millstone Grit of North Wales. *Proc. Lpool. Geol. Soc.*, 3, 152-205, 299-325, 371-428.
- Morton, G.H., 1879. The Carboniferous Limestone and Cefn-y-Fedw Sandstone of the country between Llanymynech and Minera, North Wales. 8, London, P.41, Reprinted from Liverpool Geological Society.
- Müller, G., Irion, G. and Forstner, U., 1972. Formation and diagenesis of inorganic Ca-Mg carbonates in the lacustrine environment. *Naturwissenschaften*, 59, 158-164.
- Müller, J., 1959. Palynology of Recent Orinoco delta and shelf sediments - report on the Orinoco shelf expedition. *Micropaleontology*, 5, 1-32.
- Müller, S.C., Kai, S. and Ross, J., 1982. Curiosities in periodic precipitation patterns. *Science*, 216, 635-637.
- Murata, K.J. and Larson, R.R., 1975. Diagenesis of Miocene siliceous shales, Temblor Range, California, U.S. Geol. Survey Jour. Research, 3, no.5, 553-566.
- Murata, K.J. and Norman, M.B., 1976. An Index of crystallinity for quartz. *Am. Jour. Sci.*, 276, 1120-1130.
- Murata, K.J., Friedman, I and Gleason, J.D., 1977. Oxygen isotope relations between diagenetic silica minerals in Monterey shale, Temblor Range, California. *Am. Jour. Sci.*, 277, 259-272.
- Neves, R., 1958. Upper Carboniferous plant spore assemblages from the Gastrioceras subcrenatum horizon, North Staffordshire. *Geol. Mag.*, 95, 1-19.
- Neves, R., 1961. Namurian plant spores from the Southern Pennines, England. *Palaeontology*, 4, 247-279.

- Neves, R., 1964. The stratigraphic significance of small spore assemblage of the Camocha Mine, Gijon, N. Spain. C.R. 5th Congr. Int. Geol. Strat. Carb., 3, 1063-1069.
- Neves, R., 1968. The palynology of the Woodland Borehole, Co. Durham. Bull. Geol. Surv. Gt. Br., 28, 55-60.
- Neves, R., 1969. A review of some recent advances in the palynology of the Carboniferous. C.R. 6th Congr. Inter. Strat. Geol. Carb., Sheffield, 1967, 1, 337-349.
- Neves, R. and Dale, B., 1963. Modified filtration system for palynological preparation. Nature, Lond., 198, 775-776.
- Neves, R., Read, W.A. and Wilson, R.B., 1965. Note on recent spore and goniatite evidence from the Passage Group of the Scottish Upper Carboniferous succession. Scot. Jour. Geol., 1, 185-188.
- Neves, R., and Owens, B., 1966. Some Namurian camerate miospores from the English Pennines. Pollen et. spores, 8, 337-360.
- Neves, R. and Belt, E.S., 1970. Some observations on Namurian and Visean spores from Nova Scotia, Britain and Northern Spain. C.R. 6th Congr. Avanc. Etud. Stratigr. Geol. Carb., Sheffield, (1967), 3, 1233-1248.
- Neves, R., Gueinn, K.J., Clayton, G., Ioannides, N.S. and Neville, R.S.W., 1972. A scheme of miospore zones for the British Dinantian. C.R. 7th Congr. Int. Carb. Strat. Geol., Krefeld (1971), 1, 347-353.
- Neves, R., Gueinn, K.J., Clayton, G., Ioannides, N.S., Neville, R.S.W. and Kruszewska, K., 1973. Palynological correlations within the Lower Carboniferous of Scotland and Northern England. Trans. Roy. Soc. Edinb., 69 (2), 23-70.
- Nicholls, G.D. and Loring, D.H., 1962. The geochemistry of some British Carboniferous Sediments. Geochim. Cosmochim. Acta, 26, 181-223.
- Nickel, E., 1978. The present status of cathode luminescence as a tool in sedimentology. Minerals Science Engineering, 10, 73-100.
- Nissenbaum, A., Presley, B.J. and Kaplan, I.R., 1972. Early diagenesis in a reducing fjord, Saanich Inlet British Columbia. I. chemical and isotopic changes in major components of interstitial water. Geochim. Cosmochim. Acta, 36, 1007-1027.

- Oglesby, T.W., 1976. A model for the distribution of manganese, iron and magnesium in authigenic calcite and dolomite cements in the Upper Smackover Formation in eastern Mississippi. Master's thesis, Univ. of Missouri, 122 p.
- Oomkens, E., 1974. Lithofacies relations in the Late Quarternary Niger delta complex. *Sedimentology*, 21, 195-222.
- Orme, G.R., 1974. Silica in the Visean limestones of Derbyshire, England. *Proc. Yorks. Geol. Soc.*, 40, part 1, No.5, 63-103.
- Owens, B., 1981. Palynology, its Biostratigraphic and Environmental Potential. *Petroleum Geology of the Continental Shelf of North West Europe*, 162-168.
- Owens, B. and Burgess, I.C., 1965. The stratigraphy and palynology of the Upper Carboniferous outlier of Stainmore, Westmorland. *Bull. Geol. Surv. Gt. Br.*, 23, 17-44.
- Owens, B., Mishell, D.R.F. and Marshall, J., 1976. Kraeuselisporites from the Namurian of Northern England. *Pollen et. spores*, 18, 145-156.
- Owens, B., Neves, R., Gueinn, K.J., Mishell, D.R.F., Sabry, H.S.M.Z. and Williams, J.E., 1977. Palynological division of the Namurian of Northern England and Scotland. *Proc. Yorks. Geol. Soc.*, 41, 381-398.
- Owens, B., Loboziak, S. and Teteriuk, V.K., 1978. Palynological subdivision of the Dinantian to Westphalian deposits of North-West Europe and the Donetz Basin of the U.S.S.R. *Palynology*, 2, 69-91.
- Parker, A., 1974. The clay mineralogy and some trace element contents of the speeton clay. *Proc. Yorks. Geol. Soc.*, 40, part 2, no.10, 181-190.
- Parry, C.C., Whitley, P.K.J. and Simpson, R.D.H., 1981. Integration of palynological and sedimentological methods in facies analysis of the Brent Formation. *Petroleum Geology of the Continental Shelf of North-West Europe*, 205-215.
- Pearson, M.J., 1979. Geochemistry of the Hepworth Carboniferous sediment sequence and origin of the diagenetic iron minerals and concretions. *Geochim. Cosmochim. Acta*, 43, no.6, 927-941.
- Peppers, R.A., 1964. Spores in strata of late Pennsylvanian cyclothems in the Illinois Basin. *Ill. St. Geol. Surv. Bull.*, 90, 1-89.

- Peppers, R.A., 1970. Correlation and palynology of coals in the carbondale and Spoon Formations (Pennsylvanian) of the north-eastern part of the Illinois Basin. Ill. St. Geol. Surv. Bull., 93, 1-173.
- Percival, C.J., 1981. Carboniferous quartz arenites and ganisters of the northern Pennines. Ph.D. thesis. University of Durham, 353 p.
- Perry, E.D. and Hower, J., 1970. Burial diagenesis in Gulf Coast Pelitic Sediments. Clays and Clay Min., 18, 165-177.
- Perry, E.D. and Hower, J., 1972. Late stage dehydration in deeply buried pelitic sediments. Am. Assoc. Petrol. Geol. Bull., 56, 2013-2021.
- Pettijohn, F. J., 1975. Sedimentary Rocks. 3rd Ed. Harper and Row, New York, 628 p.
- Pettijohn, F.J., Potter, P.E. and Siever, R., 1973. Sand and Sandstone: New York, Springer-Verlag, 618 P.
- Phillip, W., Drong, H.J., Fuchtbauer, H., Haddenhorst, H.G. and Jankowsky W., 1963. The history of migration in the Grifhorn Trough (NW-Germany). 6th World Petroleum Congr. Proc., Sec. 1, Pap. 19, 457-481.
- Philippi, G.T., 1974. The influence of marine and terrestrial source material on the composition of petroleum. Geochim. Cosmochim. Acta, 38, 947-966.
- Pierson, B.J., 1978. Control of cathodoluminescence of dolomite by iron and manganese (abs.) Am. Assoc. Petrol. Geol. Bull. 62, 553-554.
- Pisciotta, K.A., 1981. Diagenetic trends in the siliceous facies of the Monterey shale in the Santa Maria region, California. Sedimentology, 28, 547-571.
- Pisciotta, K.A. and Mahoney, J.J., 1981. Isotopic survey of diagenetic carbonates. DSDP, Leg 63, Initial Reports of the DSDP63, 595-609, Washington, D.C., U.S. Government Printing Office.
- Pittman, E.D., 1972. Diagenesis of quartz in sandstones as revealed by scanning electron microscopy. Jour. Sed. Pet., 42, 507-519.
- Pittman, E.D., 1979. Porosity, diagenesis and productive capability of sandstone reservoirs. In: Aspects of Diagenesis. Spec. Publ. Soc. Econ. Palaeontol. Mineral. Tulsa, 26, 159-173.

- Pittman, E.D. and Lumsden, D.N., 1968. Relationship between chlorite coatings on quartz grains and porosity, Spiro Sand, Oklahoma, Jour. Sed. Pet., 38, 668-670.
- Playford, G., 1962. Lower Carboniferous microfloras of Spitsbergen. Pt.1, Palaeontology, 5, 550-618.
- Pollastro, R.M., 1985. Mineralogical and morphological evidence for the formation of illite at the expense of illite/smectite. Clays and Clay Miner., 33, no.4, 265-274.
- Potter, K.W. and Weimer, R.J., 1982. Diagenetic sequence related to structural history and petroleum accumulation; Spindle field, Colorado. Amer. Assoc. Petrol. Geol. Bull., 66, 2543-2560.
- Potonié, R. and Kremp, G.O.W., 1954. Die Gattungen der palaeozoischen sporae dispersae und ihre stratigraphie. Beih. Geol. Jb., 69, 111-194.
- Potonié, R., and Kremp, G.O.W., 1955. Die sporae dispersae des Ruhrkarbons, ihre Morphographie und stratigraphie mit Ausblicken auf Arten anderer Gebiete und Zeitabschnitte: Teil I. Palaeontographica, B98, 1-136.
- Potonié, R. and Kremp, G.O.W., 1956. Idem; Teil II. Ibid. B99, 85-191.
- Powell, T.G., Cook, P.J. and McKirdy, D.M., 1976. Organic geochemistry of phosphorites: Relevance to petroleum genesis. Am. Assoc. Petrol. Geol. Bull., 4, 618-632.
- Powers, M.C., 1967. Fluid release mechanisms in compacting marine mudrocks and their importance in oil exploration. Am. Assoc. Petrol. Geol. Bull., 51, 1240-1254.
- Presley, B.J. and Kaplan, I.R., 1968. Changes in dissolved sulphate, calcium and carbonate from interstitial water of near shore sediments. Geochim. Cosmochim. Acta, 32, 1037-1048.
- Pye, K., 1985. Electron microscope analysis of zoned dolomite rhombs in the Jet Rock Formation (Lower Toarcian) of the Whitby area, U.K. Geol. Mag., 122(3), 279-286.
- Raistrick, A., 1934-5. The correlation of coal seams by miospore content, pt.1. The seams of Northumberland, Trans. Inst. Min. Engrs. Lond., 88, 142-153 and 249-264.

- Raistrick, A., 1937. The microspore content of some lower carboniferous coals, *Trans. Leeds Geol. Ass.* 5, 221-226.
- Raistrick, A., 1938. The correlation of coal seams by microspore content, pt. II. The Trencherbone Seam. *Trans. Inst. Min. Engrs. Lond.*, 97, 425-437, and 98, 95-99 and 171-175.
- Ramsbottom, W.H.C., 1967. The use of goniatites in the zonation of the Namurian. *Proc. Int. Subcomm. Carb. Strat.* (Sheffield, 1965) 23-5.
- Ramsbottom, W.H.C., 1969. The Namurian of Britain. *C.R. Congr. Stratigr. Geol. Carbonif.*, Sheffield 1967, 1, 219-232.
- Ramsbottom, W.H.C., 1969a. Interim report of the Namurian Working Group. *C.R. 6me Cong. int. strat. Geol. Carb.* (Sheffield, 1967), 1, 71-77.
- Ramsbottom, W.H.C., 1970. Carboniferous faunas and palaeogeography of the south-west England region. *Proc. Ussher Soc.*, 2, 144-157.
- Ramsbottom, W.H.C., 1974b. The Namurian in North Wales. In T.R. Owen, (Ed.). *The Upper Palaeozoic and Post-Palaeozoic rocks of Wales.* Univ of Wales Press, Cardiff, 161-167.
- Ramsbottom, W.H.C., 1977. Major cycles of transgression and regression (mesothems) in the Namurian. *Proc. Yorks. Geol. Soc.*, 41, 261-291.
- Rangin, C., Steinberg, M. and Bonnot-Courtois, C., 1981. Geochemistry of the Mesozoic bedded cherts of Central Baja, California (vizcaino-Cedros-San Benito). Implications for palaeogeographic reconstructions of an old oceanic basin. *Earth Planet Sci. Lett.*, 54, 313-322.
- Rankama, K. and Sahama, T.G., 1950. *Geochemistry.* Univ. of Chicago Press, Chicago, 912 P.
- Ravn, R.L., 1979. An introduction to the stratigraphic palynology of the Cherokee Group (Pennsylvanian) coals of Iowa. *Iowa Geol. Surv. Tech. Pap.*, 6, 1-117.
- Ravn, R.L. and Fitzgerald, D.J., 1982. A Morrowan (Upper Carboniferous) microspore flora from eastern Iowa, U.S.A. *Palaeontographica, Abt. B.*, 183, 108-172.
- Reading, H.G., 1967. Sedimentation sequences in the Upper Carboniferous of North Western Europe, 1401-1411.

- Riezebos, P.A., 1974. Scanning electron microscopical observations on weakly cemented Miocene sands. *Geologie en Mijnbouw*, 53, 109-122.
- Robin, P.Y.F., 1978. Pressure solution at grain to grain contacts. *Geochim. Cosmochim. Acta*, 42, 1383-1389.
- Rogers, M.A., 1979. Panel discussion PDI. 10 Int. Petrol. Cong.
- Ross, C.S. and Kerr, P.F., 1930. The kaolin minerals. *U.S. Geol. Surv.*, 165-E, 151-176.
- Ruppert, L.F., Cecil, C.B., Stanton, R.W. and Christian, R.P., 1985. Authigenic quartz in the Upper Freeport Coal Bed, West-Central Pennsylvania. *Jour. Sed. Pet.*, 55, no.3, 334-339.
- Rutter, E.H., 1976. The kinetics of rock deformation by pressure solution. *Proc. Roy. Soc.*, A283, 203-219.
- Sabry, H.S.M.Z. and Neves, R., 1970. Palynological evidence concerning the unconformable carboniferous basal measures in the Sanguhar Coalfield, Dumfriesshire, Scotland. *C.R. 6th Congr. Int. Strat. Geol. Carb.*, 4, 1441-1458.
- Sargent, H.C., 1921. The Lower Carboniferous chert formation of Derbyshire. *Geol. Mag.*, 59, 265-278.
- Sargent, H.C., 1927. The stratigraphical horizon and field relations of the Holywell Shales and 'Black Limestone' of North Flintshire. *Geol. Mag.*, 63, 252-263.
- Sarkisyan, S.G., 1971. Application of the scanning electron microscope in the investigation of oil and gas reservoir rocks. *Jour. Sed. Pet.*, 41, 289-292.
- Sayles, F.L. and Manheim, F.T., 1975. Interstitial solutions and diagenesis in deeply buried marine sediments: results from the DSDP. *Geochim. et Cosmochim. Acta*, 39, 103-127.
- Schmidt, V. and McDonald, D.A., 1979a. The role of secondary porosity in the course of sandstone diagenesis. In: P.A. Scholle and P.R. Schluger (Eds.), 1979. *Aspects of Diagenesis. Spec. Publ. Soc. Econ. Paleontol. Mineral.*, Tulsa, 26, 127-207.

- Schmidt, V and McDonald, D.A., 1979b. Texture and recognition of secondary porosity in sandstone. In: P.A. Scholle and P.R. Schluger (Eds.), 1979. Aspects of diagenesis. Spec. Publ. Soc. Econ. Paleontol. Mineral., Tulsa, 26, 209-225.
- Scholle, P.A., 1979. A color illustrated guide to constituents, textures, cements and porosities of sandstones and associated rocks. Am. Ass. Petrol. Geol. Mem. No.28, 201 P.
- Schopf, J.M., 1938. Spores from the Herrin (No.6) coal bed of Illinois. Rep. Invest. Ill. Geol. Surv., 50, 1-55.
- Schopf, J.M., Wilson, L.R. and Bentall, R., 1944. An annotated synopsis of Paleozoic fossil spores and the definition of generic groups. Rep. Invest. Ill. Geol. Surv., 91, 1-66.
- Schultz, L.G., 1978. Mixed-layer clay in the Pierre shale and equivalent rocks, Northern Great Plain region. U.S. Geol. Surv. Prof. paper. 1064A.
- Shaw, G. and Yeadon, A., 1964. Chemical studies on the constitution of some pollen and spore membranes. Grana palynol., 5, 247-252.
- Shaw, H.F., 1980. Clay minerals in sediments and sedimentary rocks. In: G.D. Hodson (Ed.) Development in Petroleum Geology, Vol.2, Applied Science Publ. Barking, Essex, U.K., 53-85.
- Sheppard, R.A. and Gude, A.J., 3d, 1974. Chert derived from magadiite in a lacustrine deposit near Rome, Malheur County, Oregon, U.S. Geol. Surv. Jour. Research, 2, 625-630.
- Sibley, D.F. and Blatt, H., 1976. Intergranular pressure solution and cementation of the Tuscarora orthoquartzite. Jour. Sedim. Petrol., 46, 881-896.
- Siever, R., 1962. Silica solubility 0°-200°c and the diagenesis of siliceous sediments. Jour. Geol., 70, 127-150.
- Siever, R., Beck, K.C. and Berner, R.A., 1965. Composition of interstitial waters of modern sediments. Jour. Geol. 73, 39-73.
- Siffert, B. and Wey, R., 1961. Reactions de la silice monomoléculaire en solution avec les ions Al^{3+} et Mg^{2+} . Genèse et synthèse des argiles. Coll. Intern. C.N.R.S. 105, 11-23.
- Sippel, R.F., 1968. Sandstone petrology evidence from luminescence petrography. Jour. Sed. pet., 38, 530-554.

- Sippel, R.F. and Glover, E.D., 1965. Structures in carbonate rocks made visible by luminescence petrography. *Science*, 150, 1283-1287.
- Smith, A.H.V., 1957. The sequence of microspore assemblages associated with the occurrence of crassidurite in coal seams of Yorkshire. *Geol. Mag.*, 94, 345-363.
- Smith, A.H.V., 1962. The palaeoecology of Carboniferous peats based on the miospores and petrography of bituminous coals. *Proc. Yorks. Geol. Soc.*, 33, 423-474.
- Smith, A.H.V. and Butterworth, M.A., 1967. Miospores in the coal seams of the Carboniferous of Great Britain. *Spec. Pap. Palaeontol.*, No.1, 324 P.
- Smith, J.V. and Stenstrom, R.C., 1965. Electron-excited luminescence as a petrologic tool. *Jour. Geol.*, 73, 627-635.
- Somers, Y., 1971. Etude palynologique du Westphalien du Bassin de Campine et revision du genre *Lycospora*. These de Doctorat, Univ. Liege (privately published).
- Sosman, R.B., 1927. The properties of silica. American Chemical Society Monograph Series, The Chemical Catalog Co, Inc., New York, 856 P.
- Spears, D.A. and Amin, M.A., 1981. Geochemistry and mineralogy of marine and non-marine Namurian black shales from the Tansley Borehole, Derbyshire. *Sedimentology*, 28, 407-417.
- Sprunt, E.S., 1981. Causes of quartz cathodoluminescence colors: Scanning Electron Microscopy, 1, 525-535.
- Sprunt, E.S., and Nur, A.A., 1976. Reduction of porosity by pressure solution: experimental verification. *Geology*, 4, 463-466.
- Sprunt, E.S., Dengler, L.A. and Sloan, D., 1978. Effects of metamorphism on quartz cathodoluminescence. *Geology*, 6, 305-308.
- Stanton, G.D., 1977, Secondary porosity in sandstones of the Lower Wilcox (Eocene), Karnes County, Texas. *Trans. Gulf Coast Assoc. Geol. Soc.*, 27, 197-207.
- Staplin, F.L., 1960. Upper Mississippian plant spores from the Golata formation, Alberta, Canada. *Palaeontographica*, B107, 1-40.
- Staplin, F.L., 1969. *Bull. Can Petrol. Geol.*, 17 (1), 47-66.

- Staplin, F.L. and Jansonius, J., 1964. Elucidation of some Paleozoic densospores. *Ibid.*, 114, 95-117.
- Staplin, F.L., Bailey, N.J.L., Pocock, S.A.J. and Evans, C.R., 1973. *Am. Assoc. Petrol. Geol. Sym. Anaheim (Ms).*
- Steinberg, M. and Mpodozis, M.C., 1978. Classification géochimique des radiolarites et des sédiments siliceux océaniques, signification paleo-océanographique. *Oceanologica Acta* 1, 3, 359-367.
- Steinberg, M., Bonnot-Courtois, C. and Tlig, S., 1984. Geochemical contribution to the understanding of bedded chert. In: A.Lijima, J.R. Hein and R. Siever (Eds.). *Siliceous Deposits in the Pacific Region*. Elsevier, Amsterdam, 193-210.
- Stevenson, I.P. and Gaunt, G.D., 1971. Geology of the country around Chapel-en-le-Frith. *Mem. Geol. Surv., U.K.*, 444 P.
- Strakhov, N.M., 1967. Principles of Lithogenesis (trans. from 1962 Russian original), New York, Consultants Bureau, 245 P.
- Sulaiman, A., 1972. Geochemistry of the Namurian argillites. Unpubl. Ph.D. thesis, Southampton University.
- Sullivan, H.J., 1962. Distribution of miospores through coals and shales of the coal Measures sequence exposed in the Wernddu Clay pit, Caerphilly (South Wales). *Quart. Jour. Geol. Soc. Lond.*, 118, 353-373.
- Sullivan, H.J., 1964. Miospores from the Drybrook Sandstone and associated Measures in the Forest of Dean basin, Gloucestershire. *Palaeontology*, 7, 351-392.
- Sullivan, H.J., and Marshall, A.E., 1966. Viséan spores from Scotland. *Micropaleontology*, 12, 265-285.
- Sullivan, H.J. and Mishell, D.R.F., 1971. The Mississippian-Pennsylvanian boundary and its correlation with Europe. *C.R. 6th Congr. Inter. Strat. Geol. Carb.*, Sheffield 1967, 4, 1533-1540.
- Sweatman, T.R. and Long, J.V.P., 1969. Quantitative electron probe microanalysis of rock forming minerals. *Jour. Petrol.*, v.10, 332-379.
- Sweeney, M.A., 1985. Diagenetic processes in ore formation with special reference to the Zambian copperbelt and Permian Marl Slate. Unpubl. Ph.D. thesis. University of Aston in Birmingham, vol.I and II.

- Swett, K., 1964. Petrology and paragenesis of the Ordovician Manitou Formation along the Front Range of Colorado. *Jour. Sed. Pet.*, 34, 615-624.
- Taylor, J.C.M., 1978. Control of diagenesis by depositional environment within a fluvial sandstone sequence in the Northern North Sea Basin. *Jour. Geol. Soc. Lond.*, 135, 83-91.
- Taylor, J.M., 1950. Pore-space reduction in sandstones. *Bull. Am. Assoc. Petrol. Geol.*, 34, 701-716.
- Tchoubar, V.D., 1966. *C.R. Acad. Sci. Paris*, 263, 1030.
- Teichmüller, M., 1958. Métamorphisme du charbon et prospection du pétrole. *Rev. Ind. Minérale, Numero Special*, 1-15.
- Teichmüller, M., 1962. Die Genese der Kohle. *Congr. Avan. Etudes stratigraph. Geol. Carb. C.R.*, 4, 699-722.
- Teteriuk, V.K., 1976. Namurian stage analogues in the Carboniferous period of the Donetz Basin (based on palynological data). *Geol. Jour.*, 36, 110-122 (in Russian).
- Thiessen, R. and Wilson, F.E., 1924. Correlation of coal beds of the Allegheny formation of western Pennsylvania and Eastern Ohio. *Ibid.* 10, 1-56.
- Tillman, R.W. and Almon, W. R., 1979. Diagenesis of Frontier Formation offshore bar sandstones, Spearhead Ranch Field, Wyoming. In: Scholle, P.A. and Schluger, P.R. (eds.) *Aspects of Diagenesis. Spec. Publ. Soc. Econ. Miner. Paleont.*, Tulsa, 26, 337-378.
- Ting, T.C., 1975. Reflectivity of disseminated vitrinites in the Gulf Coast region. *Petrographie de las matiere organique des sediments relations avec la paleo-temperature et le potential petrolier*. Paper presented to the Centre National de la Recherche Scientifique, September 15-17, 1973, Paris.
- Tourtelot, H.A., 1964. Minor element composition and organic carbon content of marine and non-marine shales of Late Cretaceous age in the Western interior of the United States. *Geochim. et Cosmochim. Acta*, 28, 1579-1604.
- Towe, K.M., 1962. Clay mineral diagenesis as a possible source of silica cement in sedimentary rocks. *Jour. Sed. Pet.*, 32, 26-28.

- Turner, P., 1980. Continental Red Beds. Development in Sedimentology. No. 29, Elsevier, Amsterdam, 562 p.
- Turner, P., 1982-1986. Personal Communication.
- Twenhofel, W.H. and Tyler, S.A., 1941. Methods of study of sediments. McGraw-Hill company. 183 p.
- Urban, J.B., 1971. Palynology and the independence shale of Iowa. Bull. Am. Paleont., 60, 103-189.
- Van Krevelen, D.W., 1961. "Coal". Elsevier, Amsterdam.
- Van Leckwijck, W.P., 1960. Report of the Subcommittee on Carboniferous stratigraphy. C.R. 4me Cong. Int. Strat. Geol. Carb. (Heerlen 1958) 1, xxiv-xxv.
- Van Praagh, G., 1947. Synthetic quartz crystals. Geol. Mag. 84, 98-100.
- Van Praagh, G., 1949. The hydrothermal crystallization of vitressil at constant temperature. Discussions of the Faraday Soc., 5, 338-341.
- Van Wijhe, D.H. and Bless, M.J.M., 1974. The Westphalian of the Netherlands with special reference to miospore Assemblages. Geol. Mijnbouw, 53, (6), 295-328.
- Vassoyevich, N.B., Korchagina, Y.I., Lopatin, N.V. and Chernyshev, V.V., 1970. Principal phase of oil formation. Moskov. Univ. Vestnik, no.6, 3-27 (in Russian); Eng. transl: Internat. Geology Rev., v., 12, 1276-1296.
- Venkatachala, B.S., 1980. Differentiation of Amorphous organic matter types in Sediments. Proceedings of a symposium held at the 5th international Palynological Conference, Cambridge, England, 177-200.
- Venkatachala, B.S. and Bharadwaj, D.B., 1964. Sporological study of the coals from Falkenburg (Faulquemont) Colliery, Lothringen (Lorraine), France. Palaeobotanist, 11, 159-207.
- Wallace, C.A., 1976. Diagenetic replacement of feldspar by quartz in the Unita Mountain Group, Utah and its geochemical implications. Jour. Sed. Pet., 46, 847-861.
- Walker, A.L., McCulloh, T.H., Petersen, N.F. and Stewart, R.J., 1983. Anomalously low reflectance of vitrinite, in comparison with other petroleum source rock maturation indices, from the Miocene Modelo

- Formation in the Los Angeles Basin, California. Soc. Econ. Paleon. Miner. Pacific Section, 185-190.
- Walker, T.R., 1962. Reversible nature of chert-carbonate replacement in sedimentary rocks. Bull. Geol. Soc. Am., 73, 237-42.
- Walker, T.R., Waugh, B. and Crone, A.J., 1978. Diagenesis in first cycle desert alluvium of Cenozoic age, southwestern United States and northwestern Mexico. Geol. Soc. Am. Bull., 89, 19-32.
- Watson, J., 1979. Carboniferous miospores from the Prestatyn District, North-East Wales. M.Sc. thesis, Sheffield University.
- Waugh, B., 1970a. Formation of quartz overgrowths in the Penrith Sandstone (Lower Permian) of northwest England as revealed by scanning electron microscopy. Sedimentology, 14, 309-320.
- Waugh, B., 1970b. Petrography, provenance and silica diagenesis of the Penrith sandstone (Lower Permian) of northwest England. Jour. Sed. Pet., 40, 1226-1240.
- Weaver, C.E., 1960. Possible uses of clay minerals in the search for oil. Bull. Am. Assoc. Petrol. Geol., 44, 1505-1518.
- Wedd, C.B., Smith, B. and Wills, L.J., 1927. The geology of the country around Wrexham. Part. 1, Lower Palaeozoic and Lower Carboniferous rocks, Mem. Geol. Surv. Gt. Britain.
- Wedepohl, K.H., 1969. Handbook of Geochemistry. Vol. 1. Springer-Verlag, Berlin, 442 p.
- Weyl, P.K., 1959. Pressure solution and the force of crystallization - a phenomenological theory. Jour. Geophys. Res., 64, 2001-2025.
- Whitaker, M.F. and Butterworth, M.A., 1978. Palynology of Carboniferous strata from the Ballycastle area, County Antrim, Northern Ireland. Palynology, 2, 147-158.
- Whitaker, M.F. and Butterworth, M.A., 1979. Palynology of Arnsbergian (Upper Carboniferous) strata in County Leitrim, Ireland. Jour. Earth Sci. R. Dubl. Soc., 1, 163-171.
- Whitehurst, J., 1778. An enquiry into the original state and formation of the earth. London.
- Williams, L.A., Parks, G.A. and Crerar, D.A., 1985. Silica Diagenesis, I. Solubility controls. Jour. Sed. Pet., 55, No.3, 301-311.

- Wilson, L.R., 1976. Desmoinsian Coal seams of north-eastern Oklahoma and their palynological content. *Okl. Geol. Surv. and Univ. Okl.* 1, 19-31.
- Wilson, L.R., and Kosanke, R.H., 1944. Seven new species of unassigned plant microfossils from the Des Moines series of Iowa. *Proc. Iowa Acad. Sci.*, 51, 329-32.
- Wilson, L.R. and Hoffmeister, W.S., 1956. Plant microfossils of the Croweburg Coal. *Circ. Okla. Geol. Surv.*, 32, 1-57.
- Wilson, M.D. and Pittman, E.D., 1977. Authigenic clays in sandstones: Recognition and influence on reservoir properties and palaeo-environmental analysis. *Jour. Sed. Pet.*, 47, 3-31.
- Wilson, P., 1978. Quartz overgrowths from the Millstone Grit Sandstones (Namurian) of the Southern Pennines as revealed by scanning electron microscopy. *Proc. Yorks. Geol. Soc.*, 42, part 2, no.15, 289-295.
- Wilson, R.C.L., 1966. Silica diagenesis in Upper Jurassic limestones of southern England. *Jour. Sed. Pet.*, 36, 1036-1049.
- Wollast, R., 1967. Kinetics of the alteration of k-feldspar in buffered solutions at low temperature. *Geochim. Cosmochim. Acta*, 31, 635-648.
- Wood, A., 1936. Goniatic zones of the Millstone Grit Series in North Wales. *Proc. Lpool. Geol. Soc.*, 17, 10-28.
- Zetzsche, F. and Kalin, O., 1932. Untersuchungen uber die Membranen der sporen und Pollen VII. Eine Methode zur Isoierung des polymerbitumens aus kohlen. *Braunkohle*, 31, 345-351 and 363-366.
- Ziegler, P.A., 1982. Geological Atlas of Western and Central Europe. Shell internationale Petroleum Maatschappij B.V.
- Zinkernagel, U., 1978. Cathodoluminescence of quartz and its application to sandstone petrology. *Contributions to Sedimentology*, 8, 69 p.